Proceedings

IIBEC 2022 - Building for the Future

International Convention and Trade Show

March 17–22, 2022 | Orlando, FL

Proceedings of the IIBEC International Convention and Trade Show

March 17-22, 2022

TABLE OF CONTENTS

3:45 pm – 5:15 pm

Monday, March 21, 2022

8:45 am – 10:15 am

10:30 am – 12:00 pm

2:15 pm – 3:45 pm

4:00 pm – 5:30 pm

Nondestructive Testing Methods in Structural and Building Enclosure Assessment

Maziyar Bolour

Walter P Moore | Toronto, ON

mbolour@walterpmoore.com

Michael Brown, PhD

Walter P Moore | Austin, TX

mdbrown@walterpmoore.com

IIBEC 2022 - Building for the Future

International Convention and Trade Show

March 17–22, 2022 | Orlando, FL

ABSTRACT

In recent years, nondestructive testing methods have evolved as important tools for assessing both building enclosure and structural components. At the same time, many practicing engineers and architects are unaware of these methods or their capabilities. This presentation covers selected nondestructive testing methods that are currently in use in North America, and it includes a case study for each method presented to demonstrate how the nondestructive testing investigation guided the design team to an appropriate repair strategy. Attendees will gain an overview of select techniques for potential use in assessments.

SPEAKERS

Maziyar Bolour

Walter P Moore | Toronto, ON

Focusing on building sciences, Maziyar Bolour is a senior project manager and leads Walter P Moore's Diagnostics Group in Toronto, Ontario, Canada. Having joined the architecture, engineering, and construction industry in 1997, he is experienced in structural design, evaluation, and rehabilitation of building structure and enclosure systems. He has completed more than 100 detailed condition assessments and technical audits for insurance companies, private property owners, and developers, and routinely performs audit and condition assessments of existing structures, parking structures, and window or curtainwall systems commonly used in North America. Bolour's extensive knowledge of the National Building Code of Canada/Ontario Building Code and the related design standards for various construction materials, along with a combination of structural engineering and enclosure consulting expertise, make him an excellent resource for any complex repair and restoration project.

Michael Brown, PhD

Walter P Moore | Austin, TX

Michael Brown is a project manager within Walter P Moore's Diagnostics Group, operating out of the Austin, Texas office. Having joined the industry in 2000, he specializes in the evaluation and repair of reinforced and prestressed concrete buildings and has extensive experience in nondestructive testing. Brown is a member of the American Concrete Institute Committee 228, Nondestructive Testing.

Nondestructive Testing Methods in Structural and Building Enclosure Assessment

Several common methods for nondestructive testing and evaluation are currently in use for building condition assessments carried out in both greenfield and brownfield projects. However, recent experiences have suggested that the integration of the nondestructive testing results into the evaluation process is lagging, and the results of the nondestructive testing program often end up as little more than colorful or distracting attachments to a report of findings.[1] Awareness of this trend is emerging in the property condition assessment and building performance audit communities. Thus, the purpose of this paper is to provide introductory level knowledge of a variety of nondestructive testing and evaluation techniques so that readers may begin to incorporate these methods into their work in a way that brings value.

Nondestructive testing methods do not produce direct answers to questions. Rather, nondestructive testing provides reliable supplemental information that a licensed design professional can use when making founded conclusions or determinations needed as part of an evaluation. The distinction between nondestructive testing, which is typically performed by a laboratory or technician, and nondestructive evaluation, which is typically performed by a licensed design professional, is a common source of misunderstanding and frustration. In a nondestructive evaluation, the design professional uses nondestructive testing, along with calculation, experience, and judgment, to develop and implement a plan of action.

This paper presents a series of nondestructive testing techniques at a conceptual level. After these techniques are discussed, we present three case studies in which these techniques were used to evaluate and repair existing building enclosure systems in Houston, Texas.

NONDESTRUCTIVE TESTING TECHNIQUES

Several techniques that show potential for building enclosure assessments are presented conceptually in the following sections. These techniques are not the only ones that could be applied; rather, they are techniques the authors have used during the course of their assessments and investigations.

Visual Assessment

Visual assessment is the most basic nondestructive testing technique, and it is often dismissed as trivial and inconsequential. However, a properly trained and experienced professional can visually assess large volumes of space quickly and efficiently. Subtle visual indications such as variations in color; variations in gaps or joints; staining; and cracking are all readily visible in many cases. If nothing else, the indicator can provide information to identify locations where further assessment is warranted.

Infrared Thermography

Infrared (IR) thermography is the science of acquisition and analysis of thermal information from noncontact thermal imaging devices. As it offers real-time, two-dimensional results using remote sensing, IR thermography is an extremely powerful tool for building diagnostics. IR thermographic survey of building elements and components can identify the following:

- Areas of energy losses associated with missing, inadequate, or uneven insulation
- Sources of air leakage and water penetration
- Anomalies that may cause long-term degradation of building structure
- Anomalous structural and material performances based on thermal mass of construction materials
- "Hot" electrical panels, breakers, switches, and wire connections
- Heating and cooling duct placement
- Pipe location
- Pest infestation

IR thermography detects emitted radiation in the IR range of the electromagnetic spectrum. This corresponds to wavelengths longer than the visible light portion of the spectrum. IR thermography is unique compared to the other two heat transfer mediums (conduction and convection) in that it does not require a transfer medium, that is, it can occur through a vacuum.

In a nondestructive evaluation, the design professional uses nondestructive testing, along with calculation, experience, and judgment, to develop and implement a plan of action.

IR cameras detect radiation energy and convert it to a temperature. However, not all energy detected from an object is related to its temperature. There are also components of absorbed and transmitted radiation.

When an IR camera detects radiation from a source, it detects not only emitted radiation but also reflected and transmitted radiation. Because the camera does not differentiate among emitted, reflected, and transmitted radiation amounts, its resulting temperature reading is skewed by the reflected and transmitted radiation components. Thus, those objects that register a temperature on an IR camera closest to their true temperature are those materials

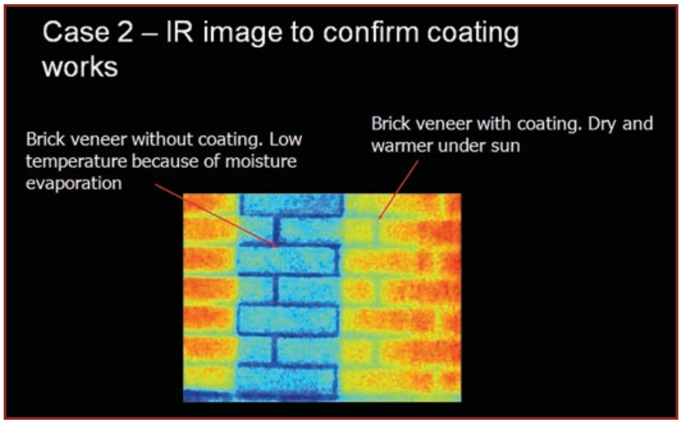

Figure 1. Sample of infrared thermography to detect a coating.

with higher emissivity. Most common building materials are suitable for IR thermography, but special attention is needed when dealing with metals due to their surface reflectivity.

Figure 1 presents an IR thermograph of a brick-veneer wall. The assessment associated with the thermograph aimed to determine the limits and confirm the efficacy of a coating to prevent moisture ingress in the brick surface. A portion of the surface was coated while the remainder remained uncoated. IR thermography confirmed the thermal variations associated with moisture ingress in the uncoated areas shown in blue in Fig. 1.

Short Pulse Radar

Short pulse radar (SPR) is a cost-effective, nondestructive, and reliable tool for scanning and imaging of subsurface defects, voids, and objects. Commonly referred to as ground penetrating radar, SPR was initially developed and used in geophysics and geology for subsurface scanning and imaging. However, the method has been successfully adapted in many other disciplines, including civil engineering and building sciences.

SPR is a nondestructive technique that emits a short pulse of electromagnetic energy, which is radiated into the subsurface. When this pulse strikes an interface between layers of materials with different electrical properties, part of the energy reflects, and the remaining energy continues to the next interface. SPR evaluates the reflection of electromagnetic waves at the interface between two different dielectric materials. The penetration of the waves into the subsurface is a function of the relative dielectric constants of the media. If a material is dielectrically homogeneous, the wave reflections will indicate a single thick layer. If the layers are dielectrically heterogenous, a strong wave reflection will be identified.

SPR directs electromagnetic energy into the subsurface. Concrete and masonry materials are low-conductivity, nonmetallic media that are ideal for SPR signal propagation. However, concrete and masonry typically have steel reinforcement, which is metallic and therefore completely reflects the SPR signal and shadows anything directly below.

Figure 2 provides the results of an SPR scan on a partially grouted and reinforced concrete masonry unit wall. In the figure, the scanned surface is at the top of the image. The scan represents an SPR depiction of the cross section of the wall. The red dashed lines represent head joints, and the locations of the reinforcing bars and empty cells are identified as well. Interpretation of these signals requires training and experience, but to a properly trained person, the results are quite clear.

Ultrasonic Pulse Velocity

Ultrasonic pulse velocity (UPV) is a nondestructive test method for determining the relative condition and quality of concrete or grouted masonry elements. UPV measures the time it takes for an ultrasonic pulse to travel through an element. The velocity of the waves depends on the density and elastic properties of the media as well as the presence of any discontinuities or anomalies within. This test generally requires access to both sides of the test element, but one-sided testing is also possible. The test is used to detect locations with interior cracking, honeycombing, and delaminations that may not be visible at the surface. In general, the longer the travel time of the ultrasonic pulse through a medium is, the more likely it is that an anomaly is present within the material.

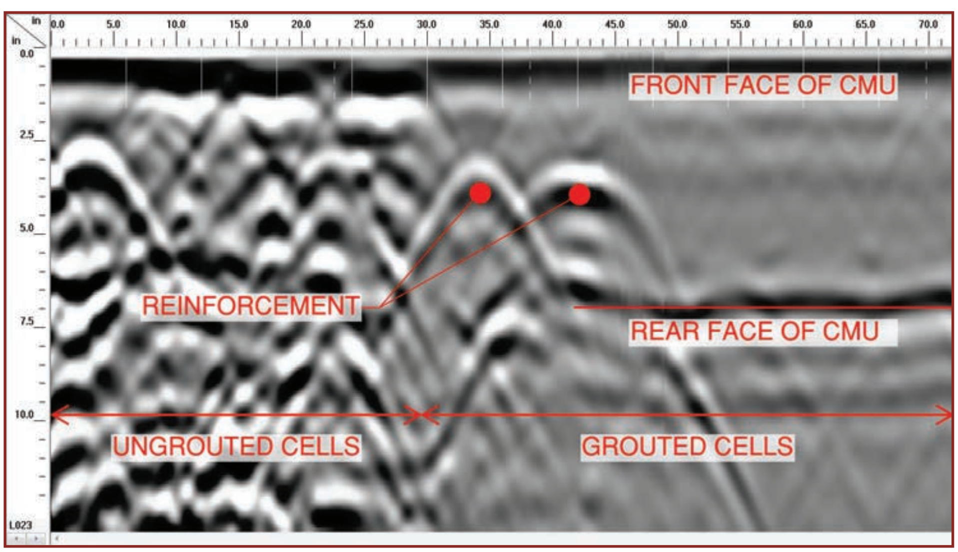

Figure 2. Sample short pulse radar image of a concrete masonry unit (CMU) wall.

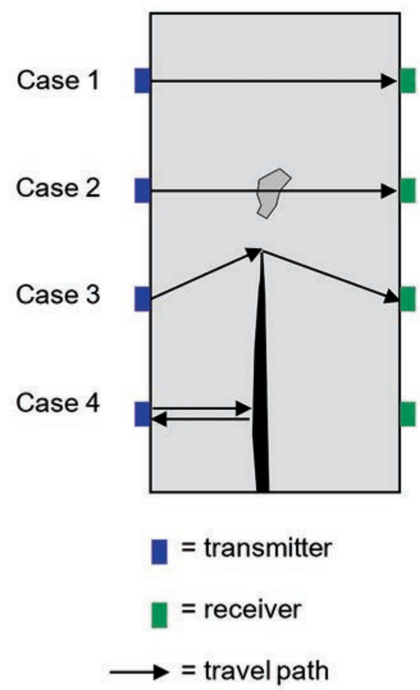

Figure 3. Schematic representation of ultrasonic pulse velocity. Case 1 = ultrasonic pulse traveling through sound concrete; Case 2 = ultrasonic pulse traveling through a portion of concrete that is inferior in quality, such as when unconsolidated concrete is present; Case 3 = ultrasonic pulse traveling around a crack or void; Case 4 =ultrasonic pulse being reflected due to the presence of a significant void.

Figure 3 illustrates four possible cases that can be inferred using the UPV method. Case 1 represents an ultrasonic pulse traveling through sound concrete. In this case, the measured travel time is the shortest of the four cases because the ultrasonic pulse travels directly through the media without interruption. Case 2 represents an ultrasonic pulse that travels through a portion of concrete that is inferior in quality, such as when unconsolidated concrete is present. In this case, the measured travel time is greater relative to the time measured for Case 1. Case 3 represents an ultrasonic pulse that has to travel around a crack or void. Due to the longer travel path, the measured travel time is greater relative to Case 1. Case 4 represents a scenario where the ultrasonic pulse is reflected due to the presence of a significant void. In this case, the travel time cannot be recorded and is measured as an out-of-range value.

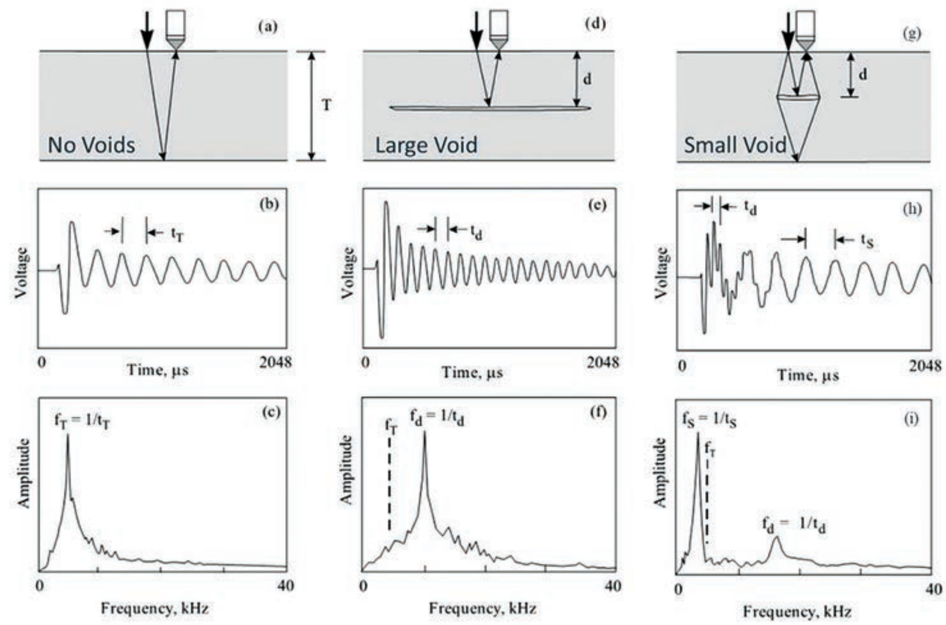

Figure 4. Sample of impact-echo signals for a thin element with no voids (a, b, and c); a thin element with a large defect (d, e, and f); and a thin element with a small void (g, h, and i). T = thickness; d = depth to flaw; t_T = characteristic period of full thickness echo; t_D = characteristic period of partial thickness echo; t_S = characteristic period of full thickness echo around a flaw; f_T = thickness frequency; f_d = thickness frequency at flaw; f_S = shifted full-thickness frequency. (Adapted from Sansalone and Street, 1997.[2])

Impact-Echo Technique

The impact-echo technique is based on the use of transient stress waves generated by a short-duration elastic impact of a small steel sphere on a concrete, masonry, or asphalt surface. This impact generates low-frequency stress waves that propagate into the structure and are reflected by flaws, external surfaces, or both. Surface displacements caused by the reflections of these waves are recorded by a displacement transducer located adjacent to the impact. The resulting displacement-versus-time signals are transformed into the frequency domain, and plots of amplitude versus frequency (spectra) are obtained. Multiple reflections of stress waves between the impact surface, flaws, and other external surfaces give rise to patterns of wave reflection and transient resonances, which can be identified in the spectrum and used to evaluate the integrity of the structure or to determine the location of flaws. It is the patterns present in the waveforms and spectra that provide information about the existence and locations of flaws or the dimensions of the cross section of the structure where a test is performed, such as the thickness of a concrete pavement. If flaws such as cracks, voids, or delaminations are present, these patterns are disrupted and changed in ways that provide qualitative and quantitative information about the existence and location of flaws. **Figure 4**[2] provides examples of typical signals for element with and without voids.

The impact-echo technique can be used to determine the thickness of plate-like structural members, such as slabs and facade panels; detect flaws in plate-like structural members, as well as beams, columns, and hollow cylindrical structural members; assess the quality of bond in overlays; and measure crack depths.

Using an impact to generate a stress pulse is an old technique that does not require a bulky transmitting transducer, and it provides a stress pulse with great penetration ability. However, the stress pulse generated by impact at a point is not focused like a pulse from an ultrasonic transducer. Instead, waves propagate into a test object in all directions, and reflections may arrive from many directions.

Since the early 1970s, impact methods—usually referred to as seismic-echo (or sonic-echo) methods—have been widely used for evaluation of concrete piles and drilled shaft foundations.[3] Beginning in the mid-1980s, the impact-echo technique was developed for testing of concrete structural members.[4,5]

Impulse Response

Impulse response is a nondestructive test used to evaluate the integrity of concrete elements. A low-strain impact is applied to excite the structure, and the response of the structure is measured. The concrete element is struck with a 1-kg hammer, which has a built-in load cell that measures the impulse imparted. The response (vibration) of the concrete element is monitored by a velocity transducer (geophone) placed adjacent to the impact location (**Fig. 5**).

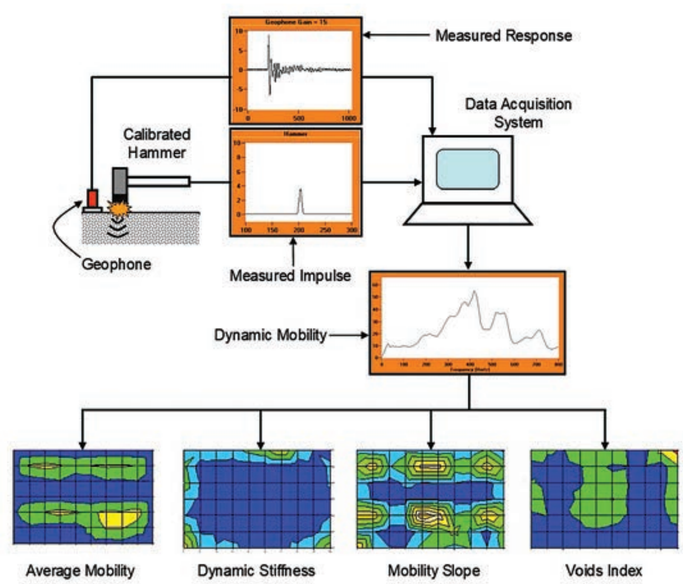

Figure 5. Schematic of impulse-response test.

Half-cell potential versus Cu/CuSO4(1)	Probability of corrosion
More positive than -200 mV	Low likelihood
Between -200 and -350 mV	Uncertain
More negative than -350 mV	High likelihood

Table 1. Interpretation of half-cell potential readings[6]

The hammer and the geophone are connected to a data acquisition and processing system, which calculates the dynamic mobility as a function of the frequency of the excitation. The dynamic mobility is analyzed to characterize the condition of the concrete and support conditions, and the probabilities of internal delaminations and voids in the concrete, which may not be visible at the surface.

Based on the analysis of the mobility plot, the following characteristics are obtained:

- Average mobility: The average mobility is a function of the density and thickness of the element. Cracking in concrete might affect the stability of the mobility plot.
- Dynamic stiffness: The dynamic stiffness is a function of the concrete quality, the element thickness, and the element support conditions.
- Mobility slope: The mobility slope is a function of concrete consolidation and structural shape changes.
- Voids index: The voids index is the ratio between the peak mobility and the average mobility. A high voids index indicates a higher probability of delaminations within a concrete member.

The testing is performed on a grid pattern, and contour plots are developed for the respective characteristic factors. Based on the analysis of these contour plots, probable locations of defects are determined.

Corrosion Testing

Corrosion testing in concrete and masonry elements is typically performed with a suite of techniques. The most widely used of these techniques are half-cell corrosion potential testing, linear polarization resistance (LPR), concrete resistivity, chloride ion content, and carbonation tests.

Half-Cell Corrosion Potential Measurement

Half-cell corrosion potential and corrosion rate tests are performed to determine the probability of corrosion activity on the reinforcing steel. The corrosion potential represents the tendency of a metal to corrode in a given environment. Half-cell corrosion potential testing is typically performed in accordance with ASTM C876, *Standard Test Method for Half-Cell Potentials of Uncoated Reinforcing Steel in Concrete*.[6]

The corrosion potential of reinforcing steel is measured relative to the potential of a reference electrode (such as copper-copper sulfate or silver-silver chloride). For potentials measured relative to the same reference electrode, the more negative the corrosion potential is, the greater the tendency of the metal to corrode is. **Table 1** shows the interpretation of the half-cell corrosion potential according to reference 6.

Concrete Resistivity

Corrosion of steel embedded in concrete or masonry is an electrochemical process. If the electrical resistance of the media is excessively low, corrosion will not occur. Thus, direct measurement of the electrical resistivity of the media provides insight into the likelihood of corrosion.

The most common technique to determine surface resistivity is the four-electrode method (**Fig. 6**).[7] In this test, the exterior electrodes emit an alternating current while the inner probes measure the resulting voltage. Based on the applied current and the measured voltage, the electrical resistance can be calculated.

Linear Polarization Resistance

LPR equipment uses the galvanostatic pulse method, a rapid nondestructive polarization technique, to determine the corrosion rate of the reinforcing steel. In the galvanostatic pulse method, a short-anodic current pulse is impressed galvanostatically to the reinforcing steel from a counter electrode placed on the concrete surface. A reference electrode placed in the center of the counter electrode measures the change in the electrochemical potential (polarization) of the reinforcement as a function of polarization time. A guard ring limits the length of the reinforcing bar that is affected by this polarization to a known quantity, which is essential to the calculation of the corrosion rate. The classification of the corrosion activity based on the measured corrosion rates depends on the equipment used to obtain the measurements. The interpretation of the corrosion rate measurements from a typically commercially available test system is presented in **Table 2**.[8]

Chloride Ion Content

Chlorides diffusing into concrete from an external source form a chloride profile (**Fig. 7**). The profile typically shows more chlorides near the top, indicating the need to sample the chlorides at the level of the reinforcing, either at the top or bottom layer of steel, or at both levels.

Chlorides have a dual effect within concrete, both of which contribute to corrosion of

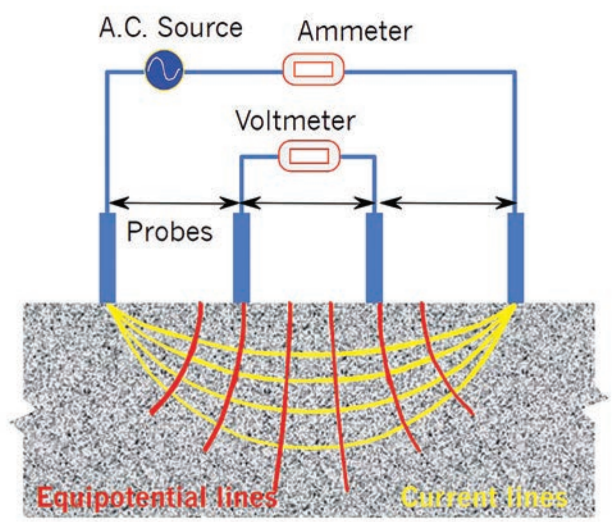

Figure 6. Schematic view of the four-electrode method for concrete surface resistivity.

Current density, μA/cm²	Thickness loss, mm/y	Corrosion level
<0.1	<0.001	Negligible
0.1–0.5	0.001–0.005	Low
0.5–1.0	0.005–0.001	Moderate
>1.0	>0.001	High

Table 2. Levels of corrosion activity from corrosion rate measurements[8]

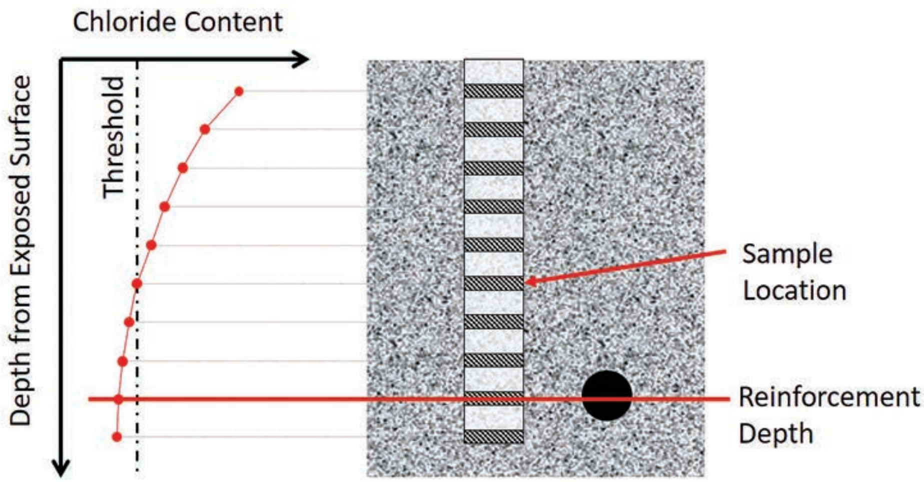

Figure 7. Chloride ion content profile in a core. Chloride profiles are often useful when determining the depth of concrete to be removed.

Figure 8. Example of concrete section with phenolphthalein staining for carbonation. The free calcium hydroxide is stained pink, and carbonation depth is approximately 7 mm.

embedded steel. They act to break down the passive layer and also increase conductivity of the concrete. If the concrete chloride content at the level of steel is at or above the threshold value, steel corrosion can start. How quickly corrosion occurs depends on available levels of oxygen and moisture. Cracking and spalling are not noticeable when the chloride content of the concrete at the steel reaches the threshold value. Deterioration usually is not noticed until chloride contents reach about 4 to 5 pounds of chloride per cubic yard of concrete at the steel.

The most common method for measuring chloride contents is laboratory testing of powdered concrete samples. To obtain powdered samples, a rotary hammer can be used, or a core can be removed and then sliced and ground. Representative samples at various locations and different depths within the concrete are usually obtained. The powdered concrete sample is tested for either water-soluble or acid-soluble chloride ion content.

The chloride ion content in concrete is most often reported as a percentage by weight of concrete. But it also can be reported using other units:

- Percentage by weight of cement
- Pounds of chloride per cubic yard of concrete
- Parts per million

Carbonation Testing

Carbonation is the process free calcium hydroxide ($Ca[OH]_2$), which is common in portland cement products, reacts with atmospheric carbon dioxide (CO_2) and water to produce calcium carbonate ($CaCO_3$).[9] Carbonation in itself does not cause concrete to deteriorate, but its effects can be deleterious. The primary deleterious effect of carbonation is a reduction in the alkalinity of the pore water within concrete elements. Generally, concrete pore water is initially quite alkaline, with a pH of 12.5 to 13.5. After carbonation, which can take years or decades, the pH can be as low as 9. As the pH reduces, the corrosion protection of embedded steel elements is also reduced. Thus, carbonation of the concrete reduces the durability of the embedded steel.

To determine the depth of concrete carbonation, a freshly cut concrete sample is stained with a solution of phenolphthalein in diluted alcohol. The solution stains free calcium hydroxide pink, while the calcium carbonate, which is a product of carbonation, remains its original gray color (**Fig. 8**).

General Comments Related to Corrosion Testing

Values obtained for corrosion potential, resistivity, and corrosion rate measurements are instantaneous measurements at a single point in time and space. Corrosion testing on a member is typically performed on a grid at multiple points on the member. The actual layout of the testing grid for each member varies based on the geometry of the member, the area available, and the orientation of the reinforcing steel within the concrete. Corrosion rates must be taken directly over the reinforcement, and the size of the reinforcement must be known for accurate readings.

Additionally, values depend on a variety of factors such as seasonal variation in temperature and relative humidity. Measurements taken at precisely the same point in space but at different times of year will result different measurement values. Thus, results of corrosion testing should always be reviewed by an experienced professional capable of interpreting the readings.

Petrographic Examination

Petrographic examination of concrete is a microscopic assessment of a sample of concrete. Typically, a concrete sample is removed for assessment and transported to laboratory where the sample is sectioned into small pieces and polished to reveal the internal components. Based on a microscopic examination of the polished surface, various features of specimen—including hardness, carbonation, air content, aggregate mineralogy, cement content, and deterioration mechanisms—are revealed (**Fig. 9**).

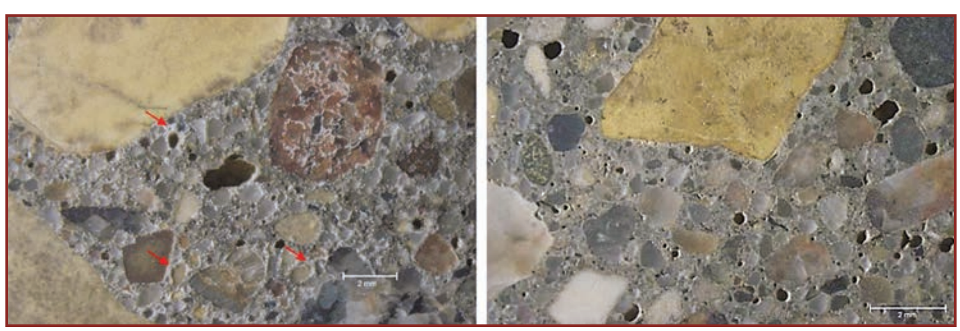

Figure 9. A saw-cut and lapped cross section of the concrete showing white efflorescence (red arrows), halite and sylvite, that has emanated from the paste at depth within the concrete sample (left); and hardened air void system (right).

Figure 10. Extent of visible wall bowing (left) and efflorescence at crack in panel (right).

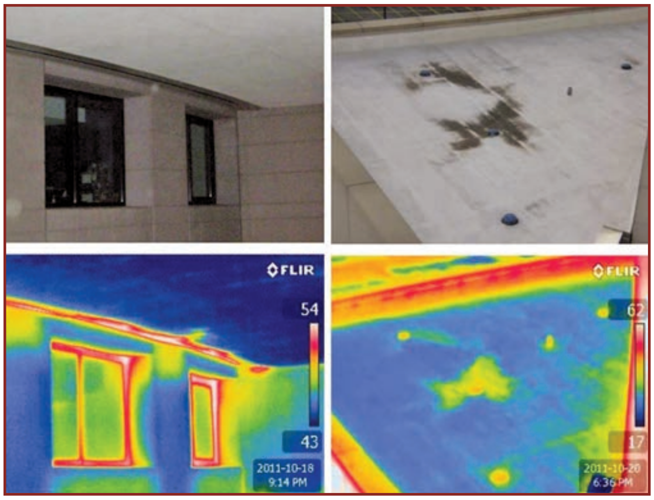

Figure 11. The referenced thermograms illustrate heat loss along the perimeter of nonthermally broken exterior windows, including the window washing track (left); and typically anomalous conditions at exhaust vents (where in operation), roof drains, and roof anchors, as well as thermal bridging along the parapet wall (right).

CASE STUDY 1: TILT-UP CONCRETE WAREHOUSE

The building was constructed circa 1974 and currently serves as a storage facility for medical supplies. The structural system of the building consisted of reinforced concrete tilt-up wall panels (approximately 5.5 in. thick) supporting the steel roof framing and the roof deck system. The building enclosure system also consisted of a concrete tilt-up wall panel system, with joint sealants between adjacent panels. The facility enclosed a space of approximately 44,000 ft^2.

The initial distress identified by the client was related to visible lateral deflection (bowing) in a particular wall panel that supported the primary electrical service panels for the building. Upon initial review, investigators observed that several cracks in the panel were exhibiting efflorescence, which is indicative of waterflow through a crack.

Given the observed conditions, investigators initiated a thorough assessment of the wall panels to determine the extent of corrosion. The evaluation consisted of visual assessment, IR thermography, half-cell potential corrosion measurements, chloride ion content measurement, and petrographic examination of concrete cores.

Visual Assessment

Visual assessment of the interior and exterior surfaces of the facade panels indicated cracking through most panels (**Fig. 10**). In most cases, the cracks were aligned with the internal reinforcement, and many cracks exhibited signs of water infiltration. Overall, the pattern of the visible distress indicated that deterioration was widespread throughout the facade panels, but no obvious cause of the distress was visibly identifiable.

Infrared Thermography of Building Enclosure Systems

Partial visual survey of building interior and exterior, IR thermographic scanning of exterior wall and roof systems, and hygrothermal analysis of the as-built construction at select locations were performed in this case study. As shown in **Fig. 11**, the observed anomalous conditions were found to be a result of one or a combination of the following:

- Incomplete or defective interior air and/or exterior weather seals at the perimeter of the windows
- An area of missing, inadequate, uneven, or discontinued thermal insulation
- An area of loose insulation resulting in air circulation around the thermal insulation and a localized reduction in the thermal resistance
- Wet insulation resulting in a localized reduction in the thermal resistance
- Thermal bridges at numerous locations

Infrared Thermography of Precast Concrete Panel

IR thermography was performed from the exterior of a building for identifying any anomalous conditions on exposed concrete surfaces. Through IR thermography, many areas of delaminated concrete were identified (**Fig. 12**). Concrete delaminations typically consist of planar separation within the concrete that is roughly parallel to the surface. These locations typically corresponded with locations where steel connection elements bridged between panels. The correlation between the delaminations and connector elements suggested corrosion of the embedded steel elements could be driving the visible distress.

Half-Cell Corrosion Potential Mapping of Exposed Concrete Surfaces

To assess the state of corrosion within the facade panels, the corrosion potentials were measured relative to a copper-copper sulfate electrode. Measurements were taken at a grid spacing of approximately 2 ft by 2 ft so that trends and contours within the measured data could be developed and reviewed. The photograph of a typical panel in **Fig. 13** has been annotated to indicate the locations of cracks, delaminations, and a previously infilled wall opening. Figure 13 also includes a contour plot of the half-cell corrosion potentials measured on the panel. Areas in contour are color coded per the categories presented in Table 1, with the red and green areas exhibiting the greatest and least probabilities for corrosion, respectively, and the yellow areas representing corrosion probabilities between those of the red and green areas.

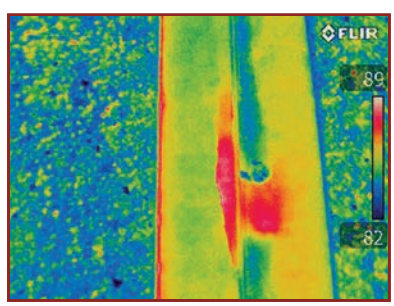

Figure 12. Infrared thermogram at panel-to-panel connector.

As shown in Fig. 13, the areas of mapped corrosion potential correspond with the visible cracked areas. The most heavily cracked areas exhibited the greatest potential for active corrosion. However, it must be noted that measurement of half-cell corrosion potentials is greatly dependent on measurement conditions. Dry conditions generally produce lesser corrosion potentials than wet conditions. Thus, the assessor should focus on trends within the data rather than precise values of the measured half-cell corrosion potentials.

In this case, the visible damage, IR thermography survey, and the measured half-cell corrosion potentials consistently indicated the presence of a deleterious mechanism within these facade panels.

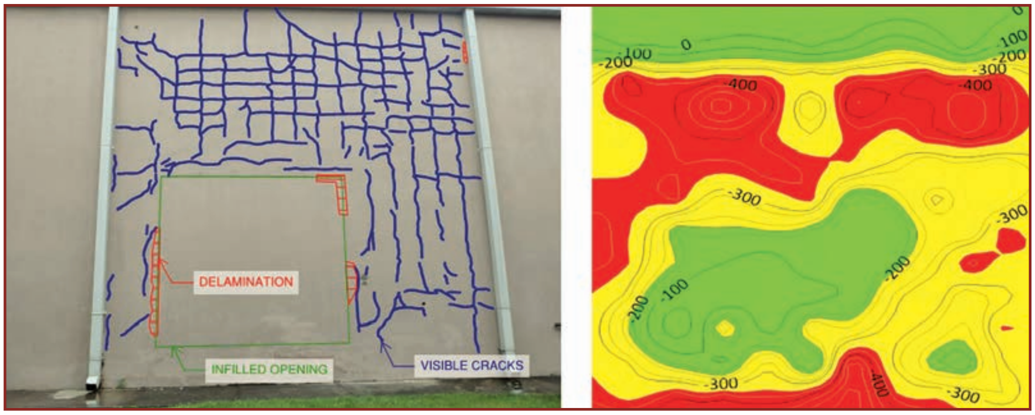

Figure 13. Annotated photograph of wall panel at exterior (left), and half-cell corrosion potential contour map (right). In the map, red and green areas have the greatest and least probabilities for corrosion, respectively, and yellow areas represent corrosion probabilities between those of the red and green areas.

Petrographic and Chloride Ion Content Analysis

To supplement the in situ testing, several samples of the facade panels were removed for laboratory analysis. Laboratory testing for this work included petrographic examination per ASTM C856, *Standard Practice for Petrographic Examination of Hardened Concrete*,[10] and measurement of the water-soluble chloride content of the concrete per ASTM C876.[6]

Petrographic examination indicated that the concrete comprising the facade panels had variable water content in the concrete mixture and there was cracking and microcracking throughout the samples. The samples were otherwise unremarkable.

The chloride ion content of the cores removed from the facade panels was also tested. Specifically, the cores, which were removed from the entire thickness of the panels, were subdivided into smaller components. By subdividing the core, chloride content in various segments can be measured, and comparison of those chloride contents can provide information as to their source. For example, a structure exposed to deicing salts would have an elevated chloride content at the exterior face with a much lower chloride content at an interior face.

Generally, a chloride ion content between 1.0 and 1.5 pounds of chloride per cubic yard of concrete (250 to 380 parts per million of chloride) is considered the threshold to initiate chloride-induced corrosion per the American Concrete Institute's *Guide to Protection of Reinforcing Steel in Concrete Against Corrosion* (ACI 222R-19).[11] The measured chloride ion contents in the samples removed from the structure ranged from 190 to 1550 ppm. Additionally, the chloride content throughout the panel thickness was fairly uniform, which suggests that chlorides were mixed in with the fresh concrete.

At the time of construction of the building, chloride was used to accelerate the set of fresh concrete without consideration for durability. This practice has long since been abandoned for concrete structures containing steel reinforcement in North America.

Summary

This facade assessment began with a relatively small scope to assess localized concrete damage. As the assessment developed, a series of testing techniques were implemented in an attempt to identify the source of the damage so that a proper repair could be implemented. Each nondestructive technique provided some insight into the source of the problem until the actual cause, chloride ion–contaminated concrete, was identified.

Based on the results of the testing and the costs associated with remediating chloride ion–contaminated concrete, the building occupant chose to make short-term repairs to maintain use of the facility for three to five years. In that time, the occupant plans to identify and transition to a new space.

CASE STUDY 2: HIGH-RISE CONDOMINIUM BUILDING

The second case study involves a twin-tower, 30-story condominium building constructed in the early 1980s. The exterior wall system consisted primarily of precast concrete panels of various sizes and shapes connected to the concrete frame structure through embedded plates and welded connector plates.

One of the homeowners within the condominium building reported a visible increase in a joint between adjacent facade panels near their unit on the 20th floor, which suggested that a concrete facade panel had shifted. Given the information provided, an emergency response team was quickly mobilized to site to observe the conditions and assess potential life safety concerns.

Upon arriving on the site, we observed the distress shown in **Fig. 14**. We advised the client to immediately barricade the area below this panel to prevent injury to anyone on the

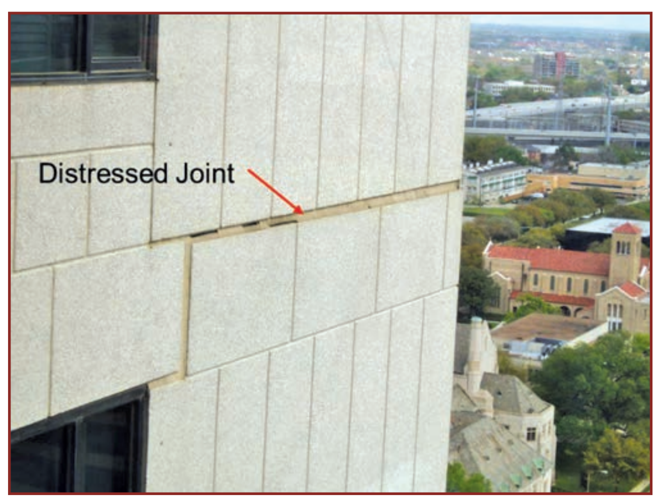

Figure 14. Apparent panel movement at a joint.

building plaza level below. A contractor was quickly mobilized to temporarily stabilize the affected panel using the lifting elements that had been used to lift the panels during the original construction of the building. With the immediate hazard temporarily addressed, assessment of the panel movement began.

Visual Assessment

Because of the emergency nature of the response, scaffolding or swing stages were not available to assess the displaced panel. Instead, the initial assessment was performed by removing the finishes from interior space to access the facade panel connectors. After the interior finishes were removed, the source of the displacement was readily identifiable. The precast concrete panel connection consisted of a steel plate welded to a series of steel studs, which had been cast into the panel's fresh concrete. The welds at the base of the studs had failed, and the concrete panel was displaced due to gravity loading (**Fig. 15**). While the cause of the displaced panel was apparent, the larger question was to determine whether other locations within the structure were similarly affected. Neither accessing each connection from interior residential space nor removing all panels from the building was a feasible assessment technique. Thus, nondestructive methods were needed.

Impact-Echo Testing

Impact-echo testing was the technique chosen to initially assess the facade panels. This technique could be applied entirely from the exterior of the building using swing stages. To verify the use of impact-echo testing, pilot testing was conducted at the known failed connection. Unfortunately, the pilot tests did not distinguish between the connectors that were known to have failed and those that were known to be in serviceable condition. By performing the pilot testing, the viability of the technique was assessed before significant time and effort were invested in widespread testing.

Impulse Response Testing

Impulse response testing is conceptually similar to impact-echo testing in that an impact produces vibrations that are measured by a transducer. Based on the movements recorded at the transducer, inferences can be made about the conditions of the impacted structure. Whereas impact-echo testing uses a relatively small impact that produces vibrations at a material level, impulse response testing uses a much larger impact that produces vibrations at a member level.

The construction documents for the building identified the locations of the steel connectors at each facade panel. Using those locations, a series of impulse response soundings were performed from swing stages on the exterior of the building on and around the connector locations.

Figure 16 presents typical results for single panel with two gravity connectors. In the figure, the red portion of the spectrum represents relatively high stiffness while the blue end of the spectrum represents relatively low stiffness. In the lower right inset, stiffness is concentrated at a small, red area at the location of the panel connector, which indicated that the connector was still attached and provided the desired support. In the lower left portion of the figure, there is no discernible change in stiffness at the connector location. Based on these measured responses, investigators concluded that the lower left connector was still intact while the connector in the lower right had failed.

Summary

Using impulse response testing, the investigators identified several failed or partially failed connectors throughout the structure. Proper selection of a nondestructive technique was essential to identifying the locations of the distress. After the locations of distress were identified, supplementary steel plates and anchors were installed to repair the damage.

CASE STUDY 3: MIDRISE MEDICAL BUILDING

This case study involves a medical building that was originally designed in 1951. In 1986, an addition to the original building was designed, replacing portions of the east, west, and south elevations.

The six-story building is clad in a combination of marble panels and aluminum spandrel panels with some exposed concrete details. The structural system of the original building is a cast-in-place reinforced concrete frame with perlite block infill walls. The structural system of the addition is cast-in-place reinforced concrete with concrete masonry unit infill walls.

Georgia [Etowah Fleuri] Pink marble was specifically chosen for this building. Due to its highly figurative coloration, the marble was only available in narrow slabs, making a thin

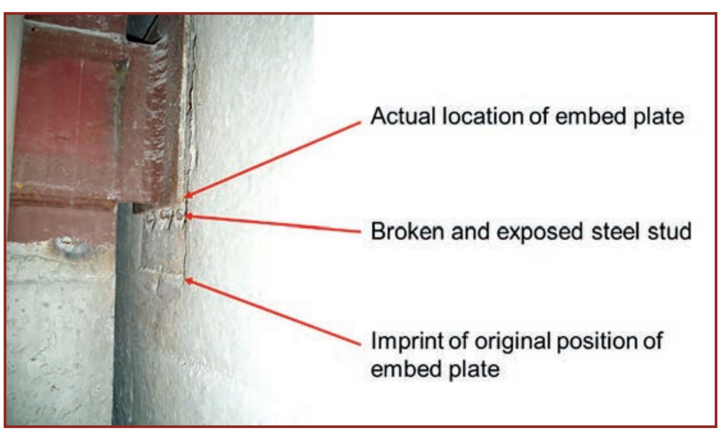

Figure 15. Broken facade panel connectors.

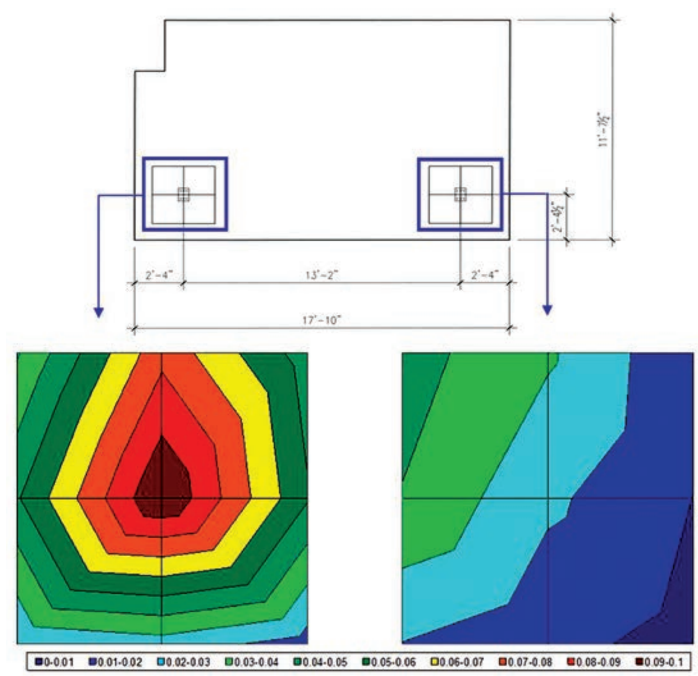

Figure 16. Sketch of a typical panel (top); typical impulse response of an intact connection (lower left); and typical impulse response of broken connector (lower right).

Figure 17. Area of panel detachment.

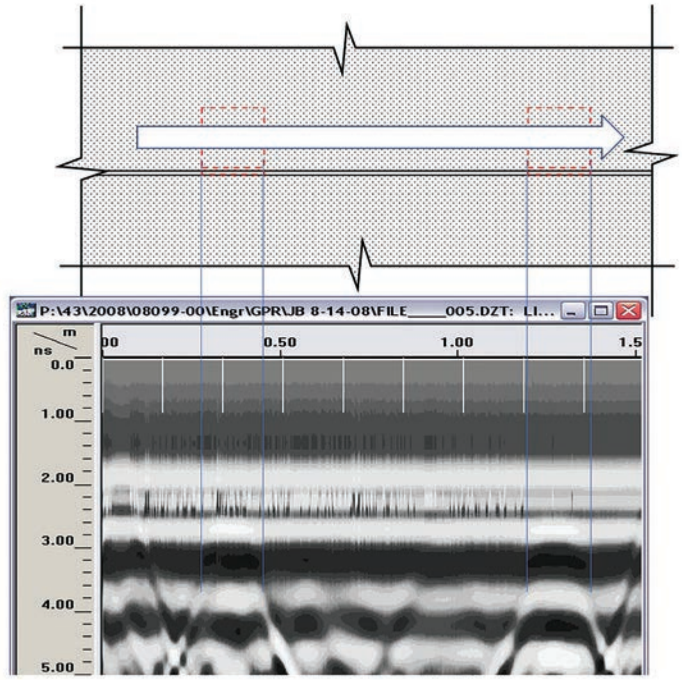

Figure 18. Short pulse radar scans above and below a horizontal panel joint.

stone veneer the only option for the building. At the time of construction, the local building code did not allow for veneer systems. A petition was successfully made to the local authority having jurisdiction to alter the building code to allow this veneer system to be used.

After the building had been in service for more than 50 years, seven marble panels detached from the south face of an exterior penthouse wall and fell onto the roof of the building (**Fig. 17**). We were tasked with conducting an assessment program to first evaluate the immediate life safety concerns and then comprehensively evaluate the hand-set marble panel cladding system. Based on our initial response and site assessment, we recommended overhead fall protection at all pedestrian areas to mitigate risk posed by potential systematic concerns with the panel support system.

Visual Assessment

Visual assessment of the marble cladding system was done shortly after the panels fell. Investigators observed each accessible marble panel individually and recorded detailed notes about observations on field sheets. Approximately 80% of the cladding system was accessible for evaluation. However, about 20% of the cladding system could not be closely evaluated due to restrictions created by an adjacent construction site and preexisting overhead protection along the west elevation.

In the visual assessment, investigators observed and categorized several modes of deterioration: spalls, panel deformation, vertical movement, horizontal movement, corner cracking, midspan cracking, and edge damage, Many of the individual panels on the building exhibited some form of distress.

Nondestructive testing was then implemented to supplement the visual assessment.

Short Pulse Radar

SPR was used to locate the various gravity-supporting elements and lateral wire ties and dowels. According to the limited drawings available, the support for the marble panels consisted of discontinuous shelf angles with dowel pins that were placed into discrete holes drilled into the edges of the panel. By performing SPR along the horizontal panel joints, investigators could identify both of the shelf angles (**Fig. 18**). Thus, the presence and location of the angles were confirmed nondestructively and without direct access to the elements. However, confirmation of the presence of these elements was not sufficient to confirm with integrity.

Impulse Response Testing

After the SPR assessment, investigators performed impulse response testing on selected panels to characterize the relative conditions of the panel connections qualitatively. As previously described, impulse response can be used to assess relative support stiffness of panel elements and that stiffness is typically resolved into a contour plot to indicate differences in stiffness within the field of testing.

Figure 19 depicts the contour plot results for panel stiffness as determined by impulse response testing on four individual stone

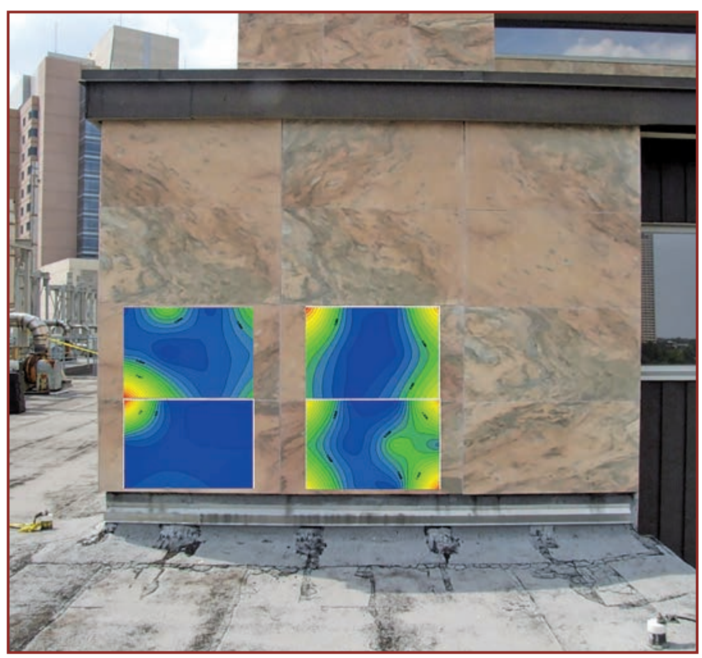

Figure 19. Select impulse response results overlaid on photograph of a testing area. Colors on the blue and red ends of the spectrum indicate lower and higher stiffness values, respectively.

panels. Colors on the blue end of the spectrum indicate lower stiffness values, and those on the red end of the spectrum represent higher stiffness values. The contour plots inset within the photograph represent the dynamic stiffnesses of the facade elements. In both of those panels, the stiffness increases significantly at each panel corner, which is consistent with an intact panel support mechanism. In the contour plots for the two panels on the left, the measured stiffness is relatively constant and at a relatively low level of stiffness, with one hot spot of higher stiffness. Thus, the plots for the two left panels indicate a loss of support within the panels.

Using the impulse response test results, the relative condition of the panel supports could be quantified and classified without direct observation of the supports. By basing the impulse response testing grid on the SPR data, investigators ensured that stiffness measurements were performed at the critical locations.

Summary

In this case study, investigators used both SPR and impulse response to perform the assessment. SPR was used to locate the connection elements. Once they were located, investigators used impulse response testing to assess the stiffness of those elements. From the stiffness measurements, the investigators determined which panels needed additional investigation and repair without having to remove all the facade panels.

It is noteworthy that SPR and impulse response testing were used in this case study on stone panels rather than concrete elements. Many of the nondestructive testing methods developed for concrete can be applied to natural stone elements, which is an important aspect of building enclosure assessments.

CONCLUSION

Many nondestructive testing methods have become mainstream within building condition assessment methodologies. Visual assessment is the most basic nondestructive testing technique and should form the basis of any assessment. In addition, various other nondestructive testing techniques, if used judiciously and properly, can enhance understanding of concealed or latent problems. Nondestructive tests may be conducted by certified technicians and technologists; however, professional engineers or building science experts should interpret and assess test results to validate the findings and determine next steps.

For each of the case studies presented, the extent of the problems could not be completely assessed based on visual inspection alone. In the Case Study 1, it would have been simple to perform localized repairs at the points of damage. However, localized repairs would have left the underlying causes in place and damage would have continued over time, leading to more repairs in the future. For Case Study 2, only a small number of facade panels were visibly damaged, and it was not possible to determine if similar, but hidden, damage was present throughout the system. Use of impulse response testing expanded the visual assessment to allow for the appropriate scope of repairs. Lastly, for Case Study 3, a combination of methods was needed to locate and then assess the facade panel connections. This combination allowed the strengths of two techniques to complement one another to assess the existing conditions.

REFERENCES

1. Kesner, K., and M. Brown. 2009. "Integration of NDT Results into the Evaluation of Distressed Structures." ASCE Fifth Forensic Engineering Congress. doi: 10.1061/41082(362)65.
2. Sansalone, M., and W. Streett. 1997. *Impact-Echo Nondestructive Evaluation of Concrete and Masonry.* Jersey Shore, PA: Bullbrier Press.
3. Steinbach, J., and E. Vey. 1975. "Caisson Evaluation by Stress Wave Propagation Method." *Journal of Geotechnical and Geoenvironmental Engineering* 101 (4). doi: 10.1061/AJGEB6.0000161.
4. Sansalone, M., and N. J. Carino. 1986. *Impact-Echo: A Method for Flaw Detection in Concrete Using Transient Stress Waves*. NBSIR 86-3452. Washington, DC: National Bureau of Standards.
5. Sansalone, M. 1997. "Impact-Echo: The Complete Story." *Structural Journal* 94 (6): 777-786.
6. ASTM International. 2015. *Standard Test Method for Corrosion Potentials of Uncoated Reinforcing Steel in Concrete*. ASTM C876-15. West Conshohocken, PA: ASTM International. doi: 10.1520/C0876-15.
7. American Concrete Institute (ACI) Committee 228. 2013. *Report on Nondestructive Test Methods for Evaluation of Concrete in Structures.* ACI 228.2R-13. Farmington Hills, MI: ACI.
8. Andrade, C., and Alonso, C., 2004, "Test Methods for On-Site Corrosion Rate Measurement of Steel Reinforcement by Means of the Polarization Resistance Method," *Materials and Structures* 37: 623-643.
9. Neville, A. M. 2011. *Properties of Concrete*. 5th ed. London, UK: Pearson.
10. ASTM International. 2020. *Standard Practice for Petrographic Examination of Hardened Concrete*. ASTM C856/C856M-20. West Conshohocken, PA: ASTM International. doi: 10.1520/C0856_C0856M-20.
11. ACI Committee 222. 2019. *Guide to Protection of Reinforcing Steel in Concrete Against Corrosion*. ACI 222R-19. Farmington Hills, MI: ACI.

Cladding Attachment Strength for Wood-Framed Structures

J. Lawrence Elkin, PE

Elkin Engineering & Diagnostics LLC | Charleston, SC

jlelkin@elkineng.com

Lee Fischer, PE

Elkin Engineering & Diagnostics LLC | Charleston, SC

lfischer@elkineng.com

IIBEC 2022 - Building for the Future

International Convention and Trade Show

March 17–22, 2022 | Orlando, FL

ABSTRACT

This presentation discusses the standards and building code requirements that govern the attachment of exterior wall claddings to wood-framed structures as compared with common installation practices and in situ performance. The presenters consider stucco, fiber-cement siding, and vinyl siding. Topics include:

- Industry standards, building codes, and applicable installation requirements and their origins
- Common installation practices that do not strictly comply with building code and manufacturer's installation requirements
- The presenters' mock-up testing of fastener withdrawal capacities and cladding attachment capacities; resulting reasonable allowable loads; and the most likely modes of failures for the various claddings
- Recommendations for modifying the current installation requirements

SPEAKERS

J. Lawrence Elkin, PE

Elkin Engineering & Diagnostics LLC | Charleston, SC

Larry Elkin has nearly 30 years of experience in design, commissioning, and forensics. He graduated from the Rose-Hulman Institute of Technology with both bachelor and master of science degrees in mechanical engineering. Later, he obtained a master of civil engineering with an emphasis in structural engineering from Norwich University. Elkin initially learned about stucco in the 1990s while diagnosing moisture issues with exterior insulation and finish systems. This led him to attend Sto's certified installer training in 1996. Since then, he has inspected thousands of stucco-clad structures to diagnose the causes of failures and provide repair solutions.

Lee Fischer, PE

Elkin Engineering & Diagnostics LLC | Charleston, SC

Lee Fischer is a professional engineer who oversees structural building enclosure and fenestration investigations using a multitude of diagnostic tools and test methods. He frequently serves as an expert witness in litigation. His experience extends across residential, multifamily, and light commercial structures and components. Fischer holds FenestrationMaster certification from the Fenestration and Glazing Industry Alliance (FGIA) and is in the process of getting Elkin Engineering to become the only FGIA-certified field testing agency in South Carolina. He is an Infrared Training Center Level I infrared thermographer and has completed the Exterior Design Institute's EIFS Third Party Inspector Certification, Quality Control and Moisture Analyst Training Course.

Cladding Attachment Strength for Wood-Framed Structures

Many building code requirements are not based on research or engineering judgment. An example is the requirement for a 1-in. air space behind brick veneer. As the apocryphal story goes, a group of people in the masonry industry sought to create a standard for the installation of brick veneer. They all agreed that the industry standard was to leave a "thumb-width" between the back of the veneer and the substrate. Realizing that they needed to include something more precise in their standard, they measured their thumbs and the average was about an inch. Now, a 1-in. air space is the minimum requirement in the building code. Given that building codes form the basis of design decisions, are the standard for accepting new work, and are the benchmark for multimillion dollar lawsuits, our building codes should be based on proven engineering methods.

The 2015 *International Building Code*[1] (and its predecessors (dating to the 1994 *Standard Building Code*[2]) require portland cement stucco to be designed and installed in accordance with ASTM C926, *Standard Specification for the Application of Portland Cement-Based Plaster*,[3] and ASTM C1063, *Standard Specification for the Installation of Lathing and Furring to Receive Portland Cement-Based Plaster*.[4] These standards indicate that lath should be fastened at 7 in. on center along the framing. This requirement has no engineering basis. Rather, as Innocenzi[5] reports, this requirement dates back to the use of rod-ribbed lath installed over open framing (that is, no structural sheathing). This lath was produced in 28-in.-wide sheets, and nails were to be applied along the ribs spaced at the quarter points of the lath (hence 7 in. on center). Advancements in analytical and testing methods have made it possible to develop engineering-based values for how stucco lath should be attached to a structure.

In the recent years, several documents have been published that, when used together, create the rationale to form an engineering basis for the attachment of stucco lath to buildings. In 2010, the American Plywood Association (APA, now known as APA—The Engineered Wood Association) released Technical Note TT-109,[6] which provided guidance for using APA-rated structural sheathing as a nail base for cladding systems with dead loads up to 11 lb/ft^2. APA has determined that some claddings can only be fastened to sheathing and cannot be fastened through sheathing and into studs. APA indicated that additional consideration should be given when cladding dead loads exceed 11 lb/ft^2. However, Newkirk,[7] who observed that many stucco installations were attached primarily to oriented strand board (OSB) sheathing, concluded that stucco attached only to sheathing was not likely to fail. In 2015, the American Wood Council's (AWC's) *National Design Standard for Wood Construction*[8] included new relationships for calculating the withdrawal capacity of grip-shank fasteners. Grip-shank fasteners have a greater resistance to withdrawal than smooth-shank fasteners, which, historically, have been used to fasten stucco. Finally, in March 2018, ASTM International adopted ASTM C1860, *Standard Test Methods for Measurement of Tensile Strength or Bond Strength of Portland Cement-Based Plaster by Direct Tension*.[9] Though earlier publications suggested ways to use existing testing methods for cladding testing, there is now a consensus standard for pull-testing of stucco claddings.

A useful tool for designers would be a table that shows the allowable load capacities of stucco lath fasteners. This paper discusses a project that used testing and engineering analytical methods to develop such a table.

Description	Shank length (in.)	Shank diameter (in.)	Head diameter (in.)
Senco 16-gauge electrogalvanized staple, 1-in. crown	2.000	2 @ 0.051	1.000
Wind-lock ULP 302 3WLM1 #7	1.625	0.151	1.750
Simpson 304 stainless, barbed roofing nail	1.250	0.131	0.375
B&C CR-112 15-degree coil collated smooth roofing nail	1.500	0.120	0.375

Table 1. Fastener summary

METHODOLOGY AND DATA

Testing was conducted in three phases. The first phase tested fastener withdrawal only from a variety of substrate conditions with no lath present. The second phase pull-tested samples of lath attached to the substrates with the same types of fasteners used in the first phase. ASTM D1761, *Standard Test Methods for Mechanical Fasteners in Wood*,[10] was used as a guide for fastener and lath testing. In the third phase of testing, full-scale stucco panels were constructed using the previously tested

Figure 1. View of a fastener being extracted from an oriented strand board panel with a digital pull tester.

A. Senco staple

Substrate	Mean force (lbf)	Maximum force (lbf)	Minimum force (lbf)	Standard deviation	Coefficient of variation
Stud	181	225	151	15.74	8.7%
Sheathing	53	72	32	9.46	17.8%
Stud and sheathing	192	270	145	29.69	15.5%

B. Wind-lock screw

Substrate	Mean force (lbf)	Maximum force (lbf)	Minimum force (lbf)	Standard deviation	Coefficient of variation
Stud	522	588	408	49.69	9.5%
Sheathing	173.3	229	109	37.46	21.7%
Stud and sheathing	550	716	479	52.82	9.60%

C. Simpson barbed nail

Substrate	Mean force (lbf)	Maximum force (lbf)	Minimum force (lbf)	Standard deviation	Coefficient of variation
Stud	135	191	110	19.15	14.2%
Sheathing	84	182	56	22.06	26.3%
Stud and sheathing	139	203	101	22.94	16.5%

D. B&C smooth nail

Substrate	Mean force (lbf)	Maximum force (lbf)	Minimum force (lbf)	Standard deviation	Coefficient of variation
Stud	97	161	61	22.74	23.5%
Sheathing	37	54	24	9.18	24.8%
Stud and sheathing	79	146	47	19.68	24.9%

Table 2. Force at failure data from fastener pull-tests

fasteners and lath. Samples of the walls were pull-tested in accordance with ASTM C1860.

Phase I: Fastener Pull-Testing

Initially, a variety of common stucco fasteners (Table 1) were driven into substrate samples and pulled using a Force Test Model SP1 Digital Pull Tester (Fig. 1). Substrates included No. 2 southern yellow pine (SYP) 2 × 4 wall studs, 7⁄16 APA-rated OSB, and a composite of sheathing attached to wall studs. In the test, 30 of each type of fastener were installed into each of the three substrates using a hammer. Stop pieces were used to ensure fasteners were installed at consistent depths. An effort was made to ensure fasteners were installed into consistent substrate conditions. Table 2 summarizes the fastener pull data.

Phase II: Lath Pull-Testing

Lath samples were also pull-tested (Fig. 2). The purpose of testing the lath, in addition to the fasteners, was to determine whether the mode of failure under loading would be

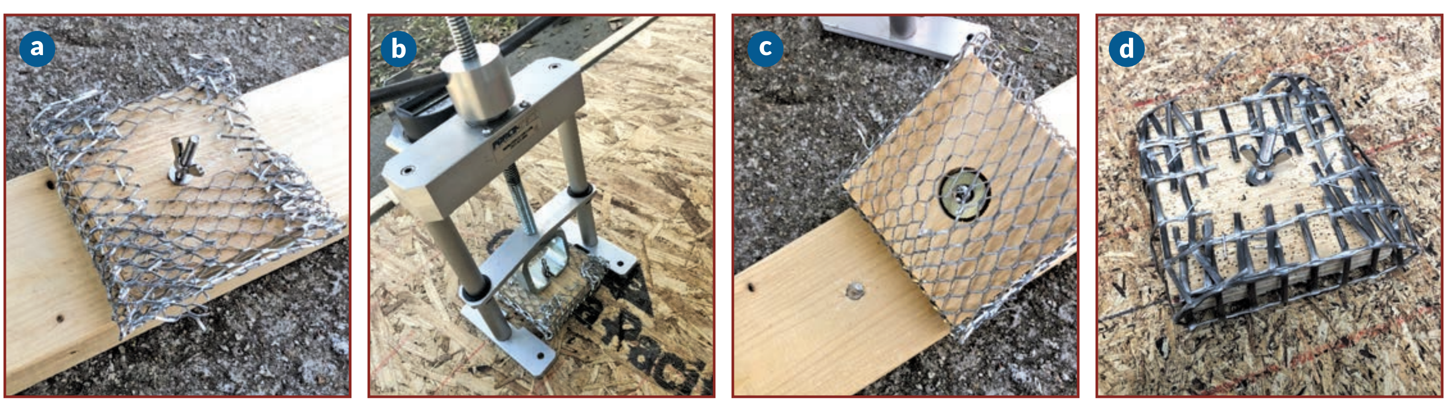

Figure 2. The configuration and process for lath pull-testing. (a) A sample of lath was affixed with a fastener to one of the substrates. (b) A plywood test blank, with a recessed screw and fender washer, were placed over the lath. Edges of the lath were tightly bent up an over the plywood where they were stapled in place. (c) The fastener puller engaged the exposed end of the screw and was used to apply force to the lath-fastener combination. Note that the lath pulled away from the blank in a conical shape prior to failure.

A. Metal lath/smooth nail

Substrate	Mean force (lbf)	Maximum force (lbf)	Minimum force (lbf)	Standard deviation	Coefficient of variation	Mode of failure*
Sheathing	44	64	26	9.38	21.3%	Fastener
Stud and sheathing	105	134	71	15.55	14.9%	Lath

B. Metal lath/barbed nail

Substrate	Mean force (lbf)	Maximum force (lbf)	Minimum force (lbf)	Standard deviation	Coefficient of variation	Mode of failure*
Sheathing	63	108	11	24.44	40.0%	Mixed
Stud and sheathing	72	127	10	31.40	43.5%	Mixed

C. Metal lath/staples

Substrate	Mean force (lbf)	Maximum force (lbf)	Minimum force (lbf)	Standard deviation	Coefficient of variation	Mode of failure*
Sheathing	64	94	22	18.68	21.3%	Fastener
Stud and sheathing	158	258	109	36.60	23.2%	Lath

D. Fiberglass lath/screw

Substrate	Mean force (lbf)	Maximum force (lbf)	Minimum force (lbf)	Standard deviation	Coefficient of variation	Mode of failure*
Sheathing	66	141	30	25.00	37.8%	Fastener
Stud and sheathing	96	165	21	34.92	36.2%	Lath

E. Fiberglass lath/staple

Substrate	Mean force (lbf)	Maximum force (lbf)	Minimum force (lbf)	Standard deviation	Coefficient of variation	Mode of failure*
Sheathing	50	71	29	10.93	22.0%	Fastener
Stud and sheathing	91	123	48	19.53	19.5%	Lath

*Fastener = fastener withdrawal; Lath = lath pullover; Mixed = fastener withdrawal and lath pullover modes of failure were evenly represented.

Table 3. Force at failure data from pull-testing of laths

fastener withdrawal or lath failure. To perform the lath testing, the 6 × 6 in. lath samples were secured to substrate materials with a single fastener. The substrate was limited to APA sheathing only and a composite of sheathing attached to studs.

After the lath was secured to the substrate, a 3.5 × 3.5 in. block of ¾-in.-thick plywood was centered over the fastener. The test sample size was selected to fit between the legs of the pull tester. The edges of the lath were folded up and over a plywood block and was stapled to the block of wood with ½-in.-long T-38 staples. A no. 10 screw with a 1-in.-diameter fender washer extended through the center of the plywood block. The screw provided a stud to engage the pull tester. The test used 30 of each lath/fastener/substrate combination.

Two types of lath were considered:

- AMICO Self-Furred Diamond Mesh Lath, Galvanized, 2.5 lb/yd (Fig. 2[a], [b], and [c])
- BASF PermaLath 1000, Self-Furring, Fiberglass, 8.8 oz/yd (Fig. 2[d])

In addition to the force at failure, the mode of failure was documented. The two modes of failure were fastener withdrawal and lath pullover. Table 3 reports the most frequently observed modes of failure. If the modes of failure were evenly represented, the mode of failure is reported as "mixed." A mode of failure of "Fastener" indicates fastener withdrawal, and "Lath" indicates lath pullover.

Significant Lath Test Observations

The primary modes of failure for fasteners driven through sheathing only was fastener withdrawal. The primary modes of failure for fasteners driven through studs and sheathing was lath pullover with one exception; metal lath with barbed nails had a mixed mode of failure.

Lath Test versus Fastener Test Comparisons

Table 4 shows the average ultimate failure loads of the fastener and lath tests. The average ultimate load in the lath test was atypically greater than the fastener test in the following scenarios: metal lath/smooth nail combination in both substrate conditions and metal lath/staple combination in sheathing-only

Substrate	Sheathing		Sheathing and stud	
Lath/fastener	Fastener test	Lath test	Fastener test	Lath test
Metal/smooth nail	37	44	79	105
Metal/barbed nail	84	63	139	72
Metal/staple	53	64	192	158
Fiberglass/screws	173	66	550	96
Fiberglass/staples	53	50	192	90

Table 4. Fastener and lath average ultimate failure loads (lb)

Figure 3. The arrangement of several stucco panels during initial curing.

substrate. However, the modes of failure were consistent with the other tests. This indicated possible issues with lath test in these scenarios.

For the metal lath/staple combination in studs and sheathing substrate, the average ultimate load in the lath test was significantly stronger than the other fastener/lath/substrate combinations. This indicates the staples may be able to hold the lath better and prevent lath failure.

For the metal lath/barbed nail combination in studs and sheathing substrate, the average ultimate load in the lath test was significantly weaker than the other fastener/lath/substrate combinations. This mixed mode of failure indicated either the ultimate strength of the lath was not reached, or there were issues with the nail/lath interaction.

Phase III: Stucco Pull-Testing

Twenty stucco wall panels were prepared using the same five lath/fastener combinations that were tested previously. Two panels of each combination were constructed with fasteners driven only into APA-rated wall sheathing. Two additional panels of each lath/fastener combination were constructed where fasteners passed through the sheathing and into 2 × 4 wall studs.

Each panel was 48 in. wide by 96 in. tall. Framing consisted of No. 2 SYP studs and 7/16 OSB. The wall panels were wrapped with a commercially available polyolefin weather-resistive barrier. A layer of no. 15 building paper was applied to the face receiving stucco. Amico polyvinyl chloride (PVC) casing bead, 3/4 in. deep, was applied along the perimeter of each panel as a stucco ground. Lath was fastened at 16 in. on center horizontally and 7 in. on center vertically. The stucco consisted of BASF Acrocrete StuccoBase Premix. This product was used for both a 3/8-in.-thick scratch coat and a 3/8-in.-thick brown coat. No finish was applied. Bituminous self-adhering flashing was applied as a coping over the top of each wall panel to shed rain. The panels were placed on top of pressure-treated sleepers to raise them above grade but were otherwise exposed to natural weather conditions. Initially, the stucco was moist cured for 72 hours to reduce curing stress and shrinkage cracking (**Fig. 3**). The stucco was allowed to cure for a minimum of 30 days before pull-testing commenced.

In accordance with ASTM C1860, a 26 × 26 in. panel of 3/4-in.-thick plywood was adhered to the stucco. A diamond saw was used to cut the stucco around the perimeter of the stucco down to the OSB sheathing. A second plywood panel was attached to the first panel with twenty-four 7/8-in.-long no. 14 wood screws.

Stucco samples were then pull-tested using the methods in ASTM C1860[9] to determine the validity of the tabulated values (**Fig. 4–6**). The force applied to each panel with the pull-testing rig was measured using an Omega Engineering LFCD-1K 1000-lb load cell.

Table 5 shows the average force at failure for each lath/fastener/substrate combination. The mode of failure followed the lath test mode

One theory why stucco pull-test loads were less than the lath test loads is that lath deflections change the loading characteristics when not embedded in stucco. As the lath deflected, lath strands became tensile dominant.

Figure 4. Stucco panels being prepared for testing. The panels were removed from the support stands and laid flat. Per ASTM C1860, nine ¾-in.-thick plywood panels were adhesively attached to the stucco.

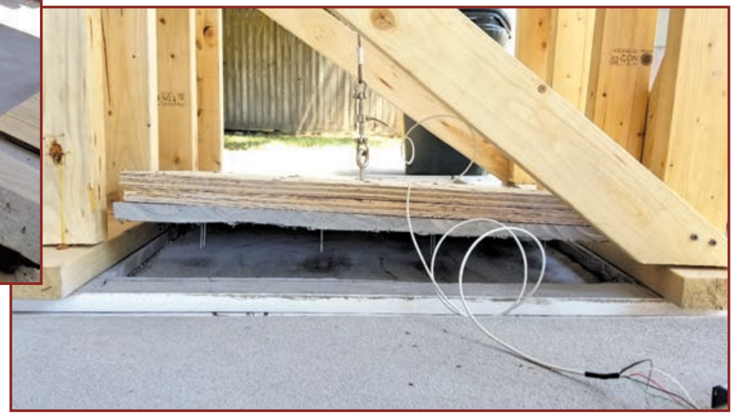

Figure 6. View of a sample profile showing the load cell connected to the eyebolt and a stucco sample pulled from a panel.

Figure 5. The overall arrangement of the stucco pull-test rig. A worm-gear-driven winch was used to apply tension to a cable connected to an eyebolt in the plywood blank. A 1000-lb load cell was placed in line between the tension cable and the eyebolt.

of failure. Six test malfunctions occurred; three of the metal lath/staple combination and three of the fiberglass/screw combination. The failures occurred when the top layer of plywood (connected to the winch) pulled away from the bottom layer of plywood (adhered to the stucco) when the screws connecting the layers stripped through the wood. In no case did the plywood debond from the stucco, nor did the stucco fail between scratch coat and brown coat. The average of the ultimate failure loads were calculated, and the resulting pressures at failure in pounds per square foot (lb/ft^2) were calculated by dividing the average ultimate failure loads by the areas of the test specimen.

Lath/fastener	Sheathing		Sheathing and stud	
Metal/smooth nail	424.0 lb	90.2 lb/ft^2	499.7 lb	106.3 lb/ft^2
Metal/barbed nail	343.3 lb	73.0 lb/ft^2	497.8 lb	105.9 lb/ft^2
Metal/staple	363.0 lb	77.2 lb/ft^2	617.7 lb	131.6 lb/ft^2
Fiberglass/screws	666.0 lb	141.9 lb/ft^2	711.5 lb	151.6 lb/ft^2
Fiberglass/staples	345.8 lb	73.6 lb/ft^2	419.3 lb	89.2 lb/ft^2

Table 5. Stucco average ultimate failure values

Stucco Test versus Lath Test versus Fastener Test Comparisons

In addition to the mode of failure for each stucco pull, the number of fasteners in each stucco specimen was recorded. To provide a comparison between each of the testing protocols, the load per fastener was calculated for the stucco pulls. **Table 6** presents the average ultimate failure load per fastener for each testing protocol.

For metal lath/smooth nails in sheathing only, the stucco test load was atypically greater than both fastener and lath test loads. This suggests the results may be unreliable.

For fiberglass lath/screws in sheathing only, the stucco test load was great than the lath test load, but less than the fastener test load, and the stucco test mode of failure was consistent with the fastener and lath test modes of failures. This indicates there was likely an issue with lath test; however, the stucco test results are likely reliable.

For metal lath/barbed nails in studs and sheathing, the stucco test load was slightly

Substrate	Sheathing			Sheathing and stud		
Lath/fastener	Fastener*	Lath	Stucco	Fastener*	Lath	Stucco
Metal/smooth nail	37	44	47	79b	104	59
Metal/barbed nail	84	63	59	139	72	79
Metal/staple	53	64	45	192	158	92
Fiberglass/screws	173	66	89	550	96	89
Fiberglass/staples	53	50	43	192	90	50

*The values are for fastener pulls only. No lath or stucco was included.

Table 6. Stucco ultimate force (lb) per fastener

Substrate	Sheathing		Sheathing and stud	
Lath/fastener	Fastener	Stucco	Fastener	Stucco
Metal/smooth nail	10	13	22	17
Metal/barbed nail	24	17	39	22
Metal/staple	15	13	54	26
Fiberglass/screws	49	25	154	25
Fiberglass/staples	15	12	54	14

Table 7. Calculated allowable loads (lb) using US Department of Agriculture Forest Products Laboratory[12] safety factor and American Wood Council National Design Standard[8] *load duration factor*

higher than the lath test load. As previously explained, the lath test results were likely unreliable. The stucco test mode of failure was consistent with the fastener and lath test modes of failures. This indicates the stucco test results are reliable.

For metal lath/barbed nails in sheathing only, metal lath/staples in both substrates, fiberglass lath/screws in stud and sheathing, and fiberglass lath/staple in sheathing only, the stucco test loads were less than the fastener and lath test loads. The stucco test mode of failure was consistent with the fastener and lath test modes of failures. This indicates the results are reliable.

For metal lath/smooth nails and fiberglass lath/staple in stud and sheathing, the stucco test loads were significantly less than the lath test loads. The stucco test mode of failure was consistent with the fastener and lath test modes of failures. This indicates the stucco test results are unreliable. Additional testing should be performed.

One theory why stucco pull-test loads were less than the lath test loads is that lath deflections change the loading characteristics when not embedded in stucco. As the lath deflected, lath strands became tensile dominant. The presence of stucco resisted lath deflections, and the lath strands were loaded primarily in shear. The results indicate that the predominately tensile strength in lath tests was stronger than the shear strength in the stucco tests.

ANALYSIS

Determination of Allowable Capacities

Most undergraduate civil and mechanical engineering students are introduced to the concepts of allowable stress, yield stress, and ultimate stress in a mechanics of materials course. Although engineers appreciate the concept of assigning an allowable limit that results in a factor of safety for structural designs, there is no universally accepted standard for how allowable capacities are derived from ultimate strength data. ASTM D5457, *Standard Specification for Computing Reference Resistance of Wood-Based Materials and Structural Connections for Load and Resistance Factor Design*,[11] offers some insight. This standard provides methodologies for converting existing NDS reference values from the allowable stress design (ASD) format to load and resistance factor design (LRFD). It also discusses how to calculate reference design values for wood and timber for test-based data. Specifically, it requires a minimum sample size of 30. It further recommends considering only the lower tail of a distribution for analysis because the upper tail is irrelevant for reliability estimates. ASD reference values are based on the bottom fifth percentile of such a distribution. Overall, this standard is more applicable to wood members and the structural connections described in the NDS as compared with assemblies that are secured to wood framing.

The NDS provides methods for calculating the design withdrawal values for fastener based on an empirical relationship developed by the US Department of Agriculture Forest Products Laboratory (FPL).[12] The AWC's equation adds a safety factor of 5.7 to the FPL relationship. Therefore, one method for calculating allowable loads is dividing the average ultimate forces by the NDS/FPL safety factor of 5.7. However, according to the NDS, additional factors affect the allowable loads based on a variety of installation conditions. A factor of 1.0 was assumed for all factors except the factor for wind, which used the load duration factor $C_D = 1.6$. Table 7 presents the calculated allowable values using the following equation:

*Average Ultimate Failure Loads/5.7 * C_D*

Another standard, ASTM D7147, *Standard Specification for Testing and Establishing Allowable Loads of Joist Hangars*,[13] offers further insight. This specification is useful because its intent is to address the interaction of wood and nonwood elements and it assumes small sample sizes. For sample sizes less than six, allowable loads are deemed to be the lowest ultimate strength value measured divided by three. For a sample size of six or more, the allowable load is the average ultimate strength divided by three. Table 8 presents the calculated allowable values using ASTM D7147. Eight of the ten stucco tests had a sample of six and utilized the following equation:

Average Ultimate Failure Load/3

Two of the ten stucco tests had testing failures, and only three test samples were considered. Those tests are marked in Table 9 and used the following equation:

Minimum Ultimate Failure Load/3

Calculated NDS Withdrawal Capacities

The NDS ASD withdrawal design capacities were calculated to compare with the calculated fastener and stucco allowable loads. First, the unfactored withdrawal capacity W was calculated for each fastener based on the substrate type, fastener dimensions, and depth

Substrate	Sheathing		Sheathing and stud	
Lath/fastener	Fastener	Stucco	Fastener	Stucco
Metal/smooth nail	12.5	15.7	26.4	19.6
Metal/barbed nail	27.9	19.8	46.2	26.2
Metal/staple	17.6	15.1	64.1	22.3*
Fiberglass/screws	57.8	29.8	183.2	25.5*
Fiberglass/staples	17.6	14.5	64.1	16.6

*Test malfunction resulting in sample size less than 6.

Table 8. Calculated allowable loads (lb) using ASTM D7147, Standard Specification for Testing and Establishing Allowable Loads of Joist Hangers[13]

Type	Fastener dimensions (in.)		Fastener depth (in.)		Unfactored withdrawal capacities, *W* (lb)		
	Diameter	Shank	Stud	Sheathing	Stud	Sheathing	Stud and sheathing
Smooth	0.12	1.5	0.9	0.475	33.4	13.9	47.3
Barbed	0.131	1.25	0.65	0.475	34.4	28.0	62.4
Staple	0.051	2	1.4	0.475	22.1	11.8	33.9
Screw	0.151	1.625	1.025	0.475	99.0	51.1	150.1

Table 9. Unfactored withdrawal capacity for each fastener type in each substrate

into each substrate. A specific gravity *G* of 0.55 was used for SYP studs, and *G* = 0.50 was used for OSB.

Next, the following ASD adjustment factors were applied to the unfactored withdrawal capacity to determine the factored withdrawal capacity *W'* for each fastener:

C_M = wet service factor
C_t = temperature factor
C_{eg} = end grain factor
C_{tn} = toe-nail factor
C_D = load duration factor

Based on the conditions of the testing, C_M, C_t, C_{eg}, and C_{tn} are all equal to 1.0. The load duration factor C_D is 1.6 based on wind pressures. Therefore, $W' = W * C_D = W * 1.6$. **Table 10** shows the NDS ASD factored withdrawal capacity for each fastener and substrate.

Calculated Allowable Fastener and Stucco Load Comparisons

Table 11 shows the calculated allowable fastener loads compared with the NDS ASD design values. The NDS/FPL method was slightly more conservative than ASTM D7147 method. The calculated allowable staple loads were nearly or exactly the same as the NDS design capacities, indicating accurate testing results. Calculated allowable loads for the smooth nail, barbed nail, and screws were significantly less than the NDS design values. Based on the results of the testing, it may be underconservative to assume NDS capacities.

Next, the same methods were used to calculate the allowable stucco loads and tabulated with the NDS design capacities (**Table 12**). The calculated allowable stucco loads were significantly less than the NDS design capacities with the exception of metal lath/smooth nails, metal lath/staples, and fiberglass lath/staples in sheathing only. Using the ASTM D7147 for allowable loads is likely to be overconservative as the minimum ultimate load was used in lieu of the average ultimate load due to sample

Fastener	Sheathing	Stud and sheathing
Smooth	22	76
Barbed	45	100
Staple	19	54
Screw	82	240

Table 10. American Wood Council National Design Standard[8] factored fastener withdrawal capacities W' (lb)

Substrate	Sheathing			Sheathing and stud		
Lath/fastener	Per ASTM D7147	Per NDS/FPL	NDS	Per ASTM D7147	Per NDS/FPL	NDS
Smooth nail	12	10	22	26	22	76
Barbed nail	28	24	45	46	39	100
Staple	18	15	19	64	54	54
Screws	58	49	82	183	154	240

Note: ASTM D7147 = *Standard Specification for Testing and Establishing Allowable Loads of Joist Hangers*[13]; NDS/FPL = US Department of Agriculture Forest Products Laboratory[12] safety factor and American Wood Council (AWC) *National Design Standard*[8] load duration factor; NDS = AWC *National Design Standard*.[8]

Table 11. Calculated allowable fastener loads (lb) using ASTM D7147, NDS/FPL, and NDS design capacities

Substrate	Sheathing			Sheathing and stud		
Lath/fastener	Per ASTM D7147	Per NDS/FPL	NDS	Per ASTM D7147	Per NDS/FPL	NDS
Metal/smooth nail	16	13	22	20	17	76
Metal/barbed nail	20	17	45	26	22	100
Metal/staple	15	13	19	22	26	54
Fiberglass/screws	30	25	82	25	25	240
Fiberglass/staples	14	12	19	17	14	54

Note: ASTM D7147 = *Standard Specification for Testing and Establishing Allowable Loads of Joist Hangers*[13]; NDS/FPL = US Department of Agriculture Forest Products Laboratory[12] safety factor and American Wood Council (AWC) *National Design Standard*[8] load duration factor; NDS = AWC *National Design Standard*.[8]

Table 12. Calculated allowable stucco loads (lb) using ASTM D7147, NDS/FPL, and NDS design capacities

Fastener	Sheathing	Sheathing and stud
Staple	11	10
Screw	57	80
Smooth Nail	45	50
Barbed Nail	40	60

Table 13. Maximum allowable bearing loads (lb)

size. Overall, the use of NDS design capacities without considering the effects of lath failure is underconservative for design.

Alternate Failure Mode Consideration

Stucco lath fasteners secure the cladding to the structure to resist wind suction loads. However, they also resist vertical loads imparted by gravity. During testing, samples of lath and stucco were weighed after pull-testing. The average weight of the stucco was approximately 10 lb/ft^2. This value was comparable to the dead-load values ranging between 10 and 15 lb/ft^2 for lath and plaster assemblies published in ASCE/SEI 7-10, *Minimum Design Loads for Buildings and Other Structures*.[14] The analytical methods in APA TT-109[6] limit cladding fasteners to supporting no more than 11 lb/ft^2 of cladding.

The shear capacity of the metal fasteners is much greater than the bearing capacity of the wood substrate. Therefore, only an analysis of the bearing capacity of the wood is needed to resist the gravity loads. The AWC's national design standard[8] has methods for calculating the bearing capacity of wood-supporting fasteners subjected to shearing loads. Table 13 presents the maximum dead load that each type of fastener can support based on the AWC standard. When specifying a fastener spacing for stucco attachment, the designer should ensure that the tributary load for each fastener is within the allowable values shown in Table 13.

EXAMPLE CALCULATIONS

Consider a single-family residence, 30 × 40 ft in plan with a mean roof height of 30 ft. The stucco selected weighs 10 lb/ft^2. In our example calculations, we will select the stucco lath attachment for this type of structure at a sheltered site in Terre Haute, Ind., and an exposed site in Charleston, S.C. Because the examples analyze a single-family residence, we will calculate the wind loads using methods in the 2015 *International Residential Code* (IRC).[15]

Terre Haute, Indiana

For the home located in Terre Haute, suction pressures on cladding can be determined using IRC Tables R301.2(2) and R301.2(3) along with Fig. 302.2(4)A. The following parameters applied:

Ultimate design wind speed, V_{ult} = 115 mph (from Fig. R301.2[4])A]
Exposure category B adjustment factor = 1 (from Table R301.2[3])
Component and cladding load = –11 lb/ft^2 (from Table R301.2[2])

The cladding suction pressure is low, and therefore the attachment method can be largely driven by economy. Attachment directly to sheathing saves the cost of locating studs. Table 13 shows that metal lath with smooth nails and metal lath with staples both have low allowable loads. Dividing the allowable loads in Table 11 by the cladding loads determines the maximum area of stucco that can be supported by each fastener.

Metal lath/smooth nail: 16 lb/11 lb/ft^2 = 1.45 ft^2
Metal lath/staple: 15 lb/11 lb/ft^2 = 1.36 ft^2

However, staples are limited to supporting 10 lb/ft^2 of stucco in bearing. Staples are limited to 1 ft^2 of stucco.

Metal lath/smooth nail spacing = $\sqrt{(1.45 \text{ ft}^2 * 144 \text{ in.}^2/\text{ ft}^2)}$ = 14.4 in.

Therefore, the stucco applied to the home in Terre Haute can be attached with smooth nails at 14 in. on center horizontally and vertically into sheathing or staples at 12 in. on center horizontally and vertically into sheathing.

Charleston, South Carolina

For the home located in Charleston, IRC Figure 302.2(4)A indicates that a wind design performed in accordance with ASCE 7[14] is required. The following parameters applied:

Risk category: II
Basic wind speed: 148mph (ASCE 7-10 Fig. 25.5-1A)
Exposure category: C
Velocity pressure coefficient K_z: 0.98 (ASCE 7-10 Table 30.3-1)
Topographic factor K_{zt}: 1 (no local topographic features)
Direction factor K_d: 0.85 (ASCE 7-10 Table 26.6-1)
Enclosure classification: Enclosed (assumed for example)
Internal pressure coefficient: ±0.18 (ASCE 7-10 Table 26.11-1)
End zone width, $a = 0.4h$ or 10% least horizontal
a = 3 ft
Effective area = a * wall height = a * 20 ft = 60 ft^2
End Zone 5 external pressure coefficient based on effective area: –1.18 (ASCE 7-10 Fig. 30.4-1)
Velocity pressure = 46.7 lb/ft^2 (ASCE 7-10 Eq. [30.3-1])
Design wind pressure = 63.5 lb/ft^2 (ASCE 7-10 Eq. [30.4-1])
For ASCE (ASD) load combination = $1.0D + 0.6W$
Therefore, the ASD design wind pressure = (0.6) * –63.5 lb/ft^2 = –38.1 lb/ft^2

Try the following lath/fastener/substrate combinations using Table 12 allowable loads:

Metal lath/barbed nails in sheathing and stud:
Per Table 11, allowable load = 26 lb
Fastener area = 26 lb/38.1 lb/ft^2= 0.68 ft^2
Vertical fastener spacing (using 16 in. on center horizontal) = (0.68 ft^2* 144 in./ft^2 * ¹⁄₁₆ in.) = 6.1 in.
Fiberglass lath/screws in sheathing only:
Per Table 12, allowable load = 30 lb
Fastener area = 30 lb/38.1 lb/ft^2 = 0.79 ft^2
Fastener spacing (vertical) and (horizontal) = $\sqrt{(0.79 \text{ ft}^2 * 144 \text{ in.}^2/\text{ft}^2)}$ = 10.7 in.

It is interesting to note that the traditional selection of metal lath/barbed nails into studs and sheathing would require more fasteners than is currently required by the building code (which requires fasteners at 7 in. on center along framing).

CONCLUSION

The findings from this study demonstrate the potential benefits of stucco lath attachment tables. In regions where design wind speeds are lower, the ability to use fewer fasteners and attaching stucco only to structural sheathing would be an economic improvement. In regions with higher wind speeds, the attachment of stucco can be specified to meet the correspondingly higher wind loads.

To fully develop this concept for industry practice, further research is needed in the following areas:

- Additional stucco pull-testing should be performed. This project pulled only six samples of each stucco assembly, which leads to greater uncertainty in the statistical analysis of the stucco pull-test data. The methods used for determining allowable loads would have reduced the allowable loads in Table 12 significantly below the NDS design capacities. However, these values do not correlate with the author's 25 years of experience evaluating stucco or the evidence provided by Newkirk[7]—most stucco does not blow off in storms. Therefore, the values in Table 12 seem more overly conservative. Nevertheless, additional testing would result in more-robust allowable load values. In addition, there are other lath and fastener combinations that could be evaluated.
- The protocol for pull-testing of lath should be reevaluated. This battery of testing was included to provide insight regarding the mode of failure when stucco pulls off from a structure. However, lath tested without being embedded in cured plaster deforms, and the loading on the lath strands becomes primarily tensile. When fastener heads pull through lath in actual failures, the lath strands fail primarily in shear. Further consideration should be given to methods for lath testing.
- Additional testing specific to stainless steel assemblies (stainless steel lath, lath accessories, and fasteners) should be conducted. Stainless steel is a popular material in coastal regions where salt-rich air accelerates corrosion of metal building components. These same regions are subject to higher wind loads. Data from this project, as well as industry literature, indicate that load capacities of some stainless steel connections are lower than those of carbon steel fasteners.

ACKNOWLEDGMENTS

The authors gratefully acknowledge the support of the many people who provided guidance, insight, and encouragement for the completion of this work. Specific thanks are extended to:

- C. Reid Phillips of the Citadel for his assistance with pull-testing duties. Phillips has since graduated with a bachelor of science in mechanical engineering and is an engineer at Elkin Engineering & Diagnostics.
- J. Reed Elkin of Embry-Riddle Aeronautical University for his assistance with pull-testing duties.
- Bill Egan and BASF Wall Systems for donating Acrocrete stucco products and PermLath fiberglass lath.
- Doug Lindsay and AMICO Lath for donating expanded metal lath and PVC casing bead.

REFERENCES

1. International Code Council (ICC). 2014. *International Building Code, 2015 Edition*. Country Club Hills, IL: ICC.
2. ICC. 1994. *Standard Building Code*. Country Club Hills, IL: ICC.
3. ASTM International. 2014. *Standard Specification for the Application of Portland Cement Based Plaster*. ASTM C926-14. West Conshohocken, PA: ASTM International. https://doi.org/10.1520/C0926-14.
4. ASTM International. 2014. *Standard Specification for the Installation of Lathing and Furring to Receive Portland Cement-Based Plaster*. ASTM C1063-14. West Conshohocken, PA: ASTM International. https://doi.org/10.1520/C1063-14.
5. Innocenzi, M. 2018. "How Stuck Is the Stucco? A Method for Measurement and Analysis." IIBEC website. https://iibec.org/stuck-stucco.
6. APA—The Engineered Wood Society. 2010. *Wood Structural Panels Used as Nailable Sheathing*. APA Technical Topic 109. Tacoma, WA: APA.
7. Newkirk, B. D. 2010. "Questioning the Stucco Lath Fastening Requirements of ASTM C1063." *Journal of Architectural Engineering* 16 (1). https://doi.org/10.1061/(ASCE)AE.1943-5568.0000016.
8. American Wood Council (AWC). 2015. *National Design Specification for Wood Construction, 2015 Edition*. Leesburg, VA: AWC.
9. ASTM International. 2018. *Standard Test Methods for Measurement of Tensile Strength or Bond Strength of Portland Cement-Based Plaster by Direct Tension*. ASTM C1860-18. West Conshohocken, PA: ASTM International. https://doi.org/10.1520/C1860-18.
10. ASTM International. 1988. *Standard Test Methods for Mechanical Fasteners in Wood*. ASTM D1761-88. West Conshohocken, PA: ASTM International.
11. ASTM International. 2019. *Standard Specification for Computing Reference Resistance of Wood-Based Materials and Structural Connections for Load and Resistance Factor Design*. ASTM D5457-19B. West Conshohocken, PA: ASTM International. https://doi.org/10.1520/D5457-19B.
12. U.S. Department of Agriculture Forest Products Laboratory (FPL). 2010. *Wood Handbook, Wood as an Engineering Material*. FPL-GTR-190. Madison, WI: FPL. https://www.fpl.fs.fed.us/documnts/fplgtr/fpl_gtr190.pdf.
13. ASTM International. 2011. *Standard Specification for Testing and Establishing Allowable Loads of Joist Hangers*. ASTM D7147-11. West Conshohocken, PA: ASTM International. https://doi.org/10.1520/D7147-11.
14. American Society of Civil Engineers (ASCE). 2013. *Minimum Design Loads for Buildings and Other Structures*. ASCE/SEI 7-10. Reston, VA: ASCE.
15. ICC. 2014. *International Residential Code, 2015 Edition*. Country Club Hills, IL: ICC.

Air Infiltration and Its Consequences for Building Enclosures in Hot/Humid Climate Zones

David Finley

Finley Consulting Group LLC | Macedonia, OH

dave@finleycg.com

Manfred Kehrer

Wiss, Janney, Elstner Associates Inc. | Northbrook, IL

MKehrer@wje.com

IIBEC 2022 - Building for the Future

International Convention and Trade Show

March 17–22, 2022 | Orlando, FL

ABSTRACT

The consequences of unintentional air leakage through building enclosures for hygrothermal performance depend on many parameters such as climate zone and airtightness. The presenters recently published studies to quantify the risk of microbial growth in cold climate zones for building enclosures having a split insulation arrangement to meet code requirements. In this study, they focus on quantifying the risk in those zones of microbial growth and potential deterioration of interior gypsum wallboard for exterior walls in hot and humid climate zones because of unintentional exterior air infiltration. Several partially unknown parameters—namely air infiltration rates depending on airtightness, actual indoor temperatures, perm ratings of interior paints and exterior water-resistive air barriers, and their impact on the hygrothermal performance—are considered.

SPEAKERS

David Finley

Finley Consulting Group LLC | Macedonia, OH

David Finley is involved in a wide range of architectural investigations. His building enclosure experience includes water infiltration testing of windows, curtainwalls, masonry facades, and plaza and below-grade waterproofing, as well as condensation and air leakage testing of glazed fenestrations and masonry facades.

Finley is well versed in performing hygrothermal analyses using steady- and transient-state techniques. Additionally, he is capable of analyzing window and wall systems for two-dimensional thermal conduction.

Manfred Kehrer

Wiss, Janney, Elstner Associates Inc. | Northbook, IL

Manfred Kehrer is a senior associate at Wiss, Janney, Elstner Associates Inc. (WJE), who has been active in the field of building science for more than 30 years. After more than 20 years at Fraunhofer IBP, Germany, where he was active in the laboratory and leading development of WUFI software, he worked for the Oak Ridge National Laboratory for five years as a senior researcher and then served for one year as president of the start-up consulting company justSmartSolutions LLC. At WJE, Kehrer is in charge of building science solutions for a variety of problems in construction practice. He is a voting member, chair, and vice chair for several American Society of Heating, Refrigerating and Air-Conditioning Engineers and ASTM International committees, serves on the editorial board of the journal *Frontiers in Built Environment*, and has won several awards.

Air Infiltration and Its Consequences for Building Enclosures in Hot/Humid Climate Zones

To maximize the efficacy and performance of building enclosure walls, the four major building enclosure control layers (liquid water, air, water vapor, and thermal) should be designed and installed with continuity. The position of these control layers within a wall assembly can also significantly affect the hygrothermal performance (movement of heat and moisture) of an exterior wall. In a previous study,[1,2] we reviewed the risk of microbial growth within energy code–compliant exterior walls that use a split insulation arrangement, both exterior continuous insulation and batt insulation within the stud cavities, located in Climate Zones 4 and higher, as defined in the *International Energy Conservation Code* (IECC).[3]

In this study, we focus on quantifying the risk of microbial growth and potential deterioration of the interior gypsum wallboard for energy code–compliant exterior walls in hot and humid climate zones (such as Climate Zones 1 and 2) because of unintentional exterior air infiltration.

EFFECTS OF INSULATION

Because the introduction of insulation in any exterior wall system reduces the heat flow through the wall assembly, the surface temperature of materials inboard of the insulation are reduced in hot and humid climates (especially when air conditioning is used). In addition to the temperature drop in the interior space caused by the insulation, a subsequent and greater reduction in the saturation vapor pressure P_{ws} occurs, as shown in **Eq. (1)**, which can cause the development of condensation.

$$P_{ws} = 1000e^{\left(52.58-\frac{6790.5}{T}-5.028\ln T\right)}$$

where

T = temperature (°K)

Note that P_{ws} will drop exponentially relative to T.

Equation 1

Saturation vapor pressure is the maximum pressure of water vapor, or absolute humidity, that can exist within the air. Relative humidity (RH) is the ratio of actual water vapor in the air to the maximum amount of water vapor at saturation (**Eq. [2]**). Therefore, the RH of saturated air (that is, actual vapor pressure equal to the saturation vapor pressure) is 100%.

$$RH = \frac{P_w}{P_{ws}}$$

where

P_w = vapor pressure

Equation 2

Because of the relationship between the significant drop in saturation vapor pressure associated with thermal gradients via insulation, increased RH as well as the inherent reduction in surface temperatures inboard of the insulation layer is expected. Therefore, it is important and ideal to place the thermal control entirely outboard of the other building enclosure control layers, thereby protecting the structure and moisture-sensitive finishes from elevated RH and potential condensation development. However, the energy codes allow either splitting the thermal control layer so that it sandwiches some of the other control layers or placing it entirely inboard of the control layers within the stud cavity. If the insulation is placed in a split or inboard position, it is imperative to control or reduce the vapor and air transport into and through the insulation layer to avoid condensation development or increased surface RH that can promote microbial growth.

Condensation can occur on surfaces when the surface temperature drops below the dew point temperature of the ambient air, which occurs when the vapor pressure reaches the saturation vapor pressure, or an RH of 100% (**Eq. [3]**).

$$T_{dp} = \frac{B\left[\ln\frac{RH}{100}\right]+\frac{A\cdot T_i}{B+T_i}}{A-\ln\frac{RH}{100}-\frac{A\cdot T_i}{B+T_i}}$$

where

T_{dp} = dew point temperature (°C)

T_i = interior temperature (°C)

A = 17.62

B = 243.12

Equation 3

For interstitial spaces, such as within a wall system, the necessary moisture (vapor) for condensation or elevated surface RH typically comes from two sources: vapor diffusion and air leakage. Both of these mechanisms should be considered when evaluating the anticipated hygrothermal performance of a proposed exterior wall assembly.

DIFFUSIVE CONDENSATION

Diffusive condensation occurs when moisture migrates from air with a higher vapor pressure to air with a lower vapor pressure. Diffusion is a much slower method of transferring moisture than airflow. As a result, it is typically a less significant contributor to moisture migration associated with condensation problems than airflow. Nonetheless, the placement of vapor retarders within an exterior wall assembly with respect to the location of the insulation warrants careful consideration.

As previously discussed, insulation causes a significant change in the thermal gradient and a corresponding drop in saturation vapor pressure. If the predicted vapor pressure at any

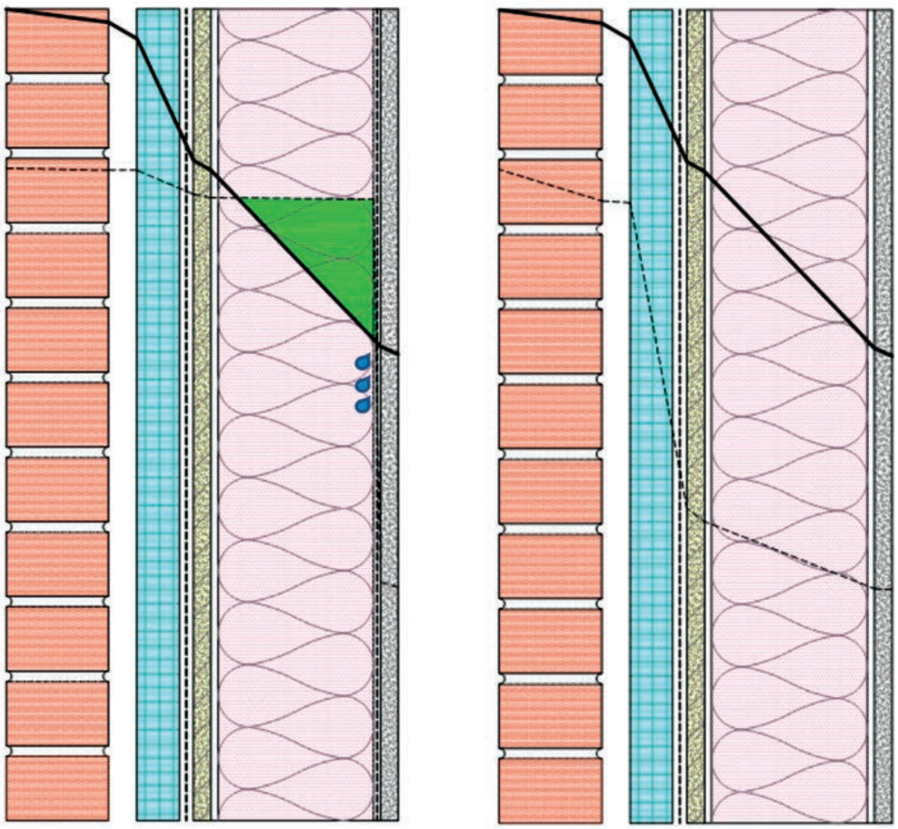

Figure 1. Predicted vapor pressure profile of a typical split insulation system in a hot and humid climate. The dashed lines represent the predicted vapor pressure, and the solid lines represent the saturation vapor pressure. The green shaded region indicates the area where the predicted vapor pressure exceeds the saturation pressure or where the predicted relative humidity exceeds 100% (left). The pressure profile for the same assembly but with a vapor-impermeable water-resistive air barrier (right).

point across the moisture-sensitive portion of the wall assembly were to exceed the saturation vapor pressure, condensation would be predicted to occur to satisfy equilibrium (**Fig. 1**). It should be noted that the rate of condensation development is typically extremely low.

To control diffusive condensation, a vapor retarder (typically the water-resistive air barrier), should be generally placed on the warm side of all insulation, outboard of the inherent drop in saturation vapor pressure, to locally reduce vapor pressure; however, split insulation assemblies make this challenging in hot-humid climates (Fig. 1).

CONVECTIVE CONDENSATION

Because airflow through discontinuities can carry moisture into a wall assembly at a much greater rate than diffusion through materials can, air leakage is often the primary source of moisture transfer associated with condensation within a wall assembly.

Airflow occurs when there is an air pressure differential across an assembly. The differential may be caused by wind, mechanical pressurization, stack effect, or other factors, and the airflow travels from a higher to a lower air pressure. Depending on the direction of airflow, ambient air temperatures, and the RH of the air and wall system materials, airflow may cause either wetting of the assembly's materials via condensation or drying of the materials through evaporation.

For example, if hot and humid exterior air flows into the exterior wall assembly due to a pressure differential, moisture can condense on surfaces of wall components that are below the dew point of the infiltrating interior air. With air-permeable batt insulation within the stud cavity, it can be expected that some infiltrating exterior air will be able to reach the inboard face of the gypsum wallboard, which may have a surface temperature below the dew point temperature of the outdoor air, and that could promote condensation. Paths for this type of airflow include discontinuities within the water-resistive air barrier and exterior sheathing; such discontinuities are commonly found around penetrations and along terminal edges at interfaces with floors, roofing assemblies, and fenestration.

In general, there are two primary air leakage paths: direct and circuitous. Direct paths, like the one shown on the left in **Fig. 2**,[4] are typical of a through-wall connection or penetration, where the air flows directly from the outside to the inside or vice versa. In this case, the air usually carries enough thermal energy to warm up or cool down the component surfaces along the flow path. This typically keeps the surface temperature of the contacted elements within the flow path above the dew point, which means that there will be no condensation along the path. Depending

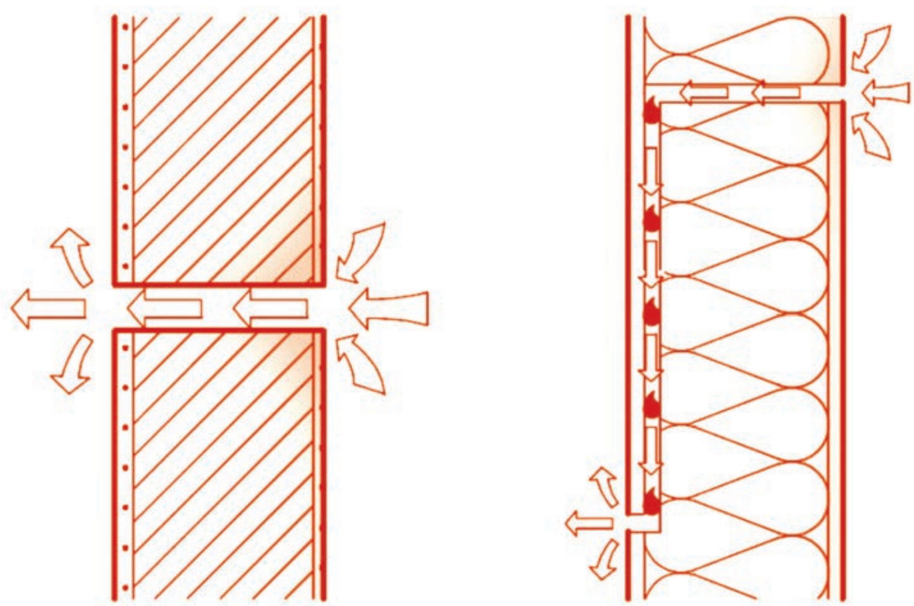

Figure 2. Diagram showing direct airflow paths (left) and circuitous airflow paths (right) for a cold weather situation. Figure: Reprinted from reference 4.

on climatic conditions, liquid condensation may develop on either the interior or exterior surface of the wall assembly. The primary concern with direct leakage paths is typically thermal shorts ("energy leaks") within the building enclosure.

Conversely, circuitous flow patterns, as shown on the right in Fig. 2, do not sufficiently warm or cool the greater area of the crossed surfaces; therefore, there is a potential for moisture-laden air to contact surfaces that are below the dew point temperature of the air. This type of air leakage path can result in the deposition of significant amounts of condensate within the wall system.

To prevent direct and circuitous air paths, all materials, components, and assemblies should be integrated to provide a continuous air-control layer. However, even with a "continuous" air-control layer, construction practices and general operation and service of the building will allow some unintended air leakage, which will likely increase during the service life of the building as materials age and weather. But how much is too much, and are there energy code–compliant wall assemblies that fare better when some air leakage occurs?

To provide insight on these questions for hot and humid climates, we conducted transient hygrothermal analyses that considered several combinations of partially unknown parameters, namely air infiltration rates depending on airtightness, actual indoor temperatures, perm ratings of interior paints and exterior water-resistive air barriers, and their impact on the hygrothermal performance.

HYGROTHERMAL MODELING

In our study, we used WUFI Pro 6 (WUFI), which is modeling software that can assess the response of a multilayered system in terms of one-dimensional simultaneous heat and moisture transport. Using historical climatic conditions for a given geographic location, WUFI can model trends in the moisture content and wetting and drying cycles of each component in the system over a period of multiple years.

The model we developed—which is similar to the air exfiltration model in cold climate zones that is incorporated in WUFI—can account for the effects of air leakage. Our approach takes pressure difference due to stack effect and global building air leakage rates, which can be derived by blower door measurements, into account. It should be noted that this air infiltration model is not yet validated, although the authors of the air exfiltration model agree that it is viable.

Index	Description of Growth
0	No growth
1	Small amounts of mold on surface (microscope), initial stages of local growth
2	Several local mold growth colonies on surface (microscope)
3	Visual findings of mold on surface, <10% coverage, or <50% coverage of mold (microscope)
4	Visual findings of mold on surface, 10%–50% coverage, or >50% coverage of mold (microscope)
5	Plenty of growth on surface, >50% coverage (visual)
6	Heavy and tight growth, coverage about 100%

Source: Adapted from reference 6.

Table 1. Mold indices

In our study, we used WUFI simulations to characterize the influence of air leakage rates and elevated surface RH on a prototype wall assembly in an example location. A brick masonry–clad, framed wall section with a vapor-impermeable (0.1 perm) water-resistive air barrier over glass-matt faced gypsum board as the exterior sheathing was assumed to be oriented south in Houston, Tex., which is in Climate Zone 2. Further, *R*-20 batt insulation placed between 2 × 6 wood studs and interior gypsum wallboard was modeled. The combination of the following conditions resulted in more than 500 combinations simulated with WUFI:

- Interior temperatures from 65°F to 72°F
- Interior RH 50% and 60%
- Building airtightness at 75 Pa from 0 to 1 $ft^3/min/ft^2$
- Interior finish: latex paint (7 and 1 perm), vinyl wallpaper

The output data were analyzed and are conveyed in terms of ANSI/ASHRAE 160-2016, *Criteria for Moisture-Control Design Analysis in Buildings*,[5] at the interior paper-faced gypsum board. The main criterion is based on a mold growth model developed by TEKES (the Finnish Funding Agency for Technology and Innovation) and VTT (the Technical Research Council of Finland),[6] which has been validated on actual laboratory and field measurements on mold growth and takes the temperature, RH, time, and substrate class into account. This main criterion is based on the mold index values in Section 6 of ASHRAE 160 (**Table 1**), and it defines values equal to greater than 3 as unacceptable.

RESULTS

We compiled the resulting mold growth index (MGI) to provide a more detailed assessment of the hygrothermal performance of

Depending on climatic conditions, liquid condensation may develop on either the interior or exterior surface of the wall assembly. The primary concern with direct leakage paths is typically thermal shorts ("energy leaks") within the building enclosure.

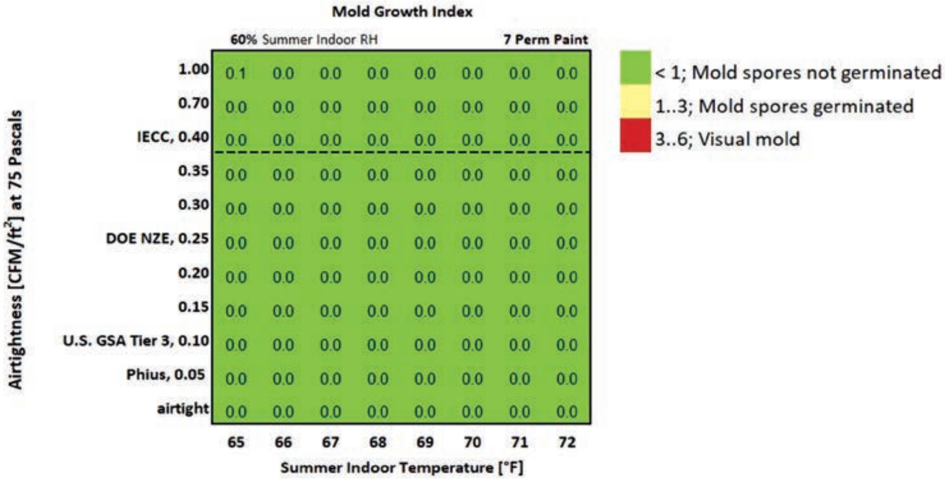

Figure 3. Maximum mold growth index values for variable air leakage rates and interior temperatures with 7-perm latex paint. DOE NZE = U.S. Department of Energy, Net Zero Energy Buildings; IECC = International Energy Conservation Code*; Phius = Passive House Institute; U.S. GSA Tier 3 = U.S. General Service Administration, Level Tier 3.*

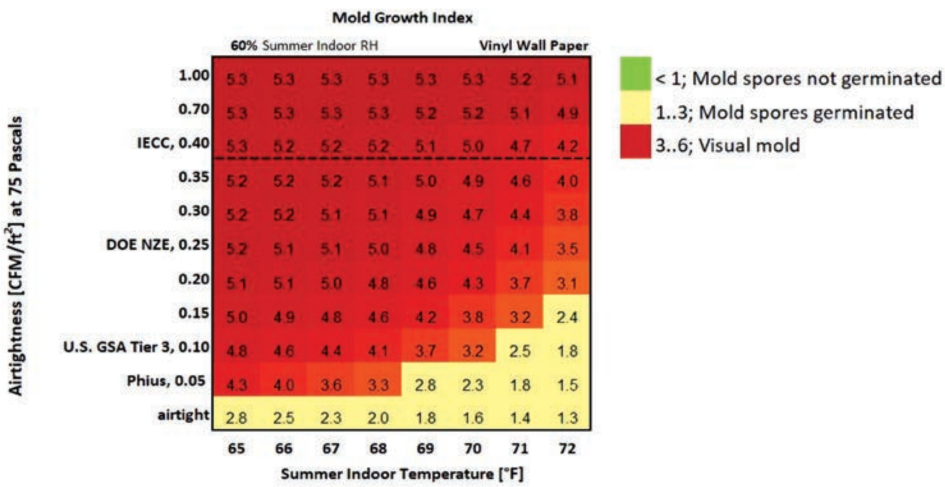

Figure 4. Maximum mold growth index for variable air leakage rates and interior temperatures with vinyl wallpaper. DOE NZE = U.S. Department of Energy, Net Zero Energy Buildings; IECC = International Energy Conservation Code*; Phius = Passive House Institute; U.S. GSA Tier 3 = U.S. General Service Administration, Level Tier 3.*

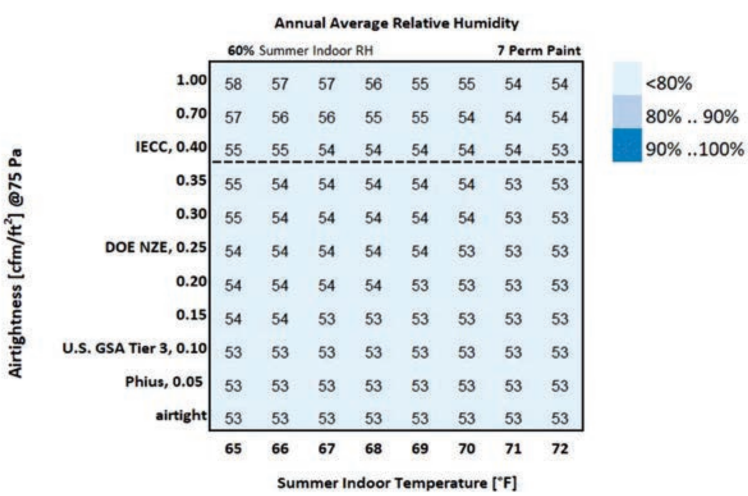

Figure 5. Maximum relative humidity for variable air leakage rates and interior temperatures with 7-perm latex paint. DOE NZE = U.S. Department of Energy, Net Zero Energy Buildings; IECC = International Energy Conservation Code*; Phius = Passive House Institute; U.S. GSA Tier 3 = U.S. General Service Administration, Level Tier 3.*

code minimum *R*-values in ASHRAE 90.1, *Energy Standard for Buildings Except Low-Rise Residential Buildings*,[7] and the IECC.[3] For example, **Fig. 3** through **8** illustrate the results after a 10-year simulation on the exterior surface of the interior paper-faced gypsum wallboard example wall with either a 7-perm latex paint or vinyl wallpaper finish under 60% interior RH. The diagrams show the predicted maximum MGI, maximum RH, and maximum water content (percent by weight) depending on the air leakage rate and the indoor temperature. The figures also identify the air leakage requirements from the IEEC and from the following organizations and programs: the Passive House Institute, the U.S. Department of Energy Net Zero Energy Buildings, and the U.S. General Service Administration Level Tier 3 Sources can be found at https://www.buildingscience.com/documents/digests/bsd-104-understanding-air-barriers and http://www.phius.org/Tools-Resources/TechCorner/201508-Airtightness-Karagiozis.pdf. Other results can be found in Fig. A.1 through A.6 in the **Appendix**.

All the diagrams show a similar basic and predictable behavior: Wall assemblies at higher airtightness levels and higher interior temperatures are at lower risk for development of mold (as represented by the green colors in the lower right corners of the diagrams). Altering conditions toward the upper left corners of the diagrams, meaning higher airtightness levels and lower interior temperatures, results in higher risk for development of mold, as represented by the colors turning from yellow/orange to red.

It is obvious from the results in the Appendix that decreasing air leakage leads to better-performing assemblies. Further, increased interior operating temperatures also help the exterior wall perform better: because the interior drywall will be at a higher temperature, the risk of condensation for the example wall assembly in Climate Zone 2 is lower, assuming the levels of airtightness are at least code compliant (0.4 $ft^3/min/ft^2$ at 75 Pa) to achieve acceptable ASHRAE 160 criterion.

Finally, from the results in the Appendix, we can establish that use of a Class I or II vapor retarder (less than 1 perm) is associated with a significantly higher risk for mold development in all the combinations when compared with the use of variable latex paint permeances (greater than or equal to 1 perm). This validates the code restriction on the use of Class I vapor retarders on the interior side of framing in Climate Zones 1 and 2.

CONCLUSION

Figures 4 through 8 show that even if construction follows the energy code, a hygrothermal safe performance is associated with higher interior temperatures and lower air leakage rates. Our findings suggest that compliance with the energy code does not guarantee condensation- or mold-free wall performance.

Hygrothermal performance of wall assemblies is exceptionally complex, a function of numerous variables and assumptions. Thus, simplified empirical design guides may not provide prudent direction.

This study focused on a single city in Climate Zone 2. Additional simulations to include more geographic locations and prototype wall assemblies would provide a more encompassing design guideline for designers to comply with the current energy codes and avoid moisture accumulation and microbial growth due to condensation.

REFERENCES

1. Finley, D., and M. Kehrer. 2019. "ASHRAE 90.1 and Cold Weather Condensation." In: *Proceedings of the 2019 IIBEC Building Enclosure Symposium, Louisville, KY*, pp. 64–72.
2. Finley, D., and M. Kehrer. "ASHRAE 90.1: Codified Condensation for Cold Climates." In: *2020 Residential Building Design & Construction Conference Proceedings*, pp. 39–54. https://www.phrc.psu.edu/assets/docs/Publications/2020RBDCCPapers/2020-RBDCC-Whole-Proceedings.pdf.
3. International Code Council (ICC). 2021. *International Energy Conservation Code*. Country Club Hills, IL: ICC.
4. Künzel, H. M., D. Zirkelbach, and B. Schafaczek. 2012. "Modelling the Effect of Air Leakage in Hygrothermal Envelope Simulation." *National Institute of Building Science 2012—Proceedings BEST3 Conference, Atlanta (2012)*. https://wufi.de/literatur/K%C3%BCnzel,%20Zirkelbach%20et%20al%202012%20-%20Modelling%20the%20Effect%20of%20Air.pdf.
5. American Society of Heating, Refrigerating and Air-Conditioning Engineers (ASHRAE). 2016. *Criteria for Moisture-Control Design Analysis in Buildings*. ANSI/ASHRAE 160-2016. Peachtree Corners, GA: ASHRAE.
6. Ojanen, T., H. Viitanen, R. Peuhkuri, K. Lähdesmäk, J. Vinha, and K.

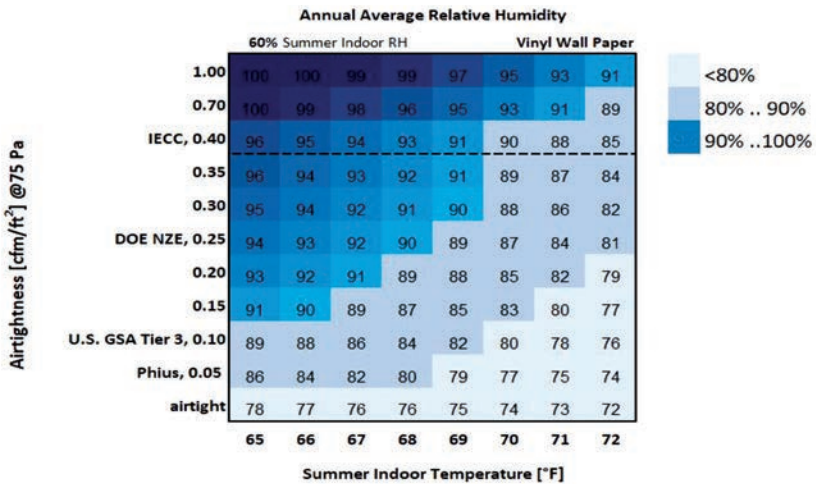

Figure 6. Maximum relative humidity for variable air leakage rates and interior temperatures with vinyl wallpaper. DOE NZE = U.S. Department of Energy, Net Zero Energy Buildings; IECC = International Energy Conservation Code; Phius = Passive House Institute; U.S. GSA Tier 3 = U.S. General Service Administration, Level Tier 3.

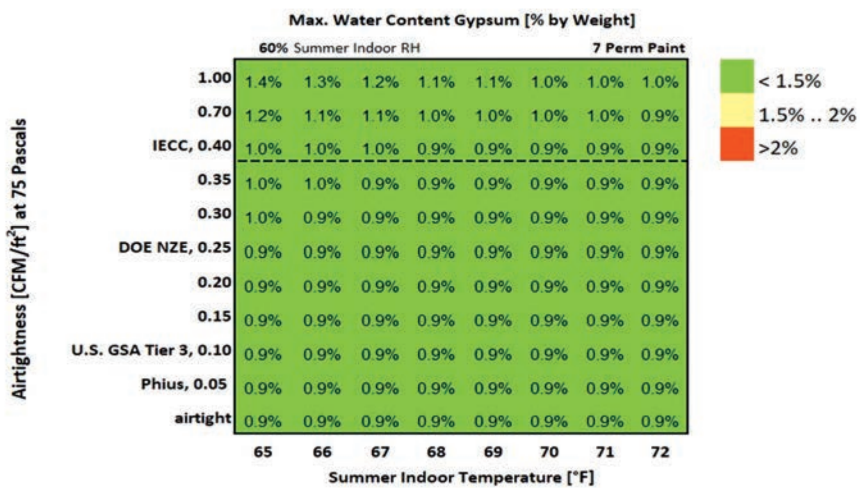

Figure 7. Maximum water content for variable air leakage rates and interior temperatures with 7-perm latex paint. DOE NZE = U.S. Department of Energy, Net Zero Energy Buildings; IECC = International Energy Conservation Code; Phius = Passive House Institute; U.S. GSA Tier 3 = U.S. General Service Administration, Level Tier 3.

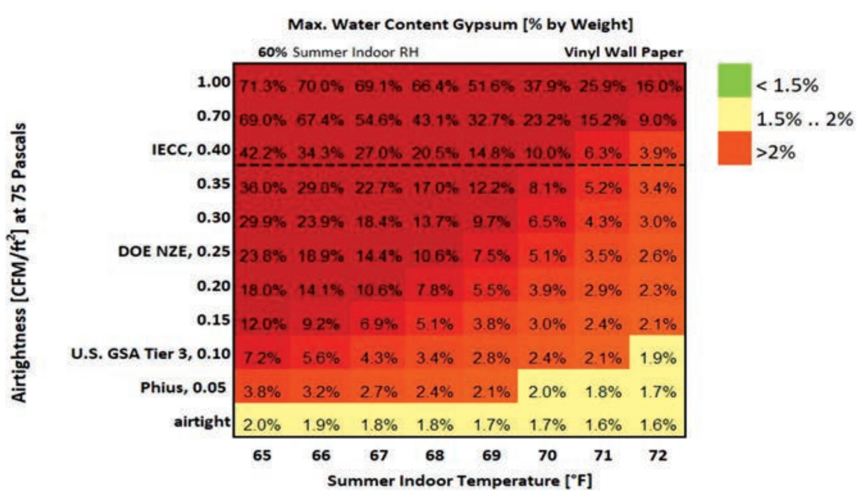

Figure 8. Maximum water content for variable air leakage rates and interior temperatures with vinyl wallpaper. DOE NZE = U.S. Department of Energy, Net Zero Energy Buildings; IECC = International Energy Conservation Code; Phius = Passive House Institute; U.S. GSA Tier 3 = U.S. General Service Administration, Level Tier 3.

Salminen. 2010. "Mold Growth Modeling of Building Structures Using Sensitivity Classes of Materials." In: *Proceedings of the Thermal Performance of the Exterior Envelopes of Whole Buildings XI Conference, Clearwater, Florida*. https://web.ornl.gov/sci/buildings/conf-archive/2010%20B11%20papers/104_Ojanen.pdf.

7. ASHRAE. 2019. *Energy Standard for Buildings Except Low-Rise Residential Buildings*. ASHRAE 90.1-2019. Peachtree Corners, GA: ASHRAE.

APPENDIX:
HYGROTHERMAL MODELING RESULTS

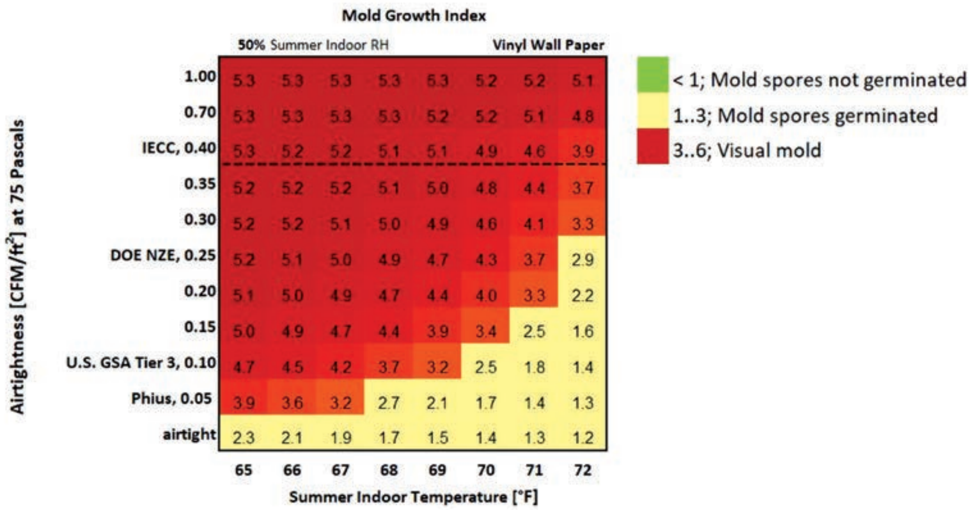

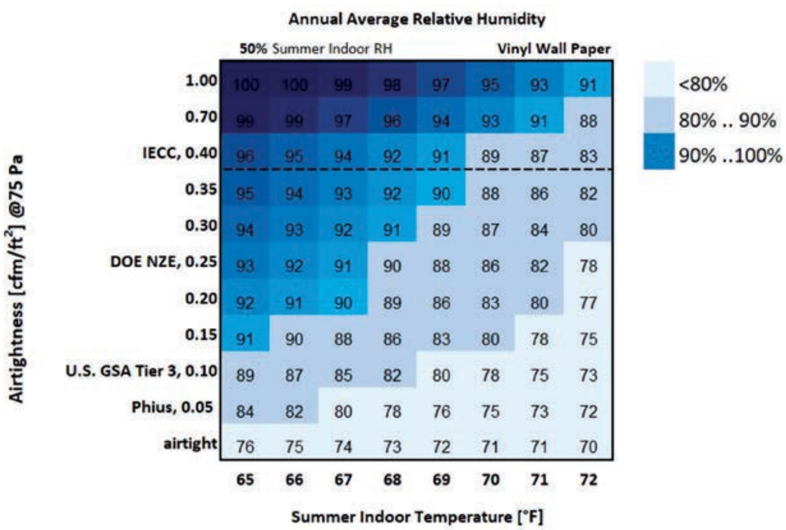

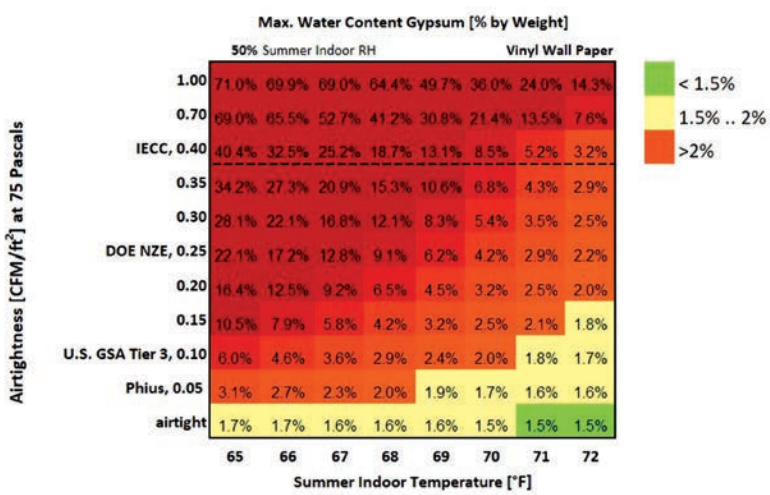

Figure A.1. Interior gypsum wallboard with vinyl wallpaper under 50% relative humidity: (a) mold growth index, (b) maximum relative humidity, and (c) maximum water content (percent by weight). DOE NZE = U.S. Department of Energy, Net Zero Energy Buildings; IECC = International Energy Conservation Code; Phius = Passive House Institute; U.S. GSA Tier 3 = U.S. General Service Administration, Level Tier 3.

APPENDIX:
HYGROTHERMAL MODELING RESULTS

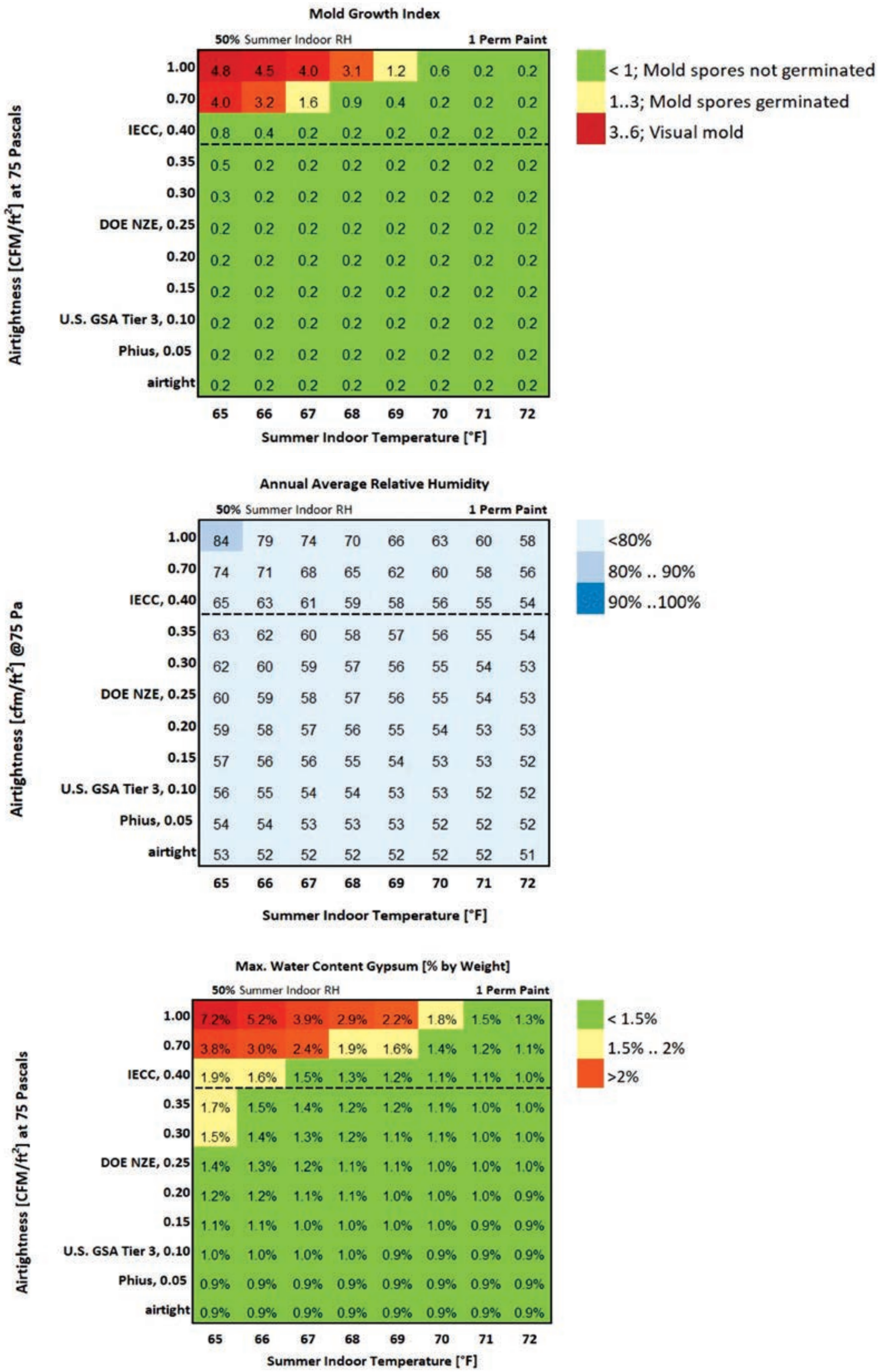

Figure A.2. Interior gypsum wallboard with 1-perm latex paint under 50% relative humidity: (a) mold growth index, (b) maximum relative humidity, and (c) maximum water content (percent by weight). DOE NZE = U.S. Department of Energy, Net Zero Energy Buildings; IECC = International Energy Conservation Code*; Phius = Passive House Institute; U.S. GSA Tier 3 = U.S. General Service Administration, Level Tier 3.*

APPENDIX:
HYGROTHERMAL MODELING RESULTS

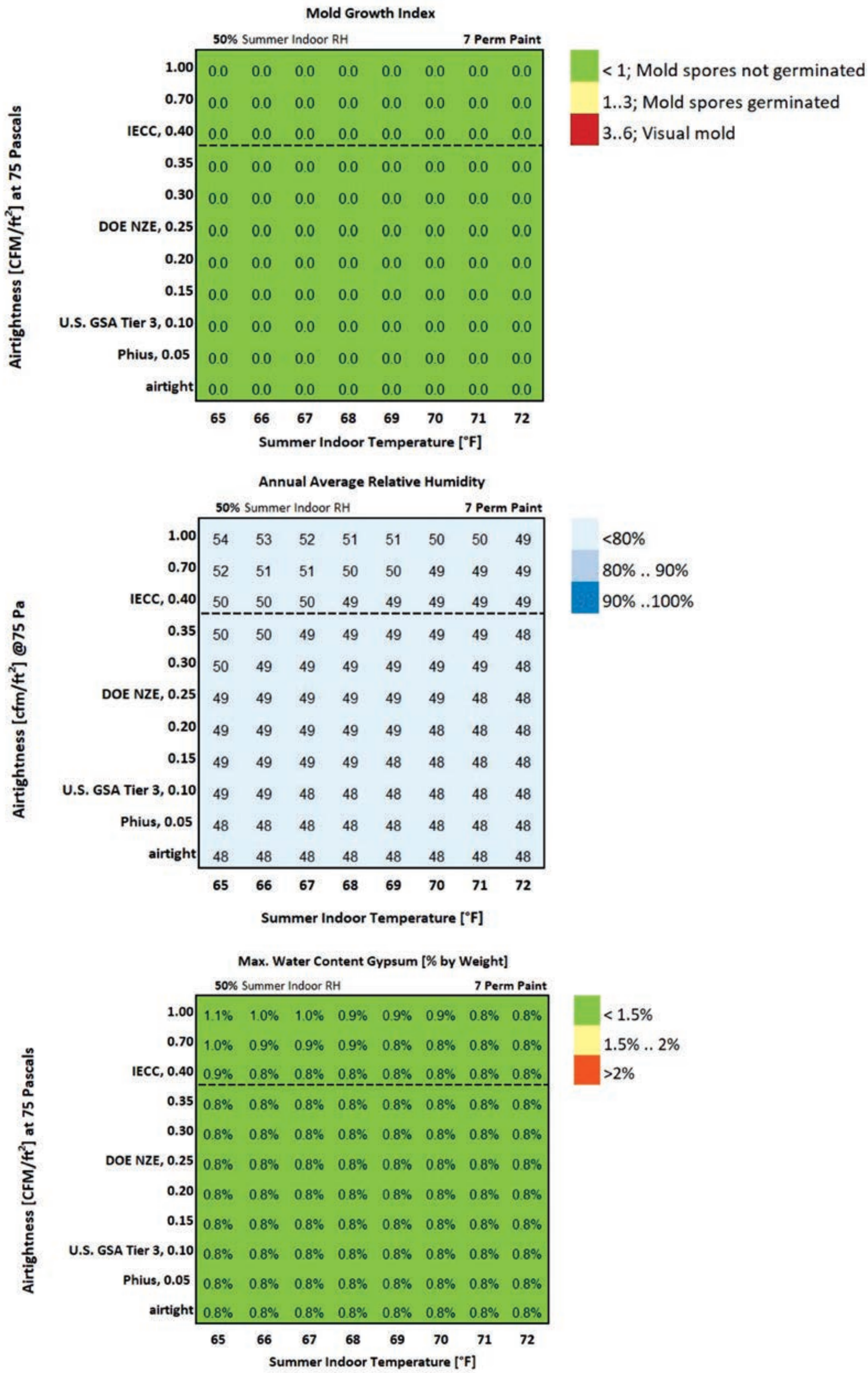

Figure A.3. Interior gypsum wallboard with 7-perm latex paint under 50% relative humidity: (a) mold growth index, (b) maximum relative humidity, and (c) maximum water content (percent by weight). DOE NZE = U.S. Department of Energy, Net Zero Energy Buildings; IECC = International Energy Conservation Code; *Phius = Passive House Institute; U.S. GSA Tier 3 = U.S. General Service Administration, Level Tier 3.*

APPENDIX:
HYGROTHERMAL MODELING RESULTS

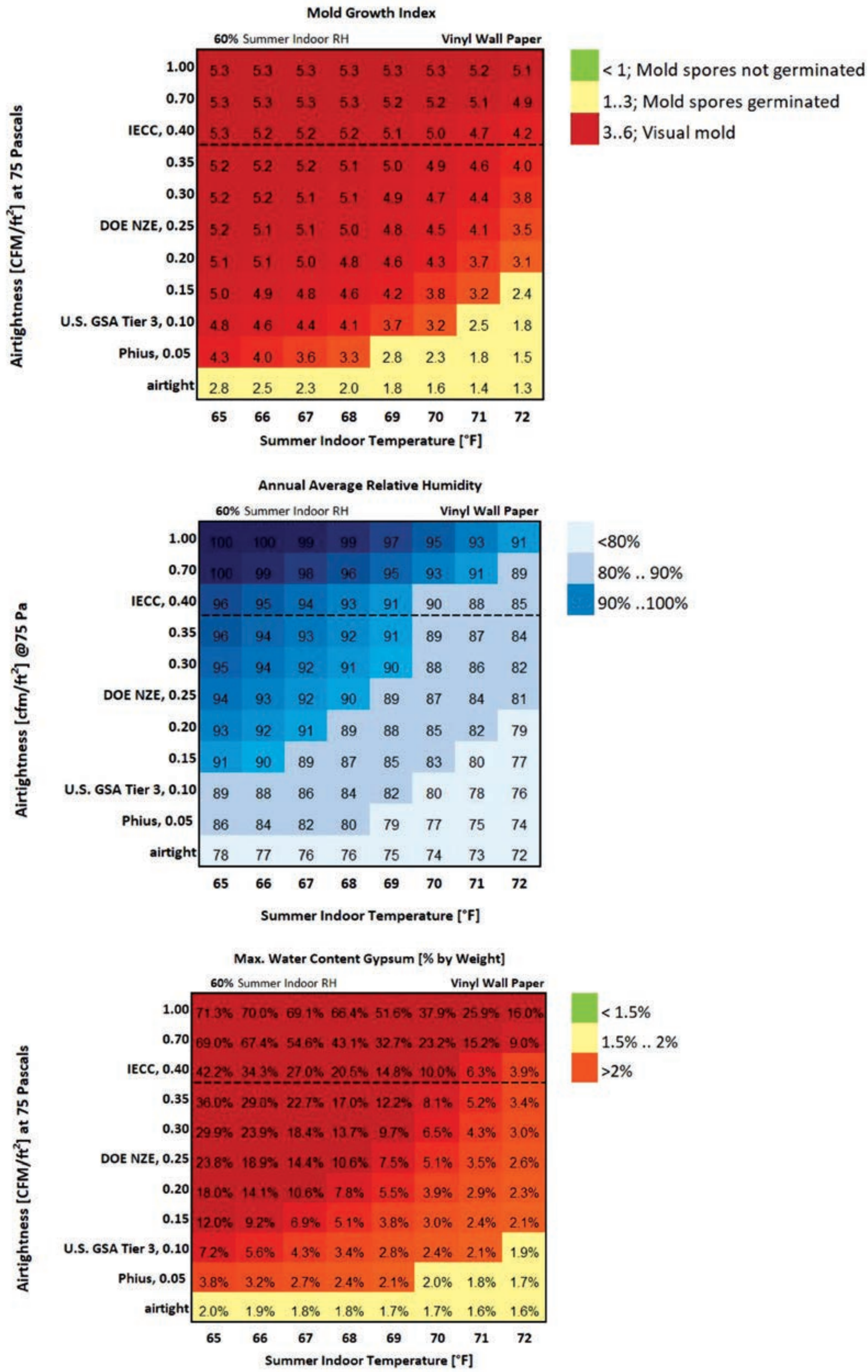

Figure A.4. Interior gypsum wallboard with vinyl wallpaper under 60% relative humidity: (a) mold growth index, (b) maximum relative humidity, and (c) maximum water content (percent by weight). DOE NZE = U.S. Department of Energy, Net Zero Energy Buildings; IECC = International Energy Conservation Code; Phius = Passive House Institute; U.S. GSA Tier 3 = U.S. General Service Administration, Level Tier 3.

APPENDIX:
HYGROTHERMAL MODELING RESULTS

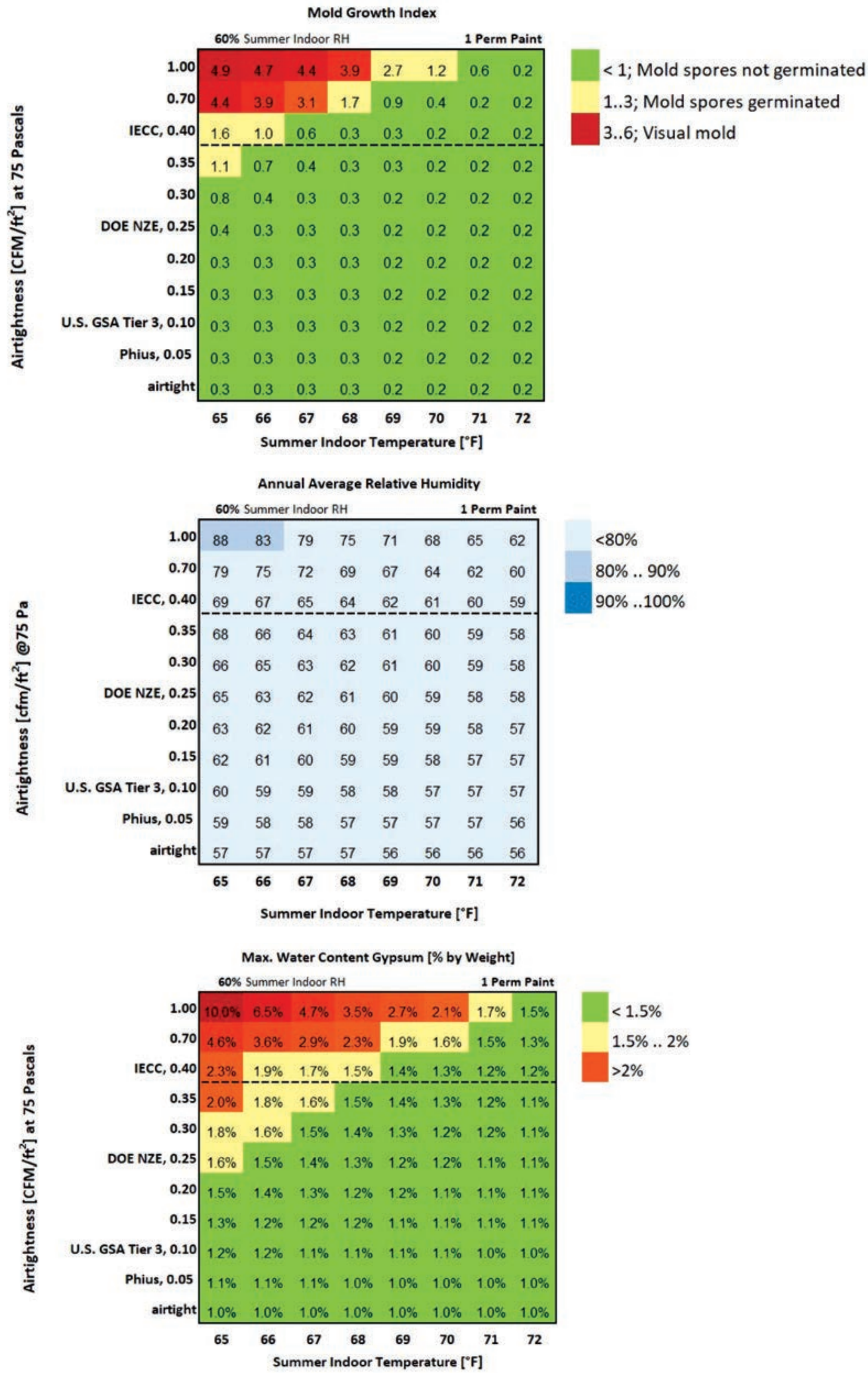

Figure A.5. Interior gypsum wallboard with 1-perm latex paint under 60% relative humidity: (a) mold growth index, (b) maximum relative humidity, and (c) maximum water content (percent by weight). DOE NZE = U.S. Department of Energy, Net Zero Energy Buildings; IECC = International Energy Conservation Code; Phius = Passive House Institute; U.S. GSA Tier 3 = U.S. General Service Administration, Level Tier 3.

APPENDIX:
HYGROTHERMAL MODELING RESULTS

Mold Growth Index

60% Summer Indoor RH — 7 Perm Paint

Airtightness [CFM/ft²] at 75 Pascals	65	66	67	68	69	70	71	72
1.00	0.1	0.0	0.0	0.0	0.0	0.0	0.0	0.0
0.70	0.0	0.0	0.0	0.0	0.0	0.0	0.0	0.0
IECC, 0.40	0.0	0.0	0.0	0.0	0.0	0.0	0.0	0.0
0.35	0.0	0.0	0.0	0.0	0.0	0.0	0.0	0.0
0.30	0.0	0.0	0.0	0.0	0.0	0.0	0.0	0.0
DOE NZE, 0.25	0.0	0.0	0.0	0.0	0.0	0.0	0.0	0.0
0.20	0.0	0.0	0.0	0.0	0.0	0.0	0.0	0.0
0.15	0.0	0.0	0.0	0.0	0.0	0.0	0.0	0.0
U.S. GSA Tier 3, 0.10	0.0	0.0	0.0	0.0	0.0	0.0	0.0	0.0
Phius, 0.05	0.0	0.0	0.0	0.0	0.0	0.0	0.0	0.0
airtight	0.0	0.0	0.0	0.0	0.0	0.0	0.0	0.0

Summer Indoor Temperature [°F]

< 1; Mold spores not germinated
1..3; Mold spores germinated
3..6; Visual mold

Annual Average Relative Humidity

60% Summer Indoor RH — 7 Perm Paint

Airtightness [cfm/ft²] @75 Pa	65	66	67	68	69	70	71	72
1.00	58	57	57	56	55	55	54	54
0.70	57	56	56	55	55	54	54	54
IECC, 0.40	55	55	54	54	54	54	54	53
0.35	55	54	54	54	54	54	53	53
0.30	55	54	54	54	54	54	53	53
DOE NZE, 0.25	54	54	54	54	54	53	53	53
0.20	54	54	54	54	53	53	53	53
0.15	54	54	53	53	53	53	53	53
U.S. GSA Tier 3, 0.10	53	53	53	53	53	53	53	53
Phius, 0.05	53	53	53	53	53	53	53	53
airtight	53	53	53	53	53	53	53	53

Summer Indoor Temperature [°F]

<80%
80% .. 90%
90% ..100%

Max. Water Content Gypsum [% by Weight]

60% Summer Indoor RH — 7 Perm Paint

Airtightness [CFM/ft²] at 75 Pascals	65	66	67	68	69	70	71	72
1.00	1.4%	1.3%	1.2%	1.1%	1.1%	1.0%	1.0%	1.0%
0.70	1.2%	1.1%	1.1%	1.0%	1.0%	1.0%	1.0%	0.9%
IECC, 0.40	1.0%	1.0%	1.0%	0.9%	0.9%	0.9%	0.9%	0.9%
0.35	1.0%	1.0%	0.9%	0.9%	0.9%	0.9%	0.9%	0.9%
0.30	1.0%	0.9%	0.9%	0.9%	0.9%	0.9%	0.9%	0.9%
DOE NZE, 0.25	0.9%	0.9%	0.9%	0.9%	0.9%	0.9%	0.9%	0.9%
0.20	0.9%	0.9%	0.9%	0.9%	0.9%	0.9%	0.9%	0.9%
0.15	0.9%	0.9%	0.9%	0.9%	0.9%	0.9%	0.9%	0.9%
U.S. GSA Tier 3, 0.10	0.9%	0.9%	0.9%	0.9%	0.9%	0.9%	0.9%	0.9%
Phius, 0.05	0.9%	0.9%	0.9%	0.9%	0.9%	0.9%	0.9%	0.9%
airtight	0.9%	0.9%	0.9%	0.9%	0.9%	0.9%	0.9%	0.9%

Summer Indoor Temperature [°F]

< 1.5%
1.5% .. 2%
>2%

Figure A.6. Interior gypsum wallboard with 7-perm latex paint under 60% relative humidity: (a) mold growth index, (b) maximum relative humidity, and (c) maximum water content (percent by weight). DOE NZE = U.S. Department of Energy, Net Zero Energy Buildings; IECC = International Energy Conservation Code*; Phius = Passive House Institute; U.S. GSA Tier 3 = U.S. General Service Administration, Level Tier 3.*

Testing Built-up and Modified Bitumen Roofs for Hail Damage

Stephen L. Patterson, RRC, PE

ROOFTECH | Fort Worth, TX

spatterson@rooftechusa.com

Jordan Beckner, PE

ROOFTECH | Fort Worth, TX

jbeckner@rooftechusa.com

IIBEC 2022 - Building for the Future

International Convention and Trade Show

March 17–22, 2022 | Orlando, FL

ABSTRACT

Although there is currently no ASTM method specifically for testing built-up and modified bitumen (bituminous) roof systems for hail-caused damage, laboratories routinely test bituminous roof systems for hail-caused damage. This presentation discusses the ASTM test methods that are commonly referenced in these laboratory testing reports. This presentation also includes findings from research the author's company has performed using ASTM D3746, *Standard Test Method for Impact Resistance of Bituminous Roofing Systems*, to illustrate what hail-caused damage of bituminous roofs looks like and to compare our ASTM D3746 test results to actual hail-caused damage to bituminous roofs. The intent is to provide exemplar photographic examples for visual comparative purposes.

SPEAKER

Stephen L. Patterson, RRC, PE

ROOFTECH | Fort Worth, TX

Stephen L. Patterson has been in the roofing industry for almost 50 years. He founded Roof Technical Services Inc. (ROOFTECH) in 1983 and has been an active consulting engineer and roof consultant ever since. ROOFTECH has provided laboratory testing, including testing for hail damage, since the late 1980s. Patterson has been technical director/director of engineering for two roofing manufacturers and managed a roof contracting company for four years.

Nonpresenting Coauthor

Jordan Beckner, PE

Jordan Beckner is a senior engineer with Roof Technical Services Inc. in Fort Worth, Texas.

Testing Built-up and Modified Bitumen Roofs for Hail Damage

There are numerous testing laboratories across the country that test built-up and modified bitumen roof (bituminous roof) samples for evidence of hail damage. The problem is that there is no specific ASTM International standard test method for performing these tests. As a result, testing labs are using a variety of test methods for testing bituminous roof samples for hail damage. Roof Technical Services Inc. (Rooftech) has been testing bituminous roof samples for evidence of hail damage since the 1980s. Most of the testing from different laboratories that we have reviewed has adapted test protocols from ASTM D2829, *Standard Practice for Sampling and Analysis of Existing Built-Up Roof Systems*,[1] and/or ASTM D3746, *Standard Test Method for Impact Resistance of Bituminous Roofing Systems*.[2] Additionally, there are acceptance criteria that are sometimes referenced in the laboratory reports included in Factory Mutual (FM) Class Number 4470, *Single-Ply, Polymer-Modified Bitumen Sheet, Built-up Roof (BUR) and Liquid Applied Roof Assemblies for Use in Class 1 and Noncombustible Roof Deck Construction*[3,4] (Appendix F: Susceptibility to Hail Damage Test Standard), ANSI FM 4473, *Impact Resistance Testing of Rigid Roofing Materials by Impacting with Freezer Ice Balls*,[5] and Underwriters Laboratory (UL) 2218, *Standard for Safety—Impact Resistance of Prepared Roof Covering Materials*.[6]

This paper has two broad objectives. The first is to provide an understanding of the test methods in ASTM D2829 and ASTM D3746 and how they relate to testing bituminous roofs for hail-caused impact damage, as well as the acceptance criteria in UL 2218, FM 4470, and FM 4473. The second is to provide a method for evaluating test samples for evidence of hail damage based on laboratory testing. To accomplish these objectives, we performed ASTM D3746 tests on insulated and noninsulated bituminous roofs. The purpose of this testing was to simulate hail-caused impact damage on these samples, to document the resulting hail-caused impact damage, and to provide a comparative visual standard to evaluate bituminous test samples for hail damage. This is an ongoing project, which will be expanded to more varieties of bituminous roof systems.

ASTM D3746

ASTM D3746[2] is a test protocol used to assess the hail resistance of bituminous roofing, such as built-up and modified bitumen roofing. This test procedure utilizes a free-falling steel missile to replicate the impact energy of a 2 in. (50 mm) hailstone. This test method provides a standard protocol for analyzing the bituminous roofing for resistance to hail-caused impact damage to bituminous roofs.

ASTM D3746 Section 10.7, "Damage Assessment," establishes a test protocol for evaluating the roof for impact damage as follows. Section 10.7 establishes a standard for desaturating felts for evaluation. The process uses a solvent bath to remove the bituminous material from the reinforcement. Reinforcements typically include fiberglass felts; polyester mats; combination fiberglass and polyester; and, in the case of older roofs, organic or asbestos felts. The desaturation process makes it easier to evaluate the felts for evidence of hail-caused damage.

> ***Section 10.7 Damage Assessment***
>
> *10.7.1 Remove any slag or gravel surfacing from the specimen carefully with a hot scraper, such as a putty knife.*
>
> *10.7.2 Record the extent of obvious damage to the membrane, such as dents or fractures, by photograph or sketch and written description.*
>
> *10.7.3 Cut the four Impact Areas from the specimen using a hot knife. Staple the felts in each area together and extract the bitumen by immersing in warm 1,1,1 trichloroethane in a fume hood. <u>Do not heat the trichloroethane to boiling.</u> (For tarred felt and pitch membranes, use xylene in place of trichloroethane.)*

ASTM D3746 Section 10.8, "Rating of Impact Damage," establishes a protocol for rating the impact damage as follows. There is only a protocol for rating the samples based upon the evidence of dents and cracks or splits. There is nothing in the protocol that establishes a pass or fail rating, so the interpretation is left to the reader of the report.

> ***Section 10.8 Rating of Impact Damage***
>
> *10.8.1 Rate the impact damage which occurs in each ply in each of the four quadrants by assigning the number which most accurately describes the impact damage, as follows:*

There are numerous testing laboratories across the country that test built-up and modified bitumen roof (bituminous roof) samples for evidence of hail damage. The problem is that there is no specific ASTM International standard test method for performing these tests.

0 = no damage;
2 = dents, indentations only;
4 = any cracks or splits

10.8.2 After assigning the numbers to all plies within each quadrant, add up all the numbers and divide by four times the number of plies to obtain an average for the membrane. (Note: No passing or failing criteria are provided.)

ASTM D2829

ASTM D2829[1] is a test for the analysis of existing built-up roofs to determine whether the roof sample contained the appropriate number of plies, the appropriate amount of asphalt or coal tar pitch (bitumen), an appropriate flood coat, and an appropriate gravel surfacing, and whether there are excessive installation voids in the interply. The following section from ASTM D2829 describes the test. There is nothing in the scope of this test method that deals with hail-caused impact damage. It is a test protocol for "determining *approximate* quantities of the various components."

1. Scope

1.1 This practice is a guide for removing test specimens from existing built-up roofing systems in the field and for determining the "approximate" quantities of the components of that specimen (Note 1). Components determined may be: 1.1.1 Insulation components when they are part of the roof membrane system, 1.1.2 Plies of roofing felt, 1.1.3 Interply layers of bituminous material,1.1.4 Top coating, and 1.1.5 Surfacing.

NOTE 1—This procedure is for the investigation of existing roofs and is not intended for new construction inspection.

1.2 This practice is applicable to both 914-mm (36-in.) and 1000-mm (39⅜-in.) wide felt rolls.

1.3 The values stated in SI (metric) units are to be regarded as standard.

1.4 This standard does not purport to address all of the safety concerns, if any, associated with its use. It is the responsibility of the user this standard to establish appropriate safety and health practices and determine the applicability of regulatory limitations prior to use.

For specific precautionary information, see 6.3.2.1

The test protocol includes methods for extracting samples from the field and for delaminating the felts, both of which are commonly used in testing bituminous roofs for hail-caused impact damage. Section 8, "Report," describes the reporting protocol as follows. Again, the report is based on analyzing the roof components and is not related to testing for hail-caused impact damage.

8. Report

8.1 Describe the built-up roof, including the type and class of bituminous material, type of surfacing, type of insulation, type of roof decking, and the type and number of felts or roofing sheets.

8.2 Fully identify the origin and roof location of each specimen.

8.3 Report the mass per unit area of surfacing, average interply bituminous material, top coating bituminous material, total applied bituminous material, and the total specimen (minus insulation). See Table 3 for summary of results and conversion to conventional units of measurement.

8.4 Diagram the felt lapping to show the number of plies and the lap relationship, if determined (6.8).

FM 4470

The requirements for hail damage resistance are included in FM 4470 Section 4.4, "Hail Damage Resistance Test."[3] The test is included in Appendix F, "Susceptibility to Hail Damage Test Standard," which was included in the older standard[4] and is only referred to as "Susceptibility to Hail Damage Test Standard" in the newer standard. The FM test is similar to ASTM D3746[2] in that the test method includes dropping steel balls to simulate hail. The acceptance criteria are included in FM 4420 Section 4.4.1, "Conditions for Hail Damage Resistance," as follows.

4.4.1 Conditions for Hail Damage Resistance

Both unconditioned (unweathered) and conditioned (weathered) samples of roof cover are inspected for damage. Neither the roof cover nor the field seam (if present) shall show any signs of cracking or splitting. The field seam shall not show any signs of cracking, splitting, separation, or rupture when examined closely under 10X magnification. Under adhered conditions, minor separations of the roof cover from the substrate (directly under the Impact Areas) is acceptable for monolithic decks only (i.e. structural concrete or gypsum) or lightweight insulating concrete insulation.

ANSI FM 4473

ANSI FM 4473[5] standard utilizes ice balls to simulate hail impact. The ice balls are propelled at a velocity that simulates the kinetic energy established for the various sizes of hail. Ice ball testing is generally more representative of actual hail impact than steel balls. Steel balls are a simple way of simulating impact energy—for example, drop a 1 lb (0.5 kg) steel ball 1 ft (0.305 m) and one gets 1 ft-lb (0.14 kg-m) of impact energy. A good example is clay and concrete tile roofing. Steel balls that generate the same impact energy as hail will break tile, while ice balls with the same impact energy will not, as ice shatters upon impact and steel does not. The difference is related to the difference in momentum between ice balls and steel balls. The acceptance criteria are included in Section 4, "Pass/Fail Criteria," as follows:

4.1.1 The test specimen shall show no evidence of visible cracking or breakage or any damage such as splits, punctures, fractures, disengagement of lap elements or exposure of materials not so intended.

4.1.2 When a test specimen fails to meet the acceptance criteria for a tested classification, two consecutive test specimens must successfully meet the acceptance criteria to qualify for the given classification

UL 2218

UL 2218[6] is similar to ASTM D3746[2] in that steel balls are dropped to simulate hail impact. UL 2218 utilizes 1.25-in.- (32-mm-), 1.5-in.- (38-mm-), 1.75-in.- (44-mm-), and 2.00-in.- (50-mm-) diameter steel balls that are dropped from 12.0 ft (3.7 m), 15.0 ft (4.6 m), 17 ft (5.2 m), and 20.0 ft (6.1 m), respectively, to simulate the impact energy of 1.25-in-., 1.50-in.-, 1.75-in.-, and 2.00-in.-diameter hail. The acceptance criteria are included in Section 7, "Acceptance Criteria," as follows:

7.1 The prepared roof covering material is to be examined after being subjected to the test procedure described in Section 6. The prepared roof covering material exposed surface, back surface and underneath layers shall show not evidence of tearing, fracturing, splitting, rupture, crazing or other evidence of opening through any prepared roof covering layer.

7.2 For asphalt shingles, a visible crack of the asphalt on the back of the shingles shall be determined to be a failure.

7.3 For wood, tile, concrete, fiber-cement, plastic and metal roof coverings, a surface crack shall not be determined to be a failure. A crack that extends through the cross-section of the roof covering material layer shall be determined to be a failure.

7.4 Cosmetic damage in and of itself shall not be determined to be a failure. Cosmetic damage such as denting, damage not extending through the cross-sectional area of a roof covering material layer, crack of any paint finish, etc. shall not be determined to be a failure.

TESTING PROTOCOL

We utilize a modified version of ASTM D3746[2] for analyzing hail-caused impact damage and the methodology for delamination and desaturating the felts to evaluate the samples to determine whether there is damage. In general, the protocol includes the following:

1. Visually examining the top and bottom of the samples for evidence of impact damage to the surface of the roof. This would include evidence of spatter marks, denting, displaced granules or gravel, and evidence of crushed or cracked bitumen.
2. Delaminating the samples in general accordance with ASTM D2829[1] and visually examining the interply bitumen for evidence of denting, crushed interply, and/or fracturing of the reinforcement.
3. Desaturating the samples in general accordance with ASTM D3746[2] and visually examining the desaturated reinforcements for evidence of denting and fracturing of the reinforcement. It should be noted that some labs do not desaturate the samples and rely on the examination of the delaminated plies for evidence of fracturing. However, desaturation is part of the ASTM D3746 protocol and provides for a more reliable assessment of the reinforcement.
4. The samples are also examined under various magnifications, including 10-power magnification, at each step of the testing in general accordance with Susceptibility to Hail Damage Test Standard, Section 4.4.1.[7]

The following is an excerpt from a typical report describing our testing protocol.

Each of the six mineral granule surfaced modified bitumen roof membrane samples was logged, visually inspected under various magnifications and photographed top and bottom. The roof membrane samples were then delaminated, inspected, and photographed. The roof membrane samples were desaturated and evaluated in general accordance with ASTM D3746, Impact Resistance Analysis of Bituminous Roofing Systems. *Each individual ply was photographed top and bottom and visually inspected. Plies were examined under microscope at various magnifications. Any anomalies detected were photographed and recorded.*

Our intent is to visually document each step of the testing to provide transparency in our reporting. Each step of the testing protocol is photographed, including photographs of the front and back of the sample upon arrival, the individual plies after delamination, and the individual plies after desaturation, along with magnified views of points of interest. A diagram of the sample configuration in general accordance with ASTM D2829[1] is also provided.

ANALYSIS AND INTERPRETATION OF THE DATA

The next step is to analyze and interpret the data, which can be subjective. As noted earlier, the general guidelines included in ASTM D3746[2] are as follows:

Rate the impact damage which occurs in each ply in each of the four quadrants by assigning the number which most accurately describes the impact damage, as follows:

0 = no damage;
2 = dents, indentations only;
4 = any cracks or splits

We do not provide a rating analysis as described. Our reports document evidence of granule or gravel loss, denting of the surface and/or the reinforcement, cracks or splits in the reinforcement, and crushed bitumen at the point or points of interest. ASTM D3746 provides an unambiguous description of impact damage. Are the desaturated felts dented or fractured? No dents or fractures receive a rating of 0; dents receive a 2, and fractures receive a 4. The test method does not consider the surfacing or the interply bitumen for damage. The issues of what constitutes damage may become subjective, depending on the various definitions of damage—for example, the definition of damage included in an insurance policy.

It is important to consider that ASTM D3746 is designed to test and rate a bituminous roof sample for resistance to hail. Typically, the test samples used are from new construction and often prepared for the purpose of testing. In the case of these samples, the area of impact is known, and the impacted area can be analyzed and compared with the nonimpacted areas. This is not the case of test samples taken from existing roofs.

Existing bituminous roofs have been subjected to construction traffic; maintenance traffic; and, in many cases, years of weathering. Bituminous roofs are typically installed with heat (hot asphalt and torches) and are susceptible to foot and general construction traffic during the installation of the roof, particularly when the roof is hot. Anomalies from installation traffic are common to virtually all bituminous roofs, and these anomalies are often confused with impact damage from hail.

The intent of our ASTM D3746[2] testing was to provide clear visual examples of impact damage to bituminous roofs—that is, what hail-caused impact damage looks like on bituminous roofs.

ASTM D3746 TESTING

We performed ASTM D3746[2] testing on aged aggregate-surfaced fiberglass asphalt built-up roof samples and on new and aged granule-surfaced SBS modified bitumen roof samples. The built-up roofing samples were tested on insulated (relatively soft) and noninsulated (firm) substrates. The new granule-surfaced modified bitumen samples were tested on a firm substrate of 0.5 in. (13 mm) gypsum cover board and an insulated (relatively soft)

Figure 1. A test sample positioned on the platform.

Figure 2. A missile was dropped onto the approximate center of each of the four quadrants.

substrate. The aged granule-surfaced modified bitumen samples were tested on insulated and noninsulated substrates. ASTM D3746 uses a 2.0 in. (50 mm) diameter missile to replicate the impact energy of 2.0 in. hail. Many bituminous roof systems are resistant to 2.0 in. hail. The fundamental purpose of our testing was to replicate hail-caused damage. Therefore, we modified the missile size to replicate 2.5 in. (64 mm) hail and to develop 57.48 ft-lb of impact energy as defined by the National Bureau of Standards.[3]

The modified missile was 2.5 in. (64 mm) in diameter and 6 in. (152 mm) long, and weighed 7.67 lb (3.48 kg). A 24 × 24 in. (610 × 610 mm. testing table was constructed using two-by-fours placed on edge and bolted together in accordance with ASTM D3746. The test sample was placed on the testing table, and the missile was dropped from 87⅞ in. (2232 mm) onto the approximate center of each of the four quadrants. A test sample positioned on the platform is shown in **Fig. 1**.

A missile was dropped onto the approximate center of each of the four quadrants, as shown in **Fig. 2**.

Testing was performed on test samples taken from an aged aggregate-surfaced asphalt fiberglass built-up samples and from new and aged granule-surfaced SBS-modified bitumen samples. Each sample was examined and photographed in accordance with the our protocol described previously.

TEST RESULTS FROM AGGREGATE-SURFACED BUILT-UP ROOF SAMPLES

Evaluation of Surfacing at Impact Area

The test results related to surface damage were consistent. The impact from a 2.5 in. (64 mm) missile resulted in surface damage to the samples on both the insulated and noninsulated substrates. The results of the laboratory impact damage to the surface were compared with test samples of roofs that had been damaged by hail and to examples included in Haag Engineering's *Built-up Roofing: A Pictorial Guide*.[8] The test sample before the missile drop in shown in **Fig. 3**. The test sample after the missile drop and after the loose gravel was removed is shown in **Fig. 4**. The red arrows identify the area of impact in Fig. 4.

Figure 4. The test sample after the missile drop and after the loose gravel was removed.

Figure 3. The test sample before the missile drop.

Figure 5. The test sample after the missile drop showing crushed gravel at point of impact.

Figure 6. Localized crushing of the asphalt flood coating at the point of impact is shown in this 10-power photograph.

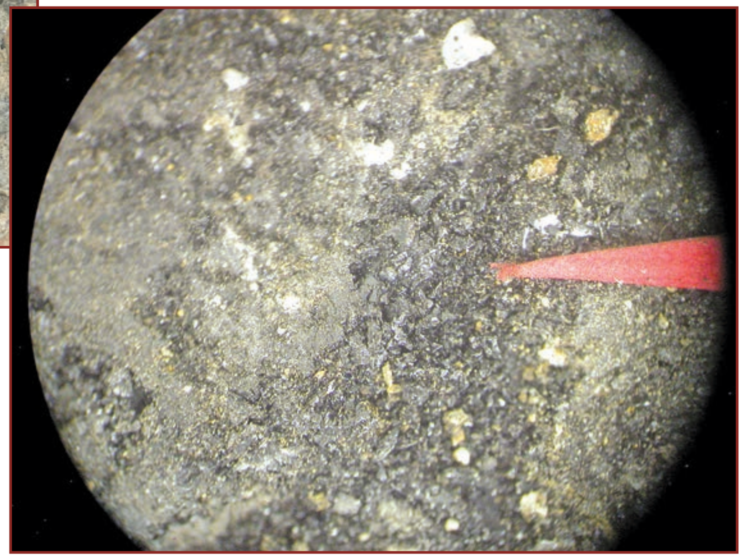

The areas of impact were very similar on all tests. There was a general displacement of the imbedded aggregate and exposure of the asphalt flood coat. The aggregate at the point of impact was crushed at some of the impacts (**Fig. 5**). In no case did the impact result in aggregate being driven into the sample, affecting the felts below. The crushed aggregate was likely the result of using a steel missile rather than an ice ball for testing, as hail typically shatters on impact and steel does not.

There was localized crushing of the asphalt flood coat at the point of impact, as shown in **Fig. 6**.

The area of impact in our simulated testing is also consistent with roof samples that we have tested from roofs damaged by hail. **Figure 7** shows a test sample taken from a roof that was damaged by hail. The meteorological and physical evidence indicated that the hail was in the 2.5 in. (64 mm) and larger range.

The surface damage occurring at each of the impact areas from our testing was consistent in appearance, was consistent with surface damage from actual hail observed in the field and in the laboratory, and was consistent with the photographs included in *Built-up Roofing: A Pictorial Guide*.[8] Our conclusion is that these illustrations of surface damage to aggregate-surfaced built-up roofs are representative of actual hail damage and can be used for comparative analysis.

Evaluation of Interply Bitumen—Insulated and Noninsulated Samples

There is no protocol for the evaluation of the interply bitumen in ASTM D3746.[2] The rating system protocol for evaluation of damage is limited to the desaturated felts. Therefore, crushed or disturbed interply is not a factor in the evaluation process of ASTM D3746. In the case of the noninsulated samples, there was no denting or cracking of the desaturated felts, so, based upon ASTM D3746, this roof would have been rated as having no hail-caused impact damage.

The sample was desaturated and the felts were evaluated using the rating protocol in ASTM D3746. Early on, the vast majority of our testing focused on ASTM D2829[1] and ASTM D3617.[9] Both standards were used to determine whether the roof system was installed in accordance with industry standards. These testing standards consisted of weighing and measuring the components of the roof and comparing the results to a recommendation or guideline, either a manufacturer's or the National Roofing Contractors

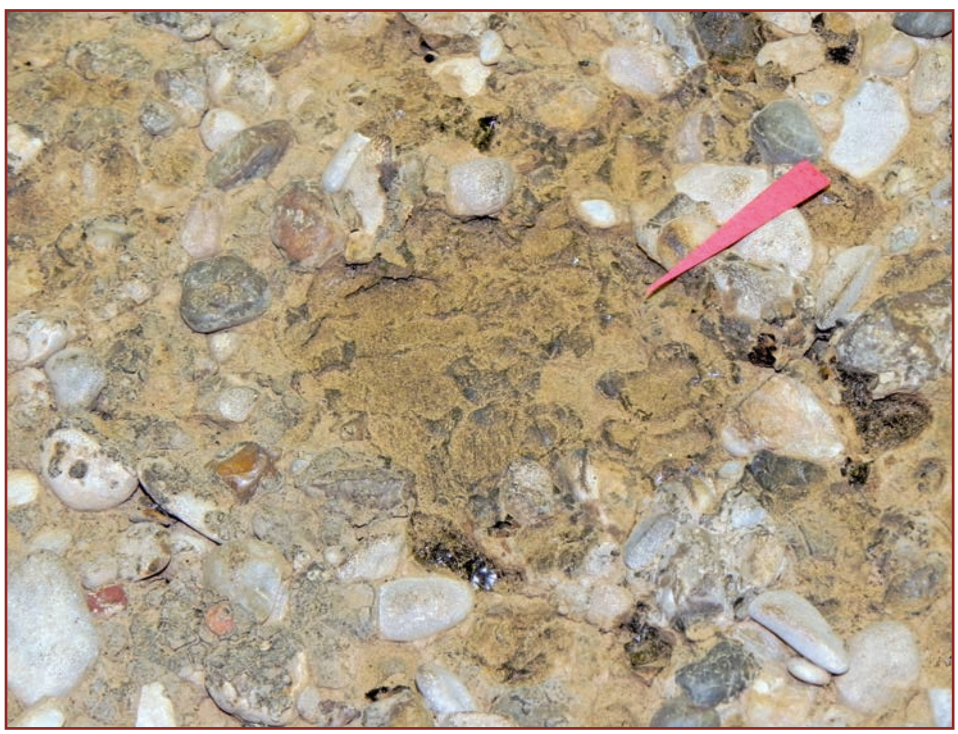

Figure 7. A test sample taken from a roof that was damaged by hail.

Figure 9. Close-up of impact 2 with no evidence of crushed or disturbed interply.

Figure 8. The back side of the top ply of felt, which was partial lap-ply.

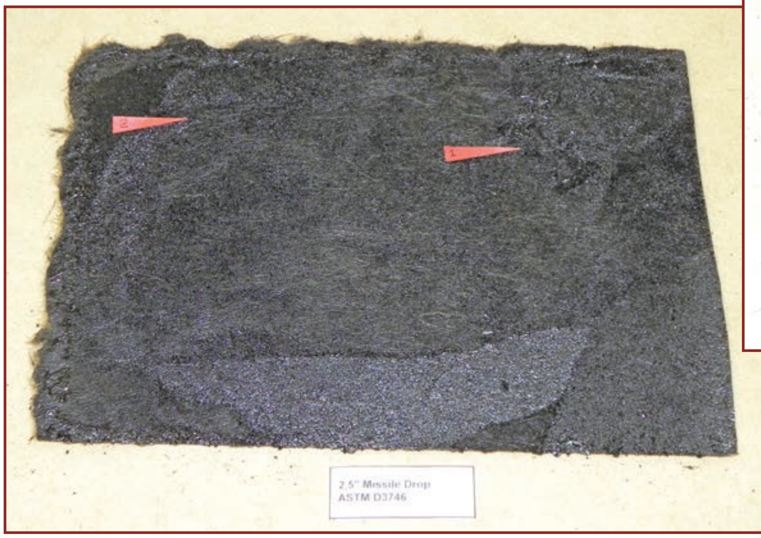

Association's. These tests were used for quality assurance or forensic purposes. Part of the protocol included the delaminating the felts to determine the lap-ply configuration. In addition, we examined the interply for evidence of voids or dry spots.

We began testing roof samples for evidence of hail damage in the 1980s. Our standard test protocol for evaluating hail damage utilized ASTM D2829 testing standards for removal of the samples, for preparation of the samples, and for delamination of the felts. The delaminated felts were then desaturated and evaluated using the ASTM D3746 protocol for assessment. On rare occasions, in the case of very large hail, we observed crushed interply asphalt between the plies and began including these observations in our reports. It should be noted that crushed interply was never observed in coal tar pitch samples, which is likely the result of the self-healing properties of coal tar pitch.

Observations regarding crushed or disturbed interply bitumen were included in our study. Our study was based on evaluating damage from 2.5 in. (64 mm) missiles representing very large hail. Crushed interply bitumen was observed at each area of impact on the insulated samples. Crushed interply was observed at some of the impact areas on the noninsulated samples. **Figure 8** shows the back side of the top ply of felt, which was partial lap-ply. The sample was only impacted by test drops 1 and 2. There was no evidence of crushed interply at this level within the sample.

Figure 9 shows a close up of impact 2 with no evidence of crushed or disturbed interply.

Figure 10 shows the impact area at 10-power with no evidence of crushed asphalt.

There was evidence of crushed interply in the lower layers of felt. **Figure 11** shows impact area 4 on the back of the first full ply.

Figure 12 shows impact area 4 at 10-power and the crushed interply asphalt at the point of impact.

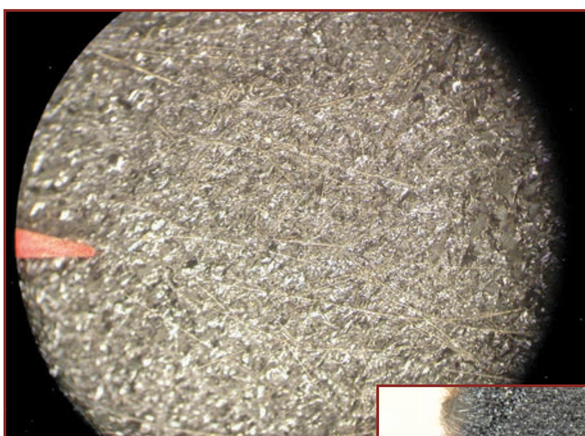

Figure 10. Impact area at 10-power with no evidence of crushed asphalt.

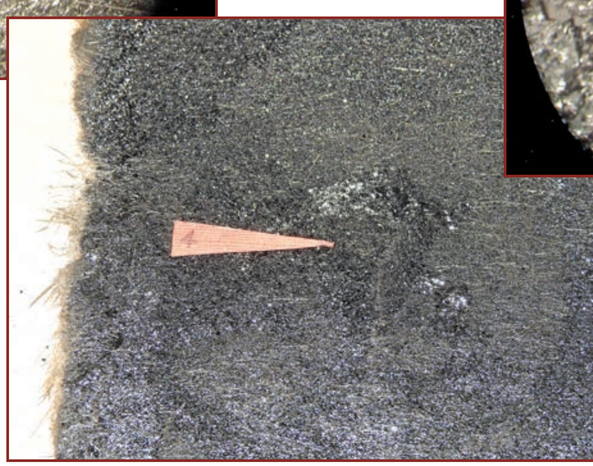

Figure 11. Impact area 4 on the back of the first full ply.

Figure 12. Impact area 4 at 10-power and the crushed interply asphalt at the point of impact.

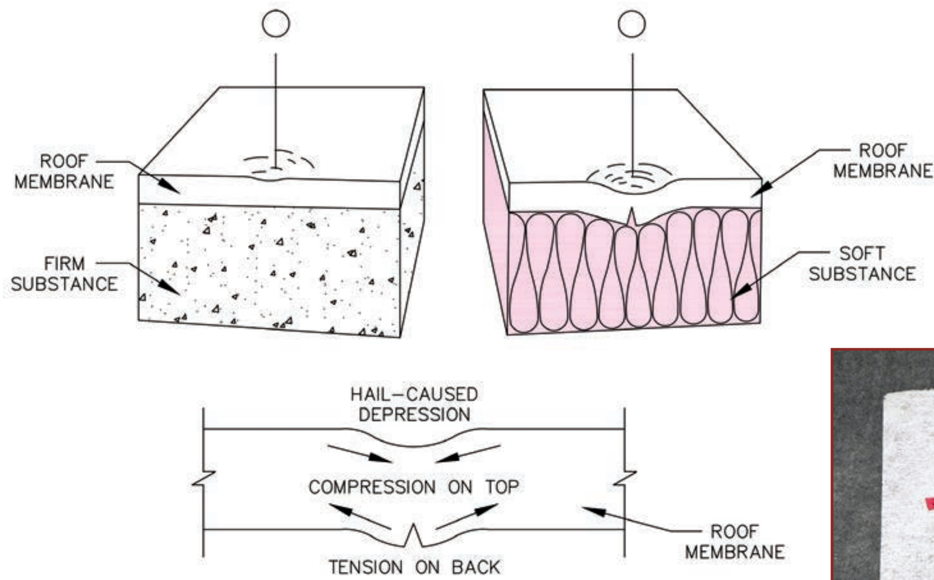

Figure 13. The softer substrate allows for more deflection in the membrane, resulting in tension in the bottom layers of the felts. Figure: Adapted from Haag Engineering's **Built-up Roofing: A Pictorial Guide.**

Figure 15. Bottom full ply with impact fractures identified by red arrows.

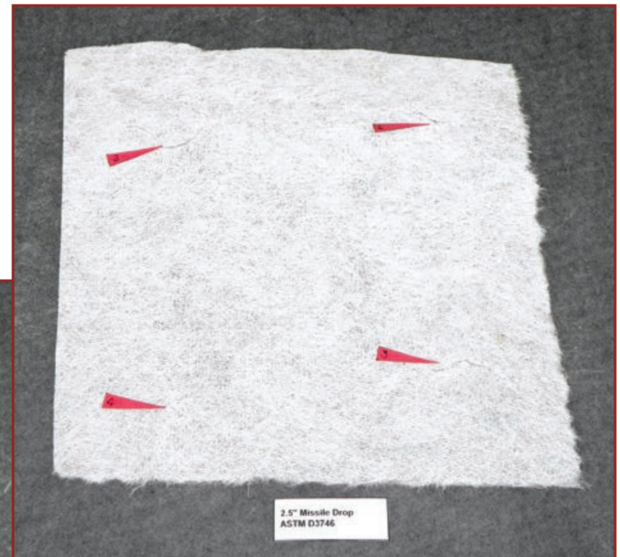

Figure 14. Desaturated bottom ply of felt in the noninsulated (firm substrate) sample.

The crushed interply in our simulated testing was also consistent with roof samples we have tested from roofs damaged by hail. One example is a roof designed by us that was approximately 15 years old at the time of the event. The hail was in the 2.5 in. (64 mm) and larger range.

There was evidence of crushed interply in all of the areas of impact on the insulated samples. There was evidence of crushed interply in some of the areas of impact on the noninsulated samples. In general, the softer the substrate (typically insulated), the more susceptible the roof is to hail damage. Crushing of the interply may also be a function of the thickness of the asphalt. The crushed interply bitumen occurring at each of the impact areas from our testing was consistent in appearance and was also consistent with crushed interply bitumen from actual hail observed in the field and laboratory.

Evaluation of Desaturated Felts—Insulated and Noninsulated Samples

The protocol for evaluating hail-caused impact damage to desaturated felts is clearly defined as dents or cracks or splits (fractures) in ASTM D3746.[2] The desaturated felts were examined for evidence of damage at each of the four impact areas. The results of the laboratory impact damage to the surface were compared with our test samples of roofs that had been damaged by hail and to examples included in Haag Engineering's *Built-up Roofing: A Pictorial Guide*.[8]

Our study showed that there were fractures in the felts at each of the impact areas on the insulated samples, but there were no fractures in the felts at each of the impact areas on the noninsulated samples. There were no dents or indentations in the felts in any of the impact areas. The denting criterion is probably a holdover from testing on organic or asbestos felts, as it has been our experience that hail impact does not typically result in dents in fiberglass felts. Dents and other anomalies in the top layer of felt commonly occur as a result of construction traffic during installation, particularly from loose aggregate stepped on during construction before the flood coat has been applied.

Our test results confirm the importance of the substrate in the hail resistance of bituminous roofs. In general, the softer the substrate (typically insulated), the more susceptible the roof is to hail damage. Impact from very large hail can cause localized deflection in the membrane at the point of impact. **Figure 13** illustrates how the softer substrate allows for more deflection in the membrane, resulting in tension in the bottom layers of the felts.

Figure 14 shows the desaturated bottom ply of felt in the noninsulated (firm substrate) sample. The tension is greatest in the bottom ply, so the bottom ply is the most likely ply to fracture. The tension in the felt was limited by the firm substrate, and there was no fracturing. Also, there was no denting in the fiberglass felts on the insulated and noninsulated sample.

There were fractures at all impact areas in the insulated sample. **Figure 15** shows the bottom full ply with impact fractures identified with the red arrows.

Figure 16 shows a magnified view of the fracture in the felt at impact area 3.

The fractures at the areas of impact in our simulated testing are also consistent with roof

Figure 16. Magnified view of the fracture in the felt at impact area 3.

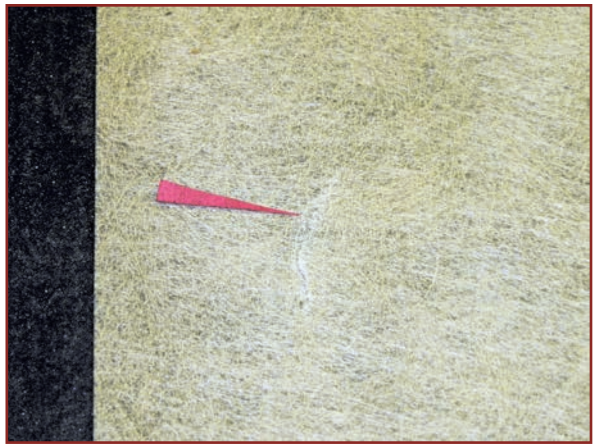

Figure 17. Fractured felts in a test sample from a roof that was damaged by hail.

samples we have tested from roofs damaged by hail. **Figure 17** shows fractured felts in a test sample from a roof that was damaged by hail. This was a roof that was designed by us and was approximately 15 years at the time of the hail event. The hail was in the 2.5 in. (64 mm) and larger range.

The area of impact in our simulated testing is also consistent with the hail-caused impacts illustrated in reference 8.

There was no evidence of fracturing in the desaturated felts in the noninsulated sample. The was evidence of fractured felts at all of the areas of impact on the insulated samples. There was no evidence of denting in the insulated or noninsulated samples. The fractured felts occurring at the impact areas from our testing were consistent with fractures occurring as a result of actual hail and consistent with published literature.[8]

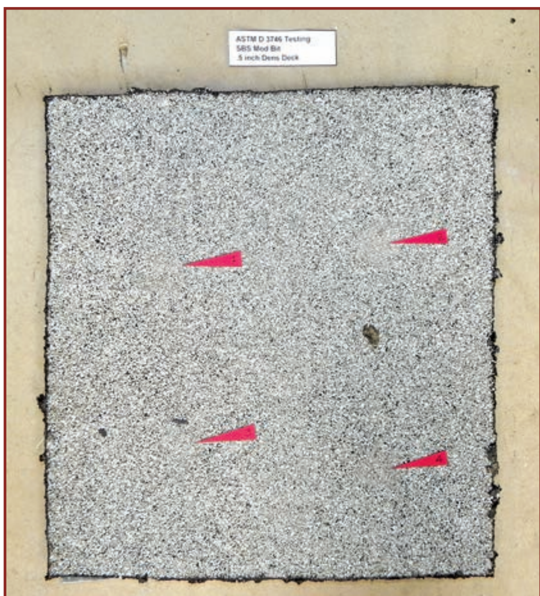

Figure 18. The new modified bitumen sample on noninsulated substrate after the sample was impacted by the four missile drops.

TEST RESULTS FROM NEW GRANULE-SURFACED SBS MODIFIED BITUMEN ROOF SAMPLES

Evaluation of Surfacing at Impact Area

The test results related to surface damage to the granule-surfaced modified bitumen samples varied. There was very little evidence of displaced granules on the new samples on insulated or noninsulated substrates. It should be noted that the noninsulated samples were supported by 0.50 in. (13 mm) gypsum cover board, which was not as firm as the wood test table but is considered to be a firm substrate. The insulated samples were supported by 0.75 in. (19 mm) perlite, which is considered to be a soft substrate. The samples were positioned and impacted as described in the protocol for the aggregate-covered built-up roofs.

Figure 18 shows the new modified bitumen sample on noninsulated substrate after the sample was impacted by the four missile drops.

Figure 19 shows a closer view of impact area 1. There is a slight difference in the color of the granules.

Figure 20 shows a 10-power view of impact area 1. There are no discernible displaced granules. The change in color is the result of localized crushing of the granules at the point of impact.

Figure 21 shows a 10-power view of a typical

Figure 20. 10-power view of impact area 1. There are no discernible displaced granules. The change in color is the result of localized crushing of the granules at the point of impact.

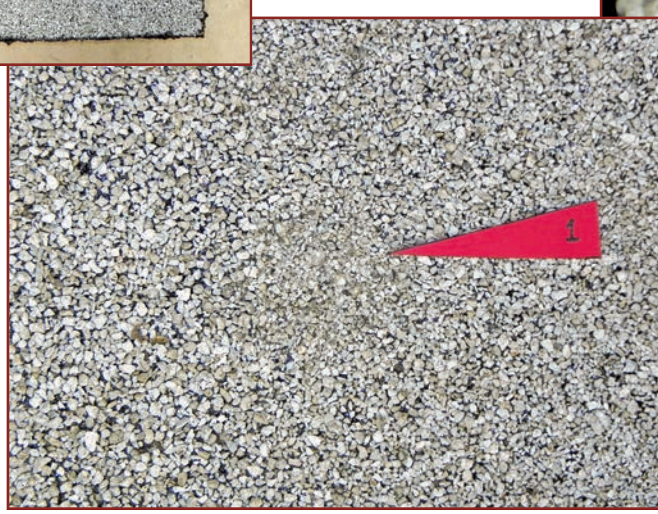

Figure 19. A closer view of impact area 1. There is a slight difference in the color of the granules.

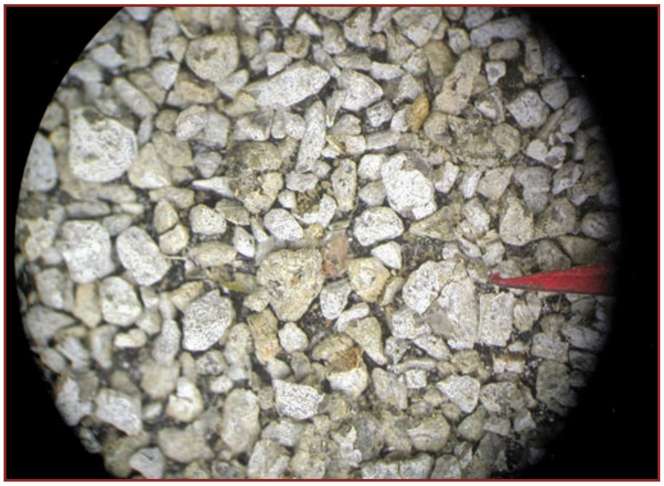

Figure 21. 10-power view of a typical impact area on the insulated sample. There are no discernaile displaced granules. There is no evidence of localized crushed granules on the insulated samples.

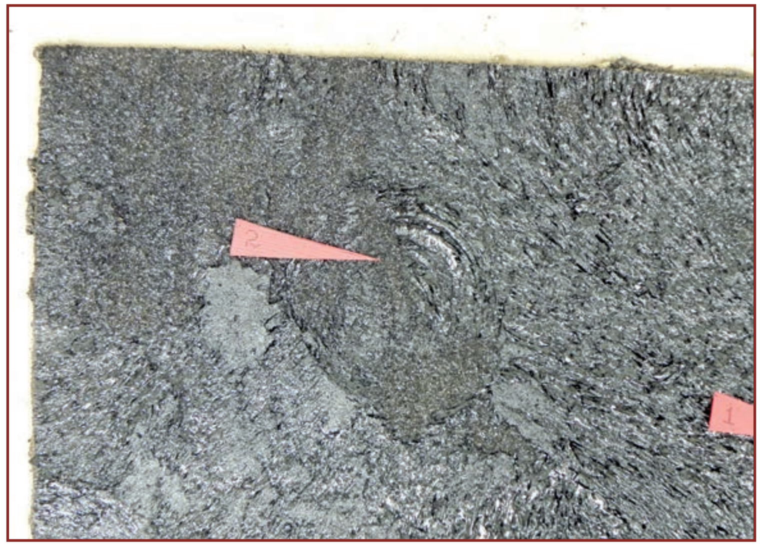

Figure 22. Example of crushed interply on the insulated sample.

impact area on the insulated sample. There are no discernible displaced granules. There is no evidence of localized crushed granules on the insulated samples.

The area of impacts on the new modified bitumen exhibited no displaced granules. The crushed granules were likely the result of the steel missile and were unlikely to occur on simulated ice balls or natural hail. We have observed similar results on newer installations that were impacted by large hail. The adhesion of the granules on new SBS modified bitumen roofs is generally very good and limited or no granule loss may occur on newer installations of modified bitumen roofs. The crushed granules may weather away over time and result in an area of localized granule loss, but this was not verified.

Evaluation of Interply Bitumen—Insulated and Noninsulated Samples

As stated previously, there is no protocol for the evaluation of the interply bitumen in ASTM D3746.[2] However, the interply bitumen was examined on the modified bitumen samples. Crushed interply bitumen was observed on the insulated sample but not on the noninsulated sample. The lack of crushed interply is possibly the result of the quantity of interply asphalt. It has been our experience that thicker applications of interply asphalt are more prone to crushed interply. **Figure 22** shows an example of crushed interply on the insulated sample.

There was evidence of crushed interply in all of the areas of impact on the insulated samples. There was no evidence of crushed interply in the areas of impact on the noninsulated samples. In general, the softer the substrate (typically insulated), the more susceptible the roof is to hail damage. Crushing of the interply may also a function of the thickness of the asphalt. The crushed interply bitumen occurring at each of the impact areas from our testing was consistent with crushed interply bitumen from actual hail observed in the field and laboratory.

Evaluation of Reinforcement—Insulated and Noninsulated Samples

The modified bitumen membrane had a dual-carrier mat with a combination of polyester and fiberglass reinforcement. **Figure 23** shows the dual-carrier mat with no fractures or denting.

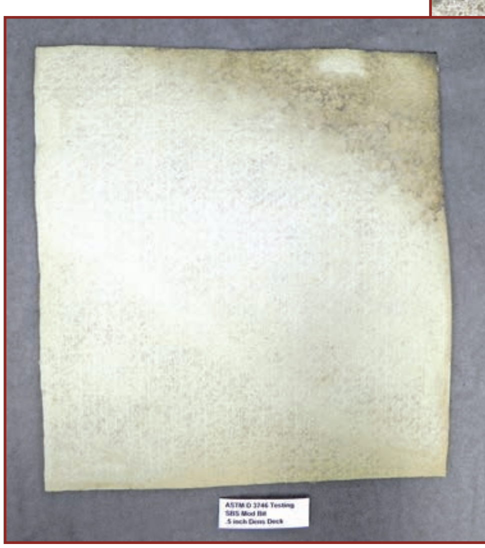

Figure 23. Dual-carrier mat with no fractures or denting.

The second ply was fiberglass asphalt felt. There were fractures in the fiberglass felt at all four missile drops on both the insulated and noninsulated samples. In should be noted that there was a depression at the area of impact in the gypsum cover board, which resulted in more tension in the bottom ply than the built-up samples on the wood testing table. **Figure 24** shows a fracture in the bottom ply (fiberglass felt) on the noninsulated sample. The fractures on the insulated samples were more pronounced than on the noninsulated samples.

The fractured felts occurring at the impact

Figure 24. Fracture in the bottom ply (fiberglass felt) on the noninsulated sample.

areas from our testing were with fractures occurring as a result of actual hail, and consistent with published literature.[8]

Figure 25. Aged modified bitumen roof on the noninsulated substrate after the sample was impacted by the four missile drops.

TEST RESULTS FROM AGED GRANULE-SURFACED SBS MODIFIED BITUMEN ROOF SAMPLE

Evaluation of Surfacing at Impact Area—Noninsulated Substrate

The aged modified bitumen sample was only tested over a noninsulated (wood) substrate. The exact age of the sample is unknown but is believed to be at least 10 years old.

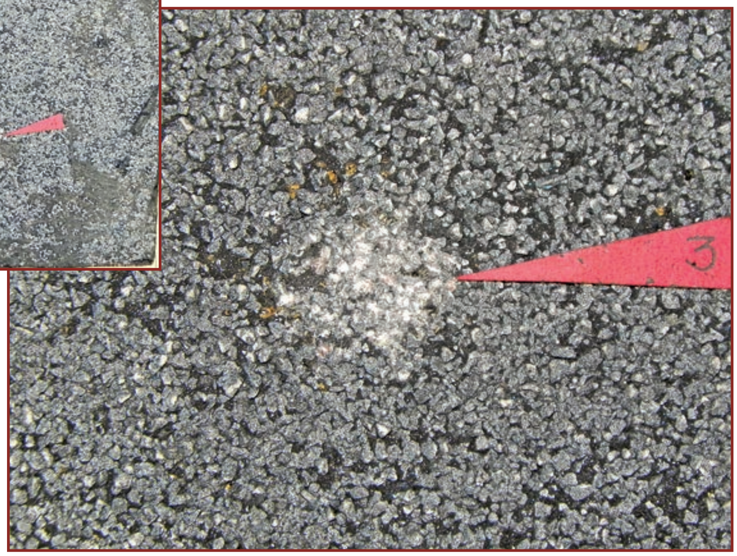

Figure 26. Close-up of impact area 3.

The test results related to surface damage to the granule-surfaced modified bitumen samples were similar to results for the noninsulated new modified bitumen sample, with the exception that there was some granule displacement at the point of impact on the aged sample. **Figure 25** shows the aged modified bitumen roof on the noninsulated substrate after the sample was impacted by the four missile drops.

Figure 26 shows a close-up of impact area 3. There are crushed granules similar to the crushed granules on the new modified bitumen sample on the firm substrate as well as some granule displacement not evident in the sample of the new roof.

Figure 27 shows a 10-power view of impact area 3.

Figure 28 shows a close up of impact area 4. There are crushed and displaced granules. Exposed reinforcement is also visible.

Figure 29 shows impact area 4 at 10-power. The area of impacts on the aged modified bitumen exhibited crushed granules and some displaced granules. It is possible that additional granule loss would occur over time if the sample were exposed to normal weathering.

Figure 27. 10-power view of impact area 3.

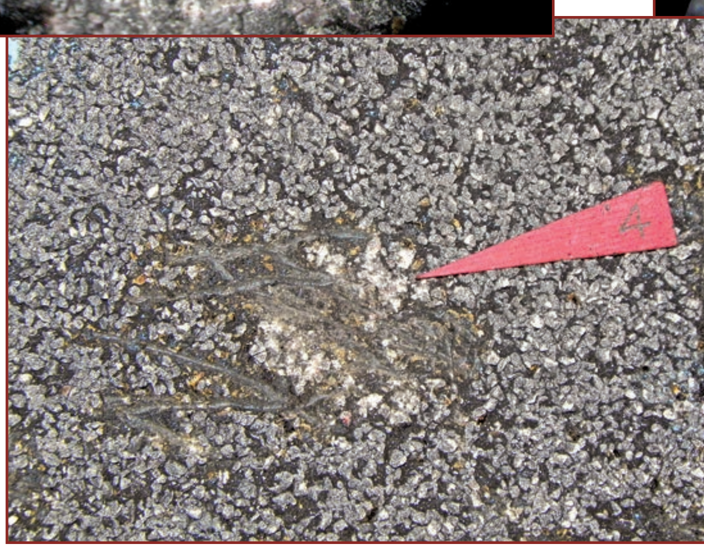

Figure 29. Impact area 4 at 10-power.

Figure 28. Close-up of impact area 4.

Figure 30. An example of localized granule loss on an aged modified bitumen roof.

Figure 31. A closer view of the hail-caused granule loss on the same project as Fig. 30.

We have observed localized granule loss at impacts from actual hail on aged modified bitumen roofs. **Figure 30** shows an example of localized granule loss on an aged modified bitumen roof. The pattern of granule loss was consistent with the random distribution of the large hail that fell and matched the pattern of the larger hail-caused impacts on the air-conditioning units and larger spatter marks.

Figure 31 shows a closer view of the hail-caused granule loss on the same project.

Figure 32 shows the impact at 10-power. There are visible fractures in the surface at the point of impact. Also, note that the surface of the exposed modified bitumen is relatively smooth. There is no evidence of shrinkage cracking or oxidized bitumen typically seen on older modified bitumen roofs.

Figure 33 shows a test sample from a modified bitumen roof with an area of localized granule loss at the point of interest noted. This type localized granule loss is also often confused with localized granule loss from hail impact. In some cases, a close examination of the area of granule loss will exhibit signs of weathering, as shown in Fig. 33, indicating that the granules loss occurred prior of the hail event.

Figure 34 shows a closer view of the point of interest. There is evidence of shrinkage cracking in the surface. There is localized granule loss in areas where the shrinkage cracking has converged. The point of interest is the largest area of localized granule loss visible on the sample.

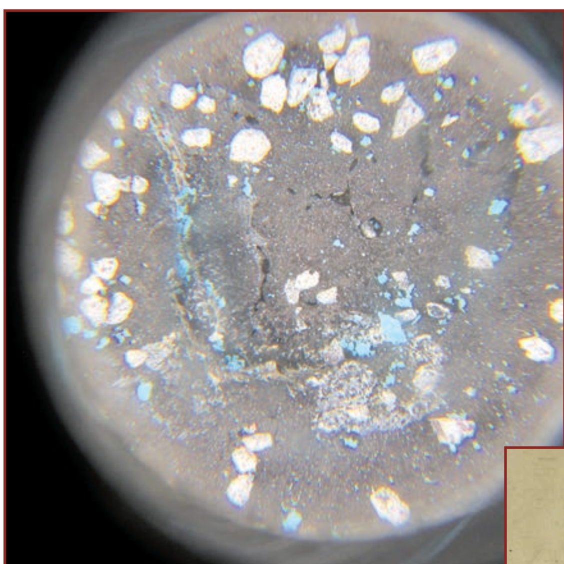

Figure 32. Impact at 10-power.

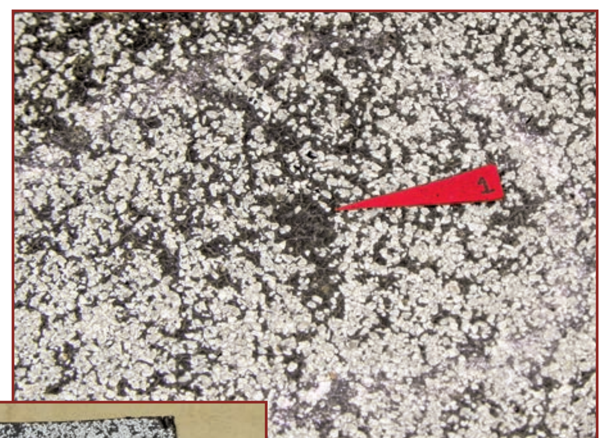

Figure 34. A closer view of the point of interest.

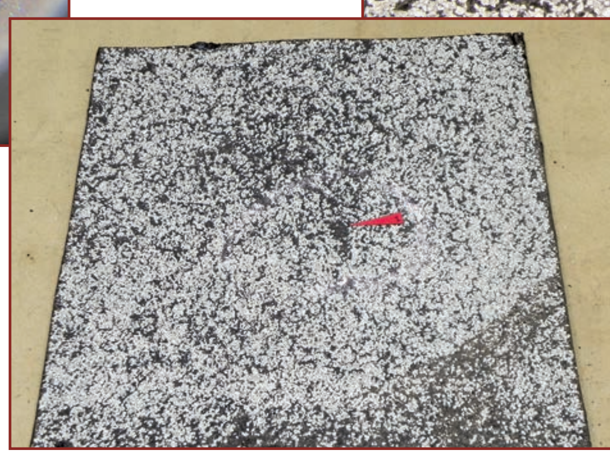

Figure 33. Test sample from a modified bitumen roof with an area of localized granule loss at the point of interest noted.

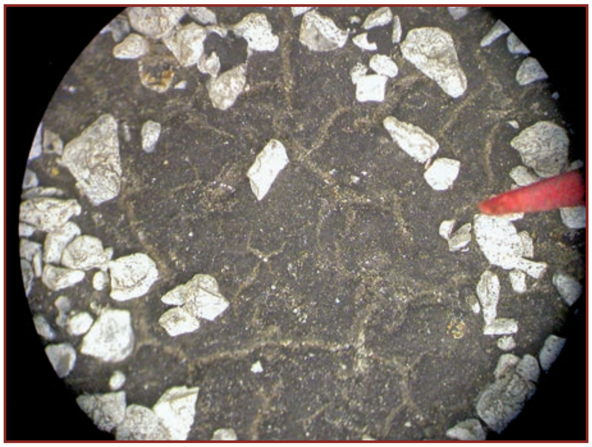

Figure 35. Point of interest at 10-power.

Figure 35 shows the point of interest at 10-power. The oxidized modified bitumen and shrinkage cracking in the modified bitumen surfacing are visible. There is no evidence of impact damage to the surface, and there were no fractures of crushed interply below the point of impact. There was no evidence of any other damage to the sample consistent with hail-caused impact. This type localized granule loss is often confused with granule loss from hail-caused impact.

Another type of localized granule loss is related to contaminants such as bird droppings. This type of localized area of granule loss tends to be in specific areas where birds congregate, as shown in **Fig. 36**. This type of localized granule loss is often confused with granule loss from hail-caused impact.

Figure 37 shows a closer view of granule loss of localized granule loss occurring as a result of contaminants from bird droppings.

Figure 38 shows the progression of granule loss occurring as a result of the bird droppings. Remnants of the bird droppings are visible. The granules typically continue to come off over time.

Figure 39 shows the progression of granule loss from small semicircular areas of granule loss to complete circular granule loss.

The surface damage occurring as a result of our impact testing of the granule-surfaced modified bitumen ranged from no displaced or crushed granules on the new modified bitumen on insulated (soft) substrate to crushed granules on firm substrates with no discernible granule loss. This is consistent with field observations on relatively new modified bitumen roofs that were impacted by large hail.

The aged modified bitumen sample tested on a firm substrate resulted in crushed granules and some displaced granules. The displaced granule loss observed on the aged sample tested was not as pronounced as observations of granule loss on aged modified bitumen roofs impacted by large hail. The age and degree of surface deterioration are likely contributing factors, as well as the angle of strike from actual hail.

Evaluation of Interply Bitumen—Noninsulated Samples

The interply bitumen was examined on the modified bitumen samples. Crushed interply bitumen was observed on the sample at all four areas of impact.

Figure 36. Localized areas of granule loss tend to be in specific areas where birds congregate.

Figure 37. A closer view of granule loss of localized granule loss occurring as a result of contaminants from bird droppings.

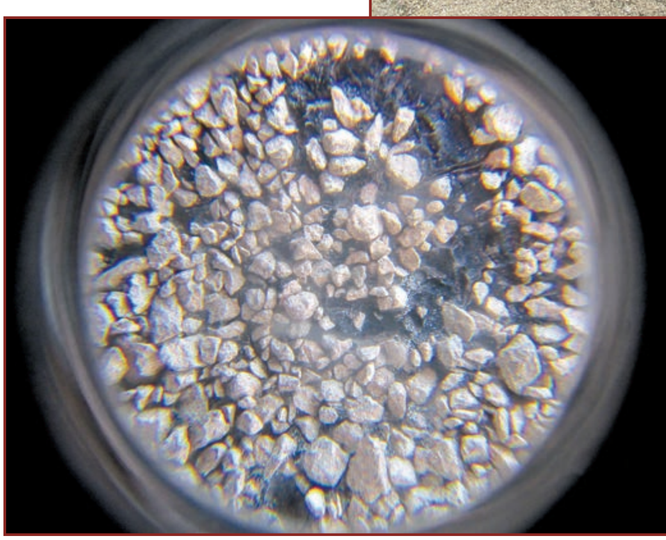

Figure 38. Progression of granule loss occurring as a result of the bird droppings.

Figure 39. Progression of granule loss from small semicircular areas of granule loss to complete circular granule loss.

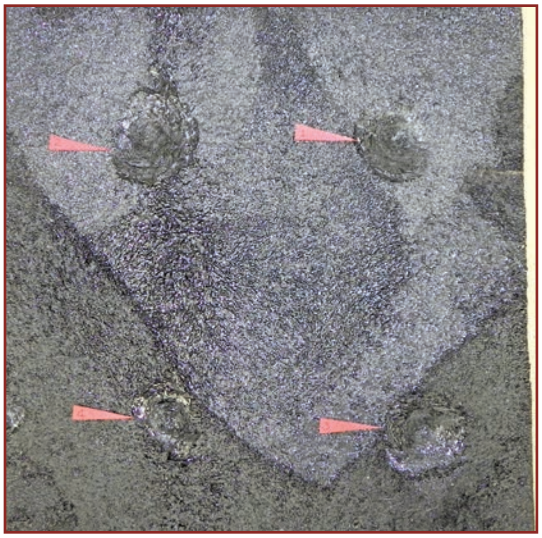

Figure 40. An example of crushed interply on the insulated sample.

Figure 40 shows an example of crushed interply on the insulated sample.

There was evidence of crushed interply in all of the areas of impact on the samples. The crushed interply bitumen occurring at each of the impact areas from our testing was consistent in appearance and was also consistent with crushed interply bitumen from actual hail observed in the field and laboratory.

Evaluation of Reinforcement—Noninsulated Substrate

The membrane was a fiberglass-reinforced modified bitumen installed over two plies of glass felt. There was no denting or fracturing of the modified bitumen reinforcement. There were fractures in the bottom ply at all four impact areas. **Figure 41** shows the fractured bottom ply of the membrane. The fractures were small and difficult to see without desaturating the felts.

Figure 41. Fractured bottom ply of the membrane.

The testing results of the aged modified bitumen sample were consistent with the testing of the new modified bitumen samples, with the exception that there was discernible granule displacement on the aged modified bitumen sample.

DISCUSSION

The use of highly magnified photographs of samples and particularly desaturated felts and reinforcements to demonstrate damage has become increasingly prevalent. By way of demonstration, We performed desaturation on a new roll of Type IV fiberglass felt. A 12 × 12 in. (305 × 305 mm) sample was removed and placed on a light table, illustrating the normal holes in the new felt, as shown in **Fig. 42**.

Figure 43 shows the portion of the felt in the red box (test area) of Fig. 42 at a magnification showing the normal holes in a typical fiberglass felt.

Figure 44 shows the desaturated test area. The individual fibers can be seen. We have seen an increasing number of this type of photograph, which is represented as evidence of hail-caused damage to bituminous roofs. The holes like the one circled in red are often represented as being the result of hail impact. Anomalies resulting from construction or maintenance damage are also often represented as evidence of hail-caused damage. It is important to distinguish normal surface anomalies and normal holes in felts from actual hail-caused impact damage.

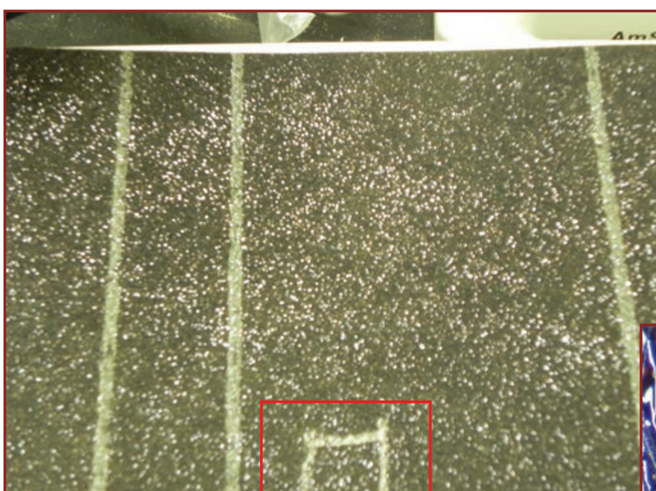

Figure 42. A 12 × 12 in. sample was removed and placed on a light table illustrating the normal holes in the new felt. Note: 1 in. = 25.4 mm.

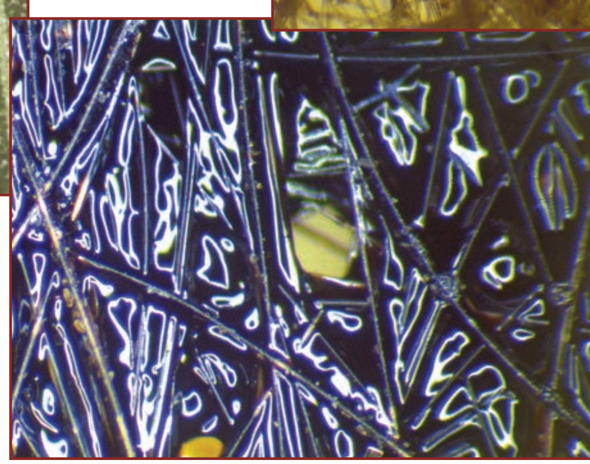

Figure 43. The portion of the felt shown in the red box (test area) of Fig. 42 taken at magnification showing the normal holes in a typical fiberglass felt.

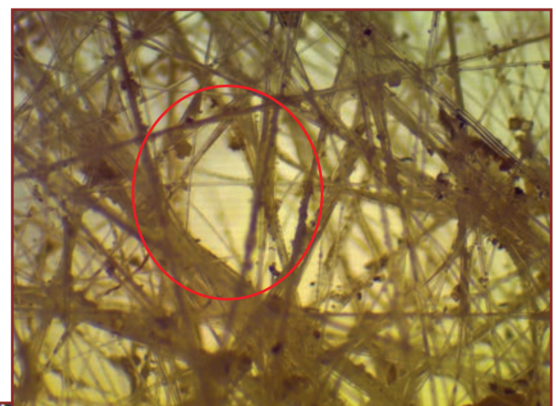

Figure 44. Desaturated test area.

CONCLUSION

The use of the assessment protocol in ASTM D3746[2] is an appropriate method for evaluating impact damage to the reinforcements of bituminous roofs. The assessment protocol in ASTM D3746 does not address impact to the surfacing of the sample or to the interply bitumen. The results of our testing utilizing ASTM D3746 impact testing protocol to simulate hail-caused impact damage provide a graphic example of what hail-caused damage looks like. The results of our testing were consistent with observations and testing of bituminous roofs that have been damaged by hail, are consistent with the research performed by Haag Engineering,[8] and are consistent with testing reports by others that we have reviewed over the years.

Hail-caused impact damage has a specific signature, as demonstrated by this testing, and the results of this testing provide a graphic comparative standard for hail-caused damage to bituminous roofs. The results of this testing provide a way to distinguish actual hail-caused damage to bituminous roofs from normal anomalies common on bituminous roofs, including construction traffic, maintenance traffic, and contaminants. Most bituminous roofs are resistant to 1.5 in. (38 mm) hail, and many are resistant to 2.0 in. (50 mm) or larger hail, so it takes large hail to damage this type of roof. We are continuing to research different types of roofing to provide standards for assessing hail-caused damage on various combinations of roofing.

There are a variety of testing standards that provide protocols for addressing hail-caused impact. Unfortunately, there is no specific ASTM test method for evaluating hail damage to existing roof systems. The lack of a specific standard has led to confusion in the industry and the use of widely varying in test methods for analyzing hail-caused impact damage. A new ASTM test standard that specifically addresses testing for hail-caused impact damage to existing roofs would help eliminate the confusion in the industry and provide more consistent testing and analysis.

REFERENCES

1. ASTM International. 2019. *Standard Practice for Sampling and Analysis of Existing Built-Up Roof Systems.* ASTM D2829M-07(2019)e1 West Conshohocken, PA: ASTM International.
2. ASTM International. 2015, *Standard Test Method for Impact Resistance of Bituminous Roofing Systems.* ASTM D3746M-85 (2015)e1 West Conshohocken, PA: ASTM International.
3. Factory Mutual Insurance Company (FMIC). 2012. *Single-Ply, Polymer-Modified Bitumen Sheet, Built-Up Roof (BUR) and Liquid Applied Roof Assemblies for use in Class 1 and Noncombustible Roof Deck Construction.* FM Class Number 4470. Johnson, RI: FMIC.
4. FMIC. 2002. *Single-Ply, Polymer-Modified Bitumen Sheet, Built-Up Roof (BUR) and Liquid Applied Roof Assemblies for use in Class 1 and Noncombustible Roof Deck Construction.* FM Class Number 4470. Johnson, RI: FMIC.
5. FMIC. 2005. *Impact Resistance Testing of Rigid Roofing Materials by Impacting with Freezer Ice Balls.* ANSI FM 4473. Johnson, RI: FMIC.
6. Underwriters Laboratories (UL). 2020. *Standard for Safety—Impact Resistance of Prepared Roof Covering Materials.* UL 2218. Northbrook, IL: UL.
7. FM Approvals. 2010. *Approval Standard for Class 1 Roof Covers Appendix 7: Susceptibility to Hail Damage Test Standard.* Norwood, MA: FM Approvals.
8. Haag Engineering Co. 2004. *Built-up Roofing: A Pictorial Guide.*
9. ASTM International. 2017. *Standard Practice for Sampling and Analysis of Built-Up Roof Systems During Application*, ASTM D3617. West Conshohocken, PA: ASTM.

"To Be or Not To Be": A Case Study of the Wind Impact Analysis of an Aged Curtainwall

Mallory Buckley, EIT, RRO

Walter P Moore | Dallas, TX

mbuckley@walterpmoore.com

Kimani Augustine, PE

Walter P Moore | Houston, TX

kaugustine@walterpmoore.com

IIBEC 2022 - Building for the Future

International Convention and Trade Show

March 17–22, 2022 | Orlando, FL

ABSTRACT

As extreme weather events are becoming both more frequent and intense, essential facilities face a dual threat of increased wind pressures and airborne debris impacts, particularly at facilities with glazed curtainwall systems. Furthermore, the structural and waterproofing elements of these curtainwalls may have experienced age-related deterioration. This case study considers an existing medical office building with a 1960s curtainwall system. Investigators evaluated whether it could accommodate current code-level wind pressure impacts, and the evaluation was used to develop conceptual schemes to implement hardening retrofits or other appropriate restoration options that would better allow the facility to functionally remain operational during extreme weather wind events. The presentation addresses building codes and industry consensus standards used during this evaluation such as ASCE 7-16, *Minimum Design Loads and Associated Criteria for Buildings and Other Structures*, and ASTM E1996, *Standard Specification for Performance of Exterior Windows, Curtain Walls, Doors, and Impact Protective Systems Impacted by Windborne Debris in Hurricanes.* Particular focus will be placed on current technologies to both understand and improve the resiliency and sustainability of existing curtainwall systems.

SPEAKERS

Mallory Buckley, EIT, RRO

Walter P Moore | Dallas, TX

Mallory Buckley is an associate in Walter P Moore's Diagnostics Group in Dallas, Texas. Her experience focuses on the field of building enclosure consulting, and her areas of expertise include assessing and designing repairs for distress conditions related to facade systems, building enclosure moisture management, roofing systems, and below-grade waterproofing on concrete substrates. Her portfolio includes developing work scopes, repair details, repair procedures, and technical specifications for waterproofing, restoration, and rehabilitation projects.

Kimani Augustine, PE

Walter P Moore | Houston, TX

Kimani Augustine is a principal in Walter P Moore's Diagnostics Group in Houston, Texas. He has been in the engineering industry since 2004 and has experience in diversified aspects of enclosure diagnostics consulting, including managing a wide variety of building enclosure projects and preparing design documents to address identified distress conditions. Augustine is a leader in Walter P Moore's Enclosure Diagnostics Practice, which is dedicated to developing step-by-step processes for finding solutions to building enclosure issues. He is on the board of the IIBEC Gulf Coast Chapter, where he actively serves to enhance building enclosure knowledge in the Houston area.

Nonpresenting Coauthor

Lukas Hayter, EIT

Lukas Hayter is an associate in Walter P Moore's Diagnostics Group in Washington, DC.

“To Be or Not To Be”: A Case Study of the Wind Impact Analysis of an Aged Curtainwall

Buildings with aged exterior wall systems are vulnerable to impacts from extreme weather events. Aged exterior wall systems on essential facilities are particularly problematic because damage to the wall system may disrupt ongoing operations at times when it critical for these facilities to remain fully functional to serve their affected communities. There are numerous essential facilities across the United States with curtainwall systems that have been in service for more than 50 years, and many of those systems have not been proactively maintained. Furthermore, the structural and waterproofing components of these curtainwalls have experienced age-related deterioration over time.

As extreme weather events are becoming both more frequent and intense, facilities with aged curtainwall systems may be exposed to a dual threat from increased wind forces and wind-borne debris damage. The case study presented in this paper focuses on the evaluation of an existing medical office building with a 1960s curtainwall system in Houston, Texas. We assessed the vulnerabilities of the curtainwall based on current code wind pressures and wind-borne debris during a high-wind event. Then, we studied conceptual schemes to implement hardening retrofits or other appropriate restoration options that would better allow the facility to remain operational during extreme weather events. Industry consensus standards referenced by the building code used during this evaluation include the American Society for Civil Engineers' *Minimum Design Loads and Associated Criteria for Buildings and Other Structures* (ASCE/SEI 7-16),[1] the National Council of Structural Engineers Associations' 2018 *NCSEA Engineering Structural Glass Design Guide*,[2] and the ASTM International's *Standard Specification for Performance of Exterior Windows, Curtain Walls, Doors, and Impact Protective Systems Impacted by Windborne Debris in Hurricanes* (ASTM E1996).[3] In this study, we emphasize current technologies to both understand and enhance the resiliency and sustainability of existing curtainwall systems.

RECENT EXTREME WEATHER EVENT TRENDS

This paper focuses on curtainwall systems in hurricane-prone regions, which are defined in the 2018 *International Building Code* (IBC)[4] as the U.S. Atlantic Ocean and Gulf of Mexico coasts where the ultimate design wind speed is greater than 115 mph for Category II buildings. According to the National Oceanic and Atmospheric Administration (NOAA),[5] in the Southern region of the United States (Louisiana, Mississippi, and Texas), there were 4523 severe weather reports (394 tornado reports, 1310 hail reports, and 2819 wind reports) in 2020. In the Southeast region (Alabama, Georgia, Florida, North Carolina, South Carolina, and Virginia), NOAA reports that there were 3843 severe weather reports during 2020; that was more than 130% of the median annual frequency of 2936 reports during 2000–2019. Strong thunderstorm winds accounted for 85% (3256 of 3843) of the severe weather reports and caused at least 10 fatalities and 34 injuries across the Southeast region.[5]

Looking at the trends for weather events for the United States as a whole, NOAA weather data collected from 1960 to 2010[6] demonstrate a positive trend of increased precipitation (**Fig. 1**). Overall, the NOAA data[6] regarding landfalling tropical storm extremes show a varying spread from 1910 to 2020 (**Fig. 2**). The tropical storm data also show isolated upticks in tropical storm events around 1995 and 2020 compared with the average across the 20th century.

The Federal Emergency Management Agency (FEMA)[7] published a map recognizing specific areas of the United States prone to high-wind events, including hurricanes (**Fig. 3**). The map highlights the Southern and Eastern coasts as hurricane-prone regions and also shows other areas scattered throughout the United States that are prone to wind events.

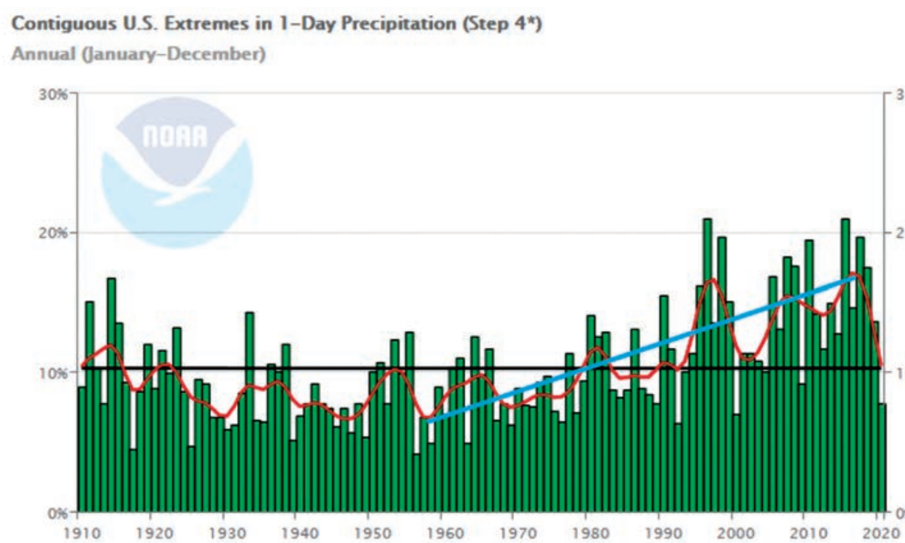

Figure 1. Precipitation extremes in the United States from 1910 to 2020. The index is calculated as the arithmetic average of values from a specified set of extreme events, weighted by the percent area that experienced the defined conditions. The long-term variation or change of this index represents the tendency for extremes of climate to either decrease, increase, or remain the same. Figure: National Oceanic and Atmospheric Administration. n.d. "U.S. Climate Extremes Index." Accessed October 6, 2021. https://www.ncdc.noaa.gov/extremes/cei/graph.

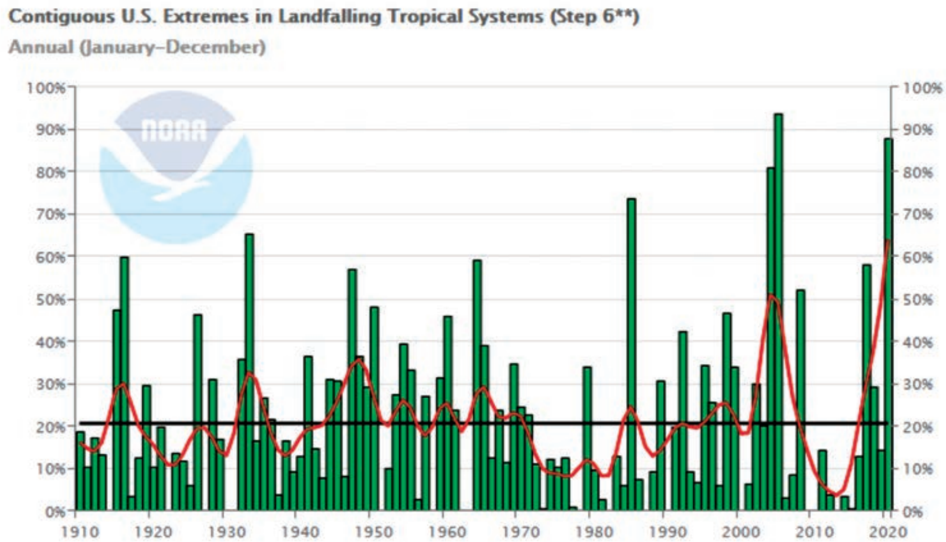

Figure 2. Landfalling tropical storm extremes in the United States, 1910–2020. The index is calculated as the arithmetic average of values from a specified set of extreme events, weighted by the percent area that experienced the defined conditions. The long-term variation or change of this index represents the tendency for extremes of climate to either decrease, increase, or remain the same. Figure: National Oceanic and Atmospheric Administration. n.d. "U.S. Climate Extremes Index." Accessed October 6, 2021. https://www.ncdc.noaa.gov/extremes/cei/graph.

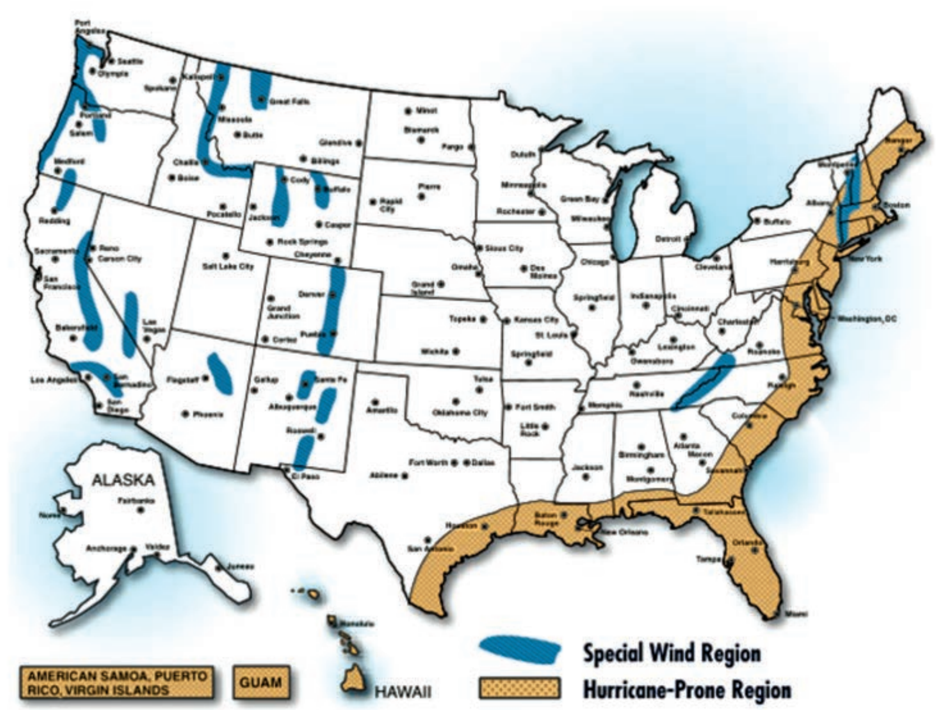

Figure 3. Hurricane-prone and special wind regions. Figure: Adapted from Reference 7 for use in https://www.wbdg.org/resources/wind-safety-building-envelope.

As the prevalence of high-wind events and other extreme weather events continues, it is important to assess the vulnerabilities aged curtainwalls face, particularly in high-wind regions of the United States.

HISTORY OF GLAZING MATERIALS USED IN CURTAINWALLS

The history of curtainwalls in the United States can be divided into a few defining eras. The first era generally includes curtainwalls built from the early 1900s to the 1950s. This era of curtainwall construction consisted of simple stick-built metal framing and generally single-pane plate glass. The first curtainwall system in the United States was constructed at the Boley Building in Kansas City, Mo., in 1908 (**Fig. 4**). The curtainwall design used single-pane annealed glass (also commonly referred to as flat glass or plate glass).[8]

The Hallidie Building (**Fig. 5**), which was constructed in 1918 in San Francisco, Calif., is another early example of a building featuring a curtainwall with single-pane annealed glass.[9] In 2010, the Hallidie Building was renovated to include new laminated safety glazing to improve the integrity of the curtainwall system.

More than 30 years after construction of the Hallidie Building, the Lever Building (**Fig. 6**) was constructed in New York City in 1952, featuring a 21-story curtainwall system and blue-green colored plate glass. By the mid-1990s, almost all the original glass had been replaced, and in 2001 a full renovation of the curtainwall system was implemented.[10]

The second era generally includes curtainwalls built in the 1960s to 1980s. This era of curtainwall construction consisted of simple stick-built metal framing with the use of various glazing systems such as strengthened glass, insulated glass, composite panels, and metal panels. The curtainwall industry began using custom aluminum extrusions, which allowed for efficient manufacturing of curtainwall systems. Furthermore, the 1964 *Uniform Building Code* (UBC) introduced safety glazing requirements based on glass impact loads. In 1970, the John Hancock Tower (**Fig. 7**) , featuring double-pane annealed glass framed with extruded aluminum, was constructed in Boston.[11] Soon after construction, in 1972, curtainwall glazing panels fractured and fell. The fracturing of the glazing was determined to be caused by the design of the original glazing system and exacerbated by high wind speeds. In 1973, every glazing panel was replaced with high-strength monolithic glass.[12]

The modern era generally includes curtainwalls built from the late 1980s to the present day. This era of curtainwall construction consists of a combination of unitized and stick-built assemblies and primarily uses safety glazing in the form of heat-strengthened, laminated, and fully tempered glass for the vision portions of these systems.

The building codes varied by region of the United States in the early 20th century. The predominant U.S. building codes before the IBC were the *Basic National Building Code* (BOCA), *Standard Building Code* (Southern Building Code), and the UBC. In general, the

Figure 4. Boley Building in Kansas City, Mo. Figure: Photograph by Cole Woodcox. Originally published in SAH Archipedia (http://sah-archipedia.org/buildings/MO-01-095-0001). Reprinted with permission from the Society of Architectural Historians and University of Virginia Press.

Figure 5. Hallidie Building in San Francisco, Calif.

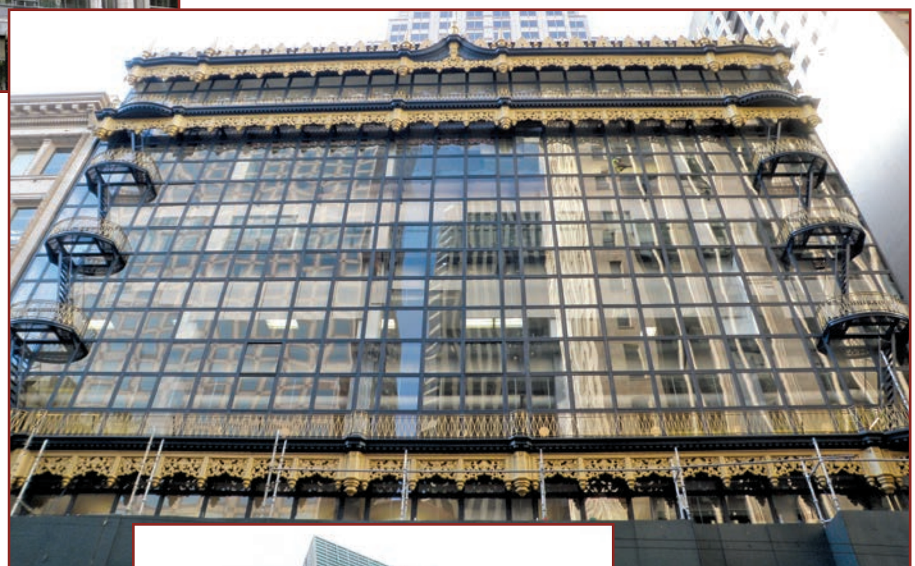

UBC was commonly used in the Western United States, the Southern Building Code was commonly used in the Southeast and the BOCA was commonly used in the Northeast. However, many large cities adopted codes that were not consistent with the standard code adopted by the state and added their own building code regulations. For example, Texas adopted the Southern Building Code, but the city of Houston adopted the UBC, overruling the state standard.

The requirements for designing and selecting glazing materials based on loads in the UBC were developed in the early 1960s with the introduction of the glass-thickness recommendation based on glass type. The 1964 UBC introduced a dedicated code section to Glass and Glazing and stated requirements of glass thickness based on glass type and size. The 2000 IBC with reference to the ASCE 7-98 was the first model code to address wind-borne debris requirements for glazing in buildings located in hurricane-prone regions.

HISTORY OF WIND DESIGN STANDARDS IN HOUSTON, TEXAS

The State of Texas did not adopt a state-wide implemented building code until 2001, when it adopted the IBC. Before the statewide basic code requirement was implemented, individual Texas municipalities, including Houston, had their own building codes.[13] In Houston, the UBC was the base code to guide the city's construction standards until the IBC became the basis for Texas code.

In 1945, the American National Standards Institute (ANSI) published the first consensus wind load design criteria in ANSI A58, *Minimum Design Loads for Buildings and Other Structures*.[14] The ANSI A58.1 standard was subsequently revised in 1955, 1972, 1982, and 1988 as ASCE 7,[15] which

Figure 6. Lever Building in New York, N.Y. Figure: ArchDaily. Gallery of AD Classics: Lever House/SOM - 10. archdaily.com.

Photo by Janine Robinson on Unsplash

Figure 7. John Hancock Tower in Boston, Mass. Figure: Architect Magazine. https://www.architectmagazine.com/project-gallery/john-hancock-tower.

Design standard	Year published	Wall wind pressure,* lb/ft^2
1958 UBC	1958	-20
1970 UBC	1970	-55
ANSI A58.1-1972	1972	-35 (interior)/-75 (corner)
ASCE 7-05	2005	-43 (interior)/-79 (corner)
ASCE 7-10	2012	-44 (interior)/-80 (corner)
ASCE 7-16†	2016	-44 (interior)/-80 (corner)

UBC = *Uniform Building Code*.

*All wind pressures are shown as allowable stress design values. For purposes of comparison, the wind pressures shown for ASCE 7-10 and ASCE 7-16 were converted from strength design values to allowable stress design values. All wind pressures shown are leeward wind pressures.

†ASCE 7-16 is an anticipated future code design standard for Houston, Texas.

Table 1. Negative wind pressure comparisons based on historic codes and standards for a 150-ft-tall, Risk Category IV (essential facility) building

the IBC adopted as the reference standard for design wind loads. The 2000 edition of the IBC was the first model code to address wind-borne debris requirements for buildings located in the hurricane-prone regions, via reference to the ASCE-7 standard.

Table 1 provides a limited overview of the Houston code changes in design wind pressures for components and cladding assemblies in exterior wall systems from 1958 to 2016.[16] The wind pressure analysis in Table 1 is based on a 150-ft-tall, Risk Category IV (essential facility) building in Houston, using Exposure Category C, where applicable. The wind pressure is specific to the 55 × 55 in. window referenced in the case study analysis as part of this paper.

The wind load design in the 1958 UBC was based on the building height.[17] The code provided standard wind pressures, which depended on whether the portion of the building analyzed was positioned equal to or greater than 60 ft above the ground or less than 60 ft above the ground. In the case study of the 150-ft-tall building, the design wind pressure for the window would be 20 lb/ft^2.

The wind load design in the 1970 UBC was based on building location and height.[18] The code identified allowable resultant wind pressures for the geographical location of a building, and then these basic wind pressures were translated into design wind pressures according to the various height zones of a building. For the case study window, the design wind pressure would be 55 lb/ft^2 because the 150-ft-tall building was located in Houston.

ANSI A58.1-1972[14] provided a basic wind speed, which was dependent on the building location, building height, exposure category, and fenestration openings. For a building in Houston, the basic wind speed was 90 mph. ANSI A58.1-1972 also introduced a distinction between corner zones and interior zones. For the case study window, the design wind pressure would be 35 lb/ft^2 for a window in the interior zone and 75 lb/ft^2 for a window in the corner zone.

ASCE 7-05[19] specified the basic wind speed for Risk Category III/IV (essential facilities) in Houston as 108 mph. ASCE 7-05 took building height and exposure category into design consideration, similar to ANSI A58.1. ASCE 7-05 also introduced the classification categories for buildings still used in current IBC code. For the case study window, the design wind pressure would be 43 lb/ft^2 if the window were in the interior zone or 79 lb/ft^2 if it were in the corner zone.

ASCE 7-10[20] shifted from allowable stress design to strength design. For purposes of comparison in Table 1, the wind pressures shown for ASCE 7-10 and ASCE 7-16[1] were converted from strength to allowable stress values.

ASCE 7-10 and ASCE 7-16 have similar analysis methodologies for components and cladding wind pressures. In ASCE 7-10, the basic wind speed was 145 mph. However, the City of Houston building code amendments for the 2012 IBC require a basic wind speed of 150 mph for Risk Category IV. ASCE 7-16 reintroduced a separate return period map for Risk Categories III and IV. For ASCE 7-16, the basic wind speed is 150 mph for Risk Category. For the case study window, the design wind pressures from either ASCE 7-10 modified for the 150 mph requirement in the Houston building code or ASCE 7-16 would be 44 lb/ft^2 if the window were in the interior zone or 80 lb/ft^2 if it were in the corner zone.

VULNERABILITIES OF AGED CURTAINWALLS

As a result of the changes in code and industry standards, the design wind pressures used today are higher than those specified for pre-1972 curtainwalls under earlier building codes and consensus standards. The outdated design requirements of older curtainwall systems are an increasing concern in coastal regions where tropical storms are becoming more prevalent on average when compared with the early 20th century. Furthermore, the federal Disaster Mitigation Act of 2000 encouraged states and communities to identify critical facilities and evaluate their vulnerabilities against severe weather events. Along with high winds, these curtainwalls are exposed to potential wind-borne debris impacts.

The impact of wind-borne debris is conditional on wind speed, the size and weight of the wind-borne object, and the strength of the curtainwall glazing. Depending on the glass type used in the design of the curtainwall,

The outdated design requirements of older curtainwall systems are an increasing concern in coastal regions where tropical storms are becoming more prevalent on average when compared with the early 20th century.

the aged curtainwall may be more susceptible to impact damages. In 2007, the Federal Emergency Management Agency (FEMA) issued FEMA 543, *Design Guide for Improving Critical Facility Safety from Flooding and High Winds*.[21] The publication highlights the need to design exterior glazing at essential facilities to withstand impacts and provides case studies of essential facilities that experienced global glazing failures during hurricane events from airborne debris. FEMA 543 recommends the design of exterior glazing for essential facilities to include laminated glass designed to resist test missiles and wind load pressures.

Upkeep with general maintenance requirements is another important factor that can affect the resiliency of a curtainwall in a high-wind event. Gaskets dry out, shrink, and crack as they age (**Fig. 8**). Subjected to sun exposure and freezing-and-thawing cycles, the elastic material degrades. Without the support of gaskets, the glass may lose stability within the curtainwall assembly. Like gaskets, structural glazing will deteriorate over time and begin to shrink, discolor, and become brittle. Gasket and sealant replacement should be part of a planned preventive maintenance program. Lack of proactive upkeep with industry- and manufacturer-recommended maintenance can reduce the service life and integrity of curtainwall components, leaving these exterior wall systems more vulnerable to impact and damage during extreme weather events.

Figure 8. Example of gasket cracking deterioration in a 1965 curtainwall.

CASE STUDY: INVESTIGATION OF AN AGED CURTAINWALL

This case study is based on an actual project but has been modified for the purposes of this paper. The building under review in this study is a 150-ft-tall Houston medical facility constructed in 1965. The client wanted to understand the vulnerabilities of the existing curtainwall system and upgrade the system as necessary to meet current design loads that are anticipated in an extreme weather event such as a hurricane. The purpose of the study was to evaluate the capacity of the existing curtainwall glazing panels at the medical facility to withstand "uniform wind pressure load" per the requirements of ASCE 7-16[1] as well as the 2018 *NCSEA Engineering Structural Glass Design Guide*.[2] For the study (and for this paper in particular), two representative single-pane glazing panels were analyzed at two different wind zone locations (**Fig. 9** and **10**).

As part of the investigation, the original construction drawings were reviewed to understand the existing curtainwall system

Figure 9. Representative photo of curtainwall glazing panels within the interior wind zone. The blue dashed lines frame the interior zone window analyzed in the case study.

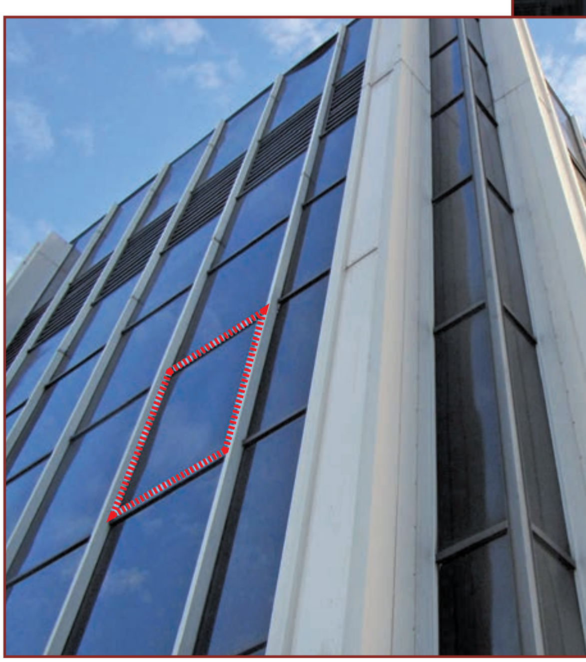

Figure 10. Representative photo of curtainwall glazing panels within the corner wind zone. The red dashed lines frame the corner zone window analyzed in the case study.

Figure 11. Glazing thickness measurement (¼ in.) at curtainwall glazing panels.

transitions, terminations, and anchorage. A site investigation was necessary to obtain field measurements and collect as-built construction documentation of representative glazing panels. An MIG MG1500 Laser Glass Thickness Gauge was used to measure the cross-sectional thickness of the glazing panels (Fig. 11).

Two representative types of single-pane glazing panels at two different wind zone locations were identified. Refer to Table 2 for the in-field measurements and locations of the representative glazing panels.

The glazing panels presented in the case study are single-pane and likely annealed glass, based on the era of construction and known design history of glazing applications in curtainwalls during that period.

Overview of Analysis Methodology

There are three parts to the curtainwall wind impact study analyses presented in this paper:

- **Part 1: Stress and deflection criteria.** The allowable stress and maximum deflection criteria of the glazing were calculated in accordance with the 2018 *NCSEA Engineering Structural Glass Design Guide.*[2]
- **Part 2: Finite element analysis.** ASCE 7-16[1] uniform wind loading was applied using SJ Mepla, a finite element analysis software for structural glass design, to determine the glazing stresses and deflections. The glazing stresses and deflections were then compared with the allowable stress and maximum deflection criteria determined in Part 1.
- **Part 3: Wind-borne debris load.** The maximum static point load that could be applied to the center of the glass with a uniform pressure wind loading was determined using a finite element analysis. The maximum static point load was then converted to an impact load that had mass and velocity for each test missile type prescribed in ASTM E1996.[3] A pass-fail criterion was then used to evaluate the representative glazing panel cases against a governing test missile type.

Single-pane glazing panels were used for the analysis. The wind impact analyses parameters for glazing panels analyzed are shown in Table 2.

For the purposes of this study, analyses were performed assuming the following types of glass-strengthening treatments: annealed, heat-strengthened, and tempered. Glazing allowable stress and maximum deflection were then calculated based on these assumptions and in accordance with the 2018 *NCSEA Engineering Structural Glass Design Guide.*[2]

Representative glazing panel	Glazing height, in.	Glazing width, in.	Glazing thickness, in.	Wind zone (External pressure coefficient zone)
A	55	55	0.25	Corner
B	55	55	0.25	Interior

Table 2. Parameters for the curtainwall glazing wind impact study analysis

Representative glazing panel	Wind zone	ASCE 7-16		UBC 1958
		Positive pressure wind load, lb/ft^2	Negative pressure wind load, lb/ft^2	Design wind pressure, lb/ft^2
A	Corner	72.6	-132.8	-20
B	Interior	72.6	-72.7	-20

UBC = *Uniform Building Code.*

Table 3. Components and cladding wind pressures per ASCE 7-16 and applicable code at time of original building construction (1958 UBC)

Representative glazing panel	Wind zone	Glazing stress demand–capacity ratio (per glass treatment type)			Glazing deflection demand–capacity ratio*
		Annealed	Heat strengthened	Tempered	
A	Corner	1.89†	0.98	0.49	1.42†
B	Interior	0.73	0.37	0.18	0.47

*Glazing deflection results are independent of glass treatment type.

†The ratio did not meet the wind-borne debris impact analysis acceptance criteria demand-capacity ratio threshold of equal to or less than 1.10.

Table 4. Findings from uniform wind load analyses

Uniform Wind Load Analysis

Wind loads were calculated per ASCE 7-16.[1] Wind pressures were determined based on the following criteria:

- Building location: Houston, Texas
- Ultimate design wind speed V_{ult}: 150 mph (3-second gust)
- Building risk category: IV
- Exposure category: C
- Building height: 150 ft
- Least horizontal dimension: 150 ft
- Angle of roof from horizontal: 0 degrees
- Internal pressure coefficient GC_{pi}: +0.18/-0.18
- Directionality factor K_d: 0.85.
- Width of end zone/edge/corner strip: 15 ft

Table 3 presents components and cladding wind load analyses findings for the curtainwall glazing panels.

Component and cladding pressures act normal to the surface. Positive pressures act toward the surface, and negative pressures act away from the surface. The effective wind area is the span length multiplied by an effective width that is not less than one-third the span length.

Temperature differential loads were also considered for three cases: "without temperature" loading, "summer temperature" loading, and "winter temperature" loading. The results did not vary within two significant digits between load cases; therefore, only the "without temperature" differential loading results are presented as part of this case study analysis.

A finite element analysis was performed with SJ MEPLA to determine the glazing stresses and deflections under the applicable ASCE 7-16[1] load combination for dead and wind loads. (See **Fig. 12** for a SJ MEPLA model of a typical finite element analysis stress result for the uniform wind analysis.)

The finite element analysis considered geometric nonlinearity to account for the significant deflections the glazing would experience under a code-level, high-wind load event. The glazing stress and deflection analysis demands were compared with the allowable glazing stress for the referenced glass-strengthening treatments and maximum deflection capacities to generate demand-capacity ratios. For the purposes of this study, demand-capacity ratios less than 1.10 for glazing stress and deflection criteria were considered to be a passing result for existing lateral load-carrying structural elements in accordance with the 2018 *International Existing Building Code*,[22] Section 806.3. Refer to **Table 4** for the findings of the uniform wind pressure impact analyses.

Impact Load Analysis

The maximum static point load was determined by iterative analysis until the glazing stress was within 2% of the allowable glazing stress. A uniform wind pressure was simultaneously applied to the analysis, using the ASCE 7-16[1] load combination for wind, and, for the purposes of this study, a load factor of 1.0 was assumed for impact loads. The static point load was then converted to an impact load with mass and velocity.

To convert the static point load to an impact load, the wind-borne debris kinetic energy was assumed to be transferred entirely to the glazing and is thus equivalent to the strain energy of the glazing. This is a conservative assumption because some energy will be dissipated during impact and wind-borne debris may bounce off the glazing, thereby retaining some of its energy.

The strain energy of the glazing was considered equivalent to the effect of a static load

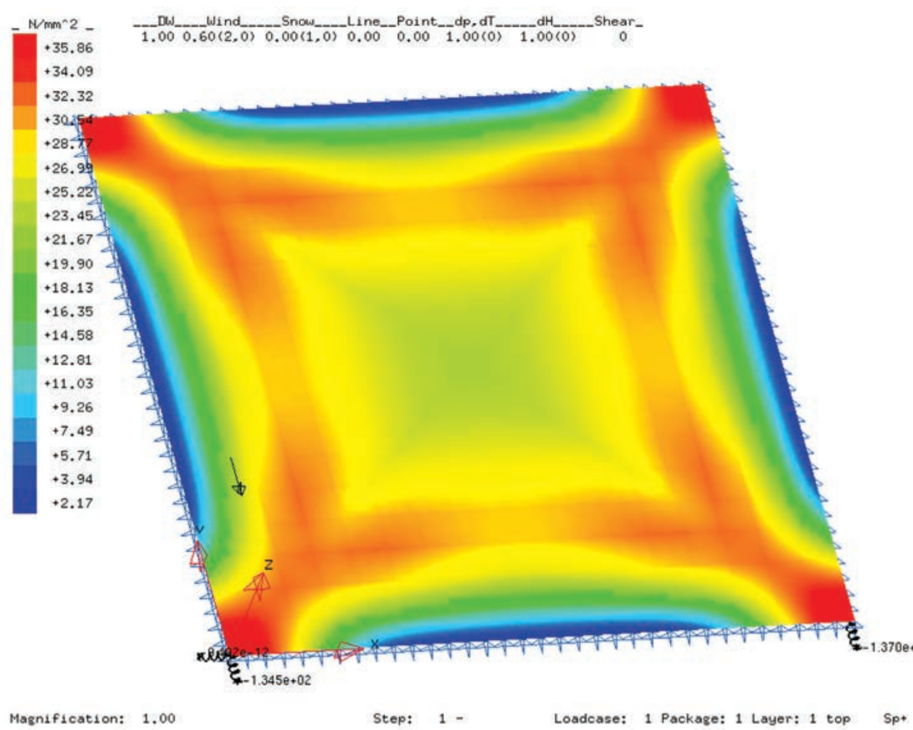

Figure 12. Model of the finite element analysis stress result for the uniform wind analysis of representative glazing panel A. The colors represent the relative stresses across the glazing panel: red represents a stress result closer to the maximum value, green represents a stress result closer to the median value, and blue represents a stress result closer to the minimum value.

Representative test missile	Mass	Cross-sectional area	Impact (threshold) velocity, mph	Description
A	33 grains	0.36 in.^{2}	89	10x steel balls
B	2.25 lb	2 × 4 in.	34	2x lumber
C	4.25 lb	2 × 4 in.	27	2x lumber
D	9.25 lb	2 × 4 in.	34	2x lumber
E	9.25 lb	2 × 4 in.	55	2x lumber

Table 5. ASTM E1996 test missile parameters

deflecting the glazing. The velocity was determined from the maximum static point load and the mass of wind-borne debris.

ASTM E1996[3] prescribes a laboratory test method for impacting a fenestration assembly infill panel with small and large missiles. The ASTM E1996 laboratory testing parameters were used as a guideline basis of analysis for the assessment methodologies in this evaluation. One "small" and three "large" missile sizes and weights, as prescribed in the ASTM E1996 consensus standard, were used as representative wind-borne debris cases in the analysis. Table 5 presents the sizes, weights, and test impact velocities of the ASTM E1996 representative missiles considered in this study.

The impact load was applied to the center of the glazing using the full cross-sectional area of the representative wind-borne debris. In reality, the contact area may be only a portion of the cross-sectional area, depending on the angle of impact and geometry of the debris. A smaller contact area would increase the impact of glazing stresses.

The contact area assumption is one of several used to analyze the glazing for wind-borne debris impact loads; therefore, the results are not a precise representation of the glazing's impact resistance during a high-wind event. Instead, the impact load analysis results are intended to approximately forecast how the glazing might perform against typical wind-borne debris missile impacts, as defined by ASTM E1996.[3] Furthermore, it is important to note that the ASTM E1996 consensus standard was first issued in 2001. Therefore, the original construction date of the existing curtainwall system predates this standard, and the window technology in place during original installation should not be expected to conform with modern industry consensus guidelines and building code requirements.

The ASTM E1996 governing missile type was used as a pass/fail criterion to evaluate the representative glazing panels considered in the analyses. The governing missile type depends on the building's importance factor, the basic wind speed for the geographic location, and the panel elevation. Per the standard, the governing missile type is 'E' for glazing panels equal to or less than 30 ft of elevation and 'D' for glazing panels above 30 ft. If the maximum applied impact velocity of the governing missile type determined from the finite analysis were greater than the threshold velocity prescribed in ASTM E1996 for missile impact–resistant curtainwall assemblies, the representative glazing panel would pass or meet the impact load analysis requirements. Refer to Table 6 for the findings of the wind-borne debris missile impact analyses.

Summary of Analysis Findings

Structural analyses, per the applicable ASCE 7-16[1] wind loading criteria and 2018 *NCSEA Engineering Structural Glass Design Guide*[2] consensus standard guidelines, including assumptions as referenced in the report, determined the following.

- **Uniform wind load analyses**:
  - Analysis of the annealed glass treatment found that representative glazing panel A, installed at the corner wind pressure zone, exceeded the allowable stress demand–capacity ratio of 1.10 (see Table 4).
  - Analysis of the heat-strengthened or tempered glass treatment found that all representative glazing panels were below the allowable stress demand–capacity ratio of 1.10 (see Table 4).
  - Additionally, representative glazing panel A did not meet the allowable glazing deflection demand–capacity ratio of 1.10; this finding is irrespective of the type of glass treatment in place as all the assumed glass treatment types have the same section modulus. Excessive deflection of glazing panels can result in dislodgement or reduced performance of the gasket components securing and sealing the glass to the curtainwall framing.
- **Wind-borne debris impact analyses**:
  - Analysis of glazing panels below 30 ft of elevation involved the

Representative glazing panel	Elevation > 30 ft (Type E missile†)			Elevation ≤ 30 ft (Type D missile†)		
	Annealed	Heat strengthened	Tempered	Annealed	Heat strengthened	Tempered
A	Failed‡	3 mph	7 mph	Failed‡	3 mph	7 mph
B	1 mph	4 mph	8 mph	1 mph	4 mph	8 mph

*None of the results met the wind-borne debris impact analysis acceptance criteria for threshold impact velocity, as defined in the Impact Load Analysis section of the case study. Results shown indicate impact velocity resulting in failure.

†The threshold impact velocity for Type E missiles is 55 mph. The threshold impact velocity for Type D missiles is 34 mph.

‡The glazing panels did not meet the analysis's pass criteria when only positive wind pressure, per ASCE 7-16, was applied without the wind-borne debris missile impact load.

*Table 6. Pass/fail results per glass type from wind-borne debris impact analyses of glazing panels**

Type E test missile, which is the governing wind-borne debris missile type for glazing panelsequal to or less than 30 ft of elevation; the threshold impact velocity for this type of test missile is 55 mph. The glass treatment types considered in this study (annealed, heat-strengthened, and tempered) did not meet the referenced wind-speed threshold pass criteria for this missile type for either of the representative glazing panels.

- Analysis of glazing panels above 30 ft of elevation involved the Type D test missile, which is the governing wind-borne debris missile type for glazing panels above 30 ft of elevation; the threshold impact velocity for this type of test missile is 34 mph. The glass treatment types considered in this study (annealed, heat-strengthened, and tempered) did not meet the referenced wind-speed threshold pass criteria for this missile type for either of the representative glazing panels.

Based on the field documentation, engineering analyses, and the evaluation assumptions stated, the facility may be susceptible to global and systemic curtainwall glazing panel failures resulting in significant facility operational disruptions if a code-level high-wind event occurs at the building's geographical location. Specifically, based on the analysis and the referenced assumptions, the glazing panels do not seem to conform with the modern ASTM E1996[3] standards for wind-borne debris impact resistance for all glass treatment types.

Additionally, the analysis indicates that under uniform wind pressure loading, one of two representative glazing panels, if annealed, does not meet the allowable stress demand–capacity ratio requirements, and one of the two representative glazing panels does not meet the allowable glazing deflection demand–capacity pass criteria.

Failure of one or more glazing units will progressively result in an amplification of the wind pressures applied to the curtainwall system with each subsequent glazing panel failure as the building enclosure transitions from an enclosed type of construction to a partially enclosed type to an open type. This scenario will result in progressive acceleration of the glazing panel failure rate and continued operational impacts to the facility.

Furthermore, if the wind event is accompanied by rain, loss of glazing panels will result in water infiltration into the building's interior occupied spaces. This scenario will further significantly affect the building's functional operational capacity because multiple rooms will likely need to be abandoned until temporary measures are implemented.

In summary, the study determined that the facility may be vulnerable to systemic wind impact and related operational disruptions during a code-level wind event based on the findings referenced.

CONCEPTUAL RESTORATION RECOMENDATIONS

There are a few viable options used in the industry to strengthen curtainwall systems to meet wind-borne debris code requirements or to reduce the vulnerabilities of the curtainwall per FEMA 543[21] recommendations. These options may provide wind-borne debris impact resistance and deflection control capacity for meeting the referenced wind loading criteria. Two options relevant to the case study are as follows.

- **Option 1:** Replace the curtainwall system with a new system that meets the applicable City of Houston wind loading criteria for allowable stress and deflection and missile-impact criteria per ASTM E1996.[3] The new curtainwall design would need to meet current *International Energy Conservation Code*[23] requirements, including energy performance and more stringent air infiltration requirements. This option may be cost prohibitive and will result in impactful disruptions to the facility during construction. However, this option would provide the opportunity to refresh the aesthetic features of the curtainwall system to modern architectural detailing standards and, if designed appropriately, will better allow the essential facility to remain operational during an extreme weather event.
- **Option 2:** Install safety and security window film to increase the debris impact resistance of the glazing panels to meet ASTM E1996[3] test missile impact criteria. Films are available in a wide range of shades, styles, and grades that can be implemented to reduce the impact of wind and debris. The films can be designed and retrofitted to fit the existing window geometry and are typically mechanically attached to the window frame. However, the integrity of the window framing and attachment of the frame to the building would need to be analyzed and may require retrofitting. This would be a less-expensive option, with a lower degree of operational disruption to the facility, but it could require ongoing maintenance and reapplications. With this option, the existing exterior-facing aesthetic features of the curtainwall system would remain the same and would not be upgraded. However, the films and corresponding sealants would be reoccurring as well as long-term maintenance items. For example, as glazing panels are replaced, new glazing panels will also require installation of the security window film to provide wind borne-debris protection and aesthetically match other curtainwall panels.

The goal of restoration of these aged curtainwalls is to perform repairs to strengthen the curtainwall or replace the curtainwall before failure occurs. Professional assessments and analysis will determine the vulnerabilities of the curtainwall and help identify the best course for remediation. Installing laminated glazing or security film may be sufficient to address impact vulnerabilities; however, if the glazing is already damaged or water infiltration is also observed, full replacement may be a more financially viable option for the building owner.

Restoration of an aged curtainwall system may strengthen and extend the service life of the existing system, but it does not resolve all the existing distress issues. Whether replacement or restoration of the curtainwall is pursued, the building owner must keep up with general maintenance.

CONCLUSION

Since 1965, Houston, Texas, has not regularly experienced sustained wind speeds above 65 mph, but there have been a few extreme weather events. Based on NOAA historical weather data, the maximum sustained wind-level event experienced by the building in this case study was 100 mph in 1983.[24]

To date, the curtainwall system in the case study has not experienced widespread damage to the glazing panels. However, it was not designed to meet the modern ASTM E1996[3] wind debris impact criteria, and it is therefore vulnerable to glazing failures in future extreme weather events.

It is vital that essential facilities such as the one that is the focus of this study remain functional, particularly during extreme weather events. Therefore, aged curtainwalls should be assessed using modern codes and standards to identify their susceptibilities to high winds and debris impact, and to determine appropriate strategies to reduce the risk of glazing failures.

Curtainwalls designed and constructed before the publication of the ANSI 58.1 standard[14] in 1972 may be particularly vulnerable because they were designed for at least 25% lower wind pressures compared to ANSI A58.1 and ASCE 7[1] standards. Facilities with aged curtainwalls are particularly susceptible because the systems were not designed to modern ASTM E1996[3] standards. Furthermore, several of the aged curtainwall components may not have been proactively maintained or replaced.

We have the opportunity to minimize the risk of future potential failures by preparing our aged curtainwall systems for more powerful extreme weather events, which seem to be occurring at a greater frequency. It is critical that we evaluate these curtainwall systems to determine the need for possible retrofits to mitigate potential operational disruptions now—rather than when it is too late.

REFERENCES

1. American Society for Civil Engineers (ASCE). 2016. *Minimum Design Loads for Buildings and Other Structures*. ASCE 7-16. Reston, VA: ASCE.
2. March, M., and F. Lancaster. 2018. *NCSEA Engineering Structural Glass Design Guide*, edited by P. Khalil. Chicago, IL: National Council of Structural Engineers Associations.
3. ASTM International. 2020. *Standard Specification for Performance of Exterior Windows, Curtain Walls, Doors, and Impact Protective Systems Impacted by Windborne Debris in Hurricanes*. ASTM E1996-20. West Conshohocken, PA: ASTM International. https://doi.org/10.1520/E1996-20.
4. International Code Council (ICC). 2018. *International Building Code*. Country Club Hills, IL: ICC.
5. National Oceanic and Atmospheric Administration (NOAA). 2021. "State of the Climate: National Climate Report for Annual 2020." https://www.ncdc.noaa.gov/sotc/national/202013.
6. NOAA. n.d. "U.S. Climate Extremes Index." Accessed October 6, 2021. https://www.ncdc.noaa.gov/extremes/cei/graph.
7. Federal Emergency Management Agency (FEMA). 2021. *Protect Your Property from High Winds: Wind Retrofit Guide for Residential Buildings*. FEMA P-804, Washington, DC: FEMA.
8. Woodcox, C., and K. Eggener. 2018. "Boley Building." In *SAH Archipedia*. Society of Architectural Historians website. https://sah-archipedia.org/buildings/MO-01-095-0001.
9. https://aiasf.org/about/about-us/hallidie-restoration/.
10. Perez, A. 2010. "AD Classics: Lever House/SOM." ArchDaily website. https://www.archdaily.com/61162/ad-classics-lever-house-skidmore-owings-merrill.
11. Weaver, A. E. 2013. "John Hancock Tower Named a Notable Historical 'Failure by Design.'" BostInno website. https://www.bizjournals.com/boston/inno/stories/news/2013/08/19/john-hancock-tower-design-failure-falling-windows.html.
12. Goldberger, P. 1988. "Architecture View; a Novel Design and Its Rescue from Near Disaster." *New York Times* April 24, 1988, https://www.nytimes.com/1988/04/24/arts/architecture-view-a-novel-design-and-its-rescue-from-near-disaster.html.
13. Leon, R., and J. Rossberg. 2012. "Evolution and Future of Building Codes in the USA." *Structural Engineering International* 22 (2): 265–269. https://doi.org/10.2749/101686612x13291382991047.
14. American National Standards Institute. 1972. *Building Code Requirements for Minimum Design Loads in Buildings and Other Structures*. ANSI A58.1-1972. New York, NY: ANSI.
15. ANSI/ASCE. 1988. *Minimum Design Loads for Buildings and Other Structures* (abstract). ANSI/ASCE 7-88. https://ascelibrary.org/doi/book/10.1061/9780872627420.
16. City of Houston Department of Public Works and Engineering Building Code Enforcement Branch. 2016. "Houston Code Adoption History." https://www.publicworks.houstontx.gov/sites/default/files/code_publications/1204_code_adoption_history_for_houston_codes.pdf.
17. International Conference of Building Code Officials. 1958. *Uniform Building Code*. Whitter, CA: International Conference of Building Code Officials.
18. International Conference of Building Code Officials. 1970. *Uniform Building Code*. Whitter, CA: International Conference of Building Code Officials.
19. ASCE. 2005. *Minimum Design Loads for Buildings and Other Structures*. ASCE 7-05. Reston, VA: ASCE.
20. ASCE. 2010. *Minimum Design Loads for Buildings and Other Structures*. ASCE 7-10. Reston, VA: ASCE.
21. Federal Emergency Management Agency. 2007. *Design Guide for Improving Critical Facility Safety from Flooding and High Winds*. FEMA 543. https://www.fema.gov/sites/default/files/2020-08/fema543_design_guide_complete.pdf.
22. ICC. 2018. *International Existing Building Code*. Country Club Hills, IL: ICC.
23. ICC. 2021. International Energy Conservation Code. Country Club Hills, IL: ICC.
24. NOAA. 2021. "Storm Events Database." https://www.ncdc.noaa.gov/stormevents.

Deflection and Drift Considerations for the Enclosure Design of Prefabricated Facade Panels

Brad Carmichael, PE, CPHC

4EA Building Science | Seattle, WA

bradc@team4ea.com

IIBEC 2022 - Building for the Future

International Convention and Trade Show

March 17–22, 2022 | Orlando, FL

ABSTRACT

Building structures are not entirely static, as they are designed to deflect and move under various loading conditions such as live loads, wind loads, and seismic loads. Some movement locations such as building expansion joints, cladding expansion joints, and curtainwall stack joints are typically well defined by the architectural design of the building. In many instances, however, the movement of a building structure occurs at more subtle interface and transition conditions that are not always clearly defined architecturally. Determining the location of this movement can become increasingly complex with unitized and panelized wall systems in seismic areas that have airtightness requirements.

This presentation provides background on how building structures move and the impact that movement has on enclosure systems and their geometry. This presentation also suggests design approaches for identifying building movement locations to address control layer continuity.

SPEAKER

Brad Carmichael, PE, CPHC

4EA Building Science | Seattle, WA

Brad Carmichael has been consulting on building enclosures throughout North America for more than 15 years; his work has included complex new construction and rehabilitation projects. He is passionate about good design and the role it can play in social and environmental stewardship. He believes that durable and efficient building enclosures are critical for a built environment that is low consumption and long lasting.

Deflection and Drift Considerations for the Enclosure Design of Prefabricated Facade Panels

The structures that hold up our buildings are not infinitely rigid. Instead, building structures are intentionally designed to undergo a limited amount of movement under wind loads, live loads, seismic loads, and other forces. The magnitude of this movement can often be fairly small (in the order of several inches). However, even small movements can affect continuity in the building structure unless the design accounts for them. Therefore, when one is maintaining the performance of a continuous air- and water-control layer, it is important to consider the impact of structural movements on the building enclosure.

In particular, the movement of building structures has unique implications for panelized enclosure systems that are designed to move along with the structure. This paper focuses on the deflection and interstory drift considerations of panelized framed wall systems. Other types of movement from sources such as thermal movement, creep, and column shortening are outside the scope of this paper but should be considered in design as well.

LIVE-LOAD DEFLECTION

Building structures experience some level of vertical deflection whenever load is applied. One common location that is affected is where floor lines intersect with the enclosure—particularly when panelized facades are attached along floor lines. The deflection of the floor under loading is then transmitted through the enclosure, where it needs to be accommodated.

In the *International Building Code* (IBC),[1] limits on the magnitude of live-load deflections are provided in Chapter 16, "Structural Design." In IBC, structural members supporting floors are often limited to deflecting $\frac{1}{360}$th of their span, although the limitation can vary. Ultimately, the project's structural engineer is responsible for establishing the designed deflection of the superstructure, but the implications of that design carry through to the design of components and cladding. On a project-specific basis, we commonly see a need for the components and cladding in the enclosure to account for a design deflection of of $\pm\frac{1}{2}$ in. to $\pm\frac{3}{4}$ in.

Floor-line deflection is typically expressed as plus or minus a distance because the movement is relative to the floors above and below. When a given floor is loaded and deflects, the distance between it and the floor above increases and floor-line joints open (see Case 1 for panels in **Fig. 1**). Conversely, the difference between a loaded floor and the floor below decreases and floor-line joints close (Case 2 in Fig. 1). Therefore, when this deflection translates through to enclosure elements, accommodation for deflection at floor lines must occur in both the upward and downward directions.

INTERSTORY DRIFT

Buildings structures are designed to move laterally, particularly during seismic events, such that one floor will displace relative to the floors above and below in what is referred to as interstory drift. In seismic regions, this differential displacement can affect the design of components and cladding systems.

When designing components and cladding systems for drift, there are two types of interstory drift to account for: inelastic and elastic drift limits. The inelastic drift limits are larger values that generally represent the extent to which permanent displacement or deformation of the structure can occur without jeopardizing the serviceability of the building structure. Under these circumstances, it is important that the building not present a risk to the safety of the public or the serviceability of the structure. For example, breaking glass, falling cladding, or other hazardous phenomena should not occur during these levels of drift.

The elastic drift limits are smaller values that generally represent the displacements that are permitted to occur within the regular operation of the building. Below the elastic drift limit, the building and its components should continue to perform as designed. For the enclosure in particular, this means that design levels for airtightness, watertightness, and thermal efficiency should be maintained throughout movements within these limits.

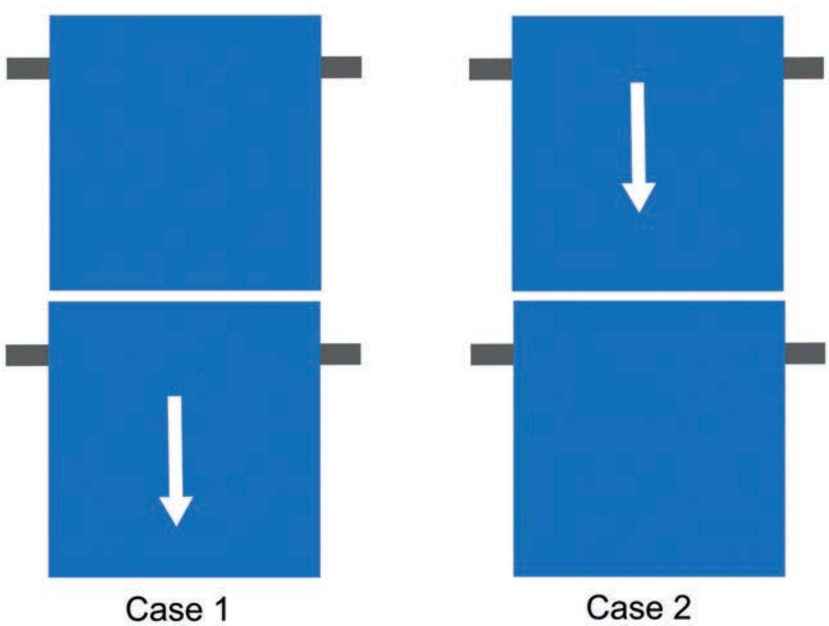

Figure 1. Load cases for facade panels under live-load deflection.

	RISK CATEGORY		
	I or II	III	IV
Structures, other than masonry shear wall structures, <4 stories above the base, with interior walls, partitions, ceilings, and exterior wall systems designed for drifts	2.5% of story height	2.0% of story height	1.5% of story height
Masonry cantilever shear wall structures	1.0% of story height	1.0% of story height	1.0% of story height
Other masonry shear wall structures	0.7% of story height	0.7% of story height	0.7% of story height
All other structures	2.0% of story height	1.5% of story height	1.0% of story height

Table 1. Allowable inelastic drift limits per ASCE 7[2]

The amount of inelastic design story drift is prescribed in the American Society of Civil Engineers' *Minimum Design Loads for Buildings and Other Structures* (ASCE 7)[2] and is generally a function of the occupancy risk of a building, the type of structural system, and the floor-to-floor height (see **Table 1**). For example, using a common commercial floor-to-floor height of 15 ft, the maximum inelastic design story drift can range from ±1.26 in. to ±4.5 in.

The maximum allowed amount of elastic interstory drift δ_{xe} is prescribed as a fraction of the inelastic design story drift δ_x. The magnitude varies by building because it depends on the ratio of the deflection amplification factor to the importance factor. The deflection amplification factor C_d is specific to the seismic force–resisting system and generally ranges from 1 (for example, for ordinary reinforced concrete) to 6 (for example, for dual systems with steel and concrete composite shear walls). The seismic importance factor I_e relates to the use of the building and ranges from 1 (typical buildings) to 1.5 (essential facilities).

The relation between the elastic drift limits and the inelastic drift limits is prescribed by ASCE 7[2] as follows:

$$\delta_x = \frac{C_d \delta_{xe}}{I_e}$$

For example, a commercial office building with a 15-ft floor-to-floor height and a steel buckling–restrained brace frame structure, occupied as Risk Category II, would have a maximum allowed inelastic story drift of ±3.6 in. at each floor. The elastic story drift for this structure would be ±0.9 in., which in absolute terms is a total design movement of 1.8 in. These magnitudes are not unusual for commercial buildings in seismic regions.

Building enclosures should be designed to maintain the performance of the air- and water-control layers under movements within the elastic range. Because the enclosure is required to maintain performance within the elastic range, it can be challenging to create a design capable of accommodating both the live-load deflection and the elastic story drift while also maintaining airtightness and watertightness. The following sections will review some of the design considerations.

FACADE CONSIDERATIONS

The two most common ways of designing facade systems to accommodate drift is to translate (**Fig. 2** Cases 1 and 2) or to rack (Fig. 2 Cases 3 and 4).

Unitized Curtainwalls

The building movement discussed in the previous section should ultimately be accommodated by the facade and other enclosure components. Some systems such as unitized curtainwall systems are designed and tested to accommodate these movements in a manner that is well established and has been tested over time. In some cases, early curtainwall systems did not accommodate building movement, and the effects can be seen in out-of-plane and dislodged glass at floor lines (**Fig. 3** and **4**).

Contemporary unitized curtainwall panels have features that accommodate movement better than their early predecessors. Contemporary panels are typically hung from a slab edge, and they interface with the panels on the lower floor at the stack joint. The geometries of the various stack joints in these systems are designed to accommodate both drift and deflection of the structure, as the "chicken head" gasket connection is allowed to move up and down, translate side to side, and rock back and forth under building movement. This gasket and similar gaskets at the sides of the panels also allow the units to maintain airtightness and watertightness across the facade even while the facade moves.

This type of movement accommodation is commonly tested in a performance mock-up using the American Architectural Manufacturers Association's full AAMA 501 testing protocol, which includes options for testing for vertical deflection (AAMA 501.7[3]), interstory drift (AAMA 501.4[4]), and dynamic seismic movement (AAMA 501.6[5]), among other tests.

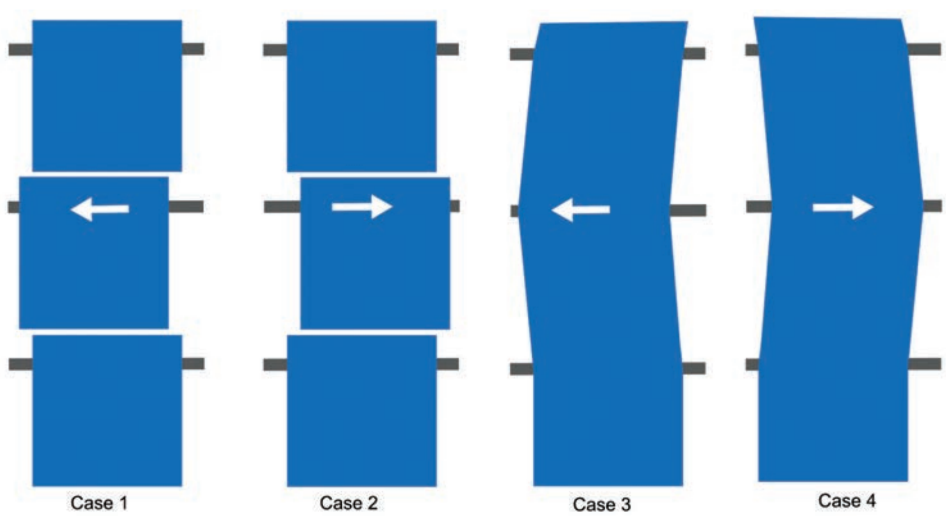

Figure 2. Schematic of in-plane panel movement under interstory drift.

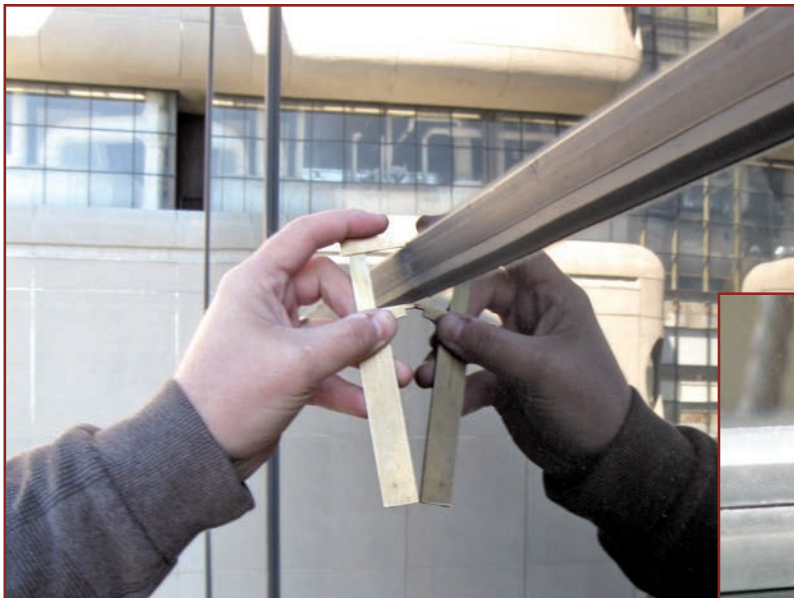

Figure 3. Out-of-plane glass across a floor line in an early curtainwall.

Figure 4. Dislodged glass below a floor line in an early curtainwall.

While the testing sequences for different AAMA 501 performance mock-ups may vary slightly among projects, one common characteristic is that when structural and movement tests are performed in the elastic range, the curtainwall is then tested for air and water resistance afterward to confirm that performance is maintained. The final structural tests of a performance mock-up are typically in the inelastic range, and testing of air and water resistance is typically not performed afterward. This underscores the expectation that airtightness and watertightness are to be maintained within the elastic movement range, but they are not expected to be maintained in the inelastic movement range.

Panelized Framed Wall Systems

As energy codes increasingly reduce glazing percentages, prefabricated panelized framed wall systems are emerging as an alternative to curtainwall systems for projects that require greater insulated opaque wall area and yet are of the height or scale that makes the use of field-assembled stud wall sections less practical. The advent of factory-applied air and water barriers onto sheathing boards has also improved the efficiency of off-site panelized framed walls, greatly reducing the amount of fieldwork needed once panels arrive on site. These systems are well suited for high-rise construction (**Fig. 5**) because the framed wall panels can be hung from slab edges in a manner that is similar to curtainwall.[6,7] Panels can be fairly large in size and encompass more than one story if desired. Because there are many different configurations for the components, layouts, attachment methods, and other variables, designers have a high degree of flexibility when designing with panelized framed wall systems.[8] This paper focuses primarily on panelized framed walls that have framing, sheathing, and weather barriers applied off site; however, many of the implications discussed here may also apply to other similar panelized wall types and field assembles walls as well.

Panelized framed wall systems fixed to floor lines are subject to the same types of building movement from the supporting structure as unitized curtainwalls, and they also have the same need for continuous air- and water-control layers. In comparison with unitized curtainwalls, panelized framed walls are less product-driven and do not have as extensive a history of performance mock-up testing using the AAMA 501 testing sequence. As a result, care must be taken on a project-by-project basis to review how the panels will interact with the moving structure, and how the movement joints are designed to remain airtight and watertight.

One method of constructing a panelized framed wall to accommodate building movement is to attach an extrusion for a unitized curtainwall system onto the perimeter of the

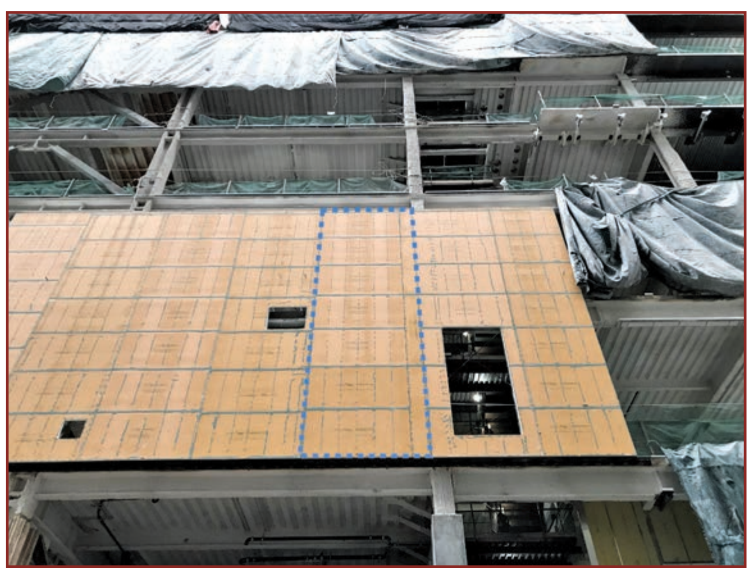

Figure 5. Large-format panels on a commercial high-rise building. Panel size is indicated by the blue dashed lines.

Panelized wall parapets are often balloon framed past the roofline because the added stiffness provides structural efficiency and because installation is easy.

framed panel. This will allow the panel to behave similar to a curtainwall under deflection and drift conditions.[6] One downside of this approach is the higher cost of aluminum extrusions relative to cold-formed steel; another is the thermal bridging that comes with adding an aluminum extrusion around the perimeter edge of the framing panel. An upside to this approach is that the joints do not require treatment after installation, so the panels could be prefabricated with exterior insulation and cladding already installed.

The alternative to using unitized curtainwall extrusions is to leave clearance gaps at joints between panels that can accommodate the anticipated amount of movement. This approach will require project-specific design of the movement joints. The following sections review design considerations for these types of joints.

Drift and Deflection Joint Design Considerations

The layout of drift and deflection joints in panelized framed walls is important to understand during the design phase because the joints will likely need to be continuous through the wall assembly—from interior finishes through the cladding—and the layout will therefore affect the aesthetics, finishes, and structure. Layout considerations include the following:

- Locating horizontal joints near floor lines can reduce the potential need for a moving joint through the interior finishes. Installing drift joints slightly below floor lines can place the joint in a location less visible at the interior (such as a ceiling cavity).
- Intersecting drift and deflection joints away from punched window rough openings will negatively affect the water-control layers of the rough opening as well as the attachment of the frame.
- Drift at outside and inside corners occurs in two orthogonal directions. To maintain sheathing and cladding on the same plane, consider a one-piece L-shaped corner, if possible.

Parapet Considerations

Panelized wall parapets are often balloon framed past the roofline because the added stiffness provides structural efficiency and because installation is easy. However, there are implications for how the roofing ties into the parapet because the joint between the roof deck and parapet could then be subject to live-load deflection as well as interstory drift.

Many roofing and waterproofing systems have details for simple roof-to-wall joints that can accommodate some movement due to deflection of the roof deck, but not all roofing and waterproofing systems can accommodate the total differential translational movement of 1.5 to 2 in. that would occur with interstory drift. In particular, fluid-applied roofing systems do not perform well when subject to this kind of movement, and if sheet membranes are used, the seams can be stressed during repeated movement.

One way to address this differential movement is to eliminate it at the roof by platform-framing the parapets, pouring the parapets in concrete, or dead-loading the panels to the roof deck. These techniques will fix the parapet to the roof deck and eliminate differential movement. A downside to this approach is that it results in having to move the drift/deflection joint to another location that may be less convenient for the overall design.

A variety of roofing-grade expansion joints can accommodate both drift and deflection, although they are often intended to be used as building expansion joints for larger joint sizes and larger ranges of movement. These types of joint systems are a good option, but they tend to be costlier and require longer lead times than field-fabricated alternatives.

It is important to note that in many conventionally insulated roof assemblies, particularly in colder climates, the roof membrane layer is not the only control layer in a roof assembly—there is a separate air- and vapor-barrier layer at the roof-deck level. A roofing membrane expansion joint at this transition will address the water-control layer, but the air-control layer might be a separate layer. In this case, the air barrier should also maintain continuity during building movements. It is important to review whether drift/deflection provisions are needed at just the roof membrane layer or if they are also necessary at the air-barrier layer, in which case you may need two movement joints at the roof intersection with the parapet.

Use of expansion joint membranes at the deck level can also place an expansion joint integration detail that can be more prone to leaks at a roof elevation where it may be in contact with more water (**Fig. 6** Case 1). Another approach, which is commonly used

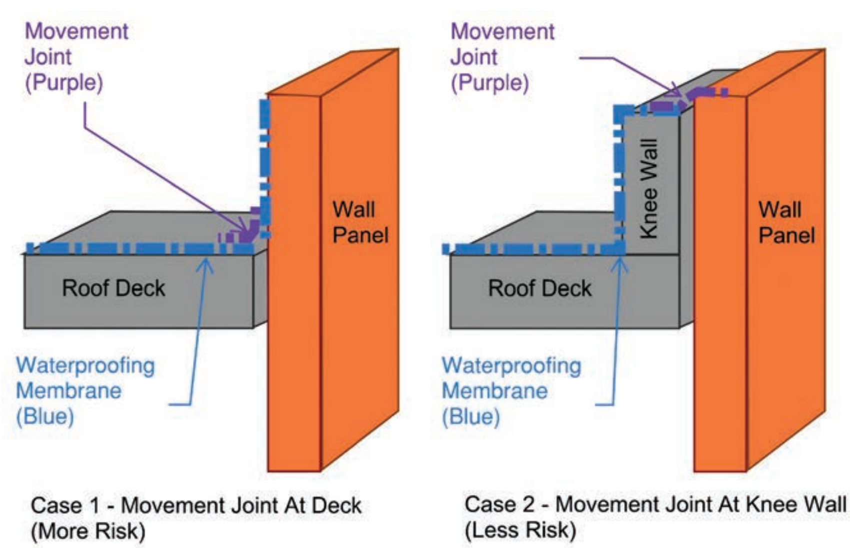

Figure 6. Roof-to-parapet joint considerations.

with unitized curtainwall parapets, is to construct a small knee wall on the interior side of the parapet (Fig. 6 Case 2). While this does not eliminate the need for a movement joint altogether, it moves the joint to a place above the deck level where water collects and where the movement can be accommodated with a field-fabricated silicone sheet and self-adhered membrane. An additional benefit with conventionally insulated roof systems is that that the air-control layer at the roof deck can reintegrate with the water-control layer at the roof membrane flashing such that there is a need for only one movement joint instead of two.

Corners

As noted in the earlier design considerations, panelized corners behave uniquely under deflection and drift for several reasons. One reason that panelized corners behave uniquely is that the drift movement occurs in two orthogonal directions. A panel designed to translate along with floor drift movement can clash with a panel at the corner because each panel is designed to translate in plane with the elevation when drift occurs. Therefore, at least one movement joint, and preferably two, should be considered at corners.

For corners with a single movement joint between panels, drift can translate panels out of plane if the direction of the drift is out of plane with the joint.

Mitered joints are one option at corners, but this strategy can result in a larger joint and increase the complexity of panel fabrication and cladding detailing at the corner.

A one-piece corner can result in an improved condition because having a joint in each plane will allow for adjacent panels to translate while staying in plane with the respective elevations. Refer to the green panel in **Fig. 7**.

Care should be taken to consider how these joints terminate at the bottoms of walls (soffits) and tops of walls (parapets) as the movement may need to be accommodated at the parapet coping as well as the backside of the parapet wall. This complicates matters as the vertical wall drift joints at the panel connections will need to intersect with the live load and drift joints already at the parapet as shown in **Fig. 8**. This intersection of multiple joints becomes more apparent in saddle conditions.

Parapet Saddle Conditions

Parapet saddles can be geometrically complex under normal circumstances, but the complexity compounds when panelized walls that drift and deflect are involved. **Figure 9** demonstrates some of the geometry of these types of conditions and the layout of the movement joints that results.

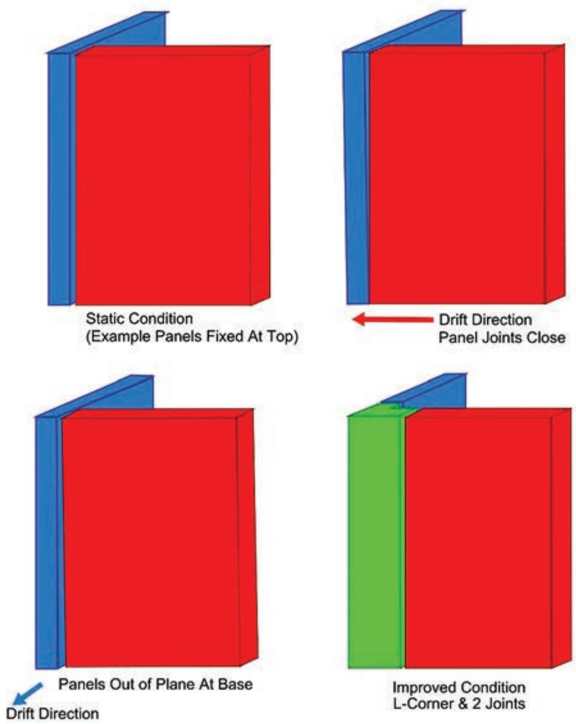

Figure 7. Drift cases at outside corners.

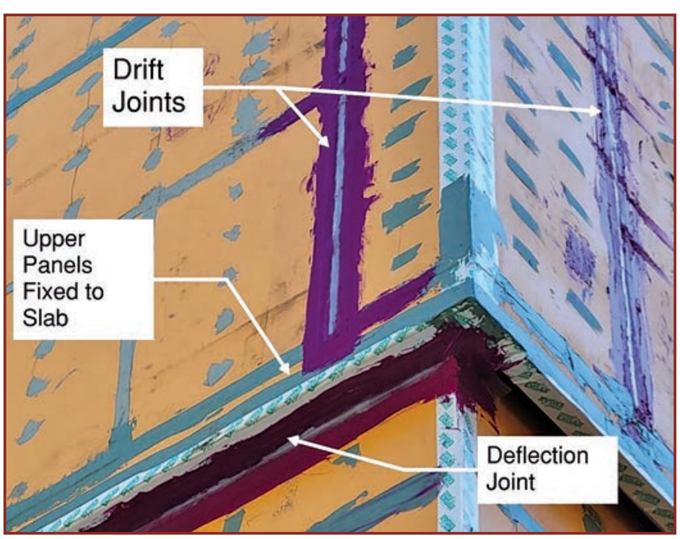

Figure 8. Drift and deflection joints at outside corners and floor lines.

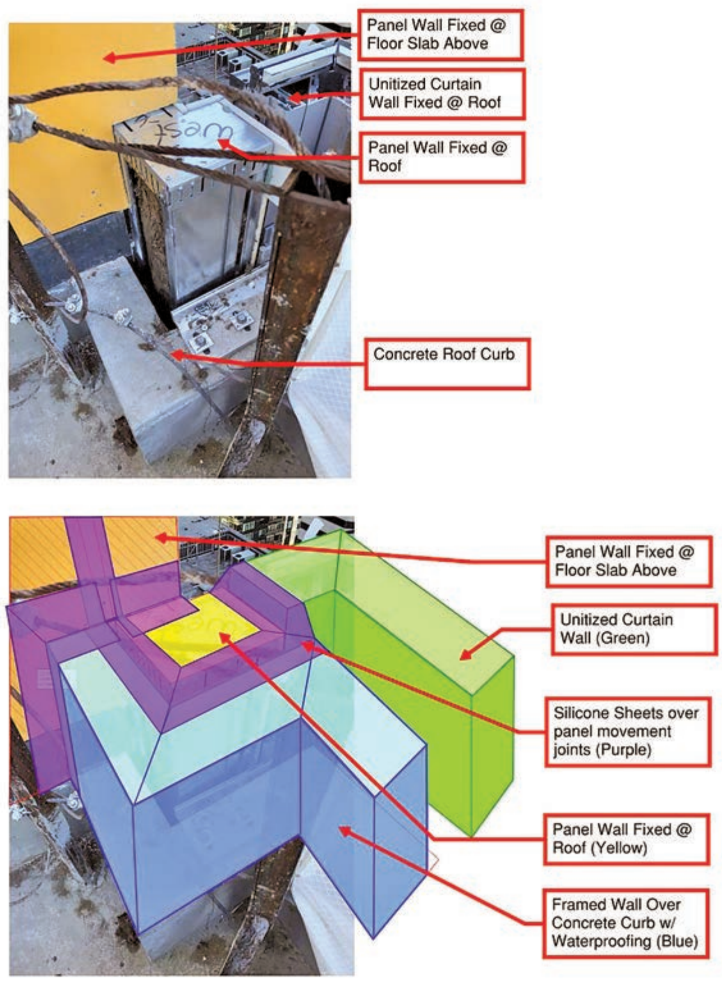

Figure 9. Schematic drift/deflection joint layout at parapet saddle.

Jambs at Curtainwalls and Window Walls

As discussed earlier in this paper, prefabricated wall panels typically have similarities to unitized curtainwalls; these similarities are also shared with window walls. However, prefabricated wall panels, curtainwalls, and window walls may not bear on the structure in the same way. For example, if a panelized frame wall is fixed to a floor slab at its base and is adjacent to a unitized curtainwall that is hung from the floor slab above, the two systems will deflect and translate differentially with each other, and the movement should be accounted for.

Similar conditions can occur with adjacent precast concrete panels, window wall systems, and other types of facade assemblies depending on how each one is connected to the structure.

Stick-built curtainwalls can also drift and deflect differentially from panel systems because the curtainwalls are often dead-loaded at a given floor and designed so that they rack with building movement rather than translate. Sufficient clearance should be provided between translating wall panels and racking curtainwall mullions.

Wall Panel Joint Waterproofing Material Selection and Sizing

The movement joints between panels are commonly waterproofed at the sheathing layer with materials designed to be compatible with the surrounding water-control layer. The materials used at this layer need to accommodate movement while still maintaining airtightness and watertightness.

Compression gaskets can be a very effective approach to consider when designing movement joints—and they have a proven track record of success with unitized glazing systems. In our experience, these gaskets work best when integrated with aluminum extrusions that mount to the perimeter of panels, as discussed earlier in this paper as well as in papers by Gannon[6] and Loush.[7]

Self-adhered membranes that have foil or polyethylene facers have been used to bridge these joints, but they often have limited movement capacity due to the facers. Although forming a bellows with these membranes over a backer rod can add a degree of movement flexibility, the range of allowable movement is often limited when joints are subject to both deflection and drift in more than one direction.

Sealant joints are another method of treating the panel movement joints. However, this approach can result in larger joints because sealant joints do not fully compress (they typically compress 25%–50%). Recalling the earlier example of drift joints that have elastic movement of ±0.9 in., if backer rod and sealant are used for waterproofing, those joints would need to be approximately 1.8 in. wide for sealant with 50% compression and designed to expand up to 2.7 in.

If sealants are used for drift joints at the cladding layer, the same movement should be accounted for. Note that the result could be wide and rather visible sealant joints at corners, jambs, and other transitions.

There are alternatives to consider to reduce the width of movement joints. Extruded silicone sheets are a suitable material that can be used for these types of joints because these sheets allow for multidirectional movement and can compress more than 50%. Care should be taken with the use of extruded silicone sheets as they can be subject to tears and punctures.

At the cladding layer, there are other options available beyond large sealant joints, but they need to be carefully considered. Open-joint cladding systems can allow for drift and deflection with adequate clearance gaps,. and closed-joint systems can use joints that rely on shiplap-type slip connections, splice plates, and other means of accommodating movement without the use of sealant. This can allow for smaller joints that are less conspicuous on the facade (see **Fig. 10**).

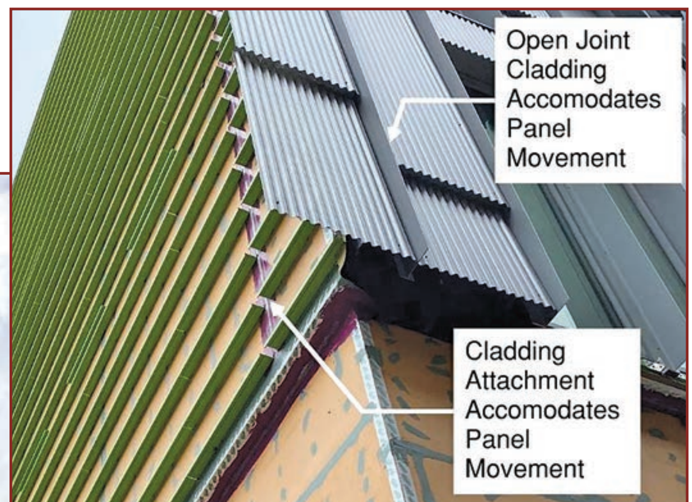

Figure 10. Open-joint cladding and furring spaced to accommodate drift.

Figure 11. Panelized wall facade nearing completion.

All of these steps—from determining the magnitude and directions of movement to laying out the panels and their joints to accommodate the movements, to designing waterproofing and cladding systems that work—are often necessary for the successful execution of a high-performance enclosure (see **Fig. 11**).

CONCLUSION

Building structures are designed to move, and this movement of the structure can affect the design of enclosure systems. This is especially the case in seismic regions and when panelized wall systems are used. Projects with these characteristics require careful attention during design.

Once the layouts and sizes of the movement joints are established in panelized walls and their cladding systems, thoughtful and intentional design can accommodate the movements of a facade system while still achieving an elegant aesthetic. The use of prefabricated panelized frame walls allows for faster installation on site, factory-controlled quality, and more-efficient project delivery. As such, we expect this emerging form of enclosure construction to become more broadly used in the future.

ACKNOWLEDGMENTS

The author of this paper would like to thank the members of the design, fabrication, and construction teams for their work on various projects using panelized walls, and for the high caliber of our regional industry practices without which this paper would not be possible. Some of the key team members on these various panelized facade projects include the Miller Hull Partnership, Graphite Design Group, Lease Crutcher Lewis, Sellen Construction, Performance Contracting Inc., and Northshore Exteriors Inc.

REFERENCES

1. International Code Council (ICC). 2018. *2018 International Building Code*. Washington, DC: ICC.
2. American Society for Civil Engineers (ASCE). 2016. *Minimum Design Loads for Buildings and Other Structures*. ASCE 7-16. Reston, VA: ASCE.
3. American Architectural Manufacturers Association (AAMA). 2017. *Recommended Static Test Method for Evaluating Windows, Window Wall, Curtain Wall and Storefront Systems Subjected to Vertical Inter-Story Movements*. AAMA 501.7-17. Schaumburg, IL: AAMA.
4. AAMA. 2018. *Recommended Static Test Method for Evaluating Window Wall, Curtain Wall and Storefront Systems Subjected to Seismic and Wind-Induced Inter-Story Drift*. AAMA 501.4-18. Schaumburg, IL: AAMA.
5. AAMA. 2018. *Recommended Dynamic Test Method for Determining the Seismic Drift Causing Glass Fallout from Window Wall, Curtain Wall and Storefront Systems*. AAMA 501.6-18. Schaumburg, IL: AAMA.
6. Gannon, K. 2018. "Ultra High Performance Concrete Panels for Prefabricated Wall Assemblies." *BEST Conference Building Enclosure Science and Technology*. https://www.brikbase.org/sites/default/files/Gannon.paper_.pdf.
7. Loush, K. C. 2018. "Prefabricated Exterior Wall Panels for Commercial Building Enclosures." *BEST Conference Building Enclosure Science and Technology*. https://www.brikbase.org/content/prefabricated-exterior-wall-panels-commercial-building-enclosures.
8. Lopes, G. C., R. Vicente, M. Azenha, and T. M Ferreira. 2017. "A Systematic Review of Prefabricated Enclosure Panel Wall Systems: Focus on Technology Driven for Functional Requirements." *Conference Proceedings of the 12th Conference of Advanced Building Skins*. https://doi.org/10.1016/j.scs.2017.12.027.

Are Air Barriers, Vapor Barriers, and Water-Resistive Barriers the Same?

Laverne Dalgleish

Air Barrier Association of America | Walpole, MA

ldalgleish@buildingprofessionals.com

IIBEC 2022 - Building for the Future

International Convention and Trade Show

March 17–22, 2022 | Orlando, FL

ABSTRACT

People use the terms "weather barrier," "vapor barrier," "air barrier," and "water-resistive barrier" interchangeably, which results in confusion in the industry. For example, design professionals may be critical of the water vapor transmission rate of a barrier material when the real problem is the air control area. To address this confusion, the presenter explains that the industry should first define these barrier terms as functions and then look at materials to determine whether they can provide the intended function. Proper understanding of these terms and what their function is in a building enclosure is becoming more critical as we move to higher-performing buildings.

SPEAKER

Laverne Dalgleish

Air Barrier Association of America | Walpole, MA

Laverne Dalgleish has spent most of his life in the construction business. As the executive director of the Air Barrier Association of America (ABAA), he has been involved in all their research projects, starting with a major one to demonstrate the energy savings of airtight buildings. Dalgleish is the coordinator for developing material specifications for air and water-resistive barriers and test methods to determine the material properties. As the developer of ABAA's Site Quality Assurance Program, he saw the problems caused by water intrusion and poor workmanship.

Are Air Barriers, Vapor Barriers, and Water-Resistive Barriers the Same?

There is no easy answer to the question, "Is a material a water-resistive barrier, an air barrier, or a vapor retarder?" Building science will tell you, "It depends" The answer depends on the material properties, the quality of the installation, and how and where the material is used in a building. The answer is further complicated by the range of terms used in building codes and construction standards to describe the various control layers within the building enclosure. For example, the *International Building Code* (IBC),[1] *International Residential Code* (IRC),[2] and *International Energy Conservation Code* (IECC)[3] use the terms "weather-resistant barriers," "water-resistive barriers," "air barriers," and "vapor retarders" (formerly called "vapor barriers") to identify different types of control layers. The IBC and IRC do not use the term "thermal insulation"; instead, they refer to "thermal isolation," "*R*-value" (thermal resistance), and "thermal transmittance" or "U-factor." This paper aims to help readers understand how the various control layers in a building enclosure are defined and cut through some of the confusion surrounding the key concepts and requirements related to control layers.

THE BASICS

Control layers are *not* materials. Each control layer serves a different function in a building enclosure assembly (**Fig. 1**) and is not defined by specific types of materials. The IBC,[1] IRC,[2] and IECC[3] have performance requirements that a material must meet to fulfill a specific control function. Specifically, for a material to be used within a control layer, the material must meet the material performance requirements, be designed to serve the control function in the building enclosure, and then be installed in a manner that ensures that the material will work either as a part of or individually as the control layer.

The building enclosure is composed of all control layers and is defined as an assembly designed to resist the loads imposed by all elements of the weather, including solar exposure, wind, windborne debris, heat, flooding, liquid water, and water vapor transmission. The Air Barrier Association of America (ABAA) has defined the control layers as follows (see **Appendix A** for related terms):

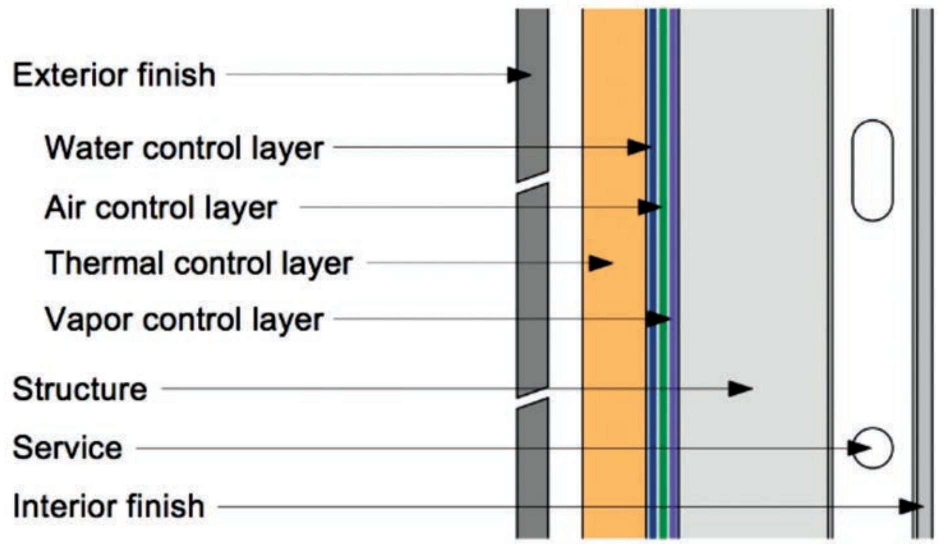

Figure 1. Control layers in a wall assembly.

- Air barrier: Plane of airtightness to provide a continuous barrier to the movement of air through building enclosures made up of air barrier materials, accessories, components and assemblies
- Water-resistive barrier: Assembly of materials and accessories behind an exterior wall covering that is intended to resist the further intrusion of liquid water that has penetrated the exterior covering into the exterior wall assembly
- Thermal insulation (heat barrier): Materials of relatively low heat conductivity used to shield against loss or entrance of heat by radiation, convection, or conduction
- Vapor retarder: Material designated to reduce the water vapor transmission rate through the material

A material may be able to function as more than one control layer. For a single material to serve multiple control-layer functions in a building enclosure, it must meet the performance requirements for each control layer.

The building enclosure is composed of all control layers and is defined as an assembly designed to resist the loads imposed by all elements of the weather, including solar exposure, wind, windborne debris, heat, flooding, liquid water, and water vapor transmission.

	Fluid-applied membranes	Self-adhered membranes	Gypsum-based materials	Mechanically fastened membranes	Closed-cell cellular plastic insulating board stock	Closed-cell, medium-density spray polyurethane foam
Water-resistive barrier	Yes	Yes	No	Yes	Yes	Yes
Air barrier	Yes	Yes	Yes	Yes	Yes	Yes
Vapor retarder	Yes	Yes	No	No	Yes	Yes
Thermal insulation	No	No	No	No	Yes	Yes

Table 1. Examples of standard building materials that may perform as multiple control layers

ABAA Material Specifications

The following are material specifications from the Air Barrier Association of America (ABAA):

ABAA S0001, *Standard for Air and Water-Resistive Barriers—Medium Density Closed Cell Rigid Spray Polyurethane Foam—Material Specification*

ABAA T0002, *Standard Test Method for Pull-Off Strength of Adhered Air and Water Resistive Barriers Using an Adhesion Tester*

ABAA S0003, *Standard for Air Barrier Material—Light Density Open Cell Semi-Rigid Spray Polyurethane Foam—Material Specification*

ABAA T0004, *Standard Test Method for Determining Gap Bridging Ability of Air and Water Resistive Barrier Materials*

ABAA S0005, *Standard for Air Barrier Material—Non-Insulating Sheathing—Gypsum Based—Material Specification*

ABAA S0006, *Standard for Air Barrier Material—Mechanically Fastened Engineered Polymer Film—Material Specification*

ABAA S0007, *Standard for Air and Water-Resistive Barriers—Self-Adhered Sheet Membrane, Bitumen Based—Material Specification*

ABAA S0008, *Standard for Air and Water-Resistive Barriers—Fluid Applied Membrane—Material Specification*

ABAA S009, *Standard for Air and Water-Resistive Barriers Fluid Applied Coating—Material Specification*

ABAA T00010, *Standard Method for Building Enclosure Airtightness Compliance Testing*

ABAA S0011, *Standard for Air Barrier Material—Low Density Open Cell Rigid Spray Polyurethane Foam—Material Specification*

ABAA S0012, *Standard for Air and Water-Resistive Barriers—Factory-Bonded Membranes to Sheathing—Material Specification*

ABAA S00013, *Standard for Air and Water-Resistive Barriers—Mechanically Fastened Commercial Building Wraps—Material Specification*

ABAA S0014, *Standard for Air and Water-Resistive Barriers—Rigid Cellular Thermal Insulation Board—Material Specification*

Table 1 illustrates generally how standard building materials may be able to perform as multiple control layers when properly installed. For each material in the table, ABAA has material specifications that provide material property performance requirements (see sidebar **ABAA Material Specifications**). Materials not evaluated by ABAA may have different requirements. The table is focused on the materials only; it should be noted that the materials are subject to application and installation requirements when used for the functions listed.

The objective for Table 1 is simply to show examples of materials that have the properties and meet the performance requirements to serve as multiple types of control layers. Note that some materials will only meet the control-layer requirements or provide the function of the control layer under specific circumstances. In the building codes, some of the performance requirements for cover-layer materials are straightforward, but others are not.

BUILDING CODE CHALLENGES

There is confusion in the industry surrounding what a vapor control layer is. One reason for this confusion is that the IBC and the IRC do not define "vapor retarder" or "vapor barrier." However, both codes include definitions for "vapor permeable membrane" and "vapor retarder class." The National Building Code of Canada[4] defines "vapour barrier" as "the elements installed to control the diffusion of water vapor."

Additionally, there are varying opinions regarding whether the vapor control layer should be defined as a retarder or as a barrier. Within the codes and standards industry, the terms "vapor barrier" and "vapor retarder" have been debated for years. In the United States in the 1970s, Professor Eric Burnett at Penn State University proposed the term "vapor retarder" as a preferable alternative to "vapor barrier" based on the opinion of some people that nothing is an absolute barrier. Furthermore, ASTM supported this position with their formal opinion that the meaning of the term "barrier" depends on the frame of reference. (For example, cars can breach a traffic "barrier" placed on a highway.) In fact, in the building enclosure industry, many people consider the terms "retarder" and "barrier" to be interchangeable.

The confusion over vapor control layers is compounded because the reasoning behind code requirements is often unstated. Prescriptive building codes must always be met. However, building codes do not provide detailed explanations of the reasons why you must follow the requirements. Sometimes, code requirements are "legacy" requirements carried over from previous building codes. Although you must comply with these requirements, understanding their rationale can be very difficult.

The confusion is exacerbated when there seem to be conflicts among requirements or definitions within a single code or between codes within the same jurisdiction. For example, the IBC[1] states that a Class III vapor retarder is rated between >1.0 perm and ≤10 perm. The same building code defines "vapor permeable membrane" as "the property of having a moisture vapor permeance rating of 5 perms (2.9×10^{-10} kg/Pa·× s·× m^2) or greater, when tested in accordance with the desiccant method using Procedure A of ASTM E96. A vapor permeable material, which is not defined, permits a greater passage of moisture vapor."

When a manufacturer requested a ruling from the International Code Council regarding what is considered a vapor retarder in the building code, the reported answer was, in part, that a vapor retarder is a material installed on the interior of a building and that the requirements in the building code only apply to interior-installed vapor retarders. The response was based on the IBC wording for vapor retarders. However, in cold climates, many buildings are constructed with the vapor retarder installed on the outside of the building on the warm side of the insulation. In hot and humid climates, the vapor retarder usually must be installed on the outside of the building's exterior sheathing, or on the outside of the thermal insulation.

To illustrate the range of specific language used in requirements for control layers, **Appendix B** summarizes relevant information from various building codes and standards. Clearly, work is needed to harmonize the requirements for the four control layers, as those layers must be considered together in the building enclosure design.

Building codes have specific requirements for what types of material can be used as vapor retarders in the various climate zones. Some people interpret these requirements to mean the vapor retarder is critical to stop moisture problems in buildings; however, they do not understand that vapor barriers stop only a small percentage of water vapor entering the building enclosure. The same building code allows you to meet the air leakage rate requirements for air barriers by demonstrating that you are using a material that meets the performance requirements for an air barrier material. There are some prescriptive requirements for air barrier installation, but you have no idea whether the material has been installed continuous on all six sides of the building. The only way to confirm a continuous air barrier system is to conduct a whole-building blower door test.

PUTTING WATER VAPOR IN PERSPECTIVE

As we compare the amount of moisture that is transported through a material by water vapor transmission to the amount of moisture that is transported through cracks, gaps and holes, there is a magnitude of difference. To illustrate this point, let us consider the magnitude of the measurements used in building codes for moisture. A perm is 57 ng per 1 $m^2 \times s \times Pa$ of water, and a nanogram is one-billionth of a gram. If the volume of a drop of water is 0.05 mL, the mass of that drop is 0.05 g. Although one drop is not a lot of water, it is the equivalent of hundreds of millions of nanograms.

The intent of the air barrier and vapor retarder code requirements is to limit how much moisture will enter the building assemblies while, at the same time, allowing the building assemblies to dry out.

The amount of water transported into the building assembly by vapor diffusion is miniscule compared to what is transported by air leakage (**Table 2**).[5] Therefore, the proper design and installation of both the air barrier and the vapor retarder are critical to these control layers' performance.

DESIGN CONSIDERATIONS

The designer is responsible for translating the owner's requirements into a functioning building. From all the requirements, the designer must incorporate the four control functions that will meet the loads being imposed: the water-resistive function, the air leakage control function, the heat flow control function, and the water vapor transport control function. For these functions, the materials are typically referred to as a water-restive barrier, an air barrier, a heat barrier (thermal insulation), and a vapor retarder, respectively.

The designer must deal with the four control layers at the same time since the material used for one function will affect other functions. Neil Hutcheson from the National Research Council (NRC) developed a list (**Fig. 2**) of the primary functions of a wall assembly. His point was that you cannot design one function without looking at all the functions.

Water-Resistive Barrier

A water-resistive barrier must be designed to resist bulk water, which continues across

Location	Volume of water vapor by air transport through a 1 in.² hole, oz. (gal.)		Volume of water vapor transmission through 39 × 39 in. of material using ASTM E96[5] desiccant method Procedure A, oz.		
	Midrise	High rise	5.7 ng (0.1 perm)	57 ng (1.0 perm)	570 ng (10 perm)
Seattle, WA	5543 (34.64)	18,120 (113.25)	0.166	1.66	16.6
San Francisco, CA	6812 (42.57)	20,738 (129.61)	0.166	1.66	16.6
Chicago, IL	5612 (35.07)	16,285 (1010.78)	0.166	1.66	16.6
Miami, FL	7941 (49.63)	17,577 (109.86)	0.166	1.66	16.6

Note: 1 in. = 25.4 mm; 1 oz. = 29.57 mL; 1 gallon = 3.785 L.

Table 2. Moisture movement: Comparing water vapor transmission through a material with air transport

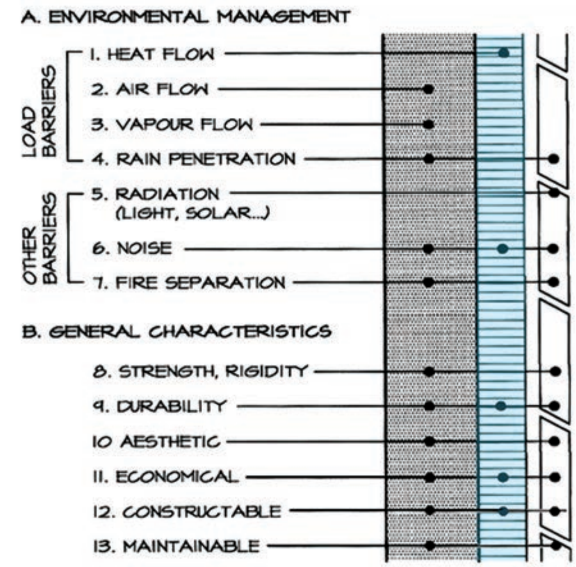

Figure 2. Primary functions of a wall assembly.

the complete structure, and to direct water to the exterior of the cladding layer. The material must be strong enough to resist any loads imposed from any hydrostatic head pressure, and it must be durable under real-life conditions such as high/low temperature cycles and high humidity in a typical building assembly cavity.

When choosing the material, you need to consider all potential modes of moisture transport. The first consideration is water resistance, where the material—when in contact with liquid water—needs to resist the passage of that water through the material. The most common test is a hydrostatic head test[6] where a 55 cm (22 in.) column of water is placed on the material for five hours (**Fig. 3**). The underside of the material is checked for drops of water coming out the other side. The limitation in this test is that it seems to work well on thin materials but not on thick materials. If you use this test method on 16 mm (⅝ in.) gypsum boards, there is a good chance that the boards will pass this test as there will not be drops of water on the underside, but the gypsum core may become mush.

Figure 3. Hydrostatic head test.

The water vapor transmission rate of water-resistive barrier materials ranges from being very low (a few ng) to being very high (over 2000 ng), but they all will resist liquid water ingress and shed liquid water. If the material is thick and the material is in a high-humidity atmosphere, the material may shed liquid water but absorb water vapor. Some of the water vapor going through a material will stay in the material and increase the moisture content of the material. The hygroscopic sorption isotherms test[7] will provide that information. To illustrate this point, let us consider the example of wood studs. An ASTM E96[5] desiccant test on no. 2 spruce studs shows the water vapor transmission rate as being less than 57 (m^2·s·Pa) or less than 1 perm. However, water vapor will build up within the wood until it reaches equilibrium. The amount of moisture content in the wood can exceed 20% by weight, which is typically the limit for wood being used in buildings.

Many water-resistive barriers do not provide any meaningful thermal insulation properties. (Closed-cell cellular plastic is an exception; this material can provide water resistance and thermal insulation.) Each material needs to be considered for their thermal insulation value, and then it must be determined whether the material will be used to provide all or some of the control layers.

Most—but not all—of the water-resistive barriers are also air barriers. House-wrap types of materials will shed liquid water and allow water vapor transmission through the material, but not all of them have the air leakage rate to be classified as an air barrier. Most of the self-adhered materials and the fluid applied materials installed as a water-resistive barrier are classified as also being an air barrier.

The water-restive barrier needs to be placed on the outside the building assembly that it is to protect. It will be placed behind the cladding system to stop further ingress of water and to then drain that water to the exterior of the building. Some designers place the water-resistive barrier on the substrate and then place insulation outside the water-restive barrier. Others place the water-resistive barrier on the outermost layer, immediately behind the cladding, on top of the insulation.

Air Barrier

An air barrier must be impervious to air leaking through the material; installed so that the entire air-barrier system is continuous (**Fig. 4**); strong enough to withstand the loads imposed by a wind/stack/mechanical effect; and durable throughout the expected life span of the building.

An air barrier material should be one of the easiest materials to choose as there are hundreds of air barrier materials already being used to construct buildings. To only provide the air control layer, the material can be placed anywhere in a building assembly. Think of a garden hose: you can pinch the hose at either end, or anywhere in between, and it will stop the water flow.

For air to leak into a building assembly, the same amount of air must leak out. The material needs to resist air leakage in either direction. Materials that are mechanically fastened need to resist the suction caused by wind on the leeward side of the building.

There are a few materials that are air barriers but not water-resistive barriers; A paper-faced gypsum board, OSB, plywood, and any wood-based products that are not treated would not be considered water-restive barriers.

All air barrier materials will have a water vapor transmission rate. The rate ranges from a few nanograms to thousands of nanograms. Depending on the water vapor transmission and the climate zone, the designer needs to consider where the air barrier material is placed in the building assembly.

Many types of the thermal insulation are not air barriers. All fibrous material has an air

Figure 4. Air barrier system for six sides of the building.

leakage rate that is greater than the maximum allowed for air barrier material. Cellulose fiber has been "dense-packed" into closed cavities to reduce the air leakage rate through the cavity, which is effective in reducing the air leakage rate but not enough to be considered an air barrier material. Most cellular plastic materials meet the requirement for air barrier materials, but some only do so at a minimum thickness. Light-density spray foam expanded polystyrene and one-component sealant foam (foam in a can), at normal thickness, will not meet the requirements for air barrier materials. Using this material can still improve the airtightness of a building assembly. Using one-component sealant foam to fill the gap between the window and the rough opening does not seal as well as using caulking, but it seals and insulates much better than stuffing glass fiber in the gap.

Thermal Insulation

Thermal insulation must control the heat flow through the assembly. All materials will have a thermal transmittance through the material. When heat flow of a building is modeled, all the materials, including the air films on the inside and the outside of the building assembly, are taken into consideration. The important thermal insulation value is that of the complete building assembly, not that of each individual material.

Where the insulation is placed is important. Insulation that keeps a surface above the dew point will reduce or eliminate condensation. Placing insulation on the outside of a building in cold climates can mean that warm moist air will not condense on the inside of the exterior sheathing.

Thermal bridging is becoming a more important consideration as we add more insulation to the building assembly. Codes for many areas of the United States require continuous exterior insulation to isolate many of the thermal bridges. In some codes, there could be up to 2% of the building enclosure area where there is no insulation. Today, as we add more insulation to the building, thermal bridging represents a larger percentage of the heat loss. A new standard—CSA Z5010:2021, *Thermal Bridging Calculation Methodology*[8]—offers a more accurate method for calculating the effect of thermal bridging.

Thermal insulation can provide a water-resistive barrier function if the material does not absorb liquid water. Closed-cell cellular plastic materials are commonly used to provide water resistance in addition to providing thermal insulation. Other types of thermal insulation such as cellulose fiber need to be fully protected from water, whereas others, like rock glass and slag wool, can withstand water intrusion as the material will allow the water to drain from the insulation.

Thermal insulation materials that provide water resistance normally are also classified as an air barrier. Fibrous insulations and light cellular plastic insulations, such as open-cell light-density spray polyurethane foam and expanded polystyrene are materials that are not classified as air barrier materials.

Each thermal insulation material will have a water vapor transmission rate, and depending on the tested value, it could be thousands of ng·s·m^2·Pa or it could be less than 10 ng·s·m^2·Pa.

Vapor Retarder

Each material in the building assembly has a water vapor transmission rate. Many design professionals want to identify a material that will have either a high water vapor transmission rate or a very low water vapor transmission rate. Keep in mind that the water vapor transmission rate of any material will vary as the environment conditions to which the material is subjected changes. Such changes will happen hour by hour.

Given that all materials have a water vapor transmission rate, there are materials that can provide both the water-resistive function and the vapor retarder function. There are also materials that are a class of vapor retarder, air barrier, and water-restive barrier. However, some materials that resist water (such as polyethylene film) are not used as a water-resistive barrier because they are susceptible to ultraviolet degradation.

All vapor retarders materials will have an air leakage rate. Materials with a high water transmission rate can have a low air leakage rate. The water vapor transmission rate of a material chosen will depend on the material chosen, the desired result of using the material, and where it is placed in the building assembly.

Many thermal insulation materials can provide the vapor retarder function at the same time that they provide thermal insulation.

There are many misconceptions about what a vapor retarder can provide. Many designers want the material to have a high water vapor transmission rate so that the building enclosure can dry out, whereas others want a very low water vapor transmission rate so moisture does not get in.

Building Assembly

Each material used in a building design will have properties that affect air leakage, water vapor transport, and heat flow through the building assembly. In most cases, the design will include materials that are only used for one function, even though those materials may be usable for more than one function. The designer must ensure that the material selected for a given function has the material properties to perform that function. Additionally, the designer must identify the material that will perform the function, design the building assembly to allow the material to perform the function, and take into consideration the impact that other materials will have on the performance of the building assembly.

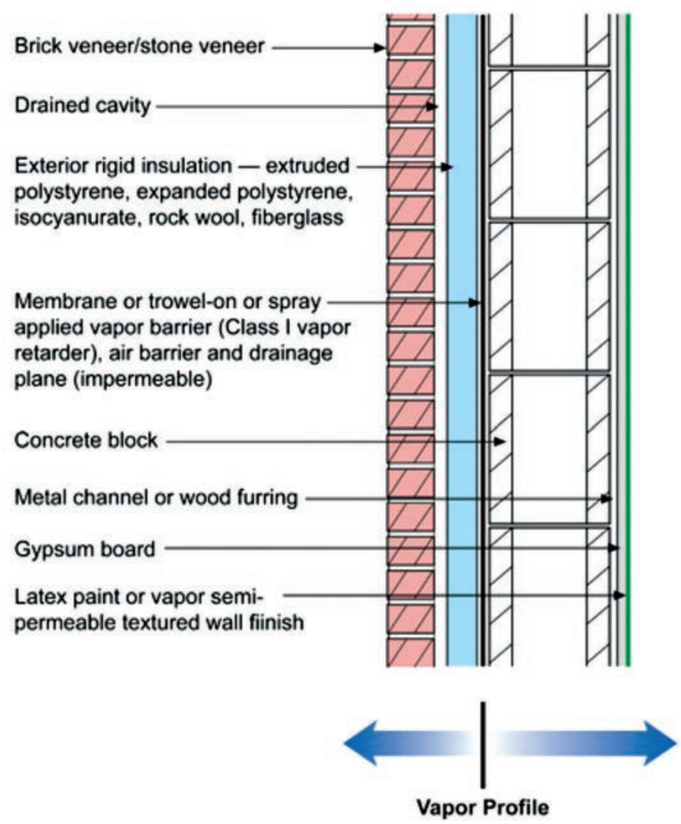

Figure 5. Basic wall construction.

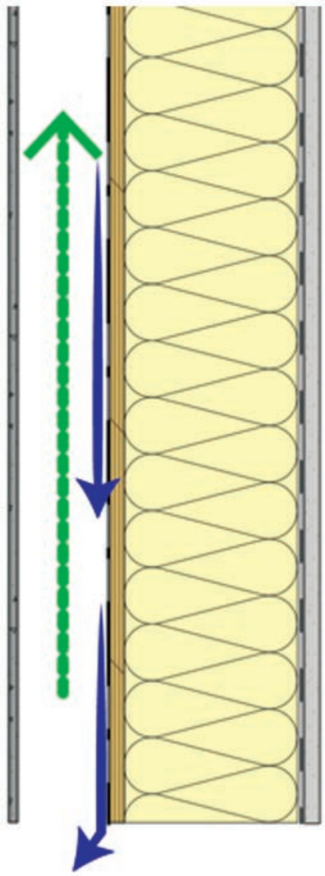

Figure 6. Drainage and ventilation of a wall.

Figure 5 presents a basic wall design to help illustrate the issues. Starting from the interior, most buildings have gypsum board to provide the interior finish. That gypsum board will be painted. The paint has water vapor transmission properties of a Class 2 vapor retarder. However, the designer could ignore the paint's water vapor transmission properties and specify a 6-mil polyethylene vapor retarder over the studs and insulation and behind the gypsum board. Even though the paint on the gypsum may meet code requirements, the designer selects the 6-mil polyethylene material to perform the function of limiting the water vapor transmission rate. In the IRC,[2] Section R703.1.2 requires that a water-resistive barrier shall be applied over studs or sheathing of all exterior walls. All water-restive barrier material will have a water vapor transmission rate. If cellular plastic is installed as part of the wall assembly, the material has a water vapor transmission rate that could qualify as meeting any local code requirements. That means there are potentially four materials that could fulfill the vapor retarder function of this simple wall assembly.

The air barrier providing the air leakage control function must be identified. The 6-mil polyethylene material used to reduce the water vapor transmission rate could also reduce the air leakage rate. To do that, the building design must include specific installation requirements. If the 6-mil polyethylene material is only serving a vapor control function, it does not need to be free of holes, lapped, sealed, and so on. However, if the material is also to provide an air leakage control function, the design and the installation process must be altered so that the material is free of holes, joints are lapped and sealed, and all penetrations through the material are sealed. It is always important to note whether a material is both an air barrier and a vapor retarder, just a vapor retarder, or just an air barrier. The interior gypsum boards—if properly installed—can provide the air-barrier function if all joints, penetrations, and terminations are properly sealed. The exterior sheathing—if properly installed—can provide the air barrier function and serve as the continuous insulation and the water-resistive barrier.

Thermal insulation is used to slow heat flow. Some insulating materials can serve more than one function. However, fibrous materials (glass fiber, rock fibers, etc.) cannot be used for the air barrier or water-restive functions of water vapor control. These materials are affected by the design and installation of all the materials in the wall assembly. Air flowing through the insulation, liquid water saturating the material, or high humidity in the cavity will affect the rate of heat flowing through the wall materials.

Various cellular plastic insulations can serve more than one control-layer function. Some types can be used for the heat flow control function, the air barrier function, the water-resistive barrier function, and the vapor control function. Even though such materials can perform multiple functions, most building enclosures are designed with the cellular plastic thermal insulation used only for the heat flow control function.

The exterior sheathing's main function is to be part of the structural support for the building enclosure. In commercial construction, glass-faced gypsum board is commonly used for sheathing. By itself, this material can be used for the air leakage control function if the board is properly installed and completely sealed. Note that the gypsum board alone does not provide the vapor control function or the water-resistive barrier function. Unless it is combined with additional materials, the gypsum material provides only minimal thermal insulation.

Cladding systems will shed most of the bulk water that might otherwise enter the building and are a critical component to a rainscreen assembly. The cladding will provide a means to shed water from the building enclosure. However, because it is expected that water will get past the cladding, a water-resistive barrier is required behind the cladding. Some cladding systems are marketed as being barrier systems or face-sealed systems. Those systems require continual maintenance to ensure that the barrier is kept intact. Most cladding systems are not designed to provide an air leakage control function, a water vapor transmission function, or a water-resistive barrier function.

Cladding systems will shed most of the bulk water from entering the building and are a critical component to a rainscreen assembly (**Fig. 6**).

In the simple wall assembly shown in Fig. 5, we can see that multiple materials can serve multiple functions. A material must be specified for each specific function, as the material selected will affect the design and installation requirements.

To evaluate the performance of the building assembly, the designer must always consider all materials that are going into that assembly, rather than considering materials individually.

The control layer that is most misunderstood is the vapor retarder. Designers may err by focusing on how a single material performs when it is tested in steady-state conditions. However, if the conditions are changed, the material's performance will also change, and that could affect the overall performance of the building enclosure.

Buildings are becoming more complicated, and some of the latest artificial materials have not been around long enough to determine how they will perform over the long term. The designer's job is therefore becoming increasing complicated.

INSTALLATION CONCERNS

As noted, the installation requirements for many materials depend on the function or functions those materials are to provide. For example, the installation requirements for a polyethylene sheet depend on whether it is to serve a vapor control function only or if it has both an air barrier function and a vapor control function. Similarly, the installation instructions for a flexible-sheet water-resistive barrier that is intended to only provide a water-resistive function are very different from the instructions for installing the material to provide both air barrier and water-resistive barrier functions.

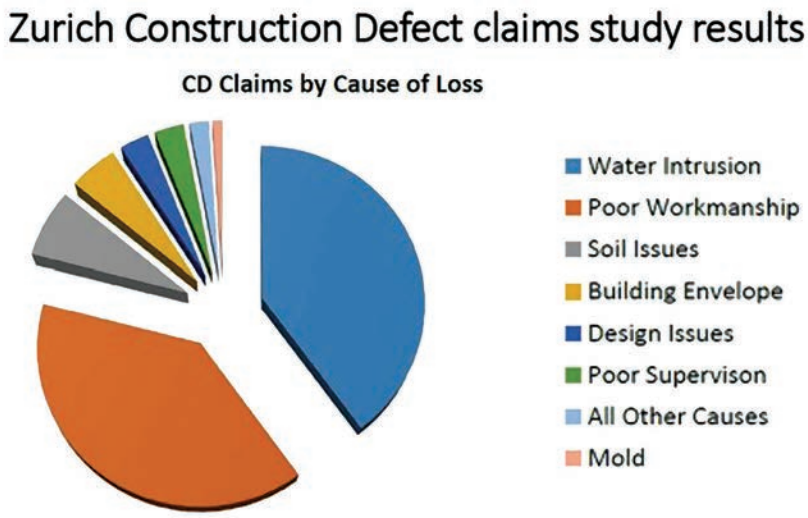

Figure 7. Construction defect (CD) insurance claims.

The performances of all materials going into a building are affected by the ways they were installed. For this reason, we should be concerned that our skilled labor force is shrinking, and few young people are entering the trades.

We are constructing more complex buildings, and using more sophisticated materials, while using a somewhat untrained workforce. This has resulted in buildings in need of repair even before the construction is completed.

Zurich, an insurance company, identifies water intrusion (including water vapor transported by air leakage) and poor workmanship as the overwhelming reasons for construction defect insurance claims (**Fig. 7**).

LOOKING FORWARD

The future is bright for the construction industry. Our communities need new buildings, and we also need to retrofit existing buildings. A key to our industry's success is ensuring that we have a workforce that is educated and ready for the challenges we face. We need trades that are properly educated, inspectors/auditors who can determine where and why materials are not performing as intended, and a whole industry that takes a systems approach using building sciences to set our guiding principles.

Another challenge that we face today is that many buildings require severe retrofits and repairs within just a few years of their construction.

Current construction projects are using sophisticated materials in complex designs with high performance requirements set for buildings. To help owners and design professionals properly design buildings, manufacturers should provide catalogs of building assemblies that have been tested as built assemblies. The documentation must provide the air leakage rate of the assembly, the thermal performance of the assembly, the water resistance of the assembly, and the water vapor transport rate of the whole assembly. With this information, we can build better buildings that will last an extended period.

REFERENCES

1. International Code Council (ICC). 2021. *International Building Code*. Country Club Hills, IL: ICC.
2. ICC. 2021. *International Residential Code*. Country Club Hills, IL: ICC.
3. ICC. 2021. *International Energy Conservation Code*. Country Club, IL: ICC.
4. National Research Council (NRC). 2019. *National Building Code of Canada*. Ottawa, ON: NRC. https://publications.gc.ca/collections/collection_2019/cnrc-nrc/NR24-28-2018-eng.pdf.
5. ASTM International. 2021. *Standard Test Methods for Gravimetric Determination of Water Vapor Transmission Rate of Materials*. ASTM E96/E96M-21. West Conshohocken, PA: ASTM International.
6. American Association of Textile Chemists and Colorists (AATCC). 2018. *Test Method for Water Resistance: Hydrostatic Pressure*. AATCC TM127-2017(2018)e. Research Triangle Park, NC: AATCC.
7. ASTM International. 2016. *Standard Test Method for Hygroscopic Sorption Isotherms of Building Materials*. ASTM C1498-04a(2016). West Conshohocken, PA: ASTM International.
8. CSA Group. 2021. *Thermal Bridging Calculation Methodology*. CSA Z5010:21. Toronto, ON: CSA Group.
9. American Society of Heating, Refrigerating, and Air-Conditioning Engineers (ASHRAE). 2019. *Energy Standard for Buildings Except Low-Rise Residential Buildings*. ANSI/ASHRAE/IES Standard 90.1. Peach Tree Corners, GA: ASHRAE.
10. ASTM International. 2017. *Standard Specification for Asphalt-Saturated Organic Felt Used in Roofing and Waterproofing*. ASTM E226-17. West Conshohocken, PA: ASTM International.
11. ICC. 2019. *Standard for Testing Airtightness of Building, Dwelling Unit, and Sleeping Unit Enclosures; Airtightness of Heating and Cooling Air Distribution Systems; and Airflow of Mechanical Ventilation Systems*. RESNET/ICC 380-2019. Country Club Hills, IL: ICC.
12. ASTM International. 2019. *Standard Test Method for Determining Air Leakage Rate by Fan Pressurization*. ASTM E779-19. West Conshohocken, PA: ASTM International.
13. ASTM International. 2011. *Standard Test Methods for Determining Airtightness of Buildings Using an Orifice Blower Door*. ASTM E1827-11. West Conshohocken, PA: ASTM International.

ADDITIONAL RESOURCES

- ASTM International. 2019. *Standard Test Method for Determining Rate of Air Leakage Through Exterior Windows, Skylights, Curtain Walls, and Doors Under Specified Pressure Differences Across the Specimen*. ASTM E283/E283M-19. West Conshohocken, PA: ASTM International.
- ASTM International. 2019. *Standard Specification for Air Barrier (AB) Material or Assemblies for Low-Rise Framed Building Walls*. ASTM E1677-19. West Conshohocken, PA: ASTM International.
- ASTM International. 2018. *Standard Test Method for Determining Air Leakage Rate of Air Barrier Assemblies*. ASTM E2357-18. West Conshohocken, PA: ASTM International.

APPENDIX A:

AIR BARRIER ASSOCIATION OF AMERICA (ABAA) STANDARD FOR AIR AND WATER RESISTIVE BARRIER—TERMINOLOGY

The air barrier industry, as represented by the Air Barrier Association of America (ABAA), has developed the following terms and definitions:

accredited

organization officially recognized or authorized that has the means to be able to complete a process to a specific requirement

accredited testing laboratory

organization accredited to ISO 17025 by a member of the IAF/ ILAC Multilateral Agreement, possessing the necessary competence to test material to the specific test method

air and water-resistive barrier assembly

combination of air and water-restive barrier materials and components, sealed together to reduce air leakage and water ingress with the use of air barrier accessories

air and water-resistive barrier component

premanufactured elements such as windows, doors and service elements that are installed in the environmental separator, which met a requirement for a maximum air leakage rate and water ingress

air and water-resistive barrier material

material that is primary element that provides a continuous barrier to the movement of air and resists liquid water that has penetrated the cladding system

air and water-resistive barrier material —adhesively backed commercial building wrap

flexible sheet material providing a plane of airtightness and a barrier to water ingress, which is intended to be mechanically attached and is generally installed behind the cladding system in exterior walls

air and water-resistive barrier material —board stock—rigid thermal insulation board

rigid insulating material providing a plane of airtightness and a barrier to water ingress, which is installed in exterior walls

air and water-resistive barrier material —factory-bonded membranes to sheathing

rigid sheathing board material where the air and water-resistive barrier material has been installed on the board in a factory

air and water-resistive barrier material —fluid-applied coating

fluid material that is not self-supporting and requires installation on a substrate for conducting the testing and is sprayed or rolled

air and water-resistive barrier material —fluid-applied membrane

liquid-based material that is sprayed, troweled, or rolled onto a continuous exterior substrate to provide the primary resistance to air leakage and water penetration

air barrier accessory

materials designated to maintain airtightness between air barrier materials, air barrier assemblies, and air barrier components, to fasten them to the structure of the building, or both (e.g., sealants, tapes, backer rods, transition membranes, nails/washers, ties, clips, staples, strapping, primers)

air barrier assembly

combination of air barrier materials and air barrier components, sealed together to reduce air leakage with the use of air barrier accessories

air barrier material

primary element that provides a continuous barrier to the movement of air

air barrier material —low-density spray polyurethane foam

rigid cellular plastic material that is formed in place by the catalyzed reaction of polymeric isocyanate and polyhydroxyl compounds, expanded with blowing agents and producing a 90%-plus open-cell product that has a density of approximately 12 to 27 kg/m^3 (0.76 to 1.74 lb/ft^3)

air barrier material —mechanically fastened commercial building wrap

flexible sheet material providing a plane of airtightness, which is intended to be mechanically attached and is generally installed behind the cladding system in exterior walls

air barrier material —medium-density spray polyurethane foam

rigid cellular plastic material that is formed in place by the catalyzed reaction of polymeric isocyanate and polyhydroxyl compounds, expanded with blowing agents and producing a 90%-plus closed-cell product that has a density of approximately 28 to 43 kg/m^3 (1.75 to 2.80 lb/ft^3)

air barrier material —noninsulating sheathing—gypsum based

panel products consisting of a noncombustible core primarily of gypsum with glass mat facers or paper facers with low air leakage rate

air barrier material —self-adhered sheet membrane

sheet/roll of material with an adhesive as part of the material that provides the primary resistance to air leakage and water penetration

APPENDIX A:

AIR BARRIER ASSOCIATION OF AMERICA (ABAA) STANDARD FOR AIR AND WATER RESISTIVE BARRIER – TERMINOLOGY

air barrier system
combination of air barrier assemblies and air barrier components, connected by air barrier accessories, that are designed to provide a continuous barrier to the movement of air through the building enclosure

air leakage
airflow through unintended openings in the building enclosure, which is driven by either, or both, positive (exfiltration) or negative (infiltration) pressure difference

air leakage rate [L/(s·m^2)] [cfm/ft^2]
airflow (L/s) [(cfm)] driven through a unit surface area (m^2) [(ft^2)] at a unit static pressure difference (Pa) [(lb)] across the material, assembly, or system

air sealing material
product used to seal up holes, gaps, and cracks in the building envelope to reduce air leakage

baseline pressure (bias, static pressure readings, and zero-flow pressure difference)
enclosure pressure with test fans off and sealed, recorded while the building is configured in the test condition

building assembly air leakage test
procedure to determine the air leakage rate of a building assembly comprised of air barrier materials and air barrier accessories

building envelope (enclosure)
assemblies consisting of roofs, walls, and foundations, and components such as skylights, windows, curtain walls, and doors that separate one environment from another environment and any adjoining unconditioned spaces using control layers

building envelope testing
defined boundary of the test sample to determine its air leakage rate of the building envelope excluding the HVAC-related devices (HVAC devices sealed)

certified
person officially recognized as possessing certain qualifications or meeting certain standards

contractor
individual, organization, or corporation who is responsible for meeting all requirements and obligations for the installation

enclosure pressure
differential pressure between the interior of the building being tested and the outdoors, measured with the outdoors as the reference

energy use test
air leakage test to determine airtightness of a building enclosure including HVAC-related penetrations in an "as used" state with minimal building envelope preparation

induced enclosure pressure
change in enclosure pressure caused by operation of fans during testing or operation

installer
individual who has the knowledge, skills, and ability to properly install materials and who is responsible for the actual installation and the site requirements under contract

licensed
official permission or permit to do, use, or own something granted by a party to another party as an element of an agreement between those parties

operational envelope test
air leakage test to determine airtightness of a building enclosure including HVAC-related penetrations

supplier
entity that provides a material or product

vapor retarder (barrier)
material with a low water vapor transmission rate

water-resistive barrier
material behind an exterior wall covering that is intended to resist liquid water that has penetrated behind the exterior covering from further intruding into the exterior wall

water vapor transmission rate
quantity of water vapor transmitted through unit area of a test specimen in unit time under specified conditions of temperature, humidity, and thickness

APPENDIX B:

DEFINITIONS AND REQUIREMENTS FOR CONTROL LAYERS FROM BUILDING CODES AND STANDARDS

This appendix focuses on requirements included in the *International Building Code*[1] (IBC), the *International Residential Code*[2] (IRC), *International Energy Conservation Code* (IECC),[3] and ASHRAE 90.1-2019.[9] The building codes and building performance standards have requirements for control layers and set performance levels. Many control layers require more than a single material. It is up to the design professional or the builder to show that they have chosen a set of materials that can provide the control layer and that these materials meet the performance requirements set forth in the code. As an example, the IECC and ASHRAE 90.1 require an air barrier and the material(s) used to provide that control function cannot have an air leakage rate greater than 0.02 L/(s·m²) at a pressure difference of 75 Pa (0.004 cfm/ft²). The designer should always designate control layer placement wherever control is needed, whether throughout the entire building or a portion thereof.

BUILDING ENCLOSURE

The complete building enclosure provides a barrier to all the elements of the weather, separating the interior environment from the outside environment and providing protection from rain, hail, snow, wind, windborne debris, floods, sun exposure, and more. The four control layers within the design of the building enclosure serve the water-resistive function, the air leakage control function, the heat flow control function, and the water vapor transport control function. The building enclosure encompasses all the building assemblies of the control layers together; these layers are made up of components and subassemblies, which in turn are made up of materials and accessories.

The building enclosure is all inclusive, but it is broken down into the four control layers. The design and installation of the control layers vary depending on the layers' location in the building. For example, how the ingress of liquid water is controlled varies depending on whether the control layer is part of the roof, wall, or foundation assembly. The design and construction of the control layer will also vary depending on the location of the building and the loads on the building.

WEATHER-EXPOSED SURFACES

The 2021 editions of the IBC and IRC do not define "weather barrier" but the IBC does define "weather-exposed surfaces" as follows:

> Surfaces of walls, ceilings, floors, soffits and similar surfaces exposed to the weather except for the following:
> — Ceilings and roof soffits enclosed by walls, fascia, bulkheads or beams that extend not less than 12 inches (305 mm) below such ceiling or roof soffits.
> — Walls or portions of walls beneath an unenclosed roof area, where located a horizontal distance from an open exterior opening equal to not less than twice the height of the opening.
> — Ceiling and roof soffits located a minimum horizontal distance of 10 feet (3048 mm) from the outer edges of the ceilings or roof soffits.

WATER-RESISTIVE BARRIER

Although much of the rain that lands on the face of the cladding is shed off, water will intentionally or unintentionally get past the cladding system. Therefore, the water-resistive barrier is intended resist the water ingress and keep the building assembly dry. The water-resistive barrier includes the use of flashings to expel the water to the exterior face of the wall and not just to the exterior face of the water-resistive barrier assembly.

The IBC[1] and the IRC[2] use the following definition of water-resistive barrier: "A material behind an exterior wall covering that is intended to resist liquid water that has penetrated behind the exterior covering from further intruding into the exterior wall assembly." However, the 2021IECC[3] and ASHRAE 90.1[9] do not use the term "water-resistiv barrier."

Both the IBC (Section 1403.2) and the IRC (Section 703.2) indicate the minimum requirements for the water-resistive barrier as "not fewer than one layer of No. 15 asphalt felt, complying with ASTM D226 for Type 1 felt or other approved [materials]."

ASTM 226-17,[10] *Standard Specification for Asphalt-Saturated Organic Felt Used in Roofing and Waterproofing*, provides the following physical requirements for Type 1 asphalt-saturated roofing felt.

- Average minimum breaking strength with fiber grain: 5.3 kN per meter of width (30 lb per inch of width).
- Average minimum breaking strength across fiber grain: 2.6 kN per meter of width (15 lb per inch of width).
- Pliability at 25°C (77°F): The 10 strips tested shall not crack when bent 90 degrees at a uniform speed over a rounded corner of 12.7 mm (½ in.) radius.
- Loss on heating at 105°C (221°F) for 5 hours: 4% maximum.

Note that the IBC and IRC list minimum requirements, but these minimum requirements may not provide the performance necessary to achieve the owner's requirements or additional requirements of the design professional. Each material type will have additional requirements to ensure that the material will perform as intended as a part of or wholly as the control layer. These requirements include additional necessary components as well as instructions for their specific installation to achieve the control-layer requirements.

AIR BARRIER

The 2021 IBC[1] does not define "air barrier," but it does define "air impermeable insulation" as follows: "An insulation having an air permeance equal to or less than 0.02 L/s × m² at 75 Pa pressure difference tested in accordance with ASTM E2178 or ASTM E283."

The IRC[2] defines "air-impermeable insulation" similarly, as "an insulation having an air permeance equal to or less than 0.02 L/s × m² at 75 Pa pressure difference tested in accordance with ASTM E2178 or ASTM E283. For the definition applicable in Chapter 11, see Section N1101.6."

In Chapter 11, Section N1101.6 (R202), Energy Efficiency—General, the IRC provides the following definitions:

APPENDIX B:

DEFINITIONS AND REQUIREMENTS FOR CONTROL LAYERS FROM BUILDING CODES AND STANDARDS

- Air impermeable insulation: An insulation that functions as an air barrier material.
- Air barrier: One or more materials joined together in a continuous manner to restrict or prevent the passage of air through the building thermal envelope and its assemblies.
- Continuous air barrier: A combination of materials and assemblies that restrict or prevent the passage of air through the building thermal envelope.

The IECC[3] defines "air barrier" as "one or more materials joined together in a continuous manner to restrict or prevent the passage of air through the building thermal envelope and its assemblies."

In ASHRAE 90.1,[9] "continuous air barrier" is defined as "the combination of interconnected materials, assemblies, and sealed joints and components of the building envelope that minimize air leakage into or out of the building envelope."

The terms and definitions regarding air barrier, vapor retarders, and water-resistive barriers included in the IBC, IRC, IECC, and ASHRAE 90.1 are somewhat harmonized. All the terms are describing control-layer functions without describing them as such.

In the criteria for Chapter 13, Energy Efficiency, the IBC requires that buildings be designed and constructed in accordance with the IECC (Section 1301.1.1).

In Section N1102.4 (R402.4), Air Leakage (Mandatory), the IRC requires the building thermal enclosure "shall be constructed to limit air leakage in accordance with the requirements of Sections N1102.4.1 through N1102.4.5."

IRC Section N1102.4.1 (R402.4.1), Building Thermal Envelope, requires that the building thermal enclosure "shall comply with Sections N1102.4.1.1 and N1102.4.1.2. The sealing methods between dissimilar materials shall allow for differential expansion and contraction."

In Sections N1102.4.1.1 and N1102.4.1.2, the IRC requires that the installation follow the manufacturer's instructions and the criteria in Table N1102.4.1.1. The building or dwelling unit must be tested to verify that the air leakage rate is not greater than (a) 5 air changes per hour in Climate Zones 1 and 2, or (b) 3 air changes per hour in Climate Zones 3 through 8. The testing is to be done in accordance with RESNET/ICC 380-2019,[11] *Standard for Testing Airtightness of Building, Dwelling Unit, and Sleeping Unit Enclosures; Airtightness of Heating and Cooling Air Distribution Systems; and Airflow of Mechanical Ventilation Systems*; ASTM E779-19,[12] *Standard Test Method for Determining Air Leakage Rate by Fan Pressurization*; or ASTM E1827-11,[13] *Standard Test Methods for Determining Airtightness of Buildings Using an Orifice Blower Door* and reported at 0.2 in. water gauge (50 Pa). The building official can require that the testing be done by an approved party with the report signed by the third party. The clause goes on to set out additional requirements.

In Section C402.5, Air Leakage—Thermal Envelope (Mandatory), the IECC requires the following: "The *building thermal envelope* shall comply with Sections C402.5.1 through Section C402.5.11.1, or the *building thermal envelope* shall be tested in accordance with Section C402.5.2 or C402.5.3. Where compliance is based on such testing, the building shall also comply with Sections C402.5.5, C402.5.6, and C402.5.7."

In Section C402.5.1.1, Air barrier construction the IECC sets out requirements for the air barrier system installation.

IEEC Section C404.5.1.3 is a material requirement, where the material can have an air permeability not greater than 0.004 cft/ft^2 (0.02 L/s ×m^2) under a pressure difference of 0.3 in. water gauge. Sixteen materials are listed as meeting this requirement for the purposes of the IRC.

IEEC Section C402.5.1.4 is an assembly requirement: "Assemblies of materials and components with an average leakage not greater than 0.04 cfm/ft^2 (0.2 L/s × m^2) under a pressure difference of 0.3 inch of water gauge (w.g.) (75 Pa) when tested in accordance with ASTM E2357, ASTM E1677, or ASTM E283 shall comply with this section." The section lists three "assemblies," but these are not really assemblies because they are simply units put together—no penetrations, terminations, or fenestrations are included.

In Section C402.5.3, Building thermal envelope testing, the IECC requires the building enclosure to be tested for air leakage and the measured air leakage shall not exceed 0.40 cfm/ft^2 (2.0 L/s × m^2) at a pressure difference of 0.3 in. water gauge (75 Pa).

ASHRAE 90.1[9] Section 5.4.3, Air Leakage, requires that "Air leakage control for the *building envelope* shall comply with this section. Materials and assemblies that are part of the *continuous air barrier* and *fenestration* and *doors* shall comply with Section 5.8.3."

In Section 5.4.3.1, Continuous Air Barrier, ASHRAE 90.1 requires that "The *exterior building envelope* and the *semiexterior building envelope* shall have a *continuous air barrier* complying with Sections 5.4.3.1.1 and 5.4.3.1.2."

In Section 5.4.3.1.1, Whole-Building Air Leakage, ASHRAE 90.1 requires that "Whole-building pressurization testing shall be conducted in accordance with ASTM E779 or ASTM E1827 by an independent third party. The measured air leakage rate of the *building envelope* shall not exceed 0.40 cfm/ft^2 under a pressure differential of 0.3 in. of water, with this air leakage rate normalized by the sum of the above-grade and below-grade building envelope areas of the *conditioned space* and *semi-heated space*." The section goes on to show compliance requirements for *conditioned space* and *semi-heated space* and then lists exceptions.

ASHRAE 90.1 Section 5.4.1.2, Continuous Air Barrier Design and Installation, lists a number of requirements for the air barrier.

In ASHRAE 90.1 Section 5.8.3, Air Leakage Section 5.8.3.1, Testing, Acceptable Materials and Assemblies, it states that "Air leakage for materials or assemblies used as components of the *continuous air barrier* shall be determined in accordance with the test method and minimum air pressure specified in Table 5.8.3.1 and shall not exceed the maximum air leakage specified in Table 5.8.3.1 when using Exception 3 of Section 5.4.3.1.1."

ASHRAE 90.1 Table 5.8.3.1 lists the test methods to be used for materials and for assemblies and the performance requirements.

VAPOR RETARDER

The vapor retarder (or vapor barrier) is the control layer intended to reduce the water vapor transmission rate both through a material

APPENDIX B:

DEFINITIONS AND REQUIREMENTS FOR CONTROL LAYERS FROM BUILDING CODES AND STANDARDS

and through an assembly. Many people think that this control layer is provided by a single material whereas the complete building assembly will affect the moisture transport into and out of the building assembly. Wetting and drying can be to the exterior or to the interior of the assembly, as all current materials allow the transfer to be in both directions. It is important to understand that as the material is tested at a single difference in atmospheres, the results are for comparison purposes only, and the results for a material will change when the atmospheres change.

The ASTM E96[5] test method is conducted at a single steady-state atmosphere difference. In the Procedure A desiccant method, there is 0% relative humidity (RH) on one side and 50% RH on the other side with a temperature of 23°C (73°F). In the Procedure B water method, there is 100% RH on one side and 50% RH on the other side with a temperature of 23°C. If the atmosphere difference (RH or temperature) is changed, the water vapor transmission also changes.

The IBC[1] and the IRC[2] do not define "vapor retarder" or "vapor barrier," but the codes do define "vapor permeable" and "vapor retarder classes" as follows:

- Vapor permeable: The property of having a moisture vapor permeance rating of 5 Perms (2.9×10^{-10} kg/Pa· s· m^2) or greater, when tested in accordance with the desiccant method using Procedure A of ASTM E96. A vapor permeable material permits the passage of moisture vapor.
- Vapor retarder classes: A measure of a material or assembly's ability to limit the amount of moisture that passes through that material or assembly. Vapor retarder class shall be defined using the desiccant method with Procedure A of ASTM E96/E96M-21, *Standard Test Methods for Gravimetric Determination of Water Vapor Transmission Rate of Materials* as follows:
    - Class I: ≤0.1 perm rating
    - Class II: >0.1 perm to ≤1.0 perm rating
    - Class III: >1.0 perm to ≤10 perm rating

The IECC and ASHRAE 90.1 do not define "vapor retarder" or "vapor barrier."

The construction industry has assigned the following names to the different vapor retarder classes:

- Class I is called "vapor barrier."
- Class II is called "vapor retarder."
- Class III is called "semipermeable."
- Class IV is called "permeable."

The IBC and IRC do not have a Class IV, but any material with water vapor transmission greater than 10 perm is considered a "vapor-permeable" material. Air barrier material manufacturers market their products as "vapor permeable" even though there is no consensus-based term and definition for "vapor permeable."

IBC Section 1404.3, Vapor Retarders, requires that "a vapor retarder shall be provided on the interior side of framed walls in accordance with Tables 1404.3(2) and 1404.3(3)."

IBC Table 1404.3(2) indicates that a Class I and II vapor retarders are not permitted in Zones 1 and 2. Class I vapor retarders are not permitted in Zones 3 and 4 (except Marine 4). Class I, Class II, and Class III, in certain assemblies, are permitted in Zones 5, 6, 7, 8, and Marine 4."

IBC 1404.3.2, Class III Vapor Retarders. states that "Only Class III vapor retarders shall be used on the interior side of frame walls where foam plastic insulating sheathing with a perm rating of less than 1 is applied in accordance with Table 1404.3.2 on the exterior side of the frame wall."

IBC 1404.3.3 deems some materials to meet the requirement for the three classes.

IBC R702.7, Vapor Retarders, requires Class I or II vapor retarders on the interior side of frame walls in Climate Zones 5, 6, 7, and 8 and Marine 4 and then lists three exceptions.

IBC 702.7.1 states that Class III vapor retarders are permitted when any one of the conditions in Table R702.7.1 is met.

IBC 702.7.2 then lists material that are deemed to meet one of the classes.

Wind Resistance of Standing Seam Roofs and Roof-Mounted Solar Panels

Richard J. Davis, PE, FSFPE, MASCE

FM Global | Manomet, MA

richard.davis@fmglobal.com

IIBEC 2022 - Building for the Future

International Convention and Trade Show

March 17–22, 2022 | Orlando, FL

ABSTRACT

Standing seam roofs (SSRs) behave somewhat differently than other roof coverings when exposed to wind uplift pressures. Their design came under closer scrutiny after Hurricane Andrew struck south Florida in 1992. Since then, our knowledge of SSR wind resistance has increased considerably, such that SSRs can now be properly tested, designed, and installed to meet relatively high wind design pressures, including in perimeter and corner roof areas.

This presentation explains that external seam clamps or wind clamps can substantially increase the wind uplift resistance of an SSR if they properly fit the seam profile and are installed correctly. They may change the failure mode of the SSR, and the limiting factor of the enhanced assembly will likely be the strength of the internal clip. When securing solar panels to an SSR, it is important that the clamps used to secure them be attached to each deck rib to follow the wind load path of the SSR design and prevent overloading internal clips.

SPEAKER

Richard J. Davis, PE, FSFPE, MASCE

FM Global | Manomet, MA

Richard J. Davis has been working in loss prevention engineering for 47 years. He has written and revised a number of FM Global data sheets on construction, including the ones for standing seam roofs and roof-mounted solar panels. Davis has also served on many external committees working on codes and standards development, including the ASCE 7 wind load subcommittee for the last three revision cycles. He was task committee chair for the chapter on roof-mounted equipment during the latest ASCE 7 revision, and he contributed to the 2017 revision of the Structural Engineers Association of California's *Wind Design for Solar Arrays* (SEAOC PV2). Davis has given numerous presentations on wind design, both internally for FM Global wind specialists and externally to various roofing associations.

Wind Resistance of Standing Seam Roofs and Roof-Mounted Solar Panels

The wind resistance of standing seam roofs (SSRs) came under scrutiny following Hurricane Andrew in south Florida in 1992. There were numerous SSR blowoffs during this extreme wind event (**Fig. 1**). Additional information can be found in the article "Insights on Metal Roof Performance in High-Wind Regions."[1]

Many SSRs at that time were tested in a 10 × 10 ft wind uplift test apparatus. Typically, SSR panel spans between purlins were 5 ft on center. Thus, the test allowed for testing of only two spans and, usually, five 2-ft-wide panel sections. The ends of the panels were secured to the test assembly. In practice, SSR panels were made in lengths of up to 40 ft. Structurally, they spanned continuously over four or more supports, and the flat portion (pan) of the panels between ribs was typically fastened only to the eave struts. The 10 × 10 ft test did not structurally replicate actual installations, and, consequently, this test overestimated the pressure resistance of the assembly. After some wind-loss investigations, it was shown that the failure pressures of some assemblies that had ultimate wind ratings of 90 lb/ft^2 based on the smaller 10 × 10 ft tests were actually as low as 40 lb/ft^2, considering reported nearby wind speeds and pressure coefficients in the American Society of Civil Engineers' *Minimum Design Loads and Associated Criteria for Buildings and Other Structures* (ASCE 7).[2,3]

The problem was exacerbated because most installations did not reduce the purlin spacing (or otherwise enhance the wind resistance) in Zones 2 (roof perimeter) and Zones 3 (roof corners) to account for higher wind pressures there, as quantified by ASCE 7.

RECOMMENDED TESTS

After Hurricane Andrew, attention shifted from using wind resistance pressures from the smaller 10 × 10 ft test to using findings from the Army Corp of Engineers test, which later became ASTM E1592, *Standard Test Method for Structural Performance of Sheet Metal Roof and Siding Systems by Uniform Static Air Pressure Difference*.[4] This test can be used for not only multiple widths of panels but also

Figure 1. Typical wind failure of a standing seam roof.

multiple spans. It can accept assemblies up to 12 ft wide and 24 ft long.

For wind uplift tests, a 6-mil-thick (0.006-in.-thick) pleated polyethylene air barrier is placed over the purlins on the test apparatus and the metal roof is constructed over the airbag. A positive pressure is applied to the underside of the roof panels. Sufficient pleating is provided such that the air barrier comes in complete contact with the underside of the panels. Current SSR panels typically do not exceed 2 ft in width, which allows for testing of five full-panel widths and two partial widths at the sides for proper edge sealing. Given typical spans, three or four full spans can be accommodated in the test. Each pressure increment is held for at least 1 minute. After each pressure increment is held, the pressure is zeroed out and the roof panels are checked for signs of permanent deformation.

FM 4471, *Approval Standard for Class 1 Panel Roofs*,[5] is an FM Approvals test that is used for panel roofs such as SSRs. "Class 1" refers to the fire rating based on underside fire exposure of the assembly. The test standard includes a 12 × 24 ft wind uplift test similar to the ASTM E1592 test method. A similar airbag is used; each test pressure level is held for a minimum of 1 minute; the pressure is zeroed out after each increment; and the roof panels are checked for permanent deformation.

In FM 4471, the minimum wind uplift pressure rating is 60 lb/ft^2. This is the ultimate resistance provided. It can apply in allowable strength design (such as based on an approximate 100-year MRI wind speed) where the design pressure is equal to or less than 30 lb/ft^2, resulting in a safety factor of 2.0. There are other ways to compare this rating to what is required, such as:

A. Calculate the pressure needed using ultimate wind speeds, such as per ASCE 7-16[2] or ASCE 7-22.[3] That calculation can then be converted back to an allowable pressure by multiplying by 0.6. Then the safety factor can be multiplied by the resultant.
B. Calculate the pressure needed using ultimate wind speeds, such as per ASCE 7-16, then divide that by a resistance factor Φ to get the final ultimate resistance required. Values can vary depending on the type of roof system being used. For additional information, see *Climate Change Adaption Technologies for Roofing* by Baskaran et al.[6]

The FM 4471 wind test has two pass-fail criteria. The first is that there can be no permanent deformation of the roof panels at the maximum design pressure. The second criteria is that the ultimate rating is the last pressure held for 1 minute before failure occurs. So, if

Zone	GC_p (dimensionless)	$GC_p + GC_{pi}$ for enclosed building	$GC_p + GC_{pi}$ for partially enclosed building
3	3.2	3.38	3.75
2	2.3	2.48	2.85
1	1.7	1.98	2.25
1′	0.9	1.08	1.45

GC_p = external pressure coefficient; GC_{pi} = internal pressure coefficient.

*Based on an effective wind area of 10 ft^2.

Table 1. External pressure coefficients for low-slope roofs per ASCE 7-16.[2]*

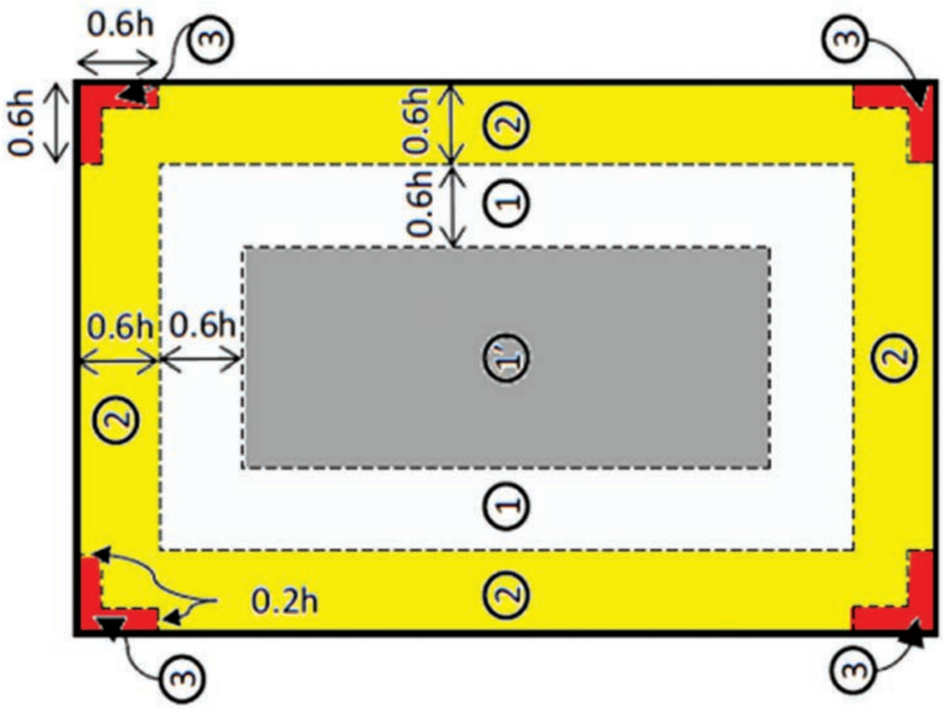

Figure 2. Plan of zone dimensions for low-slope roofs based on ASCE 7-16.[2]

an assembly withstands 45 lb/ft^2 of wind uplift pressure without permanent deformation and withstands 90 lb/ft^2 before failure, it receives a 90 lb/ft^2 wind uplift pressure rating.

There are many similarities between FM 4471 and ASTM E1592. One major difference is that ASTM E1592 requires deflection measurement at each pressure interval, with a minimum of 6 pressure intervals.

ROOF WIND ZONES

The *International Building Code* (IBC) wind load criteria in the 2018[7] and 2021[8] editions are based on the 2016 edition of ASCE 7.[2] In ASCE7-16, there are four wind zones for low-slope (≤7 degrees) roofs, which many SSRs are. It is important that SSRs provide adequate wind uplift pressure resistance for each zone. These zone dimensions, and related pressure coefficients, did not change in ASCE 7-22.[3] The zones are Zone 3 (corners), Zone 2 (perimeters), Zone 1 (field zone), and Zone 1′ (inner field zone). During the 2016 revision of ASCE 7, the external pressure coefficient GC_p of the wind design pressures for Zone 1 was increased considerably (by 70%), whereas the GC_p for Zone 1′ was decreased by 10% (**Table 1**). Another major change for low-slope roofs in ASCE 7-16 is the zone dimensions (**Fig. 2**). The values for internal pressure coefficients GC_{pi} remains unchanged at 0.18 for enclosed buildings and 0.55 for partially enclosed buildings.

While it is acceptable to use a system that meets the Zone 3 requirements throughout the entire roof, that may not be cost effective. To be cost effective and practical, the same SSR assembly could have design variations with up to four different wind ratings, one for each zone. This approach is considered a performance-based design. This can be achieved in different ways, but it is commonly done by spacing purlins closer together in the more stringent wind zones and, in some cases, by adding external seam clamps (ESCs).

A prescriptive enhancement option could also be considered, as discussed in FM Global *Property Loss Prevention Data Sheet 1-31: Panel Roofs*,[9] if it would be acceptable to the authority having jurisdiction. That approach would also consider similar methods of enhancement as described previously.

WIND PERFORMANCE OF SSRs

There are numerous variables that influence the wind resistance of SSRs. They include:

- Type of metal (steel, aluminum)
- Panel thickness and yield strength
- Rib spacing
- Rib type
- Panel embossments
- Purlin spacing
- Purlin thickness and yield strength
- Seaming methods
- Clip type
- Clip securement—number and size of screws
- ESC size and shape type

PURLINS, INTERNAL CLIPS AND THEIR ATTACHMENT

Purlins in metal building systems typically have a minimum thickness of 16 gauge (0.060 in.) and are made of high-strength steel (≥50 ksi yield stress). The number of screws per internal clip can vary from one to four, and the screw size is usually no. 10, no. 12, no. 14 (¼ in.), or ⅜ in. Obviously, using more screws and larger screws increases pullout resistance. But for cost effectiveness, all failure modes should be reasonably close to each other. Overkill on one failure mode does not necessarily increase the strength of the SSR. The screws should be as close as possible to the web (vertical portion) of the internal clip to limit prying action, which could result in premature pullout of the screw or screws. In some cases, screws are placed further away from the web to allow clearance for the screw gun; however, putting the screws closer to the web and using a bit extender may allow for a more concentric load transfer from the clip to the purlin. These variables determine the mode of failure for screw pullout from the purlin.

The strength of most single internal clips varies from about 400 to 1100 lb. SSRs must allow for normal thermal expansion. Internal clips can be one piece or two pieces. Most SSR panels are fastened between ribs to the eave strut and allowed to expand toward the roof peak. Two-piece clips are more common on larger SSRs, which require more thermal

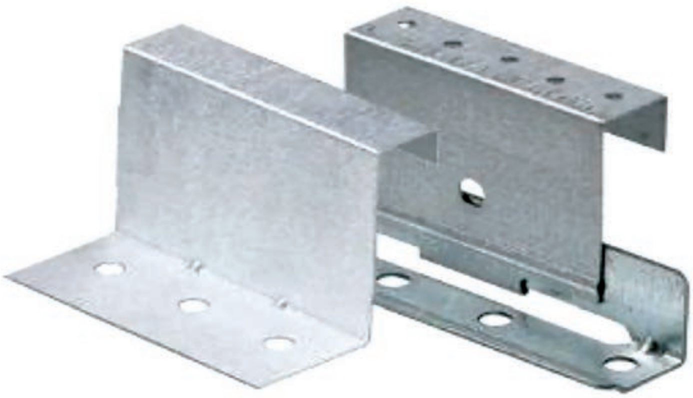

Figure 3. Examples of a one-piece internal clip (left) and a two -piece internal clip (right).

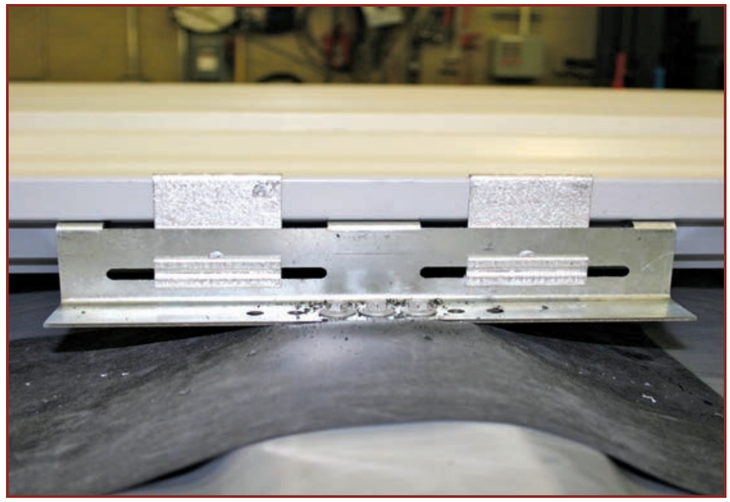

Figure 4. Double clip used to increase securement.

expansion. The top part of the clip is seamed into the mating SSR panel sections, and a slot in the bottom piece allows for thermal movement between the top and bottom parts of the clip (**Fig. 3**). The use of an automatic seaming machine and a two-piece internal clip allows for a tight seam at the ribs without restricting thermal movement. Thermal movement with one-piece clips occurs between the SSR seam and the clip; consequently, the seam may not be as tight as desired to increase wind resistance. Often, the wind load failure mode is the SSR releasing from the clip, either because of a lack of tightness of the seam or because the top part of the clip unfolds and releases the SSR.

If the slot in the internal clip that allows thermal expansion is wide and the metal is relatively thin or shallow, a two-piece clip may fail because the top part of the lower portion of the clip buckles.

In some cases, double clips can be used. That is, two pieces of internal clip (or double clip) can be seamed into the SSR and secured to an extender that is fastened to the purlin (**Fig. 4**). Continuous clips that extend the entire length from one purlin to the next can also be used for high-wind-pressure areas.

SEAMING TECHNIQUES

Seaming techniques can play a significant role in the wind uplift resistance of SSRs. Snap-on seams are sometimes used in the United States and are common in Australia. They tend to provide the least wind resistance, all else being equal.

Hand-crimped seams are typically not used in the United States. However, they have been used in Asia, where labor costs are lower.

Automatic seaming machines are most common now. In some cases, a single fold of the seam is used. Double-folding the seam further increases wind resistance, but it may complicate any necessary repairs.

EXTERNAL SEAM CLIPS

An ESC is intended to keep the seams attached to the internal clip. ESCs first became somewhat popular after Hurricane Andrew, but it took years for the industry to gain the knowledge that would improve their performance. Several well-intended after-market installations proved inadequate because the ESCs did not fit the seam shape properly. Large-scale tests have shown that ESCs that do not fit properly may increase wind resistance by only a small percentage (±20%) compared with an SSR with no ESCs (**Fig. 5**). If the ESC fits properly, it can force internal failure of the assembly. That is, either the internal clip screws will pull out of the purlin or the internal clip will break. In some cases, the top part of the internal clip may unfold and release from the seam. Large- and small-scale tests have shown that if the ESCs fit properly, they can in some cases increase strength to up to two to three times the original resistance.

The same SSR type as shown in Fig. 5 was tested again with properly fitting ESC and

Figure 5. Large-scale testing of a standing seam roof (SSR) without external seam clamps (ESCs) (above) and with ESCs that did not fit the SSR properly (at right). Compared with the failure point for the SSR with no ESCs (50 lb/ft²), the failure point for the SSR with improperly fitting ESCs only increased by 20% (to 60 lb/ft²).

Figure 6. Examples external seam clamps (ESCs): a two-piece ESC that fits a tee-shaped standing seam roof (SSR) (below); a two-piece ESC that fits a bulb-shaped SSR (at right).

failed at 150 lb/ft^2, an increase of 200%. The initial failure mode was internal clip screws pulling out of the purlin and the clip pulling over the head of the screws.

Given the large variety of ESCs available, there is one to fit almost every SSR (**Fig. 6**). This includes Australian SSR that are snap-fit type.

The ESCs must not restrict thermal expansion; therefore, for one-piece clips, one ESC on each side of the internal clip is recommended (the ESC should be about 1 in. [25 mm] away from the internal clip measured horizontally along the deck rib). For two-piece clips, one ESC immediately over the internal clip is recommended because the thermal movement will still occur between the top and bottom parts of the internal clip. Depending on the type and width of the SSR seam, a two-piece ESC (Fig. 6) may be needed to properly fit. The main piece fits over the top, and the other piece slides under the top of the seam. The ESC usually has one or two machine bolts to tighten the ESC against the SSR seam. In all cases, the ESC must be properly torqued. The torque usually ranges from 130 to 180 in.-lb, depending on the specific model and type and thickness of the SSR metal. ESCs that tighten toward the web (vertical part) of the internal clip will likely perform better than those that only tighten into the top (horizontal flange) of the internal clip.

ESCs are typically made of extruded aluminum and are quite strong. Longer ESCs (about 3 in. long) using two screws will likely resist more than 2000 lb before breaking. Shorter ESC will usually resist more than 1100 lb before breaking, which is at least as strong as most internal clips. Which type of ESC to use will depend on the limiting strength of the internal clip or its securement to the purlin.

Large-scale tests (using samples up to 12 × 24 ft) such as ASTM E1592[4] or FM 4471[5] are always recommended. But, in some cases, such as existing installations for which retrofitting with ESC is being considered, it may not be practical to conduct large-scale tests. For example, testing could be cost prohibitive, or sufficient materials may not be available for testing because the SSR assembly is no longer manufactured (testing requires about 300 ft^2 of material). Often, designers or installers do not provide reduced purlin spacing, ESCs, or an equivalent increase in resistance based on performance-based tests in higher roof wind zones (Zones 3 and 2).

When trying to determine the resulting strength with ESCs, one should not base the estimate on the strength of the ESCs alone, as the limiting factor may be the strength of the internal clip or its securement to the purlin. In such cases, conducting smaller-scale tests, such as with a tensile test machine and realistic jig, will provide a closer approximation of the resultant strength. To be realistic, a small amount of the SSR material plus clips and screws must be provided to mock-up what is installed. A short piece of purlin of a thickness and yield strength equal to that installed can be clamped to the base of the tensile tester, with the ESC directly on the seam and over the internal two-piece clip (or for one-piece clips, use two ESCs, as explained previously). The load should be applied from the top jaws of the equipment to the flat parts of the SSR panel edges (**Fig. 7**).

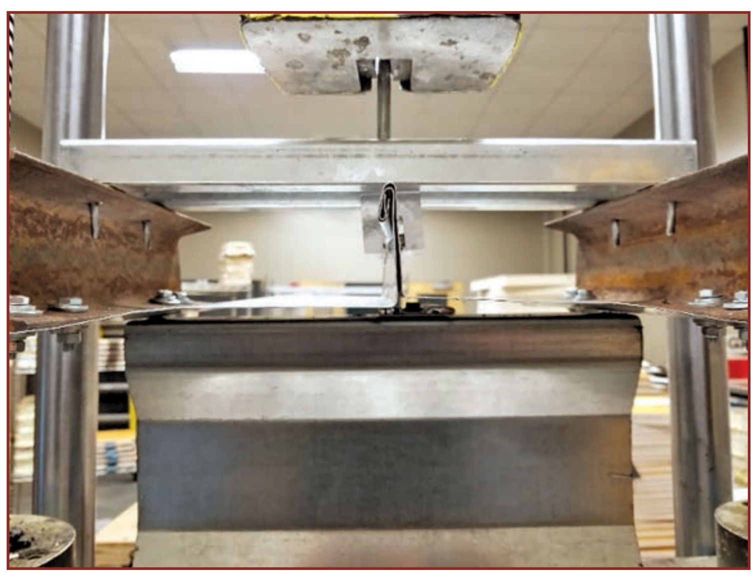

Figure 7. Small-scale test to estimate enhanced strength of a standing seam roof with external seam clamps.

ROOF-MOUNTED SOLAR PHOTOVOLTAIC PANELS

There are a variety of variables related to wind design of roof-mounted photovoltaic (PV) panels. This discussion mainly focuses on PV panels parallel to the SSR surface. That situation is common with SSRs, and it is much more simplified than other situations with regard to the determination of design wind loads on the PV panels. For situations where PV panels are parallel to the SSR surface and meet dimensional limits described, boundary layer wind tunnel (BLWT) testing is not required. For roof-mounted PV panels that are sloped with respect to the roof surface, conservative prescriptive wind pressure coefficients based on ASCE 7-16,[2] ASCE 7-22,[3] or the Structural Engineers Association of California's *Wind Design for Solar Arrays* (SEAOC PV2)[10] may be used; however, it is more common to conduct BLWT tests specific to the PV panel design.

When PV panels are parallel to SSR roof surface, the prescriptive external wind pressure coefficients used for roof coverings can also be used for the PV panels, with the following modifications:

- If the tops of the PV panels are equal to or less than 10 in. from the flat part of the SSR, and there is at least a ¼ in. gap between each PV panel in both directions, an air equalization factor ϒ of 0.8 may be multiplied by the design pressure for effective wind areas (EWA) equal to or less than 10 ft^2 (0.93 m^2). The space below and between the PV panels allows for some equalization of air pressure and reduces the wind uplift pressure on the PV panels.
- If the tops of the PV panels are equal to or less than 5 in. from the flat part of the SSR, and there is at least a ¾ in. gap between each PV panel in both directions, an air equalization factor ϒ of 0.6 for EWA equal to or less than 10 ft^2 (0.93 m^2) may be multiplied by the design pressure.

For dimensions in between the above height and gap boundaries, bilinear interpolation is allowed. That means a 20% to 40% reduction of the roof cover pressure may be used for the PV panel design. For an example calculation, see the **Appendix**.

It is important to understand the following points:

- The roof cover must be designed as if the PV panels were not there.

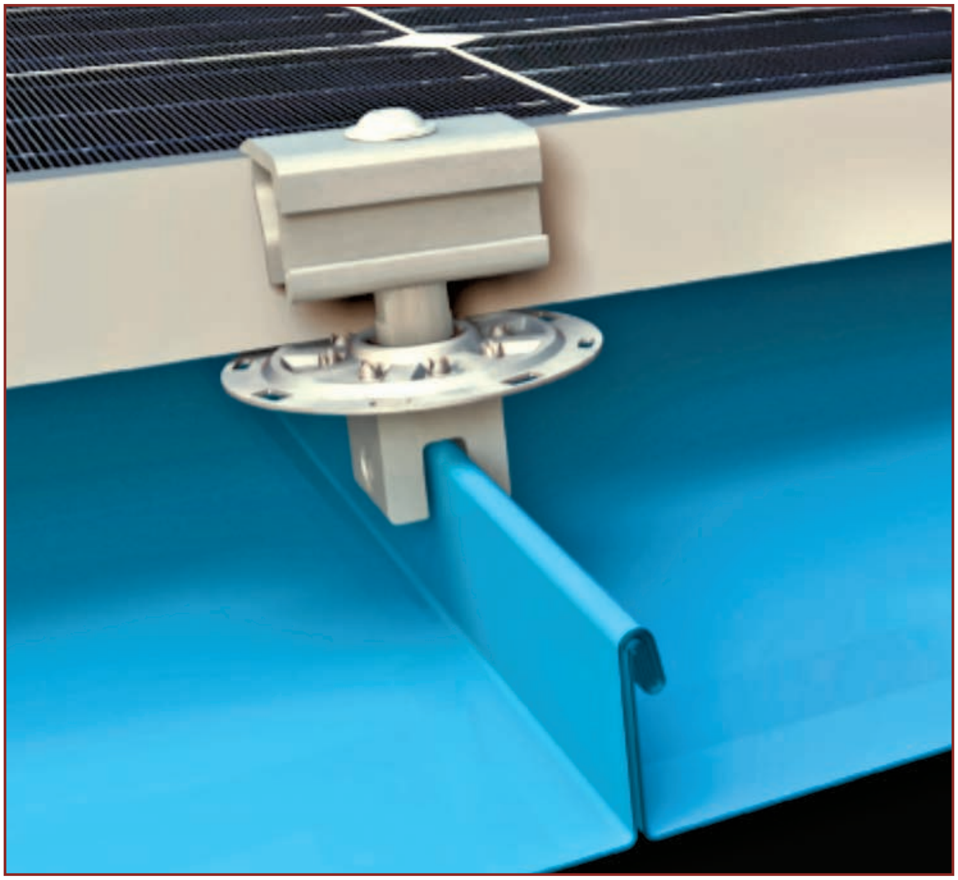

Figure 8. Photovoltaic panel attachment kit is fastened and torqued to the top of an external seam clamp that properly fits the standing seam roof's seam.

- You do *not* need the add the PV panel wind load to the roof wind load. Each is designed independently.
- The best advice is to provide mechanical securement of the PV panels at each SSR deck rib; otherwise, the wind load path used in the SSR will not be followed and the strength of the internal clip or its securement to the purlin may be exceeded. Evidence of this is noted in "Hurricanes Irma and Maria in the US Virgin Islands,"[11] published by ASCE.
- If securement is done at every other rib instead of at each rib, more deflection of the glass in the PV panel may occur. That could lead to the panel releasing from the clip, or the PV frame could buckle. Wind losses have been experienced where fastening at each rib has not been provided.

Securement of the PV panels is usually accomplished by using an ESC that properly fits the SSR seam and attaching a PV attachment kit (**Fig. 8**) to the top of ESC, with proper

When trying to determine the resulting strength with external seam clamps (ESCs), one should not base the estimate on the strength of the ESC alone, as the limiting factor may be the strength of the internal clip or its securement to the purlin.

torque applied to the screw(s) securing the ESC to the deck rib and the PV stud securing the PV panel to the attachment kit.

Laboratory wind uplift pressure tests using at least two PV panels are recommended to verify that the assembly is adequate for the PV panel wind uplift pressures needed. How well the PV attachment grips the PV panel edges may be a limiting factor in the wind resistance. When subjected to significant wind loads, the PV panels will deflect considerably (about 1 in. or more) in their center, rotation at the edge frames can occur and PV panels can be dislodged from the clamps. This is further evidenced in the Federal Emergency Management Agency publication, *Rooftop Solar Panel Attachment: Design, Installation, and Maintenance.*[12]

EXTERIOR FIRE SPREAD

Another benefit of using PV arrays (a group of PV panels together) over a metal SSR is better performance with regard to exterior fire exposure. There have been many fire losses with PV arrays used over single- and multiple-ply roof covers, with thousands of square feet of fire damage. With a metal roof, fuel does not significantly contribute to an exterior fire. For additional information, see FM Global's *Property Loss Prevention Data Sheet 1-15: Roof Mounted Solar Photovoltaic Panels.*[13]

REFERENCES

1. Smith, T. L. 1995 (February). "Insights on Metal Roof Performance in High-Wind Regions." *Professional Roofing.*
2. American Society of Civil Engineers (ASCE). 2016. *Minimum Design Loads and Associated Criteria for Buildings and Other Structures.* ASCE 7-16. Reston, VA: ASCE.
3. ASCE. 2022. *Minimum Design Loads and Associated Criteria for Buildings and Other Structures.* ASCE 7-22. Reston, VA: ASCE.
4. ASTM International. 2017. *Standard Test Method for Structural Performance of Sheet Metal Roof and Siding Systems by Uniform Static Air Pressure Difference.* ASTM E1592-05(2017). West Conshohocken, PA: ASTM International.
5. FM Approvals. 2010. *Approval Standard for Class 1 Panel Roofs.* FM 4471. Norwood, MA: FM Approvals.
6. Baskaran, B., S. Moletti, D. Lefebvre, and N. Holcroft. 2018. *Climate Change Adaptation Technologies for Roofing.* Ottawa, Canada: National Research Council of Canada.
7. International Code Council (ICC). 2018. *International Building Code.* Country Club Hills, IL: ICC.
8. ICC. 2021. *International Building Code.* Country Club Hills, IL: ICC.
9. FM Global. 2020. *Property Loss Prevention Data Sheet 1-31: Panel Roofs.* Johnston, RI: FM Global.
10. Structural Engineers Association of California (SEAOC). 2017. *Wind Design for Solar Arrays.* SEAOC PV2-2017. Sacramento, CA: SEAOC.
11. ASCE. 2021. *Hurricanes Maria and Irma in the US Virgin Islands.* Reston, VA: ASCE.
12. Federal Emergency Management Association (FEMA). 2018. *Rooftop Solar Panel Attachment: Design, Installation, and Maintenance*, FEMA 4340, US VI-RA5/April. Washington, DC: FEMA.
13. FM Global. 2021. *Property Loss Prevention Data Sheet 1-15: Roof Mounted Solar Photovoltaic Panels.* Johnston, RI: FM Global.

APPENDIX:
SAMPLE PROBLEM—PHOTOVOLTAIC PANELS PARALLEL TO ROOF

The following example is based on guidance in the American Society of Civil Engineers' *Minimum Design Loads and Associated Criteria for Buildings and Other Structures* (ASCE 7-22).[1]

EXAMPLE

A proposed photovoltaic (PV) array is to be secured to a 24-in.-wide metal standing seam roof (SSR) using extruded aluminum external seam clamps (ESCs). The roof slope is ¼ in./ft (1.2 degrees). The PV panels will be parallel to the roof surface. The distance between the flat part of the roof deck and the top edge of the 2-in.-deep integral aluminum frame of the PV module is to be 7.5 in. The PV modules are 20 ft^2 in plan area. The long dimension of the PV modules will run across the deck ribs. It is preferred that 3 ESCs be used to secure each long edge of the PV module to the roof deck ribs in accordance with **Fig. A1**. The horizontal space between modules in both directions will be equal to or less than 1 in. (52 mm). A minimum of 800 modules must be installed to provide the required electrical output. The building is just slightly above sea level. Other details are as follows:

H = roof height = 33 ft (10 m), Wind Exposure Category C
K_Z = velocity pressure coefficient = 1.0
W_L = long plan dimension of building = 246 ft
W_S = short plan dimension of building = 140 ft
V = ultimate wind speed = 138 mph, per ASCE 7-16[2]
K_{ZT} = topographic factor = 1.0
K_D = 0.85 per ASCE 7 for roof-mounted equipment
K_e = elevation factor = 1.0 per ASCE 7

ESCs are proposed to be installed at every other deck rib, which does not follow the wind load path of the SSR to which the PV modules are to be secured. The wind load path goes from the deck ribs to an internal clip, then through self-drilling screws securing the internal clips into the top flange of steel purlins. The fire department requires an aisle that is at least 6 ft wide every 100 ft. The goal is to minimize the wind load transferred to the existing roof. Determine if that will be acceptable.

Solution

- The PV modules are parallel to the roof surface, within 10 in. of the flat part of the roof deck, and meet the minimum horizontal space requirements between panels. Per ASCE 7-22[1] and SEAOC PV2-2017,[3] the wind design load may be the same as for a low-slope (≤7 degrees) gable roof. The value for GC_P is determined from ASCE 7.
- One exception is that an edge factor Υ_E = 1.5 must be applied to the exposed PV panels located along each outer row closest to the roof edge and adjacent to wide aisles (>4 ft) between arrays. The largest area supported by any ESC will be ≤10 ft^2, so the GC_P will be based on an effective wind area (EWA) ≤10 ft^2.
- For an EWA ≤10 ft^2, an air pressure equalization factor Υ_A of between 0.8 and 0.6 may be applied per ASCE 7-22 in this case. The top edge of the modules is 7.75 in. from the roof surface (h_1 = h_2), and the minimum gap G between modules in each direction is ≥¾ in. Bilinear interpolation will result in using a pressure equalization factor Υ_A of 0.65. Bilinear interpolation of the air equalization factor may be done as follows:
- Interpolate based on gap width between panels.
- Interpolate based on h_2.
- Average both values.

First evaluate factor based on gap size. Gap ≥ ¾ in., so
$\Upsilon_A = 0.6$.
Evaluate based on h_2:
$\Upsilon_A = (0.8 + 0.6)/2 = 0.7$
Find the average between the 2 factors:

$$\Upsilon_A = (0.7 + 0.6)/2 = 0.65$$

- Determine the basic pressure at roof level:

$$q_h = 0.00256\, K_z\, K_e\, K_{zt}\, K_d\, V_U^2$$

Where:
q_h = basic pressure at roof level
K_z = velocity pressure coefficient (from tables in ASCE 7)
K_{zt} = topographic factor = 1
K_d = directionality factor = 0.85
V_U = ultimate design wind speed (mph)
K_e = elevation factor (see ASCE 7-16 or ASCE 7-22) = 1.0 (default)

$$q_h = 0.00256(1.0)(1.0)(1.0)(0.85)(138)^2 = 41.4 \text{ lb/ft}^2$$

Convert to Allowable = 0.6(41.4 lb/ft^2) ~ 25 lb/ft^2

- Apply the safety factor, pressure coefficient, edge factor and air equalization factor:

$$p_s \text{ (wind pressure on solar)} = q_H\,(GC_P)(SF)\Upsilon_E\,\Upsilon_A$$

Where:
GC_P = pressure coefficient for roof zone
SF = safety factor (2.0)
A_p = PV panel area (ft^2)
Υ_E = edge factor (1.5 for edge panel, 1.0 for interior panels)
Υ_A = air pressure equalization factor

Zone 1:

- $p_s = (25)(2.0)(-1.7)(1.5)(0.65) = -82.9$ lb/ft^2 for the first row of exposed modules
- $p_s = (25)(2.0)(-1.7)(1.0)(0.65) = -55.3$ lb/ft^2 for the interior rows of modules

Zone 1′:

- $p_s = (25)(2.0)(-0.9)(1.5)(0.65) = -43.9$ lb/ft^2 for the first row of exposed modules
- $p_s = (25)(2.0)(-0.9)(1.0)(0.65) = -29.3$ lb/ft^2 for the interior rows of modules

APPENDIX:
SAMPLE PROBLEM—PHOTOVOLTAIC PANELS PARALLEL TO ROOF

Assume the purlin spacing is 5 ft on center and the SSR tested held a wind pressure of 90 lb/ft^2 before failing. If the deck ribs are spaced 2 ft on center, the minimum ultimate wind resistance held by the internal clips was (90 lb/ft^2) (5 ft) (2 ft) = 900 lb. If the ESCs are only provided at every other deck seam, the wind load transferred to the internal clips of the SSR is:

Exposed panels (edge factor = 1.5):

F = force at each ESC/PV attachment = $p_s(A_p)(1.67)$
F = (89.3 lb/ft^2)(10 ft^2)(1.67) = -1491 lb > 900 lb **no good**.
Recommend a 3rd PV/ESC attachment on both edges of exposed panels in Zone 1 (**Fig. A1**).

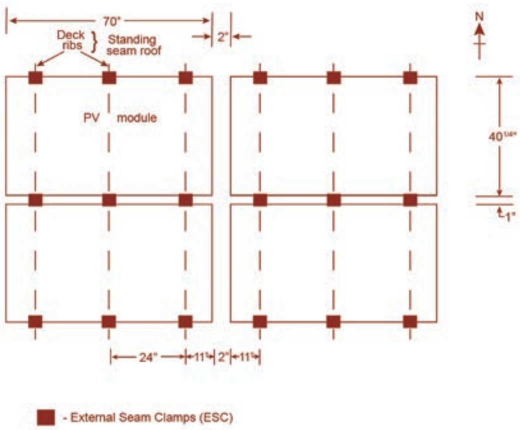

Fig. A1. Preferred securement and needed for Exposed Panels in Zone 1.

Shielded panels:

F = (55.3 lb/ft^2)(10 ft^2)(1.67) = -924 lb > 900 lb This provides a SF of 1.95. If we deduct 0.6 × dead weight of the PV panel, the SF ~ 2.0 without a third PV/ESC attachment on all Zone 1 shielded panels is close enough (**Fig. A2**).

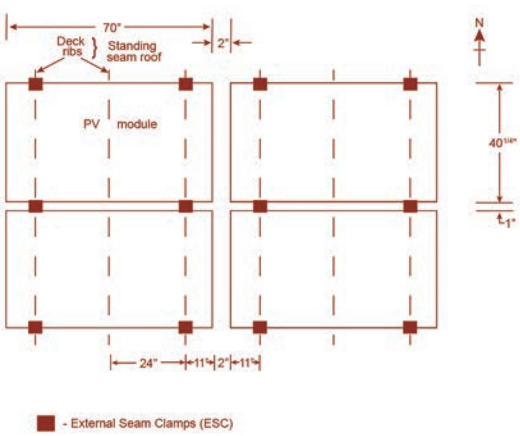

Fig. A2. Proposed and solution for all panels except those exposed in Zone 1.

Table A-1.
External pressure coefficient GC_p values per ASCE 7-16[2] for roof slope ≤7 degrees

Zone	GC_p
1	3.2
2	2.3
1	1.7
1′	0.9

Note: All GC_p values are based on an effective wind area of 10 ft^2.

Summary

1. A minimum setback of 20 ft should be used, and the modules installed per Fig. A1 or A2, depending on their location.
2. ESC and PV attachments are needed at each deck rib (3 points per PV panel) for exposed panels in Zone 1 (Fig. A1). Two points of attachment are acceptable in all other areas (Fig. A2).
3. The following modules located in an outer row or column are considered "exposed" and should be designed using the higher wind loads that include an edge factor of 1.5:
   a. The north and south edges of Arrays 1 and 2
   b. The west edge of Array 1 and the east edge of Array 2.
   c. The east edge of Array 1 and the west edge of Array 2 also require an edge factor of 1.5.

DISCUSSION

Limiting the distance between the modules and the roof surface to 7.5 in. and providing a minimum gap of ¾ in. between modules will significantly reduce the wind uplift design pressure as Υ_A is reduced to 0.65. Note that this is allowed per SEAOC PV2-2017[3] and ASCE 7-22.[1]

Another factor is by increasing the setback distance to 20 ft on all sides and placing the modules in Zones 1 and 1′, and not in Zone 2 or 3.

The local fire department required access aisles that were at least 6 ft wide at maximum distances of 100 ft. Therefore, the modules along each side of the aisle must use an edge factor of 1.5 because the aisle is more than 4 ft wide.

This arrangement will still allow enough room for the required minimum of 800 modules if the modules are installed in two approximately 100 × 100 ft arrays.

REFERENCES

1. American Society of Civil Engineers (ASCE). 2022. *Minimum Design Loads and Associated Criteria for Buildings and Other Structures*. ASCE 7-22. Reston, VA: ASCE.
2. ASCE. 2016. *Minimum Design Loads and Associated Criteria for Buildings and Other Structures*. ASCE 7-16. Reston, VA: ASCE.
3. Structural Engineers Association of California (SEAOC). 2017. *Wind Design for Solar Arrays*. SEAOC PV2-2017. Sacramento, CA: SEAOC.

Making the Connection: Fastening Through Continuous Insulation

Leah Ruther, PE

Wiss, Janney, Elstner Associates Inc. | Grand Haven, MI

lruther@wje.com

Logan Cook, PE

Wiss, Janney, Elstner Associates Inc. | Indianapolis, IN

lcook@wje.com

IIBEC 2022 - Building for the Future

International Convention and Trade Show

March 17–22, 2022 | Orlando, FL

ABSTRACT

Despite its many benefits, continuous insulation in exterior wall systems separates the cladding from the supporting structural framing (often by 2 in. or more), which can create severe demands on fasteners bridging the gap. It has become increasingly challenging to achieve connection details that reasonably resolve demands and capacities, particularly with heavier claddings and thicker continuous insulation. The industry has responded to some degree: designers are being more creative, suppliers are developing proprietary thermally improved framing or clip systems, and model building codes recently incorporated fastening requirements. However, the industry has not fully addressed the complex array of conditions that can be encountered and the associated engineering issues to efficiently provide proper performance of the exterior wall system. This presentation discusses the complex behaviors of the seemingly simple cladding connections through continuous insulation, associated design challenges, concepts for resolving demands and capacities, and current requirements recently adopted in the *International Building Code*.

SPEAKERS

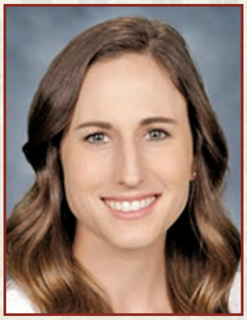

Leah Ruther, PE

Wiss, Janney, Elstner Associates Inc. | Grand Haven, MI

Leah Ruther is a licensed professional engineer at Wiss, Janney, Elstner Associates Inc. (WJE). She has a bachelor's degree in civil engineering from Calvin University and a master's degree in civil engineering from Lawrence Technological University. Since joining WJE in 2012, Ruther has been involved with numerous structural engineering and architecture-related projects. Her responsibilities include the investigation and analysis of existing and damaged structures, development of technical repair and rehabilitation documents, and construction observations. Ruther has experience with building enclosure–related failures such as water infiltration, air leakage, and condensation, as well as structural failures.

Logan Cook, PE

Wiss, Janney, Elstner Associates Inc. | Indianapolis, IN

Logan Cook is a licensed professional engineer at Wiss, Janney, Elstner Associates Inc. (WJE). He has a bachelor's degree in construction engineering and management and master's degree in engineering from Purdue University. Since joining WJE in 2012, Cook has served as project manager or project associate on hundreds of assignments related to the investigation, repair, and restoration of new and existing arenas, stadiums, museums, buildings, parking garages, and bridges. His experience includes evaluating challenges and developing solutions related to facades, roofing, waterproofing, masonry, concrete, steel, and various types of structural systems.

Making the Connection: Fastening Through Continuous Insulation

In contemporary building enclosure design, specifying continuous insulation outboard of both the exterior wall framing and water-resistive barrier has become common practice in many regions, and for good reason. In this paper, we are expanding the 2021 *International Building Code*[1] (IBC) definition of *water-resistive barrier* to include air and vapor barriers that may also be included in the exterior wall assembly.

There are many benefits to designing and installing exterior wall assemblies in this manner, including increased energy efficiency and reduced condensation potential at sensitive materials. However, for structural engineers, ensuring support for directly attached veneer systems on the exterior wall framing has become much more difficult, particularly with heavy systems (for example, terra-cotta rain screens). In this paper, we intend the term *veneer* to be equivalent to the term *cladding* when referring to facade systems (for example, terra-cotta rain screens) that are entirely supported by the backup wall system (that is, directly attached) rather than receiving gravity support independent of the backup. While the demands imposed on veneers (for example, gravity, wind, seismic, atmospheric ice) are not appreciably affected the need to make attachments through continuous insulation has greatly complicated veneer design. In particular, efficiency of resolving demands encourages the use of insulation materials as elements of the structural load paths; however, little is understood about how the relevant properties of these materials contribute to connection capacity. Although the industry has begun to recognize and respond to these challenges, there are many questions left to answer. The information provided in this paper summarizes current understanding of the demands and mechanisms of the veneer connections through continuous insulation, previous research and results, and recommended actions the industry should pursue to provide more reliable guidance on the design of veneer connections through continuous insulation.

USE OF CONTINUOUS INSULATION IN EXTERIOR WALL ASSEMBLIES

The concept of continuous insulation is not new. We have observed continuous insulation in the mass masonry walls of a circa 1920 refrigerated building (Fig. 1). In this 1920s building, the weight of heavy masonry outboard of the insulation was not supported by the interior (backup) wall system (that is, the veneer was not directly attached), but was instead supported independently by the foundation. Lateral support of the exterior masonry was provided by anchors embedded in the structural backup wall system that penetrated the insulation. This 1920s design is similar to common cavity wall construction, which can accommodate continuous insulation in the cavity between the veneer and structural backup wall framing.

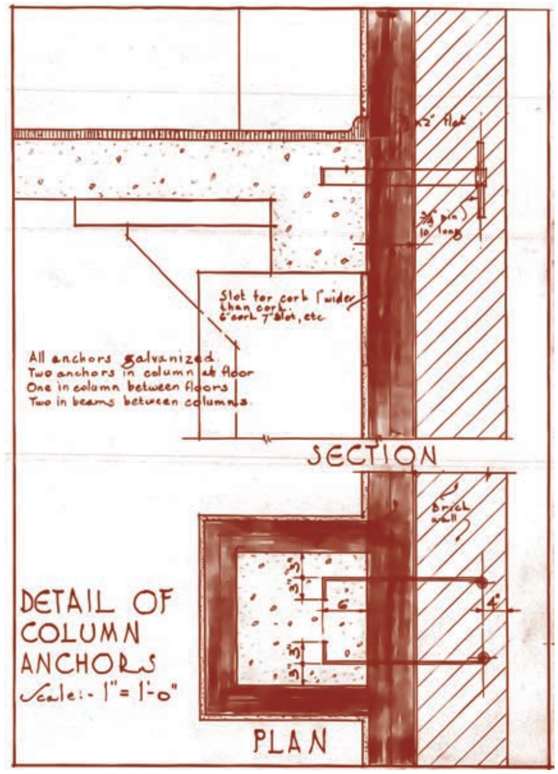

Figure 1. Section and plan of continuous insulation of a cold-storage building designed circa 1920. Note: 1" = 1 in. = 25.4 mm; 1' = 1 ft = 0.305 m.

While cavity wall construction with independent gravity support of the exterior veneer can readily accommodate continuous insulation, many veneer systems require gravity support provided by the structural backup wall by means of a connection to transfer the veneer loads directly back to the structural backup wall. The term "directly attached" is often used to describe such veneer systems. Until recently, insulation for exterior walls with directly attached veneer systems has been commonly installed within stud cavities or other spaces within the structural backup framing. Placing the insulation within the structural backup allowed veneers to be directly attached to structural backup elements with, at most, a relatively thin layer of sheathing between the veneer and its supporting structural backup (Fig. 2). The performance of common fasteners (usually screws) in such a configuration, without significant gaps, has been well understood, enabling simple, efficient, effective designs for structural engineers.

2021 *International Building Code* Definitions

The 2021 *International Building Code*[1] (IBC) defines a water-resistive barrier as "a material behind an exterior wall covering that is intended to resist liquid water that has penetrated behind the exterior covering from further intruding into the exterior wall assembly." In this paper, we are expanding the definition of *water-resistive barrier* to include air and vapor barriers that may also be included in the exterior wall assembly.

The 2021 IBC defines veneer as "a facing attached to a wall for the purpose of providing ornamentation, protection or insulation, but not counted as adding strength to the wall."

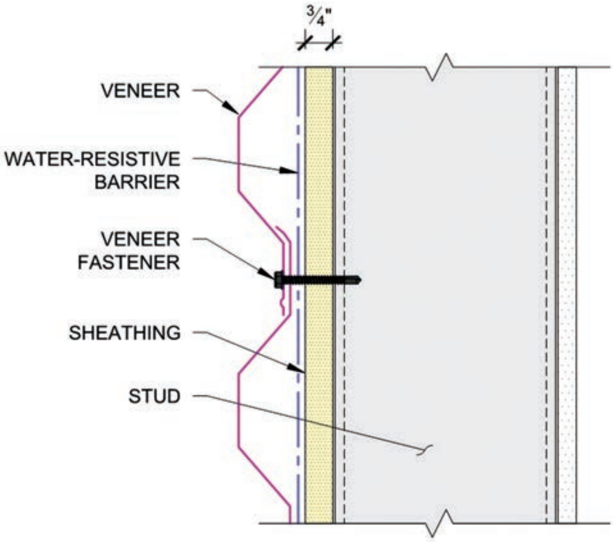

Figure 2. Direct fastening of veneer system to structural backup framing without continuous insulation. Note: 1″ = 1 in. = 25.4 mm.

Due to the numerous performance benefits and related provisions in model building codes, it is now common (and often required) practice to have layers of continuous insulation between directly attached veneers and the structural backup walls. Typical exterior wall assemblies of this type include the following components from exterior to interior:

- **Veneer:** The outermost element of the system, veneer comprises the visible exterior surface and, typically, provides some degree of protection from rain, snow, and wind. There are many common veneer materials, such as vinyl lap siding (**Fig. 3**), fiber cement boards, composite metal panels (**Fig. 4**), and terra-cotta rain screens (**Fig. 5**). Lighter-weight veneer components (for example, vinyl lap siding and cement board siding) typically weigh on the order of 1 to 5 lb/ft^2 (4.88 to 24 kg/m^2). Heavier veneer systems (for example, stucco, adhered stone/masonry, or terra-cotta rain screens) can weigh from 10 to 40 lb/ft^2 (49 to 195 kg/m^2).
- **Veneer subframing:** Veneer subframing comprises structural elements that are outboard of the insulation and attached to the structural backup wall framing. Subframing is used when veneer elements require support at locations that cannot be reliably coordinated with structural support elements in the backup wall and to promote alignment among veneer elements. Veneer subframing often comprises cold-formed steel hat channels or *z* channels that can be oriented vertically, horizontally, or both to accommodate a wide variety of panelized veneers. In subsequent discussion, veneer subframing, where used, will be considered part of the veneer.
- **Insulation:** Continuous insulation typically is made from extruded polystyrene (XPS), expanded polystyrene (EPS), foil-faced polyisocyanurate, or rigid mineral fiber. Insulation compressive strengths range from approximately 15 to 140 psi

Figure 3. Vinyl lap siding veneer over continuous insulation.

Figure 4. Panelized composite metal veneer over continuous insulation.

Figure 5. Terra-cotta rain screen veneer over continuous insulation.

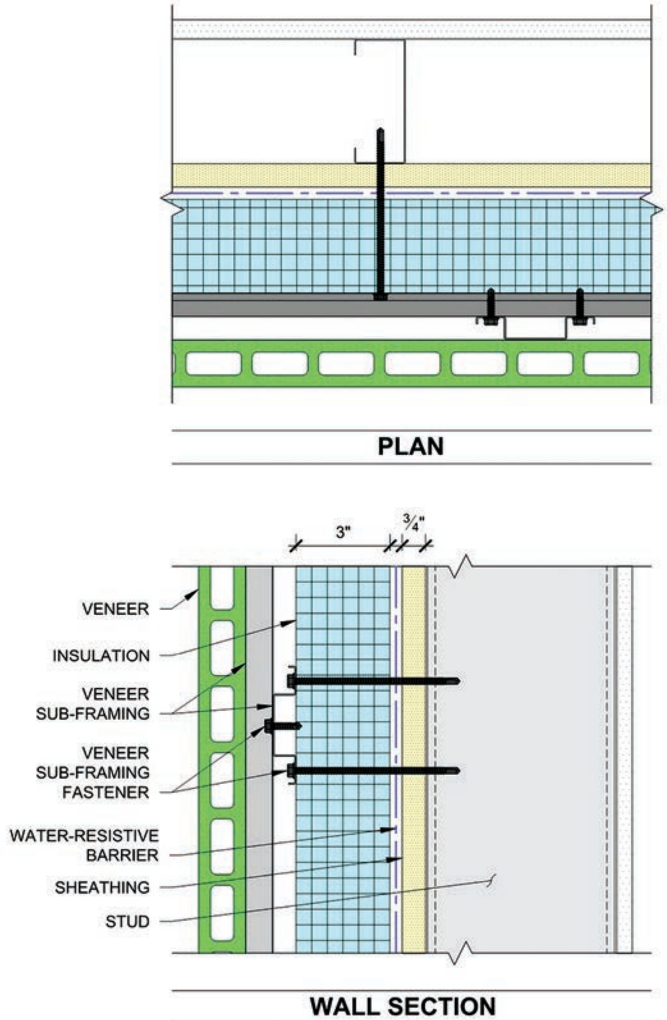

Figure 6. Surface-mounted veneer subframing connection. Note: 1″ = 1 in. = 25.4 mm.

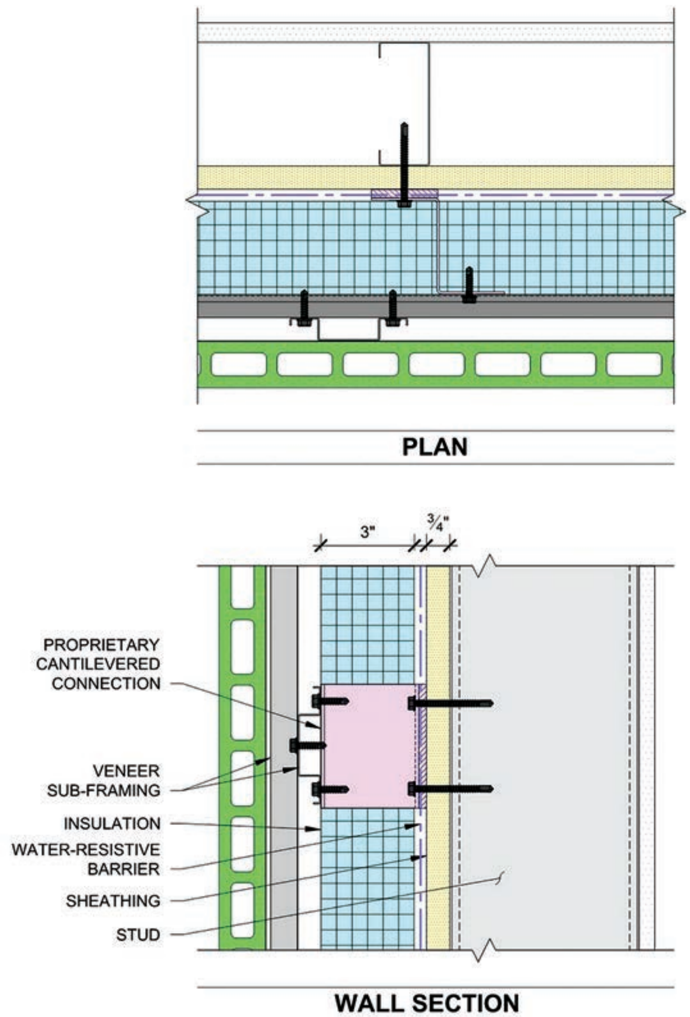

Figure 7. Cantilevered veneer subframing connection. Note: 1″ = 1 in. = 25.4 mm.

(103 to 965 kPa), depending on the insulation density. Insulation thickness commonly ranges from 1 to 4 in. (25 to 100 mm), depending on *R*-value requirements. Section 5.5 of ANSI/ASHRAE/IES 90.1-2019[2] prescribes minimum *R*-value requirements ranging from 9.8 to 31.8, depending on the type of wall and the climate zone of the building.

- **Water-resistive barrier:** There are many types of water-resistive barriers for use in exterior walls, including fluid-applied materials, sheet goods, and materials integrated within exterior sheathing. Regardless of the water-resistive barrier type, the barrier usually adds only a nominal thickness within the assembly of 60 mils (0.060 in. [1.5 mm]) or less.
- **Sheathing:** Exterior sheathing is commonly ¾ in. (19 mm) oriented strand board (OSB) or gypsum sheathing in contact with and fastened to the structural backup wall framing. Sheathing compressive strengths are generally greater than 500 psi (3500 kPa).
- **Structural backup:** The most common forms of structural backup for directly attached veneer on exterior walls include structural cold-formed steel studs, concrete masonry, and wood studs.

VENEER CONNECTION TYPES

Lighter-weight veneer cladding (for example, vinyl siding) is often directly attached to the structural backup or sheathing without veneer subframing. Heavier veneers such as terra-cotta rain screens typically have subframing that is directly attached to structural backup. In our experience, subframing connections are usually one of the following types:

- **Surface mounted:** The veneer subframing is in contact with the exterior surface of the continuous insulation and fastened with screws to the structural backup through the layers of the exterior wall assembly (**Fig. 6**).
- **Cantilevered:** The veneer subframing is supported by a bracket that is fastened to the structural backup such that the fasteners (usually screws) only penetrate the sheathing while the bracket extends through the insulation (**Fig. 7**).

Continuous insulation layers separate the veneer from the structural backup support and fill the resulting gap with material that is relatively soft and weak. For loads normal to the plane of the wall (for example, wind), this configuration has little or no effect. For loads in the plane of the wall (for example, gravity loads), the separations increase eccentricities between loads and points of support, which can severely affect the performance of various attachment details. Cantilevered connections accommodate these separations by using conventional fastening details and simple structural elements to essentially extend the

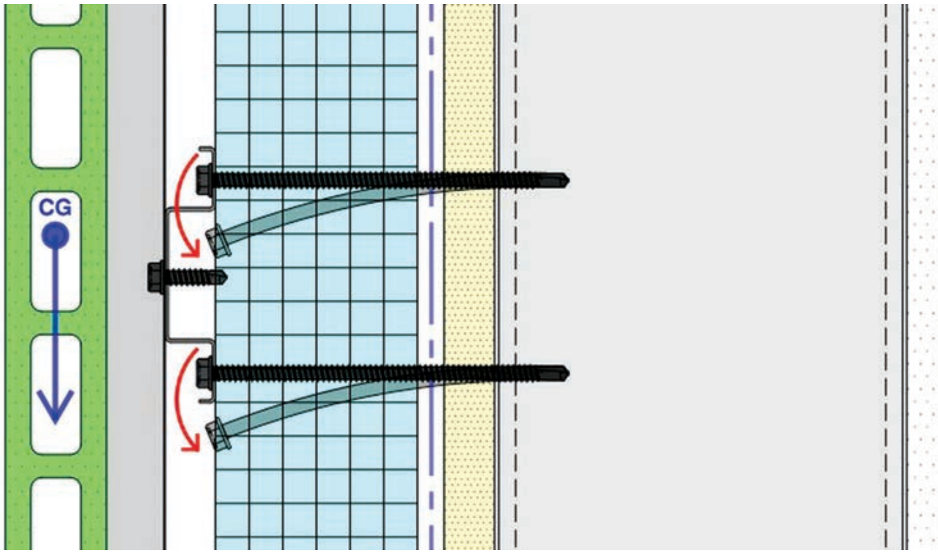

Figure 8. In-plane load-resisting mechanism 1—cantilever screw.

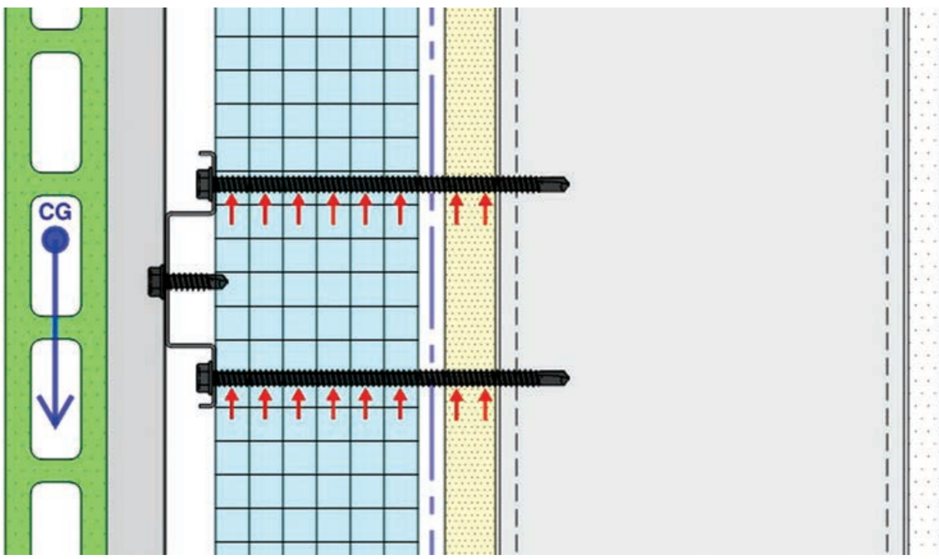

Figure 9. In-plane load-resisting mechanism 2—screw shank bearing.

structure of the backup wall to the veneer. The structural design of cantilevered connection extensions is relatively simple, and several entities have developed proprietary systems that can be used with a variety of veneer materials and configurations. While simple from a structural standpoint, cantilevered connections can provide challenges related to installation effort and hygrothermal performance.

From a structural standpoint, surface-mounted connections are quite complex. Having fasteners (typically screws) penetrate up to several inches of insulation greatly reduces the amount of shear the fasteners can carry without experiencing unacceptable deformations. Several critical factors are concurrently employed that can affect capacity; these factors include the amount of clamping force developed as well as various properties of the insulation, including bearing stiffness, shear modulus, coefficient of friction, and compressive stiffness. Establishing reliable values for material and system properties while quantifying the manner in which they influence fastener performance is a challenging task. The remainder of this article discusses the design and performance of surface-mounted connections.

SURFACE-MOUNTED CONNECTIONS

When designing connections between veneer systems and the structural framing through continuous insulation, structural engineers must determine demands in accordance with applicable building codes. As an example, Section 2603.12 of the 2021 edition of IBC[1] states, "Where used, furring and furring attachments through foam sheathing shall be designed to resist design loads determined in accordance with Chapter 16." In that chapter, applicable demands typically include dead loads (that is, weight of veneer and veneer subframing), wind pressures, seismic forces, and atmospheric ice loads. Furthermore, stresses and deformations caused by expansion and contraction of the veneer components may need to be considered, particularly when veneer components are materials with high coefficients of thermal expansion, or when joints capable of accommodating movements are widely spaced.

In surface-mounted connections, movements often become excessive before ultimate strengths are reached. Consequently, deformation tolerances must be established. Deformation limits related to factors such as movement joint performance may be relatively easy to establish, whereas identifying limits based on other factors such as visual uniformity can be more challenging and subjective. Because veneer deflection limits may often be governed by factors not addressed by building codes or even manufacturers' literature, it is critical to establish owner expectations early and state them clearly in the design documents. It is also important to avoid unrealistic and stringent movement requirements, as this may make construction unnecessarily challenging, costly, and contentious. Reviewed veneer system manufacturer's reference specifications indicate deflection tolerances ranging from approximately ½ to 1⁄64 in. (13 to 0.40 mm). One study proposed a deflection limit of 1⁄64 in. for veneer design with continuous insulation.[3] However, the basis for that deflection limit in the study was connection design values for wood framing; therefore, the 1⁄64 in. limit may be inapplicable for veneer systems fastened through continuous insulation into other structural backup materials.

When considering movement-related issues, structural engineers must also consider both short- and long-term sources of deformation. The latter are especially important for surface-mounted connections that rely to some degree on insulation to support sustained veneer gravity loads. This is particularly relevant because common continuous insulation materials (for example, XPS and EPS) are susceptible to time-dependent behaviors under sustained stress.

After demands and deflection tolerances are determined, structural engineers must provide reliable load paths between the structural backup wall and the veneer that have the strength and stiffness needed to keep the veneer properly positioned for its entire service life. The presence of thick layers of insulating materials makes this challenging.

For demands perpendicular to the plane of the wall, the capacities of resisting elements are often easily calculated using conventional approaches and well-defined material properties. For loads parallel to the plane of the wall, available mechanisms for resisting demands are much more complex, and relevant material properties are often not well defined to rationally resolve such demands. Examples of in-plane load-resisting mechanisms include the following:

- Mechanism 1—cantilever screw (**Fig. 8**): This mechanism relies on flexural properties of the screw, rotational restraint of the screw provided by the structural backup, and rotational restraint of the screw provided by the veneer.
- Mechanism 2—screw shank bearing (**Fig. 9**): This mechanism relies on the ability of the insulation and sheathing to develop and sustain stresses normal to the screw shank.
- Mechanism 3—friction (**Fig. 10**): This mechanism relies on the ability of the insulation to develop and sustain clamping forces.
- Mechanism 4—subframe bearing (**Fig. 11**): This mechanism relies on the ability of the fasteners to force framing elements into the insulation and the ability of the insulation to sustain bearing stresses.
- Mechanism 5—strut and tie (**Fig. 12**): This mechanism requires appropriately oriented slope in the screw and the ability of the insulation to develop and sustain compression stresses.

To quantify the extent to which any of these mechanisms can be mobilized and sustained, the analyst requires reliable values for material properties (for example, insulation modulus and creep parameters), material interactions (for example, rotational stiffness of screw/stud interfaces, reactions of insulation to concentrated loads), and connection geometry. For lighter-weight veneers, it may be most efficient to use conservative assumptions and provide more connections than are really required. As veneer weight increases, a point is reached where using a conservative approach is no longer practical and thus the benefit of improving connection optimization also increases. In such cases, connections must carry higher loads, which means designers need to be able to determine reliable capacities and establish realistic force-displacement characteristics. Unfortunately, there are very

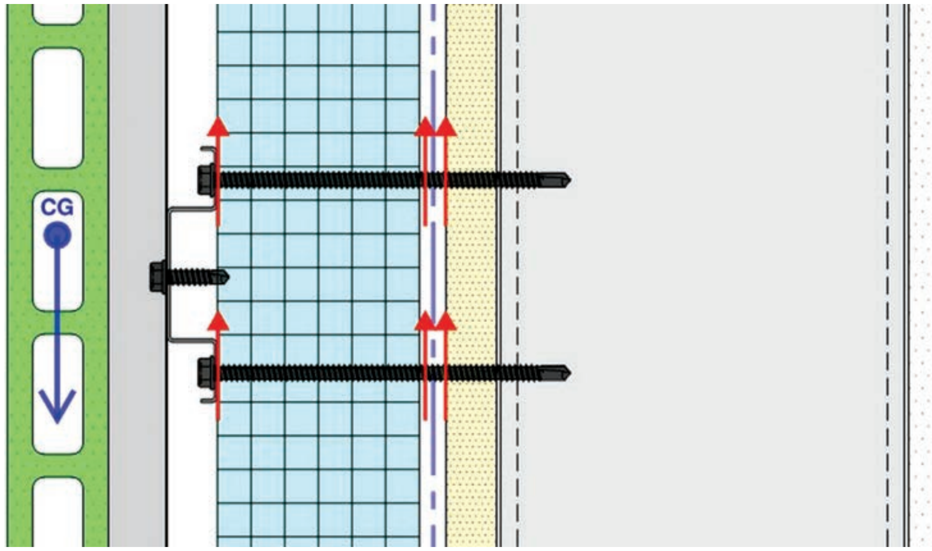

Figure 10. In-plane load-resisting mechanism 3—friction.

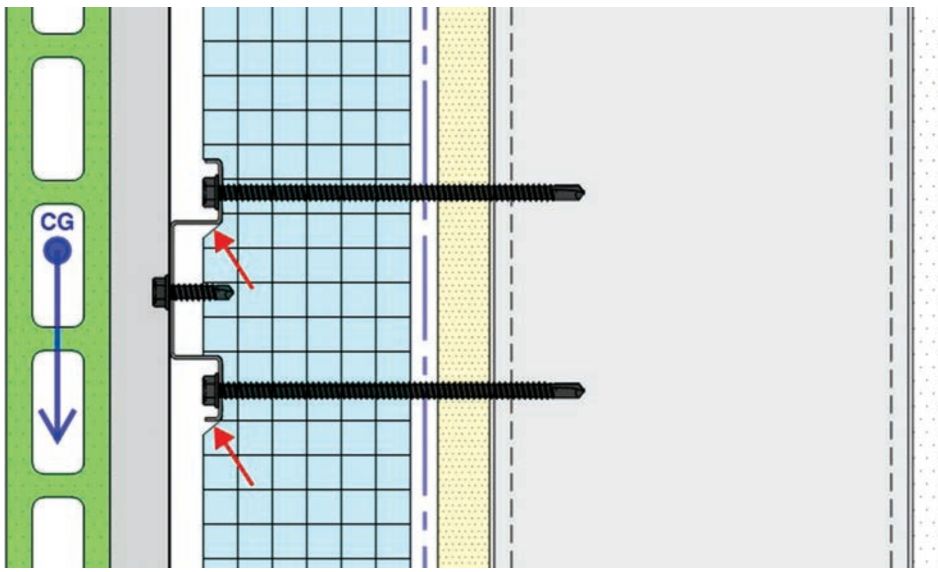

Figure 11. In-plane load-resisting mechanism 4—sub-frame bearing.

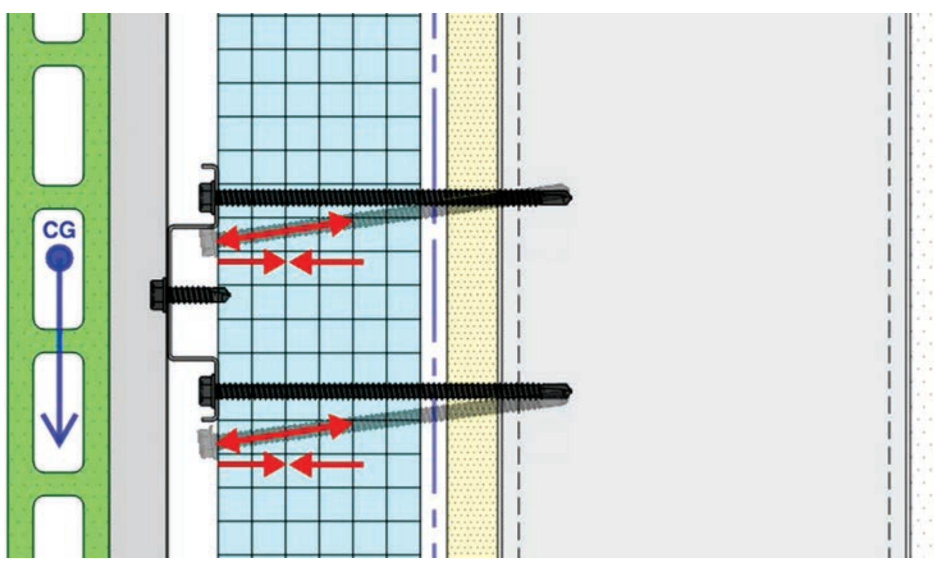

Figure 12. In-plane load-resisting mechanism 5—strut and tie.

few resources available to structural designers for reliably and efficiently quantifying the strengths, stiffnesses, and long-term deformation characteristics of the mechanisms outlined previously.

COMPLETED RESEARCH

Industry experience (that is, past performance of installed systems), project-specific testing, and manufacturer-tested proprietary systems clearly show that surface-mounted connections are viable. However, comprehensive data concerning the performance of various combinations of structural backup, connection details, insulation properties, and veneer characteristics are lacking. Reliable information related to certain individual element properties is also sparse. In other words, we know that surface-mounted connections can work, but, with the exception of simply replicating a proven system, we lack the means for analytically demonstrating good performance.

Available research studies often refer to and build upon findings from the 2010 New York State Energy Research and Development Authority (NYSERDA) study,[3] which intended to "develop attachment techniques and materials for securing building cladding and continuous insulation to above-grade, steel-framed walls of single family and multifamily buildings." The study involved many tasks, including review of building codes and performance requirements for cladding fasteners, review of options to develop plastic fasteners to eliminate thermal bridging, evaluation of constructibility of connections through continuous insulation, and limited testing of connection assemblies to develop a prescriptive capacity table for cladding attachment through continuous insulation.

Examples of research completed since the 2010 NYSERDA study include the following:

- *External Insulation of Masonry Walls and Wood Framed Walls*, published by the US Department of Energy National Renewable Energy Laboratory (NREL) in January 2013[4]
- *Expert Meeting Report: Cladding Attachment over Exterior Insulation,* published by NREL in October 2013[5]
- *Cladding Attachment Over Thick Exterior Insulating Sheathing,* published by NREL in November 2013[6]
- Applied Building Technology Group's *Attachment of Exterior Wall Coverings through Foam Plastic Insulating Sheathing (FPIS) to Wood or Steel Wall Framing*, which was most recently updated in 2019[7]

While these studies provide useful information, they leave many questions unanswered. In fact, a common conclusion is that further study and testing are necessary to develop a rational analytical method for designing efficient surface-mounted connections. For example, *Cladding Attachment Over Thick Exterior Insulating Sheathing*[6] refers to completed testing and mechanics-based analytical equation models, but the authors, Baker and Lepage, conclude that "the theorized load components that were modeled do not provide a sufficiently accurate prediction of the measured load components to be used in a reliable design model."

In attempts to make use of available test data, the concept of a "gap factor" was developed. Gap factors are applied to existing shear capacity equations to approximate the reduced capacities resulting from the creation of separations, or gaps, between connected parts that result from insertion of continuous insulation. The 2010 NYSERDA study[3] developed gap factors for connections to wood framing by using wood shear connection design formulas from ANSI/AF&PA NDS-2005, *National Design Specifications for Wood Construction,*[8] in conjunction with testing of connections through continuous insulation into wood framing. While the gap factor approach has been shown to produce useful results in some situations involving wood backup framing, gap factors have not been developed for materials that provide different degrees of restraint for surface-mount screws (for example, metal studs). Furthermore, the gap factors developed in the NYSERDA study are based on a deflection limit of 1⁄64 in. (0.4 mm), which may be overly stringent in some cases.

Baker and Lepage[6] monitored veneer deflections of test assemblies for a period of 70 days between July and September 2012. The assemblies were constructed similarly with of 4-in.-thick (100-mm-thick) panels of various insulation types (XPS, EPS, polyisocyanurate, and rigid mineral fiber). Ultimately the study concluded that loads of 30 lb (14 kg) per fastener or greater demonstrated a potential for long-term creep of the assemblies that were tested. This study did not consider many factors such as seasonal temperature variations, diurnal temperature variations during other seasons, varying insulation thicknesses or other framing materials. Considering the study's many limitations, the authors appropriately recommend further investigation of long-term creep of directly attached veneers through continuous insulation.

Despite the many limitations of studies performed to date, the information they provide has been used to develop design aids, including tables adopted by the *International Residential Code* (IRC) and IBC. The tables included in the IRC are Tables R703.15.1 and R703.15.2, which were adopted in the 2015 edition.[9] The tables included in the IBC are Tables 2603.12.1 and 2603.12.2 for cold-formed steel framing and Tables 2603.13.1 and 2603.13.2 for wood framing, all of which were adopted in the 2018 edition.[10]

These IRC and IBC tables provide limits to the thickness of insulation based on various factors, including framing member material and size, fastener size, fastener spacing, furring spacing, and weight of the cladding. The tables were specifically developed based on limited available test data to control deflection of the cladding to less than 0.015 in. (0.38 mm) under the dead load only.[10] The tables do not provide any information concerning the abilities of various connections to resist other demands. Consequently, the tables should not be used by designers as a prescriptive fastener design tool, but merely as an aid for checking dead-load deflection.

Furthermore, even using the tables to check deflections should be done with care. If deflection tolerances greater than 0.015 in. (0.38 mm) are acceptable, the tables could be overly conservative. Conversely, the tables may be unconservative as minimum requirements for a deflection tolerance of 0.015 in. because they are based only on the weight of the veneer. Other demands (for example, ice loads, cyclic thermal loads) can also cause veneers to move.

Given the current lack of sufficient information to reliably and accurately analyze surface-mounted veneer performance, designers are left with the following methods for developing connections that have a high likelihood of performing adequately:

- Replicate a design that has performed well during many years of service in similar conditions.
- Use clearly conservative assumptions concerning the capacities of various mechanisms, such as those previously discussed.
- Rely on applicable and sufficient previous testing (for example, a properly tested proprietary system).
- Perform project-specific testing for short- and long-term effects.

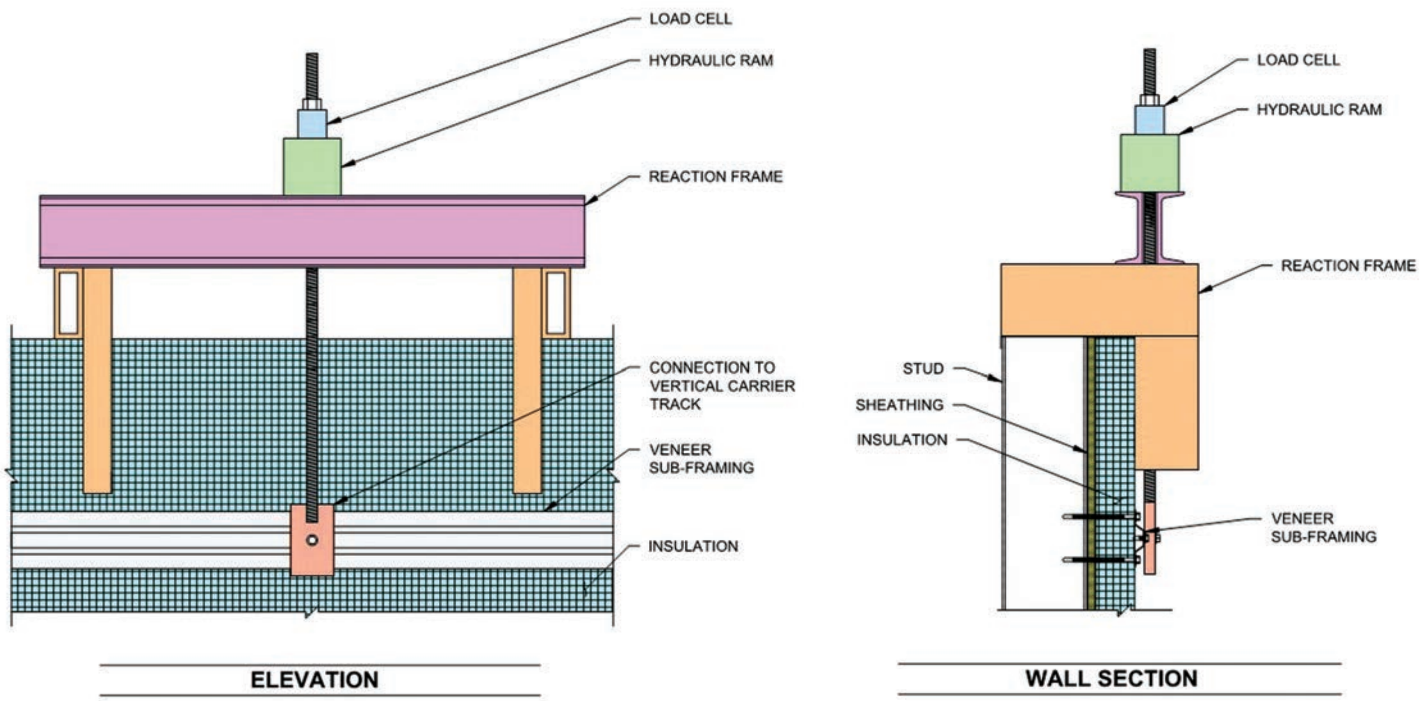

Figure 13. Schematics for a testing apparatus to quantify key performance features of surface-mounted connections on structure with a relatively heavy veneer.

TESTING

When the means for analytically quantifying structural performance are lacking, testing often provides a reasonable substitute. Testing of surface-mounted veneer connections can be used to demonstrate strength and stiffness characteristics, which can then be incorporated into the design process. Currently, there is no nationally recognized standard test method for quantifying strength and deformation characteristics of surface-mounted veneer connections that pass through continuous insulation. However, there are many practical ways to efficiently and accurately quantify relevant connection characteristics. Some researchers have adapted standard tests for wood connections, including ASTM D1761, *Standard Test Methods for Mechanical Fasteners in Wood and Wood-Based Materials.*[11] ASTM D1761 includes test procedures for quantifying properties such as withdrawal resistance and lateral load transmission of nails, staples, and screws when embedded in wood or wood-based materials. While aspects of the ASTM D1761 methods may be adaptable to veneer connections through continuous insulation, many requirements in the standard may be inapplicable or even detrimental.

Figures 13 and 14 show an apparatus the authors developed to quantify key performance features of surface-mounted connections on a completed building with a relatively heavy veneer. The project-specific testing included construction of an off-site mock-up that replicated the as-installed veneer connections and materials. The test setup comprised a load frame, hydraulic ram, load cell, and threaded rod connection to the vertical carrier track of the test specimen. The load frame legs incorporated L-shaped structural members where one leg rested horizontally on the surface of the insulation board while the other leg was vertical and reacted on the edge of the test specimen.

The testing procedure loaded the specimens monotonically to service loads and beyond while load and displacement data were collected. In these project-specific tests, deflections at service loads were consistently below the project-specified service load deflection limit of 1⁄16 in. (1.6 mm). To demonstrate adequate strength, test loads were increased

Figure 14. Testing apparatus developed by the authors to quantify key performance features of surface-mounted connections on a structure with a relatively heavy veneer.

well beyond factored demands. This test program did not include evaluation of long-term deflections under sustained dead load. Such testing was considered unnecessary given the following project-related facts: the as-built system showed no evidence of time-dependent movement during five months of service; and the ultimate strengths of the tested connections were more than 10 times the service load, which suggests that sustained stresses in creep-sensitive materials were very low.

EVOLUTION OF TEST-BASED DESIGN METHODS

Given the evident complexity of most surface-mounted veneer connections through insulation, continuing the development of test-based design equations may be the most efficient approach for providing useful and reliable design tools. Empirically derived design formulas are very common in structural engineering. Examples include equations used to quantify many types of connection behaviors such as concrete anchor breakout, reinforcing bar splice failures, bearing of structural steel bolts, and shear failure of wood screws. Prior to the last two decades, design of concrete anchors relied heavily on manufacturer-provided breakout capacities, which were often established using inconsistent methods of testing and data interpretation. In addition, the conditions tested by manufacturers often failed to include conditions of interest to structural engineers. To enhance concrete anchor design reliability and flexibility, the concrete industry instituted an intensive program of testing, which resulted in a standardized analytical approach for designing concrete anchors that can be used under an extensive array of conditions.

This approach uses a baseline capacity (that is, basic concrete breakout strength) that is modified by application of several factors that are individually associated with influential variables to appropriately adjust the calculated anchor capacity for various conditions. A similar approach could be used to develop design equations for surface-mounted veneer connections with adjustment factors to reflect relevant variables, such as insulation strength, stiffness, thickness, and creep properties; fastener type and orientation; structural framing properties; and subframing features.

CONCLUSION AND PROPOSED ACTIONS

Adding continuous insulation to the exterior wall assembly offers many benefits, and this practice is becoming more common as the industry demands higher energy performance. However, the inclusion of continuous insulation in exterior walls with directly attached veneer systems poses connection design challenges for structural engineers. Based on the experience of the industry as well as limited research conducted in the past two decades, we know that many of the connections for directly attached veneers over continuous insulation can support the necessary demands within relatively stringent deflection tolerances. However, there is no recognized rational analytical means for designers to reliably calculate the capacities and deformation characteristics of these rather complex connections.

While the industry has made modest progress in providing guidance to designers for certain veneer connection types and configurations, more extensive research is necessary to accurately identify and characterize the mechanisms and variables that contribute to capacity. Until this is done, designers are resigned to rely on crude, conservative analyses, replication of proven designs, testing of identical connections (for example, tested proprietary connections), or project-specific testing of new connections.

The authors recommend the industry pursue the following action items to build upon previous research:

- Develop a standardized test method specific to directly attached veneer through continuous insulation focused on demands parallel with the plane of the wall.
- Compile and use test data to develop formulas for calculating capacities and deformation characteristics of directly attached veneers through continuous insulation.

REFERENCES

1. International Code Council (ICC). 2021. *2021 International Building Code* Country Club Hills, IL: ICC.
2. American National Standards Institute (ANSI), American Society of Heating, Refrigerating and Air-Conditioning Engineers (ASHRAE), and Illuminating Engineering Society (IES). 2019. *Energy Standard for Buildings Except Low-Rise Residential Buildings*, ANSI/ASHRAE/IES 90.1-2019. Atlanta, GA: ASHRAE.
3. Newport Ventures. 2010. *Fastening Systems for Continuous Insulation* Albany: New York State Energy Research and Development Authority. https://www.nyserda.ny.gov/-/media/Files/Publications/Research/Other-Technical-Reports/fastening-systems-continuous-insulation.pdf.
4. Baker, P. 2013. *External Insulation of Masonry Walls and Wood Framed Walls*. Golden, CO: US Department of Energy National Renewable Energy Laboratory (NREL). https://www.nrel.gov/docs/fy13osti/54643.pdf.
5. Baker, P. 2013. *Expert Meeting Report: Cladding Attachment over Exterior Insulation*. Golden, CO: NREL. https://www.nrel.gov/docs/fy14osti/57260.pdf.
6. Baker, P., and R. Lepage. 2014. *Cladding Attachment Over Thick Exterior Insulating Sheathing*. Golden, CO: NREL. https://www.nrel.gov/docs/fy14osti/57825.pdf.
7. Applied Building Technology Group (ABTG). 2015, updated 2019. *Attachment of Exterior Wall Coverings through Foam Plastic Insulating Sheathing (FPIS) to Wood or Steel Wall Framing*, ABTG Research Report no. 1503-02. Madison, WI: ABTG. https://www.appliedbuildingtech.com/rr/1503-02.
8. ANSI and American American Forest and Paper Association (AF&PA). 2005. *National Design Specification for Wood Construction*. ANSI/AF&PA NDS-2005. Washington, DC: AF&PA.
9. International Code Council (ICC), *2015 International Residential Code* (Country Club Hills, IL: ICC, 2015).
10. International Code Council (ICC), *2018 International Residential Code* (Country Club Hills, IL: ICC, 2018).
11. ASTM International, 2020. *Standard Test Methods for Mechanical Fasteners in Wood and Wood-Based Materials*, ASTM D1761-20. West Conshohocken, PA: ASTM International. https://doi.org/10.1520/D1761-20.

You Down with VIG: A Vacuum-Insulated Glazing Primer

Sarah Sinusas, PE

Wiss, Janney, Elstner Associates Inc. | New Haven, CT

ssinusas@wje.com

Joseph M. Bukovec, RRO, PE

Walker Consultants | New Haven, CT

jbukovec@walkerconsultants.com

IIBEC 2022 - Building for the Future

International Convention and Trade Show

March 17–22, 2022 | Orlando, FL

ABSTRACT

Vacuum-insulated glazing (VIG) is an emerging technology that has been in commercial development for the past 20 to 30 years The concept was first described in a German patent application in 1913 and was more seriously studied, with the production of real units, in the 1980s. While some VIG technology has been commercially available since 1996, its presence in the United States architectural market has been minimal. The presentation includes a brief history of VIG technology, describes the typical makeup of VIG and hybrid VIG units, addresses the thermal performance of available products, and discusses considerations for evaluating various products available in the market. The presentation also offers two recent projects as case studies.

SPEAKERS

Sarah Sinusas, PE

Wiss, Janney, Elstner Associates Inc. | New Haven, CT

Sarah Sinusas is a senior associate at Wiss, Janney, Elstner Associates Inc. (WJE) in New Haven, Conn. She has specialized in building enclosure systems since beginning her career in 2008. Her primary focus is the evaluation and investigation of curtainwall and window assemblies, and she has participated in and led projects that include design, detailing, testing, and monitoring of a variety of cladding and glazing systems. Sinusas led WJE's assessment of vacuum-insulated glass for the case studies in this presentation.

Joseph M. Bukovec, RRO, PE

Walker Consultants | New Haven, CT

Joseph M. Bukovec is the director of building envelope, forensics, and restoration for Walker Consultants in New Haven, Conn. He has specialized in historic preservation and building enclosure systems since beginning his career in 2005. His primary focus is the investigation and repair design of historic facades, windows, roofing, and waterproofing systems. He has consulted on projects that include the investigation, testing, repair design, and construction administration for architecturally significant facades and roofs. With his previous firm, Bukovec was the project manager for one of the case studies in this presentation, which included the replacement of historic wood-framed windows with state-of-the-art hybrid vacuum-insulated glazing units in thermally broken aluminum frames.

You Down with VIG: A Vacuum-Insulated Glazing Primer

Glass has been used in buildings for millennia. Monolithic (single-pane) float glass was the standard for architectural glass installed in building facades for the first half of the 20th century. As architectural styles evolved and advancements were made in the production of construction materials, architects began to explore designs with aluminum and glass curtainwall facades and, in general, greater use of glass and metal. This new style of architecture, generally referred to as midcentury modern, produced many buildings where large mechanical systems were used to keep occupants warm in the winter and cool in the summer to compensate for the thermal inefficiencies in the building facade components. Glass and metal are poor insulators (the *R*-value is about R-1 for a single pane of ¼-in. -thick [6 mm] glass), and they require significantly more energy consumption than their architectural predecessors, mass masonry walls, which provide significant thermal mass and two to four times the *R*-value of glass and metal. Although insulating glass units (IGUs) were patented in the 1860s, it was not until the late 1970s, after the oil embargo, that they began to gain in popularity for their increased *R*-value, resulting in improvements in building energy consumption.

An IGU in its simplest form consists of two panes of glass separated by a captured air space. This concept approximately doubles the insulating value compared with single-pane glass. For example, a simple 1-in. -thick (25-mm-thick) IGU with a ½ in. (12 mm) air space has a thermal resistance of about R-2.

To achieve insulating performance and maintain durability and clarity of the unit, the perimeter of the IGU must be hermetically sealed to keep outside air and moisture out of the unit. Additionally, desiccant is provided in the perimeter edge spacer to absorb any slight moisture captured within the unit at the time of its manufacture. The air space dimension, typically ½ in. (12 mm) for commercial IGUs, is sized for thermal efficiency—a wider air space would result in less conductive heat loss but would allow convective loops that begin increasing heat transfer.

As IGUs have become more widely adopted over the past 50 years, there have been many improvements to the basic IGU technology to increase thermal efficiency. Today, it is common for both commercial and residential IGUs to employ low-emissivity (low-e) coatings and noble gas fills (such as argon or krypton), which can improve the *R*-values up to about R-4. There are also options to increase the number of captured air spaces to make triple or even quadruple IGUs. Increases to the number of captured air spaces and low-e coatings can improve center-of-glass *R*-values up to about R-8, but they also result in a much thicker assembly, which can require special considerations in the structural design of the frame components, anchors, and building structure.

Incorporating "high-performance" IGU technologies into new construction projects is now common practice. However, adapting these technologies for use in existing buildings presents building enclosure professionals with a long list of challenges. Addressing those issues often involves compromises in thermal performance or aesthetics, and can be costly for building owners.

WHAT ARE THE OPTIONS FOR EXISTING BUILDINGS?

While various forms of IGUs in combination with thermally broken window frames have helped improve thermal efficiency of windows and curtainwalls for the last half-century, older buildings with single-pane glass still make up a large segment of the built environment. One method commonly employed to improve thermal efficiency and occupant comfort in buildings with single-pane glass is to install exterior or interior storm windows. The application of a storm window provides a second barrier to bulk air transport (drafts) and can introduce a somewhat captured air space between the storm window and original window to improve thermal performance. However, storm windows are not always desirable; for example, they may detract from a building's aesthetics, affect access to operable features, and create a potential for condensation in the interstitial space. Installation of an IGU into a window that once contained single-pane glass can be considered; however, an IGU will be thicker than the original single-pane glass and will likely require modification to the glazing pocket and stops that hold the glass in place. A 1-in. -thick (25-mm-thick) IGU is also twice as heavy as a ¼-in. -thick (6-mm-thick) glass pane. This increase in dead load can affect the operation of operable windows and can require structural retrofit of curtainwall anchors. In these instances, reglazing options are limited. In circumstances such as these, vacuum-insulated glass (VIG) may be a suitable solution to improve thermal efficiency. This article will describe the components that make up a VIG unit, compare VIG thermal

> The vacuum space dimension and vacuum pressure within the VIG unit are designed to eliminate conductive and convective heat exchange between the two panes of glass. By reducing conductive and convective heat exchange, the thermal performance of the glazing unit improves significantly.

performance to double- and triple-pane IGUs, and present highlights from two recent projects involving VIG.

WHAT EXACTLY IS VIG?

The VIG concept was first described in a German patent application in 1913 and was more seriously studied, with the production of real units, in the 1980s.[1] Internationally, VIG technology has been commercially available since 1996,[2] but its presence in the US market has been minimal. There are ongoing challenges related to maintaining consistent vacuum pressure (and therefore consistent thermal performance), the manufacturing of VIG units in sizes (and associated strengths) desired by architects, and costs of production. Research and development are underway to resolve these concerns.

A VIG unit consists of two panes of glass separated by a very thin space between them. Typically, this space is between 0.008 and 0.012 in. (0.2 to 0.3 mm). During fabrication of the VIG unit, the residual air that is within this thin space is pumped out, rendering a partial vacuum within the VIG unit.

To maintain the vacuum over time, the edges of the VIG unit glass panes are sealed together, usually with a metal or glass solder. A vacuum port, which is typically located at one corner of the unit, provides an access hole into the unit to extract the air. It is subsequently sealed, often with the same material as the edge seal. Because the pressure of the vacuum will be great enough to draw the two panes of glass together and collapse the VIG, it is critical to maintain the thin space between the glass panes. This is accomplished with a grid of small mircospacers or pillars, which are placed between the glass panes (**Fig. 1** and **2**). Often, these pillars are 0.02-in.-diameter (0.5-mm-diameter) oblong spheres placed in a grid (for example, 2 x 2 in. [50 × 50 mm]) within the vacuum space. Also within the vacuum space, a "getter"—a specially formulated mixture of metals intended to absorb or dissolve impurities (gases or particles) within the vacuum space—is placed at corners.

Although manufacturers' specifications vary, the vacuum space dimension and vacuum pressure within the VIG unit are designed to eliminate conductive and convective heat exchange between the two panes of glass. In a standard double-pane IGU with low-e coating, the convection/conduction component of heat exchange can account for about 70% of the total heat exchange through the unit.[3] By reducing conductive and convective heat exchange, the thermal performance of the glazing unit improves significantly.

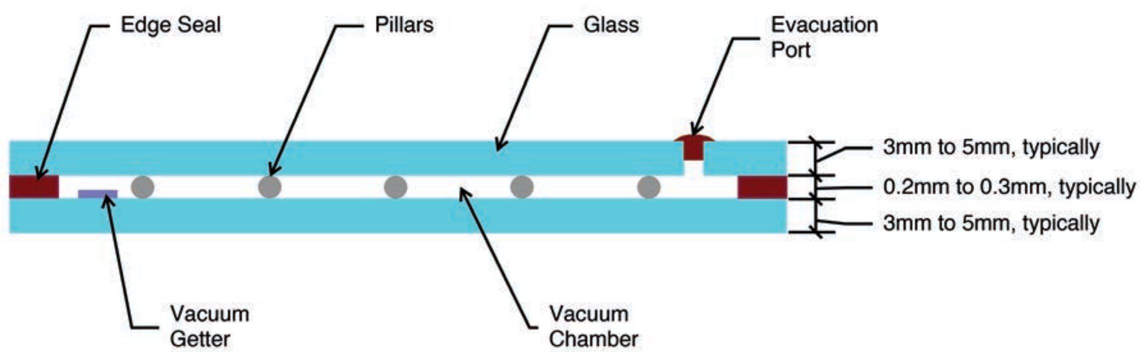

Figure 1. Diagram of typical vacuum-insulated glass unit construction. Note: 1 mm = 0.0394 in.

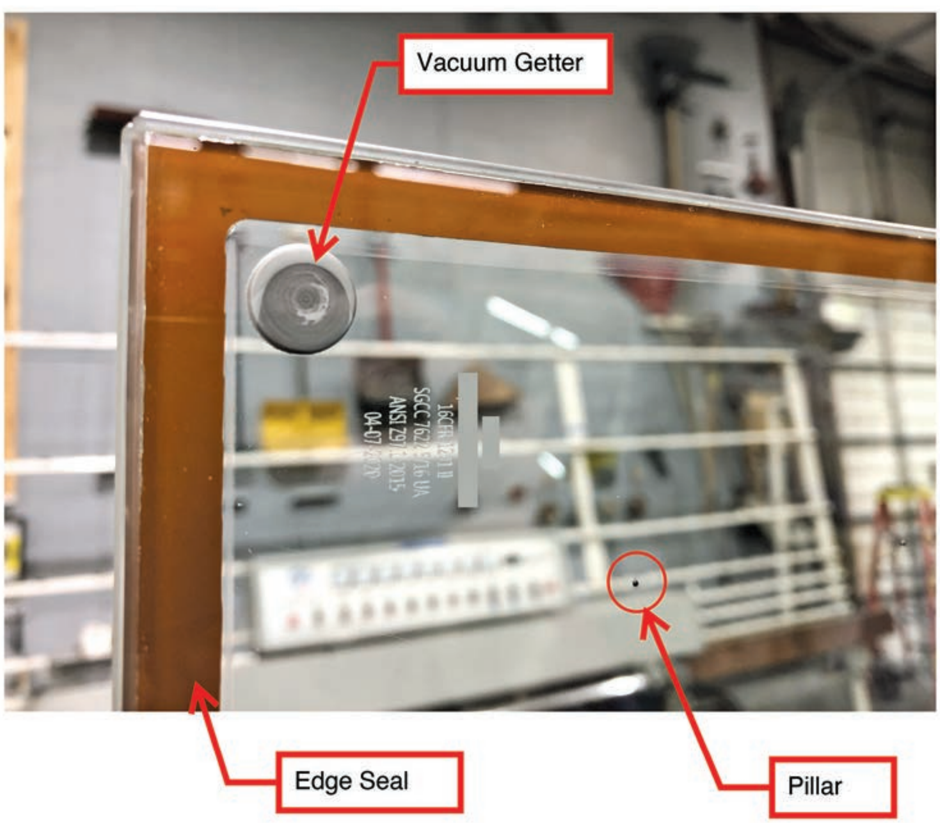

Figure 2. A corner of a vacuum-insulated glass unit.

For further improvements in thermal efficiency, VIG units can also be glazed into IGUs to create hybrid-VIG units. In a hybrid-VIG unit, the VIG serves as one pane of the IGU (**Fig. 3**). Traditional mechanisms to improve thermal performance of IGUs, including the

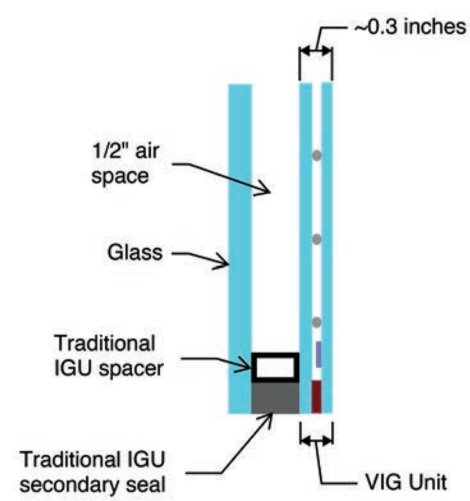

Figure 3. Diagram of typical hybrid-VIG unit. Note: IGU = insulating glass unit; VIG = vacuum-insulated glass. 1 in. = 25.4 mm.

application low-e coatings and alternate noble gas fills (such as argon or krypton) can also be employed in hybrid-VIG units.

HOW GOOD IS VIG THERMAL PERFORMANCE?

Table 1 highlights the center-of-glass thermal performance of single-pane glass and typical IGU assemblies compared with VIG and hybrid-VIG units. **Figure 4** illustrates the conventional numbering of glass surfaces used in the table.

Please note that Table 1 should be used for general comparison purposes only. There are many types of low-e coatings, glass colors, and glazing assemblies available in the marketplace, and actual performance of a specific assembly may be less than or greater than the example glass makeups and performance values listed.

One item that should stand out in Table 1 is that not all VIG units are created equal. For example, the two 5⁄16 in. (8 mm) VIG units listed in the table (R-5.5 and R-11) are from different manufacturers and include different pillar arrays (pillar spacings) and low-e coatings. Variables that specifically affect the thermal performance of VIG units include the low-e coating, pillar spacing, and vacuum pressure within the unit, which vary by manufacturer and product line.

CONSIDERATIONS IN THE USE OF VIG: TRUST BUT VERIFY

Unique to VIG units, the unit's thermal transmittance (U-factor) may change as the unit ages and as there are small changes in the vacuum pressure. Similar to any vacuum (including your stainless steel vacuum-walled water bottle), the VIG edge seal can remain intact, but the vacuum pressure can decrease as a result of discharge of material surface particles facing the vacuum space. Air leakage through the edge seal would also significantly affect the vacuum pressure. ISO 19916-1, *Glass in Building—Vacuum Insulating Glass—Part 1: Basic Specification of Products and Evaluation Methods for Thermal and Sound Insulating Performance*,[4] permits a 10% change between the initial U-factor and the U-factor following exposure testing (for example, temperature cycling, ultraviolet light exposure). It is therefore important to ask for test reports to support the manufacturer's reported U-factor, and to gain an understanding of the manufacturer's longest in-service units. The authors recently

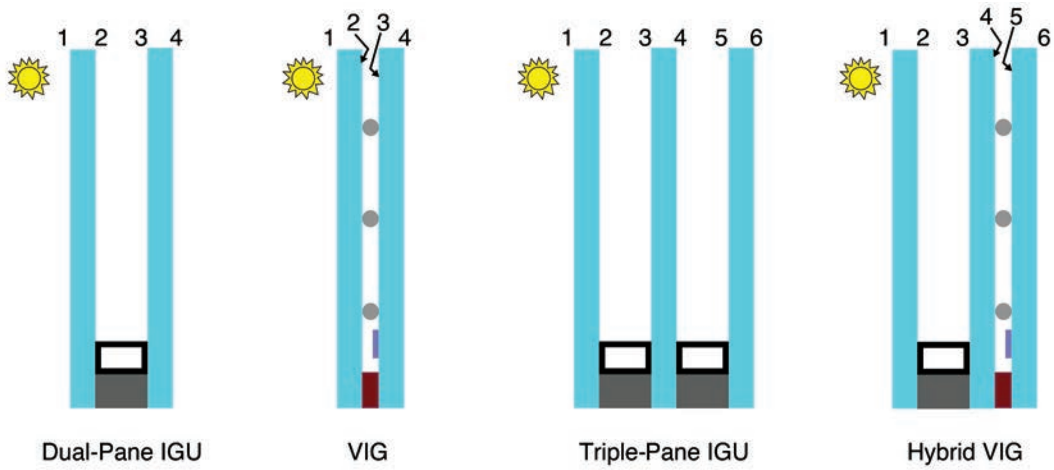

Figure 4. Glass surface nomenclature. Note: IGU = insulating glass unit; VIG = vacuum-insulated glass.

Description†	Approximate U-Factor‡ (BTU/h-ft²-°F)	Approximate *R*-Value‡
¼ in. (6 mm) clear glass	1.03	R-1
1 in. (25 mm) IGU with low-e on no. 2 surface, with air fill	0.29	R-3.5
1 in. (25 mm) IGU with low-e on no. 2 surface, with argon fill	0.25	R-4
1¾ in. (44 mm) triple-pane IGU with low-e on no. 2 and no. 5 surfaces, with argon fill	0.12	R-8
5⁄16 in. (8.2 mm) VIG (3 mm clear, 0.2 mm vacuum, 5 mm clear with low-e on no. 2 surface)	0.18	R-5.5
5⁄16 in. (8.2 mm) VIG (4 mm clear with low-e on no. 2 surface, 0.3 mm vacuum, 4 mm clear)	0.09	R-11
1¹⁄16 in. (27 mm) hybrid-VIG (4 mm clear with low-e on no. 2 surface, 0.3 mm vacuum, 4 mm clear, 12.7 mm in. argon fill, 6 mm glass with low-e on no. 4 surface)	0.07	R-14

IGU = insulating glass unit; low-e = low emissivity; VIG = vacuum-insulated glass. *R*-value = 1/U-factor. 1 mm = 0.0394 in.

*There are many different low-e coatings, glass colors, and glazing assemblies available in the marketplace. This table should be used for general comparison purposes only. Actual performance of a specific assembly may be less than or greater than the values listed.

†In the descriptions, low-e coatings on the no. 2, no. 4, and no. 5 surfaces are described. Glass surfaces are conventionally numbered from exterior to interior (see Fig. 4).

‡The U-factors and *R*-values in this table are center-of-glass values, which were calculated using Lawrence Berkeley National Laboratory's WINDOW software or derived from manufacturer's literature where applicable. The center-of-glass U-factors and *R*-values do not account for conductive heat loss at the edge of glass due to the spacer and/or the window/curtainwall frame.

*Table 1. Thermal transmittance of selected glazing products**

oversaw testing according to the National Fenestration Research Council's *Procedure for Measuring the Steady Thermal Transmittance of Fenestration Systems* (NFRC 102)[5] and found that the actual center-of-glass U-factor (before exposure testing) correlated to the manufacturer's published center-of-glass U-factor but was approximately 15% greater (worse performing) than the manufacturer's initially advertised center-of-glass U-factor.

It is also important to note that the center-of-glass U-factor (or *R*-value) is typically the highest-performing measurement of thermal transmittance for a VIG unit; in this way, VIG units are similar to traditional IGUs. Edge effects of the VIG unit, potentially compounded by non–thermally broken framing, increase the overall thermal transmittance of the assembly. For this reason, the impact of retrofitting with VIG units on overall thermal transmittance increases with the unit size (that is, the larger the ratio of center-of-glass is compared with the total window area, the greater the impact is). In the NFRC 102 testing overseen by the authors, we have found edge effects in VIG can extend 2.5 to 5 in. (64 to 125 mm) into the glass daylight opening; however, the effects may vary by specific product. Additionally, a non–thermally broken frame will further increase thermal transmittance. Most buildings with single-pane exterior glass also employ non–thermally broken window or curtainwall framing. Thermally improving the framing, in conjunction with improved glazing performance, will provide the greatest overall thermal improvement.

POSSIBLE VIG APPLICATIONS

VIG for Retrofit Application

The authors recently evaluated VIG units for a retrofit application involving the reglazing of a 22-story office building. The office building is clad in a non–thermally broken aluminum curtainwall with monolithic glass and uninsulated metal and glass spandrel panels. In this project, the installation of exterior storm windows would not be practical, interior storm windows are not desired, and the curtainwall cannot accommodate the added weight (approximately 2 times the weight of the existing glass) of IGUs without structural modification. Therefore, the project team explored VIG technology. Along with the installation of VIG, the project team is also planning to thermally improve accessible areas of the framing and insulate spandrel areas.

Thermal modeling using the Lawrence Berkeley National Laboratory's THERM software (**Fig. 5**) and NFRC 102[5] physical testing of a project-sized VIG specimen (4 ft 9 in. wide by 6 ft 9 in. high [1.5 m wide by 2 m high]) found that whole-window thermal transmittance increased by approximately 75% (indicating worse performance) when the VIG specimen was installed in a thermally improved aluminum frame, compared with the VIG manufacturer's reported center-of-glass value. Whole-window thermal transmittance increased by about 250% when the VIG specimen was installed in a non–thermally broken aluminum frame replicating the existing project frame conditions. Findings can be summarized as follows:

- The manufacturer's reported center-of-glass *R*-value is R-11.
- The approximate *R*-value of the mock-up assembly with a ½ in. (12 mm) edge of VIG captured in insulation (representing a *theoretical* fully "thermally broken" frame) was R-10.
- The approximate *R*-value of the mock-up assembly with VIG installed in a thermally improved project frame (Fig. 5) was R-6.
- The approximate *R*-value of the mock-up assembly with VIG installed in a non–thermally improved project frame (Fig. 5) was R-3.

These findings indicate that, as with all fenestration and insulating glass, the conductivity of the framing has a significant impact on overall assembly thermal performance.

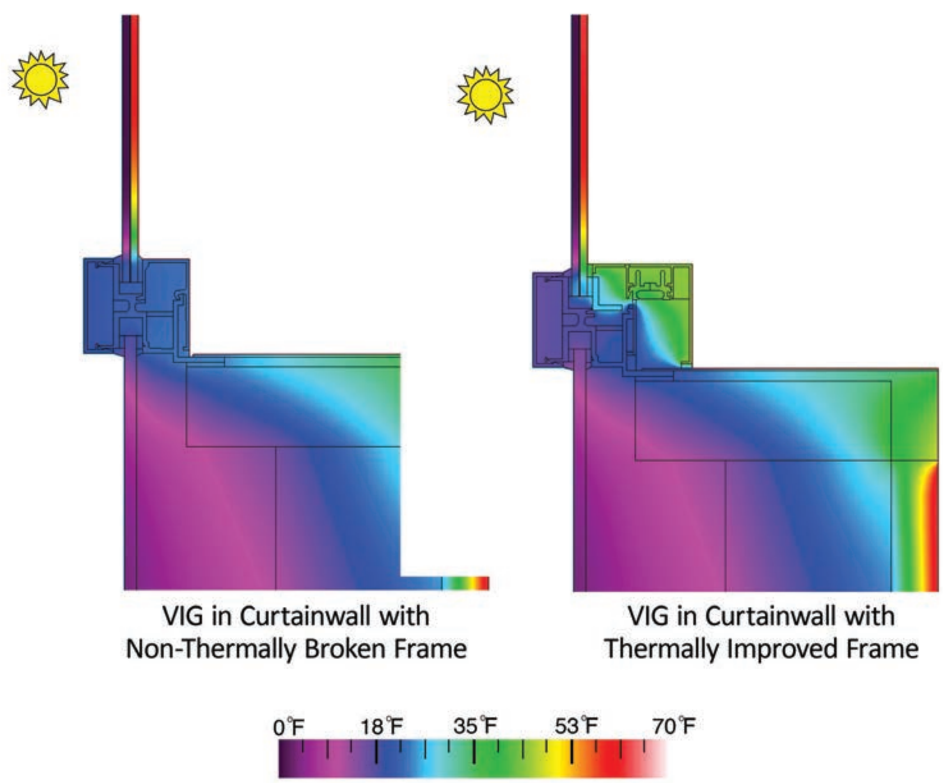

Figure 5. Comparison of vacuum-insulated glass (VIG) installed in an existing curtainwall frame and a thermally improved frame. Note that in this project, given the existing frame configuration, thermal breaks can only be provided at the interior side.

Hybrid VIG for High-Performance Windows

The track record for commercially available VIG units is limited. ISO 19916-1,[4] published in 2018, defines parameters for accelerated aging of VIG units; however, consensus testing parameters are relatively new and we therefore expect that they will continue to be refined. As the technology further evolves and VIG gains a stronger track record, hybrid-VIG units may also be considered for improved glazing performance in buildings with high window-to-wall ratios and correspondingly stringent energy code requirements (for example, in those projects that currently consider triple glazing), or in buildings with high sustainability and energy consumption goals.

Hybrid VIG in Historical Applications

The authors recently completed a project where hybrid-VIG units were installed in thermally broken aluminum-frame replacement windows in a four-story building whose owner was pursuing significant energy reductions. This building was constructed in the early 20th century and featured large wood-framed window assemblies. Before the project began, the existing wood-framed windows exhibited distress and decay, which had resulted in water intrusion and a negative aesthetic. When considering the repair or replacement of the wood-framed windows, the owner set aggressive goals for improved energy consumption (in combination with mechanical system upgrades) and ease of maintenance for the windows. Because of these requirements, as well as other project limitations, the restoration of the wood-framed windows and the installation of exterior storm windows were not viable options, and so the option of window replacement was pursued. Working with multiple window manufacturers and the contractor's team, the authors specified a thermally broken aluminum-framed assembly that included a hybrid-VIG unit. The hybrid-VIG units used on the project included the VIG unit as the interior pane of the IGU (similar to Fig. 3), with low-e coatings on the no. 2 and no. 4 glass surfaces. **Figure 6** shows the corner of the installed window. The center-of-glass *R*-value of the installed glass was reported by the manufacturer to be R-15. Installation of the hybrid-VIG units in the project window frames followed standard window-glazing procedures. The project was completed in late December 2020, and performance metrics such as energy savings and occupant comfort are still being gathered. We look forward to gathering these data for industry consumption.

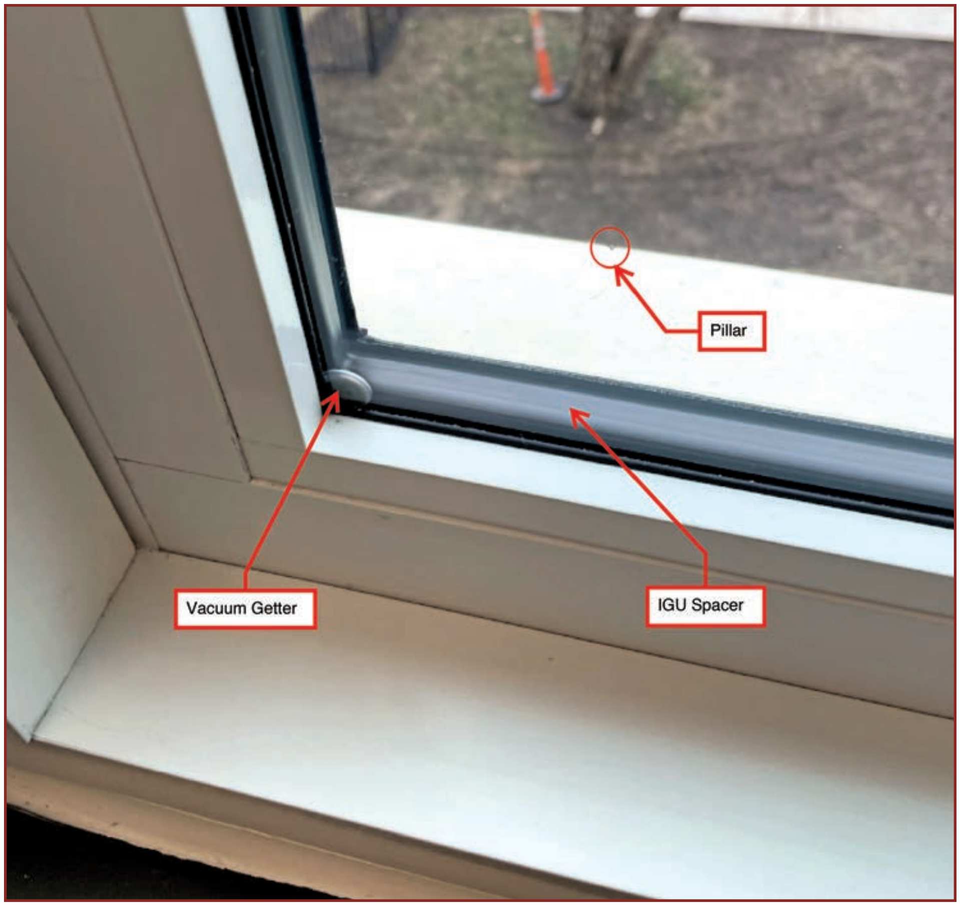

Figure 6. A corner of a hybrid–vacuum-insulated glass unit. Note: IGU = insulating glass unit.

CLOSING REMARKS

Although commercial installation of VIG and hybrid-VIG units in the United States is currently limited, the opportunities and advancements in VIG technology continue to grow. Older buildings with single-pane glass curtainwalls have proven a challenge to thermally improve, particularly in cases where storm windows are undesirable. There is an opportunity for the specifier to explore VIG as a suitable solution to improve thermal efficiency in these buildings. Hybrid-VIG units also present an opportunity to introduce higher center-of-glass U-factors to high-performance buildings and allow for the use of glazing while also improving energy consumption.

As described in the retrofit case study example, and as is typical with all fenestration, the conductivity of the framing has a significant impact on overall assembly performance. Therefore, the benefits of using VIG in a small fenestration (with a correspondingly small center-of-glass area) may be limited, particularly if the framing is also not thermally broken. Many VIG manufacturers, like IGU manufacturers, recommend a wept glazing pocket to minimize moisture in contact with the edge seal. Achieving this recommendation may be a challenge in retrofit projects and should be reviewed with the VIG manufacturer and project stakeholders to understand the corresponding impact on unit durability.

VIG may not be the silver bullet to solve thermal issues related to windows and curtainwalls, but it can provide impressive improvements to the assembly's U-factor when used appropriately.

REFERENCES

1. Lawrence Berkeley National Laboratory. 2019. "Vacuum Insulated Glazing (VIG)." https://windows.lbl.gov/vacuum-insulated-glazing-vig.
2. Collins, R. 2019. "Vacuum Insulating Glass—Past, Present and Prognosis." Paper first presented at Glass Performance Days (GDP) 2017. https://www.glassonweb.com/article/vacuum-insulating-glass-past-present-and-prognosis.
3. Pilkington North America. 2018. "Vacuum Insulated Glazing—Pilkington Spacia" (product brochure). https://www.pilkington.com/en/us/products/product-categories/thermal-insulation/pilkington-spacia.
4. International Organization for Standardization (ISO). 2018. *Glass in Building—Vacuum Insulating Glass—Part 1: Basic Specification of Products and Evaluation Methods for Thermal and Sound Insulating Performance*. ISO 19916-1:2018. Geneva, Switzerland: ISO.
5. National Fenestration Research Council (NFRC). 2020. *Procedure for Measuring the Steady Thermal Transmittance of Fenestration Systems*. NFRC 102-2020[E0A0]. Greenbelt, MD: NFRC. https://cdn.ymaws.com/nfrccommunity.org/resource/resmgr/2020_tech_docs/nfrc_102-2020_e0a0_redline_o.pdf.

Water, Wind, Windows, and Walls with Continuous Insulation

Jay H. Crandell, PE

ARES/ABTG Consulting | Shady Side, MD

jcrandell@aresconsulting.biz

IIBEC 2022 - Building for the Future

International Convention and Trade Show

March 17–22, 2022 | Orlando, FL

ABSTRACT

New research and building code provisions have improved appropriate means to continuously insulate walls and integrate fenestration in punched openings for optimal performance. This presentation reviews structural wind resistance and water resistance research supporting various detailing options in the context of new provisions in the latest editions of the *International Building Code* and *International Residential Code*. The presenter also discusses the thermal efficiency and thermal bridging implications of various details to integrate punched openings with continuous insulation on walls. In addition, the presentation includes a sneak preview of new research on wind-driven-rain hazard characterization to guide design, specification, and detailing decisions for water resistance of building enclosures and components.

SPEAKER

Jay H. Crandell, PE

ARES/ABTG Consulting | Shady Side, MD

Jay H. Crandell has over 30 years of experience in construction, engineering, and innovative building technology research for private and public sector clients. He has conducted benchmark studies of major natural disasters and conducted research to address significant structural, energy, and building science challenges. His work has helped propel many innovative technologies into international codes and consensus standards. He is widely published on various engineering, construction, and building science topics. For additional information, visit www.aresconsulting.biz and www.appliedbuildingtech.com.

Water, Wind, Windows, and Walls with Continuous Insulation

Continuous insulation (ci), as shown in **Fig. 1**, is a prescribed insulation component for energy code compliance and is commonly used for high-performance wall assemblies. It is defined as follows in the *International Energy Conservation Code* (IECC)[1] and ASHRAE Standard 90.1, *Energy Standard for Buildings Except Low-Rise Residential Buildings*[2]:

> Insulation that is uncompressed and continuous across all structural members without thermal bridges other than fasteners and service openings. It is installed on the interior or exterior or is integral to any opaque surface of the building envelope.

Although ci is primarily used for energy code compliance, its appropriate use must be considered together with various other wall components and functional requirements for a complete, building code–compliant wall assembly. These integrated design considerations include water vapor control, cladding installation, fire performance, and water, wind, and air-leakage resistance. The author has addressed many of these topics—including multifunctional applications of ci to optimize a wall assembly's constructability, cost, and performance—in previous IIBEC papers.[3-5] For additional information on these matters, including technical guidance, design resources, research, and code compliance listings, visit continuousinsulation.org.

This paper provides an update on new and forthcoming building code and energy code requirements related to the use of ci on above-grade walls for thermal and moisture control. Next, it addresses the latest research into installation practices and the installed performance of integrally flanged fenestration (typical for punched openings) on light-frame steel or wood walls with ci of foam plastic insulating sheathing (FPIS). In relation to fenestration installation details, the paper discusses the impact of thermal bridging at the window-to-wall interface with a view toward use of appropriate detailing with ci to limit thermal bridging. Finally, the paper presents preliminary insights from a new research project to evaluate wind-driven-rain hazards as they vary across the United States. All of these topics relate to the water and wind resistance of a complete wall assembly and particularly the interface of FPIS ci and fenestration components.

Although continuous insulation is primarily used for energy code compliance, its appropriate use must be considered together with various other wall components and functional requirements for a complete, building-code-compliant wall assembly.

EVOLVING CODE REQUIREMENTS

Although various types of insulation materials may be used as ci, this paper focuses on FPIS materials, which include expanded polystyrene (EPS), extruded polystyrene (XPS), and

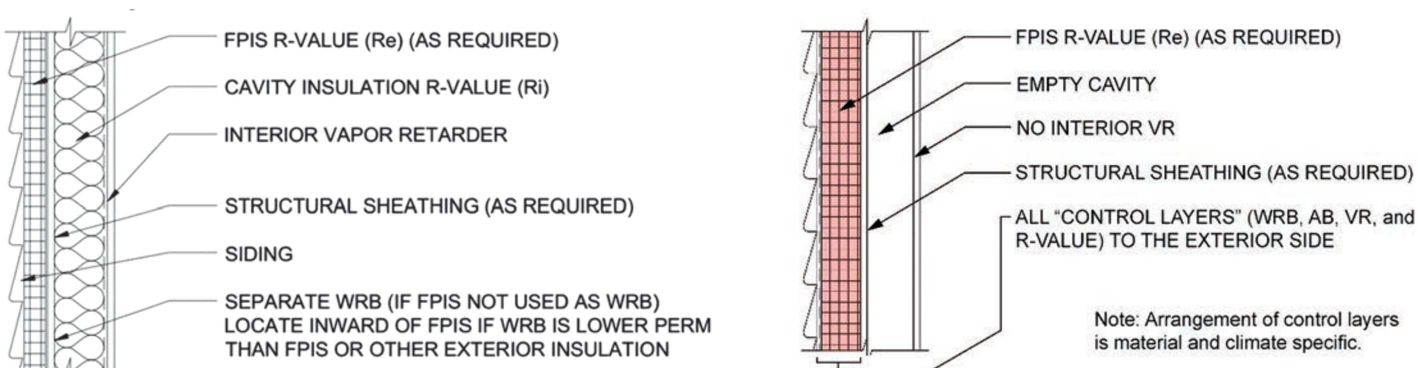

Figure 1. Example wall assemblies with continuous insulation. AB = air barrier; FPIS = foam plastic insulating sheathing; VR = vapor retarder; WRB = water-resistive barrier. Figure: Reference 25 and Crandell, J. H. 2017. "Assessment of Hygrothermal Performance and Design Guidance for Modern Light-Frame Wall Assemblies." In **Advances in Hygrothermal Performance of Building Envelopes: Materials, Systems and Simulations**, *P. Mukhopadhyaya and D. Fisler, eds., 362–394. ASTM STP1599. West Conshohocken, PA: ASTM International. https://doi.org/10.1520/STP159920160097.*

<table>
<tr><th rowspan="2">Climate zone</th><th rowspan="2">Building use</th><th colspan="2">Metal framed</th><th colspan="2">Wood framed</th></tr>
<tr><th>2018 IECC</th><th>2021 IECC</th><th>2018 IECC</th><th>2021 IECC</th></tr>
<tr><td rowspan="2">0 and 1</td><td>All other</td><td rowspan="3">R-13 + 5ci (U-0.077)</td><td rowspan="3">R-13+5ci (U-0.077)</td><td rowspan="9">R-13 + 3.8ci or R-20 (U-0.064)</td><td rowspan="8">R-13 + 3.8ci or R-20 (U-0.064)</td></tr>
<tr><td>Group R</td></tr>
<tr><td rowspan="2">2</td><td>All other</td></tr>
<tr><td>Group R</td><td rowspan="10">R-13 + 7.5ci (U-0.064)</td><td rowspan="5">R-13 + 7.5ci (U-0.064)</td></tr>
<tr><td rowspan="2">3</td><td>All other</td></tr>
<tr><td>Group R</td></tr>
<tr><td rowspan="2">4 except Marine</td><td>All other</td></tr>
<tr><td>Group R</td></tr>
<tr><td rowspan="2">5 and Marine 4</td><td>All other</td><td rowspan="2">R-13 + 10ci (U-0.055)</td><td rowspan="6">R-13 + 7.5ci or R-20 + 3.8ci (U-0.051)</td></tr>
<tr><td>Group R</td><td rowspan="5">R-13 + 7.5ci or R-20 + 3.8ci (U-0.051)</td></tr>
<tr><td rowspan="2">6</td><td>All other</td><td rowspan="3">R-13 + 12.5ci (U-0.049)</td></tr>
<tr><td>Group R</td></tr>
<tr><td rowspan="2">7</td><td>All other</td></tr>
<tr><td>Group R</td><td>R-13 + 15.6ci (U-0.052)</td><td>R-13 + 15.6ci (U-0.042)</td></tr>
<tr><td rowspan="2">8</td><td>All other</td><td>R-13 + 7.5ci (U-0.064)</td><td rowspan="2">R-18 + 18.8ci (U-0.037)</td><td rowspan="2">R-13 + 15.6ci or R-20 + 10ci (U-0.036)</td><td rowspan="2">R-13 + 18.8ci (U-0.032)</td></tr>
<tr><td>Group R</td><td>R-13 + 17.5ci (U-0.045)</td></tr>
</table>

ci = continuous insulation; IECC = *International Energy Conservation Code*.

*Table is based on IECC Commercial Provisions, Tables C402.1.3 and C402.1.4.

*Table 1. Comparison of 2018 and 2021 IECC prescriptive insulation requirements for light-frame, above-grade walls—commercial buildings**

polyisocyanurate (PIR). Code-compliant FPIS products are manufactured in accordance with ASTM C578, *Standard Specification for Rigid, Cellular Polystyrene Thermal Insulation*,[6] and ASTM C1289, *Standard Specification for Faced Rigid Cellular Polyisocyanurate Thermal Insulation Board*.[7] These standards provide a foundation for complying with various building code and energy code provisions governing the use of FPIS in residential and commercial building construction.[1,2,8,9]

Energy Code Updates for Above-Grade Walls

Tables 1 and 2 compare prescriptive *R*-values and U-factors required for above-grade walls of light-frame construction in the 2018 and 2021 editions of the IECC for commercial and residential construction. For commercial buildings (Table 1) with cold-formed steel frame ("metal framed") walls, the 2021 IECC[1] specifies improved thermal performance in Climate Zones 5 through 8, including Marine 4. For wood-framed walls, the 2021 IECC requires thermal performance improvements for Climate Zone 5/Marine 4 (for non–Group R buildings only) and Climate Zone 8. Thus, these improvements focus on colder climate zones where energy savings tend to be more significant. In all of these cases, the IECC approach has relied on a "hybrid" use of ci with cavity insulation (see Fig. 1).

<table>
<tr><th rowspan="2">Climate zone</th><th colspan="2">Wood-frame walls</th></tr>
<tr><th>2018 IECC</th><th>2021 IECC</th></tr>
<tr><td>0, 1, and 2</td><td>R-13 (U-0.084)</td><td>R-13 or R-0 + 10ci (U-0.084)</td></tr>
<tr><td>3</td><td rowspan="3">R-20 or R-13 + 5ci (U-0.060)</td><td>R-20 or R-13 + 5ci or R-0 + 15ci (U-0.060)</td></tr>
<tr><td>4 except Marine</td><td rowspan="4">R-30 or R-20 + 5ci or R-13 + 10ci or R-20ci (U-0.045)</td></tr>
<tr><td>5 and Marine 4</td></tr>
<tr><td>6</td><td rowspan="2">R-20 + 5ci or R-13 + 10ci (U-0.045)</td></tr>
<tr><td>7 and 8</td></tr>
</table>

ci = continuous insulation; IECC = *International Energy Conservation Code*.

*Table is based on IECC Residential Provisions, Tables R402.1.2 and R402.1.3.

*Table 2. Comparison of 2018 and 2021 IECC prescriptive insulation requirements for light-frame, above-grade walls—one- and two-family dwellings**

For one- and two-family dwellings and low-rise multifamily construction (Table 2), the 2021 IECC revised the prescriptive insulation requirements in two ways. First, in all climate zones, options to use cavity insulation only, cavity insulation and ci (hybrid), and ci only were added. These options represent the three main strategies for insulation placement on light-frame walls and are evaluated to provide equivalent thermal performance (U-factor) for the total wall assembly. These options also provide flexibility to optimize other performance functions such as moisture control in coordination with building code requirements. The U-factor and appropriate calculation methods (such as the parallel path procedure for wood-frame walls) can be used to justify many other equivalent variations.

Second, as shown in Table 2, the 2021 IECC requires significant improvements or increases in thermal performance for above-grade walls for Climate Zones 4 and 5 (matching requirements only applied to Climate Zones 6–8 in the 2018 IECC). *R*-value solutions are provided for cavity-only insulation (R-30), hybrid 2 × 4 and 2 × 6 assemblies with cavity insulation and ci (R-13 + 10ci or R-20 + 5ci), and ci-only assemblies (R-20ci). Use of these assemblies in any given climate must be coordinated with the vapor-retarder provisions in the building code, as addressed in the next section.

Finally, there is a seemingly small but significant change in the 2021 IECC commercial building provisions' definition of above-grade wall. The updated definition (with new text underlined) reads as follows:

> **WALL, ABOVE-GRADE.** A wall associated with the *building thermal envelope* that is more than 15 percent above grade and is on the exterior of the building or any wall that is associated with the *building thermal envelope* that is not on the exterior of the building. <u>This includes, but is not limited to, between-floor spandrels, peripheral edges of floors, roof knee walls, dormer walls, gable end walls, walls enclosing a mansard roof and skylight shafts.</u>

This revised definition makes it clear that the effects of thermal bridging caused by various assemblies and components intersecting with the above-grade wall must be considered in determining compliance with the thermal performance requirements (for example, *R*-values and U-factors) for the above-grade wall. Thus, mitigating thermal bridges with improved detailing has become more important for code compliance and is often a more cost-effective solution than ignoring the thermal bridge and attempting to offset it by adding more insulation or using some other type of tradeoff. In many cases, appropriate use and detailing of ci (which is also used on the wall assembly to address thermal bridging caused by framing members in the assembly) is an efficient way to satisfy the code requirement and improve building thermal enclosure performance. This topic is addressed in a later section with regard to thermal bridging at the window-to-wall interface.

The ASHRAE 90.1[2] provisions have explicitly required consideration of thermal bridging, particularly in the whole building modeling compliance path, where thermal bridges are somewhat mislabeled as "uninsulated assemblies."

Building Code Updates for Water Vapor Control with CI

Building codes are continuing to evolve to better address the three rules for moisture control that should never be broken[10]:

- Keep water vapor (humid air) away from cool surfaces.
- Minimize air leakage.
- Avoid rainwater intrusion.

These rules may not be equally important, but breaking any one of them can cause significant performance problems. Any wall assembly can break one or more of these rules if it is not properly designed, especially if the designer only follows older "rules of thumb" that rely exclusively on specification of an interior vapor retarder while ignoring the thermal and moisture-related properties of other material layers on the interior and exterior sides, and within a given wall assembly in a given climate.

This section addresses updated code provisions providing multiple ways of using FPIS ci to control water vapor by controlling the temperature within a frame wall assembly and maintaining drying potential. As I have addressed in a 2020 IIBEC paper,[4] the 2021 *International Building Code* (IBC)[8] and 2021 *International Residential Code* (IRC)[9] have already made significant strides forward in providing a framework for water vapor control in coordination with the energy code insulation requirements and strategies discussed in the previous section. These building code provisions provide a simple and effective prescriptive water vapor control "design check" for use of ci and interior vapor retarders.[11] (Users should be aware that several errata were published for the vapor retarder provisions in Section 1404.3 in the first printing of the 2021 IBC to correct errors in correlating various approved code changes.[12] The 2021 IRC vapor retarder provisions in Section R702.3 are not similarly affected.)

Energy code insulation requirements and building code vapor retarder requirements have been automated by online wall calculator tools to support a broad array of energy code– and building code–compliant wood- and steel-frame wall solutions. Two code compliance calculators for cold-formed steel-framed and wood-frame wall assemblies can be found at www.continuousinsulation.org.

Further improvements based on the sum effect of currently approved code changes are forthcoming for the 2024 IBC, as shown in Appendix A. (For information on code change proposals affecting Section 1404.3 of the 2024 IBC, see reference 13.) Similar improvements are expected for the 2024 IRC. The major improvements over the 2021 IBC and IRC provisions will include the addition of requirements to address the "perfect wall" application of ci whereby all or most of the insulation is continuous and located on the exterior side of the wall assembly (see Fig. 1); no interior vapor retarder will be required for maximized inward drying potential. This added insulation approach maximally leverages the three moisture control rules mentioned previously, maximally separates the structural frame and interior of the building from the outdoor environment for improved durability, and minimizes thermal bridging through wall framing, which can significantly erode thermal performance and also cause moisture-durability problems. Additional code improvements will include adding a definition for responsive vapor retarders (also known as "smart" vapor retarder) and further improvements to the format and usability of the provisions.

Building Code Updates for Water-Resistive Barriers

For the 2024 IBC, the water-resistive barrier (WRB) provision will be updated in two ways based on currently approved code changes, as shown in the following preliminary code text (with changes underlined):

> **1403.2 Water-resistive barrier.** Not fewer than one layer of *water-resistive barrier* material shall be attached to the studs or sheathing, with flashing as described in Section 1404.4, in such a manner as to provide a continuous *water-resistive barrier* behind the exterior wall veneer. <u>The *water-resistive barrier* material shall be continuous to the top of walls and terminated at penetrations and building appendages in a manner to meet the requirements of</u>

the exterior wall envelope as described in Section 1402.2. *Water-resistive barriers* shall comply with one of the following:

1. No. 15 felt complying with ASTM D226, Type 1,
2. ASTM E2556, Type I or II,
3. foam plastic insulating sheathing WRB systems complying with Section 1402.2 and installed in accordance with manufacturer's installation instructions,
4. ASTM E331 in accordance with Section 1402.2, or
5. other approved materials installed in accordance with the manufacturer's installation instructions.

The first underlined change coordinates with similar language in the IRC, which clarifies the intent and function of the WRB. In the second underlined change, FPIS WRB systems are specifically recognized as a code-compliant option. In previous editions of the codes, use of FPIS WRB systems relied on a third-party code evaluation process and local building department approval. However, these systems have been in successful use for several decades and are increasingly common. It is important to recognize that, like many WRB approaches, FPIS WRBs are "systems." Consequently, the 2024 IBC will require that the manufacturer's instructions be followed (and enforced). This ensures that tested and compatible components as specified by the manufacturer are used to meet the intended code performance level. Substitute or alternative components are not permitted unless they are included in the manufacturer's instructions—for example, it is impermissible to use off-the-shelf joint tape to seal the sheathing joints or flash windows to the FPIS WRB surface. Finally, it is important to recognize that FPIS WRB systems are held to the highest level of water-resistance performance criteria of current code-recognized or approved WRB materials or systems.[14]

Improvements to Fenestration Flashing Provisions

For the 2024 IBC, the flashing provisions will be updated as follows to include a new subsection for fenestration flashing that is modeled after provisions in the IRC (see underlined text for changes):

1404.4 Flashing. Flashing shall be installed in such a manner so as to prevent moisture from entering the wall or to redirect that moisture to the surface of the exterior wall finish or to a water-resistive barrier complying with Section 1403.2 and that is part of a means of drainage complying with Section 1402.2. Flashing shall be installed at the perimeters of exterior door and window assemblies in accordance with Section 1404.4.1, penetrations and terminations of *exterior wall* assemblies, *exterior wall* intersections with roofs, chimneys, porches, decks, balconies and similar projections and at built-in gutters and similar locations where moisture could enter the wall. Flashing with projecting flanges shall be installed on both sides and the ends of copings, under sills and continuously above projecting *trim*. Where self-adhered membranes are used as flashings of *fenestration* in wall assemblies, those self-adhered flashings shall comply with AAMA 711. Where fluid applied membranes are used as flashing for *exterior wall* openings, those fluid applied membrane flashings shall comply with AAMA 714.

1404.4.1 Fenestration flashing. Flashing of the fenestration to wall assembly interface shall comply

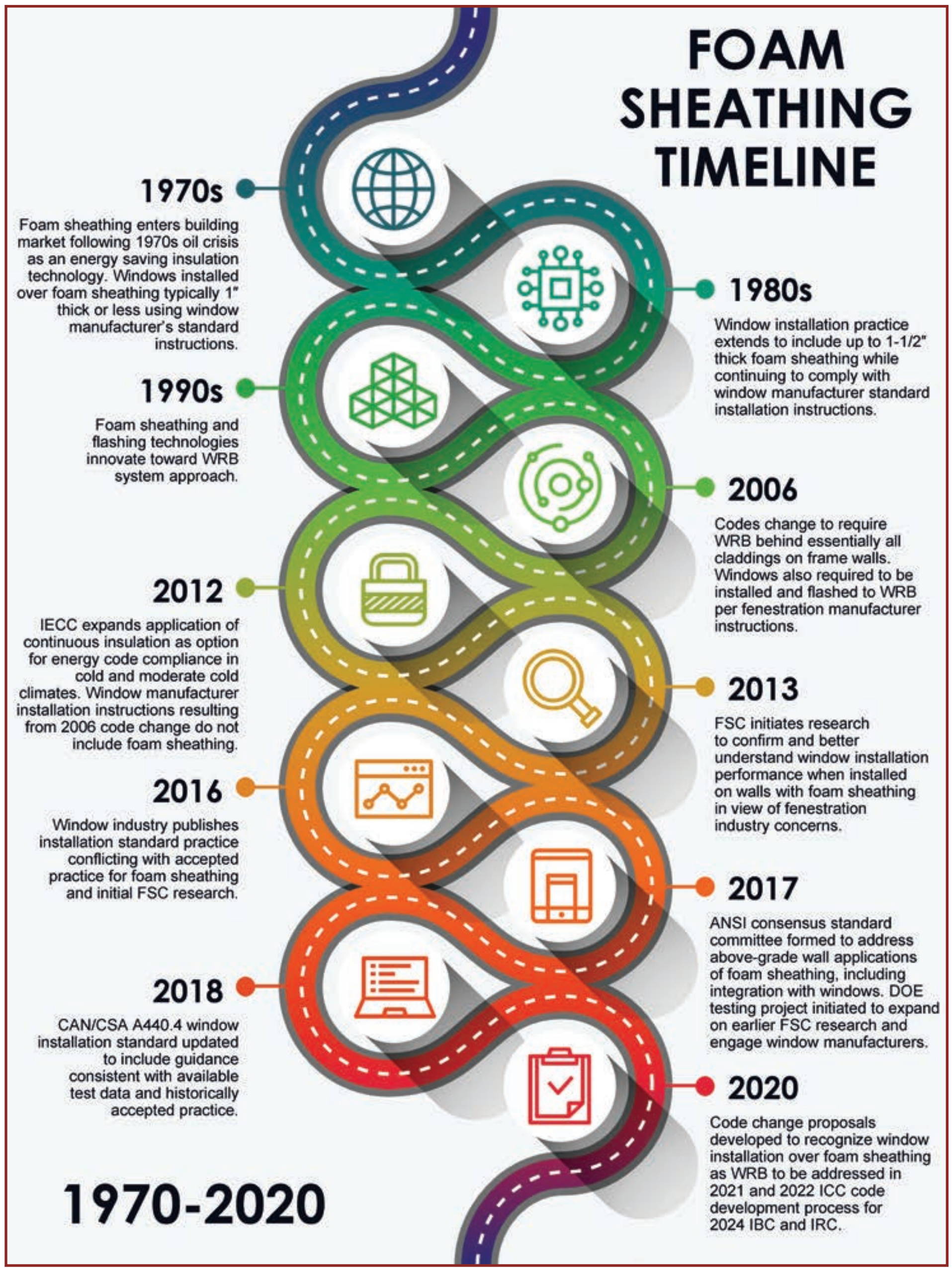

Figure 2. A timeline for foam sheathing showing the evolution of accepted window installation practices, code requirements, research, and standards development.

with the fenestration manufacturer's instructions or, for conditions not addressed by the fenestration manufacturer's instructions, shall comply with one of the following:

1. The water-resistive barrier manufacturer's flashing instructions;
2. The flashing manufacturer's flashing instructions;
3. A flashing design or method of a registered design professional; or
4. Other approved methods.

Although the updated provisions establish the fenestration manufacturer's instructions as the primary source for flashing, the update also provides four options for frequent cases where conditions do not match those addressed in the fenestration manufacturer's instructions. One of those options is use of the WRB manufacturer's flashing instructions.

Many WRB manufacturers, including manufacturers of FPIS WRB systems (as discussed in the previous section), include window openings and other penetrations in their WRB performance tests to ensure appropriate flashing methods are used with their WRB systems, just as window manufacturers desire appropriate flashing methods for their fenestration components. Ultimately, these components of a wall are joined together and must all work together for a common goal: keeping the water out of the wall (see the "three rules for moisture control" listed previously). Avoiding water intrusion is generally understood to be the most important moisture control item to get right for building resiliency, durability, and risk management (although breaking any one of the three rules for moisture control can be the demise of a building over time).

FENESTRATION INSTALLATION AND PERFORMANCE IN WALLS WITH FPIS CI

Fenestration has been installed on walls with FPIS ci for many decades. Techniques for fenestration installation on walls with ci originally resulted from the evolution of accepted field practices, then were subject to code requirements, and finally became a focus for research to refine codes and better define accepted practice, particularly regarding matters of conflicting installation instructions, differing opinions, and confusion. This trajectory is unsurprising—it is what innovation often looks like in the construction industry (see **Fig. 2**). Key findings along this journey have supported some of the code change proposals mentioned previously, generally confirmed successful field practices (within limits), and provided useful insights into the tested structural, water-resistance, and durability performance of typical integral-flanged fenestration units installed in frame walls with FPIS ci. These findings are summarized from a more detailed research report on the topic.[15]

Field Experience

In the 1970s, the practice of installing windows on walls with FPIS ci started with the use of window manufacturers' product-specific installation instructions supplemented by some obvious adjustments, such as use of longer flange fasteners to accommodate the FPIS thickness. For special conditions, such as large window units, door thresholds, and FPIS thickness greater than 1½ in., the installation instructions were further modified or enhanced by use of blocking or other devices (such as a window buck) for support and anchorage.

Because accepted practices often develop from "lived experience," the primary sources for their documentation are the people who applied them in the field. For example, in a 2011 blog post, Holladay[16] recounts a conversation with Joseph Lstiburek about the development of the historically accepted installation practice:

> "Back then [1982], we weren't using OSB [oriented strand board] or plywood sheathing—just XPS foam sheathing [...] with diagonal metal strapping for bracing," Lstiburek told me recently. "At first, we would run a horizontal 1-inch-thick board under the bottom flange of the window, to help support the weight of the window. Under the other three flanges, there was nothing but foam. We attached the windows to the studs with screws through the foam. We built thousands of houses this way, using foam up to 1½ inch thick. We never experienced any problems....
>
> "In the late 1980s, I took that practice with me to the U.S.," said Lstiburek. "Then we stopped installing the horizontal board underneath—except for wide windows. If the window was wider than 4 feet, we'd still install a board under the bottom flange. But most of the windows we installed were basically hung from the flange fasteners....
>
> "I don't have enough of a track record with 2-inch foam, so when we go above 1½-inch-thick foam, I recommend using side straps," Lstiburek told me.

In another example, Arn McIntyre of McIntyre Builders Inc. described his successful experience with installation of windows on walls with FPIS in an April 5, 2019, email to the author: "We have been installing vinyl double pane windows over 1½" XPS foam with no OSB for over six years and before that over 1"

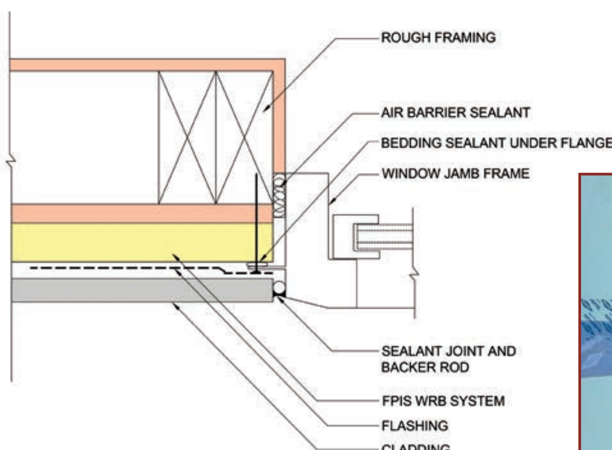

Figure 3. Typical installation of a flanged window directly over foam plastic insulating sheathing on a wood-frame home.

Figure 4. Adhered flashing and joint tapes used for foam plastic insulating sheathing water-resistive barrier systems and window flashing.

foam for almost 30 years and have seen no issues with window movement."

Consistent with these accounts, **Fig. 3** shows a typical example of flanged window installation over FPIS where, in this 2014 construction project, the FPIS served as ci and the WRB system. The window and door installations followed the manufacturer's installation instructions with the following modifications:

- Window flanges were installed over and flashed directly to the FPIS WRB surface.
- Longer flange fasteners were used to maintain required embedment in wood framing.
- Wood blocking was used to provide full support of door thresholds. (Inswing exterior doors were used so that door frame or hinge anchor screws could be securely driven into the rough opening framing without added jamb blocking.)

In parallel with development of the accepted installation practice for structural support and anchorage, joint tape and adhered flashing materials saw major technological advancements and greater market acceptance throughout the 1990s.[17] These flashing and joint-sealing technologies were applied to various applications, including FPIS WRB systems and fenestration flanges (see **Fig. 4**), for continuity of the water-control layer or drainage plain of a wall. They had become an important part of accepted practice by the early 2000s. These flashing practices became necessary for building code compliance when Section R703 of the 2006 edition of the IRC included requirements for WRB installations and window flashing to the WRB.

Before the 2006 IRC code change, so-called self-flashing flanged fenestration units were commonly mounted directly to wall sheathing materials such as fiberboard, plywood, OSB, and FPIS without the presence of any type of WRB. Instead, bedding sealant applied under the fenestration flange was the sole defense against water intrusion at the fenestration perimeter. This minimum code-allowed practice of building frame walls without a continuous WRB, flashing, and a means of drainage was found to be unacceptable based on experience gained in the 1990s.[18]

Figure 5 shows an installation detail for a net zero energy house with 4-in.-thick FPIS ci. In this case, a ½-in.-thick plywood window buck was used to support fenestration placed in alignment with the exterior FPIS ci for architectural reasons (a window flush with the exterior facade) and to minimize thermal bridging at the window-wall interface (see later section). Because plywood was used as the buck, anchor straps commonly used for block-frame windows were used to anchor the fenestration unit, and the fenestration flanges were used only as a flashing plane to the FPIS at the jambs and head of the window (flange fastening to the narrow edge of plywood is not feasible). This detail is an example of the historically accepted practice of providing additional support where the FPIS thickness exceeds 1½ in. Other accepted practices include use of a 2× wood window buck in lieu of plywood, which also provides a means to attach fenestration flanges to the buck.

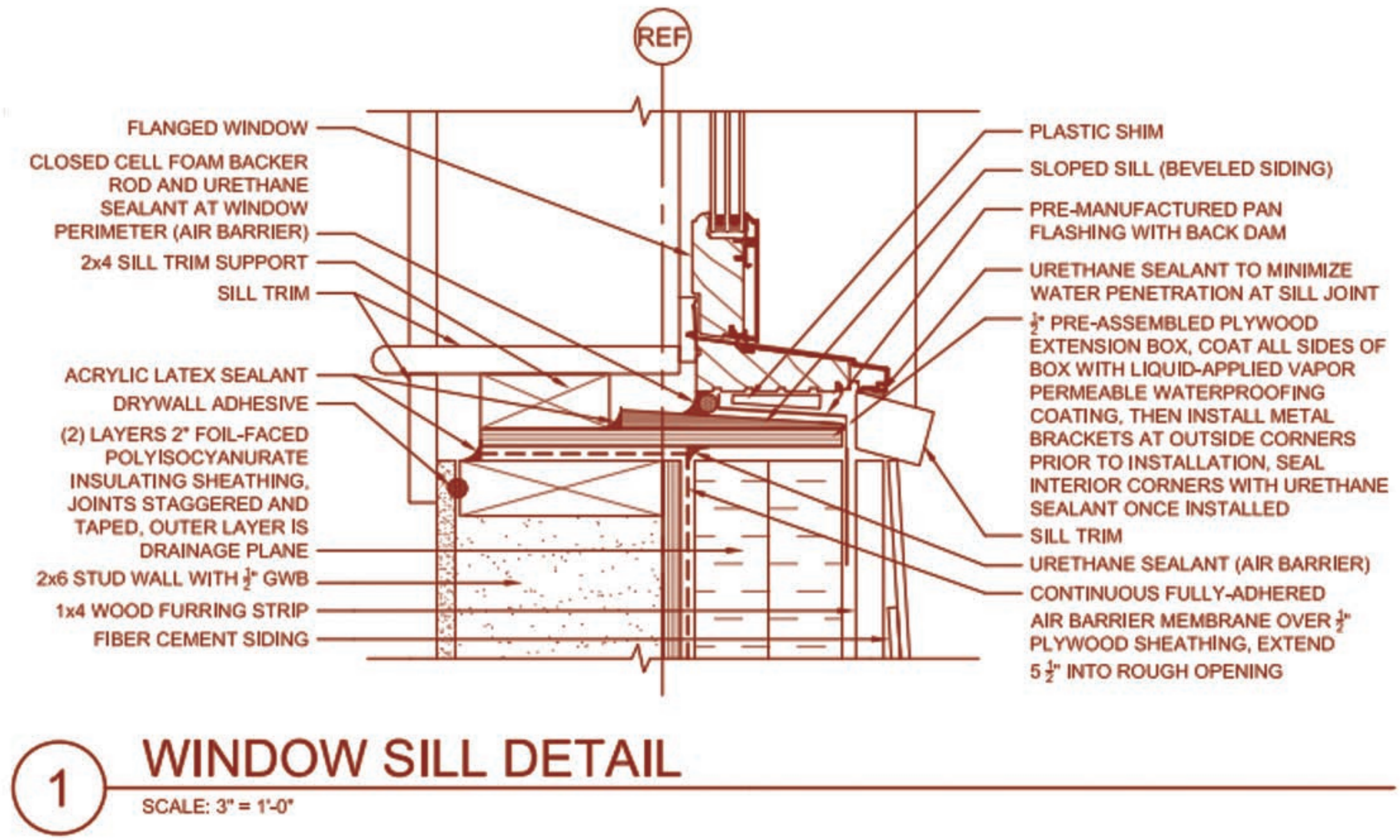

Figure 5. Plywood window buck detail for fenestration installation in alignment with 4-in.-thick foam plastic insulating sheathing. Figure: Building Science Corporation. 2009. "National Institute of Standards and Technology Net Zero Energy Residential Test Facility. Window Details and Installation Sequence." https://www.nist.gov/system/files/nzertf-architectural-plans3-june2011.pdf.

Performance Testing Experience

General

More than 140 tests have been conducted on a total of 21 wall assembly specimens.[15] The wall assembly specimens evaluated included:

- four types of windows (single hung, double hung, casement, and horizontal slider) from multiple manufacturers,
- two window frame types (vinyl and wood),
- two window configurations (single and mulled 2-unit),
- rough opening sizes up to 6 ft wide, and
- wall configurations with and without FPIS of three material types (XPS, EPS, and PIR) with thicknesses up to 2 in. and 15 or 25 psi of compression resistance.

FPIS was included on 19 of the wall assembly specimens, where it was detailed to serve as the WRB system, including joint tapes and various types of flexible adhered flashings at the window-wall interface as specified by the FPIS manufacturer's installation instructions. One of the 19 FPIS wall specimens used a 2× wood buck for window installation, but it was otherwise flashed in the same way as the other 18 specimens. For the two wall specimens without FPIS, a building wrap or no. 15 felt was used as the WRB and similarly flashed to the window flange using adhered flashings. These two wall specimens were used as a comparative baseline.

In general, and with some variation in test sequence or focus of testing, the testing employed test methods consistent with those included in the Fenestration and Glazing Industry Alliance's (FGIA's) *Voluntary Laboratory Test Method to Qualify Vertical Fenestration Installation Procedures* (AAMA-TIR-504),[19] which is specifically "intended to examine the performance and durability of the integration of a fenestration product with the building envelope."

The sequence of testing for evaluation in accordance with AAMA TIR-504 is as follows:

1. Test initial air leakage resistance per ASTM E283.[20]
2. Test initial water penetration resistance per ASTM E331.[21]
3. Perform thermal (temperature) cycling per ASTM E2264[22] Method A (level 1).
4. Repeat air and water testing (steps 1 and 2).
5. Perform design pressure (DP) load test per ASTM E330.[23]
6. Repeat water penetration resistance test (step 2).
7. Perform structural test pressure (STP) load test per ASTM E330.

AAMA TIR-504 applies the following performance criteria:

- Air leakage resistance tests (steps 1 and 4)—report values.
- Water resistance tests (steps 1, 4, and 6)—no water penetration around the fenestration unit beyond the defined drainage path.
- DP load test (step 5)—no damage to fenestration unit that prevents normal operation.
- STP load test (step 7)—no damage to the fenestration unit or installation method that results in failure to sustain the specified structural test pressure load (for example, 1.5 × DP) such as a breach resulting in depressurization. Any damage or operability impact is to

Figure 6. Adhered flashing as installed at window perimeters in test specimens with a building wrap water-resistive barrier (left) and with foam plastic insulating sheathing water-resistive barrier system (right).

> be reported, but it is not considered as a basis for failure where the structural test pressure was sustained.

Additionally, AAMA TIR-504 permits structural pressure testing to be performed separately from the water-resistance and durability conditioning steps because, in many cases, the only installation condition under consideration may relate only to a change in structural anchorage and support without a change to methods of flashing for water resistance (or vice versa).

Water Penetration Resistance

None of the ASTM E331-tested[21] fenestration installations experienced water intrusion at the flashed fenestration-to-wall interface at a pressure difference of up to 5.4 lb/ft^2. (The 5.4 lb/ft^2 value was chosen to be consistent with the maximum water resistance criteria required by the design pressure rating of the specified fenestration units. It is approximately 15% of the maximum 35 lb/ft^2 design wind pressure rating for fenestration units included in the testing program.) This finding held for walls with building wrap and walls with FPIS WRB systems (see **Fig. 6**). It also held for various window types, as well as various FPIS types, thicknesses, and compressive strengths (EPS, XPS, and PIC of 1 and 2 in. thickness and 15 to 25 psi compressive strength), and various flexible adhered flashing materials used in accordance with the WRB system (FPIS or wrap) manufacturer's flashing instructions and flashing material specifications. In addition, this finding held for water-penetration-resistance tests that were repeated after exposure to thermal cycling (ASTM E2264[22]) and service-level wind pressure loading of not less than 80% of the DP loading. In all cases, window flange bedding sealant was not used so that any observed water penetration could be directly associated with the adhered flashing approach commonly used with FPIS WRB systems. Bedding sealant, as commonly required by fenestration manufacturer installation instructions, would have provided a redundant water resistance measure.

With rare exceptions, water was typically driven up behind the unsealed bottom flange (which also excluded the external adhered flashings) and onto the rough-opening sill pan used for all tested specimens, with or without FPIS ci. This occurrence was expected because the specified ASTM E331[21] water spray test pressure differential (5.4 lb/ft^2) was sufficient to drive water up approximately 1 in. and onto the sill pan. Sill pan installations were particularly vulnerable to this phenomenon where the rough-opening gap was not pressure equalized (that is, no spray-foam air sealant was applied to the interior side of the rough-opening gap in the test specimens to allow for observation). Consequently, for the purposes of these tests, water intrusion onto the sill pan through the unsealed bottom flange was not considered a failure of the window-WRB perimeter flashing system.

Uniform Pressure (Wind Load) Resistance

Figure 7 shows the two ASTM E330[23] test apparatuses used in this investigation. In general, both positive- and negative-pressure

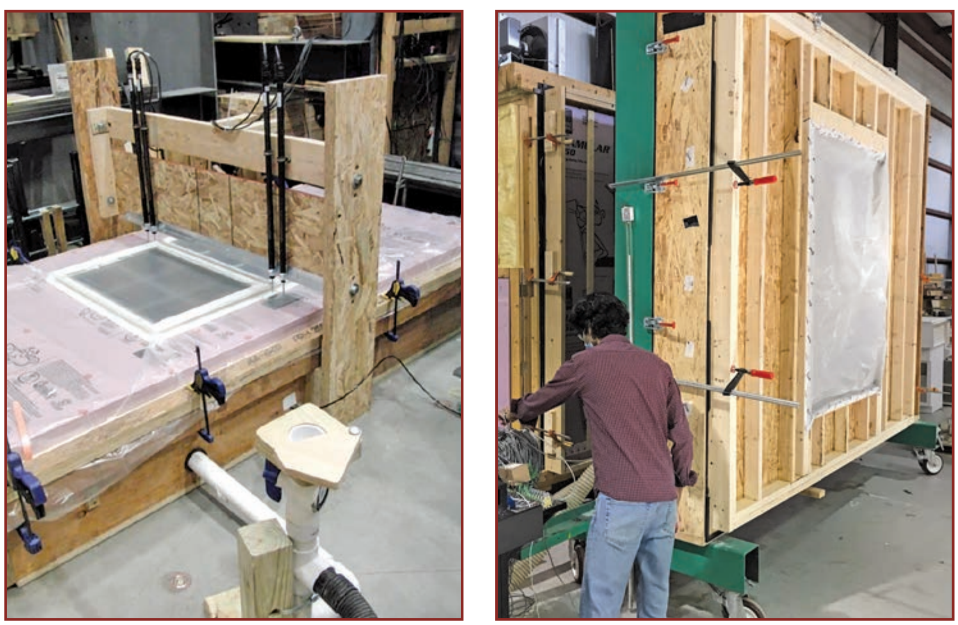

Figure 7. ASTM E330[23] test apparatuses used to evaluate uniform pressure resistance. Figure: Qualtim/Center for Building Innovation (left); Home Innovation Research Labs (right).

tests were conducted on the same specimen with positive-pressure testing conducted first. With two exceptions, all tests were conducted in a sequence of targeted pressure levels: 0.5 × DP (preload), 1.0 × DP (design pressure), 0.75 × DP, and 1.5 × DP (STP). For each targeted pressure level, the load was held for 10 seconds, released for a pause, and then the next pressure level was applied. For two test specimens, the test pressure was ramped to failure (above the window's STP) to determine the ultimate capacity and failure mode rather than just a "pass/fail" proof load test.

In general, the test conditions resulted in a more stringent evaluation than is used to rate and label the fenestration units themselves. Unlike the historically accepted installation practice discussed previously, many installations had significant weakening variances from the window manufacturer's structural anchorage and support installation requirements. Flange bedding sealant was intentionally omitted to avoid any structural "bonding" of the fenestration flange to the wall sheathing or WRB material that could have improved structural performance. In addition, most of the specimens were tested to a conservative STP load of about 1.58 times the labeled DP load rating of the fenestration product (instead of 1.5 times the labeled DP rating).

Based on the test results and observations, none of the fenestration specimens experienced structural failures directly associated with installation over foam sheathing. In the two cases where a structural failure did occur before the specimen reached the STP load level, the failure was related to a premature failure of a fenestration component (for example, wood cross-rail splitting or locking hardware) or significant installation variances from the fenestration manufacturer's installation instructions (for example, no shims and reduced flange fastening) leading to a premature failure. For these cases, successful follow-up tests were conducted after the installation variances were eliminated by following the manufacturer's installation instructions and the installation description in the window product's labeled certification test report.

Operability Performance

Operability checks were conducted as part of the ASTM E330[23] structural testing sequence. Of the various types of windows represented, there were two window types that tended to experience operability incidents. One was a horizontal slider window, which experienced a window hardware failure at the DP test level. The other operability incident was observed for several double-hung windows installed with a weakening installation variance and was observed only after completing the STP test level, which is not considered an operability failure in accordance with AAMA-TIR-504.[19] It involved a metal sash pin becoming dislodged from the balance/braking mechanism such that the upper sash would slide down under its own weight when unlocked after the final STP test level was completed without structural failure. This operability impact was easily repaired by reinserting the sash pin into the receiver of the balance/braking mechanism. In this case, the operability issue was resolved by conducting additional window tests, with the installation variances resolved by the following methods:

- Providing the manufacturer's required flange nail group at midheight of the jambs (where the sash pins and brake/balance mechanism were located during testing with the window closed and locked). This is a location where concentrated forces are passed from the sashes to the window frame and then into the flange and flange connection to the wall substrate.
- Providing a low-expansion spray-foam air sealant 1 in. deep from the interior side of the rough-opening gap, which was included in the installation description in the window product's labeled DP rating test report. The application followed the manufacturer's air-sealing instructions.

With these two installation corrections, no operability impact was observed after completing the DP and STP test levels. This finding speaks to the importance of complying with the window manufacturer's installation instructions, as was done in the historically accepted practice for installations over FPIS ci discussed earlier.

Sustained Dead Load and Creep Resistance

In addition to structural wind pressure testing and water resistance testing, investigators conducted tests to evaluate the movement of the fenestration unit when subject to a period of sustained dead load (window self-weight). **Figure 8** shows an example test setup. Maximum downward (negative) movements of 0.000 to −0.032 in. were recorded for monitoring durations of 20 days (two specimens) and 6 months (all other specimens) for installations including up to 2 in. of FPIS and window weights ranging from 27 to 384 lb. There were no obvious trends relative to weight, size, or type of window, or foam thickness and compressive resistance. In some cases, periods of positive (upward movement) occurred, which indicates that some portion of the measured positive and negative movements may be

Figure 8. Sustained dead load tests for creep and stability. Figure: Qualtim Inc. 2013.* Creep of Fasteners Installed into Windows over Foam Sheathing Panels and OSB.** ***Madison, WI: Qualtim Inc.

Figure 9. Window installation shear load test setup.

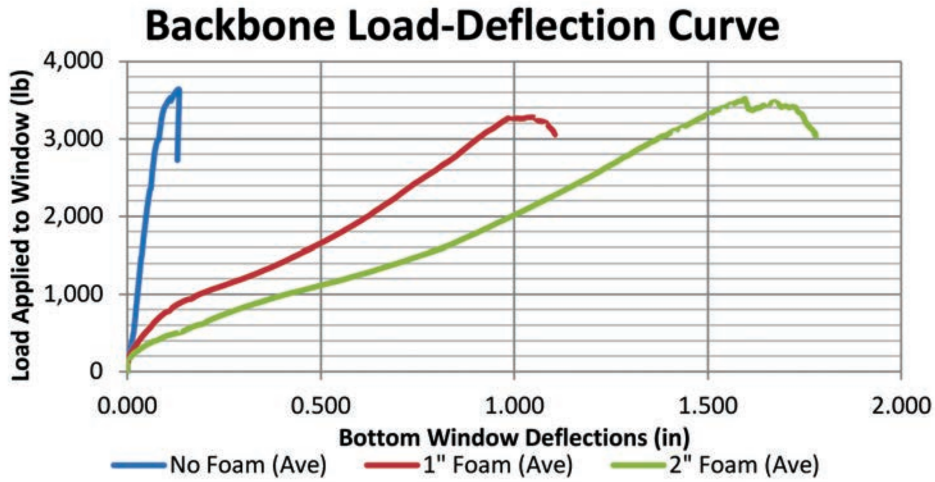

Figure 10. Load deflection plots for vinyl, integral-flange window installations over wood, 1 in. foam plastic insulating sheathing (FPIS), and 2 in. FPIS substrates.

associated with normal response of wall and window materials to temperature, humidity, and moisture content changes. It should be noted that these sustained dead load tests were conducted with the same window installation weakening variances described earlier, as applicable to some specimens.

Flange Fastener Shear Resistance

In three additional structural tests, installed single-hung vinyl frame windows were subjected to an applied downward load at the head of the window to study the shear capacity and stiffness of flange fasteners installed through 1- and 2-in.-thick FPIS of 15-psi compressive resistance.[24] For the purpose of these tests, the windows were installed with no shims, which meant that the resistance to the applied load was transferred entirely through the flange and the flange fasteners penetrating through the FPIS. These tests were used to evaluate whether an engineering method developed for evaluating fastener shear capacity of connections with an intervening layer of FPIS would be able to predict the flange fastener shear behavior. The method also served as the technical basis for cladding and furring connections through FPIS in US model building codes[25] and was addressed in a previous IIBEC paper.[5]

Figure 9 shows the test setup with a wood blocking used at the head of the window to distribute the downward-applied load uniformly into the window frame. Load and deflection of the window units were monitored as the flange fasteners and flange material responded in reaction to the downward shear load. **Figure 10** illustrates the results of these tests as load deflection plots. It is clear that the ultimate shear capacity of the flange connections, ranging from 3300 to 3600 lb, is relatively unaffected by the presence of FPIS up to 2 in. thick. However, the stiffness response became predictably more ductile with increasing FPIS thickness, as expected. With proper design, this improved ductility can result in resilient support, allowing building and window-frame differential movement to be accommodated without damaging or warping fenestration components while, at the same time, providing adequate support and stability to the fenestration unit.

As mentioned, these test results were compared to an engineering methodology used to design cladding, furring, and structural component connections through FPIS to wood and steel framing. The performance target for the design method limits fastener design shear capacity to that which produces no more than about 0.015 in. deflection and controls long-term creep. The comparison is shown in **Table 3**, and it confirms that the design methodology can be conservatively applied to design window flange connections to support fenestration dead loads and even additional applied shear load while restraining fenestration movement to not more than about 0.015 in.

Fenestration Size Effect on Installed Performance

Most of the previously mentioned assembly tests were conducted using window specimens at or near to the "gateway size" as required by code and window industry standards for evaluation of window units. The gateway size is generally the largest fenestration unit available in a given product line and, therefore, conservatively represents the entire size range of the product line to simplify the amount of product testing needed for labeling and code compliance purposes.

Structural pressure tests were conducted on two assembly specimens to evaluate window-size effects as addressed in FGIA's *Comparative Analysis Procedure for Window and Door Products* (AAMA 2502),[26] a standard referenced in US model building codes. These two tests used single-hung, vinyl frame, integral-flange windows at a size of 30 in. wide × 42 in. high. The gateway size unit serving as the basis for the product line's DP rating

Foam thickness (in.)	Applied load (lb) in addition to window weight	Load per flange fastener (lb) at 0.015-in. deflection	Design load prediction (lb)*
2	158	6	5
1	280	10.7	9

*Predictions are from reference 25.

Table 3. Comparison of test data to design predictions for flange fastener shear behavior

was 42 in. wide × 66 in. high. In addition, the windows were installed without shims, which are required by the fenestration manufacturer's installation instruction. Shims were omitted so that the structural support and anchorage relied exclusively on flange bearing on, and flange fasteners through, a layer of 2-in.-thick, minimum 15-psi FPIS. For comparison, an identical window installation was applied directly to wood framing without a layer of FPIS. Other installation conditions included (a) no use of bedding sealant (which the manufacturer's instructions noted as being necessary to maintain DP rating) and (b) use of a maximum permitted rough-opening gap of ⅜ in. in accordance with the manufacturer's "non-DP-rated" instructions (separate "DP-rated" installation instructions limited the rough opening gap to a maximum of ¼ in.).

The previously described installations were tested to an ultimate structural test pressure of 4.7 to 6.0 times the labeled 25 lb/ft^2 DP rating of the fenestration unit. The STP target load resistance of 1.5 × DP was exceeded by 300% to 400%. The failure mode was associated with the sash check rail dislodging from the window frame for the positive-pressure-loading direction in both specimens. These results indicate that typical-sized windows installed on walls with and without FPIS (and even with significant weakening installation variances) can resist structural test pressures well above the labeled DP rating and the required 1.5 safety factor for window sizes that are commonly smaller than the gateway size window used to evaluate and rate an entire window product line. These tests demonstrate that size effects are a significant factor in determining and explaining the actual structural performance of an installed fenestration unit.

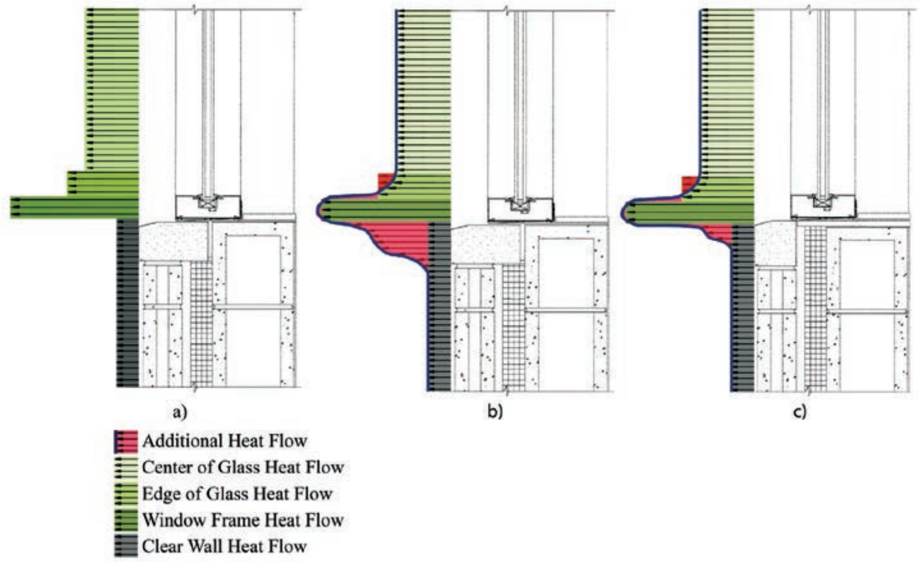

Figure 11. Window sill detail illustrating heat flow through window and wall elements where (a) perimeter thermal bridging is ignored, (b) perimeter thermal bridging is not ignored as in detail (a), and (c) perimeter thermal bridging is mitigated. Figure: Barnes, B., J. Yu, A. Pagán-Vázquez, N. Alexander, and R. Liesen. 2013. "Window Related Thermal Bridging." In **Proceedings of Thermal Performance of the Exterior Envelopes of Whole Buildings XII International Conference.** *Peachtree Corners, GA: ASHRAE. https://web.ornl.gov/sci/buildings/conf-archive/2013%20B12%20papers/120-Barnes.pdf.*

Recommended Installation Instructions

Based on the review of field installation experience and tested installed performance, a recommend installation practice for integrally flanged windows on walls with FPIS ci was developed (see **Appendix B**).[27] These practices generally follow the historically accepted field practice, but they are limited to conditions clearly confirmed by the test data described previously.

As noted in the first step of installation instructions in Appendix B, it is important to follow the window manufacturer's installation instructions for conditions that are addressed in those instructions. Similarly, it is also important to follow the FPIS WRB system manufacturer's installation instructions. Otherwise, the installation instructions in Appendix B provide appropriate guidance for effective installation of integral-flanged windows in walls with FPIS ci up to 1.5 in. thick having a minimum compressive strength of 15 psi per ASTM C578[6] or ASTM C1289.[7] For thicker or lower-compressive-strength FPIS materials, a window buck is recommended, although the test data presented earlier indicate that the installation instructions may work for up to 2-in.-thick FPIS subject to future additional tests to confirm appropriate limitations.

THERMAL BRIDGING IMPACTS OF FENESTRATION INSTALLATION

Figure 11 illustrates differences in heat flow resulting from mitigated and unmitigated thermal bridges at the window perimeter (including the case where these heat flows are completely ignored or assumed to be insignificant). These

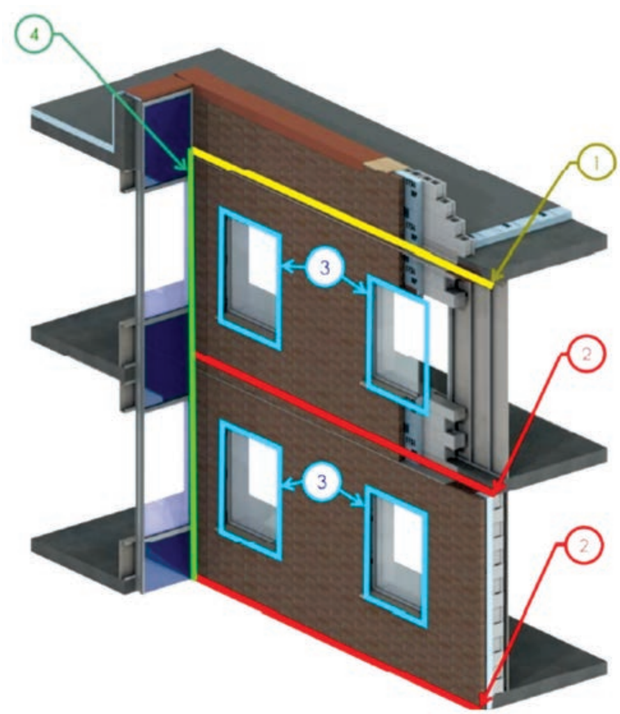

Figure 12. Illustration of linear thermal bridges caused by roof (1), floor (2), window (3), and wall (4) intersections with the clear-field area of an above-grade wall. Figure: Morrison-Hershfield Ltd. 2020. "Building Envelope Thermal Bridging Guide, V1.5." BC Hydro Power Smart website. https://www.bchydro.com/content/dam/BCHydro/customer-portal/documents/power-smart/business/programs/BE-Thermal-Bridging-Guide-v1-5.pdf.

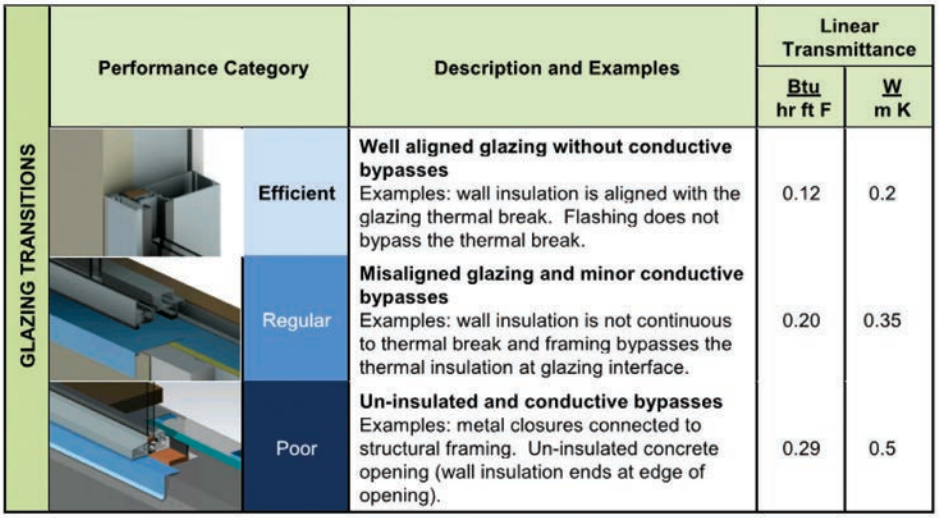

GLAZING TRANSITIONS	Performance Category	Description and Examples	Linear Transmittance Btu/hr ft F	Linear Transmittance W/m K
	Efficient	**Well aligned glazing without conductive bypasses** Examples: wall insulation is aligned with the glazing thermal break. Flashing does not bypass the thermal break.	0.12	0.2
	Regular	**Misaligned glazing and minor conductive bypasses** Examples: wall insulation is not continuous to thermal break and framing bypasses the thermal insulation at glazing interface.	0.20	0.35
	Poor	**Un-insulated and conductive bypasses** Examples: metal closures connected to structural framing. Un-insulated concrete opening (wall insulation ends at edge of opening).	0.29	0.5

Figure 13. Representative (default) linear thermal transmittance values for various levels of thermal bridging detailing for window-wall interfaces. Figure: Morrison-Hershfield Ltd. 2020. "Building Envelope Thermal Bridging Guide, V1.5." BC Hydro Power Smart website. https://www.bchydro.com/content/dam/BCHydro/customer-portal/documents/power-smart/business/programs/BE-Thermal-Bridging-Guide-v1-5.pdf.

heat flows can be characterized as lines defining the perimeter of windows, as shown in Fig. 12. Hence, they are called linear thermal bridges. They are not accounted for in the window's U-factor rating or in the wall's U-factor or *R*-value.

As shown in Fig. 13, window perimeter installation details that interface with the wall assembly have a representative Psi-factor (linear thermal transmittance) ranging from ~0.3 BTU/hr-ft-°F when unmitigated to ~0.1 BTU/hr-ft-°F when mitigated with efficient detailing.[28,29] This range corresponds to a factor-of-three difference in heat flow per unit length of a window perimeter. Thus, thermal bridging details at fenestration perimeters can have a significant impact on the installed thermal performance of the window-to-wall interface (which can be a significant part of the building thermal enclosure); the exact impact will depend on a number of factors, including the window characteristics, wall characteristics, and detailing at the rough-opening interface. The impact also varies based on the amount of window-perimeter length per unit area of the opaque wall assembly.

As an example, the impacts of "poor" and "efficient" thermal bridging detailing are quantified in Table 4. Use of a "poor" thermal bridging detail at the window-to-wall interface (see Fig. 11b and 13) can result in the entire opaque wall thermal performance (effective *R*-value) being overestimated (energy loss/gain underestimated) by as much as 100% if the thermal bridging effect is ignored. Even with an "efficient" detail, the wall thermal performance may be overestimated by 36%, but the reduction in thermal performance is much less than that from the "poor" detail. Obviously, these thermal bridging impacts and detailing considerations should be factored into the design of the building thermal enclosure. Generally, this is required by modern energy codes such as ASHRAE 90.1[2] and the 2021 IECC.[1]

WIND-DRIVEN-RAIN RESEARCH

As noted previously, water intrusion into wall assemblies (often at the window-to-wall interface) has major implications for the wall's performance and the building's durability. Wind-driven rain is the primary culprit or hazard because little rain will hit the wall if there is no wind to direct it onto the wall surface. More importantly, wind tends to create a negative pressure inside the whole building and a positive pressure on the windward-facing facade. This creates a pressure differential that drives water from the wetted side of a windward wall assembly into the assembly through small cracks or holes or over vertical legs of flashing that are too short. Thus, it is necessary to understand how the wind-driven-rain climate hazard (namely, coincidental rainfall rates and wind speeds) varies across the United States.

Properly characterizing the wind-driven-rain climate hazard is important because

Thermal bridge condition		Clear-field wall thermal performance (R-13 + 7.5ci steel frame)†		Adjusted wall thermal performance including window-wall interface		Reduction in wall thermal performance
Detailing practice‡	Linear thermal transmittance (Psi-factor, BTU/h-ft-°F)	U-factor (BTU/h-ft^2-°F)	Effective *R*-value (1/U)	U-factor (BTU/h-ft^2-°F)	Effective *R*-value (1/U)	
"Poor"	0.3	0.064	R-15.6	0.134	R-7.5	52%
"Efficient"	0.1	0.064	R-15.6	0.088	R-11.4	27%

*Table is based on a typical three-story office building (168 × 109 ft) with 21,400 ft^2 of gross above-grade wall area of cold-formed steel-frame construction having R-13 cavity insulation and R-7.5 continuous insulation (ci) on the exterior (that is, R-13 + 7.5ci wall per code, as is typical for moderate climate zones). The window-to-wall area ratio is assumed to be 33% for ribbon windows or 20% for punched window openings, resulting in about 3200 ft of window perimeter interface with the wall assembly.

†As a point of reference, a similar wall without the R-7.5ci and having only R-13 cavity insulation would have a U-factor of 0.125 BTU/hr-ft^2-°F (effective *R*-value of 8) because in that case the steel-frame thermal bridging in the clear field of the assembly would not be mitigated. If additional framing at fenestration openings had been considered in the clear-field wall U-factor calculation, the wall thermal performance would be further decreased.

‡Refer to Fig. 13.

*Table 4. Comparison of "poor" and "efficient" thermal bridging details at the window-to-wall interface**

without such hazard information there is no solid technical basis for the criteria used to judge acceptable and risk-consistent performance of building assemblies and components. In particular, the wind-driven-rain hazard at a given building site should determine the pressure differential (and perhaps also the water-spray rate) used in ASTM E331[21] tests to qualify, rate, and properly specify various building enclosure components and systems such as fenestration products, flashing methods for penetrations and windows, and WRB materials and systems as they are intended to be installed.

Recently, a new research project has been funded by the Florida Building Commission on the recommendation of the Florida Hurricane Research Council. The project will be conducted by Forrest Masters, PhD, PE, at the University of Florida with the principal investigator being Art DeGaetano, PhD, with the National Oceanic and Atmospheric Administration's Northeast Regional Climate Center at Cornell University. The author of this paper helped develop the research plan and also participated in a pilot study sponsored by the Insurance Institute for Business and Home Safety.

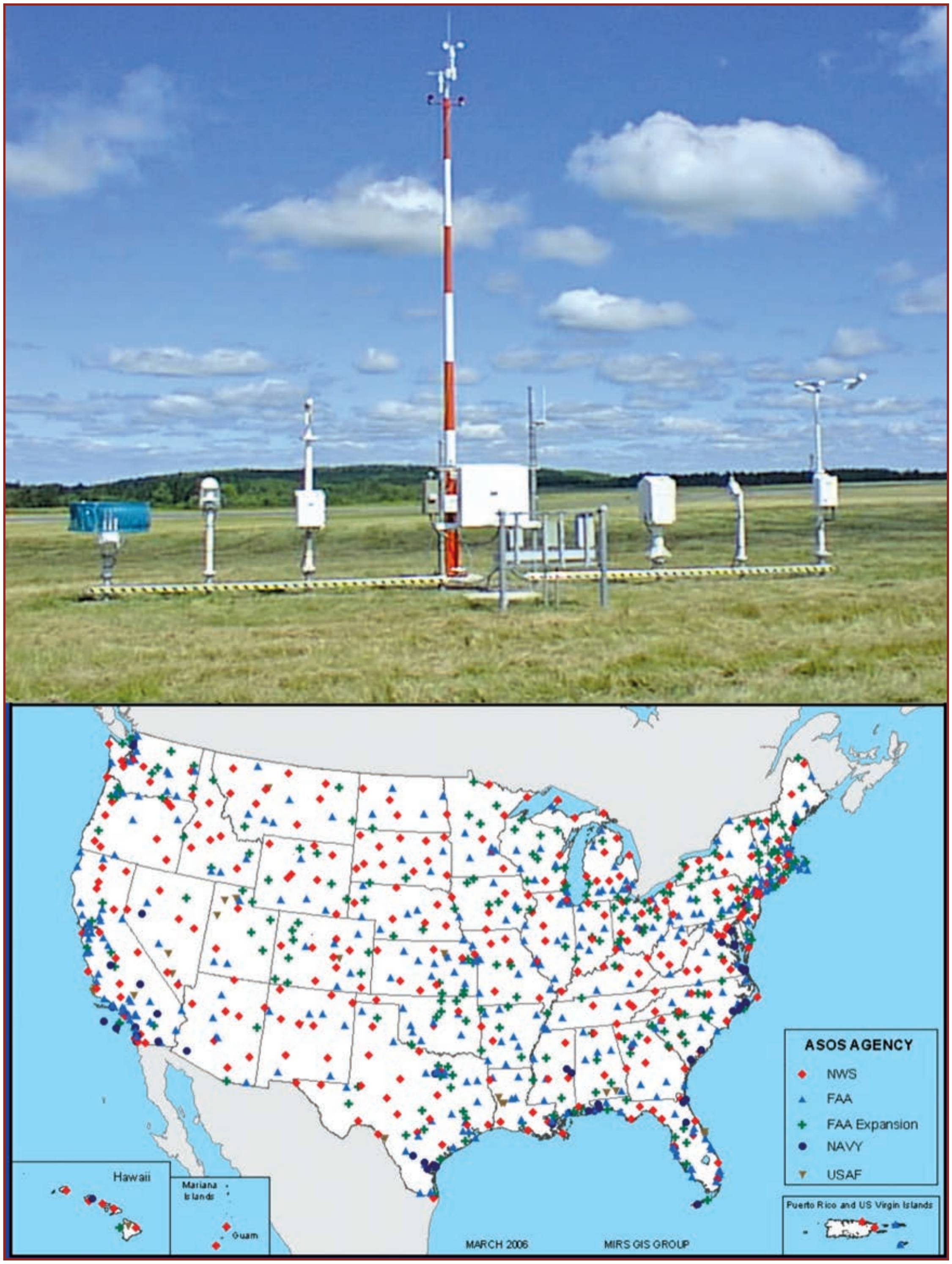

Figure 14. A typical weather station and weather station distribution across the United States.

While the project is intended to focus on the wind-driven-rain climate hazard in Florida, it will evaluate coincidental rainfall and wind data for weather stations (**Fig. 14**). Data from these weather stations, including peak gust wind speed and rainfall receipt, are available at a 5-minute resolution. Thus, it is possible to correlate wind and rainfall to a much higher degree than has been possible in the past.

The data will be evaluated to determine wind-speed return period statistics for a given rainfall rate for each weather station. Thus, it will be possible to plot the data on a US map for different return periods and rainfall-rate thresholds that are of concern for leaks in building enclosures associated with different performance objectives or consequences. These objectives might include avoidance of nuisance leaks that may be of little consequence, routine leaks that might be considered a durability concern, and especially significant leaks from extreme events that might transfer sufficient volume of water to affect building contents and not just the exterior building enclosure assembly itself. Of course, structural failures that would open large pathways for water ingress due to fenestration failure and building assembly failures caused by extreme wind pressure or windborne debris are a different matter, but these types of failures are certainly addressed by building code design requirements and product performance testing for code compliance.

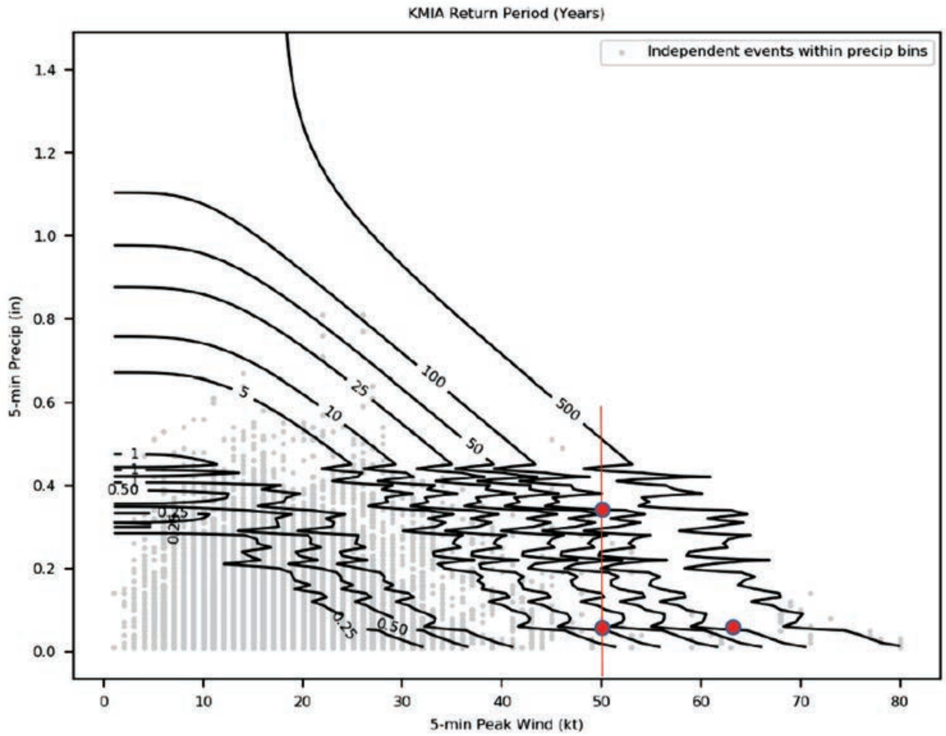

Figure 15. Coincidental wind and rain data for Miami, Fla., with return period statistics from preliminary analyses.

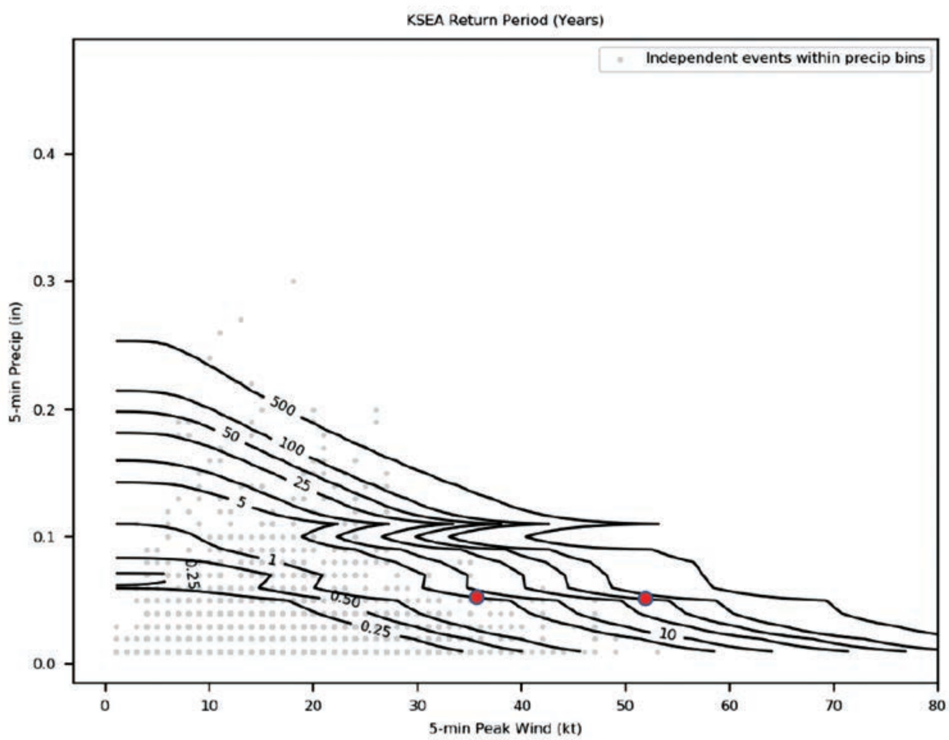

Figure 16. Coincidental wind and rain data for Seattle, Wash., with return period statistics from preliminary analyses.

While the data are very preliminary, some findings from the pilot study are shown in Fig. 15 and 16. (The author also presented these findings during an education session at the ASHRAE 2021 virtual summer meeting.) As an example of applying these data, Fig. 15 shows the 5-minute rainfall receipt (in.) and coincidental wind speeds for data from a Miami, Fla., weather station. For a 5-minute precipitation of 0.05 in. (0.6 in/hour rainfall rate for a 5-minute period), the correlating 10- and 100-year mean recurrence interval (MRI) gust wind speeds are 50 knots (57.8 mph) and 64 knots (73.6 mph), respectively. Conversely, for the Seattle, Wash., weather station data shown in Fig. 16, the same 5-minute precipitation of 0.05 in. is associated with 10- and 100-year MRI gust wind speeds of 40 knots (46 mph) and 58 knots (66.7 mph), respectively. While both weather stations have a similar wind-driven-rain hazard from an annual average wind-driven-rain receipt basis (see Fig. 17), the actual hazards in terms of the wind speed associated with rainfall differ considerably between the two sites. Of course, in regions of the country with less-extreme wind and rain conditions, it is expected that the hazards will be very different from these two examples.

Fig. 15 also shows that use of a 5-minute precipitation of 0.05 in. and a 10-year MRI wind speed as hypothetical performance criteria would also provide protection against events of much greater rainfall rates that have a corresponding 100-year return-period wind speed. This observation is based on an understanding of vulnerability to a water leak whereby small leakage paths tend to admit water mainly as a result of pressure differential and not the rate of rainfall above that required to initiate a leak. This observation also is evident in the climate hazard data themselves. The independent coincidental wind-rain event data points plotted in Fig. 15 and 16 show a trend of decreasing peak gust wind speed with increasing rainfall rate.

CONCLUSION

Major conclusions and "take-aways" from this paper include the following:

- Continuous insulation is playing an increasing role in the advancement of newer energy conservation codes and standards, particularly in moderately cold to very cold climates.
- The use of FPIS ci for energy code compliance is well supported by improved building code provisions addressing other related functional matters such as water resistance of building enclosure assemblies and water vapor control.
- The proper coordination of FPIS ci and window installation can achieve robust and durable installed performance for:
  - — structural support and anchorage of integral-flange window products to resist wind loads,
  - — wind-driven-rainwater-intrusion resistance, and

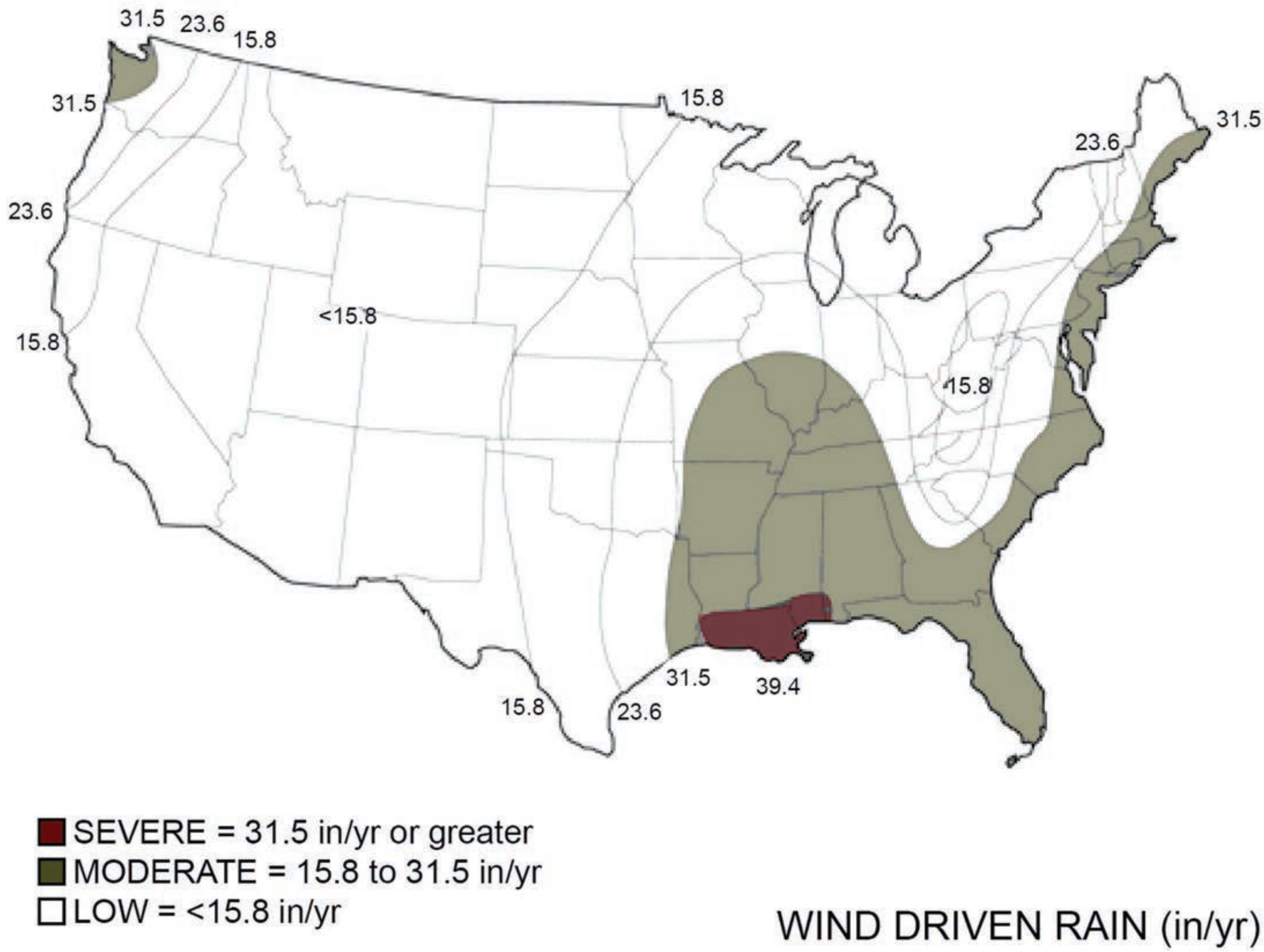

Figure 17. Annual wind-driven-rain statistics map of the United States (inches of horizontal rain receipt per year). Figure: Underwood, S. J. 1999. "A Multi-scale Climatology of Wind-Driven Rain for the Contiguous United States," PhD Dissertation, University of Georgia, Athens. US Department of Housing and Urban Development, Office of Policy Development and Research. 2015. "Durability by Design, 2nd Edition: A Professional's Guide to Durable Home Design." https://www.huduser.gov/portal/publications/reports/Guide-Durability-by-Design.html.

    — resistance to other loading conditions that can cause fenestration movement or creep.
- Efficient detailing of fenestration installations, including the positioning and location of the fenestration relative to insulation components such as FPIS ci, can significantly reduce thermal bridging at the window-to-wall interface and avoid significant impacts to the thermal performance of above-grade walls.
- New wind-driven-rain research is underway and promises to provide improved hazard data with which to evaluate and specify building enclosure components intended to provide a water-resistant system of protection to the building structure and its contents.

REFERENCES

1. International Code Council (ICC). 2021. *International Energy Conservation Code*. Country Club Hills, IL: ICC.
2. American National Standards Institute (ANSI), ASHRAE, and Illuminating Engineering Society (IES). 2019. *Energy Standard for Buildings Except Low-Rise Residential Buildings*. ANSI/ASHRAE/IES Standard 90.1. Peachtree Corners, GA: ASHRAE.
3. Crandell, J. H. 2019. "Continuous Insulation: Research, Applications, and Resources for Walls, Roofs, and Foundations." In *Proceedings of the RCI International Convention and Trade Show*. https://iibec.org/wp-content/uploads/2019-cts-crandell.pdf.
4. Crandell, J. H. 2020. "Applying Recent Building and Energy Code Advancements for Durable and Energy-Efficient Building Envelopes." In *Proceedings of the IIBEC 2020 International Convention and Trade Show*.
5. Crandell, J. H. 2021. "Cladding and Building Enclosure Component Connections Through Foam Plastic Continuous Insulation: Design and Prescriptive Code Compliance." *Proceedings of the 2021 IIBEC International Convention and Trade Show*.
6. ASTM International. 2019. *Standard Specification for Rigid, Cellular*

Polystyrene Thermal Insulation. ASTM C578-19. West Conshohocken, PA: ASTM International. https://doi.org/10.1520/C0578-19.
7. ASTM International. 2021. *Standard Specification for Faced Rigid Cellular Polyisocyanurate Thermal Insulation Board*. ASTM C1289-21. West Conshohocken, PA: ASTM International. https://doi.org/10.1520/C1289-21.
8. ICC. 2021. *International Building Code*. Country Club Hills, IL: ICC.
9. ICC. 2021. *International Residential Code*. Country Club Hills, IL: ICC.
10. Applied Building Technology Group (ABTG). 2021. "Facts on CI: Moisture Control for Wall Assemblies." https://www.continuousinsulation.org/sites/default/files/uploads/attachments/node/210/ci-factssheetmoisturecontrolfinal.pdf.
11. ABTG. 2021. "Quick Guide: 3 Steps for Code-Compliant Use of Water Vapor Retarders and Foam Plastic Insulating Sheathing (FPIS) Continuous Insulation (ci)." https://www.continuousinsulation.org/sites/default/files/uploads/attachments/node/214/ci-quickguidewatervaporcontrol.pdf.
12. ICC. n.d. "Errata Central." Accessed November 13, 2021. https://www.iccsafe.org/errata-central.
13. ICC. n.d."2021/2022 Code Development: Group A." Accessed November 13, 2021. https://www.iccsafe.org/products-and-services/i-codes/code-development-process/2021-2022-group-a.
14. ABTG. 2015. "Water-Resistive Barriers: Assuring Consistent Assembly Water-Penetration Resistance." ABTG research report no. 1504-03. https://www.appliedbuildingtech.com/rr/1504-03.
15. ABTG. 2021. "Installation and Performance of Flanged Fenestration Units Mounted on Walls with Foam Plastic Insulating Sheathing." ABTG research report no. 2104-01 https://www.appliedbuildingtech.com/rr/2104-01.
16. Holladay, M. 2011. "Musings of an Energy Nerd: Nailing Window Flanges through Foam" (blog post). GreenBuilding Advisor. https://www.greenbuildingadvisor.com/article/nailing-window-flanges-through-foam.
17. Lstiburek, J. 2013. "Stuck on You." Insight 067. Building Science Corporation. https://www.buildingscience.com/documents/insights/bsi-067-stuck-on-you.
18. Crandell, J. H., and J. Smart. 2004. "Lessons from EIFS: Past, Present, and Future Challenges for Exterior Envelope Design and Construction." In *Proceedings of Woodframe Housing Durability and Disaster Issues Conference, Las Vegas, NV, October 4-6, 2004*. Madison, WI: Forest Products Society.
19. Fenestration and Glazing Industry Alliance (FGIA). 2020. *Voluntary Laboratory Test Method to Qualify Vertical Fenestration Installation Procedures*. AAMA TIR-504-20. Schaumburg, IL: FGIA.
20. ASTM International. 2019. *Standard Test Method for Determining Rate of Air Leakage Through Exterior Windows, Skylights, Curtain Walls, and Doors Under Specified Pressure Differences Across the Specimen*. ASTM E283/E283M-19. West Conshohocken, PA: ASTM International. https://doi.org/10.1520/E0283_E0283M-19.
21. ASTM International. 2016. *Standard Test Method for Water Penetration of Exterior Windows, Skylights, Doors, and Curtain Walls by Uniform Static Air Pressure Difference*. ASTM E331-00(2016). West Conshohocken, PA: ASTM International. https://doi.org/10.1520/E0331-00R16.
22. ASTM International. 2013. *Standard Practice for Determining the Effects of Temperature Cycling on Fenestration Products*. ASTM E2264-05(2013). West Conshohocken, PA: ASTM International. https://doi.org/10.1520/E2264-05R13.
23. ASTM International. 2014. *Standard Test Method for Structural Performance of Exterior Windows, Doors, Skylights and Curtain Walls by Uniform Static Air Pressure Difference*. ASTM E330-14. West Conshohocken, PA: ASTM International. https://doi.org/10.1520/E0330_E0330M-14.
24. Qualtim Inc. 2013. *Resistance of Fasteners Installed into Windows over Foam Sheathing Panels and OSB*. Madison, WI: Qualtim Inc.
25. ABTG. 2002. "Attachment of Exterior Wall Coverings Through Foam Plastic Insulating Sheathing (FPIS) to Wood or Steel Wall Framing." ABTG research report no. 1503-02. https://www.appliedbuildingtech.com/rr/1503-02.
26. FGIA. 2019. *Comparative Analysis Procedure for Window and Door Products*. AAMA 2502-19. Schaumburg, IL: FGIA.
27. ABTG. 2021. "Quick Guide: Window Installation Instructions for Walls with Continuous Insulation." https://www.continuousinsulation.org/sites/default/files/uploads/attachments/node/214/ci-quickguidewindowinstallation.pdf.
28. Barnes, B., J. Yu, A. Pagán-Vázquez, N. Alexander, and R. Liesenet. 2013. "Window Related Thermal Bridging." In *Proceedings of Thermal Performance of the Exterior Envelopes of Whole Buildings XII International Conference*. Peachtree Corners, GA: ASHRAE. https://web.ornl.gov/sci/buildings/conf-archive/2013%20B12%20papers/120-Barnes.pdf.
29. Morrison-Hershfield Ltd. 2020. "Building Envelope Thermal Bridging Guide, V1.5." BC Hydro Power Smart website. https://www.bchydro.com/content/dam/BCHydro/customer-portal/documents/power-smart/business/programs/BE-Thermal-Bridging-Guide-v1-5.pdf.

APPENDIX A

PRELIMINARY DRAFT OF 2024 IBC VAPOR RETARDER PROVISIONS BASED ON APPROVED CODE CHANGE PROPOSALS

Section 202 – Definitions

RESPONSIVE VAPOR RETARDER. A vapor retarder material complying with a vapor retarder class of Class I or Class II but which also has a vapor permeance of 1 perms or greater in accordance with ASTM E96, water method (Procedure B).

Chapter 14 – Exterior walls

...

1404.3 VAPOR RETARDERS. Vapor retarder materials shall be classified in accordance with Table 1404.3(1). A vapor retarder shall be provided on the interior side of frame walls in accordance with Table 1404.3(2) and Tables 1404.3(3) or 1404.3(4) as applicable, or an approved design using accepted engineering practice for hygrothermal analysis. Vapor retarders shall be installed in accordance with 1404.3.3. The appropriate climate zone shall be selected in accordance with Chapter 3 of the *International Energy Conservation Code.*

Exceptions:

1. Basement walls.
2. Below-grade portion of any wall.
3. Construction where accumulation, condensation, or freezing of moisture will not damage the materials.
4. A vapor retarder shall not be required in Climate Zones 1, 2, and 3.
5. In Climate Zones 4 through 8, a vapor retarder on the interior side of frame walls shall not be required where the assembly complies with Table 1404.3(5).

1404.3.1 SPRAY FOAM PLASTIC INSULATION FOR MOISTURE CONTROL WITH CLASS II OR III VAPOR RETARDERS. For purposes of compliance with Tables 1404.3(3) and 1403.3(4), spray foam with a maximum permeance of 1.5 perms at the installed thickness applied to the interior side of wood structural panels, fiberboard, insulating sheathing or gypsum shall be deemed to meet the continuous insulation moisture control requirement in accordance with one of the following conditions:

1. The spray foam *R*-value meets or exceeds the specified *continuous insulation* R-value.
2. The combined *R*-value of the spray foam and *continuous insulation* is equal to or greater than the specified continuous insulation *R*-value.

1404.3.2 VAPOR RETARDER INSTALLATION. Vapor retarders shall be installed in accordance with the manufacturer's instructions or an approved design. Where a vapor retarder also functions as a component of a continuous air barrier, the vapor retarder shall be installed as an air barrier in accordance with the *International Energy Conservation Code.*

Table 1404.3(1).
Vapor retarder materials and classes

Vapor retarder class	Acceptable materials
I	Sheet polyethylene, nonperforated aluminum foil, or other approved materials with a perm rating of less than or equal to 0.1
II	Kraft-faced fiberglass batts or vapor retarder paint or other approved materials, applied in accordance with the manufacturer's instructions for a perm rating greater than 0.1 and less than or equal to 1.0
III	Latex paint, enamel paint, or other approved materials, applied in accordance with the manufacturer's instructions for a perm rating of greater than 1.0 and less than or equal to 10

Table 1404.3(2).
Vapor retarder options

Climate zone	Vapor retarder class		
	Class I[a]	Class II[a]	Class III
1,2	Not permitted	Not permitted	Permitted
3	Not permitted	Permitted[c]	Permitted
4 (except Marine 4)	Not permitted	Permitted[c]	See Table 1404.3(3)
Marine 4, 5, 6, 7, 8	Permitted[b,c]	Permitted[c]	

[a]A *responsive vapor retarder* shall be allowed on the interior side of any frame wall in all climate zones.

[b]Use of a Class I interior vapor retarder, that is not a *responsive vapor retarder*, in frame walls with a Class I vapor retarder on the exterior side shall require an *approved* design.

[c]Where a Class I or II vapor retarder is used in combination with foam plastic insulating sheathing installed as *continuous insulation* on the exterior side of frame walls, the *continuous insulation* shall comply with Table 1404.3(4) and the Class I or II vapor retarder shall be a *responsive vapor retarder.*

APPENDIX A

PRELIMINARY DRAFT OF 2024 IBC VAPOR RETARDER PROVISIONS BASED ON APPROVED CODE CHANGE PROPOSALS

Table 1404.3(3). Class III vapor retarders

Climate zone	Class III vapor retarders permitted for[a,b]:
4	Vented cladding over wood structural panels
	Vented cladding over fiberboard
	Vented cladding over gypsum
	Continuous insulation with *R*-value ≥ R-2.5 over 2 × 4 wall
	Continuous insulation with *R*-value ≥ R-3.75 over 2 × 6 wall
5	Vented cladding over wood structural panels
	Vented cladding over fiberboard
	Vented cladding over gypsum
	Continuous insulation with *R*-value ≥ R-5 over 2 × 4 wall
	Continuous insulation with *R*-value ≥ R-7.5 over 2 × 6 wall
6	Vented cladding over fiberboard
	Vented cladding over gypsum
	Continuous insulation with *R*-value ≥ R-7.5 over 2 × 4 wall
	Continuous insulation with *R*-value ≥ R-11.25 over 2 × 6 wall
7	*Continuous insulation* with *R*-value ≥ R-10 over 2 × 4 wall
	Continuous insulation with *R*-value ≥ R-15 over 2 × 6 wall
8	*Continuous insulation* with *R*-value ≥ R-12.5 over 2 × 4 wall
	Continuous insulation with *R*-value ≥ R-20 over 2 × 6 wall

[a]Vented cladding shall include vinyl lap siding, polypropylene, or horizontal aluminum siding, brick veneer with airspace as specified in this code, rainscreen systems, and other approved vented claddings.

[b]The requirements in this table apply only to insulation used to control moisture in order to permit the use of Class III vapor retarders. The insulation materials used to satisfy this option also contribute to but do not supersede the thermal envelope requirements of the *International Energy Conservation Code*.

Table 1404.3(4). Continuous insulation with a Class I *OR* II responsive vapor retarder

Climate zone	Permitted conditions[a]
3	*Continuous insulation* with *R*-value ≥2
4, 5, and 6	*Continuous insulation* with *R*-value ≥3 over 2 × 4 wall
	Continuous insulation with *R*-value ≥5 over 2 × 6 wall
7	*Continuous insulation* with *R*-value ≥5 over 2 × 4 wall.
	Continuous insulation with *R*-value ≥7.5 over 2 × 6 wall
8	*Continuous insulation* with *R*-value ≥7.5 over 2 × 4 wall
	Continuous insulation with *R*-value ≥10 over 2 × 6 wall

[a]The requirements in this table apply only to insulation used to control moisture in order to permit the use of Class I or II vapor retarders. The insulation materials used to satisfy this option also contribute to but do not supersede the thermal envelope requirements of the *International Energy Conservation Code*.

Table 1404.3(5). Continuous insulation on walls without a Class I, II, *OR* III interior vapor retarder[a]

Climate zone	Permitted conditions[b,c]
4	*Continuous insulation* with *R*-value ≥ 4.5
5	*Continuous insulation* with *R*-value ≥ 6.5
6	*Continuous insulation* with *R*-value ≥ 8.5
7	*Continuous insulation* with *R*-value ≥ 11.5
8	*Continuous insulation* with *R*-value ≥ 14

[a]The total insulating value of materials to the interior side of the exterior *continuous insulation*, including any cavity insulation, shall not exceed R-5. Where the *R*-value of materials to the interior side of the exterior *continuous insulation* exceeds R-5, an *approved* design shall be required.

[b]A water vapor control material layer having a permeance not greater than 1 perm in accordance with ASTM E96, Procedure A (dry cup) shall be placed on the exterior side of the wall and to the interior side of the exterior *continuous insulation*. The exterior *continuous insulation* shall be permitted to serve as the vapor control layer where, at its installed thickness or with a facer on its interior face, the exterior *continuous insulation* is a Class I or II vapor retarder.

[c]The requirements in this table apply only to insulation used to control moisture in order to allow walls without a Class I, II, or III interior vapor retarder. The insulation materials used to satisfy this option also contribute to but do not supersede the thermal envelope requirements of the *International Energy Conservation Code*.

APPENDIX B

WINDOW INSTALLATION QUICK GUIDE[27]

QUICK GUIDE
Foam Plastic Applications for Better Building

WINDOW INSTALLATION INSTRUCTIONS FOR WALLS WITH CONTINUOUS INSULATION:

Integral Nail-Flange Windows on Walls with Maximum 1½"-Thick Foam Plastic Insulating Sheathing (FPIS)[1]

05.19.21

IMPORTANT! READ ALL INSTRUCTIONS BEFORE BEGINNING INSTALLATION

STEP 1: KNOW YOUR RESPONSIBILITIES

The user of this document is responsible for the following: (1) determining the suitability of this document for the intended use; (2) complying with the local building code; (3) providing the necessary skill to execute a proper window installation; (4) following the component manufacturers' installation instructions for the user-specified window product, flashing materials, water-resistive barrier (WRB), foam plastic insulating sheathing (FPIS), sealants, and other materials as required for a complete an effective installation; and (5) addressing any variances from manufacturers' instructions and product warranty stipulations, including consultation with the applicable product manufacturers or a design professional as needed.

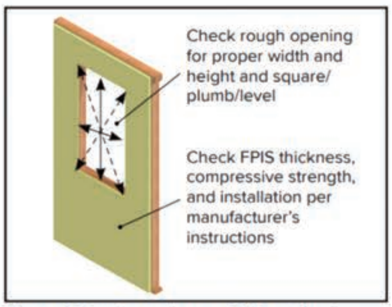

Figure 1. Rough opening and FPIS verification.

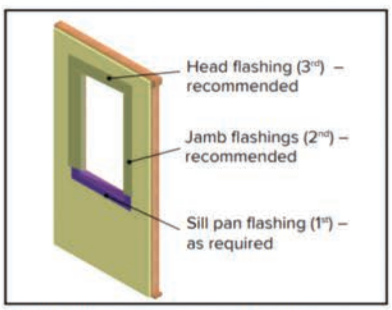

Figure 2. Install rough opening flashing, lapping shingle-fashion (bottom to top of opening).

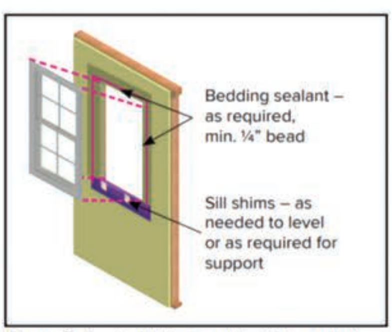

Figure 3. Apply sill shims and bedding sealant, set window into center of opening, and temporarily secure with flange nail.

STEP 2: BEFORE YOU INSTALL THE WINDOW

a. Verify that the rough opening is level, plumb, square, and the size required for the specified window product plus clearance for a rough opening gap as recommended by the window manufacturer (typically the rough opening width and height are ½" to ¾" greater than the window unit dimensions). See Figure 1.

b. Verify that the FPIS is not greater than 1½" thick, has a minimum compressive strength of 15 psi per ASTM C578 or ASTM C1289, and is installed in accordance with the FPIS manufacturer's installation instructions for a code-compliant WRB application. Where a separate WRB material is provided, the thickness of FPIS is greater than 1½", or for other special conditions, refer to the section **SPECIAL CONDITIONS & ADDITIONAL RESOURCES**.

c. Window sill pan flashing with back-dam, rough opening jamb flashings, and head flashings are a recommended installation best practice. Where used or required, install the rough opening flashing elements in shingle-lap fashion (see Figure 2). **NOTE:** Self-adhering and fluid-applied flexible flashings (or equal) are typically used for this purpose. Verify that the rough opening size can accommodate the additional thickness of flashing materials and maintain the required rough opening gap (see Item a).

STEP 3: INSTALLING THE WINDOW

a. Apply the window manufacturer's recommended bedding sealant (min. ¼" bead) to the rough opening perimeter approximately ½" to ¾" from the edge of the rough opening (see Figure 3). **DO NOT** apply bedding sealant to sill flange where sill pan flashing is used (see Step 2, Item c).

b. Where sill shims are required by the manufacturer or where the sill is not level, shims may be placed and tacked into level position prior to setting the window unit. See Figure 3.

c. With the window closed and in locked position, set into the center of the rough opening and fasten the center nail hole of the top flange to the rough opening with the manufacturer's recommended flange fastener, or initially secure as otherwise recommended by the manufacturer (See Figure 3). Verify that the required gap between the window head and header is present.

d. Install sill shims (if not previously installed) and jamb shims at locations as required by window manufacturer. Adjust shims as necessary to achieve a square, plumb, and level window installation. Apply shims at window head only where required by the manufacturer.

e. Check operation of the window and then install remaining nail flange fasteners as recommended by the manufacturer. A maximum fastener spacing of 6" is recommended. **NOTE:** The length of fasteners will need to accommodate the thickness of FPIS and maintain the required penetration into rough opening framing materials. Do not over- or under-drive flange fasteners. Flanges should be firmly

APPENDIX B

WINDOW INSTALLATION QUICK GUIDE[27]

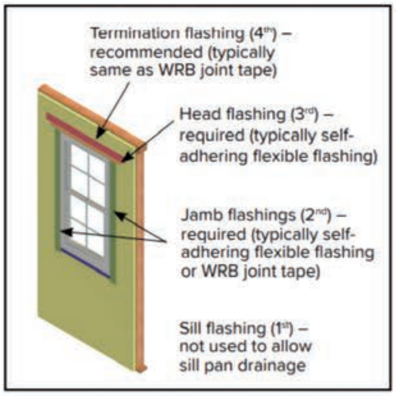

Figure 4. After permanently securing the flange, install exterior flashing in shingle fashion (bottom to top) on sill, jamb, and head flanges and to WRB surface. DO NOT apply sill flashing if rough opening sill pan is installed (as shown).

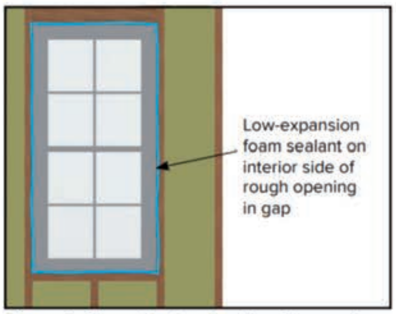

Figure 5. Air seal the interior side of the rough opening gap with low-expansion foam sealant.

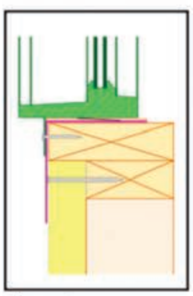

Figure 6.
Rough opening "window buck"

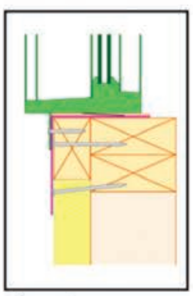

Figure 7.
Rough opening "picture frame"

bedded in sealant and not warped out of plane. Clean off any excess sealant. Install any additional frame anchorage as required by the window manufacturer.

f. Apply exterior flashing per manufacturer's instructions to window perimeter in shingle-lap fashion, starting at the bottom and ending with the head flashing (see Figure 4). **DO NOT** install flashing over flange at sill where a sill pan has been installed in the rough opening. Use compatible flashing materials recommended by the window manufacturer or WRB manufacturer and ensure conditions are appropriate for application (clean, dry, suitable temperature, etc.). **NOTE:** Self-adhering and fluid-applied flexible flashings (or equal) are typically used for this purpose and must have sufficient width to lap window flange and extend a minimum of 2" onto WRB surface.

g. Air seal the interior side of the rough opening gap with low-expansion foam sealant intended for window installation. Avoid gaps or voids in the air seal. A tight interior air seal of the rough opening gap will promote proper drainage and prevent drafty window installations (see Figure 5).

SPECIAL CONDITIONS & ADDITIONAL RESOURCES

- Where the FPIS material is greater than 1½" thick or less than 15 psi compressive strength, or where additional window or door support may be required (e.g., opening width > 6' or design wind load > 35 psf), it is recommended that a rough opening extension be applied to the rough opening. This can be done by use of 2x wood buck (see Figure 6) installed into the rough opening (which must be planned during rough framing) or by a "picture frame" furring (see Figure 7) installed around the perimeter of the rough opening of the same thickness as the FPIS for a flush installation (which can be installed at any time prior to window installation). In both cases, the window installation and flashing follow the same steps as indicated above. For additional installation guidance on this practice refer to: continuousinsulation.org/window-installation.
- A similar practice may be applied to integral flange door installations; however, door thresholds must be fully supported by blocking or rough opening extension as described above. In addition, where door frame or door hinges are required to be anchored to rough opening framing, ensure the FPIS thickness can be accommodated such that the anchorage fasteners (typically screws) embed into framing material with the minimum required edge distance.
- Where a separate WRB membrane layer is installed over or under the FPIS, refer to FMA/AAMA/WDMA 500-16 Standard Practice for the Installation of Mounting Flange Windows into Walls Utilizing Foam Plastic Insulating Sheathing (FPIS) with a Separate Water-Resistive Barrier (WRB) for appropriate installation and flashing details.

RECOMMENDED TOOLS AND ACCESSORIES

- Tape measure
- Level
- Hammer
- Power screw driver with clutch
- Shims
- Sealant*
- Flashing*
- Fasteners*

*Follow manufacturer's specifications and installation recommendations as applicable.

Additional Resources

- Window Installation in Walls with Foam Sheathing
- Water-Resistive Barrier
- Continuous Insulation for Residential Windows
- Continuous Insulation for Commercial Windows

Owned and operated by the Applied Building Technology Group with support from a grant provided by the Foam Sheathing Committee (FSC) of the American Chemistry Council, **continuousinsulation.org** provides informational resources intended to assist the foam plastic insulating sheathing industry, using sound science to develop research supporting the reliable, efficient, and economic design and installation of foam sheathing.

Contact us.

Content originally produced for continuousinsulation.org with support from ACC's Foam Sheathing Committee.

QG1_WindowInstallation_05.2021 • Page 2 of 2

Low-Rise Foam Adhesive Research Project

Randy Adams

Midwest Roofing Contractors Association | Indianapolis, IN

randy_a@radamsroofing.com

Richard S. Koziol

Wiss, Janney, Elstner Associates Inc. | Northbrook, IL

rkoziol@wje.com

IIBEC 2022 - Building for the Future

International Convention and Trade Show

March 17–22, 2022 | Orlando, FL

ABSTRACT

This presentation describes a testing and research project to determine how the bond capacity of low-rise foam adhesive between insulation panels at varying adhesive ribbon spacings was affected when the adhesive was applied to both fiberglass and organic-faced polyisocyanurate insulation boards. The project scope included design and fabrication of custom 4×4 ft aluminum frames; testing of eighteen 4-ft square specimens in direct tension until failure; testing six companion, small-scale (12×12 in.) specimens in direct tension until failure; evaluation of test results; and development of key observations from the test program.

SPEAKERS

Randy Adams

Midwest Roofing Contractors Association | Indianapolis, IN

Randy Adams is chair of the Midwest Roofing Contractors Association Technical and Research Committee. He has more than 40 years of specialized experience in the roofing industry and is owner and president of R. Adams Roofing Inc., Environmental Greenscapes Inc.

Richard S. Koziol

Wiss, Janney, Elstner Associates Inc. | Northbrook, IL

Richard S. Koziol is a principal at Wiss, Janney, Elstner Associates Inc. He has more than 35 years specialized experience in investigating and testing roofing systems. He has developed and designed repairs for water infiltration and condensation problems in new and existing building enclosures. Koziol is a graduate of the University of Illinois at Chicago and a licensed architect in five states.

Low-Rise Foam Adhesive Research Project

The research and testing program outlined in this paper was developed based on a request for proposal (RFP) titled "Low Rise Foam Research Project," which was issued by the Midwest Roofing Contractors Association (MRCA) Technical Research Committee in May 2019. It has been recognized in the industry that the handheld wand and cartridge application technique for field installation of low-rise foam adhesives is unlikely to produce consistent ribbon spacing. Thus, the problem statement presented in the MRCA RFP states, "What impact does variation in foam ribbon spacing have on ultimate roof uplift capacity?"

The problem defined in the MRCA RFP states that typical manufacturer installation instructions provide for low-rise foam adhesive ribbons to be applied at 6 and 12 in. spacings. Accordingly, the program was ultimately refined to include testing of insulation adhesion at these spacings, as well as ribbons spaced at 18 in. on full-size, 4 × 4 ft square specimens. In addition, investigators performed supplemental testing of adhesion on 1 × 1 ft square companion specimens, as well as tensile testing of adhesive-only samples.

OBJECTIVE

The objective of this research project was to determine the effect on bond capacity of low-rise foam adhesive between insulation panels at varying adhesive ribbon spacings, with the adhesive applied to both glass fiber and organic-faced polyisocyanurate insulation boards. The project scope included:

- Development of a testing plan and protocol in collaboration with the MRCA Technical and Research Committee.
- Design and fabrication of custom aluminum loading frames to apply uniform forces to the 4 × 4 ft square test specimens.
- Preparation of 18 specimens, each comprised of two 4 × 4 ft square, 2-in.-thick polyisocyanurate insulation boards adhered together with low-rise foam adhesive ribbons. Three sets of six panels were prepared with ribbons applied at spacings of 6, 12, and 18 in. centers. Within each set of six specimens, three specimens featured cellulosic felt-faced insulation boards and three featured polymer-coated glass fiber-faced insulation boards. The insulation boards were attached to nominal ¾-in.-thick plywood base layers fitted with special tee-lock connectors to accommodate anchorage of the specimens to the test frames.
- Testing of the 18 specimens in direct tension until failure, while simultaneously monitoring loads, measuring specimen elongation, and recording relative displacements at edges of specimens.
- Testing of six companion, small-scale (12 × 12 in.) insulation specimens in direct tension until failure. These specimens—three each for organic-faced and glass fiber-faced insulation—were fabricated with a single foam adhesive ribbon.
- Testing two companion, small-scale (12 × 12 in.) insulation specimens fabricated with full-coverage foam adhesive between insulation boards—one each for organic-faced and glass fiber-faced insulation.
- Direct tension testing of the low-rise foam adhesive. Tests were conducted of cured foam specimens that were either approximately ⅛-in. thick or approximately 1⁄32-in. thick.
- Evaluation of test results and development of key observations from the test program.

MATERIALS

The polyisocyanurate insulation boards and foam adhesive cartridges used for the testing were supplied to Wiss, Janney, Elstner Associates Inc. (WJE) by an MRCA member roofing contractor. Four pallets of insulation with factory-protective wrapping were received approximately 30 days before testing and stored in a warehouse building with the wrapping removed. Two types of insulation were used for the 18 full-size tests: nine of the specimens used ASTM C1289[1] Type II, Class 1, Grade 2 polyisocyanurate boards (glass-fiber-reinforced cellulosic felt facers and 20 psi compressive strength), and nine specimens used ASTM C1289 Type II, Class 2, Grade 2 boards (coated polymer-bonded glass fiber mat facers and 20 psi compressive strength). The dimensions of the insulation boards for all full-size specimens were nominally 48 × 48 in. with a thickness of 2 in. The insulation boards were delivered to our lab with these dimensions; no larger boards were cut to size. For this test program, polymer-coated glass fiber– and cellulosic felt–faced insulation specimens were designated Type A and Type B, respectively.

The objective of this research project was to determine the effect on bond capacity of low-rise foam adhesive between insulation panels at varying adhesive ribbon spacings, with the adhesive applied to both glass fiber and organic-faced polyisocyanurate insulation boards.

Figure 1. Lines were drawn on the insulation boards (with spacings centered on boards) to guide the application of the low-rise foam adhesive ribbons. The lines were centered so that application of the adhesive would be symmetrical. The photo shows the line layout for a 12 in. ribbon spacing.

Figure 2. Grid of low-rise foam adhesive being applied to plywood panels to achieve an approximate 6 in. grid onto which one of the insulation boards would be placed.

A two-component, low-rise polyurethane foam adhesive was used to adhere the insulation boards. The adhesive was provided in dual-chambered cartridges with attached mixing tips that combined the two components. The adhesive was applied with an electrically powered applicator in beads spaced as required by each test series. To create a base layer for specimens, the same two-component low-rise adhesive was used to attach insulation boards to $\frac{3}{4}$-in.-thick, 48 × 48 in. sanded BC plywood panels.

FABRICATION OF SPECIMENS

Full-Size Specimens

Low-rise foam adhesive was applied by a skilled roofing tradesperson to all plywood panels and insulation boards using a power-actuated applicator inside the conditioned testing facility. Each of the plywood base-layer panels was drilled with $\frac{29}{64}$-in.-diameter holes at 26 locations to match the locations of the attachment points on the top and bottom of the custom-fabricated aluminum stiffening frames. Into each of these holes, a nominal $\frac{3}{8}$-in.-diameter twist-resistant tee nut with a 1-in.-diameter flange was inserted and embedded into the plywood.

Polyisocyanurate insulation specimens were sorted to separate the Class 1 boards from the Class 2 boards and put into six groups of three. The boards were inspected for labeling that read "This Side Up" or "This Side Down" and were placed appropriately. A permanent marker was used to highlight the applicable insulation board facer surfaces with line markings at the test spacings of 6, 12, or 18 in. (**Fig. 1**). The "knit line" orientation on the insulation boards was identified and placed in positions so that the knit lines of the top insulation board were oriented in perpendicular position relative to the bottom insulation board for each pair of boards comprising a test specimen.

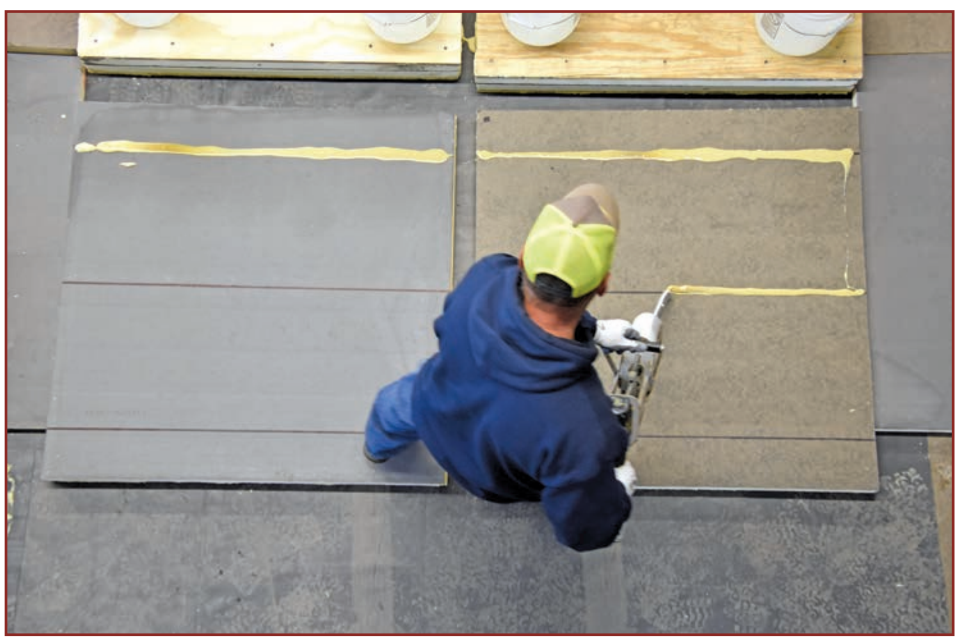

Figure 3. Typical low-rise foam adhesive bead width being applied to two separate insulation boards with 18 in. ribbon spacing lines.

Figure 5. A cross section of an insulation and plywood specimen.

Figure 4. Typical weights used as ballast until the foam adhesive set up, typically for 10 to 15 minutes per specimen.

The two-part polyurethane foam adhesive was initially installed onto the plywood board surfaces in ribbons approximately 6 to 9 in. on center in each direction (**Fig. 2**). Immediately after placement of the adhesive, insulation boards were installed on the prepared plywood boards. Five weighted buckets, approximately 26 lb each, were placed on the insulation boards, one at each corner and one in the center. The buckets remained in place for approximately 10 to 15 minutes while the adhesive cured. The adhered plywood and insulation halves for each of the specimens were allowed to set up and cure between 12 to 24 hours before final assembly.

After setup and curing, the two-part polyurethane adhesive was applied in ribbons onto half of the specimen along the highlighted markings at designated ribbon spacing. The foam adhesive ribbons were applied at an initial application width of approximately ¾ in. (**Fig. 3**). The foam ribbons were installed in straight, parallel lines from one end of the insulation board to the other, in lieu of a serpentine pattern. Effort was made to keep the bead width as uniform as possible; however, some variation in adhesive bead width did occur. In addition, in some instances, a small amount of adhesive accumulated at the ends of the boards because of the nature of the applicator tool and the handheld process used.

Immediately after placement of the adhesive ribbons, the top insulation board was positioned on top of the ribbons, and weighted buckets (approximately 26 lb each) were placed on the plywood panels at the corners and in the center (**Fig. 4**). The buckets remained in place for approximately 10 to 15 minutes while the adhesive cured. **Figure 5** presents a cross-sectional view of a typical completed specimen assembly.

Companion Specimens

Companion tests were performed on two small-scale specimen configurations to provide supplemental information of bond strength of the adhesive between the polyisocyanurate insulation layers as well as the tensile strength of the two-part polyurethane foam adhesive.

1 × 1 ft Specimens

Eight 1 × 1 ft square companion specimens were made with the same plywood and insulation materials as the full-sized specimens (**Fig. 6**). Six test specimens were made by adhering insulation with a centrally positioned single 12-in.-long ribbon of foam adhesive. Three of the six specimens were made with coated glass fiber facers (Type A) and three with cellulosic felt facers (Type B). The remaining two specimens, one made with Type A insulation and the other made with Type B, were fabricated with a continuous film of foam adhesive to effectively provide full coverage over the 1 ft^2 surface area.

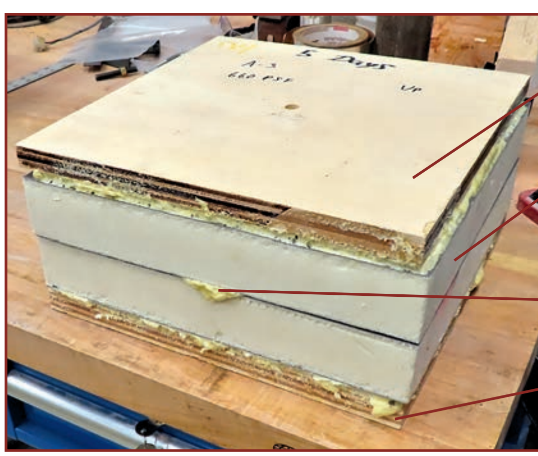

Figure 6. A 12 × 12 in. insulation board specimen with a single ribbon of adhesive.

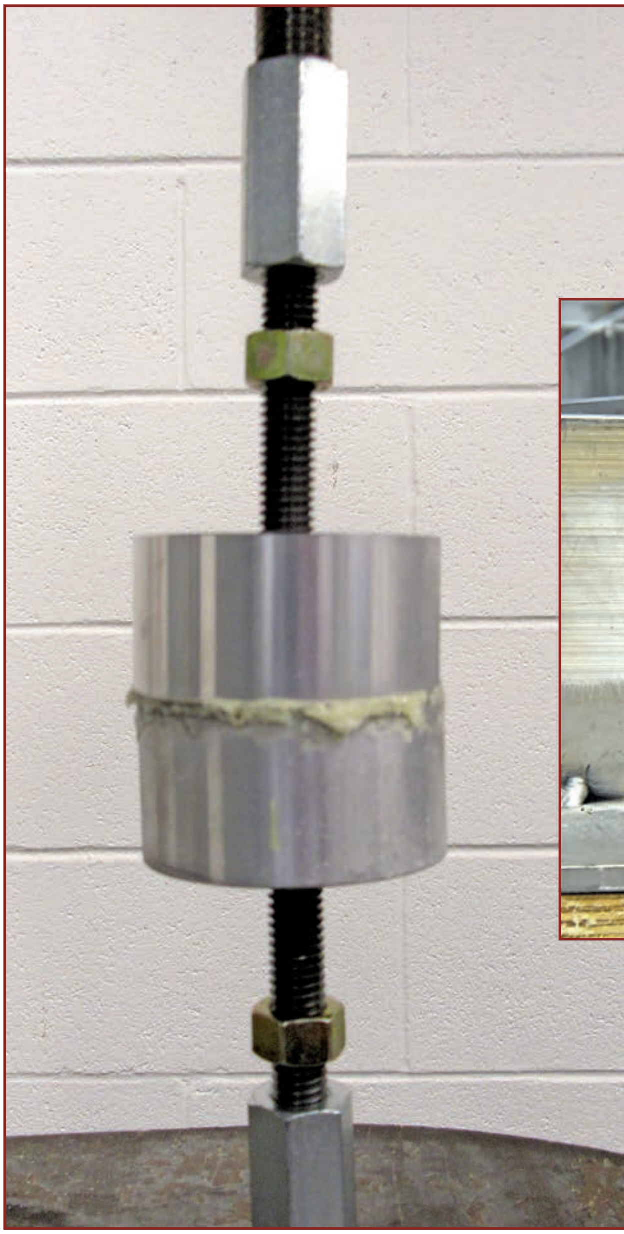

Figure 7. Two pucks with a ⅛-in.-gap space filled with foam adhesive.

Figure 8. Example of the alphanumeric system and label used to identify the insulation specimens. B-18-3 indicates a cellulosic felt facer (B) with 18 in. ribbon spacing, and specimen number 3.

Adhesive-Only Specimens

To assess the tensile strength of only polyurethane foam adhesive, we used a controlled, thin-layering methodology in which the material was placed and adhered between two aluminum pucks (**Fig. 7**). The pucks have a machined surface on one side and a threaded hole on the other side to receive a threaded rod used to apply tensile test loads. Six specimens were prepared by initially cleaning and abrading the flat face of the aluminum puck. A layer of the project's two-part polyurethane foam was then applied to the face and inserted into a fabrication jig that holds and secures both pucks while maintaining a ⅛ in. gap between their planar surfaces. Subsequent expansion of the foam produces a controlled ⅛ in. separation of the pucks, ensuring appropriate resistance and simulating the effects of restraining ballast for actual installations. These specimens were intended to determine tensile strength of the foam adhesive at a thickness judged to be representative of typical use.

Three additional specimens were fabricated in a similar configuration as the first series, except that the pucks were adhered with a minimal space between the two puck surfaces (1⁄32 to 1⁄16 in. thickness). This specimen was intended to evaluate tensile strength of the foam adhesive in a thin-film configuration, possibly representing a condition of maximum confinement and restraint.

DESIGNATION AND IDENTIFICATION OF SPECIMENS

Full-Size Specimens

To provide unique identification of the 18 full-size test specimens, investigators developed an alphanumeric system consisting of letters to represent the facer type—polymer-coated glass fiber (A) and cellulosic felt (B)—followed by the ribbon spacing measurement, and the specimen test number (**Fig. 8**). For example, specimen number B-18-3 indicates a cellulosic felt–faced insulation board with 18-in. adhesive ribbon spacing, and specimen no. 3. **Table 1** summarizes the test matrix for all 18 specimens.

Facer type	Ribbon spacing (in.)	No. of specimens
Type A Polymer-coated glass fiber	6	3
	12	3
	18	3
Type B Cellulosic felt (organic)	6	3
	12	3
	18	3

Table 1. Test matrix for the full-size specimens

Companion Specimens

Of the six 1 × 1 ft square companion specimens fabricated with a single ribbon of adhesive, three were made with polymer-coated glass fiber facers (A) and three with cellulosic felt facers (B). The three specimens with polymer-coated glass fiber facers were numbered A-1, A-2, and A-3, and the three with cellulosic felt facers were numbered B-1, B-2, and B-3.

The two additional 1 × 1 ft square companion specimens with full-coverage foam adhesive applied between insulation boards were numbered FCA-1 and FCB-1.

Adhesive Specimens

The six puck specimens fabricated for tensile strength testing of the foam adhesive were identified as specimens TBS-1 through TBS-6. All six specimens were fabricated in a manner that allowed for a ⅛ in. gap between the pucks. Specimens TBS-1, TBS-2, and TBS-3 were allowed to cure for two days, and specimens TBS-4, TBS-5, and TBS-6 were allowed to cure for five days before testing.

Three additional pucks fabricated with the thin-film configuration were identified as ABS-1 through ABS-3.

AGE AND CONDITIONING OF SPECIMENS

The insulation boards and polyurethane foam adhesive were delivered to the laboratory on September 17, 2019, by an MRCA member contractor. The materials were delivered in unopened packaging, and after they were relocated into a warehouse building, the coverings were initially cut to allow for air movement. The materials remained in this location until assembled into the test specimens (approximately 30 days).

The environmental conditions in the warehouse during the time that the 4 × 4 ft square specimens were adhered with low-rise foam adhesive were 55°F to 67°F with relative humidity (RH) varying between 42% and 50%. The adhered specimens were kept in the warehouse building for two days; then they were moved to the conditioned laboratory space and allowed to acclimate to space environment of 70°F temperature and 30% RH for three additional days (five days total), prior to the start of testing on October 22, 2019.

The six 1 × 1 ft square insulation specimens, A1 through A3 and B1 through B3, and six pucks, TBS-1 through TBS-6, were fabricated in the warehouse building under similar conditions as full-size specimens. A single cartridge of low-rise foam adhesive was used to adhere the insulation boards to the plywood panels, and a separate cartridge was used to adhere the insulation boards together into adhered layered specimens for testing. This same cartridge was also used to adhere pucks TBS-1 through TBS-6. After setup, these samples were then relocated to the laboratory building and allowed to cure for five days. Pucks TBS-4 through TBS-6 were fabricated in a similar fashion but were allowed a cure time of two days before testing.

TEST APPARATUS AND INSTRUMENTATION

It was the intent of the program to subject the full-size adhered insulation specimens to direct axial tension force to effectively determine ultimate bond strength without inadvertent introduction of eccentric loading, prying, or peeling actions. This was accomplished by fabricating a custom test frame that secured the test specimen to an upper and lower aluminum plate system. These aluminum frames served as stiffening elements to the insulation specimens and ensured near-uniform axial loading to the adhered, layered specimen during testing.

The frames consisted of an upper and lower grillage of orthogonally oriented 6-in.-deep aluminum plates welded to a 4 × 4 ft square, ⅜-in.-thick aluminum base plate. Refer to Fig. 9 for an overall schematic of the test frame. The lower frame was anchored to and supported by four steel tube legs on 3 ft spacings, while the upper aluminum frame was fitted with a steel yoke that served to transfer a single vertical force to the center of the 4 × 4 ft square grillage. Attachment of the assembled insulation test specimen to the frames was accomplished by a series of 26 anchor bolts each at the top and bottom sections of the specimen. The ⅜ inch studs were threaded into the tee nuts installed in the upper and lower plywood backers and passed through mating holes within the aluminum base plates and secured uniformly with wing nuts. Refer to Fig. 10 for an overall view the upper test frame with an attached insulation specimen.

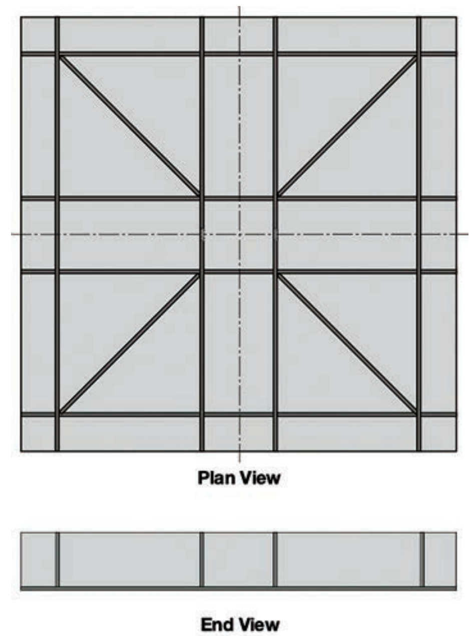

Figure 9. Schematic of stiffened upper aluminum test frame. All plates are ⅜ in. thick.

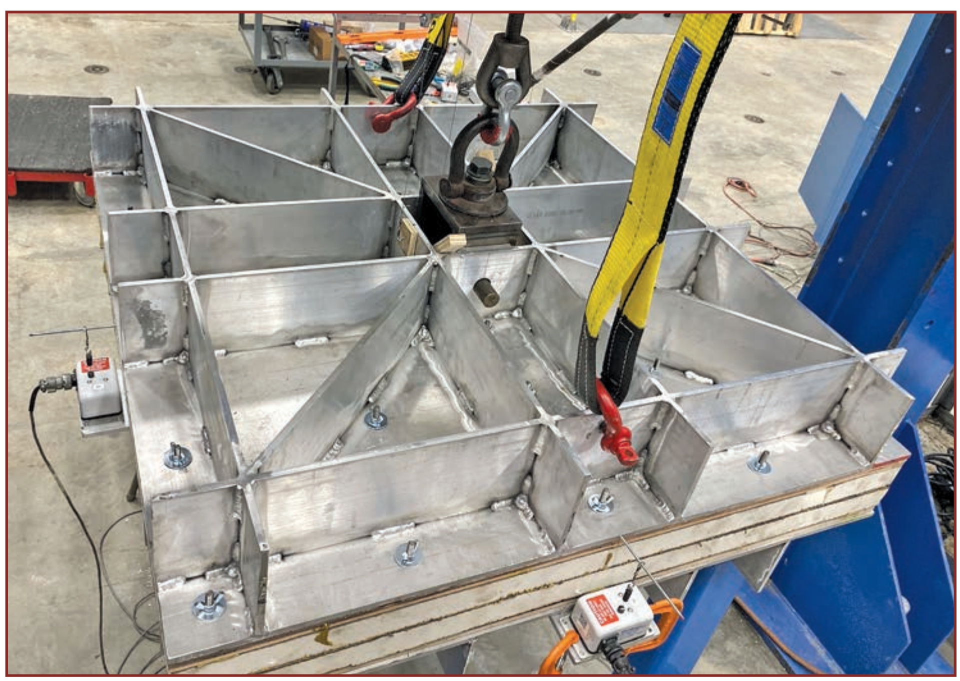

Figure 10. A stiffened aluminum test frame and secured insulation board test specimen.

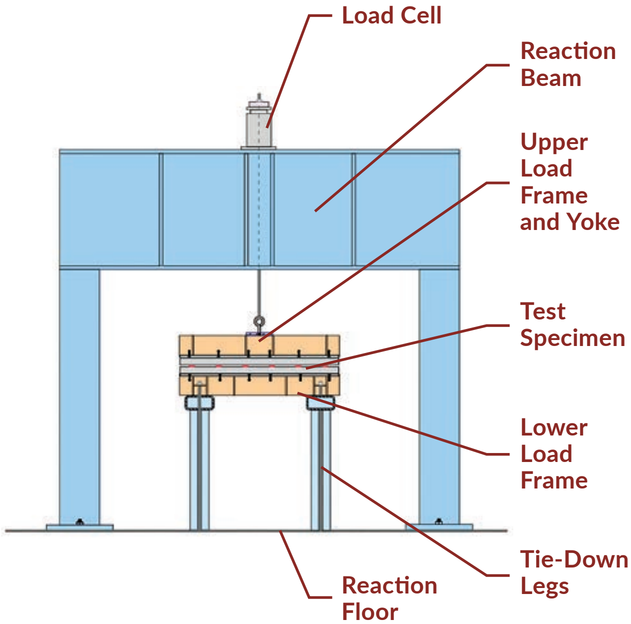

Figure 11. Schematic of existing steel reaction frame for application of load to specimen.

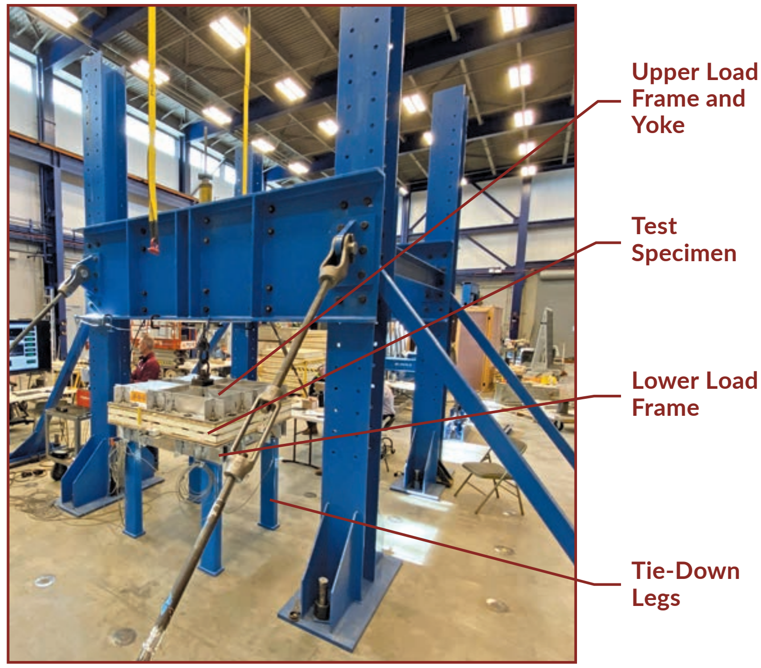

Figure 12. Existing steel reaction frame for application of load to specimen.

The aluminum test assemblies were positioned in an existing load reaction frame within the laboratory. The load reaction frame is a steel assembly used to support and apply loads and consists of steel columns and overhead steel back-to-back wide-flange beams secured to the laboratory's reinforced concrete reaction floor system. A 20,000-lb-capacity hydraulic actuator was positioned on top of the reaction frame and connected to the captured test specimen via a high-strength coil rod with end swivels. For schematic and overall views of the existing reaction frame with aluminum test frame setup, see **Fig. 11** and **12**.

A key performance parameter to evaluate relative behavior of the full-size test specimens is the load-deformation relationship. Accordingly, displacement of the specimens during tension loading was measured by four discrete displacement transducers (string potentiometers) positioned at the midpoint of each of the four edges of the specimens to measure movement between the upper and lower aluminum test frames (**Fig. 13**). The displacement transducers measured the combined effects of axial strain (stretching) of the two 2-in.-thick insulation layers, as well as separation and elongation of the low-rise foam adhesive during loading. The displacement transducers at each edge location had a total stroke of 2 in. and an accuracy of 0.001 in. For overall test fixture monitoring and measurement of any flexural deformation of the upper aluminum load frame, displacements near the center of the frame were additionally measured relative to the reaction frame at two locations.

Figure 13. Displacement transducer positioned at the edge of a test specimen to measure separation and elongation of insulation during testing.

Applied load provided by the hydraulic ram was monitored by a 20,000-lb-capacity electronic load cell. Output from all six displacement transducers and the load cell were captured by a computer-controlled data acquisition system that scanned sensors at approximately 1-second intervals. Displacements and loads were visually displayed on a large light-emitting diode screen to facilitate monitoring during testing.

TESTING PROCEDURES

Full-Size Specimens

Procedures for subjecting each of the 18 full-size specimens to uniform axial load were based on applicable provisions of ANSI/SPRI IA-1, *Standard Field Test Procedure for Determining the Uplift Resistance of Insulation and Insulation Adhesive Combinations over Various Substrates.*[2] Procedure IA-1 is commonly used to determine the uplift resistance of an installed roofing/insulation system in the field, and it provides for a loading protocol of incremental pressure increases and a dwell, or holding period, at each load stage. Investigators believed that this regimen would appropriately provide for a combination of incremental and sustained loading to effectively determine stiffness response and any short-term, nonlinear deformation tendencies. It is recognized that this modest loading rate may produce slightly lower ultimate load capacities compared with a more rapid application of load (such as a load application simulating wind gusts).

The general testing sequence of each full-size specimen consisted of the following:

1. Placing the adhered insulation specimen onto the lower aluminum test frame
2. Lowering the upper aluminum test frame onto the specimen
3. Securing the specimen to the upper and lower load frames by hand-tightening the wing nuts
4. Attaching the loading pin and pull-rod assembly to the loading yoke of upper frame
5. Attaching the north, south, east, and west edge displacement transducers
6. Attaching the two center-frame displacement transducers
7. Zeroing the displacement transducers and load cell and initiating data logging
8. Applying the preload/starting load of 30 lb/ft^2 plus tare weight
9. Maintaining the load for 1 minute
10. Incrementally increasing the load by 15 lb/ft^2 (240 lb)
11. Maintaining the load for 1 minute
12. Repeating incrementally increased loading until failure

Figures 14, **15**, and **16** present overall representative views of test setups and in-progress testing.

Companion Specimens

Companion tests were performed on two different small-scale insulation board specimen configurations to provide supplemental information about bond strength of polyisocyanurate insulation layers as well as the tensile strength of the low-rise foam adhesive.

1 × 1 ft Insulation Board Specimens

Nominal ⅜ in. threaded pull rods were anchored to each plywood back to facilitate load

Figure 14. Positioning the upper aluminum load frame onto a test specimen.

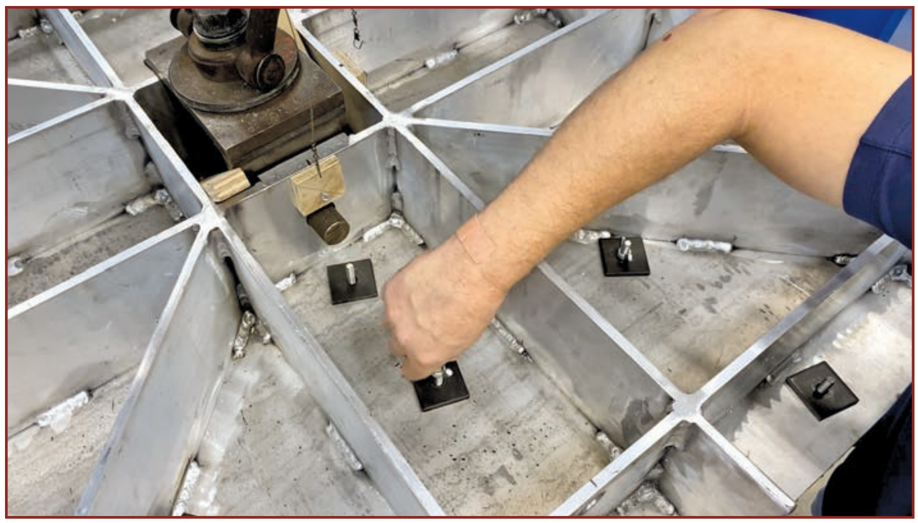

Figure 15. Securing the upper load frame to a test specimen with a plate and wing nuts onto threaded rods.

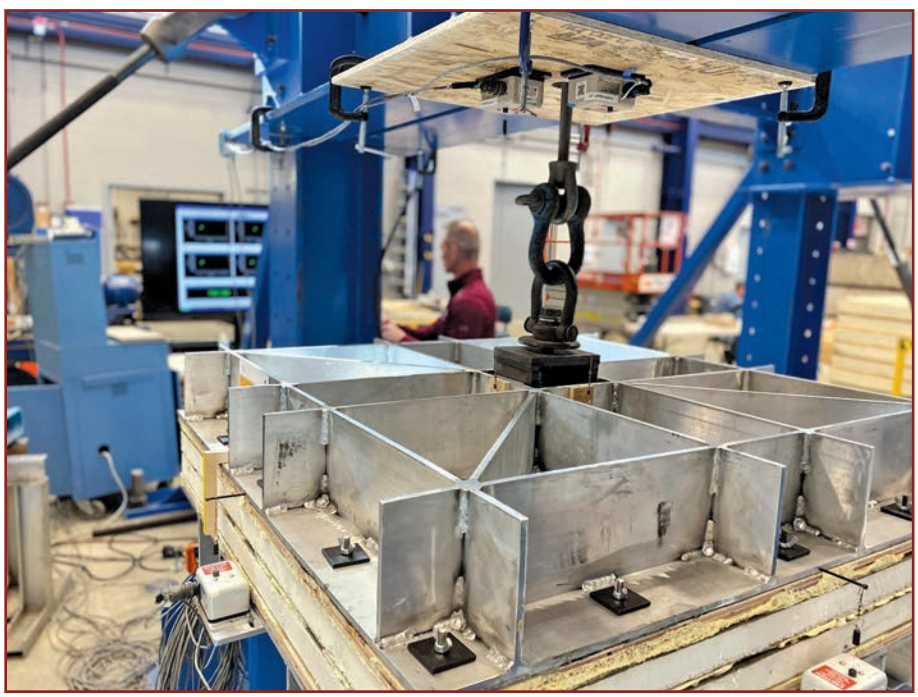

Figure 16. Application of axial load to a test specimen.

Figure 18. A 2-in.-diameter aluminum puck specimen with ⅛-inch-thick low-rise foam adhesive being tested in the hydraulic test machine.

Figure 17. Testing of a 1 ft^2 insulation board specimen with a single ribbon of adhesive in the hydraulic test machine.

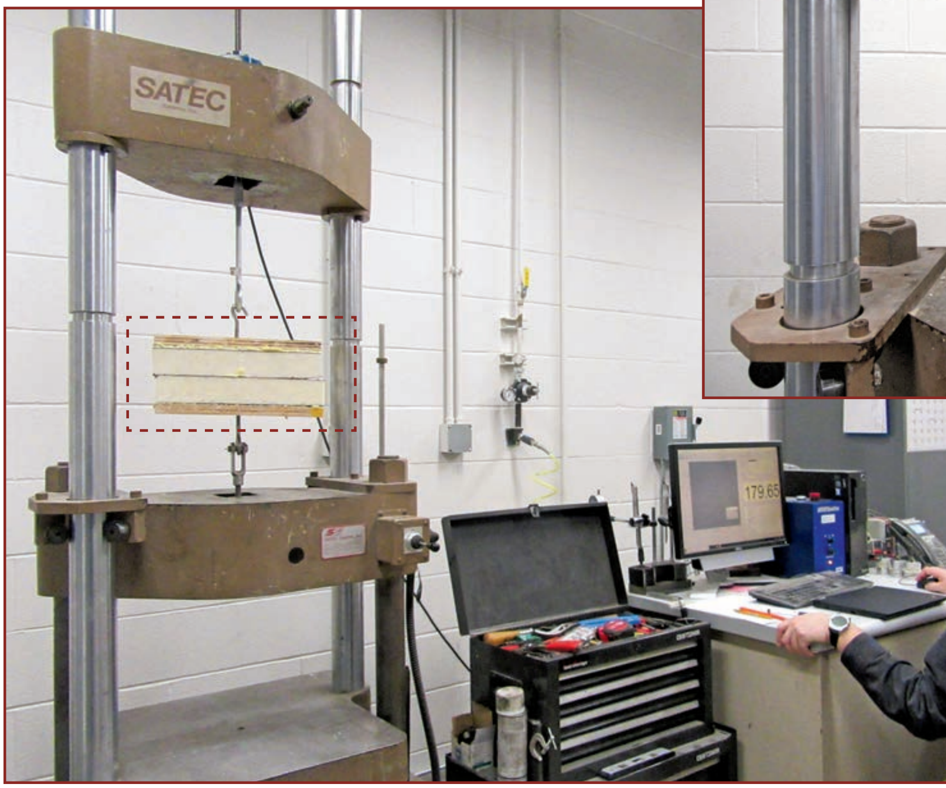

application. Specimens were installed in a hydraulic test machine, which provided application of a direct tensile load (Fig. 17). Load was applied in a similar manner as was employed for the full-size specimens: a preload of 30 lb/ft^2 was held for 1 minute, followed by incremental loading of 15 lb/ft^2 with 1-minute hold periods. The load was incrementally increased until failure occurred.

Puck Specimens

The nine aluminum puck specimens were tested in tension in the hydraulic test machine (Fig. 18). Load was applied in a similar manner as for other tests: a preload of 30 lb/ft^2 was held for 1 minute, followed by incremental loading of 15 lb/ft^2 with 1-minute hold periods. The load was incrementally increased until failure occurred.

TEST RESULTS

Full-Size Specimens

Direct tension testing of the 18 full-size specimens was performed at our structural laboratories from October 22 to October 24, 2019. Portions of the testing were witnessed by Mark Langer, representing MRCA. Specimens were tested at an age ranging from four to six days from assembly. Each specimen was loaded in 15 lb/ft^2 (240 lb) increments followed by 1-minute hold periods until separation failure occurred, in accordance with the previously described test protocol. Total test time per specimen ranged from approximately 27 to 67 minutes, depending on the magnitude of the failure mode. Continuous readings of applied load, the four displacement transducers at the specimen

Figure 19. Relationship between measured failure loads and adhesive spacing for Type A (coated glass fiber) and Type B (cellulosic felt) facers.

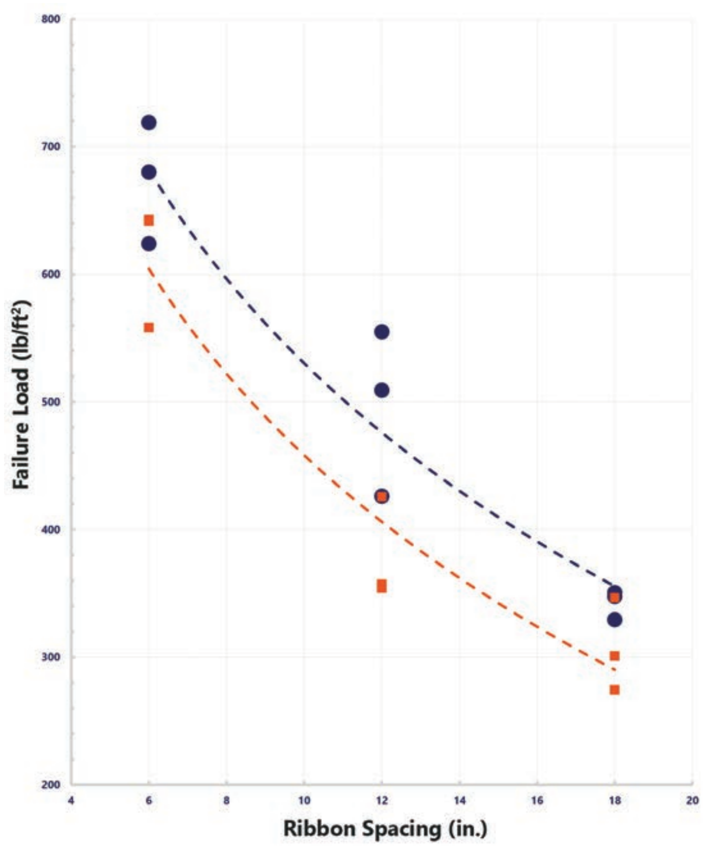

Ribbon spacing (in.)	Specimen ID	Test age (days)	Test strength (lb/ft²)	Average test strength (lb/ft²)	Coefficient of variation
6	A-6-1	4	719	674	7.1%
	A-6-2	5	680		
	A-6-3	6	624		
12	A-12-1	5	426	497	13.1%
	A-12-2	5	555		
	A-12-3	4	509		
18	A-18-1	4	348	342	3.4%
	A-18-2	5	329		
	A-18-3	5	351		

Table 2. Summary of test results for specimens with Type A (polymer-coated glass fiber) facers

Ribbon spacing (in.)	Specimen ID	Test age (days)	Ribbon spacing (in.)	Test strength (lb/ft²)	Average test strength (lb/ft²)	Coefficient of variation
6	B-6-1	5	6	558	614	7.9%
	B-6-2	6	6	643		
	B-6-3	6	6	642		
12	B-12-1	5	12	354	379	10.7%
	B-12-2	4	12	426		
	B-12-3	5	12	357		
18	B-18-1	4	18	274	307	11.9%
	B-18-2	5	18	301		
	B-18-3	5	18	347		

Table 3. Summary of test results for specimens with Type B (cellulosic felt) facers

edges, and two at the center were recorded for the duration of each test.

Direct tension strengths for each specimen were computed by subtracting the tare weight of the upper load assembly (consisting of the pull rod, shackles, the aluminum load frame, and a single layer of foam/plywood) from the maximum measured test load and dividing the result by the nominal cross-sectional area of the specimen (16 ft²).

Average test strengths for Type A (polymer-coated glass fiber) specimens for ribbon spacings of 6, 12, and 18 in. were 674, 497, and 342 lb/ft², respectively. Average test strengths for Type B (cellulosic felt) specimens for ribbon spacings of 6, 12, and 18 in. were 614, 379, and 307 lb/ft², respectively. Tables 2 and 3 summarize the testing results The relationship between measured failure loads and adhesive spacing for Types A and B facers is depicted in Fig. 19.

Separation Displacements

Displacements between the upper and lower aluminum load frames were measured during each test and represented the combined effects of axial strain (stretching) of the two 2-in.-thick insulation layers as well as separation and elongation of the polyurethane foam adhesive during loading. Figure 20 shows the plot of applied load versus average edge displacement (P-∂ plot) for specimen A-12-3. The curve is fairly linear up to failure load, at which time displacements rapidly increase due to large separation of the insulation layers.

The P-∂ relationships provide two distinct performance indicators for the tested tensile specimens: (a) maximum displacement/separation at failure and (b) stiffness. The data reveal that

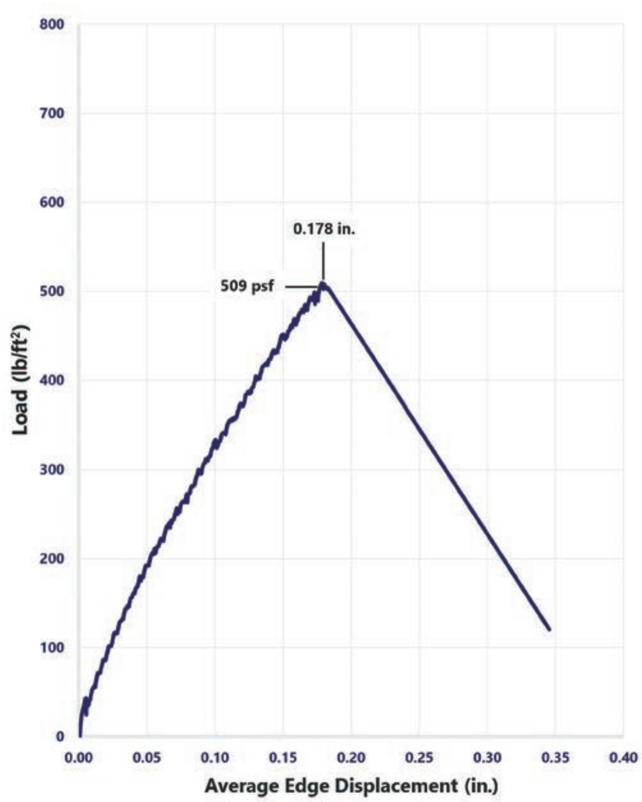

Figure 20. Load displacement plot measured for specimen A-12-3.

Facer type	Ribbon spacing (in.)	Maximum average edge displacement at failure load (in.)
A	6	0.21
	12	0.20
	18	0.17
B	6	0.15
	12	0.18
	18	0.24

Table 4. Maximum average edge displacements at failure load

the average edge displacements at failure for specimens made with adhesive ribbon spacings of 6, 12 and 18 in. were 0.16, 0.19, and 0.23 in., respectively. As expected, greater displacements were achieved at higher ultimate loads; no significant difference in maximum displacements was noted between specimens with coated glass fiber or organic facers. Table 4 summarizes the measured maximum average displacements for the test specimens.

Stiffness

The structural stiffness of a component is a strong indicator of the overall performance of an element. Stiffness is defined as the resistance of a body to deflection or deformation from an applied force—that is, elements with greater stiffness will deflect or deform less than those with lower fundamental stiffness properties. For the adhered insulation test specimens, axial stiffness was calculated for each specimen as the ratio of applied tensile load to average separation displacement between stages corresponding to 10% and 50% of ultimate loads, as shown schematically in Fig. 20.

Computed axial stiffnesses for the six specimen groups ranged from 40 to 65 ksi (Table 5). The relationships of spacing versus stiffness exhibit similar trends as that noted for ultimate strength values, with coated glass fiber–faced specimens having a somewhat higher (10% to 19%) stiffness than organic–faced specimens. The higher stiffness values for tighter adhesive ribbon spacing may be associated with the greater amount of contact adhesive area for 6 in. spacing as compared with 12 in. spacing. When there is less spacing, forces are distributed over more of the insulation surface, reducing overall axial strain at comparable loads.

Posttest Observations

The failure mechanisms in the full-size specimens were predominately delamination and separation of the facers (either the cellulosic felt or the coated glass fiber facers) and some cohesive failure of the foam core. Cohesive failure of the foam core was most prevalent in the specimens with 6 and 12 in. ribbon spacings and occurred to a lesser extent in the specimens with 18 in. ribbon spacing. For the specimens with 18 in. ribbon spacing, the primary failure plane was delamination and separations from the insulation facers. After testing, each specimen was placed on a table for examination and documentation. Representative examples are shown in Fig. 21, 22, and 23.

Companion Specimens

1 × 1 ft Square Specimens

Direct tension testing of the six 1 × 1 ft square specimens (A1, A2, A3, B1, B2, and B3) was performed after a five-day cure period. Each specimen was loaded in 15 lb/ft^2 (240 lb) increments followed by 1-minute hold periods until separation failure occurred. Test strengths were computed as the maximum measured load divided by the nominal area of the specimen (1 ft^2). Average test strengths were 673 lb/ft^2 for Type A (polymer-coated glass fiber) specimens and 484 lb/ft^2 for Type B (cellulosic felt) specimens. Table 5 summarizes the testing results.

Testing of specimens FCA-1 (polymer-coated glass fiber facer) and FCB-1 (cellulosic felt facer) fabricated with full coverage of adhesive over the entire 1 ft^2 insulation surface had failure loads of 896 and 838 lb/ft^2, respectively.

General posttest observations for the specimens A1, A2, A3, B1, B2, and B3 included the following:

- Cellulosic felt facers: The predominant failure mechanism in the three specimens with a single adhesive ribbon was delamination and separation of the facers from the foam body of the insulation.
- Coated glass fiber facers: The predominant failure mechanism in the three specimens with a single adhesive ribbon was delamination and separation of the facers from the foam body of the insulation boards in conjunction with varying degrees of cohesive failure within the foam core.

General observations for the specimens FCA-1 and FCB-1 included the following:

- Cellulosic felt facers: The failure mechanism in the specimen with the full-coverage adhesive layer was cohesive delamination and separation within the facer.

Facer type	Ribbon spacing (in.)	Axial stiffness (ksi)
A	6	65
	12	50
	18	44
B	6	58
	12	42
	18	40

Table 5. Average axial stiffness for Type and Type B specimens

Facer type	Specimen ID	Test strength (lb/ft^2)	Average test strength (lb/ft^2)	Coefficient of variation
A	A1	700	673	3.4%
	A2	660		
	A3	660		
B	B1	660	485	32.2%
	B2	435		
	B3	360		

Table 5. Test strength results for 12 × 12 in. panels with single low-rise foam adhesive ribbon

- Coated glass fiber facers: The predominant failure mechanism in the specimen with the full-coverage adhesive layer was delamination and separation of the facer from the foam body of the insulation.

Puck Specimens

Direct tension testing of the six aluminum puck specimens (TBS-1 through TBS-6) that featured the ⅛-in.-wide foam layer was performed after a two- or five-day cure period. Each specimen was loaded in 15 lb/ft² (240 lb) increments followed by 1-minute hold periods until separation failure occurred. Test strengths were computed as the maximum measured load divided by the nominal area of the specimen (3.14 in.²). Average test strengths were 1355 lb/ft² for two-day-old specimens and 3361 lb/ft² for five-day-old specimens.

The data clearly show that for the configuration tested, the adhesive gained appreciable strength between curing ages of two to five days for the nominal 70°F storage environment. Table 6 summarizes the testing results.

Specimens ABS-1, ABS-2, and ABS-3 were tested at an adhesive age of four days, and their average measured strength was 295 psi (42,480 lb/ft²). These values are substantially greater than for specimens fabricated with ⅛ in. of adhesive.

General posttest observations for specimens TBS-1, TBS-2, and TBS-3 (two-day-old adhesive) revealed the failure mechanism to be cohesive failure of the foam adhesive.

In testing of specimens ABS-1, ABS-2, and ABS-3 with thin film adhesive (foam thickness less than 1⁄16 in.), the failure mechanism was a cohesive failure between the adhesive and the aluminum puck.

SUMMARY AND FINDINGS OF TEST PROGRAM

We have completed a research and testing program for the MRCA to determine the effect on bond capacity for various low-rise foam adhesive ribbon spacings used to adhere layers of polyisocyanurate roofing insulation boards. The program evaluated both polymer-coated glass fiber–faced and cellulosic felt–faced insulation board specimens prepared with 6, 12, and 18 in. ribbon spacings. The work featured fabrication of a custom test rig to accommodate and apply direct tension loading of full-size (4 × 4 ft) adhered insulation specimens, as well as testing on small-scale companion specimens and tensile tests of cured foam material.

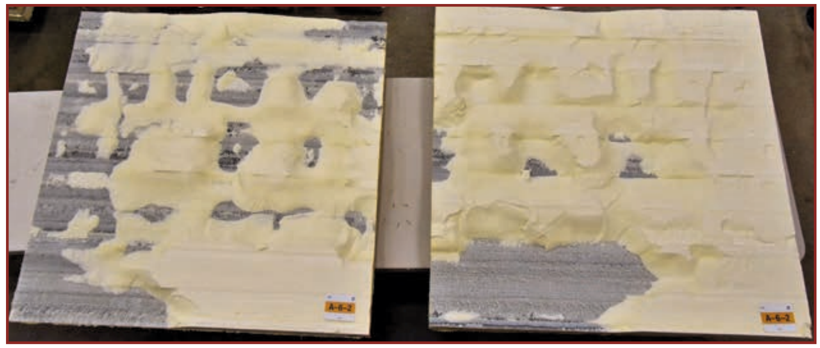

Figure 21. Specimen A-6-2 shown in separated fashion, similar to an opened book. The plane of failure was primarily within the foam core of the top facer of the insulation board (left image), with some delamination at the bottom glass fiber facer of the board (right image).

Figure 22. In specimen A-18-2, the primary failure was separation of the top facer of the bottom board from the foam core, with some cohesive bond separation within the foam core.

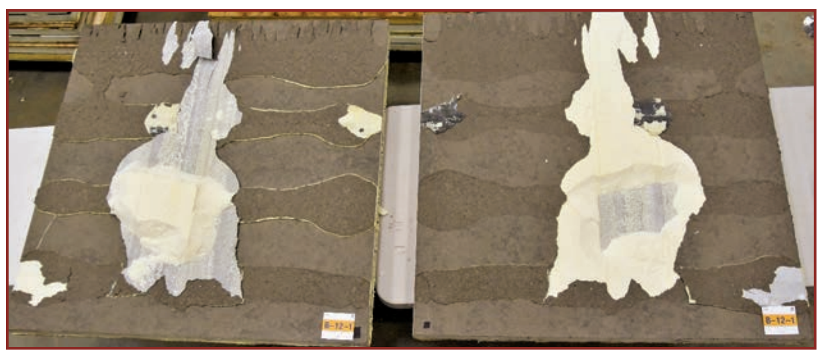

Figure 23. In specimen B-12-1, the failure planes were the bottom facer of the top board and top facer of the bottom board, with cohesive separation within the organic facer along the foam ribbons. The failure included some cohesive separation of the foam core.

Age (days)	Specimen ID	Test load (lb-f)	Test strength (psi)	Test strength (lb/ft²)	Average strength (lb/ft²)	Coefficient of variation
2	TBS-1	36	11.4	1640	1355	33.9%
	TBS-2	35	11.1	1601		
	TBS-3	18	5.7	825		
5	TBS-4	80	25.5	3667	3361	8.0%
	TBS-5	69	22.0	3163		
	TBS-6	71	22.6	3254		

Table 6. Results for low-rise foam adhesive tensile test with ⅛-in.-wide foam beads

Key findings of the test program include:

- Average measured direct tension strengths for full-size polymer-coated glass fiber–faced specimens tested at ribbon spacings of 6, 12, and 18 in. were 674, 497, and 342 lb/ft^2, respectively. Average test strengths for cellulosic felt–faced specimens for ribbon spacings of 6, 12, and 18 in. were 614, 379, and 307 lb/ft^2, respectively. These test results were fairly uniform based on computed coefficient of variation of 7% to 13% for each facer type.
- The test data clearly show that direct tension strength increased as adhesive foam ribbon spacing decreased, for both the polymer-coated glass fiber–faced and cellulosic felt–faced insulation specimens. This strong correlation confirms and quantifies industry knowledge and practice that greater adhered insulation board uplift resistance is achievable with closer foam adhesive spacings.
- For the specific polyisocyanurate insulation and foam adhesive used in this test series, boards with polymer-coated glass fiber facers exhibited approximately 9% to 24% greater strengths than cellulosic felt–faced specimens at equal adhesive spacings.
- Failure of the specimens primarily occurred as separations and/or delaminations of the insulation board facers from the foam body core along the lines of the adhesive ribbons, with secondary failures within the body of the insulation noted in some instances.
- As expected, specimens with greater ultimate strengths at decreased adhesive ribbon spacing also exhibited higher axial tensile stiffness characteristics. For a given uplift load, specimens with closer ribbon spacings would have less axial stretch or displacement than systems with greater adhesive spacing.
- As expected, the measured ultimate strength values of the full-size insulation-to-insulation adhered specimens tested in this program were found to be significantly greater than typical uplift ratings for complete roof systems.
- Testing of the 1 × 1 ft adhered insulation companion specimens, each with a single adhesive ribbon, revealed that polymer-coated glass fiber–faced specimens were 28% stronger than those specimens with cellulosic felt facers, with average strengths of 673 and 485 lb/ft^2, respectively. Companion specimens fabricated with full coverage of adhesive over the entire 1 ft^2 surface had substantially higher strengths of 833 lb/ft^2 for the cellulosic and 896 lb/ft^2 for the glass fiber. These comparative test results confirm that, when greater amounts of adhesive are present over a given area, larger portions of the facer/insulation interfacial zone are mobilized to transfer loads between adhered boards.
- In general, strengths derived from companion tests are higher and not well correlated with the results for the full-size specimens with 12 in. adhesive spacings. Testing using larger (4 × 4 ft) specimens is considered more representative of real-world installations than testing using smaller (1 or 2 ft^2) specimen sizes because the larger specimens have greater surface areas.
- Tensile testing of the 2-in.-diameter pucks with ⅛-inch-thick foam adhesive indicated substantial strength gains between test ages of two and five days. Average measured strengths were 1355 lb/ft^2 at two days and 3361 lb/ft^2 at five days. As expected with two-part polyurethane-based adhesive, chemical cure and associated strength development continues well after initial setting, depending on environment conditions at the time of dispensing and thereafter.
- In limited testing, pucks with adhesive of minimal thickness (less than ¹⁄₁₆ in.) had substantially greater adhesive tensile strength than those specimens made with ⅛-in.- thick adhesive. This behavior is not necessarily unexpected, but it reinforces the value of restraining normal foam expansion by appropriate ballasting to minimize adhesive thicknesses (and also producing wider contact zones of the ribbons) in real-world installations.

The test values derived from this program are specific to the types of insulation boards and foam adhesive used. While overall general trends indicated by test data may be similar and characteristic of other manufacturers' products, the limitations of the values presented specifically in this report should be noted.

RECOMMENDATIONS FOR FURTHER TESTING AND RESEARCH

To help put these test results into the context of industry practice and expectations, we recommend additional testing that can narrow other environmental, product, and installation variables inherent to insulated roofing systems. Such additional testing may include assessment of insulation boards of varied thickness, as well as insulation and foam adhesives from additional product manufacturers; testing of installation and curing in other environmental conditions; and investigation of other factors that may influence adhesion and overall strength in the adhered foam interfacial regions. Panel orientations and cure times may also be explored in greater depth to obtain a better understanding of short- and longer-term performance.

As the assessment of additional testing is considered, we recommend that a careful review of safety factors for adhesives in insulation-to-insulation applications, as well as overall roofing applications, be included. Similarly, a review of ribbon spacings specified in fully tested and rated assemblies for uplift should be part of any further review.

REFERENCES

1. ASTM International. 2019. *Standard Specification for Faced Rigid Cellular Polyisocyanurate Thermal Insulation Board.* ASTM C1289-19. West Conshohocken, PA: ASTM International. https://doi.org/10.1520/C1289-19.
2. American National Standards Institute (ANSI) and Small-Ply Roofing Industry (SPRI). 2015. *Standard Field Test Procedure for Determining the Uplift Resistance of Insulation and Insulation Adhesive Combinations Over Various Substrates.* ANSI/SPRI IA-1 2015. Waltham, MA: SPRI.

The Building Enclosure Commissioning (BECx) Process and Its Keys to Success

Petersen Lambert, PE, BECxP CxA+BE, Certified Air Barrier Specialist

Allana Buick & Bers Inc. | Seattle, WA

plambert@abbae.com

IIBEC 2022 - Building for the Future

International Convention and Trade Show

March 17–22, 2022 | Orlando, FL

ABSTRACT

Historically, the most common area of building failure is the exterior enclosure. When applied systematically, building enclosure commissioning (BECx) services can significantly reduce the risk of future water infiltration; improve facility operation and maintenance; and reduce the life-cycle cost of the facility for the life of the building. The BECx process confirms that building enclosure system and assembly functionality, durability, and constructability, design and installation quality, and interoperability will meet the owner's project requirements. BECx services, however, can vary greatly and are commonly misunderstood. The presentation explains step by step how BECx can outline a comprehensive control process that is fully integrated into project delivery. Through case studies, the presenter provides specific steps to scope, lead, plan, schedule, and execute BECx.

SPEAKER

Petersen Lambert, PE, BECxP CxA+BE, Certified Air Barrier Specialist

Allana Buick & Bers Inc. | Seattle, WA

Petersen Lambert is a principal and division manager for the Pacific Northwest and director of testing at Allana Buick & Bers Inc./ABB Testing. He has more than 20 years of industry experience and is a frequent presenter at in-house and industry events. He specializes in identifying and resolving enclosure waterproofing issues during construction. As a Building Enclosure Commissioning Process Provider (BECxP), he is a technical leader in building enclosure commissioning, quality control/quality assurance, construction administration services, and various types of building enclosure performance testing.

The Building Enclosure Commissioning (BECx) Process and Its Keys to Success

Historically, one of the most common and most expensive areas of building failure is the exterior enclosure. When applied systematically and geared toward the project's specific needs, the building enclosure commissioning (BECx) process can significantly reduce the risk of future water infiltration; improve facility operation and maintenance; and reduce the life-cycle cost of the facility. The process confirms building enclosure system and assembly functionality, durability, constructibility, design and installation quality, and interoperability to meet the owner's project requirements.

The appropriate level and comprehensiveness of BECx services should match the complexity of the project. For example, a warehouse project with a $5 million budget and four typical enclosure assemblies needs a much different set of BECx commissioning services than a hospital with a $100 million budget and dozens of typical enclosure assemblies.

BECx commissioning requirements currently extend from the federal level (General Services Administration, US Army Corps of Engineers) to state (New York, California, Oregon, Indiana, Washington) and local (New York City; Seattle, Wash.) levels. In addition, there are sustainability-driven codes and standards (such as ASHRAE 189.1[1] or the *International Green Constrution Code*[2]), and large and small private companies have created their own internal commissioning requirements that include BECx in part or in whole. These requirements vary from full cradle-to-grave comprehensive approaches to limited or focused commissioning or testing of specific enclosure components, usually related to air barriers or energy codes.

BECx commissioning benefits the entire project team by reducing risk, improving durability, providing vetted designs, validating performance, and reducing long-term costs, including maintenance costs. These benefits explain why sustainability programs are promoting and rewarding owners for engaging in the BECx process.

WHAT'S THE INTENT?

If you have been through the BECx process before, you might think that its intent is to consume reams of paper or to fill a hard drive. But if you ask owners who have committed themselves to this process, they will tell you that the BECx process helps them make sure that they get what they intended and what they are paying for. Buildings that are properly commissioned using the BECx process typically have fewer change orders, tend to be more energy efficient, and have lower operational and maintenance costs.[1]

When a person hears the word "commissioning," concepts such as "testing and balancing," "system confirmation," and "checklists" may come to mind. This is because decades of successful mechanical commissioning processes have been distilled into guidelines for performing the specific tasks that are most frequently parts of those processes. However, this oversimplification and "taskification" of commissioning can provide an unintended focus on construction-phase testing, as well as oversimplified design review, and can lead to overly generic, non-project-specific checklists.

BECx has inherited some of this oversimplification and "taskification" from commissioning of mechanical systems. However, the unintended consequences of this taskification for the overall project can potentially be more dire for BECx than for mechanical system commissioning because building enclosure assemblies are different from mechanical systems in the following ways:

- A mechanical system's performance requirements are straightforward and less likely to be effected by other system's changes. The building enclosure's performance, however, is made of multiple control layers, materials, and environmental conditions. Therefore, it's more challenging to understand and quantify the unintended ramifications of modifying aspects of the enclosure.
- The performance verification testing of parts or of the whole mechanical system can be done with random sampling. A fully performing building enclosure assembly on a complex building has hundreds of transitions that might require verification. In addition, a misinstalled critical transition, whether occurring once or at some percentage of time, will lead to damage to the building. Therefore, given the critical nature of building enclosure transition installation, simple statistical sampling wouldn't identify this type of issue frequently enough (unless we got really lucky).
- Standard checklists for types of mechanical systems are relevant and usable across similar projects. Building enclosure checklists can provide a generic list of requirements, but the project-specific assemblies and transitions require verification via project-specific, non-generic checklists. This will help to avoid substrate/product compatibility as well as other issues that can arise from overly generic standard checklists.

BECx commissioning benefits the entire project team by reducing risk, improving durability, providing vetted designs, validating performance, and reducing long-term costs, including maintenance costs.

Another adverse effect of "taskification" of commissioning is that it encourages over-reliance on templates for deliverables critical to the execution of the BECx plan. Too often, a service-strapped building commissioning (Cx) or architectural team provides templated owner's project requirements (OPRs), basis of design (BOD) documents, quality assurance/quality control (QA/QC) logs, checklists, testing matrixes, and so on, with the hope that a project or commissioning guide can be executed without any project-specific thought. The reality is that more is not better in this context. When a commissioning process is not project specific, it creates the very thing that it is in place to avoid: a project that cannot be executed to meet the OPR. What value is a field observation checklist for an enclosure system that is not part of the project? What is the value of a BECx plan that outlines the role and responsibilities for a team member who will not be retained on the project? What value is a templated OPR that does not capture critical project-specific performance requirements? The answer to these questions is not simply "No value." Rather, the use of generic or templated commissioning tools likely costs the owner or the general contractor time and money.

While there are times when BECx can fall short of its intent, there are also times when the intention is terrific but the process is truncated or hyperfocused.

Starting the BECx process at the beginning of construction is admirable, but if the process begins then, it will be too late to fully achieve the intended benefit of confirming that project performance requirements and design documents meet the OPR. By the time construction starts, the ship has sailed, so to speak. And while there are benefits to confirming that the ship stays afloat, there is not much one can do if the ship is the wrong size or carrying the wrong cargo.

An emerging trend is to request BECx that is focused solely on either energy-related assemblies or the air barrier. This type of hyperfocused BECx is growing in popularity because energy codes and sustainability requirements incorporate design and construction oversight testing as project requirements. These limited BECx services provide value to the project, but the owner should be made aware of the limitations and risks of focusing only on one or two of the known layers (water, air, thermal, vapor) while the remaining, unvetted control layers are not part of the BECx process.

TEAMWORK MAKES THE DREAM WORK

Commissioning will always be a team-based quality process, and the makeup of the project team will be a key driver of the level of services needed to provide BECx. Projects that have a full project team that includes the owner; owner's representative; commissioning authority (CxA); building enclosure commissioning process provider (BECxP); architect; building enclosure consultant; mechanical, engineering, and plumbing consultant; general contractor; and third-party testing agency should allow for a greater stratification of roles and responsibilities than a project team limited to the owner, BECxP, architect, and general contractor only.

BECxPs should be mindful that other team members might assume that traditional building enclosure consultant activities are the BECxP's responsibility. And while the BECxP should have the technical acumen and experience to take on the consultant's roles and responsibilities, it is important that the project team understand what dual responsibilities the BECxP may be taking on. It is helpful in these situations for the BECxP team to be separate staff from the building enclosure consulting team when the same firm provides both services. There have been times when a project team has believed that this combination of duties does not fit the intent of third-party commissioning. There certainly is potential for conflict between commissioning and consulting roles. On the other hand, having an integrated firm fill both roles may be more efficient .

The keys to success are that the project owner and team are aware of the intersection of duties and that the firm filling multiple roles outlines how they plan to mitigate the potential issue of a conflict. For example, a building enclosure firm that provides design and construction consulting, BECx services, and building enclosure performance testing can provide a plan that outlines how separate personnel from their team will manage each role and that the BECx provider will engage and communicate with each team individually to avoid any conflict.

BECx STEP BY STEP

The road map for a successful BECx process will be as simple or as complex as the project that it is being used to benefit. Available guidelines have this flexible, expandable approach built into them. ASTM E2813, *Standard Practice for Building Enclosure Commissioning*,[3] and ASTM E2947, *Standard Guide for Building Enclosure Commissioning*,[4] define the fundamental (minimum) level of BECx involvement and provide guidance on enhanced levels of involvement. The National Institute of Building Sciences' NIBS Guideline 3-2012, *Building Enclosure Commissioning Process BECx*,[5] and ASHRAE Guideline 0-2019, *The Commissioning Process*,[6] both recommend that stakeholders define the scope and budget of the BECx process very early in the project; the scope should include plans for meetings and activities, details about the design peer review and validation reviews, and an outline of mock-ups, oversight, and testing expectations. This basic planning task is often overlooked because it can be unclear which team member should prepare this scope and budget. The owner, with the assistance of a commissioning provider (CxP) or BECxP, is best suited for this task.

Many BECxPs have been asked to define the scope and fee for BECx services for a proj-

CASE STUDY: Focused Assembly Consulting

Our firm was approached during the design process to provide BECx services. After meeting with the project team, we ascertained that the owner and commissioning agency were looking for focused assistance with air barrier design and testing requirement determination. Project specifications required BECx services; however, the BECx services provided for the OPR, BOD, design review, and building enclosure testing matrix were focused on only the air barrier.

Fast forward to the construction phase: The project was negatively affected by the lack of BECx services related to anything other than the air barrier and the uncoordinated building enclosure details and specifications. Changes to the air barrier were required.

ect without having a document that defines the expectations of the owner and the team. In these situations, the BECx firm usually ends up in a dance with the owner and the commissioning agent about whether they intend to use fundamental/baseline BECx, some degree of enhanced BECx, or a focused (assembly or phase) approach.

The following sections offer a road map of critical deliverables that must be provided if the intent is truly BECx—that is, if BECx starts near the beginning of the project design phase (see also **Fig. 1**). If, however, BECx services are to begin at a later milestone in the project timeline, it is a good idea to for the owner to share with the BECxP the documents and deliverables that were expected earlier in the process for retroactive review.

The Owner's Project Requirements

The first and most essential step in the commissioning and BECx process is the creation of an OPR, either by the owner alone or by the owner with the assistance of commissioning professionals. According to the Whole Building Design Guide:[8]

> The OPR defines the Owner's project goals, measurable performance criteria, cost considerations, benchmarks, success criteria, and supporting information for the project. The OPR must be developed with significant Owner and/or Owner's representative input and ultimate approval. The CxP typically facilitates the process for the Owner in identifying the facility's requirements regarding such issues as energy efficiency measures, environment and sustainability issues, security, and operation and maintenance of the building. An effective OPR incorporates input early from the design team, operation and maintenance staff and end users of the building and is updated throughout the project.

ASTM E2813-18[4] Annex A1 provides a guideline to assist Cx and BECx teams in creating an OPR by providing a two-page questionnaire. NIBS Guideline 3-2012[6] Annex J.1 provides a comprehensive checklist of factors that can be evaluated to establish the OPR.

The most critical aspect of the OPR is that the requirements are pertinent, project specific, and defined as early in the design process as possible. Like most design-phase BECx deliverables, the OPR document, is intended to evolve and expand during the design phase. Failure to get substantive input on the OPR from the owner early in the design phase can lead to inaccurate and counterproductive basis of design and design review inputs. The owner's input should be substantive enough to allow the project architect and the building enclosure consultant (if the consultant is part of the team) to define the BOD systems and generate typical details for the building enclosure section (roof, floor, soffit and wall) that represent most, if not all, locations of control layers within assemblies on the project.

BECx PLAN

As explained in Section 3.2.6 of ASTM E2947,[5] the BECx plan outlines the BECx process to meet the OPR. It should describe the organization, schedule, and allocation of resources for the process; identify the responsibilities of stakeholders; and include testing and documentation requirements (checklists and logs). This document can become a part of the project's overall Cx plan.

ASTM E2813-18[4] Annex A1 provides a guideline to assist Cx and BECx teams contributing to the creation of an OPR by providing a two-page questionnaire. NIBS Guideline 3-2012[6] Annexes D and F provide tables and matrices to assist in the development of a BECx plan.

A BECx plan should match the size and scale of the project for which it is created. The draft should be reviewed by the project stakeholders for confirmation that each party has the scope (and budget) to provide the BECx plan deliverables. This document could be provided by the CxP and reviewed by the BECxP. The requirements for BECx participation should be meet at least the minimum requirements

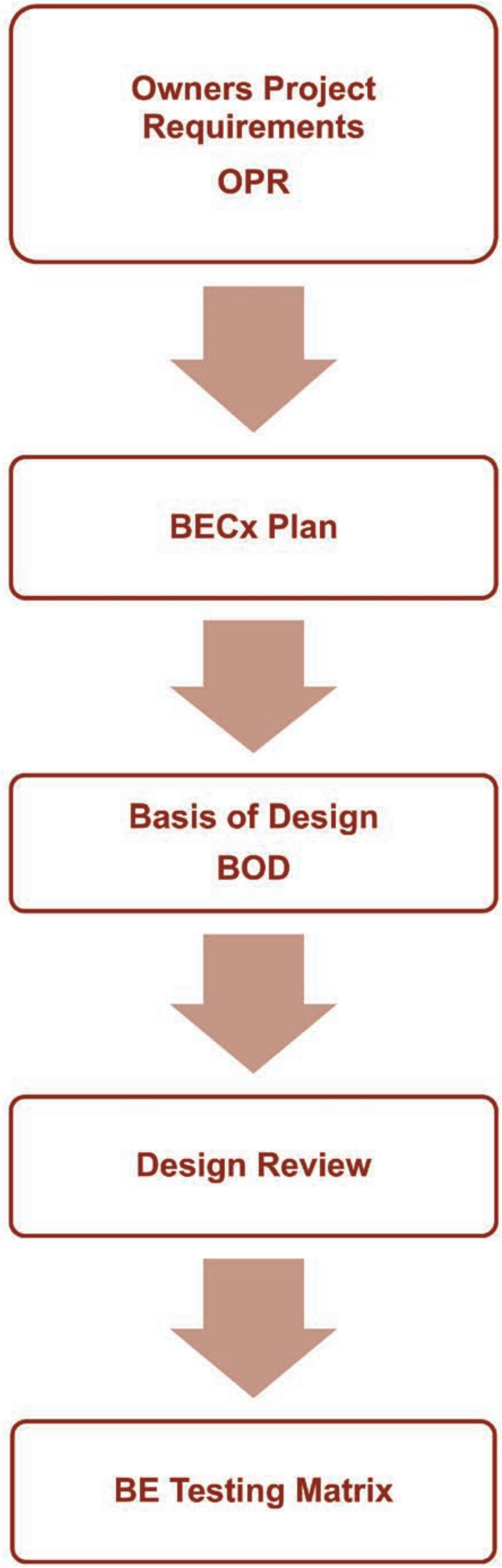

Figure 1. An example of the building enclosure commissioning (BECx) process "key to success" work flow.

outlined in ASTM E2813 for fundamental BECx. The plan should also reflect any enhanced participation required by any LEED, energy code, or air barrier–specific commissioning requirements.

Building Enclosure Basis of Design

NIBS Guideline 3-2012[6] defines the BOD as follows:

> A document that bridges the objectives conveyed in the Owner's Project Requirements (OPR) and the contract documents (construction drawings and project specifications). It records through narrative the technical concepts, performance, assumptions, decisions and product selections that fulfill the requirements of the OPR and authorities having jurisdiction.

The BOD provides the technical backbone to the OPR. It should provide adequate information such that a design review can be done using it as context. ASHRAE Guideline 0-2019[7] Informative Appendix K and NIBS Guideline 3-2012[6] Annex K offer the following (combined and simplified) list of contents:

- Specific codes, standards, and guidelines considered during design of the facility, and designer interpretations of such requirements
- Information regarding ambient conditions (climatic, geological, structural, existing construction) used during design.
- Thermal performance requirements and relevant compliance pathways
- Sustainability requirements (energy, LEED, etc.)
- Performance criteria for each building enclosure assembly and how that system was designed to meet OPR requirements

When a building enclosure consultant is part of the project's design team, the design team should do the heavy lifting of generating the BOD and then the BECx should review the document to ensure that it aligns with the OPR. If the project does not have a building enclosure consultant, the BECx can offer to provide enhanced services that include assisting the architect in generating a BOD that aligns with the OPR. Some architectural firms have technical architects who have the experience and technical acumen to provide this information internally.

Design Review

In the International Code Council's *Performance Code for Buildings and Facilities*,[9] peer review is defined as:

> An independent and objective technical review of the design of a building or structure to examine the proposed conceptual and analytical concepts, objectives and criteria of the design and construction. It shall be conducted by an architect or engineer who has a level of experience in the design of projects like the one being reviewed at least comparable to that of the architect or engineer responsible for the project.

The BECx process requires that a building enclosure specialist provide a design review of the documents, but the scope and comprehensiveness vary depending on which standard is being followed. As noted previously, it's important for the project team to establish the scope and frequency of reviews as well as which parties will be providing them.

When a building enclosure consultant is part of the design team, it can be assumed that the high-level design review will be part of that consultant's scope of work and that they will have the role as BECxS (S=specialist). At a minimum, the BECx can take a "trust but verify" approach to the design review and provide the minimum amount of verification needed to confirm that the design documents meet the OPR requirements. In the most comprehensive approach, the BECx is providing a detail by detail review of each building enclosure transition as well as identifying additional details required to be provided within the final design documents.

However, when a building enclosure consultant is not involved with design, or the project has a risk level such that the owner requires dual design reviews, the BECxP will need to take on the role of the BECxS and provide the design review. The frequency and depth of the design reviews will vary by project.

Key considerations for the BECx team are the experience level and depth of knowledge of the team member or members providing the design review. The ASTM E2947[5] and NIBS[6] BECx guidance documents indicate that a competent and knowledge person should provide the design reviews. This author further recommends that building enclosure specialists in roofing, exterior walls, glazing and fenestration, air barriers, thermal enclosure, and any distinctive project-specific enclosure assemblies or conditions review those details and applications that require such expertise.

Building Enclosure Testing Matrix

One of the clearest responsibilities of the BECxP, regardless of the level comprehensiveness of BECx services, is the establishing of building enclosure performance testing requirements. This task can be quite difficult because it requires buy-in and budgeting from the owner. The total cost for building enclosure testing—spanning laboratory tests, mockups, first works, progress testing, and completion testing for the various BE assemblies on a project—can be substantial. Owners who are unaware of the potential price tag associated with a conservative or enhanced testing protocol may end up with severe sticker shock when presented with these cost estimates in construction. Sometimes, owners do not realize that their project manual obligates them to provide third-party testing services on behalf of the project.

ASTM E2813-18[4] Annex A2 (**Table 1**) provides a guideline and a table of fundamental and enhanced requirements to assist Cx and BECx teams in creating a building enclosure testing matrix. However, the team should carefully review the guideline and table before they incorporate the requirements into a project specification; it is important to ensure that the specification does not require unneeded testing of enclosure assemblies that are not part of the project.

The key to the success of the building enclosure testing matrix during the design phase is that the matrix only includes testing for those building enclosure assemblies that require performance verification to meet the OPR. The testing matrix must be assembly specific and incorporate any building enclosure testing required by:

- building code (whole building air barrier testing),
- sustainability requirements,
- standard or enhanced manufacturer's warranty requirements (electronic leak detection or sealant adhesion),
- relevant industry organizations (Air Barrier Association of America Quality Assurance Program[10] testing; Fenestration and Glazing Industry Alliance's AAMA specifications 501,[11] 502,[12] and 503[13]),
- insurance carriers (FM Global wind uplift), or
- the owner (flood testing).

In addition to confirming the extent and scope of testing, it is important to establish who is expected to provide (pay for) the testing because this helps determine where in the documents the testing requirements will be placed. Sometimes, an owner, general contractor, subcontractor, or manufacturer is surprised to find that they are considered the responsible party for various building enclosure performance verification tests because responsibilities are not otherwise clearly identified in the specifications. One thing is for sure: If the project team's budget does not have the capacity to handle the building enclosure testing, the tests will be omitted or scaled back.

The building enclosure testing matrix is a BECx deliverable, but it should be reviewed and the information incorporated into the project specifications by the design team. The project-specific building enclosure testing matrix may conflict with a standard or templated specification. A common example of this conflict is fenestration testing requirements for curtainwalls. Most specification templates outline field-testing requirements in field QC and provide non-project-specific requirements (Fig. 2). However, these templated requirements do not provide sufficient detail to allow a third-party testing agency to provide accurate pricing for a testing scope that meets the OPR.

In contrast to the inadequate specification template, the following is an example of

Property	Standard Designation	Title	Lab System Testing	Enhanced		Fundamental	
				Field Mockup Testing	In-Situ Field Testing	Field Mockup Testing	In-Situ Field Testing
Water Penetration							
Water penetration	ASTM E331	Test Method for Water Penetration of Exterior Windows, Skylights, Doors, and Curtain Walls by Uniform Static Air Pressure Difference	L (M)	–	–	–	–
	ASTM E514/ E514M	Test Method for Water Penetration and Leakage Through Masonry	OL	(OF)	(OF)	(OF)	(OF)
	ASTM C1601	Test Method for Field Determination of Water Penetration of Masonry Wall Surfaces	–	(OF)	(OF)	(OF)	(OF)
	ASTM D5957	Guide for Flood Testing Horizontal Waterproofing Installations	–	(OF)	✓ (all horizontal surfaces)	(OF)	✓ (all horizontal surfaces)
Static water penetration	ASTM E1105	Test Method for Field Determination of Water Penetration of Installed Exterior Windows, Skylights, Doors, and Curtain Walls by Uniform or Cyclic Static Air Pressure Difference	–	✓ (1X)	✓ (2X)	✓ (1X)	✓ (2X)
Dynamic water penetration	AAMA 501.1	Water Penetration of Windows, Curtain Walls and Doors Using Dynamic Pressure	OL (M)	(OF)	✓ (1X)	(OF)	(OF)
	ASTM E2268	Test Method for Water Penetration of Exterior Windows, Skylights, and Doors by Rapid Pulsed Air Pressure Difference	OL	(OF)	(OF)	(OF)	(OF)
	AAMA 501.2	Quality Assurance and Diagnostic Water Leakage Field Check of Installed Storefronts, Curtain Walls, and Sloped Glazing Systems	–	✓ (1X)	✓ (1X)	✓ (1X)	✓ (1X)

Table 1. A portion of Table A2.1 from ASTM E2813-18, Standard Guide for Building Enclosure Commissioning.

3.7 FIELD QUALITY CONTROL

A. Testing Agency: Engage a qualified testing agency to perform tests and inspections.

B. Test Area: Perform tests on representative areas of glazed aluminum curtain walls.

C. Field Quality-Control Testing: Perform the following test on representative areas of glazed aluminum curtain walls.

1. Water-Spray Test: Before installation of interior finishes has begun, areas designated by Architect shall be tested according to AAMA 501.2 and shall not evidence water penetration.
   a. Perform a minimum of two tests in areas as directed by Architect.
2. Air Infiltration: ASTM E 783 at 1.5 times the rate specified for laboratory testing in "Performance Requirements" Article but not more than 0.09 cfm/sq. ft. (0.45 L/s per sq. m) at a static-air-pressure differential of 1.57 lbf/sq. ft. (75 Pa).
   a. Perform a minimum of two tests in areas as directed by Architect.
3. Water Penetration: ASTM E 1105 at a minimum uniform and cyclic static-air-pressure differential of 0.67 times the static-air-pressure differential specified for laboratory testing in "Performance Requirements" Article, but not less than 6.24 lbf/sq. ft. (300 Pa), and shall not evidence water penetration.

Figure 2. An example specification section outlining field testing requirements taken from our firm's archives.

information that should be provided to the team for the purposes of planning and executing the building enclosure testing requirements for exterior joint sealants; it can be updated for most types of testing.

Testing goal:	Confirm adhesion
Standard:	ASTM C1521, *Evaluating Adhesion of Installed Weatherproofing Sealant Joints*[14]
Where:	Each unique substrate type, primed and/or unprimed
Size:	Per standard
When:	Mock-up, first works, and in-progress
Frequency:	Every 1000 linear ft
Provided by:	Third-party by owner, installer by general contractor
Conducted by:	Installer and/or manufacturer at mock-up and every 1000 linear ft Third-party at mock-up, at first works, and twice during installation
Witnessed by:	None required
Failure criteria:	Per standard
Failure resolution:	Examine installation and provide input on failure reason. Retest 2 ft away from failed specimen. If results of adjacent retesting are acceptable, repair 4 ft of sealant. If adjacent retesting fails, continue to expand testing area until acceptable results are found or entire length is remediated.

CASE STUDY: Generic Building Enclosure Testing Requirements and Early Coordination of Testing

We were approached by a client to provide air barrier testing based on a testing requirement in the project specifications. The project was located in a state that does not require whole building air barrier testing. Project specifications identified air leakage rate as a performance requirement and required use of ASTM E779, *Standard Test Method for Determining Air Leakage Rate by Fan Pressurization*,[15] to confirm performance; however, the commissioning team allowed a substitution of ASTM E1186, *Standard Practices for Air Leakage Site Detection in Building Envelopes and Air Barrier Systems*.[16]

The commissioning team reached out to provide the specified testing at a point in construction where most air barrier elements were complete. The contractor was concerned about the potentially subjective nature of ASTM E1186 testing methods (infrared scanning or smoke tests). If such testing were to identify any air leakage pathways, repairs to the air barrier might be needed that would not have been required if ASTM E779 testing were provided. The building enclosure consultants also expressed concerns that infrared scanning might not be possible because of a lack of a temperature difference between the interior and exterior. There were also concerns about access to the air barrier based on the progression in construction—it was possible that any interior or exterior smoke penciling would not outline the locations of the breaches.

The building layout was reexamined, and a comprehensive testing plan was created. This gave the commissioning agent and team sufficient confidence that ASTM E779 testing could be conducted.

Two building enclosure testing requirements that should be carefully considered during the design phase are laboratory mock-up testing for curtainwalls and whole building air leakage testing. These tests provide an enormous amount of value, but they also require a considerable amount of coordination and cost.

Construction-Phase Services

When the project transitions to construction, the BECxP's role shifts toward verification. At this point, the project contract documents should meet the OPR and the general contractor is responsible for managing their team and to execute the work outlined therein. The BECxP, in accordance with the BECx plan, reviews some or all of the project documents to verify that those documents are in line with the OPR. The documents include shop drawings, requests for information, field installation checklists, and third-party testing reports of laboratory and field testing results.

Challenges can arise when the BECxP is brought into the project at this phase, without involvement in the design phase. When this happens, projects usually fall into one of two categories. In the first category are projects where the design team has not formally followed a commissioning process, but they have created a set of contract documents that generally outline the owner's project requirements and have provided acceptable building enclosure design details and specifications. These projects usually have a strong design team that includes a building enclosure consultant and a preconstruction general contractor. In the second, and more likely, category are projects where the design team has captured the owner's general project intent, but the design documents require minor or significant adjustment to meet some of the owner's specific performance requirements within the specifications.

When beginning work on projects in either category, the BECxP will need to review their scope of services with either the owner or general contractor after reviewing the project and documents to determine what is feasible.

Construction Checklists

Prefunctional checklists are a huge part of mechanical system commissioning. The requirements for checklists and logs have found their way into the BECx process as well. BECx checklists are intended to communicate the key installation requirements for meeting the OPR. They are not intended to be an installation guide for the installer's foreperson or to replace the QA or QC processes, but they are intended to help the subcontractor and general contractor verify that they are providing the work in accordance with construction documents.

Like the other BECx documents discussed previously, checklists must be updated to reflect the building enclosure assemblies and not just the products identified for the project. Quite a few manufacturers have created product-specific installation checklists. These documents are helpful but should be edited and updated to reflect the critical requirements for the project-specific assemblies. For example, a water-resistant barrier checklist should cover the actual project substrate(s), transition membrane, and cladding attachment detailing, and they should be customized to reflect the window opening detailing and any enhanced air leakage detailing requirements.

CASE STUDY: Checklists, Ugh

The general contractor and project team engaged us to provide the BECx services outlined in the project manual. The specifications required BECx, but the general contractor was brought on board after the bid phase. However, engaging a team to provide BECx services at the construction phase does not allow the entire BECx process to unfold as intended.

A focus was then placed on the specific QA/QC checklists that were outlined in the specification. Unfortunately, those checklists were not derived based on window integration and roofing, which were the project's riskiest assemblies; instead, they reflected historically challenging assemblies such as the exterior insulation and finish system (EIFS) and the air barrier. Therefore, our team diligently reviewed the 500 ft^2 of EIFS that contained the air barrier coating, while noting weeks of issues with low-slope roofing that went unobserved and were not documented through checklists.

CONCLUSION

As noted in the foreword to ASHRAE Guideline 0-2019,[7] the intent of the commissioning process is to provide a "quality-focused process for enhancing the delivery of a project by achieving, validating, and documenting the performing of facility elements that meet the objectives and criteria of the Owner." Therefore, those that venture to provide BECx services should be mindful of the overall intent of the commissioning, which is to define what the owner's expectations are for the building enclosure, to create verification mechanisms to ensure that the performance expectations are met during design and construction, and possibly to participate in the verification process. BECx must be done on a project-by-project basis with the understanding that the BECx and Cx processes are intended to be flexible to expand or contract to meet the needs of the OPR.

REFERENCES

1. American Society of Heating, Refrigerating, and Air-Conditioning Engineers (ASHRAE). 2017. *Standard for the Design of High-Performance, Green Buildings Except Low-Rise Residential Buildings.* ASHRAE/ICC/USGBC/IES Standardard 189.1-2017. Peachtree Corners, GA: ASHRAE.
2. ASHRAE. 2018. *International Green Construction Code.* Peachtree Corners, GA: ASHRAE.
3. Whole Building Design Guide Project Management Committee and Commissioning Industry Leaders Council. 2016. "Whole Building Design Guide—Building Commissioning." https://www.wbdg.org/building-commissioning.
4. ASTM International. 2018. *Standard Practice for Building Enclosure Commissioning.* ASTM E2813-18. West Conshohocken, PA: ASTM International. https://doi.org/10.1520/E2813-18.
5. ASTM International. 2021. *Standard Guide for Building Enclosure Commissioning.* ASTM E2947-21. West Conshohocken, PA: ASTM

International. https://doi.org/10.1520/E2947-21.

6. National Institute of Building Sciences (NIBS). 2012. *Building Enclosure Commissioning Process BECx*. NIBS Guideline 3-2012. https://www.wbdg.org/FFC/NIBS/nibs_gl3.pdf.
7. ASHRAE. 2019. *The Commissioning Process*. ASHRAE Guideline 0-2019. Peachtree Corners, GA: ASHRAE.
8. Whole Building Design Guide Project Management Committee and Commissioning Industry Leaders Council. 2016. "Whole Building Design Guide—Commissioning Document Compliance And Acceptance." https://www.wbdg.org/building-commissioning/commissioning-document-compliance-and-acceptance.
9. International Code Council (ICC). 2012. "Chapter 2: Definitions." *ICC Performance Code for Buildings and Facilities*. https://codes.iccsafe.org/content/ICCPC2012/chapter-2-definitions.
10. Air Barrier Association of American. n.d. "Quality Assurance Program." Accessed October 27, 2021. https://www.airbarrier.org/qap.
11. Fenestration and Glazing Industry Alliance (FGIA). 2017. *Water Penetration of Windows, Curtain Walls and Doors Using Dynamic Pressure*. AAMA 501.1-17. Schaumburg, IL: FGIA.
12. FGIA. 2021. *Voluntary Specification for Field Testing of Newly Installed Fenestration Product*. AAMA 502-21. Schaumburg, IL: FGIA.
13. FGIA. 2014. *Voluntary Specification for Field Testing of Newly Installed Storefronts, Curtain Walls and Sloped Glazing Systems*. AAMA 503-14. Schaumburg, IL: FGIA.
14. ASTM International. 2020. *Evaluating Adhesion of Installed Weatherproofing Sealant Joints*. ASTM C1521-19(2020). West Conshohocken, PA: ASTM International. https://doi.org/10.1520/C1521-19R20.
15. ASTM International. 2019. *Standard Test Method for Determining Air Leakage Rate by Fan Pressurization*. ASTM E779-19. West Conshohocken, PA: ASTM International. https://doi.org/10.1520/E0779-19.
16. ASTM International. 2017 *Standard Practices for Air Leakage Site Detection in Building Envelopes and Air Barrier Systems*. ASTM E1186-17. West Conshohocken, PA: ASTM International. https://doi.org/10.1520/E1186-17.

Waterproofing Challenges in Hydrostatic Conditions

Edward L. Lehman, AIA

Wiss, Janney, Elstner Associates Inc. | Duluth, GA

elehman@wje.com

Douglas R. Stieve, RRC, AIA

Wiss, Janney, Elstner Associates Inc. | New York, NY

dstieve@wje.com

IIBEC 2022 - Building for the Future

International Convention and Trade Show

March 17–22, 2022 | Orlando, FL

ABSTRACT

As our urban and suburban spaces are becoming increasingly congested, the building industry is designing and constructing projects in areas and conditions that were previously considered uninhabitable, including below-grade spaces under constant hydrostatic pressure. Efforts to make such spaces habitable may include the use of waterproofing systems not previously used in the region. Discussion of the application of familiar materials in unfamiliar conditions may be useful to colleagues and industry professionals to help identify potential hazards and pitfalls associated with these waterproofing applications.

In addition to the selection of waterproofing material and design detailing, this presentation explores preconstruction activities and applied strategies from the presenters' experience. Various lessons learned in the field from projects with similar hydrostatic conditions are also reviewed. These lessons include recommended considerations for concrete placement, appropriate interfaces with other building enclosure systems, and repair solutions for possible damages resulting from unanticipated field conditions.

We will also outline strategies for successfully implementing delegated designs within both traditional and modern project delivery methods. In traditional design-bid-build projects, specifications play a critical role in defining the expectations for project team members. Meanwhile, newer project delivery methods ensure that specialty designers and contractors are contracted early in the design process. With the advent of building enclosure commissioning, early project involvement of building enclosure consultants and BECx providers can add value in the form of additional quality assurance to protect stakeholder interests.

SPEAKERS

Edward L. Lehman, RWC, AIA

Wiss, Janney, Elstner Associates Inc. | Duluth, GA

Edward L. Lehman has well-rounded experience in the design and construction of various types of commercial buildings and is involved in building enclosure consulting and commissioning for new construction and existing building projects. In addition to providing consulting services, Lehman has served in multiple other roles, including contract administration for architects and quality assurance management for large-scale general contractors. He has participated in a variety of peer reviews, analyses of mock-up panels, and preinstallation meetings, and he has coordinated field performance testing on waterproofing, roofing, and glass/glazing systems.

Douglas R. Stieve, RRC, AIA

Wiss, Janney, Elstner Associates Inc. | New York, NY

Douglas R. Stieve is a building enclosure consultant who specializes in roof and waterproofing consulting as well as masonry construction. He has experience with many types of materials, including low-and steep-slope roofing as well as plaza deck, vegetative roof, and subgrade waterproofing systems. Stieve has worked on projects that have won awards from the American Institute of Architects, *Engineering News-Record*, and the National Trust for Historic Preservation, among other organizations. He has authored several articles and technical papers, and he has lectured throughout the United States on the subjects of roofing, waterproofing, and masonry construction.

Waterproofing Challenges in Hydrostatic Conditions

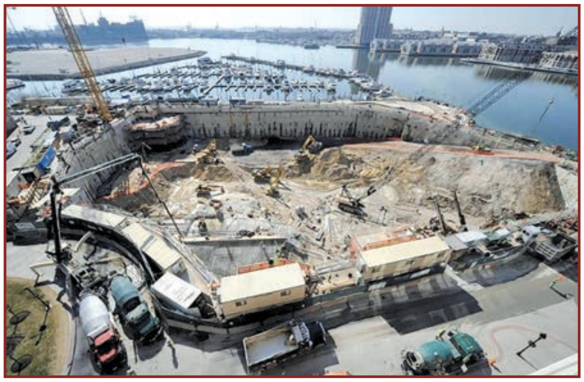

Figure 1. Construction adjacent to water.

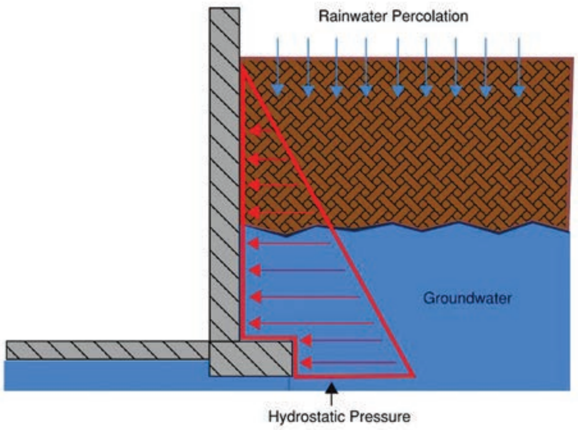

Figure 2. Hydrostatic pressure of groundwater increases with depth and volume.

Underground buildings and other structures that are constructed underground may face distinctive waterproofing challenges, and these challenges are amplified if the structure will encounter either permanent or intermittent hydrostatic pressure from groundwater through the service life of the structure, or if the project site has contaminated soils. The challenges imposed by hydrostatic pressures include the increased reliance on proper detailing of the waterproofing system and the inclusion of various redundancies in the waterproofing strategy.

Successful strategies to address these challenges are critical for several reasons: In highly populated areas, there will be a growing need of more underground construction for buildings, mass transit and water supply tunnels, tanks, and even waste storage. There could also be more pressure to develop underground properties and infrastructure in less-than-ideal geographic locations as development continues across the globe. Finally, the impacts of climate change in some areas (such as coastal regions) will increase the demands on waterproofing systems for existing and future underground structures.

HYDROSTATIC PRESSURE

Hydrostatic pressure is the stress that any fluid in a confined space exerts against adjacent bodies, including building structures. This pressure can be permanent if the structure is located well below the water table or in a coastal region (**Fig. 1**), or it can be intermittent. Causes of intermittent hydrostatic pressure include precipitation such as rainfall or snow melt, other seasonal changes, proximity to aquifers and other underground features (water reservoirs, subterranean rivers, etc.), and tidal fluctuations, particularly in marine structures.

Soil conditions can influence hydrostatic pressure. Low-impermeability strata such as rock and clay can prevent water from passing through soil, creating pockets of perched water as the buildup of water cannot pass through the ground. The hydrostatic pressure of the soil and groundwater increases relatively proportional to the depth of the structure below ground (**Fig. 2**).

In addition to hydrostatic pressure, designers and engineers must also consider the pressure that soil exerts against a structure. For example, foundations are distinctively affected by soils containing minerals such as smectite clays because these clays can retain water and will swell as they are saturated. Liquefaction of saturated soils in areas prone to earthquakes will also influence the design of a building's foundation.

Soil types and groundwater conditions are typically determined by a geotechnical engineering investigation. When the soil is below the water table, its pressure is calculated based on the weight of soil, which is then reduced by the buoyancy of the groundwater. Estimating this pressure typically requires testing and calculations by an experienced geotechnical engineer. For waterproofing design of a typical structure, a linear equation is typically used, which generally provides a somewhat conservative estimate.

Various foundation systems can be used to resist hydrostatic forces. The selection of these systems is critical for managing another effect of hydrostatic pressure: the ability of the building to resist water penetration. For example, foundations using stabilization systems such as rock and soil anchors require different

The challenges imposed by hydrostatic pressures include the increased reliance on proper detailing of the waterproofing system and the inclusion of various redundancies in the waterproofing strategy.

Figure 3. Rock anchor penetrations through foundation waterproofing.

Figure 4. Mat slab under construction.

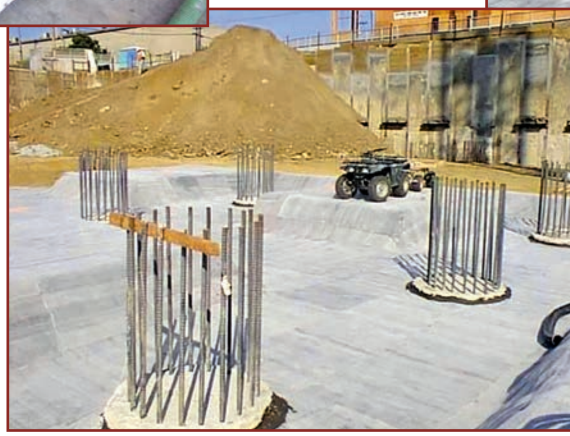

Figure 5. Pile caps.

waterproofing approaches than foundations using secondary structural elements such as "mat slabs" (thickened mat or raft foundation). Stabilization systems can include post-tensioned cables or rods grouted into the rock and/or soil. After the permanent foundation elements have been constructed, the anchors are tensioned and locked off with an anchor plate and nut (**Fig. 3**).

Secondary structural systems are another commonly used method to structurally resist hydrostatic pressure. These foundation types can be as thick as several feet to spread the load of the structure over the entire area of the building footprint (**Fig. 4**). Piles are also used to help overcome uplift pressures from either overturning of the building or hydrostatic pressure from below.

All of these structural elements can greatly influence the subgrade waterproofing system. As the number of penetrations through the waterproofing increases, the risk of water intrusion also increases because many leaks often occur at penetrations and other flashing details. Furthermore, when thickened mat slabs are used, the waterproofing system is placed below several rows of concrete reinforcement bars, making it very difficult or impossible to repair the waterproofing before concrete placement. Pile caps typically incorporate many reinforcing elements that are needed to connect the floor slab to the piles (**Fig. 5**).

GROUNDWATER MANAGEMENT

The management of groundwater under hydrostatic pressure is a challenge for almost any type of waterproofing design because the pressure can force water through a foundation. Hydrostatic pressure increases as structures are built further below the water table, and the increased pressure creates greater energy to push water through breaches at any deficiency and then through cracks and construction joints in the structure itself.

Positive-side waterproofing membrane systems are appropriate systems for hydrostatic conditions; however, even these systems are vulnerable to damage from the force of the hydrostatic pressure if the hydrostatic pressure is great enough to push the membrane up against irregular substrates such as voids and/or protrusions in the foundation. Once water leaks occur, grout repair treatment can displace the water to alternate pathways into the structure and subsequent "chasing of leaks."

The type of foundation material can also affect the management of groundwater under hydrostatic pressure. For example, if shotcrete is used as a foundation structure in hydrostatic conditions, the voids within shotcrete (such as shadowing behind reinforcement and rock pockets) can create numerous, interconnected pathways within the structure for water to travel great distances from the points of initial ingress, leading to leakage or other damage.

From a waterproofing perspective, it is almost always better to dewater than to fight the hydrostatic pressure. A common strategy to manage groundwater is to include a permanent dewatering system. This system is a subslab drainage system consisting of gravel and drainpipes. The drain piping can lead to sump pits, where the water is then pumped up and out of the structure. When a dewatering system is used, the slab can be thinner because it does not have to resist the hydrostatic pressure of the groundwater. However, there will be a long-term maintenance cost associated with operating and maintaining the pumps. Also, subslab drainage systems can become clogged over time and may not be suitable for every condition. Clean-outs should be provided in the drain lines to maintain the drain piping. Owners and designers must recognize that there is increased risk of structural damage and water intrusion if these systems are not maintained.

Another consideration for dewatering is that local ordinances may require that contaminated water be treated before it is discharged. There may be associated costs from the local utility depending on the volume of discharge.

In lieu of subslab drainage, footing drains can also be used to evacuate water from the foundation walls that are not under permanent hydrostatic conditions. However, to be effective, the footing drains must be able to discharge the water to an outlet away from the building structure or a sump pump. Otherwise, they simply fill and retain water, and are therefore unable to provide effective dewatering relief for the structure.

WATERPROOFING SYSTEMS

In addition to managing the groundwater, waterproofing systems can provide a barrier protection to prevent water from entering the structure. There are several types of waterproofing systems available, including, but not limited to, built-up bituminous (either asphalt or coal tar pitch) membranes, modified bituminous sheet membranes, composite membranes, fluid-applied membranes, bentonite-based membranes, polyvinyl chloride (PVC) membranes, and cementitious products. There are also different application methods such as fully adhering the membrane to the structure or loosely laying the membrane around the building structure. Blindside vertical applications come with additional complications of applying the waterproofing on the support of excavation and the potential damage to the waterproofing from the ensuing construction.

Each type of membrane system and each application method has advantages and disadvantages that must be considered and carefully evaluated before a system is specified for a particular use. No one product or system is without limitations. Among the issues to consider when selecting options for a particular project are the following:

- Clearance to install the waterproofing.
- Whether to use a blindside preapplied membrane or instead choose a post-construction application of the membrane. However, this is often dictated by the access to the positive side of the wall
- Whether to use an attached or loose-laid system.
- Concrete cure times.
- The quantity of joints and seams in sheet products.
- The complexity of details.
- Proposed project phasing.
- Penetrations of and proposed "tie-ins" to existing waterproofing systems.

A less-effective alternative to positive-side waterproofing systems in hydrostatic conditions is the use of a negative-side waterproofing. These methods do not prevent water penetration into the structure; rather, water may migrate through structural pores, cracks, joints, and other openings. As a result, the concrete reinforcing could be saturated with potentially contaminated groundwater. Another drawback to using a negative-side waterproofing is that it can become more easily damaged because it is often left exposed to the building interior and is also vulnerable during interior construction activities.

The application of water retardants within the structural elements (such as concrete additives) is less effective in hydrostatic conditions. Water retardants typically do not bridge larger cracks in the concrete or construction joints. Concrete admixtures, however, can be a relatively inexpensive redundant type of waterproofing to be used with a waterproofing membrane or dewatering strategy. They will densify the concrete, which provides corrosion protection to steel reinforcement.

Some subgrade structures, particularly in high-risk uses with no tolerance for water intrusion, employ redundancy in the waterproofing design. , This redundancy creates an alternative system to augment the water management of the structure. Such redundant systems may include, but are not limited to, a combination of external dewatering (subslab or perimeter walls or both) and waterproofing, compartmentalizing and grouting, or interior water collection systems used in conjunction with a waterproofing membrane (**Fig. 6**). Some waterproofing membranes also have redundancy such as composite waterproofing systems with a thermoplastic membrane combined with a swelling "bentonite type" inner fabric.

CASE STUDIES

To further elaborate on the waterproofing principles and strategies described in the previous sections, we are presenting two case studies. The first case study explores a waterproofing practice for subsurface conditions subjected to a permanent or constant hydrostatic pressure. The second case study involves waterproofing subsurface conditions subjected to a cyclic or seasonal hydrostatic pressure. Both case studies focus on new construction projects.

Case Study 1: Constant Hydrostatic Pressure

This case study involves a two-story, low-rise structure in south Florida. The project is located on the fringe of the Everglade swamp, within the Biscayne Aquifer, where many subsurface structures are subjected to constant hydrostatic pressure. The site is positioned in a suburban environment and adjacent to an interstate roadway. The building has one level on ground and one level below grade (**Fig 7**). The lower level includes a weighted

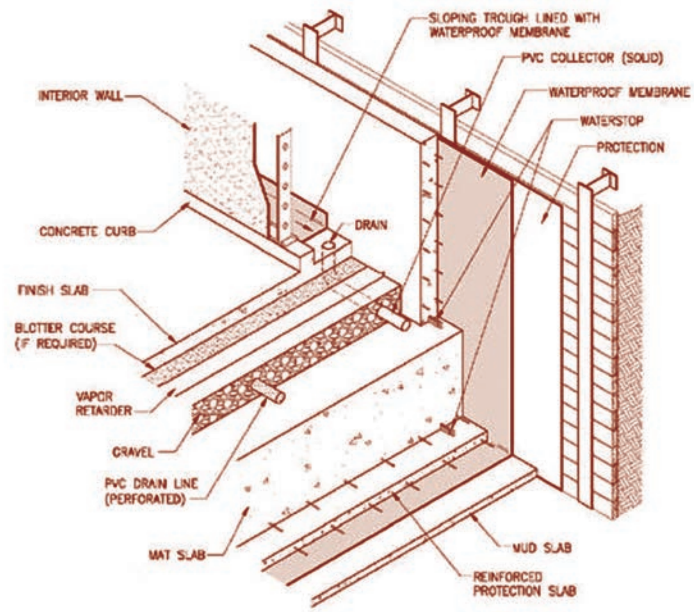

Figure 6. Internal water management strategy of a positive-side waterproofing and internal drainage system.

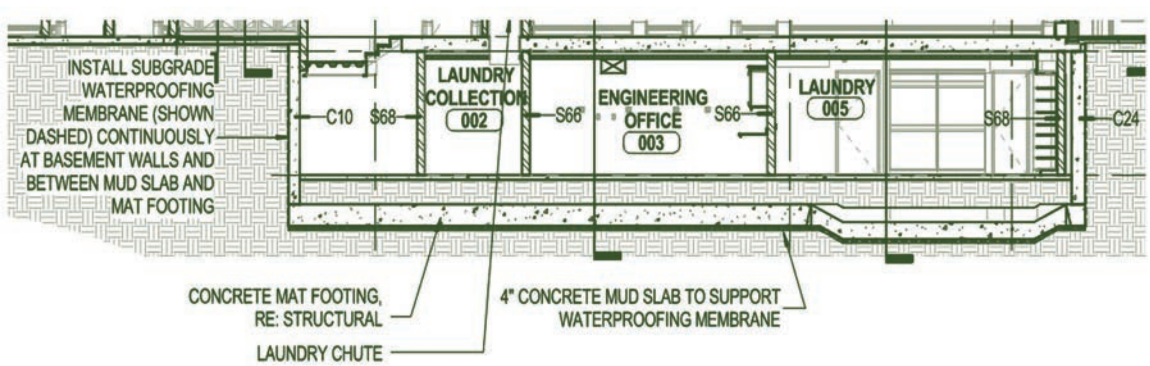

Figure 7. Architectural cross section for below-grade building area.

slab designed to resist uplift pressures, has a conditioned interior space, and is served by a holeless hydraulic elevator.

With the project being subjected to constant hydrostatic pressure, an active or expanding sodium bentonite waterproofing material was a practical choice. As soon as the waterproofing becomes submerged within the high groundwater level, the putty-like material will hydrate or expand up to seven times its original thickness. This process can occur within a week or take up to a month to happen. The swelling of the waterproofing membrane increases its material thickness and creates a compressive seal between the building structure and the surrounding soil conditions. The contact submersion in groundwater will keep the bentonite material hydrated and sealed in place.

The selected bentonite sheet waterproofing product includes a 15-mil sheet of high-density polyethylene (HDPE) and a layer of expandable, granular bentonite. A functional part of the waterproofing is the layer of granular bentonite clay material, which will "hydrate" and expand up to 7 to 10 times its original thickness once subjected to prolonged exposure to water. The HDPE is extremely resistant to chemical contaminants. This expansion of the bentonite creates a compressive seal to block the flow of groundwater.

To function properly, the compressive seal of the bentonite waterproofing must remain in constant compression between the building structure and ground conditions. Given the presence of the constant groundwater, this waterproofing system does not traditionally manage the groundwater by means of drainage.

An expanding hydrophilic water stop comprised of bentonite material, was also planned to be provided at the concrete cold joints as a secondary means of protection. The location of the expanding water stop is important within the concrete joint to properly confine the material and create the compressive seal. If the water stop is placed too close to a concrete surface, it will swell when hydrated and can displace the concrete, thereby affecting the confinement of the bentonite waterproofing at that location.

Other design considerations and strategies included sloping the surfaces at the elevator pit to ease the geometry of the structure to be waterproofed, not permitting any penetrations into the horizontal waterproofing surfaces, and coordinating specific locations of the concrete cold joints and placement of water stops.

To aid in the design of this waterproofing system, which is expected to be subjected to hydrostatic pressure, samples of the soils and groundwater were obtained and submitted to the waterproofing material manufacturer for evaluation of their pH and alkalinity levels. This testing was done because sodium bentonite swell rates are affected by pH. From the testing results, it was determined that the specified waterproofing material did not need to be modified for saltwater conditions (which had been a potential concern because the project is near the ocean).

During construction, a dewatering moat-style trench was used around the perimeter of the building pad. This trench remained filled with groundwater and was constantly serviced by a dewatering pump station (**Fig. 8**). The dewatering pump station included separate primary and secondary emergency pumps.

The bentonite waterproofing was installed horizontally on a mat or mud slab (**Fig. 9**). The building's concrete floor slab was cast onto the waterproofing, which was turned up at the vertical walls. If the material were to become displaced, gaps could form in the membrane seams, allowing groundwater and soil to breach the assembly. Therefore, critical seams were supplemented with a bentonite-based mastic to reinforce the watertight seal of the overlapping seams.

Once the foundation walls were cast in place, sheets of vertical bentonite waterproofing were mechanically attached to the outer side of the foundation walls in a postapplied condition. The seams of the vertical waterproofing were sufficiently overlapped to maintain the continuity of the compressive seal.

Lastly, the membrane detailing was especially critical for this concealed waterproofing. Transitions, terminations, and penetrations are common locations where leaks can occur in waterproofing assemblies. Also, if unconfined bentonite waterproofing hydrates and expands, it cannot perform as designed and must be replaced with new material. Taking all of this into account, and in consideration of the constant in situ hydrostatic conditions, the waterproofing detail had to be double-checked before it was concealed as a quality assurance measure.

A key lesson learned from this project occurred at the elevator pit. The horizontal mat slab was sloped to avoid additional cold

Figure 8. A dewatering pump station at a perimeter trench at the corner of the building pad.

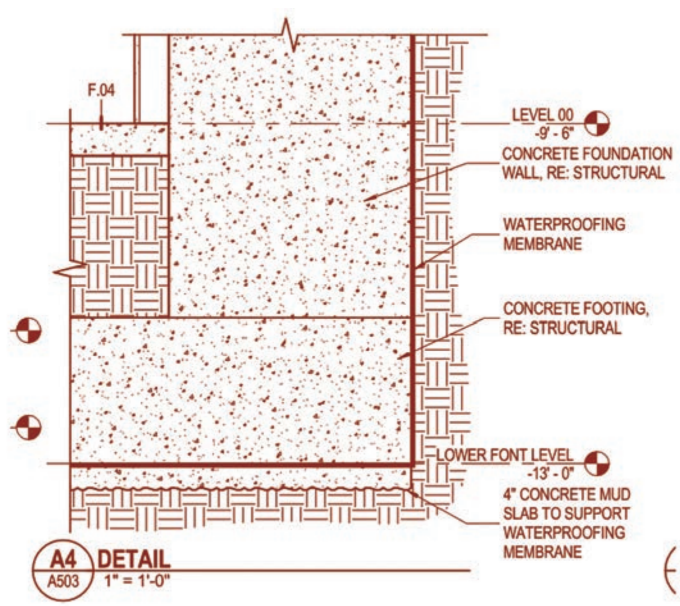

Figure 9. Enlarged design detail of horizontal waterproofing confined between the structural slab and mat slab.

Figure 10. A horizontal bentonite waterproofing sheet being placed at the elevator pit.

joints and 90-degree transitional corners at the membrane (**Fig. 10**). The reinforced horizontal concrete slab at the pit was designed to be thick enough to resist the force of the hydrostatic pressure.

During construction, water leaks were observed inside the elevator sump pit area. A repair using a modified thermoplastic membrane and perimeter sealants was developed from the negative side for this condition. The thermoplastic material was selected for its material pliability in a confined space; and acceptance from material manufacturer to include the repair condition into the project's warranty provisions for the new installation. Future leaks might be possible if the seams in the waterproofing membrane become displaced for any reason. The elevator pit was especially vulnerable to this risk because it was located near the edge of the slab where the vertical and horizontal waterproofing sheets overlapped each other.

Case Study 2: Cyclic Hydrostatic Pressure

The second case study involves a six-story, midrise structure in Boulder, Colorado, at the foothills of the Rocky Mountains, where the subsurface structures are subjected to cyclic or seasonal hydrostatic pressure. The site includes a zero-lot-line waterproofing in an urban setting. The building has four levels above grade and two levels below grade (**Fig. 11**). The lower levels include subsurface parking featuring a fully automated robotic parking system.

At this project site, the groundwater pressures and levels typically fluctuate seasonally, with the fluctuations based largely on snow melt in the mountains above. In the spring and early summer, the snow accumulation will melt, creating extensive water runoff into the creeks and streams. This runoff will cause the water table to rise and fall multiple times during the year. These pressures are usually not constant or consistent. If mountain snowfall in the winter is heavy, the resulting water table in the foothills in the spring and early summer will be high, and if the snowfall is light, the water table will be low. Given these variations, it can be beneficial to periodically monitor the water levels with piezometers.

Because the exterior face of the concrete foundation walls would be inaccessible, a preapplied or blindside waterproofing system was the most appropriate design choice for this project (**Fig. 12**). Given the inconsistent hydrostatic pressure, it would have been much more challenging to use a bentonite waterproofing because the material might have been subject to cycles of hydration. A sheet waterproofing comprised of a composite HDPE film/adhesive membrane was selected for use on the subject project. This waterproofing material selection is a reasonable choice since the heat of hydration of the concrete bonds the membrane back to the structure, which is advantageous as it mitigates the chance of water migration between the waterproofing membrane and the building structure if a breach in the membrane should occur. As in the first case study, the HDPE film is exposed to the soil and provides good chemical resistance to contaminants in the soil and water.

Unlike the first case study, on this project there were several penetrations into the hori-

Figure 11. Architectural cross section for below-grade building area.

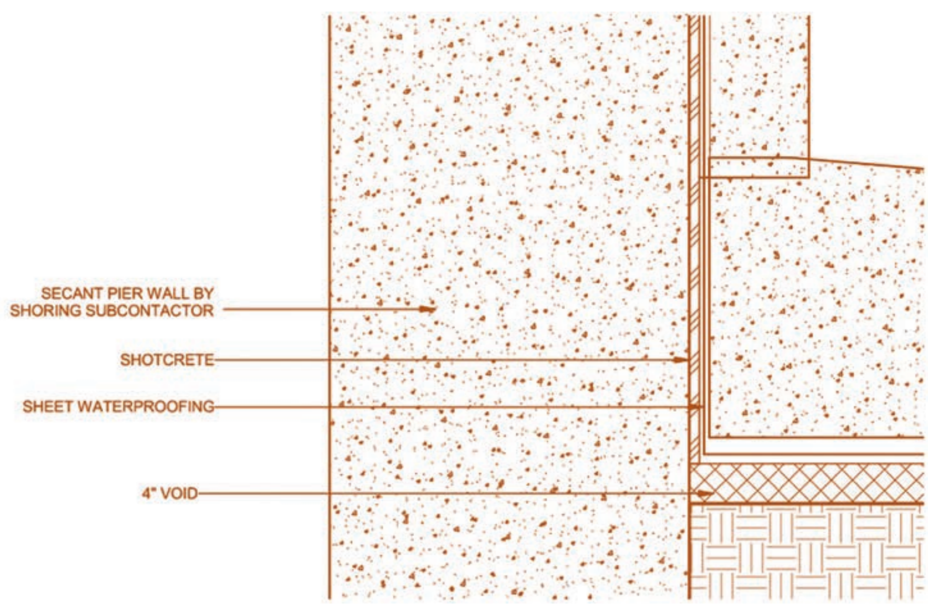

Figure 12. Enlarged design detail of blindside sheet waterproofing located between concrete shoring and concrete foundation wall.

Figure 14. Reinforcing steel being installed over the top of pre-applied sheet waterproofing.

Figure 13. View of the preapplied sheet waterproofing being installed over the support of an excavation wall at a zero-lot line condition.

zontal waterproofing at the lower slab level so the reinforcing steel could connect the slab to the deep foundation system. Most structural engineers object to waterproofing between these elements because a bond separator is formed between the concrete surfaces of the deep foundation and the horizontal structure, and that can reduce the strength of these connections. The compressive strength of the membrane can be another issue for the engineer if the membrane can compress between these two structural elements. The feasibility of flashing all the reinforcement bar penetrations is also very difficult with a sheet membrane. Given these conditions, the sheet waterproofing systems on this project required careful detailing. Most HDPE waterproofing systems also include liquid membrane flashings and mastics to assist in detailing the terminations and penetration edges in these areas. Because the exterior sides will all be inaccessible, all layers that are outboard of the waterproofing membrane had to be installed and properly secured before the concrete structure was placed. The drainage mat was only a requirement at the vertical walls of this project to help relieve the hydrostatic pressure from the fluctuating groundwater levels.

As the pit was excavated, some dewatering was required because water tables were high following a snow melt. In this region, it is preferable to schedule excavation in the early fall, if possible, to avoid the need for dewatering.

The composite HDPE film/adhesive sheet waterproofing and drainage mats were laid out before the placement of the reinforcing steel and concrete (**Fig. 13** and **14**). The waterproofing seams were all overlapped as the membrane was set into place. The selvage edge seams for the sheet waterproofing membrane were enhanced by the application of seam tape. This adhesive edge is sometimes integrated into the membrane side lap edge for added protection. Rolled tapes can be applied to reinforce the membrane seams or outright seal them.

Another key consideration during the waterproofing installation was to protect the membrane. Strategies to protect the membrane against cuts, tears, and burns from the placement of the reinforcing steel can include not locating reinforcing bar chairs on top of the horizontal membrane seams. For this project, continuous reinforcing bar chairs with plastic tips were used to support the horizontal reinforcing steel on the horizontal surface. To further protect the membrane, it was important to ensure that the reinforcing steel was not cut with torches or grinders in the vicinity of the waterproofing material.

As a cost-saving measure on concrete formwork, the design team decided to use shotcrete instead of traditional cast-in-place concrete at the foundation walls. This modification required changes to the design and installation of the sheet waterproofing. The design changes entailed confirming the appropriateness of the waterproofing material selection for shotcrete applications. Getting consistent and consolidated coverage in the shotcrete placement was also critical. Ideally, the shotcrete placement would not create voids or reinforcing bar "shadowing" in the structure.

As water leaks appeared at cold joints and cracks in the shotcrete foundation walls, an injectable polyurethane foam was used to seal the leaks. The foam was injected through ports drilled into the interior side of the concrete wall. The ports were drilled on an angle into the joint or crack in an offsetting pattern at a consistent spacing. One problem with this method of repair is that it is a "trial and error" approach and could require multiple attempts to seal the leaks at each location. It should also be noted the shotcrete can complicate the grouting repair process because there are small voids and gaps in the structural material, which facilitate the flow of water through the wall.

CONCLUSION

Groundwater pressures and activities are very "fluid" and reactive to their surroundings. Effective groundwater management in hydrostatic conditions can require a combination of drainage strategies and waterproofing protection. Managing water before it gets to the waterproofed surface by means of drainage or diversion is always the preferred option. Proper installation of an appropriate type of waterproofing system will also help ensure that the building structure remains dry.

Effects of ASCE 7-22 Wind Load Provisions on Roof Covering Design

Donald R. Scott, SE, FSEI, FASCE

PCS Structural Solutions | Tacoma, WA

dscott@pcs-structural.com

IIBEC 2022 - Building for the Future

International Convention and Trade Show

March 17–22, 2022 | Orlando, FL

ABSTRACT

The American Society of Civil Engineers (ASCE) has updated the wind design provisions in the 2022 edition of ASCE 7. Many of the updates aim to simplify the use of the component and cladding design provisions, particularly in determining roof zoning and design pressures. This presentation reviews these revisions and discusses the reasons for eliminating the tabular methods, the basis of the new tornado design provisions, and updates to the wind speed maps.

SPEAKER

Donald R. Scott, SE, FSEI, FASCE

PCS Structural Solutions | Tacoma, WA

Donald R. Scott is a senior principal with PCS Structural Solutions. He has nearly four decades of experience in the design, evaluation, and rehabilitation of building structures. He was the principal investigator for the American Society of Civil Engineers/ Structural Engineering Institute (ASCE/SEI) *Prestandard for Performance-Based Wind Design*. Scott is chair of the SEI Codes and Standards Executive Committee, chair of the ASCE 7 Wind Load Subcommittee, member of the ASCE 7 Main Committee, and past chair of the National Council of Structural Engineers Associations' Wind Engineering Committee. Scott is also a member of the SEI Board of Governors and a past president of the Board of Directors of the Applied Technology Council.

Effects of ASCE 7-22 Wind Load Provisions on Roof Covering Design

The 2022 edition of the American Society of Civil Engineers' *Minimum Design Loads and Associated Criteria for Buildings and Other Structures* (ASCE 7-22)[1] is published. This standard will be referenced in the 2024 editions of the *International Building Code* (IBC) and *International Residential Code* (IRC), and thus it will become the requirements for determining design loads and combinations of loads for the design of buildings in 2023. Some of the wind load provisions in ASCE 7-22 have been updated from those specified in previous editions of IBC, IRC, and ASCE 7. These updates aim to simplify the application of the provisions, particularly the provisions for design wind pressures for sloped roof configurations with a roof height less than or equal to 60 ft. These updates affect both the magnitude and configuration of the roof zones for the application of the wind pressures on sloped roofs. The design wind speed maps have also been modified to account for the information learned from recent hurricanes in the Gulf of Mexico, Puerto Rico, and the US Virgin Islands. However, the greatest changes in ASCE 7-22 are the tornado design provisions required for Risk Category III and Risk Category IV facilities. Also, the tabular procedures in ASCE 7-16,[2] including those in Chapter 27 Part 2, Chapter 28 Part 2, Chapter 30 Part 2, and Chapter 30 Part 3, have been eliminated from ASCE 7-22 because they were found to be confusing.

THE NEW WIND SPEED MAPS

In ASCE 7-16, the basic (design) wind speeds for the lower 48 United States were designated in two uniform sections outside of the hurricane-prone region. These two regions were divided along state boundaries, with the Western region including the states of California, Oregon, and Washington and the second region encompassing the remaining states outside of the hurricane-prone region. The wind speed maps contained in ASCE 7-16 accounted for the regional variations of wind speed across the country. In ASCE 7-22, hurricane-coastline wind speeds have been updated based on data from the most recent hurricanes making landfall in the United States. See Fig. 1 and 2 for a comparison of the hurricane-coastline contours in ASCE 7-16 and ASCE 7-22. Generally, the wind speeds along the hurricane coastlines have increased slightly in the Gulf of Mexico and Southeast Atlantic coastlines. Also included in the ASCE 7-22

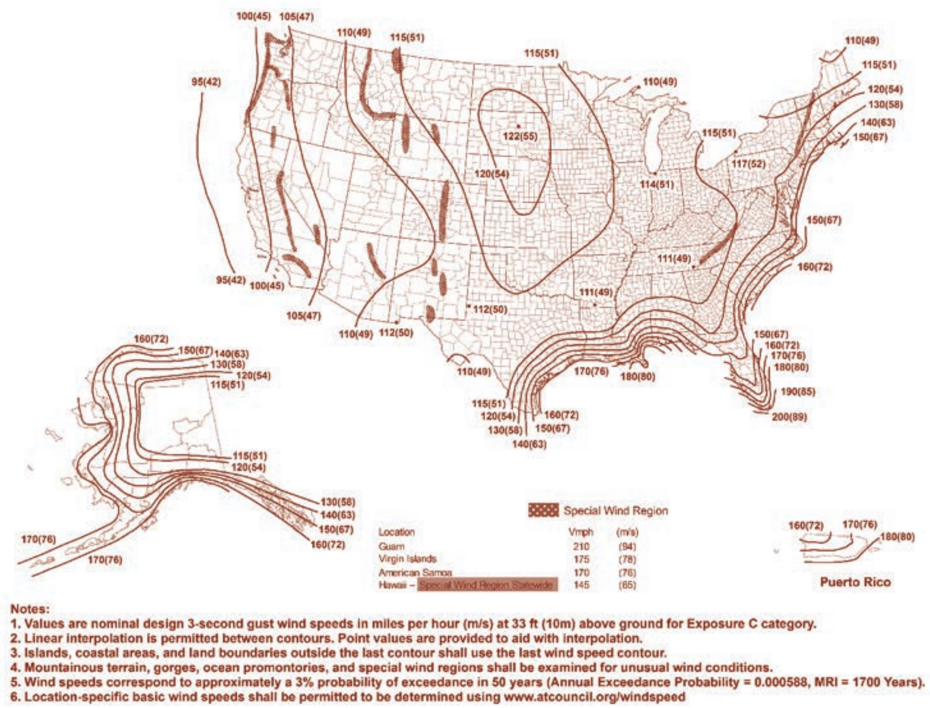

Figure 1. ASCE 7-16 wind speed map for Risk Category II buildings. Figure reprinted with permission from ASCE.

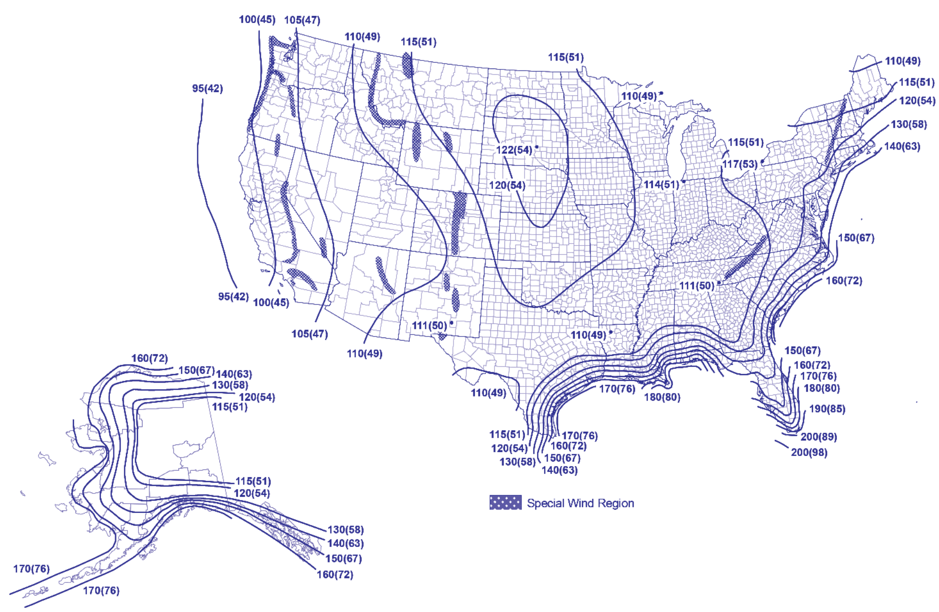

Figure 2. ASCE 7-22 wind speed map for Risk Category II buildings. Figure reprinted with permission from ASCE.

Structure Type	Directionality Factor K_d
Buildings	
Main wind force resisting system	0.85
Components and cladding	0.85
Arched roofs	0.85
Circular domes	1.0*
Chimneys, tanks, and similar structures	
Square	0.90
Hexagonal	0.95
Octagonal	1.0*
Round	1.0*
Solid freestanding walls, roof top equipment, and solid freestanding and attached signs	0.85
Open signs and single-plane open frames	0.85
Trussed towers	
Triangular, square, or rectangular	0.85
All other cross sections	0.95

*Directionality factor K_d = 0.95 shall be permitted for round or octagonal structures with nonaxisymmetric structural systems.

Table 1. Wind directionality factor K_d table from ASCE 7-22. Table reprinted with permission from ASCE.

updates are very detailed wind speed maps for Puerto Rico and the US Virgin Islands. These have been incorporated into the ASCE 7 Hazard Tool,[3] which will be available without cost for all users who purchase ASCE 7-22.

DIRECTIONALITY FACTOR K_d

The directionality factor K_d accounts for two effects: (a) the reduced possibility of maximum winds coming from any given direction, and (b) the reduced probability of the maximum pressure coefficient occurring for any given wind direction (Table 1). Research on this factor and how to incorporate it into ASCE 7 is continuing. This factor is not a variable imposed on the wind velocity pressure, but a function of the structure's orientation and location. Thus, K_d has been removed from the velocity pressure equation and incorporated into the pressure equations.

During the ASCE 7-22 revision cycle, a review of the roof pressure coefficients and roof zoning configurations was undertaken in an attempt at simplification. It was determined that zoning configuration could be combined and pressure coefficient figures could be truncated to simplify the provisions.

The ASCE 7-16 velocity pressure equations is:

$$q_z = 0.00256\, K_z\, K_{zt}\, K_d\, K_e\, V^2 \text{ (lb/ft}^2\text{)}$$

where:
q_z = velocity pressure
K_z = velocity pressure exposure coefficient
K_{zt} = topographic factor
K_e = ground elevation factor
V = basic wind speed

In ASCE 7-22, the velocity pressure equation is revised as follows:

$$q_z = 0.00256\, K_z\, K_{zt}\, K_e\, V^2 \text{ (lb/ft}^2\text{)}$$

In ASCE 7-22, the directionality factor is included in the pressure equation:

$$p = q\, K_d\, G\, C_p - q_i\, K_d\, (GC_{pi})$$

where:
p = design wind pressure
q = velocity pressure
G = gust response factor
C_p = exterior pressure coefficient
q_i = interior design wind pressure
GC_{pi} = interior pressure coefficient

ROOF PRESSURE COEFFICIENTS FOR SLOPED ROOF CONFIGURATIONS

Among the most significant changes made in ASCE 7-16 were changes to the low-rise (less than 60 ft high) roof pressure coefficients. At that time, the pressure coefficients and the roof zoning for the sloped roof configurations were developed from figures in previous editions of ASCE 7. During the ASCE 7-22 revision cycle, a review of the coefficients and roof zoning configurations was undertaken in an attempt at simplification. It was determined that zoning configuration could be combined and pressure coefficient figures could be truncated to simplify the provisions. See Fig. 3 for examples of these simplifications.

TORNADO PROVISIONS FOR RISK CATEGORY III AND RISK CATEGORY IV STRUCTURES

In ASCE 7-22, the procedures for determining tornado design pressures on components and cladding elements for Risk Category III and Risk Category IV Structures are based on the methods of ASCE 7 Chapter 30, with several modifications. Notably, tornado velocity pressures replace the velocity pressures

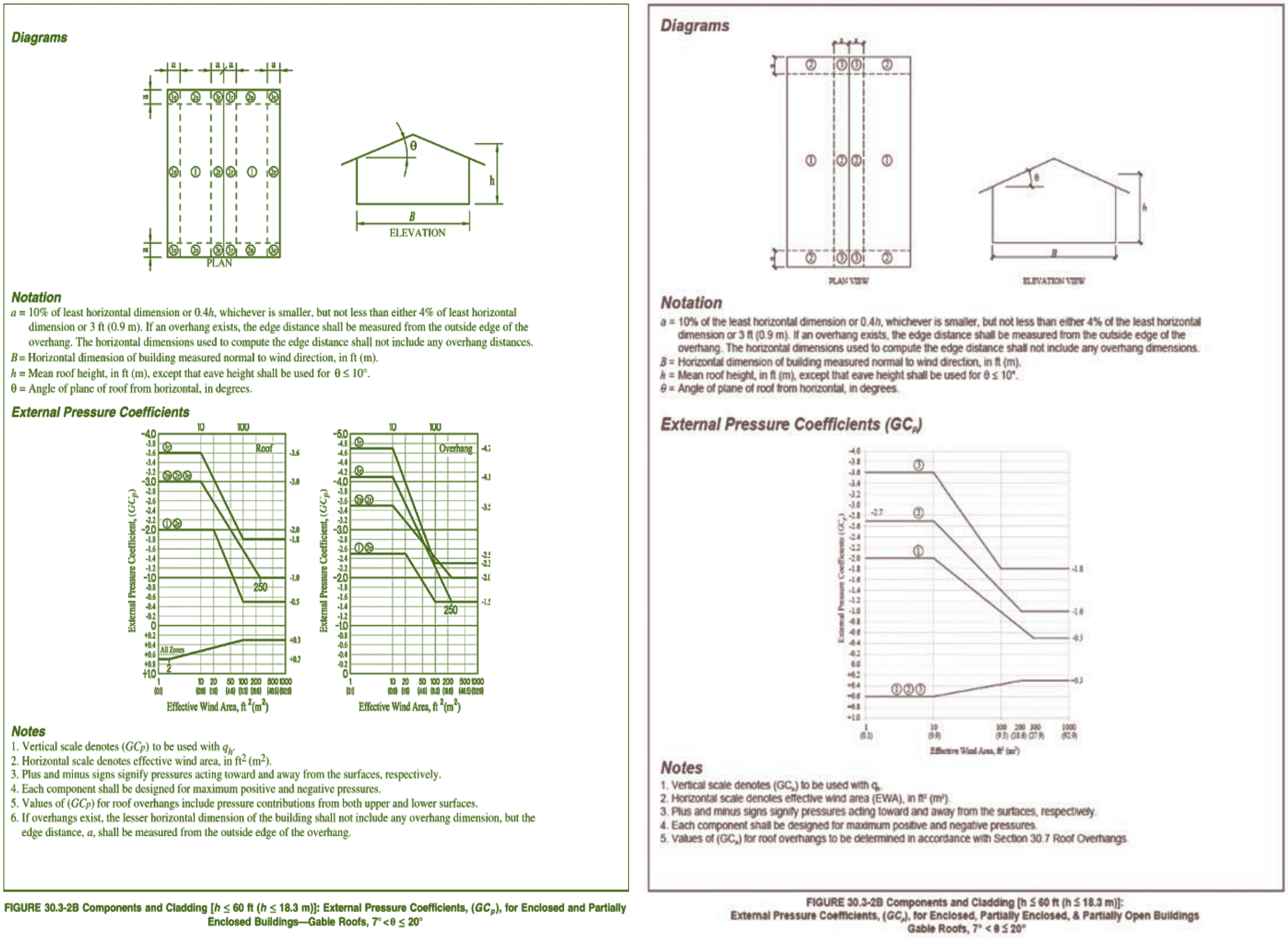

Figure 3. Comparison of ASCE 7-16 (left) and ASCE 7-22 (right) sloped-roof zoning configurations. Figures reprinted with permission from ASCE.

specified in Chapter 30. Another major modification to these procedures is the inclusion of the atmospheric pressure change (APC) that occurs with a tornado. This pressure change produces significant suction pressures on the building. Also, the wind velocity profile in a tornado is significantly different than what is found in straight-line or hurricane wind events (**Fig. 4**).

The ASCE 7-22 requirements for

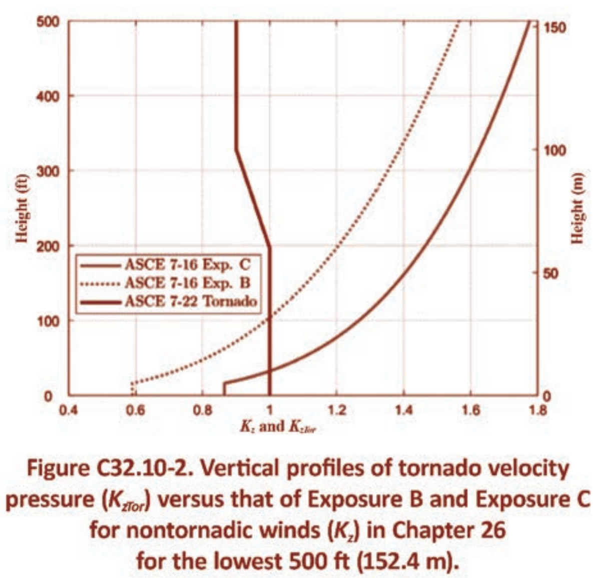

Figure 4. Vertical profiles of tornado velocity pressure versus Exposure B and Exposure C for nontornadic winds in ASCE 7-22. Figure reprinted with permission from ASCE.

Figure 5. Tornado design wind speed map in ASCE 7-22. Figure reprinted with permission from ASCE.

tornado design are based on the plan square footage of the structure being designed to account for the facility's strike risk. **Figure 5** presents an example of a tornado wind speed map for a Risk Category III structure.

CONCLUSION

The following are notable changes to the wind provisions in ASCE 7-22:

- The design wind speeds along the hurricane coastline have increased slightly based on data from the recent Gulf of Mexico hurricanes that made landfall in the United States.
- The roof design wind pressure coefficients and zoning have been simplified for easier application.
- Tornado design provisions have been incorporated for Risk Category III and Risk Category IV buildings to help protect the essential functions of these facilities.

REFERENCES

1. American Society of Civil Engineers (ASCE). 2021. *Minimum Design Loads and Associated Criteria for Buildings and Other Structures*. ASCE 7-22. Reston, VA: ASCE.
2. ASCE. 2016. *Minimum Design Loads and Associated Criteria for Buildings and Other Structures*. ASCE 7-16. Reston, VA: ASCE.
3. ASCE. n.d. "ASCE Hazard Tool." Accessed November 14, 2021. https://asce7hazardtool.online.

"Return to Glory": Restoring Safety to Tampa General Hospital's Brick Facade

E. Webb Wright, PE

Walter P Moore | Orlando, FL

wwright@walterpmoore.com

Amaris Beza, PE

Walter P Moore | Orlando, FL

abeza@walterpmoore.com

IIBEC 2022 - Building for the Future

International Convention and Trade Show

March 17–22, 2022 | Orlando, FL

ABSTRACT

Tampa General Hospital is an award-winning medical center serving Tampa Bay, Fla. The hospital first opened in 1927 and has since undergone various expansions and renovations. In 2015, facility staff observed near the West Pavilion's main entrance that brick masonry units had fallen, presenting an overhead safety hazard for hospital patients and visitors. Walter P Moore was retained to evaluate the general condition of the brick facade and recent brick failure, provide repair recommendations, and perform construction administration services during the repair work. The investigative team used more than 30 exploratory openings through the brick facade to observe concealed conditions, and identified several unique issues that necessitated widespread repairs. Unforeseen conditions also surfaced during the repair work, presenting several interesting challenges. This presentation discusses the methods of assessment and repair at the hospital, and how the team overcame the challenges of performing repairs to a facility that remained fully operational during the COVID-19 pandemic.

SPEAKERS

E. Webb Wright, PE

Walter P Moore | Orlando, FL

Webb Wright is a senior associate and senior project manager in the Walter P Moore Diagnostics Group with expertise in forensic engineering. He has more than 20 years of engineering experience in diversified aspects of structural engineering analysis, investigation, and evaluation of distressed and failed materials involving a broad range of structural, civil and architectural systems. He has also performed assessments and repairs of various facade cladding systems, reinforced concrete, masonry, prestressed concrete, steel, and timber structures. He routinely provides expert witness services on behalf of insurance companies and property owners.

Amaris Beza, PE

Walter P Moore | Orlando, FL

Amaris Beza is an engineer in the Walter P Moore Diagnostics Group. Her experience focuses on the field of building enclosure consulting and repair of existing buildings. Beza's expertise includes evaluating and designing repairs for distress related to concrete structures, building enclosure moisture management, roofing systems, and waterproofing systems. She has developed repair details, repair procedures, and technical specifications for waterproofing, restoration, and rehabilitation projects. Beza has worked on several building enclosure third-party reviews for clients, reviewing technical specifications and drawings for continuity of building enclosure systems.

“Return to Glory”: Restoring Safety to Tampa General Hospital’s Brick Facade

Tampa General Hospital (TGH) is an award-winning, nonprofit research and academic medical center serving the Tampa Bay, Fla., area. The hospital first opened its doors to the public in 1927, and in the last several decades, it has undergone various expansions and renovations. The West Pavilion building was a welcome addition to the hospital’s main campus in 1982. The campus, located on Davis Island south of downtown Tampa, currently has 1007 beds and more than 8000 team members, making it one of Florida’s largest public hospitals and one of the region’s largest employers. The West Pavilion building is a nine-story, concrete-frame structure with concrete-masonry unit (CMU) infill walls and a brick veneer facade that is mechanically attached to the backup concrete and CMU structure with brick wall ties and helical ties within the mortar joints. Ribbon windows are located throughout the building’s six elevations between sections of brick veneer. The approximate square footage of the West Pavilion building is 614,000 ft^2 gross.

In 2015, TGH facilities staff observed pieces of brick masonry units that had fallen near the main entrance to the West Pavilion building. With the safety of their patients being the highest priority, TGH retained Walter P Moore to conduct a visual assessment to evaluate both the general condition of the brick facade and the recent brick failure and provide recommendations for a future course of action. More than 30 exploratory openings were made through the brick facade to observe concealed construction and support conditions. The assessment identified several unique and unexpected issues that necessitated widespread repairs to the facade. Walter P Moore prepared construction documents for a focused program of repairs to the brick facade to address the overhead hazards and waterproofing deficiencies. During the repair work, additional unforeseen conditions surfaced, which required a quick and effective repair approach to maintain the safety of the hospital’s cladding system.

This paper discusses our assessment and repair methods at the West Pavilion building and how we overcame the logistical challenges of performing repairs to the brick facade as the facility remained active and fully operational during the COVID-19 pandemic.

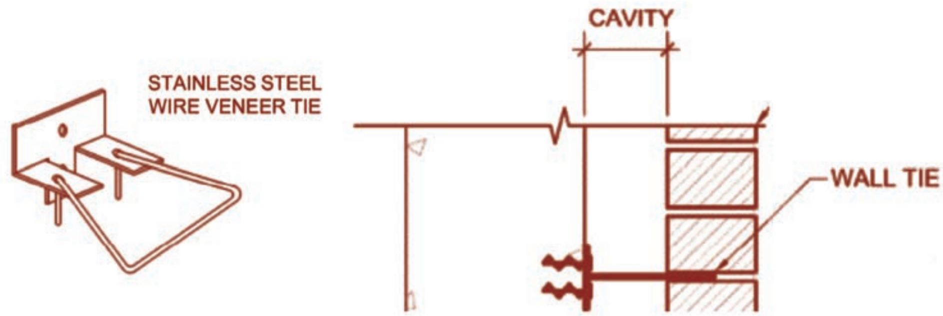

Figure 1. General detail for wall ties for a brick veneer system.

PROJECT BACKGROUND

Members of the assessment team needed to understand the history of the West Pavilion brick facade before they commenced their evaluation and developed a repair program to address the existing facade deficiencies. Team members reviewed existing documentation and interviewed building facilities personnel at the beginning of the project to understand the veneer design details, the history of brick distress, and past facade repair projects. TGH personnel stressed that the prevailing requirement for this project was ensuring the safety of the brick veneer facade.

Built to Fail: Value-Engineered Brick Veneer System

Before conducting the visual assessment of the building, the team performed a document review of the existing building drawings and available documentation to gain a general understanding of the original building construction. The assessment team also interviewed building facilities personnel to better understand the history of issues and repairs that had plagued the hospital facade system. During the review, TGH reported that 50% of the specified brick ties had been value engineered out of the project during original construction of the building. Brick wall ties are necessary to provide a connection and transfer lateral loads between the brick veneer and backup structure (**Fig. 1**).[1]

Previous Repair Attempts

Interviews with building facilities personnel revealed that previous repair attempts were performed to the building’s brick facade after its original construction in 1980. The first repair attempt was completed circa 2000 after sections of brick veneer were observed to be outwardly displaced and an approximately

Members of the assessment team needed to understand the history of the West Pavilion brick facade before they commenced their evaluation and developed a repair program to address the existing facade deficiencies.

Figure 2. General detail for helical ties for a brick veneer system.

2 × 2 ft section of the veneer had fallen. The repairs consisted of the installation of helical ties throughout the brick cavity walls in an effort to provide additional anchorage of the brick veneer and address the observed outward displacement of the brick veneer. Helical ties can be installed through existing mortar joints to reanchor brick veneers (**Fig. 2**).

A few years after the helical tie installation repairs, another brick facade repair project was completed. This project involved brick replacement, but the exact scope of work is unknown. When a piece of spalled brick fell from the building facade in 2015, it became evident that the previous repair attempts were not entirely successful at addressing the observed brick facade issues and that life safety remained a concern for hospital patrons and staff.

FACADE ASSESSMENT

The team performed a Phase 1 visual assessment of the building facade from November 30 to December 2, 2015. The field evaluation included a visual survey of the facade from the ground using binoculars, from the roof of an adjoining, lower building, and at selected locations from an aerial lift. Investigators also used metal detection equipment to perform limited nondestructive testing to identify the spacing of installed brick ties, and made exploratory openings through the veneer. Observations focused on the north-south wing of the West Pavilion because this wing (specifically, the sections of the facade near the main entrance) had experienced the recent brick failure and was more accessible than the east-west wing. The findings of the assessment indicated that the West Pavilion building had several issues that had to be addressed. It appeared that the previous repair attempts performed on the building did not resolve the source of the brick veneer problems; while sections of the brick were stabilized, brick movement had not been accommodated and thus issues persisted. The items to address included immediate issues that posed life-safety concerns, repairs to accommodate movement of the brick facade, and general maintenance repairs.

Given the deficiencies and life safety concerns associated with the condition of the brick veneer identified during our Phase 1 study, we proposed, and the owner agreed to, a more comprehensive, "global" condition assessment. The assessment involved up-close visual observations of the veneer from swing stages at multiple "drops" throughout the building facade. More than 30 exploratory openings through the brick were also included in the assessment for the purpose of evaluating the existing as-built conditions at different areas throughout the facade.

Visual Observations

The visual review of the building facade revealed multiple distress items. Our observations included the following:

- Outward displacement of brick veneer
- Shelf angle deflection (**Fig. 3**)
- Brick veneer cracking
- Mortar joint cracking (**Fig. 4**)
- Indications of veneer movement such as out-of-level shelf angles, mortar joints of excessive width, out-of-plumb soldier brick, and misaligned brick coursing

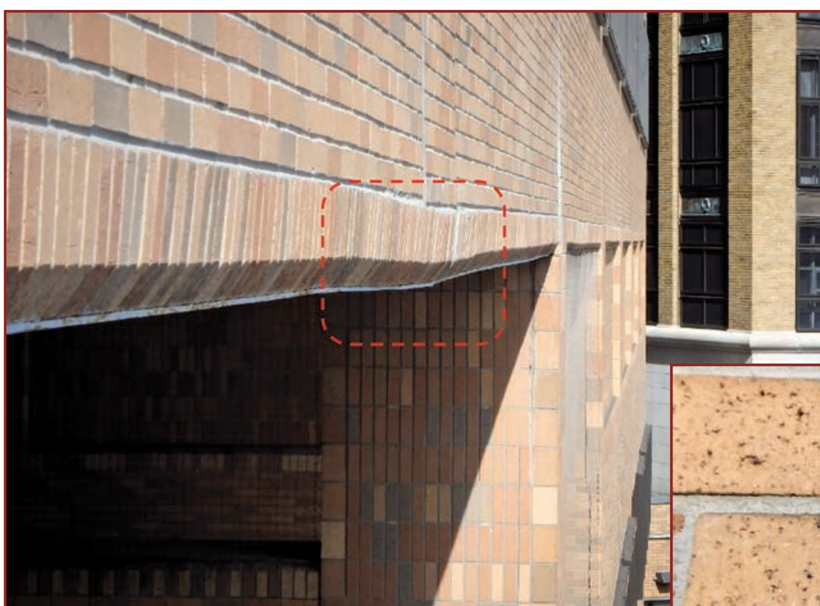

Figure 3. Shelf angle deflection.

Figure 4. Typical brick mortar joint cracking.

Identifying Safety Concerns

During the course of the visual condition assessment, it was vital to quickly identify potential overhead safety hazards so we could recommend immediate action if it were needed to protect the hospital's patrons, visitors, and staff. Distress conditions observed during our field assessments that were indicative of potential veneer instability and areas of concern were as follows:

- Loose and spalling brick
- Brick crack widths greater than ⅛ in.
- Excessive out-of-plane brick displacement

TGH installed safety netting at some locations on the building facade where loose brick, wide cracks, or out-of-plane displacements were observed (see **Fig. 5**). In the event that immediate action must be taken to temporarily secure any potential overhead safety hazards, there are multiple steps that can be taken to protect the public:

- Cordon off, and restrict pedestrians from, areas below sections of potentially unstable veneer.

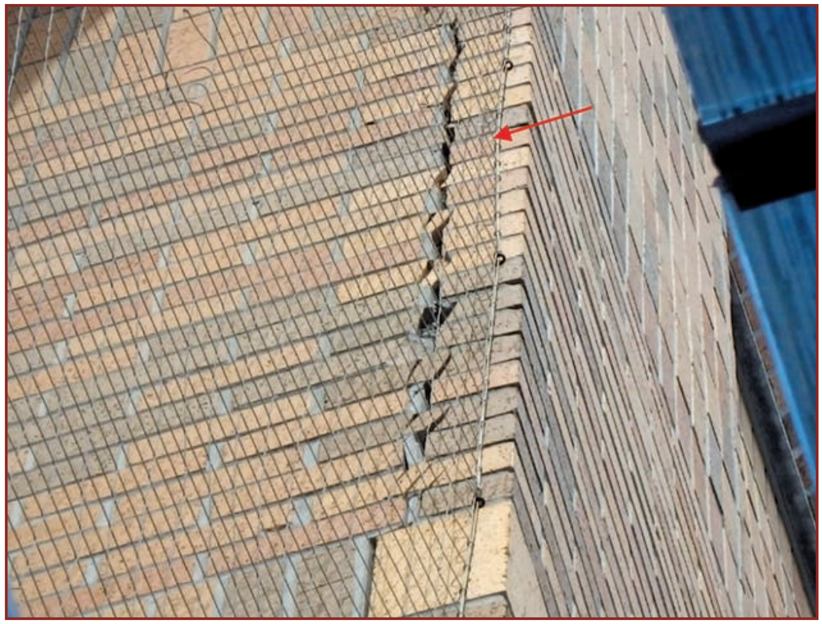

Figure 5. Cracked and spalling bricks at building corner (safety netting installed).

Observations at exploratory openings	Contribution to brick veneer distress
Vertical fractures of bricks (**Fig. 6**)	Full-depth vertical fractures (likely caused by compressive forces acting on the brick in the vertical direction) have greater potential for spalling.
No vertical expansion joints at building corners and setbacks	Without vertical expansion joints at regular intervals and at building corners, brick movement due to thermal expansion is restrained, and brick cracking and/or spalling may occur (**Fig. 7**).
No horizontal expansion joint at shelf angles	Without horizontal expansion joints at regular intervals, brick "stacking" can occur, where the dead load from the bricks' self-weight is transferred from floor to floor. This can create high compressive stresses in the brick at lower elevations of a building. Additionally, differential movement between the brick and steel shelf angle due to thermal expansion and contraction cannot be accommodated, and brick cracking may occur (**Fig. 8**).
Gaps between shelf angles up to 12 in. wide (typically at column lines)	Discontinuous shelf angles allow for sections of the brick facade to remain completely unsupported for multiple floor levels, which may lead to brick cracking and spalling. This will also cause an increase in the dead load acting on installed shelf angles, possibly exceeding their structural capacity, and contribute to excessive rotation and/or deflection of shelf angles.
Gaps between shelf angles and concrete substrate	If gaps between the shelf angles and concrete substrate are not adequately shimmed, they promote rotation of the shelf angles (**Fig. 9**).
Loose bolt connections at shelf angles	Improper anchorage of shelf angles to the concrete backup structure can contribute to excessive rotation or deflection of shelf angles.
Less than two-thirds of brick depth bearing on shelf angles (typically at column lines)	The typically specified minimum required brick-bearing area is two-thirds of the brick depth. Less than two-thirds of the brick depth bearing on shelf angles may cause increased bearing stress, higher eccentricity, and subsequent outward bowing of the brick.
Loose, detached, or broken brick wall ties and helical ties	Without adequately anchored brick wall ties, lateral loads cannot be transferred to the backup concrete structure and the veneer may become unstable.
No waterproofing or air barrier observed	Without waterproofing components such as through-wall flashings at shelf angles, the shelf angles and connections are vulnerable to deterioration and corrosion from incidental water, which inevitably enters the brick cavity wall through mortar pinholes or other brick veneer defects.

Table 1. Observed issues that contributed to brick veneer distress

Figure 6. Vertical fractures and brick bearing less than two-thirds of the brick depth.

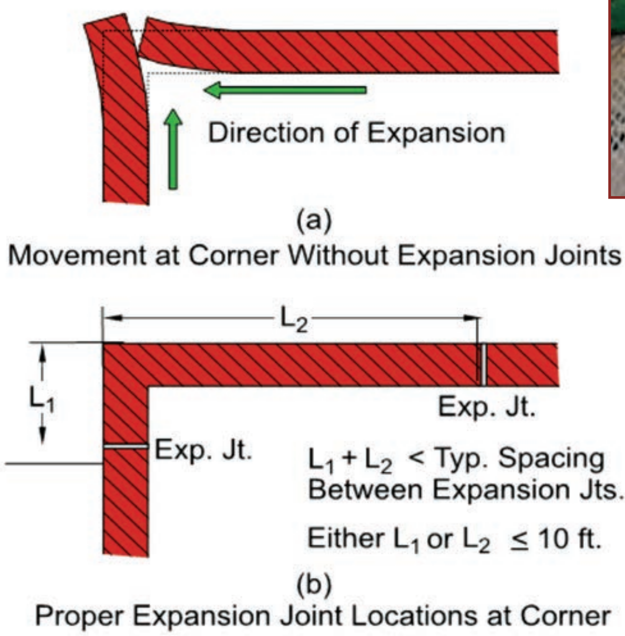

Figure 7. Vertical expansion joints at corners. Figure: Brick Industry Association Technical Note 18A, "Accommodating Brick Construction.

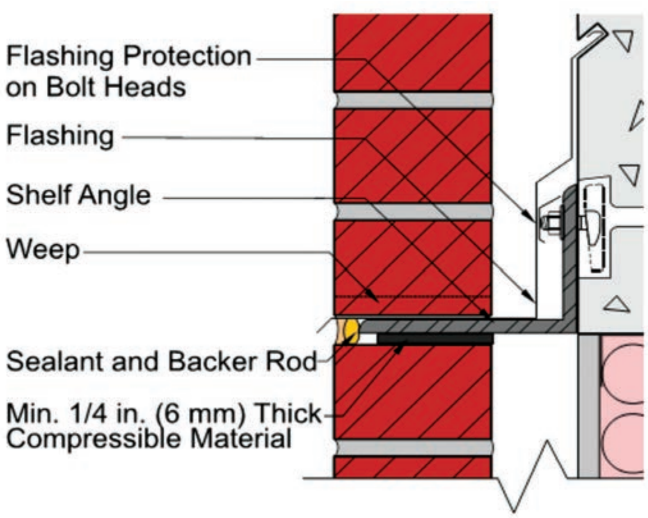

Figure 8. Expansion joint at shelf angle. Figure: Brick Industry Association Technical Note 18A, "Accommodating Brick Construction."

- Remove loose and unstable masonry.
- Install supplemental ties to reanchor and stabilize the veneer.
- Install safety netting across potential areas of concern.
- Install overhead protection scaffolding at walkways immediately adjacent to the building and at building access points.

The decision to implement a specific safety measure must be made based on specific project needs. The operational and financial impacts of implementing mitigation activities should also be considered. The owner also engaged our team to design a temporary brick stabilization/containment netting system to be used before more permanent repairs were made. However, the owner elected to not proceed with the temporary stabilization repairs, choosing instead to proceed directly with the partial brick recladding and brick repairs designed by our firm.

Exploratory Openings and As-Built Deficiencies

The team made 33 exploratory openings throughout the brick facade during the assessment to gain a better understanding of the existing as-built conditions. **Table 1** summarizes some of the as-built deficiencies observed at the exploratory openings, and how each was likely contributing to the observed distress. **Figures 6** through **9** illustrate selected concerns.

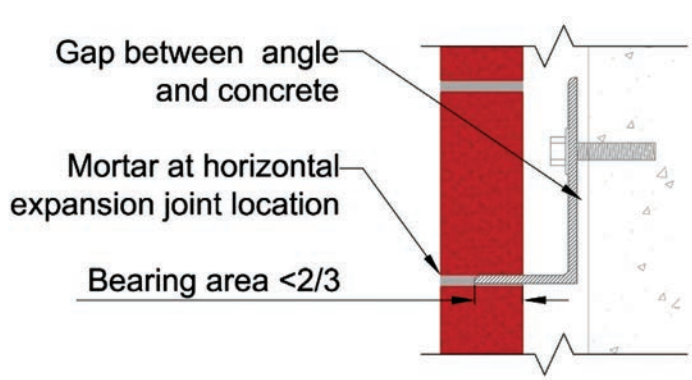

Figure 9. Typical as-built conditions at shelf angles observed through exploratory openings.

The conditions listed in Table 1 seemed to be contributing to the widespread observed brick distress in multiple ways, some of which were likely acting in tandem to exacerbate the negative effects on the veneer. The documentation obtained during the facade assessment revealed that the most severe distress conditions were present at exterior columns where the lack of horizontal expansion joints led to restraint cracking of the veneer. The team's evaluation of the field data clearly indicated that extensive facade repairs would be required to restore safety to the building facade. In addition, it was also apparent that the previous facade repair attempts had not been entirely successful because they did not include retrofitting of the existing deficient support conditions at shelf angles and because they did not include the incorporation of expansion joints into the veneer to accommodate movement.

DESIGN OF FACADE REPAIRS

Once the existing condition of the building was assessed and evaluated, our team was able to design an appropriate repair solution to address the existing distress and mitigate further deterioration of the brick veneer. The primary components of the repair design included the following:

- Removal and recladding of brick veneer in areas of excessive out-of-plane displacement (including removal of previously installed helical ties)
- Removal and replacement of shelf angles where brick veneer bearing was less than two-thirds of the brick depth (at column lines)
- Miscellaneous brick replacement and mortar joint repointing
- Installation of horizontal joints at new shelf angles
- Introduction of vertical expansion joints at building corners, offsets, and columns
- Installation of waterproofing and through-wall flashings at new shelf angles

Brick Recladding and Shelf Angle Replacement

The sections of brick with excessive out-of-plane displacement were observed at exterior columns and at select locations along floor lines in areas where the facade was fully clad with brick (areas without ribbon windows such as at stairwells). The brick veneer and existing shelf angles at these locations were demolished to install new shelf angles and brick (**Fig. 10**). In areas where brick demolition and recladding were not called for, limited brick replacement and mortar joint repointing were specified. This approach was selected so that the worst conditions were addressed without necessitating a full recladding of areas where no distress in the brick was observed. The final structural-support-repair design consisted of new shelf angles at each floor line with horizontal and vertical legs designed to support a greater amount of brick-bearing area than the original shelf angles supported.

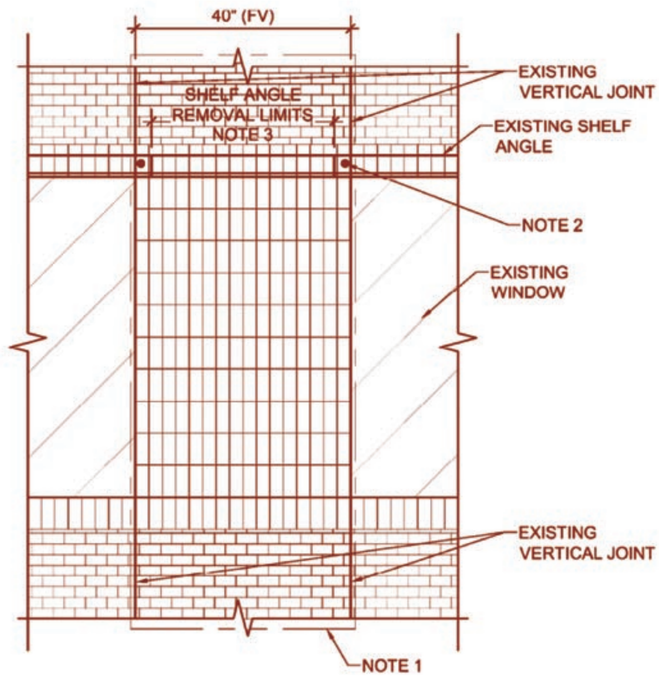

Figure 10. Example of typical detail included in repair documents for brick and shelf angle demolition at column lines.

Addition of Expansion Joints

The addition of adequately sized expansion joints in both the horizontal and vertical directions was an important aspect of the repair design to address the distress related to differential movements among the brick, steel shelf angles, and backup concrete structure. Vertical joints were located at building corners in accordance with Brick Industry Association guidelines.[2] Horizontal expansion joints were provided at each shelf angle and were sized based on total expected movement due to irreversible moisture expansion of brick, thermal expansion of brick, shelf angle deflection, and rotation of the shelf angle leg.

All building materials undergo volumetric changes due to variations in temperature and moisture. Building components move because of such volumetric changes as well as other factors such as material deformations under load. Restraint of such movement results in internal stresses and can lead to cracking of masonry elements.[3] To avoid cracks due to movement in masonry veneer construction, masonry veneer must be designed to accommodate movement without the buildup of internal stresses caused by restraint.

Irreversible moisture expansion of clay brick masonry (**Fig. 11**), thermal expansion and contraction of brick, creep of the concrete frame of the building, and shrinkage of concrete masonry and cast-in-place concrete members

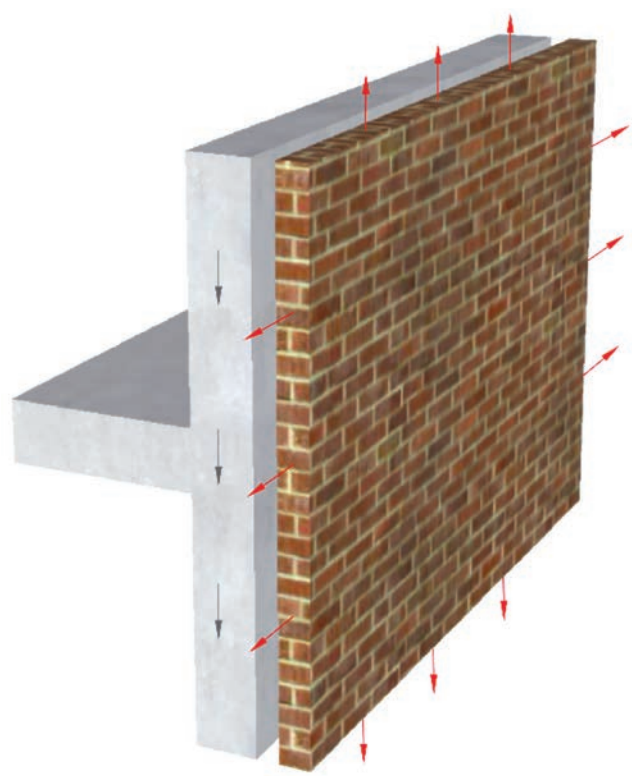

Figure 11. Brick expansion and contraction relative to structure.

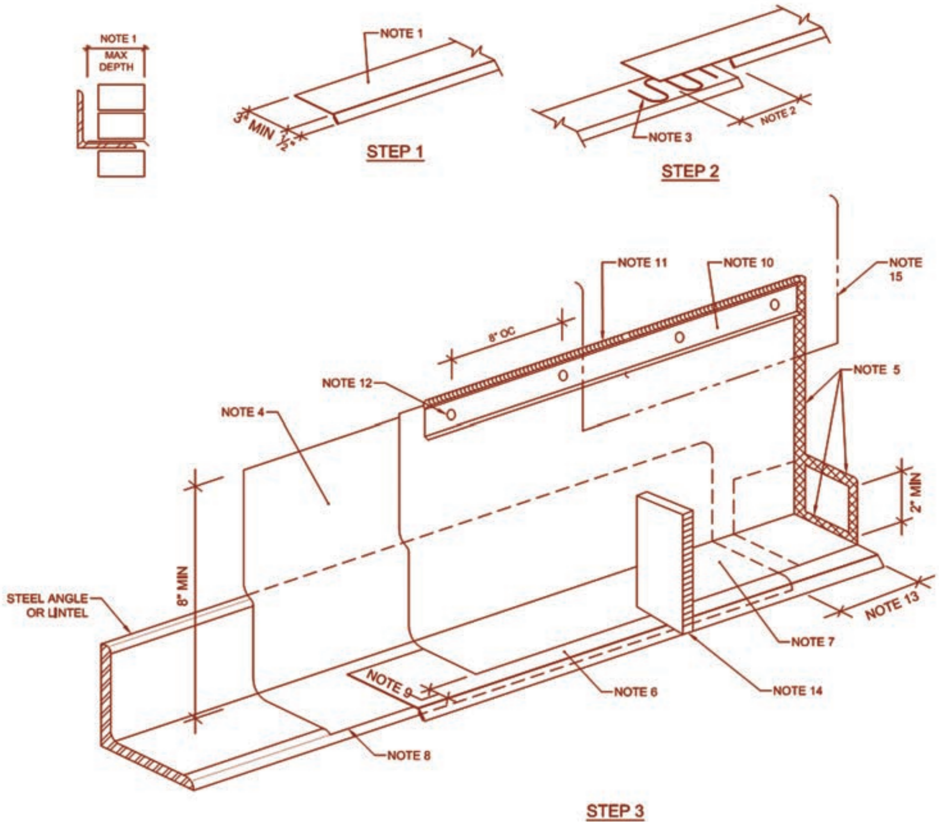

Figure 12. Shelf angle flashing detail.

were all factors in the differential movement that had occurred between the veneer and the structural backup at the West Pavilion building. Inadequate accommodation of this movement resulted in cracking, crushing, and out-of-plane displacement of the masonry.

To address these issues, the project team added vertical expansion joints at each corner and offset on the building facade. The design also included a horizontal expansion joint below each new shelf angle to ensure that movement would be accommodated where previous brick distress was observed.

Waterproofing

Installation of waterproofing was limited to new shelf angle locations to protect the angles and anchors from potential corrosion over time. Waterproofing had not been installed on the backup wall during the original construction of the building; however, removing all brick to install waterproofing at all existing shelf angle locations was not warranted or feasible given the lack of brick distress observed at areas apart from the columns and stair towers. Only at columns and at stair towers was there stacked brick over multiple floor levels, which was a primary contributor to the observed brick distress. At other areas, the brick veneer was separated by ribbon windows installed with perimeter joints, which accommodated brick movement in these areas. Thus, waterproofing installation during the repair project was limited to the locations between ribbon windows where brick recladding and shelf angle replacement was performed. It is possible that the existing shelf angles that remained in place could corrode in the future due to water that enters the brick veneer system; however, a global waterproofing installation repair program was not included in this scope of work. It is important to note that exploratory openings performed during our field assessment did not reveal corrosion of the existing shelf angles to be a problem.

The team installed waterproofing components at each new shelf angle to protect the structural supports from deterioration due to corrosion from incidental water, which could eventually enter the brick veneer system in the future. The design included through-wall metal flashings with a self-adhering membrane flashing, a termination bar, end dams, and vent-style weeps (**Fig. 12**).

CONSTRUCTION ADMINISTRATION CHALLENGES

After the brick facade repair documents were finalized, TGH sent out the design documents for bidding. Selecting a qualified contractor with prior experience related to brick veneer facade repair projects was of utmost importance. The contract was ultimately awarded to Western Specialty Contractors, a specialized restoration contractor based in Winter Park, Fla., and with offices across the United States. We provided construction administration services during the implementation of the repairs

Figure 13. Detached existing brick ties and unengaged helical ties observed at one wall section.

Description of RFI/issue	Resolution
Brick veneer section was destabilized during demolition. It was determined that existing brick ties and helical ties at large sections of brick were loose or completely detached (Fig. 13).	The contractor was directed to stop work immediately, and the brick veneer was temporarily stabilized. Extensive brick and shelf angle replacement was added to the scope of work at this section.
Positioning of existing shelf angles and shutter anchorage did not allow for standard shelf angle sizes.	Alternate shelf angle designs were provided, including inverted shelf angles and atypical horizontal leg profiles to accommodate specific existing conditions.
Existing shelf angles were installed into infill CMU walls rather than concrete framing structure.	Alternate bolt connections for the shelf angles were designed to be used in filled CMUs.
Excessive gaps were identified behind shelf angles.	Grout was installed behind the shelf angles, in lieu of installing shims, to provide greater support.
Excessive voids and gaps were found in the concrete or CMU substrate where shelf angles were to be anchored.	Concrete repair procedures were provided to the contractor on a case-by-case basis.
Brick wall cavity depths varied significantly throughout.	The contractor was required to have multiple shelf angle size options on-site to accommodate the different cavity depths.

CMU = concrete masonry unit; RFI = request for information.

Table 2. Sample of RFIs and resolutions during construction

to confirm compliance with the construction documents. Challenges faced during construction required timely responses from the owner, engineer and contractor to keep the hospital functional and safe throughout the repairs.

Inconsistent Original Construction

During demolition of the brick veneer at the specified areas on the facade, team members discovered a host of inconsistent conditions from original construction that could not be fully anticipated during the assessment phase. Because of this, several requests for information (RFIs) were issued throughout the project to address the distinctive conditions identified at multiple locations on the building facade such as detached existing brick ties (Fig. 13). Table 2 lists issues and resolutions addressed on-site through the RFI process.

Effective and organized communication among the owner, engineer, and contractor was critical to keeping the project on schedule and ensuring its success.

Hurricane Shutter Anchorage

One of the high-priority concerns that arose during construction was uncovered when the contractor noted that the hospital's hurricane panel shutters were not properly anchored to the concrete structure (Fig. 14). Considering the hospital's location on the Tampa Bay/Gulf of Mexico waterfront and the challenges associated with transporting patients, effective hurricane shutters would be important in the event of a hurricane. We quickly mobilized to the site to observe the reported deficiency and confirmed that the hurricane shutters were not adequately supported or anchored into the concrete structure. Rather, existing anchors were only secured into the brick veneer. If shutters are anchored into only the brick veneer, wind suction pressures acting on the shutters during a hurricane event will be transferred to the brick rather than the building's structural framing. This can lead to overstressing of the structural connections between the brick and concrete backup structure, leading to tie (anchor) fastener pullout, potential failure of the brick veneer and detachment of the protective shutters over windows.[4] This issue was particularly important to address for the hospital because many patients are unable to mobilize or relocate during a hurricane event.

New hurricane shutter anchorage supports were designed and included in the project scope of work over the course of a few weeks. The design consisted of new steel angles to be installed at the top and bottom of the panel shutters with bolts of sufficient length to anchor into the concrete backup structure behind the brick veneer. This repair allowed for the wind suction pressure acting on the shutters to transfer to the building's structural concrete framing, which is designed to withstand the wind pressures during a hurricane event.

Figure 14. Hurricane shutter anchorage was not attached to structure.

Overcoming COVID-19 Disruptions

In March 2020, while repairs were proceeding per schedule on the north elevation of the hospital building, Central Florida saw its first case of COVID-19. TGH serves the greater Tampa Bay area, which has suffered one of the highest rates of COVID-19 cases in Florida, and thus it was of vital importance that the construction work occurring on the building facade did not disrupt patient care. Because finishing the repairs on the building was important to restoring the safety of the building facade, the contractor did not stop work during this time and continued to push toward the scheduled project completion date. However, the repair work could no longer proceed as smoothly as before.

Several health safety measures were put into place at the hospital for all patients, visitors, staff, and vendors to help prevent the spread of COVID-19. Construction workers could no longer enter the hospital building (or its service elevators) to access the various roofs and elevations where swing stage equipment was stored and used to perform the facade repairs. Therefore, a series of multiple ladders were set up on the exterior of the building to provide access for the workers. The health safety measures also greatly restricted and made cumbersome the removal of heavy materials from demolition and overall mobilization of equipment for the workers. Because the hospital facilities staff was preoccupied with ensuring the hospital was running at its optimum level, they relied on the contractor and engineer to facilitate the repair project logistics and cooperate with new and changing on-site guidance throughout the several months that followed.

CONCLUSION

The project was completed in January 2021. TGH has expressed their gratitude and appreciation for both our and the contractor's diligent attention to restoring the hospital facade to safety throughout the project. As the hospital continues to serve the Tampa Bay area during an ongoing global pandemic, everyone can rest assured that patients, visitors, and staff are no longer vulnerable to overhead hazards from the hospital building facade.

The owner, engineer, and contractor involved with this project all learned several valuable lessons about brick veneer repairs during the assessment, design, and construction administration phases. A summary of these lessons is as follows:

- Take time to review facade design, assessment and repair documents.
- Investigate concealed conditions thoroughly before developing a repair plan.
- Integrate waterproofing and structural design of brick facades.
- Involve design professionals throughout construction to address unforeseen conditions with brick veneers that were constructed poorly.
- Design repairs that address the causes of distress.
- Establish effective communication among all parties during construction.
- Maintain project documentation for future reference.

Preventive measures taken by building owners are strongly recommended to avoid distress and the need for extensive repairs in the first place. Periodic evaluation and regular maintenance of buildings with brick veneer facades are critical to protecting the long-term durability of the structure as well as the safety of building occupants and passersby. We recommend that building owners evaluate the condition of new and existing exterior building facades once every five years to maintain the exterior walls in a safe condition. Ongoing building maintenance efforts such as joint sealant repair/replacement, brick mortar repointing, damaged brick replacement, and cleaning and coating of any exposed steel elements are also recommended to protect the structure from further deterioration.

REFERENCES

1. Brick Industry Association. 2003. "Wall Ties for Brick Masonry." Technical Note on Brick Construction 44B. https://www.gobrick.com/docs/default-source/read-research-documents/technicalnotes/44b-wall-ties-for-brick-masonry.pdf?sfvrsn=0.
2. Brick Industry Association. 2019. "Accommodating Expansion of Brickwork." Technical Note on Brick Construction 18A. https://www.gobrick.com/docs/default-source/read-research-documents/technicalnotes/tn18a.pdf?sfvrsn=0.
3. Brick Industry Association. 2019. "Volume Changes—Analysis and Effects of Movement." Technical Note on Brick Construction 18. https://www.gobrick.com/docs/default-source/read-research-documents/technicalnotes/tn18.pdf?sfvrsn=0.
4. Federal Emergency Management Agency. 2019. "Mitigation Assessment Team Report: Hurricane Harvey in Texas." Building Performance Observations, Recommendations, and Technical Guidance. https://www.fema.gov/sites/default/files/2020-07/mat-report_hurricane-harvey-texas.pdf.

Water Tower Place
Marble Facade Restoration

William D. Bast, PE, SE, SECB

SOCOTEC Engineering Inc. | Chicago, IL

wbast@lpiny.com

Lee Fink, AIA, LEED AP BD+C

SOCOTEC Engineering Inc. | Chicago, IL

lfink@lpiny.com

IIBEC 2022 - Building for the Future

International Convention and Trade Show

March 17–22, 2022 | Orlando, FL

ABSTRACT

Water Tower Place is a 74-story building constructed in 1976. The exterior facade is generally constructed of 1½-in.-thick Georgia Cherokee Solar Gray marble stone veneer panels, with flush aluminum-framed windows. The panels are typically restrained using stainless steel kerfs at the bottom corners or center of the panels, and stainless steel pins at the top and sides of the panels.

In December 2003, the owner was advised that bowing of the marble facade panels and presumed accompanying marble strength loss had accelerated after 25 years of slow but linear weakening—the marble had lost 30% of its strength in roughly 30 years.

This presentation reviews efforts to extend the facade's service life to 2025 or longer. After hundreds of strength tests were evaluated and an updated wind tunnel test was performed, nearly 17,000 custom repair anchors were installed in the building from 2007 through 2009. In the years since then, additional yearly examinations have been performed, along with additional stone testing. The repairs implemented nearly 20 years ago have kept the facade serviceable, and the future serviceable life is currently being studied.

SPEAKERS

William D. Bast, PE, SE, SECB

SOCOTEC Engineering Inc. | Chicago, IL

William D. Bast has been a practicing structural engineer for more than 35 years in Illinois, where he has led structural design teams in renovations at Wrigley Field, Navy Pier, and Willis Tower. His expertise includes building facade evaluations, renovations, and repairs. He also serves as an expert witness in disputes and lawsuits. Bast is a former president of the Structural Engineers Association of Illinois and the National Council of Structural Engineers Associations.

Lee Fink, AIA, LEED AP BD+C

SOCOTEC Engineering Inc. | Chicago, IL

Lee Fink is a senior consultant in the Building Envelope Division of SOCOTEC Engineering in Chicago, Ill. His areas of expertise include design and restoration of building enclosures that include masonry wall, glazing, metal cladding, and roofing systems. He has lead the exterior restoration of several postmodern high-rise buildings, including OneAmerica Tower and Rhodes Tower. Fink is chair leader on the Technical Issues Knowledge Committee for AIA Chicago and previously served as a professor at Northwestern University.

Water Tower Place Marble Facade Restoration

Water Tower Place is a 74-story, all-concrete structure building constructed in 1976; at 859 ft tall, it is currently the 11th tallest building in Chicago, Ill. The building was designed by architects from Loebl, Schlossman, Bennett, and Dart and Associates, along with C. F. Murphy engineers.

Thin-stone veneer construction, which was relatively new in 1976, was used for the tower facade. In 1975, the American Society of Heating, Refrigerating and Air-Conditioning Engineers (ASHRAE) published *Energy Conservation in New Building Design* (ASHRAE 90-75)[1] to help address concerns about escalating fossil fuel consumption in the United States. The standard included analysis methods and recommendations to improve the energy efficiency of buildings, including the use of insulation within exterior walls to improve thermal performance. Although the use of thin-stone veneer cladding in postmodern building designs accommodated thicker insulation layers behind the cladding, data regarding the durability of these thinner stone claddings and their associated connections were limited, as many of the support anchors were still undergoing development.

The exterior facade of Water Tower Place is generally clad with 1½-in.-thick Georgia Cherokee Solar Gray marble stone veneer panels, with flush aluminum-framed windows. The panels are typically restrained using stainless steel kerfs at the bottom corners or centers of the panels, and stainless steel pins at the tops and sides of the panels. Approximately 1 in. of insulation was placed directly behind the marble stone veneer in the original construction; much of this insulation has disintegrated over time (**Fig. 1**).

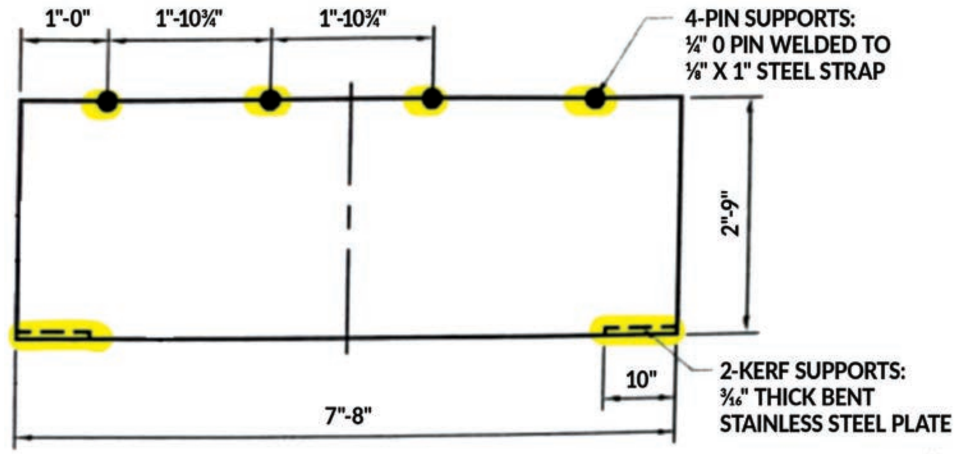

Figure 1. Elevation diagram indicating typical marble panel supports.

In 2021, the 180 East Pearson Homeowner's Association (owner) engaged LPI Inc., now known as SOCOTEC Engineering Inc., to provide a facade report for the facade of the condominium portion of Water Tower Place (floors 33 through 72) (**Fig. 2**).

The building is divided by occupancy type into three entities: the retail portion, the hotel portion, and the residential (condominium) portion. Each entity is responsible for conducting its own facade examinations to comply with the City of Chicago Exterior Wall Ordinance, Section 34(13-196-031) through 34(13-196-039), effective November 13, 2007, and the Rules and Regulations for

Figure 2. Water Tower Place's north elevation (left) and south elevation (right).

Figure 3. On-site marble bowing in relation to a straight 4 ft level.

Maintenance of High-Rise Exterior Walls and Enclosures, made effective by the City of Chicago Department of Buildings as of March 1, 2016.

Previous consultants for the owner have included Wiss, Janney, Elsner Associates Inc. (WJE), TEAM (Testing and Assessment of Marble and Limestone), Thornton Tomasetti Inc. (TT), and Raths, Raths & Johnson (RRJ). Before the 2021 evaluation project, LPI had not worked for the owner; however, the authors previously worked for TT, and they have been involved in the evaluation and maintenance of the Water Tower Place facade since 2006.

WJE served as the facade consultant to the owner and the other two entities until 2006. Based on WJE's material testing program, the owner was advised in December 2003 that bowing of the marble facade panels and presumed accompanying marble strength loss had accelerated after 25 years of slow but linear weakening.[2] In October 2004, WJE recommended pinning 100% of the 16,000 marble panels on the building, pending replacement of the marble facade in the forthcoming 3- to-5-year period, and advised that an additional 30% strength loss was predicted to occur during the next 6 to 10 years. On November 30, 2004, WJE submitted the Critical Examination to the City of Chicago in compliance with the Exterior Wall Ordinance. According to WJE's recommendations, selective marble replacement should have begun in 2005 (**Fig. 3**).

In January 2005, the owner engaged TEAM, a consortium of thin-stone marble professionals representing several leading partners in the European Union, to peer review a five-year study on marble deterioration. After performing independent stone testing from seven marble panels extracted from Water Tower Place, TEAM submitted a draft report in June 2005, stating that they expected additional strength loss of ±1% per year, rather than the loss of 30% over the next 6 to 10 years indicated by WJE.

In August 2006, the owner engaged TT to serve as the facade engineer of record. After performing two scaffold inspections in October 2006, TT prepared and submitted an Ongoing Examination Report to the City of Chicago on November 1, 2006. On December 15, 2006, TT issued their draft report, "2006 Structural Evaluation and Repair Recommendations for the Marble Facade."[3] This report concluded that repairs in the form of custom anchors laterally supporting the veneer panels could extend the panels' serviceable life for approximately 20 or more years.

Upon the recommendation of TT, the Boundary Layer Wind Tunnel Laboratory performed a wind tunnel study on Water Tower Place and published their findings on April 12, 2007.[4] The study determined the 50-year return period mean hourly gradient wind speed to be 92 mph (at a height typically 1000 to 2000 ft above the earth's surface). Corresponding wind pressures between 30 and 50 lb/ft^2, and wind suctions between 30 and 90 lb/ft^2 were predicted. Typical suctions of up to 60 lb/ft^2 were predicted for most of the facade, with the higher suctions between 60 and 90 lb/ft^2 occurring at the corners of the building.

Informed by the wind tunnel results and other findings, TT worked with Construction

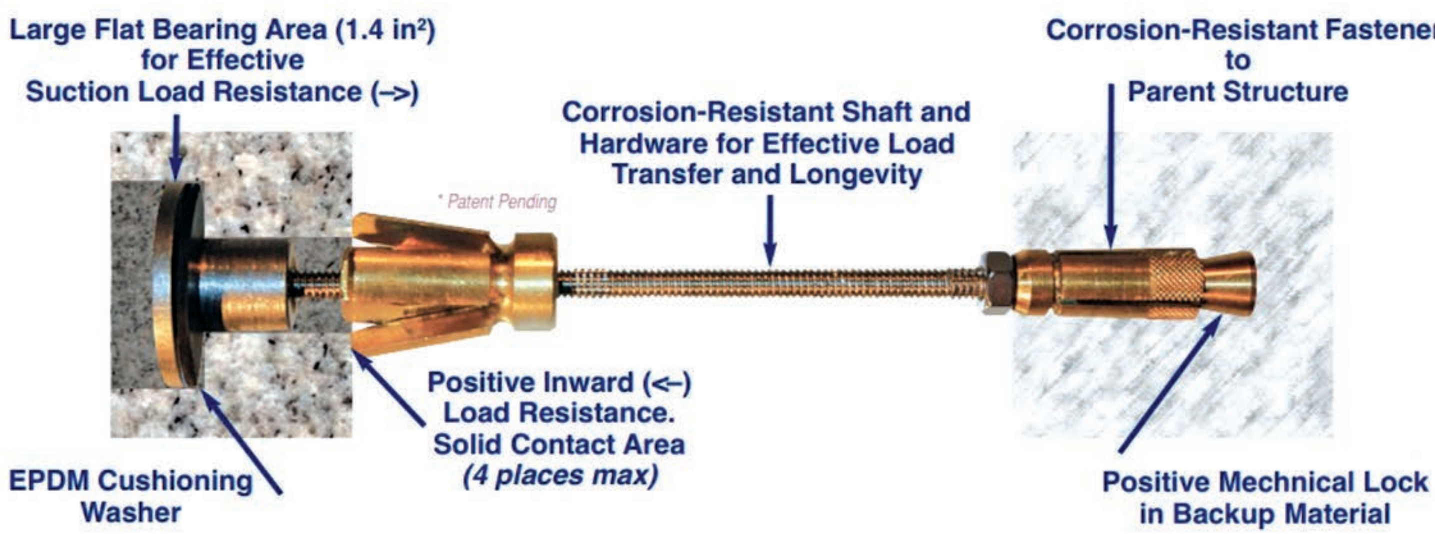

Figure 4. General diagram of the custom anchor. EPDM = ethylene propylene diene monomer (a synthetic rubber). Figure: Prosoco CTP Stone Grip-Tie (prosoco.com/product/stone-grip-tie).

Figure 5. Overview of custom stone anchors installed on the marble facade.

Tie Products (CTP) to develop a custom anchor for use on the building, rather than using the helical anchors or expansion anchors employed in WJE's previous repair campaigns. The custom anchors were designed to resist wind pressure or suction only (not gravity load) and were to be positioned within the spandrel and column panels to limit flexural stresses to 224 psi in the main field of the stone away from support conditions, and 393 psi near the stone kerfs, pins, or anchors (**Fig. 4**). The custom anchor design ignored the existing helical or expansion anchors. The flexural stresses were based on the expected average ultimate flexural strength of the stone in 2025 (447 psi), assuming a 1% degradation per year starting from 2004.

In October 2007, the first of the approximately 16,800 custom anchors were installed (**Fig. 5**). Anchor installation continued through 2008 and was completed in the summer of 2009. In September 2009, it was agreed that ongoing scaffold inspections of Water Tower Place should occur such that one-third of the total of 20 drops would be conducted each year.

In October 2009, TT had stone samples removed from the building for testing by the Tile Council of North America (TCNA) in South Carolina. The test results indicated continued deterioration of the marble strength at a rate of approximately 1% per year.

In February 2011, RRJ was engaged to replace TT as the facade engineer of record and to complete the 2008 and 2010 Ongoing Examination Reports. RRJ observed that some of the white ethylene propylene diene monomer (EPDM, a synthetic rubber) washers of the custom anchors had turned light brown, and that some washers exhibited cracking along their perimeters. In March 2012, CTP concluded that the EPDM washer material was substantially diluted with fillers and the washers were degrading as the result of environmental conditions.

TT returned as the facade engineer of record and submitted Ongoing Examination Reports from 2011 through 2020. In 2016, TCNA again conducted stone testing, and TT concluded that the test results indicated an average ultimate flexural strength of 710 psi, which represented a strength loss of 14 psi (1.2%) per year from the marble's initial ultimate strength of 1200 psi specified in 1976.[5]

REVIEW OF WJE AND TEAM TESTING AND INSPECTIONS BEFORE 2006

WJE and TEAM conducted stone testing on Water Tower Place until 2006. WJE's testing was reported on November 23, 2004, and November 17, 2006. TEAM's testing was reported on October 11, 2005.

WJE took panel bow measurements during their inspections of Water Tower Place and measured bowing up to approximately 1 in. within the panels. Except for portions of the west elevation, the bowing was within the allowable tolerance of ⅛ in. per 4 ft established by the Marble Institute of America. However, WJE recommended and provided oversight for pinning the panels on all four elevations.

In 2004, WJE removed 21 marble panels for testing and used a four-point bend test setup per ASTM C880, *Standard Test Method for Flexural Strength of Dimension Stone*.[6] This test setup produces pure bending with no shear between the middle loading points. For the 492 tests conducted, the average ultimate flexural strength was 718 psi. WJE also tested the strengths of the kerfs and pins.

In 2005, TEAM removed seven marble panels for testing and used a three-point bend test setup. This test setup produces bending with shear, and the tests generally yielded higher flexural strengths than the four-point test. For the 18 tests conducted, the average ultimate flexural strength was 1204 psi.

WJE subsequently performed additional tests and reported on November 17, 2006, that the average ultimate flexural strength in those tests was 651 psi.

REVIEW OF TT'S 2006 REPORT AND CUSTOM REPAIR ANCHORS INSTALLATION

TT did not conduct additional testing when they prepared their December 15, 2006, report. Instead, they used ASTM E122, *Standard Practice for Calculating Sample Size to Estimate, with a Specified Tolerable Error, the Average for Characteristic of a Lot or Process*,[7] to compute a "true" average from the existing test results of WJE and TEAM, considering the stone sample sizes and the measured average standard deviations. From WJE's test results in the field of the marble panels, TT considered data for samples away from the support points, where flexural stresses dominate. From TEAM's test results, TT considered data for samples near the supports, where a combination of flexural and shear stresses is present. These considerations yielded a "true" average flexural strength of 699 psi in the field of the stone, and 1066 psi in the vicinity of the pin and kerf supports.

Using this methodology, TT assumed strength degradation would continue at a rate of 1% per year and forecast that the ultimate flexural strength would be reduced to 447 psi by 2024. They further recommended a stone factor of safety of 2 be used to design supplemental anchors to resist wind pressures and suctions.

TT also created finite element model analyses to study the stone stresses under the following wind pressures or suctions:

- 33 lb/ft^2 per the original drawings and 1973 Chicago Building Code
- 46 lb/ft^2 as prescribed in 2004 during phase I repairs by WJE for typical wind zone panels
- 50 lb/ft^2 per the wind tunnel study conducted in 1973[8]
- 55 lb/ft^2 as prescribed in 2004 for the high-wind zone (corner) panels.

A thermal analysis considering a temperature change of 90°F was also conducted. Panel types F, C, E, and B were studied. Panel type F is the typical spandrel panel; Panel type C is the typical column panel, and Panel types E and B are variations on the column panel.

Based on the above analysis and considerations, TT recommended the following:

- Approximately 5600 repair anchors should be installed in 2007. This recommendation was based on the wind pressures or suctions noted previously. The number of repair anchors was later increased from 5600 to 16,800 as a result of the wind tunnel study that followed the TT report. The wind tunnel study found suctions up to 90 lb/ft^2, indicating the need for significantly more anchors than originally estimated.
- The marble facade should be monitored every year following the repairs.
- Stone testing should be done again in 8 to 10 years.
- Application of a water repellant to the stone should be considered.
- A wind tunnel study should be conducted to refine understanding of the wind pressures on the building.

Year	Examination description
2004	• WJE Critical Examination
2006	• TT ongoing examination, south and west, no specific comments noted
2008	• RRJ evaluation of Drops 1–5, 11–15, 18–20
2009	• RRJ evaluation of Drops 6–10, 16, 17
2011	• EPDM washers reviewed and torque tests performed
2012	• TT evaluation of 13 drops on north, west, and south elevations • Evaluation includes 38 locations where 53 custom anchors were installed
2013	• TT evaluation of south and east elevations, Drops 1–5, 9, and 10 • 53 repair anchors added • Cracks routed and sealed • 140 torque tests, with 9 tests <50 in.-lb
2014	• TT evaluation of Drop 11 on west elevation • Evaluation included 6 locations where 9 anchors were added
2015	• TT evaluation of north and west elevations, Drops 12–20 • Evaluation includes 6 locations where 7 custom repair anchors and 1 helical anchor were added • 180 torque tests (20 in.-lb), with 8 tests <20 in.-lb; no construction adhesive is noted at these test locations • 9 EPDM washers removed • 6 panels observed previously were removed and replaced with plywood • Observed stress cracks/propagation of existing cracks that appear through-thickness • Fissure cracks seem surficial, are pinned if necessary
2017	• TT evaluation of south and west elevations, Drops 4–11
2018	• TT evaluation of Drops 1–3, 12, 13, east and west elevations
2020	• TT evaluation of Drops 4–11 • 4 custom anchors added • 4 cracks routed and sealed • 160 torque tests, with 9 tests <20 in.-lb
2021	• LPI evaluation of Drops 1, 6, 8, 12, 15, 19 • 0 custom anchors added • 0 cracks routed and sealed • 12 cracks at top pin locations sealed • 5 custom anchor washer perimeters to be sealed • 120 torque tests, with 4 tests <20 in.-lb

EPDM = ethylene propylene diene monomer; LPI = LPI Inc.; RRJ = Raths, Raths & Johnson; TT = Thornton Tomasetti Inc.; WJE = Wiss, Janney, Elsner Associates Inc.

Table 1. Timeline of examinations, 2004–2021

SUMMARY OF INSPECTION REPORTS AND STONE TESTING SINCE 2004

Inspection Reports Since 2004

Table 1 presents a brief overview of the inspection reports available in the project files since 2004. See **Fig. 6** for a scaffold drop reference plan.

Based on our observations as well as those of the previous consultants, we conclude that the marble facade remains in a serviceable condition. Ongoing examinations and maintenance have not revealed an acceleration in the bowing or cracking of the panels, loosening of the restoration anchors, or significant deterioration of the EPDM washers of the custom restoration anchors installed between 2007 and 2009.

Bowing of the panels does not seem to have increased in severity since bowing was first observed in or before 2003, and, as previously noted, the extent of the bowing observed and measured is within the allowable tolerance of ⅛ in. per 4 ft established by the Marble Institute of America, except at portions of the west elevation. Further, one of the phenomena discovered by TEAM and subsequently accepted by WJE is that there does not seem to be a correlation between the amount of bowing and the amount of strength loss. Therefore, bowing measurements have not been taken in recent years.

Causes of the cracking observed in the marble panels typically falls into the following three categories:

- Stone anchor dowel–related cracks: At the locations where dowels or pins were used to attach the stone units around the outer perimeter, small cracks (approximately 1⁄32 in. wide × ≤2 in. long) have occasionally been observed since 2007, with the most recent observations in 2021 (Fig. 7). The dowel cracks are typically short and narrow and should be monitored during future inspections. For waterproofing purposes, the cracks have been sealed with surface-applied sealant. Routing and sealing of the cracks have not been recommended because doing so could reduce the stone capacity where it is supported by the dowels or pins. The cracking at the dowel locations at the tops and sides of the panels seems to be related to water intrusion and freezing-and-thawing damage, rather than stress related.

- Stress cracks: Stress cracks do not seem to be related to a physical attachment (dowel, kerf, etc.) (Fig. 8). The cracks can potentially be attributed to a combination of one or more of the following: propagation of preexisting cracks, the natural degradation of the marble stone, localized restraint within the stone panels from additional anchorage, thermal movement of the stone panels, or localized failure

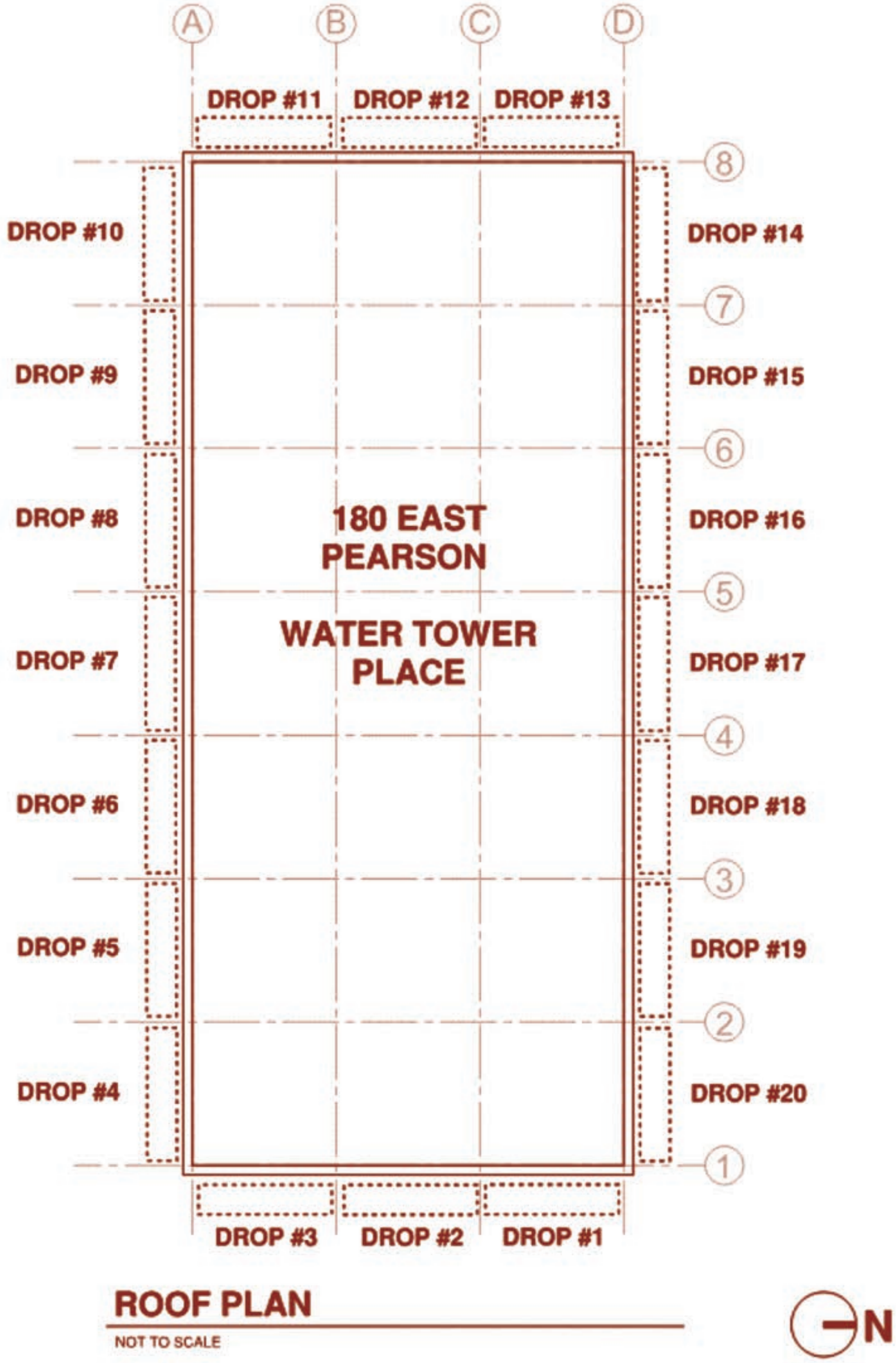

Figure 6. Scaffold drop reference plan.

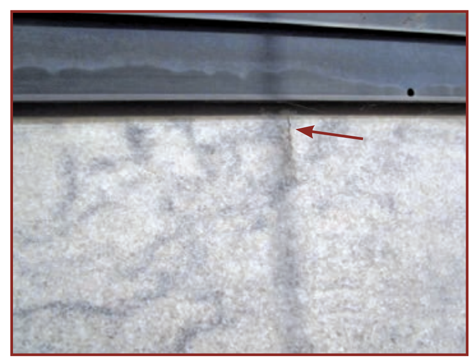

Figure 7. Typical dowel-related crack (at arrow).

Figure 8. Typical stress crack that has been routed and sealed.

Based on our observations as well as those of the previous consultants, we conclude that the marble facade remains in a serviceable condition.

when stone is subjected to wind pressure or suction. Inspectors have typically indicated that the stress cracks seem to be through-thickness cracks. The stress cracks observed have been pinned such that at least one anchor is present on either side of the crack. Anchors used for this purpose are either the CTP custom anchors or helical anchors, depending on the area of the unsupported stone.

- Fissure cracks: Marble stone naturally has veining, which is a result of variations in the different minerals that comprise the stone (**Fig. 9**). In some cases, the veins contain a concentration of minerals that create a weaker plane. A weak vein, or a striation through the marble that has weaker characteristics than the main body of the marble, is identified as a fissure. Fissure cracks typically appear to be surficial cracks. Relatively large fissure cracks have been pinned, if necessary, so that at least one anchor is present on either side of the fissure. Anchors used for this purpose are either the CTP custom anchors or helical anchors, depending on the area of the unsupported stone. Other fissure cracks should be monitored during future inspections.

Since the installation of the custom restoration anchors between 2007 and 2009, a torque wrench has been used to test the stainless steel flat heads of typically 20 custom anchors randomly selected at each drop. The wrench is equipped with a dial gauge that measures the torque. At each of the tested anchors, the torque wrench was used to measure the loosening torque (counterclockwise rotation). Each anchor was tested to a torque of a minimum of 20 in.-lb. If the anchor did not move at this torque, it was deemed as sufficiently installed. This type of testing, which has been performed typically since 2009, has demonstrated that the restoration anchors and their stainless steel flat heads have not loosened. A small percentage of the anchor heads failed to achieve the torque of 20 in.-lb. In many of those cases, it was observed that the low-viscosity construction adhesive had been applied but flowed out of the flat head receiver during installation; as a result, only a small amount of construction adhesive was in contact with the fastener components (**Fig. 10**).

Figure 9. Typical fissure crack.

Among the key concerns about the custom restoration anchors was whether they would restrain the panels from bowing and in so doing create stress cracks within the panels. TT studied this problem by inducing the observed bowing (up to 1 in.) into the analytical models to understand the magnitude of stress that such deformation would create. They found that the panels would rupture under such deformation. Because this had not occurred and signs of it had not been observed in the field, TT concluded that the panels undergo stress relief, such that the bowing occurs but does not create residual stresses within the marble. In other words, the panels bow into a certain shape, but little if any residual stress develops within the marble. Therefore, new restraints such as the custom restoration anchors would create new deformed shape patterns for the marble, but they would not induce cracking.

In previous inspections, it was reported that the white EPDM washers used as part of the CTP custom anchors had deteriorated. Based on our observations in the field, we have concluded that the apparent deterioration seems to be limited to discoloring of the EPDM surfaces, surficial or partial-depth cracking ("alligatoring") along a portion of the washer's outer exposed perimeter, and minor deterioration against spalled marble surfaces.

Figure 10. Installed custom stone anchor into the marble cladding (left) and torque testing (right).

Possible causes of the cracking include inferior EPDM material composition, ultraviolet radiation from the sun, and chemical attack (for example, from chlorine and other window-washing chemicals). The level of deterioration we observed seems consistent with that found in previous inspections and is not of concern to us at this time. Several of the most deteriorated washers were torque tested in recent inspections, including inspections in 2021, and nearly all the washers have helped hold the anchor flat head tight to the threaded rod, as intended.

Stone Testing Since 2004

As noted previously, WJE removed 21 marble panels for testing in 2004 and used a four-point bend test setup per ASTM C880.[6] This test setup produces pure bending with no shear between the middle loading points. In the 492 tests conducted, the average ultimate flexural strength was 718 psi.

In WJE's November 17, 2006, testing report, the average test result was 651 psi. The TCNA testing commissioned by TT in 2009 yielded an average test result of 624 psi.

The 2016 test results, also by TCNA and TT, yielded an average ultimate flexural strength of 710 psi (range 443 to 1165 psi). The average was derived using samples from the same 10 panels as the 2009 tests (4 north, 4 south, and 2 west panels, with the 10 pieces yielding 20 test specimens).

Figure 11 presents the graphical depiction of these results.

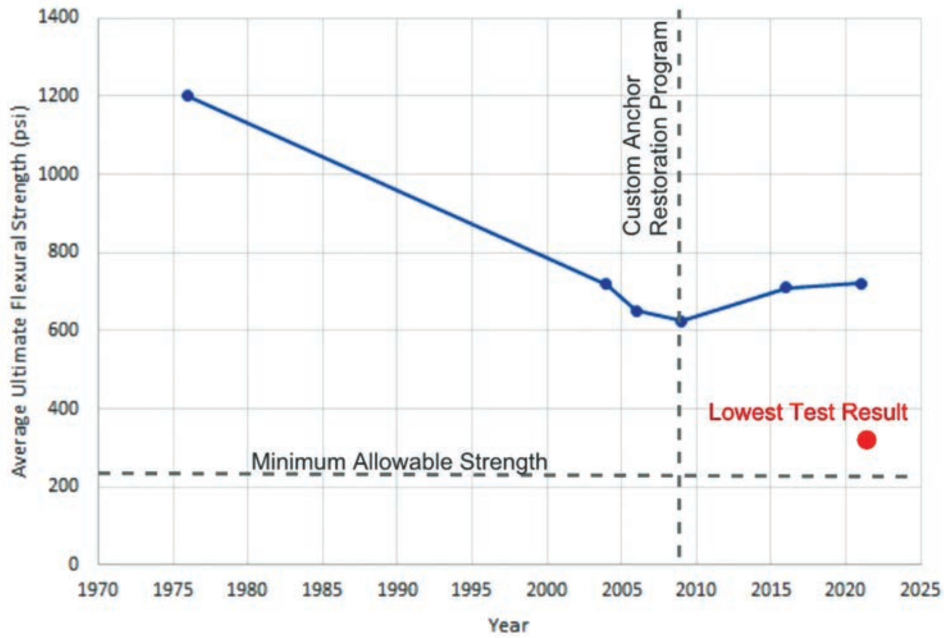

Figure 11. Average ultimate flexural strengths from stone testing.

RESULTS OF 2021 STRUCTURAL ANALYSIS AND STONE TESTING

Stone sampling was performed in April 2021 by removing 10 stone samples from the same 10 panels that had been sampled in 2009 and in 2016:

- Drop 6: floor 44, Panel C type (column); floor 63, Panel F type (spandrel)
- Drop 8: floor 56, Panel F type; floor 66, Panel C type
- Drop 12: floor 46, Panel F type; floor 71, Panel C type
- Drop 15: floor 37, Panel F type; floor 49, Panel C type
- Drop 19: floor 57, Panel C type; floor 68, Panel F type

Before the contractor, Western Specialty Contractors, removed the stone samples, LPI conducted the closehand facade examination from the six scaffold drops described previously.

Concurrent with the facade examination, LPI undertook the structural analysis of Panels C and F to update a subset of the analysis first performed by TT in 2006. This analysis included the consideration of additional removal of portions of the stone panels. The updated analysis noted that, under comparative wind suctions of 55 lb/ft^2, S_x stresses (tensile stresses in the horizontal direction of the panel) of up to 465 psi were calculated near the ends of the bottom kerf supports. This magnitude of stress is about 18% greater than the 393-psi limitation of flexural stress in the vicinity of a support condition considered in previous analyses. However, cracking of the stone panels in the vicinity of the bottom kerf supports (10 in. from the bottom edge ends of Panel F) has not been observed. It is possible that our analytical finite element modeling of the kerf supports is more rigid, and consequently more highly stressed, than the actual connection, which has some tolerance between the stone kerf cut and the stainless steel kerf support. Cracking near the top pin supports of Panel F, on the other hand, has been observed on multiple occasions by other consultants and by us, but these cracks have been relatively narrow (less than or equal to 1⁄32 in.) and they do not seem to be occurring at a significantly increasing rate. The examination of Drop 1 in 2021, where much of the elevation has estimated wind suctions up to 90 lb/ft^2, did not exhibit any observable amount of significant cracking at either the support conditions or within the main body of the panels themselves.

Ten stone samples were removed from the 10 panels noted previously. These 10 samples resulted in 20 test specimens, which were sent to TCNA in May 2021 for testing.

Using samples from the same panels as the 2009 and 2016 tests (4 north, 4 south, and 2 west panels, with the 10 pieces yielding 20 test specimens), the 2021 test results yielded an average ultimate flexural strength of 721 psi (range 377 to 1155 psi). The minimum test result was slightly lower than the minimum from 2016, and the standard deviation for these tests was relatively high due to the anisotropic and nonhomogeneous nature of the marble.

SUMMARY AND CONCLUSIONS

From the 2021 findings, we conclude that the marble strength seems to have plateaued at a strength level that represents about 58% of the initial marble strength (or a loss of 42% of initial strength, about 0.9% per year). We also conclude that this level of capacity is sufficient with the number of anchors installed between 2007 and 2009 to portend an indefinite service life.

Thin-stone cladding was a new use of an old material when it was first employed during postmodern construction, and its durability was generally unknown. Over the past few decades, postmodern building facades such as that at Water Tower Place have exhibited systemic distress due to bowing, weakening, and anchorage problems. However, not all systemic problems require full replacement of the facade. Some may be remediated with cost-effective and durable in situ solutions that maintain the general aesthetics of the original design.

REFERENCES

1. American Society of Heating, Refrigerating and Air Conditioning Engineers (ASHRAE). 1975. *Energy Conservation in New Building Design*. ASHRAE 90-75. Peachtree Corners, GA: ASHRAE.
2. Rivkin, C. T. Maintenance and Repair Chronology: 2003-2012.
3. Bast, Nacheman, and Renetskis (Thornton Tomasetti). 2006. Structural Evaluation and Repair Recommendations for the Marble Facade (draft). December 15, 2006.
4. Vis, Garnham, and Galsworthy (The Boundary Layer Wind Tunnel Laboratory). A Study of Wind Effects for Water Tower Place Chicago. April 12, 2007.
5. Prikazsky, Rohr, and Bast (Thornton Tomasetti). 2015. Facade Examination of North and West Elevations and Materials Testing. May 2, 2016.
6. ASTM International. 1998. *Standard Test Method for Flexural Strength of Dimension Stone*. ASTM C880-98. West Conshohocken, PA: ASTM International. https://doi.org/10.1520/C0880-98.
7. ASTM International. 2000. *Standard Practice for Calculating Sample Size to Estimate, With a Specified Tolerable Error, the Average for Characteristic of a Lot or Process*. ASTM E122-00. West Conshohocken, PA: ASTM International. https://doi.org/10.1520/E0122-00.
8. Loebl, Schlossman, Bennett, and Dart and Associates, and C. F. Murphy. Wind Tunnel Results—Wind Pressure Isopleths. November 26, 1973.

Assessing the Performance, Application, and Cost of Retrofit Wall Systems for Residential Buildings

André Desjarlais, FASTM

Oak Ridge National Laboratory | Oak Ridge, TN

desjarlaisa@ornl.gov

IIBEC 2022 - Building for the Future

International Convention and Trade Show

March 17–22, 2022 | Orlando, FL

ABSTRACT

The Oak Ridge National Laboratory, Pacific Northwest National Laboratory, and the University of Minnesota have been conducting a three-year study of residential retrofit wall systems. The researchers have identified, tested, and verified the hygrothermal performance of 16 wall assemblies in retrofit applications. The approach to this study includes a comprehensive literature review, the involvement of an advisory group of thermal enclosure experts, small-scale experimental in situ testing of the wall assemblies at the University of Minnesota's Cloquet Residential Research Facility, and energy and hygrothermal simulation of wall assemblies using EnergyPlus, THERM, and WUFI. Simulation and experimental results are then combined with an economic analysis to produce a techno-economic study of residential wall systems for deep energy retrofits.

This presentation summarizes the findings of this research project and is intended to guide architects and designers on how to retrofit existing wall assemblies without creating durability issues.

SPEAKER

André Desjarlais, FASTM

Oak Ridge National Laboratory | Oak Ridge, TN

André Desjarlais is the program manager for the Residential Buildings Integration Program at the Oak Ridge National Laboratory and has been involved in building enclosure research for 48 years. His areas of expertise include building enclosure energy efficiency, moisture control, and durability. Desjarlais has been a member of ASTM International since 1987, is the past chair of ASTM Committee C16, and was awarded the title of ASTM Fellow in 2011. He has been a member of ASHRAE since 1991 and is past chair of ASHRAE Technical Committee 4.4 on Thermal Insulation and Building Systems. Desjarlais is also a founding director of the RCI-IIBEC Foundation.

Nonpresenting Coauthors

Anthony Aldykiewicz
Anthony Aldykiewicz is a senior R&D staff member with Oak Ridge National Laboratory in Oak Ridge, TN.

Chrissi Antonopoulos
Chrissi Antonopoulos is an economist with Pacific Northwest National Laboratory in Portland, OR.

Cheryn Metzger
Cheryn Metzger is an advisor with Pacific Northwest National Laboratory in Helena, MT.

Jian Zhang
Jian Zhang is a mechanical engineer with Pacific Northwest National Laboratory in Richland, WA.

Tyler Pilet
Tyler Pilet is a research engineer with Pacific Northwest National Laboratory in New Orleans, LA.

Sumitrra Ganguli
Sumitrra Ganguli is an economist with Pacific Northwest National Laboratory in Richland, WA.

Travis Ashley
Travis Ashley is a cyber security engineer with Pacific Northwest National Laboratory in Richland, WA.

Harshil Nagda
Harshil Nagda is a mechanical engineer with Pacific Northwest National Laboratory in Richland, WA.

Patricia Gunderson
Patricia Gunderson is a systems engineer with Pacific Northwest National Laboratory in Upper Marlboro, MD.

Philip Jensen
Philip Jensen is a nuclear engineer with Pacific Northwest National Laboratory in Richland, WA.

Patrick Huelman
Patrick Huelman is an associate extension professor with the University of Minnesota in St. Paul, MN.

Garrett Mosiman
Garrett Mosiman is a senior research fellow with the University of Minnesota in Minneapolis, MN.

Rolf Jacobson
Rolf Jacobson is a research fellow with the University of Minnesota in Minneapolis, MN.

Fatih Evren
Fatih Evren is a research assistant with the University of Minnesota in Minneapolis, MN.

Assessing the Performance, Application, and Cost of Retrofit Wall Systems for Residential Buildings

In the United States, 39% of total energy is consumed by the building sector, and 20% of that total is attributed to residential buildings.[1] Newly constructed houses built to meet modern energy codes incorporate a combination of tight, well-insulated building enclosure components, high-performing windows, controlled mechanical ventilation, and other efficient components that deliver comfort, adequate airflow, and moisture control in addition to significantly lower energy consumption than ever before.

Older houses (those built before 1992 when the U.S. Department of Energy [DOE] Building Energy Codes Program was established) represent approximately 68% of the U.S. residential building stock,[2,3] and these structures often have significant air leakage and inadequate insulation. In residences with little to no air sealing or insulation, heating and cooling losses can represent a substantial portion of utility bills.

The residential remodeling market continues to grow, amounting to $424 billion in 2017 (up 50% from 2010). In 2017, approximately 50% of home improvement projects included upgrades to mechanical and enclosure systems in aging housing stock (made up of approximately 93% wood-framed walls, 5% masonry, and 2% steel framing).[4] These upgrades include replacement of windows and doors; siding and roofing; heating, ventilation, and air-conditioning (HVAC) systems; and insulation. Approximately one in five homeowners have invested in energy efficiency retrofits.[4] Even so, the number of existing residential buildings with little to no insulation is staggering. An estimated 34.5 million houses with wood studs have no wall insulation,[5] representing approximately 38% of existing single-family detached houses in the United States. Similarly, 71% of existing houses have air leakage rates of 10 or more air changes per hour at 1.04 lb/ft^2 (50 Pa) of pressure, indicating a significant amount of air leakage through the building enclosure.[4]

There is a significant need for cost-effective methods of increasing wall insulation and reducing air infiltration for existing houses. In current practice, wall retrofits seldom include the air, moisture, and vapor controls that are considered best practices for high-performance new home construction, and the lack of such controls could potentially create problems that put the building materials or occupants at risk. Well-tested and documented retrofit wall systems can help save substantial amounts of energy and improve home durability, comfort, health, and resilience. Done correctly, deep energy retrofits (DERs) can significantly improve the energy and air-barrier performance of a building's thermal enclosure, help manage indoor environmental pollutants, improve the building's aesthetics, and increase homeowner comfort.

This paper describes a three-year DOE-funded project to identify high-performing wall retrofit systems and provide a real-world context for their thermal, moisture, and economic performance that can aid decision makers in balancing various goals for DERs.

> Done correctly, deep energy retrofits can significantly improve the energy and air-barrier performance of a building's thermal enclosure, help manage indoor environmental pollutants, improve the building's aesthetics, and increase homeowner comfort.

INDUSTRY INPUT AND LITERATURE SURVEY

As an initial step in this project, the research team invited experts from industry, academia, the national laboratories, and other research organizations to join an expert advisory committee and participate in an expert meeting to help identify and characterize candidate wall systems. The meeting was held on April 19, 2019, in Arlington, Va., with 33 experts in attendance. A report summarizing this meeting was published.[6]

The objectives of this meeting were to bring together leading researchers and innovators to review the research methodology and to encourage suggestions, information sharing, and collaboration. The meeting's outcomes would inform potential retrofit systems to be developed and tested. Specific topics discussed in detail included data characterization for proposed wall selections, wall selection for subsequent in situ testing, and techno-economic study criteria.

The literature review[7] was conducted and published in June 2019. It provides an overview of the thermal and moisture performance of wall assemblies, identifies relevant research, and summarizes current practices for exterior wall retrofits for existing houses, focusing on retrofit applications to the exterior side of a wall assembly. Given that the vast majority of

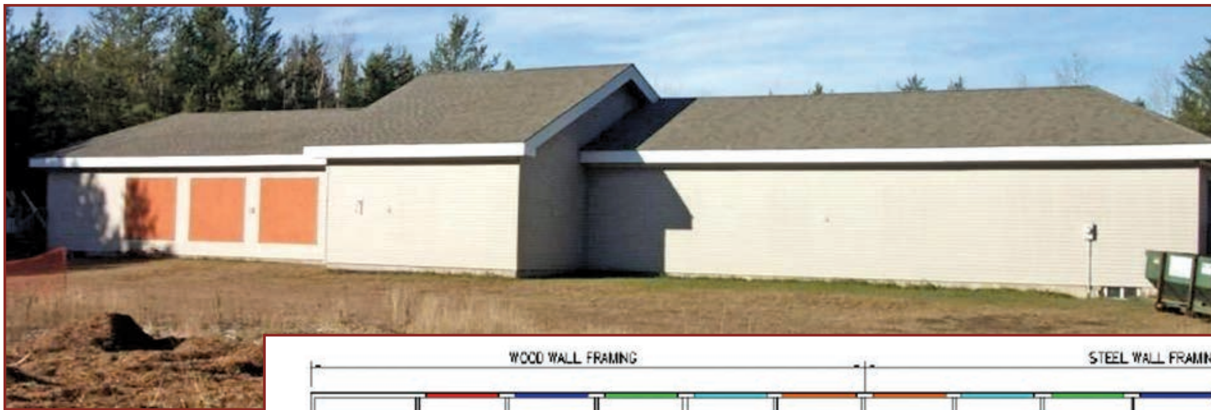

Figure 1. Cloquet Residential Research Facility was used for the in situ testing of retrofit wall assemblies.

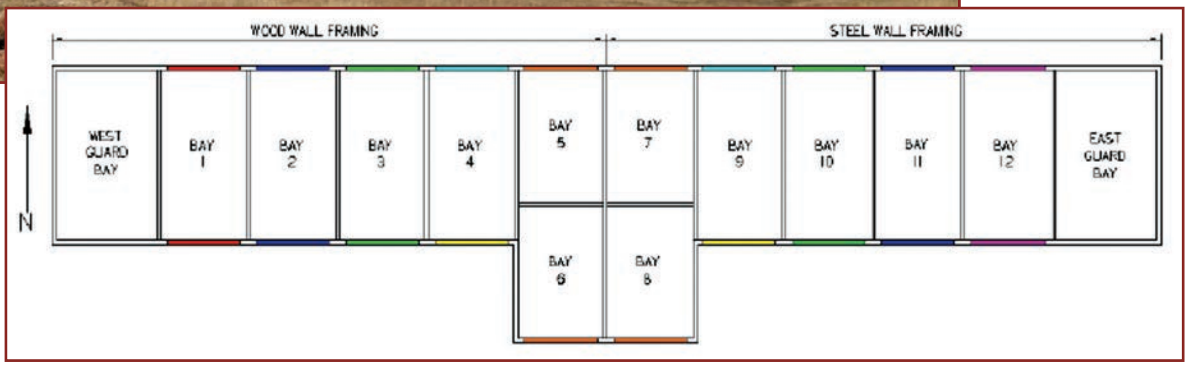

Figure 2. Floor plan of the Cloquet Residential Research Facility.

residential wall systems in the U.S. are wood framing, the report focused on this construction practice.

In addition to investigating wall assemblies, the literature review explores various innovative insulation materials and provides background for a techno-economic analysis, and the use of such analyses in building construction. A review of literature on the modeling and simulation of hygrothermal wall assembly performance is also presented, and references and links for a variety of sources of relevant information are included.

FIELD TESTING

Test Facility and Test Panels

The experimental portion of this project was carried out by the University of Minnesota at the Cloquet Residential Research Facility (CRRF), which is located on the Cloquet Forestry Center near Cloquet, Minn., approximately 20 miles (32 km) west of Duluth and in DOE Climate Zone 7. The CRRF building (**Fig. 1** and **2**) is elongated along an east-west axis to maximize the northern and southern exposures. It sits on a full basement with 12 independent above-grade test bays protected by two end-guard bays. The eight test bays that have both north and south exposures (Bays 1 to 4 and 9 to 12) were selected to conduct in situ testing for this project.

Baseline Test Panels

Two series of in situ experiments were conducted during this three-year project. The first series of test walls (Phase 1), which were developed in response to the activities associated with the literature survey and the expert meeting, were deployed in the CRRF in December 2019 and evaluated for two winter periods. After studying the results of these first tests, the research team proposed a second series of wall assemblies (Phase 2) in consultation with an advisory committee that oversaw the research project. These wall assemblies were installed in the CRRF in December 2020.

Phase 1 of this project was conducted in Bays 1 to 4 and Phase 2 used Bays 9 to 12. Each test bay has a north-facing and a south-facing wall opening. These openings are approximately 8 ft (2.4 m) wide and 7 ft (2.1 m) high, and for this project, they were divided in half to support two different test panels. Each test panel was mirrored on both the north and south orientations so eight pairs of wall assemblies were studied during each phase.

The test panels are approximately 4 ft (1.2 m) wide by 7 ft (2.1 m) high. Each test panel was divided into three wall cavities at approximately 16 in. (0.4 m) on center (oc) to represent older wood-frame construction. The center cavity of each test panel was a true 16 in. (0.4 m) oc and was designated as the test cavity. All the monitoring sensors were installed within this test cavity. The wall cavities on each side of the test cavity were designed as guard cavities. They received the exact same insulation treatment to mitigate any differential horizontal heat flows between the test and guard cavities. Both horizontal and vertical moisture flows between the test panels and test opening were controlled with the use of low-permeability membrane tapes.

To assess the impact of wall retrofits, a baseline wall assembly was designed and used as the starting point for each wall assembly and 16 identical test walls were constructed for each phase. The baseline test walls were constructed of 2 × 4 in. (51 × 102 mm) spruce, pine, or fir wood studs with 1 × 6 in. (25 × 152 mm) pine board exterior sheathing. The pine sheathing was loosely fit to reflect older construction. The sheathing was covered with a heavy no. 30 building paper lapped and stapled to the sheathing followed by 8 in. (203 mm) cedar lap siding finished with an oil-based primer, vapor-retarder primer, and latex topcoat. This exterior finish was selected to represent an older house with several coats of oil-based paints. Once the test panel was installed in the test opening and the instrumentation array was installed, an interior finish of ⅝-in.-thick (16-mm-thick) gypsum board with a vapor-retarder primer was added. The interior finish was selected to represent an older house with heavy drywall or plaster and several coats of paint. The south-facing baseline walls from Phase 2 are shown in **Fig. 3**. Team members familiar with construction practices in the local climates indicated that vapor retarders were not historically included in construction practices for the time period that was being considered for initial constructions. Since the majority of retrofits were to be performed on the exterior side of the wall assembly, access to the interior side of the cavity was unavailable and therefore vapor retarders were not included in most of the retrofits.

Figure 3. Exterior view of baseline walls depicting cedar siding before wall retrofits.

Instrumentation

Depending on the specific construction, each test cavity had between 15 and 20 sensors installed. Sensors for temperature (type-T thermocouples), relative humidity (capacitance type), heat flux (heat flux transducers), and moisture content (brass nails coated with enamel) were deployed in each test panel. Generally, temperature sensors were installed on the interior and exterior surfaces of the drywall, the interior and exterior surfaces of the sheathing, and the exterior surface of the siding. Relative humidity sensors were placed on the cavity-side surface of the drywall and the interior and exterior surfaces of the sheathing. The heat flux transducer was located on the interior surface of the drywall. The moisture content pins were inserted from the cavity side to measure the moisture content of the interior and exterior surfaces of the pine sheathing as well as the middle of the cedar siding. **Figure 4** presents a schematic of a typical instrumentation array.

The data acquisition system for this experiment was based on the Campbell Scientific CR-1000X data logger. The centrally located logger collected data from modules located in each test bay. The data acquisition system was also set up to collect interior and exterior boundary conditions. The interior temperature and relative humidity were measured in each test bay. In Phase 1, the exterior temperature, humidity, wind, and precipitation data were gathered from local weather stations. For Phase 2, a local weather station was added to the CRRF with temperature, relative humidity, wind speed and direction, rain gauge, and horizontal solar radiation instruments. Additional pyranometers were used to measure the solar radiation of the vertical wall surface on both the north and south exposures. Data were continuously collected throughout the winter periods. These data were used to validate both thermal and hygrothermal models as described in the following.

Wall Retrofits

Over the course of the three-year project, 16 baseline/retrofit strategies were evaluated. Walls "A" through "H" were instrumented and installed in the CRRF in December 2019, and Walls "I" through "P" were set up in December 2020. Data collection on each wall has been ongoing continuously since their installation. A brief description of each retrofit follows.

Wall A: Base Case Wall #1

Wall A is the baseline wall without any retrofit treatment.

Wall B: Drill and Fill (Cellulose)

For Wall B, the siding was removed in two locations just below the midpoint and near the top of the cavity, and holes were drilled through the building paper and sheathing. The cellulose was installed by a certified contractor with a target density between 3.5 to 4.0 lb/ft^3 (56 to 64 kg/m^3). The holes in the sheathing were sealed with spray foam, tape was used to repair the building paper, and the siding was replaced.

Wall C: Minimally Invasive Cavity Spray Foam

This treatment is a foam installed from the interior. The foam manufacturer's representatives managed all formulation and installation techniques, including the injection of the proprietary closed-cell polyurethane liquid foam through very small holes in the drywall. Infrared imaging was used to ensure the cavities were completely filled, and the holes in the drywall were sealed with the spray foam.

Wall D: Exterior Expanded Polystyrene Foam Panel (Siding Remains)

This wall treatment used a commercially available expanded polystyrene (EPS) insulation product that includes built-in drainage capabilities and an embedded structural ladder for attachment. A low-density fiberglass board was installed over the existing siding to remove the air channels that would be created between the existing lapped siding and the

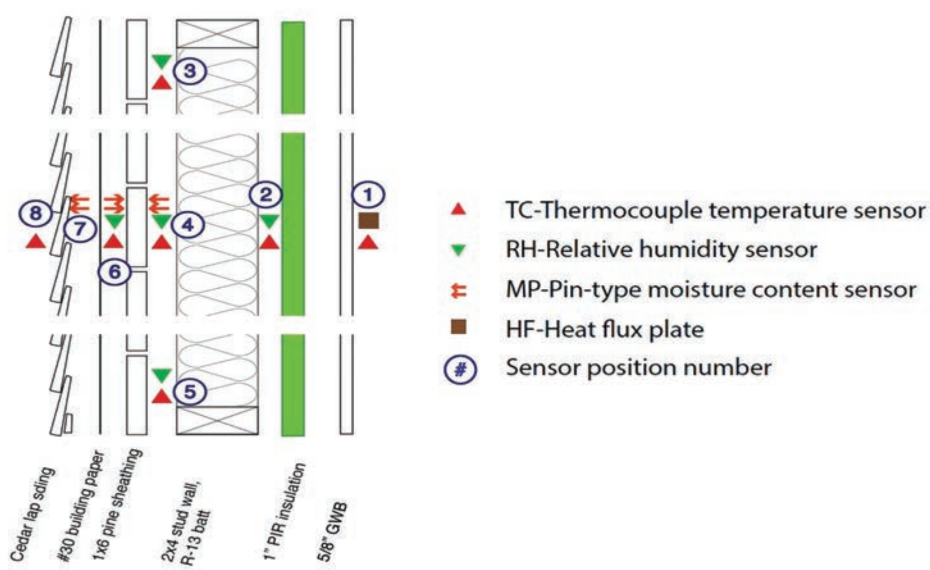

Figure 4. Typical layout of instrumentation in test panels.

rigid EPS panel. A housewrap was stretched over the fiberglass board to provide a new air- and water-control layer. Two layers of EPS (2- and 2.5-in.-thick [51- and 64-mm-thick]) were installed to the existing wall with screws using the integral fastening ladder. Vinyl siding was installed with screws to the integral fastening ladder in the second panel.

Wall E: Drill and Fill (Cellulose) with Exterior Extruded Polystyrene (Siding Removed)

For Wall E, dense-pack cellulose was installed as described for Wall B. In this case, the cedar lap siding and building paper were removed and housewrap was installed as a new air- and water-control layer. Also, 2 in. (51 mm) of extruded polystyrene foam (XPS) were held in place, and 1 × 4 in. (25 ×102 mm) furring strips were fastened to the framing through the insulation layer with washer head screws. A ¾-in.-thick (19-mm-thick) XPS layer was placed between the furring strips to support the vinyl siding cladding that was attached to the furring strips.

Wall F: Drill and Fill (Cellulose) with Exterior Vacuum Insulation Panel/Vinyl Siding (Siding Removed)

For Wall F, dense-pack cellulose was installed as described for Wall B. The cedar lap siding and building paper were removed, and a housewrap was installed as a new air- and water-control layer. A vacuum insulation panel/vinyl siding composite panel was installed to the exterior sheathing.

Wall G: Exterior Mineral Fiberboard (Siding Remains)

For Wall G, a vapor-permeable liquid-applied membrane was applied over the existing lapped siding to provide a more robust water-control layer. A 2-in.-thick (51-mm-thick) mineral wool panel was held in place, while a second 2-in-thick mineral wool layer was installed with staggered joints. Also, 1 × 4 in. (25 × 102 mm) furring strips were installed with washer head screws. A semirigid fiberglass board was installed between the furring strips to act as an insect screen that allows drainage and drying, and fiber-cement siding was fastened to the furring strips.

Wall H: Exterior Structural Graphite-Impregnated EPS Panel (Siding Remains)

For Wall H, a low-density fiberglass board was installed over existing siding to fill potential air voids between the existing lapped siding and the retrofit panel. A 1.5 in. (38 mm) structural oriented strand board (OSB) sheet was fastened with screws to the wall framing and covered with a fully adhered peel-and-stick membrane. Two layers of 2⅛-in.-thick (54-mm-thick) graphite-impregnated EPS were installed using a limited number of cap nails, and 1 × 4 in. (25 ×102 mm) furring strips were installed with washer head screws. A semirigid fiberglass board was installed between the furring strips to act as an insect screen that allows drainage and drying, and both fiber-cement siding and a metal panel siding were fastened to the furring strips. This wall treatment was envisioned to be an off-site fabricated panel, but for this study, it was installed in layers onto the existing wall.

Wall I: Base Case Wall #2

Wall I is a baseline wall without any retrofit treatment, identical to Wall A.

Wall J: Drill-and-Fill (Fiberglass)

For Wall J, the siding was removed in one location just below the midpoint and near the middle of the cavities, and holes were drilled through the building paper and sheathing. The fiberglass was installed by a certified contractor with a target density of 1.5 lb/ft^3 (24 kg/m^3). The holes in the sheathing were sealed with spray foam, a piece of building paper was used to repair the water-control layer, and the siding was replaced.

Wall K: Interior Polyiso Insulation with Fiberglass Batt

For Wall K, the drywall was removed and an unfaced fiberglass batt with an *R*-value of 13 (RSI 2.3) was carefully installed in the existing cavity. A 1-in.-thick (25-mm-thick) foil-faced polyisocyanurate foam board was installed over the studs. The drywall was reinstalled, and a sealant was used to ensure airtightness.

Wall L: Drill and Fill (Fiberglass) with Exterior Polyiso Insulation (Siding Removed)

For this wall, fiberglass was installed as described for Wall J. In this instance, the cedar lap siding and building paper were removed and the holes were filled with spray foam. A housewrap was applied and a 1-in.-thick (25-mm-thick) foil-faced polyisocyanurate foam board was installed with 1 × 4 in. (25 × 102 mm) furring strips fastened to the framing with washer head screws. A prefinished lap wood composite siding was fastened to the furring strips.

Wall M: Exterior Insulation and Finish System Panel (siding removed)

This treatment used a 6-in.-thick (152-mm-thick) piece of EPS foam finished on all six sides with a stucco material and was intended to be prefabricated. The existing siding and building paper were removed, and a coat of liquid-applied membrane was applied. All gaps and nail holes in the sheathing were filled with a proprietary caulk, and a second coat of membrane was applied. The prefinished exterior insulation and finish system (EIFS) panels were fixed in place using a gun-grade adhesive, and a temporary shelf at the bottom edge of the test panel supported the weight as the adhesive cured. The shelf supports were removed approximately 24 hours later.

Wall N: Prefabricated Polyurethane Blocks

For this prefabricated wall treatment, a housewrap was installed over the existing siding to serve as a new air- and backup water-control layer. A base plate was installed to receive the custom trim pieces at the top and both sides of the assembly. The custom metal starter strip was installed to receive the first polyurethane foam block, which was mechanically attached. Subsequent blocks engage the block below with a large tongue-and-groove shape in the foam extrusion.

Wall O: Drill and Fill (Fiberglass) with Exterior Fiberglass Board Insulation

This wall treatment uses fiberglass installed as described for Wall J. The siding was repaired, but touch-up was not required, and a sheet of housewrap was draped from the top of the panel. Two-inch-thick (51-mm-thick) semirigid fiberglass boards were installed and held in place with 1 × 4 in. (25 × 102 mm) furring strips fastened to the framing with washer head screws. A fiber-cement siding was installed on the furring strips.

Wall P: Thermal Break Shear Wall (Siding and Sheathing Removed)

For Wall P, the existing siding, building paper, and sheathing were removed and an unfaced fiberglass batt with an *R*-value of 13 (RSI 2.3) was installed in the existing cavity, followed by a 1-in.-thick (25-mm-thick) XPS board installed over the studs. A ¾-in.-thick (19-mm-thick) OSB sheet was installed over the XPS and fastened securely to the studs with 4-in.-long (102-mm-long) screws. A housewrap was installed, followed by a typical installation of vinyl siding.

ENERGY MODELING

Energy modeling have been used in many studies to evaluate enclosure performance.[8] Laboratory and field evaluations of building enclosure performance are expensive. In the past decade, modeling software programs for building energy and enclosure performance have become more robust, and the value of findings from these programs is recognized by the research community and industry. Most building modeling tools are based on solving physics-based energy and mass equations; they can provide detailed outputs on many aspects of building performance.

To capture annual energy cost savings for houses after the DERs, whole building energy modeling (BEM) tools were used. They simulate whole building energy consumption using hourly modeling of thermal loads and HVAC systems. BEM tools account for all the energy interactions involving indoor space, outdoor environment conditions, HVAC, lighting, service water heating, other appliances and equipment, and occupancy behavior. In such analyses, the energy flow through enclosure elements such as the walls, roof, and windows is treated as one dimensional, and mass flow of moisture and air and phase changes of moisture are not well captured. Among these tools, the DOE-sponsored EnergyPlus is a popular model because of its continuous research and development supported by DOE and the modeling community.

A reference set of residential building models representative of the existing national residential building stock was created to quantify the energy performance of the proposed walls. The DOE's Building Energy Codes Program has used residential prototype buildings to evaluate the energy and economic performance of residential energy codes, and to develop proposed code changes.[9] However, the prototypes represent the new construction stock and minimal compliance with the residential prescriptive and mandatory requirements of the 2018 *International Energy Conservation Code* (IECC).[10] Thus, these prototype models were modified to represent the existing building stock, and the inputs for these modifications were taken from the National Renewable Energy Laboratory's ResStock database (a large-scale housing stock database developed by combining public and private data sources, statistical sampling, and detailed building simulations).[11,12]

The baseline house was created for this study with modifications using the ResStock data to better represent the existing building stock. Based on US Census Bureau data,[3] the baseline house is a single-family, two-story house with a gross floor area of 2400 ft^2 (223 m^2) with a slab-on-grade foundation type and either an electric resistance or gas-furnace heating system type. Details about the model can be found in the technical support document by Mendon, Lucas, and Goel.[13]

Based on ResStock data, a baseline energy model was constructed with the following assumptions:

1. The uninsulated walls were framed with wood 2 × 4s at 16 in. (0.4 m) oc, and the insulated, vented ceilings had *R*-value 30 (RSI-5.3) insulation
2. Natural gas heating system with an efficiency of 80% annual fuel utilization efficiency, and a cooling system with an efficiency of seasonal energy efficiency ratio of 10
3. Ducting inside of the conditioned space, eliminating the need for duct leakage modeling
4. Standard electric water heater for Climate Zone 1 and Climate Zone 2 and gas water heaters for all other climate zones
5. Clear single-pane windows with a U-factor of 1.22 Btu/h-ft^2-°F (6.92 W/m^2•K) and a solar heat gain coefficient (SHGC) of 0.39 for Climate Zones 1–3 ,and clear double-pane windows with a U-factor of 0.62 Btu/h-ft^2-°F (3.52 W/m^2•K) and SHGC of 0.39 for Climate Zones 4–8
6. Whole house infiltration rates of 15 air changes per hour at 1.04 lb/ft^2 (50 Pa) of pressure for the baseline house

The baseline house was modified to create a set of models representing each of the climate zones as defined by the IECC. Each baseline model was then simulated with all 14 wall retrofit options using EnergyPlus

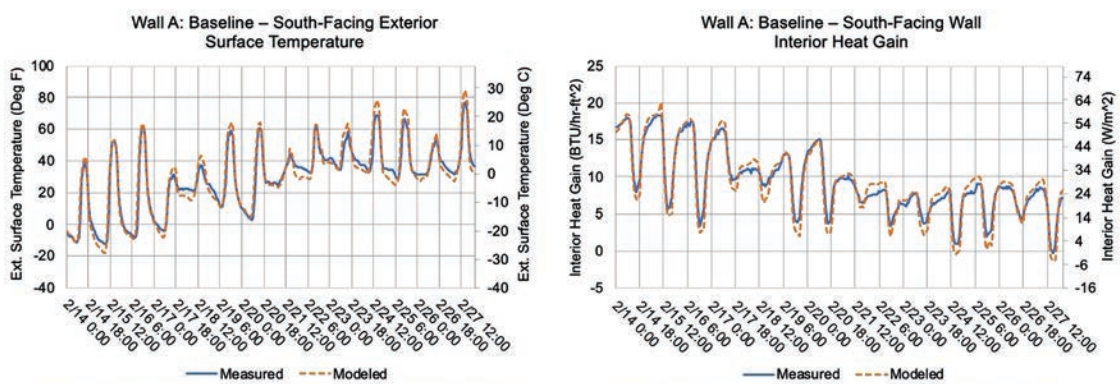

(a) Benchmarked exterior surface temperatures for Wall A.

(b) Benchmarked interior heat gain values for Wall A.

Figure 5. Energy modeling outputs compared with measured experimental data for Wall A.

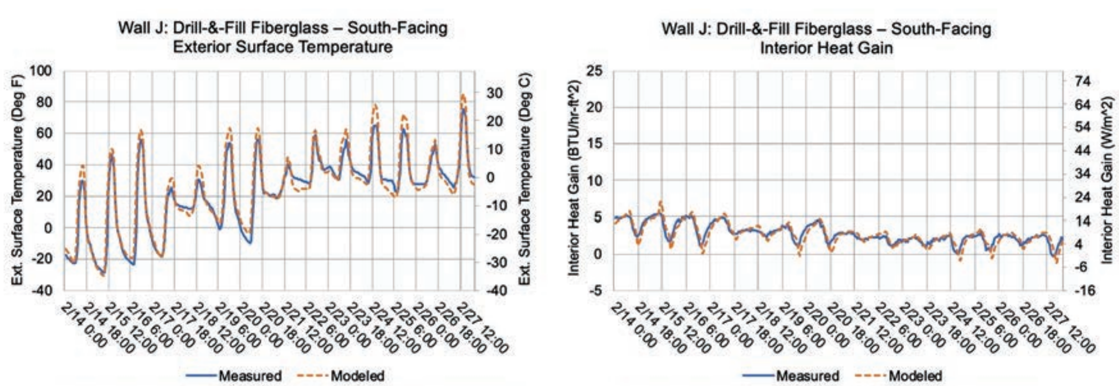

(a) Benchmarked exterior surface temperatures for Wall J.

(b) Benchmarked interior heat gain values for Wall J.

Figure 6. Energy modeling outputs compared with measured experimental data for Wall J.

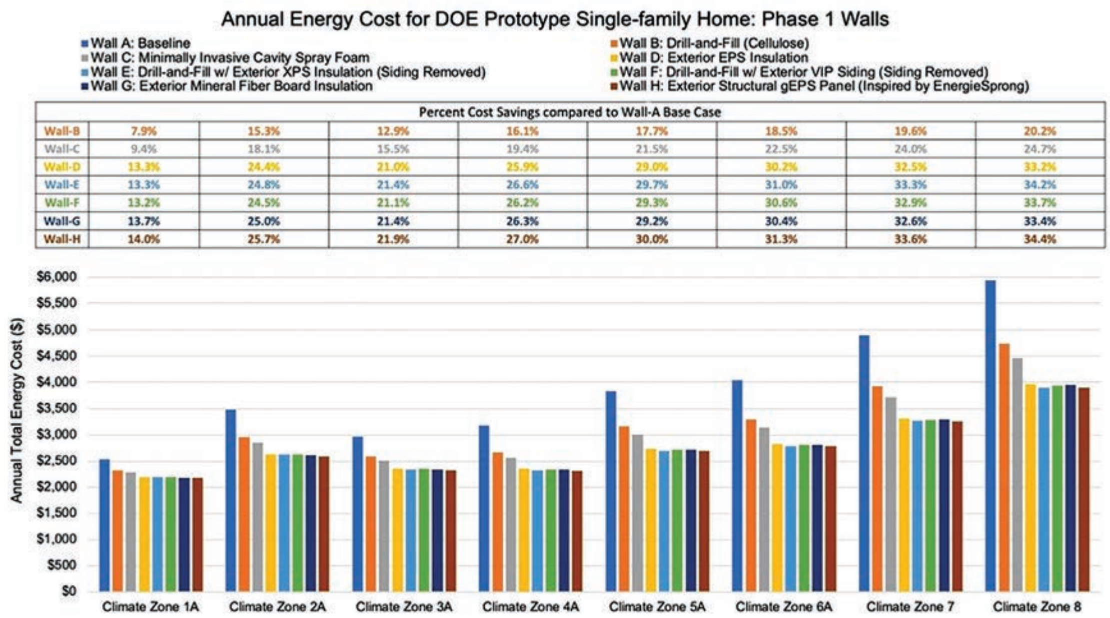

Percent Cost Savings compared to Wall-A Base Case								
Wall-B	7.9%	15.3%	12.9%	16.1%	17.7%	18.5%	19.6%	20.2%
Wall-C	9.4%	18.1%	15.5%	19.4%	21.5%	22.5%	24.0%	24.7%
Wall-D	13.3%	24.4%	21.0%	25.9%	29.0%	30.2%	32.5%	33.2%
Wall-E	13.3%	24.8%	21.4%	26.6%	29.7%	31.0%	33.3%	34.2%
Wall-F	13.2%	24.5%	21.1%	26.2%	29.3%	30.6%	32.9%	33.7%
Wall-G	13.7%	25.0%	21.4%	26.3%	29.2%	30.4%	32.6%	33.4%
Wall-H	14.0%	25.7%	21.9%	27.0%	30.0%	31.3%	33.6%	34.4%

Figure 7. The annual energy costs for the modeled residential prototype building with the Phase 1 wall retrofitted assemblies.

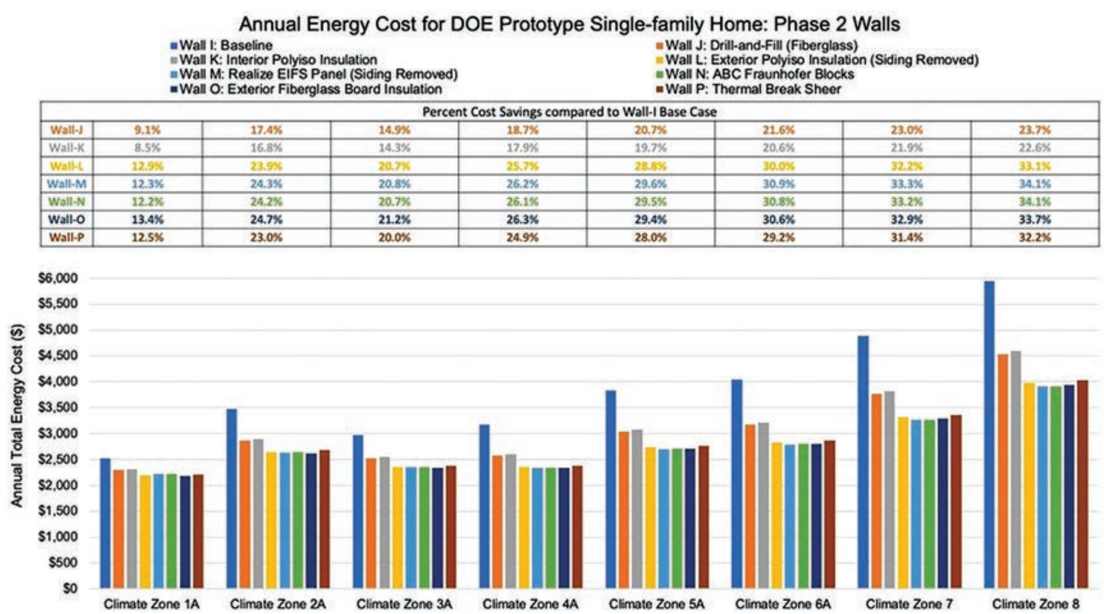

Percent Cost Savings compared to Wall-I Base Case								
Wall-J	9.1%	17.4%	14.9%	18.7%	20.7%	21.6%	23.0%	23.7%
Wall-K	8.5%	16.8%	14.3%	17.9%	19.7%	20.6%	21.9%	22.6%
Wall-L	12.9%	23.9%	20.7%	25.7%	28.8%	30.0%	32.2%	33.1%
Wall-M	12.3%	24.3%	20.8%	26.2%	29.6%	30.9%	33.3%	34.1%
Wall-N	12.2%	24.2%	20.7%	26.1%	29.5%	30.8%	33.2%	34.1%
Wall-O	13.4%	24.7%	21.2%	26.3%	29.4%	30.6%	32.9%	33.7%
Wall-P	12.5%	23.0%	20.0%	24.9%	28.0%	29.2%	31.4%	32.2%

Figure 8. The annual energy costs for the modeled residential prototype building with Phase 2 wall retrofitted assemblies.

Version 8.6. However, because EnergyPlus uses a simplified one-dimensional calculation approach for conduction heat transfer through the building enclosure, the research team applied THERM,[14] a two-dimensional conduction heat-transfer analysis program developed by Lawrence Berkeley National Laboratory, to capture the multidimensional effects of thermal bridging. A THERM model was developed for each wall section using the as-built layout and thermal properties of the wall assemblies, and overall section U-values were obtained from THERM and applied to the respective EnergyPlus models.

To use energy modeling to analyze wall performance on a national scale, it is first necessary to benchmark model results against measured data. Within this project, all 14 candidate wall retrofit assemblies were constructed and instrumented with sensors at the CRRF. To validate the energy models' enclosure calculations, multiple energy models were constructed, each representing a residential building containing the candidate retrofit wall assemblies. These energy models were run using the site-measured weather data, and the results of each of these models were compared against measured temperature and heat-flux measurements. Interior-facing wall surface temperatures, exterior-facing wall surface temperatures, and interior-facing heat fluxes were compared between the measured and modeled assemblies to validate model performance.

Figures 5 and 6 present benchmarking plot examples. In Fig. 5, the exterior surface temperature and interior surface heat-flux values for Wall A, the baseline wall, are displayed, and the measured and modeled data can be compared. For the displayed data set, the root mean square error values are 4.7°F (2.6°C) and 1.10 Btu/hr-ft^2 (3.47 W/m^2) for exterior surface temperature and interior heat-flux comparisons, respectively. Similar data are depicted in Fig. 6 for Wall J, the dense-packed fiberglass drill-and-fill wall.

Although the test assemblies at the CRRF give insight into the real-world moisture and energy performance of the proposed retrofit assemblies, physical experiments only provide context for the climate in which the experiment was conducted. Therefore, to improve understanding of the energy-saving potential of these candidate retrofit assemblies, researchers also performed simulations on the assemblies for the following cities selected from the IECC 2015 climate zones to represent a diverse set of climates: Miami, Fla. (Climate Zone 1); Houston, Tex. (Climate Zone 2); Memphis, Tenn. (Climate Zone 3); Baltimore, Md. (Climate Zone 4); Chicago, Ill. (Climate Zone 5); Burlington, Vt. (Climate Zone 6); Duluth, Minn. (Climate Zone 7); and Fairbanks, Alaska (Climate Zone 8). National energy prices were also assumed for this analysis. Energy cost values of $0.1013/kWh and $1.00/Therm were applied nationally for electricity and heating fuel, respectively.

Figures 7 and 8 depict the annual energy costs for the simulated prototype house for

Phase 1 and Phase 2 walls, respectively. Broad conclusions related to the potential savings and cost-effectiveness of climate zones can be drawn. For Climate Zone 1, the average savings for all simulated retrofit options is 12%. Wall performance for this climate zone is led by Wall H, which is also the assembly with the highest effective *R*-value. Average cost savings continue to increase from Climate Zones 1 to 8, with Climate Zone 8 having an average savings of 31%. From a national scale, these results suggest that the most influential climates for enclosure retrofits are those that are heating dominated (Climate Zones 5 through 8).

HYGROTHERMAL MODELING

Hygrothermal modeling is used to evaluate the condensation potential, moisture content, and drying capacity of the assembly, as well as the potential for mold growth and freezing-and-thawing damage. During the last two decades, several computer simulation tools have been developed to predict thermal and moisture conditions in buildings and the building enclosure. In addition to their use as forensic tools in the investigation of building failures, these computer models are increasingly used to make recommendations for building design in various climates.

WUFI modeling is a commonly used research tool in the building industry.[15-18] WUFI is an acronym for the German phrase *Wärme Und Feuchte Instationär*, which means "heat and moisture transiency." The WUFI model is based on a state-of-the-art understanding of the physics regarding sorption and suction isotherms, vapor diffusion, liquid transport, and phase changes. The model is well documented and has been validated by many comparisons between calculated and field performance data.

Hygrothermal modeling is used to verify that the proposed energy efficiency retrofit measures do not create a durability issue. The use of transient hygrothermal models for moisture control is well established in the building industry in its codes, standards, and building insulation design principles. Building enclosures are designed to naturally shed liquid water and attempt to minimize its entry into the building structure. Building enclosures should also be constructed to facilitate vapor transport so that moisture does not accumulate within the building enclosure and lead to moisture accumulation and its subsequent failure mechanisms.

Hygrothermal simulations were carried out using WUFI Pro (version 6.4). Two types of hygrothermal modeling were undertaken for this project. First, the model outputs were compared with the field measurements to verify that the models were correctly capturing all the transport phenomena occurring in the field experiments. Once the model was validated, it was employed to generalize the findings for other climate zones.

In instances where certain materials used in the wall assembly constructions were not available in the model's material property database, the thermal conductivity and water vapor permeance were measured in accordance with, respectively, ASTM C518, *Standard Test Method for Steady-State Thermal Transmission Properties by Means of the Heat Flow Meter Apparatus*,[19] and ASTM E96, *Standard Test Methods for Water Vapor Transmission of Materials*.[20] The material properties were compared to those in the model's materials database, and modifications were made accordingly. In some cases, there were no material properties, so a new material property entry was created.

Field data from the test panels were collected over two months during the winter period. Data included weather data (temperature, relative humidity, wind speed and direction, rainfall, and solar loads). From the test panels, temperature, relative humidity, moisture content, and heat flux were measured. The data were used to validate the model for that test period. Simulations were compared to the measured values from the test panels, including both south and north orientations. **Figure 9** shows the simulation results compared with the measured values for temperature and relative humidity for wall assembly A (Phase 1). Comparisons are made in locations where both temperature and relative humidity were measured.

After the validation study was completed, hygrothermal simulations of all wall assemblies were carried out in the eight DOE climate

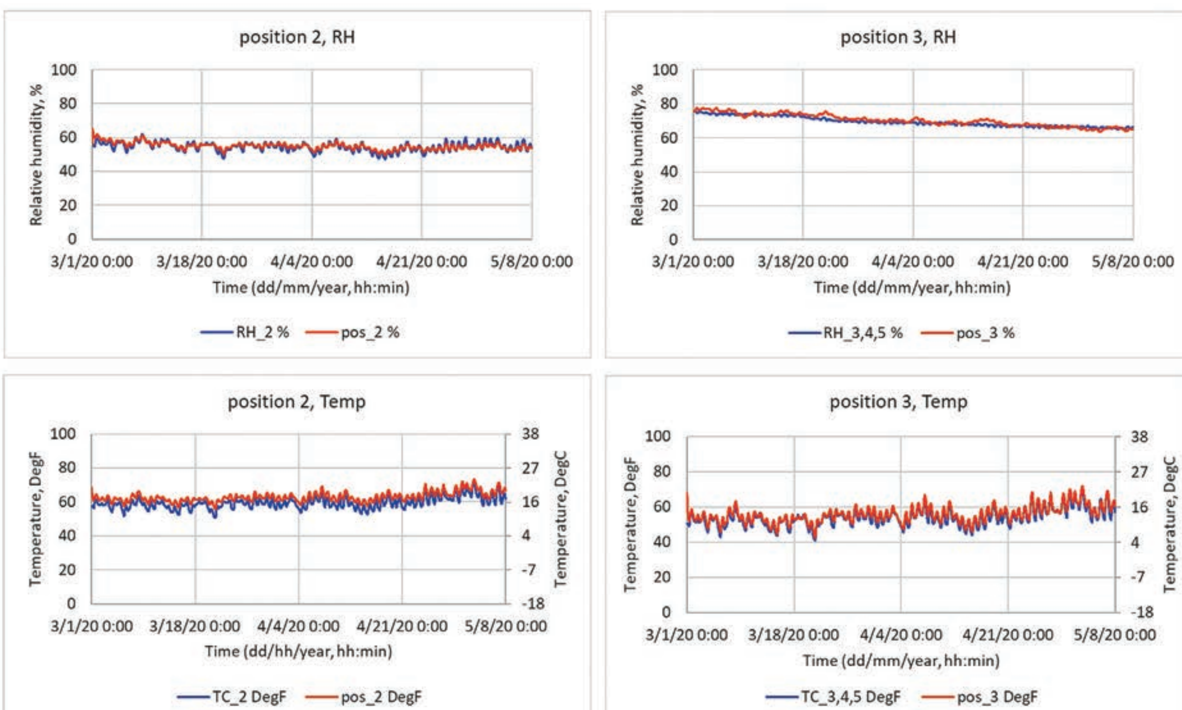

Figure 9. Comparison of measured relative humidity and temperature with calculated values using WUFI Pro (version 6.4) for Wall A (Phase 1). The simulated results are represented by pos_#, where # represents the probe position for temperature and relative humidity in the wall assembly. The measured temperature and relative humidity are represented by TC_# and RH_#, respectively, where # represents the probe position in the wall assembly.

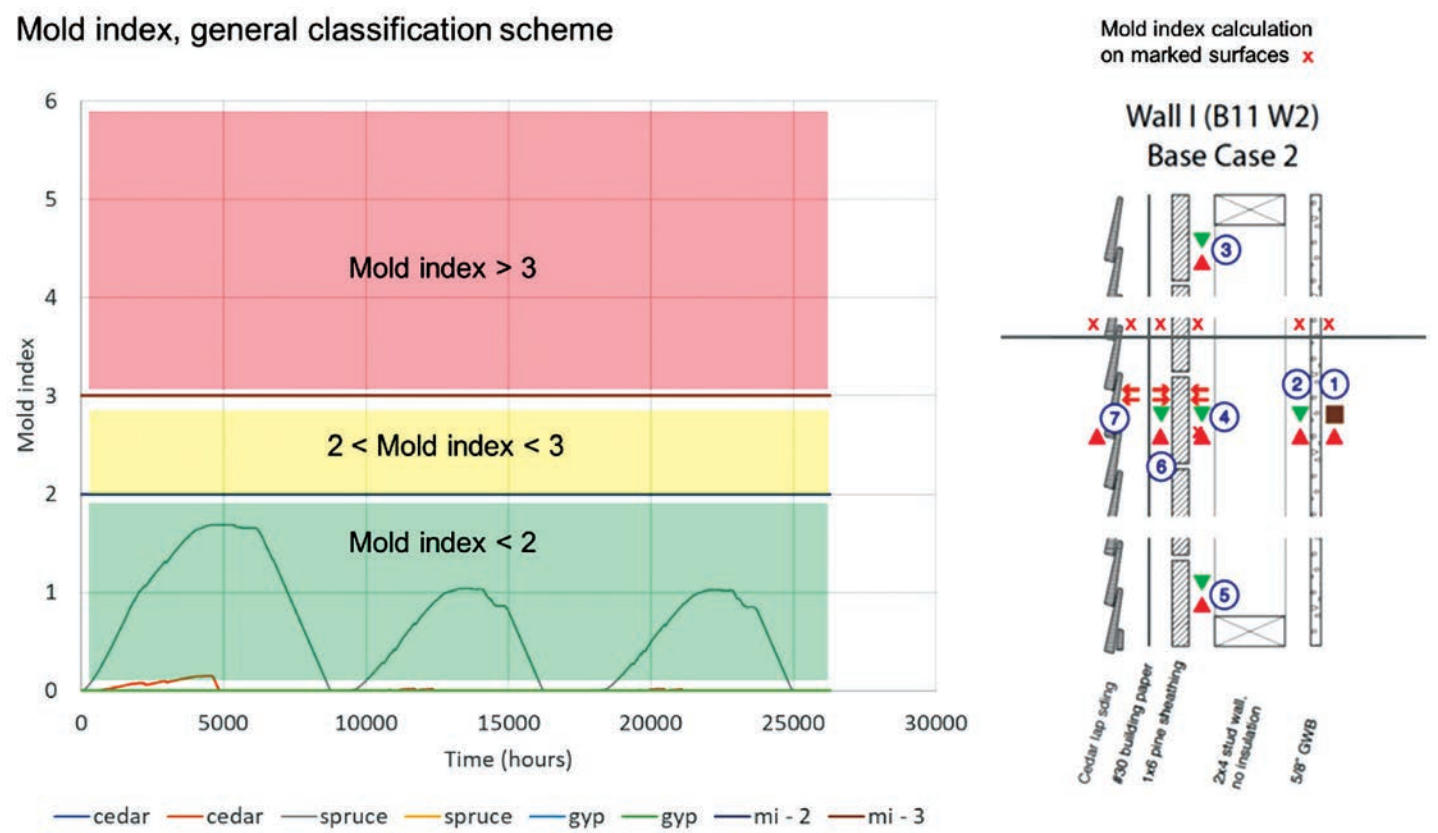

Figure 10. Classification scheme for the mold index values (left), and a wall assembly schematic showing locations where the mold index calculations were carried out (right).

zones to understand the impact of the retrofit systems on moisture performance/durability. The selected cities are Fairbanks, Alaska (subarctic); International Falls, Minn. (very cold); Boston, Mass. (cold); Charleston, S.C. (mixed humid); Amarillo, Tex. (mixed dry); Miami, Fla. (hot humid); Tucson, Ariz. (hot dry); and Seattle, Wash. (marine).

Simulations were carried out for northern exposures in accordance with ANSI/ASRHAE 160-2016, *Criteria for Moisture-Control Design Analysis in Buildings.*[21] The northern exposure was used because it represents the most severe hygrothermal conditions. The initial moisture content for the assemblies was established by using the moisture content of the base case wall. Simulation of the base case was run for three years, and the moisture content in the base case wall after the three-year simulation was used as the initial moisture content for the same elements in the retrofit construction. The equilibrium moisture content at 80% relative humidity was used for the new retrofit elements.

The mold index calculated in accordance with ASHRAE 160 was used as an indicator of moisture durability. ASHRAE 160 uses the model developed by Viitanen and Ojanen of VTT Technical Research Centre of Finland[22] to calculate a mold index for materials that make up the building enclosure. The calculation is based on experimental studies of typical building materials. According to ASHRAE 160, "to minimize problems associated with mold growth on the surfaces of components of building enclosure assemblies, the mold index shall not exceed a value of three (3.00)." The calculation was carried out for all the wall assemblies in all climate zones, and a matrix was developed using the classification presented in **Fig. 10**. The mold index takes on a value between 1 and 6. In this classification scheme, colors are assigned to the assmebly by index range: green for a mold index value less than 2; yellow for a value greater than 2 but less than 3; and red for any value greater than 3.

In the wall in Fig. 10, a line runs through the "x's" that mark the locations where mold index calculations were carried out. The mold index is calculated on all surfaces except for weather-resistive barriers. Using the VTT model in WUFI (which is the model used in ASHRAE 160), the mold index is calculated for all surfaces. The surface with the highest value is then used as the representative value for the wall assembly, and a color is assigned accordingly. To compare assemblies in all climate zones, a matrix is developed where the columns are assigned the climate zones and the rows represent the wall assemblies. **Figures 11** and **12** are the matrixes for all Phase 1 walls and all Phase 2 walls, respectively.

In most cases, all walls have building components where the mold index is less than 3; exceptions are Walls B and J, the walls that contain insulation in the wall cavity with no exterior or continuous exterior insulation. In the absence of any form of interior vapor control, the addition of exterior insulation, especially with moisture-tolerant materials, is expected to improve the hygrothermal performance of the wall assembly by pushing the point of condensation to the exterior side of the sheathing.

TECHNO-ECONOMIC ASSESSMENT

A techno-economic study refers to the analysis of a technology from both a technical and economic perspective to understand the viability of new technologies or approaches in emerging markets. Many industries use such analyses, but depending on the application, the analysis method can vary significantly. In general, a techno-economic analysis combines process modeling and engineering design with economic evaluation for a quantitative and qualitative understanding of the financial viability of an investment.[23] In the current investigation, the framework for the techno-economic analysis combines the thermal/moisture modeling results, experimental results, and economic data to investigate the opportunity for a variety of residential wall retrofit approaches in the market. For this study, the techno-economic analysis is a synthesis exercise, designed to communicate overall research findings related to wall performance, cost, and installation.

Measures of the economic performance of each wall included material, labor, and energy costs for all materials and activities associated with the wall retrofits. Cost data were derived from a local nonprofit organization that provides construction cost estimation in Portland, Ore. This organization was chosen for this activity because of its deep ties to the local residential building industry, which includes workforce training and building certification programs. These activities put the organization's team members regularly in the field, giving them access to many local contractors familiar with advanced building science approaches and principles. This connection was imperative to determine fair market costs associated with experimental approaches and installation techniques for materials not commonly used for exterior wall retrofits.

The method for gathering costs included subdividing each wall system into individual material layers and operations whose costs could be determined separately. Material and labor costs were kept separate. For each wall system, estimates for material and labor were collected from three different contractors. Upon review of the cost summaries, the research team determined that estimates from one contractor were much higher than the other two and did not seem realistic based on the team's construction experience and industry knowledge. When compared to data from the *RS Means Residential Cost Databook*,[24] this set of estimates did not appear to consistently align with real-market values. The results from this contractor were determined to be outliers and removed from consideration. The remaining two estimates were then averaged, and the costs for the wall layers were added to derive a total estimated cost. When demolition was necessary, the contractors provided an estimate, which was appended to the material list. The estimates for labor and materials were averaged and summed to produce an estimated total cost.

For the experimental wall systems, we reached out directly to manufacturers to help

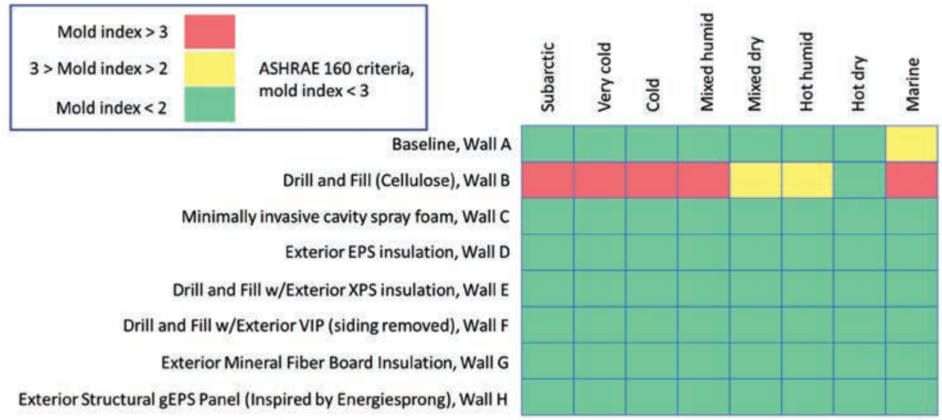

Figure 11. Mold index measures for Phase 1 walls in all eight U.S. Department of Energy climate zones.

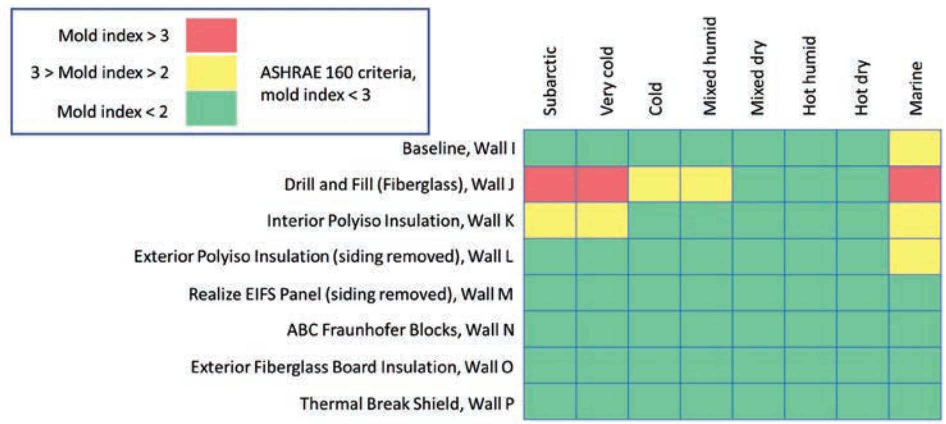

Figure 12. Mold index measures for Phase 2 walls in all eight U.S. Department of Energy climate zones.

with cost estimates. Some wall systems are highly experimental in nature, and manufacturers have not yet done detailed cost analyses. We asked the cost estimator to gather labor costs from contractors for installing these experimental materials. The labor costs for these walls represent a high-level estimate, based solely on the information provided to the contractors. It is reasonable to assume these costs will not represent a market value once the products and installation approaches are commercialized. In addition to gaining labor and material costs using a cost estimator, the RS Means databook was used to cross reference data gathered from the cost estimator. The RS Means regional indices were used to translate costs from Portland, Ore., to other regions throughout the United States.

For each wall, a siding material was identified as the final layer of the wall system. In some cases, the treatment was a cavity-only application that did not require additional siding. There were instances where the siding was integrated with the insulation in a panelized approach to the retrofits. In the cases where a new siding material was needed, the research team specified many different claddings, including vinyl, fiber cement, stucco, and metal. The choice and associated cost of cladding vary dramatically and are almost solely based on the preference of the consumer. For example, vinyl siding is significantly cheaper than stucco, but stucco might have more curb appeal to certain consumers. To control for siding cost variations, the cost analysis assumed vinyl siding for all wall systems that factored siding as a separate layer to the construction process (that is, the walls that are not cavity-fill-only or panelized systems with integrated insulation/siding). This assumption limits the cost difference to the wall structure and control layers.

Material, labor, and energy costs are presented here in absolute dollar values for two cities, which were matched to the energy modeling analysis. The project focused on the cold climates, and the cities presented here are Salem, Ore. (Climate Zone 4C), Chicago,

Title	Wall Description	Salem, OR & Chicago IL (USD)			Burlington, VT (USD)			Rank (least to most expensive)
		Material Cost	Labor Cost	Total Cost	Material Cost	Labor Cost	Total Cost	
Wall B	Drill-and-Fill (Cellulose)	867	1,423	2,289	875	1,437	2,312	1
Wall C	Minimally Invasive Cavity Spray Foam	9,000	2,134	11,134	9,090	2,155	11,245	4
Wall D	Exterior Expanded Polystyrene Foam, siding remains	16,780	35,772	52,552	16,948	36,130	53,078	11
Wall E	Drill-and-Fill (Cellulose), Exterior XPS, siding removed	8,814	27,878	36,692	8,902	28,156	37,059	9
Wall F	Drill-and-Fill (Cellulose), Exterior VIP/Vinyl Siding, siding removed	6,492	17,116	23,608	6,557	17,287	23,844	5
Wall G	Exterior mineral fiber board, siding remains	15,027	34,629	49,657	15,178	34,976	50,153	10
Wall H	Exterior Structural graphite impregnated EPS (gEPS) Panel (siding remains)	16,758	44,931	61,690	16,926	45,381	62,306	12
Wall J	Drill and Fill (Fiberglass)	867	5,110	5,976	875	5,161	6,036	3
Wall K	Interior Polyiso Insulation w/ Fiberglass Batt	1,729	3,619	5,349	1,747	3,655	5,402	2
Wall L	Drill & Fill (Fiberglass) w/ Exterior Polyiso Insulation (siding removed)	5,043	22,446	27,489	5,093	22,671	27,764	6
Wall M	EIFS Panel (siding removed)	110,000	46,678	156,678	111,100	47,144	158,244	14
Wall N	Prefabricated EPS Blocks	49,082	21,270	70,352	49,573	21,483	71,055	13
Wall O	Drill & Fill (Fiberglass) w/ Exterior Fiberglass Board Insulation	10,080	24,064	34,143	10,180	24,304	34,485	7
Wall P	Thermal Break Shear Wall (siding and sheathing removed)	7,337	27,512	34,849	7,410	27,787	35,198	8

Table 1. Material, labor, and total costs per square foot for each wall studied for Salem, Ore., Chicago, Ill., and Burlington, Vt.

Ill. (Climate Zone 5A), and Burlington, Vt. (Climate Zone 6A). In addition to labor, materials, and energy costs, simple payback and internal rate of return (IRR) were calculated to assess the viability of the initial investment.

Table 1 presents the costs per square foot for labor and materials in the two selected climate zones. Table 2 presents the IRR and simple payback for each wall system in Salem, Chicago, and Burlington. The IRR is the annual rate of growth that an investment is expected to generate. Payback is presented in years, and IRR is presented as percentages. Walls with high payback and negative IRR are not cost effective. Walls perform similarly in each ranking exercise, with the lowest-cost walls paying back in the shortest amount of time, considering energy savings.

CONCLUSION

This paper provides an overview of a three-year, multipart study of the viability of multiple retrofit approaches for residential wall systems.. The study focused on the thermal, moisture, and economic performance of 14 wall assemblies (cavity-fill, interior, and exterior approaches with and without removing existing siding) that included traditional and experimental approaches, using a typical uninsulated residential wall as a baseline.

A prototype of each wall retrofit was instrumented and installed on a test facility at the CRRF for physical testing. Data compiled during the in situ testing were then compared to energy and moisture modeling. Once validated, the hygrothermal models were employed to generalize the findings to multiple climate zones. Along with the physical performance of each wall, researchers worked with a local cost estimator to gather material and cost data to assess the techno-economic viability of the wall systems.

Wall retrofits have the potential to affect energy savings of variable magnitude across the many U.S. climate zones. It was found that the climate zones with the highest potential for retrofit savings are those that are heating dominated (Climate Zones 5–8). In these climate zones, the whole house energy savings associated with space conditioning for the simulated retrofit wall assemblies were in the range of 18% to 34%.

It was also observed that increasingly high *R*-value insulation improvements had a diminishing effect on wall conduction performance improvements. The highest potential for energy savings can be realized by going from

Title	Wall Description	Salem, OR		Chicago, IL		Burlington, VT		Rank (lowest payback to highest)
		IRR	Payback (years)	IRR	Payback (years)	IRR	Payback (years)	
Wall B	Drill-and-Fill (Cellulose)	29%	3	92%	1	80%	1	1
Wall C	Minimally Invasive Cavity Spray Foam	5%	15	5%	15	18%	6	4
Wall D	Exterior Expanded Polystyrene Foam, siding remains	-3%	50	2%	22	2%	22	11
Wall E	Drill-and-Fill (Cellulose), Exterior XPS, siding removed	-1%	35	5%	15	5%	15	7
Wall F	Drill-and-Fill (Cellulose), Exterior VIP/Vinyl Siding, siding removed	2%	22	10%	10	10%	10	5
Wall G	Exterior mineral fiber board, siding remains	-3%	47	3%	20	3%	21	10
Wall H	Exterior Structural graphite impregnated EPS (gEPS) Panel (siding remains)	-4%	57	-2%	42	-1%	33	12
Wall J	Drill and Fill (Fiberglass)	12%	6	17%	6	22%	5	3
Wall K	Interior Polyiso Insulation w/ Fiberglass Batt	13%	7	18%	6	23%	4	2
Wall L	Drill & Fill (Fiberglass) w/ Exterior Polyiso Insulation (siding removed)	1%	27	3%	19	5%	15	6
Wall M	EIFS Panel (siding removed)	-8%	107	-7%	107	-6%	84	14
Wall N	Prefabricated EPS Blocks	-5%	67	-3%	48	-1%	38	13
Wall O	Drill & Fill (Fiberglass) w/ Exterior Fiberglass Board Insulation	-1%	32	2%	24	3%	18	8
Wall P	Thermal Break Shear Wall (siding and sheathing removed)	-1%	35	1%	25	3%	20	9

Table 2. Internal rate of return (IRR) and payback period for every wall system in Salem, Ore., Chicago, Ill., and Burlington, Vt.

an uninsulated wall to a wall with cavity or continuous insulation, as opposed to a cavity-insulated wall being retrofitted to have both cavity and continuous insulation.

To determine whether the walls are moisture durable, WUFI Pro (version 6.4) was used to carry out hygrothermal simulations for northern exposures. The mold index measured in accordance with ASHRAE 160 was used as an indicator of moisture durability.

In all retrofit walls except Walls B and Wall J, the mold indices are less than 3. In the absence of any form of interior vapor control, the addition of exterior continuous insulation, especially with moisture-tolerant materials, is expected to improve the hygrothermal performance of the wall assembly by pushing the point of condensation or dew point to the exterior side of the exterior sheathing.

For Chicago, total costs for labor and materials to retrofit a 2400 ft^2 house ranged from \$1.85/ft^2 for Wall B (drill-and-fill cellulose) to \$45.45/ft^2 for Wall M (EIFS panel with the siding removed). From a materials-only perspective, the costs ranged from \$0.40/ft^2 for Wall B to \$22.50/ft^2 for Wall M. With respect to labor costs, Wall B was the least expensive at \$1.45/ft^2 whereas Wall M was most expensive at \$22.50/ft^2. Wall J (fill-and-drill fiberglass) showed the highest IRR at 25% and the shortest payback at two years. Wall M showed the lowest IRR at –5% and the longest payback at 67 years.

ACKNOWLEDGMENTS

This manuscript has been authored by UT-Battelle LLC under contract no. DE-AC05-00OR22725 with the U.S. Department of Energy. The authors acknowledge the support from Eric Werling at the U.S. Department of Energy and would like to thank him for his sponsorship, assistance, and technical discussions.

REFERENCES

1. U.S. Energy Information Administration. 2018. "Total Energy: Energy Consumption by Sector." https://www.eia.gov/totalenergy/data/browser/index.php?tbl=T02.01#/?f=A&start=1949&end=2017&charted=3-6-9-12.
2. Livingston, O., D. Elliott, P. Cole, and R. Bartlett. 2014. *Building Energy Codes Program: National Benefits Assessment*. PNNL-22610. Richland, WA: Pacific Northwest National Laboratory (PNNL). https:/doi.org/10.2172/1756522.
3. U.S. Census Bureau. 2017. "American FactFinder: Selected Housing Characteristics." https://factfinder.census.gov/faces/tableservices/jsf/pages/productview.xhtml?pid=ACS_17_5YR_DP04&src=pt.
4. Joint Center for Housing Studies of

Harvard University. 2019. "Improving America's Housing 2019." https://www.jchs.harvard.edu/sites/default/files/Harvard_JCHS_Improving_Americas_Housing_2019.pdf.

5. National Renewable Energy Laboratory. 2019. "ResStock: National Baseline (EFS v2)." https://resstock.nrel.gov/dataviewer/efs_v2_base#building-characteristics.
6. Antonopoulos, C., M. Baechler, C. Metzger, and J. Zhang, J. 2019. *Wall Upgrades for Residential Deep Energy Retrofits: Expert Meeting Report*. PNNL-28788. Richland, WA: PNNL. https://www.pnnl.gov/main/publications/external/technical_reports/PNNL-28788.pdf.
7. Antonopoulos, C., C. Metzger, J. Zhang, S. Ganguli, M. Baechler, H. Nagda, and A. Desjarlais. 2019. *Wall Upgrades for Residential Deep Energy Retrofits: A Literature Review.* PNNL-28690. Richland, WA: PNNL. https://doi.org/10.2172/1544550.
8. Dentz, J., and D. Podorson. 2014. "Evaluating an Exterior Insulation and Finish System for Deep Energy Retrofits." U.S. Department of Energy Building America Program. https://doi.org/10.2172/1123215.
9. Xie, Y., V. Mendon, M. Halverson, R. Bartlett, J. Hathaway, Y. Chen, and B. Liu. 2018. "Assessing Overall Building Energy Performance of a Large Population of Residential Single-Family Homes Using Limited Field Data." *Journal of Building Performance Simulation* 12 (4): 1–14. https://doi.org/10.1080/19401493.2018.1477833.
10. International Code Council (ICC). 2018. *International Energy Conservation Code*. Country Club Hills, IL: ICC.
11. National Renewable Energy Laboratory. n.d. ResStock website. https://resstock.nrel.gov.
12. Wilson, E., C. Christensen, S. Horowitz, J. Robertson, J. Maguire, E. Wilson, and J. Maguire. 2017. *Energy Efficiency Potential in the U. S. Single-Family Housing Stock*. NREL/TP-5500-65667. Golden, CO: National Renewable Energy Laboratory. https://www.nrel.gov/docs/fy18osti/68670.pdf.
13. Mendon, V. V., R. G. Lucas, and S. Goel. 2012. *Cost-Effectiveness Analysis of the 2009 and 2012 IECC Residential Provisions–Technical Support Document*. PNNL-22068. Richland, WA: PNNL. http://www.osti.gov/servlets/purl/1079749.
14. Lawrence Berkeley National Laboratory. 2019. "Two-Dimensional Building Heat-Transfer Modeling." https://windows.lbl.gov/software/therm.
15. Antretter, F., F. Sauer, T. Schöpfer, and A. Holm. 2011. "Validation of a Hygrothermal Whole Building Simulation Software." *Proceedings of Building Simulation 2011: 12th Conference of International Building Performance Simulation Association, Sydney, 14-16 November.* http://ibpsa.org/proceedings/BS2011/P_1554.pdf.
16. Arena, L., and P. Mantha. 2013. "Moisture Research—Optimizing Wall Assemblies." U.S. Department of Energy Building America Program. https://www.nrel.gov/docs/fy13osti/56709.pdf.
17. Lepage, R., and J. Lstiburek. 2013. "Moisture Durability with Insulating Sheathing." U.S. Department of Energy Building America Program. https://doi.org/10.1111/nph.15034.
18. Lepage, R., C. Schumacher, and A. Lukachko. 2013. "Moisture Management for High *R*-Value Walls Moisture Management." U.S. Department of Energy, Building America Program. https://www.nrel.gov/docs/fy14osti/60487.pdf.
19. ASTM International. 2017. *Standard Test Method for Steady-State Thermal Transmission Properties by Means of the Heat Flow Meter Apparatus.* ASTM C518-17. West Conshohocken, PA: ASTM International.
20. ASTM International. 2016. *Standard Test Method for Water Vapor Transmission of Materials.* ASTM E96-16. West Conshohocken, PA: ASTM International.
21. ASHRAE. 2016. *Criteria for Moisture-Control Design Analysis in Buildings*. ANSI/ASHRAE 160-2016, Atlanta, GA: ASHRAE.
22. Viitanen, H., and T. Ojanen. 2007. "Improved Model to Predict Mold Growth in Building Materials." In: *Proceedings of the Thermal Performance of the Exterior Envelopes of Whole Building X, Clearwater Beach, Florida*. https://web.ornl.gov/sci/buildings/conf-archive/2007%20B10%20papers/162_Viitanen.pdf.
23. Draycott, S., I. Szadkowska, M. Silva, and M. D. Ingram. 2018. "Assessing the Macro-Economic Benefit of Installing a Farm of Oscillating Water Columns in Scotland and Portugal." *Energies* 11(10): 2824. https://doi.org/10.3390/en11102824.
24. RS Means. 2020. "Residential Cost Data." https://www.rsmeans.com.

Wet Concrete Can Ruin a Good Roof Design: Insights to Cement Your Success

Jennifer Keegan, AAIA

GAF | Siplast | Parsippany, NJ

jennifer.keegan@gaf.com

Corey Zussman, RBEC, REWC, RWC, RRC, RRO

Pepper Construction | Barrington, IL

czussman@pepperconstruction.com

IIBEC 2022 - Building for the Future

International Convention and Trade Show

March 17–22, 2022 | Orlando, FL

ABSTRACT

With misinformation swirling around the topic of moisture in concrete roof decks, it can be difficult to know the right approach to take to mitigate risk. Key questions include:

- Are roof failures due to moisture in concrete primarily associated with the use of lightweight concrete decks?
- When can the building interior facilitate downward drying of a wet concrete roof deck?
- Is 28 days the right amount of time to let a new concrete deck cure before installing a roof?
- Are admixtures and moisture vapor–reduction additives effective in mitigating concerns around moisture in concrete roof decks?
- Are vapor retarders the answer? What about vented base sheets?
- Which adhesives and insulation and cover board facers are appropriate to use in these roof assemblies?

The presenters explore these industry-wide issues, debunk some of the myths, provide a framework to discuss the risks with the project team, review design considerations, and discuss guidelines to mitigate your risk.

SPEAKERS

Jennifer Keegan, AAIA

GAF | Siplast | Parsippany, NJ

Jennifer Keegan is the director of building and roofing science for GAF | Siplast, focusing on overall roof system design and performance. She has more than 20 years of experience as a building enclosure consultant specializing in building forensics, assessment, design, and remediation of building enclosure systems. Keegan provides technical leadership within the industry as the chair of the ASTM D08.22 Roofing and Waterproofing Subcommittee and as the education chair for IIBEC. She advocates for women within the industry, serving as an executive board member of National Women in Roofing and a board member of Women in Construction.

Corey Zussman, RBEC, REWC, RWC, RRC, RRO

Pepper Construction | Barrington, IL

Corey Zussman is a 26-year veteran in the construction industry. Since 2012, he has helped guide the leadership, design, and implementation of Pepper Construction's quality management systems and continually assesses and improves the effectiveness of the firm's processes and standards. As director of quality management, Zussman visits Pepper jobsites to plan, oversee, and promote construction quality directives. He serves as a resource to all project teams throughout the preconstruction and construction process. Zussman has a bachelor of architecture degree with a minor in construction management and business management and master of business administration degree with a specialization in quality management from the Illinois Institute of Technology.

Wet Concrete Can Ruin a Good Roof Design: Insights to Cement Your Success

Moisture-related issues in low-slope concrete roof decks continue to challenge the roofing industry. Moisture migration from the concrete roof deck into the roof system can lead to loss of adhesion of various components within the system, degradation of materials that do not perform well in moist environments, and microbial growth within the roof system. While more aggressive construction schedules may be a contributing factor, changes to the materials used and how roof systems are designed and installed have a greater impact on long-term performance. Design and installation considerations will be discussed in this paper.

TYPES OF CONCRETE ROOF DECKS

Concrete is a mixture of portland cement, aggregates, entrained air, water, and other admixtures. Concrete roof decks make up approximately 15% of the new and retrofit low-slope construction market.[1] There are several different types of concrete that are used in the construction of roof decks.

- Normalweight structural concrete decks: Typical structural concrete uses normalweight aggregate that is generally dense (typically called "hard rock"). These decks use cast-in-place concrete that becomes an integral part of the structure. Normalweight concrete is designed to carry heavy loads. Normalweight structural concrete can be installed over nonremovable vented and nonvented metal form decking.
- Lightweight structural concrete decks: Lightweight structural concrete uses lightweight, porous aggregate such as shale, which is typically prewetted and can absorb up to 30% water by weight. Because of the density difference between the aggregates used in normalweight and lightweight concrete, there are density differences between both concrete types in their finished form. Lightweight concrete reduces dead loads while improving thermal and fire-resistance properties. Lightweight structural concrete can be installed over nonremovable vented and nonvented metal form decking.
- Precast concrete decks: These decks are often constructed of prestressed or post-tensioned normalweight concrete. These T-shaped or hollow-core precast concrete components are often covered with a layer of lightweight concrete to serve as a leveling or protection layer, which can be more than 6 in. (150 mm) thick to address the camber and provide slope.
- Structural concrete composite decks: These decks are based on a steel panel deck system that is filled with normalweight or lightweight structural concrete. Loads are carried by the combination of the steel deck and concrete, which act as a single component. Typically, the steel panels are embossed to ensure mechanical coupling to the concrete.
- Lightweight insulating concrete (LWIC) decks: LWIC is a mixture of portland cement, aggregate, water, and (in cellular mixture proportions) air entrainment in the form of cellular foam. LWIC is used with expanded polystyrene insulation with open cores and can be placed over a variety of structural deck systems. LWIC decks are intended for use as an insulation and a substrate for roof membranes. LWIC can provide custom slope to drain and provide insulation that can last as long as the building. While there is a lot of water in the mixture proportions of LWIC to allow for flowability of the concrete, the moisture is managed in the design through venting. The use of LWIC has a proven design process and, when properly executed, is not typically associated with moisture-related issues; therefore, it is excluded from this discussion.

The density of concrete varies depending on the type and volume of aggregate, the water-to-cementitious materials ratio (*w/cm*), and amount of air entrainment. Concrete physical properties according to ASTM C330[2] and ASTM C332[3] are provided in **Table 1**. As shown in the table, decreasing concrete density correlates to decreasing thermal conductivity, which in turn improves the fire rating. However, as density decreases, so does compressive strength.

Both normalweight and lightweight structural cast-in-place concrete decks contain a high level of water when placed. Normalweight structural concrete uses regular aggregates with a low moisture absorption rate of up to 2%, while lightweight concrete uses shales and clays that are expanded with air to make them less dense but which have a higher moisture absorption rate of 10% to 30%. Lightweight aggregates are water soaked before they are added to the mixture so they do not absorb water needed for concrete curing.

The amount of water added to the mixture is expressed in terms of *w/cm*, which is typi-

Type of concrete	Compressive strength, psi	Density, lb/ft^3	Typical thermal conductivity, Btu·in./(hr·ft^2·°F)	Aggregate absorption rate, %
Structural concrete, normalweight	2500–5000	145–155	12.06	0.1–2
Lightweight structural concrete	>2500	90–115	4.72	10–30
Lightweight insulating concrete	100–500	15–50	0.45–1.50 (0.83)	

Table 1. Physical properties of concrete types according to ASTM C330 and ASTM C332

	Normalweight concrete with 0.5% aggregate absorption	Lightweight concrete with 10% aggregate absorption	Lightweight concrete with 20% aggregate absorption
Total cementitious material, lb/yd^3	650	710	710
Water–to–cementitious materials ratio	0.39	0.43	0.43
Added batch water, lb/yd^3	242	308	308
1% fine aggregate absorption, lb of water per yd^3	11	13	13
Coarse aggregate absorption, lb of water per yd^3	10	73	145
Total water in batch, lb/yd^3	263	394	466
Water consumed in hydration reactions, lb/yd^3	163	178	178
Water remaining after hydration, lb/yd^3	100	216	288
Water remaining in 6 in. concrete deck, 1 month after placement, quart/ft^2	0.9	1.9	2.6

*Additional water from weather or construction practices (such as, moist curing) has not been included in these calculations.
Source: Adapted from from Condren et al.[2]

*Table 2. Water added to and remaining in example concrete mixtures**

cally designed at 0.40 to 0.55 range. Water is added to the concrete mixture to hydrate the cement and to reduce the concrete's viscosity, which aids in the concrete's flowability and reduces the potential for voids in the concrete, regardless of the concrete type. The theoretical maximum amount of water needed to hydrate all cement in a mixture corresponds to a *w/cm* of approximately 0.25. Therefore, all newly placed concrete will contain surplus water that is not consumed in the hydration process if the *w/cm* is greater than 0.25, which is common for convenience of concrete placement.

Table 2[4] demonstrates the amount of water remaining in a 6 in. (150 mm) concrete roof deck one month after placement. The volume of water remaining in lightweight concrete with 10% aggregate absorption is about double that of normalweight concrete, and the volume remaining is nearly triple that of normalweight concrete when the aggregate absorption rate is increased to 20%.

ADVANTAGES OF CONCRETE ROOF DECKS

There are several advantages to the use of concrete roof decks. Primarily, they are selected based on structural requirements and desired fire ratings. Concrete can reduce air infiltration and improve wind-uplift ratings. As wind rises up and over a building, it creates uplift pressure that exerts an upward force on the roof membrane. The *International Energy Conservation Code* (IECC)[5] considers concrete to be an effective air barrier, provided that all seams and joints, as well as all the penetrations and cracks that develop, are sealed. By restricting airflow up into a roof assembly, the resistance of the roof system to that upward force is increased. This is shown in Fig. 1, which compares a concrete deck with a steel deck. When penetrations through a concrete deck are made after the concrete is placed, they must be carefully sealed to maintain the air barrier and prevent upward air movement.

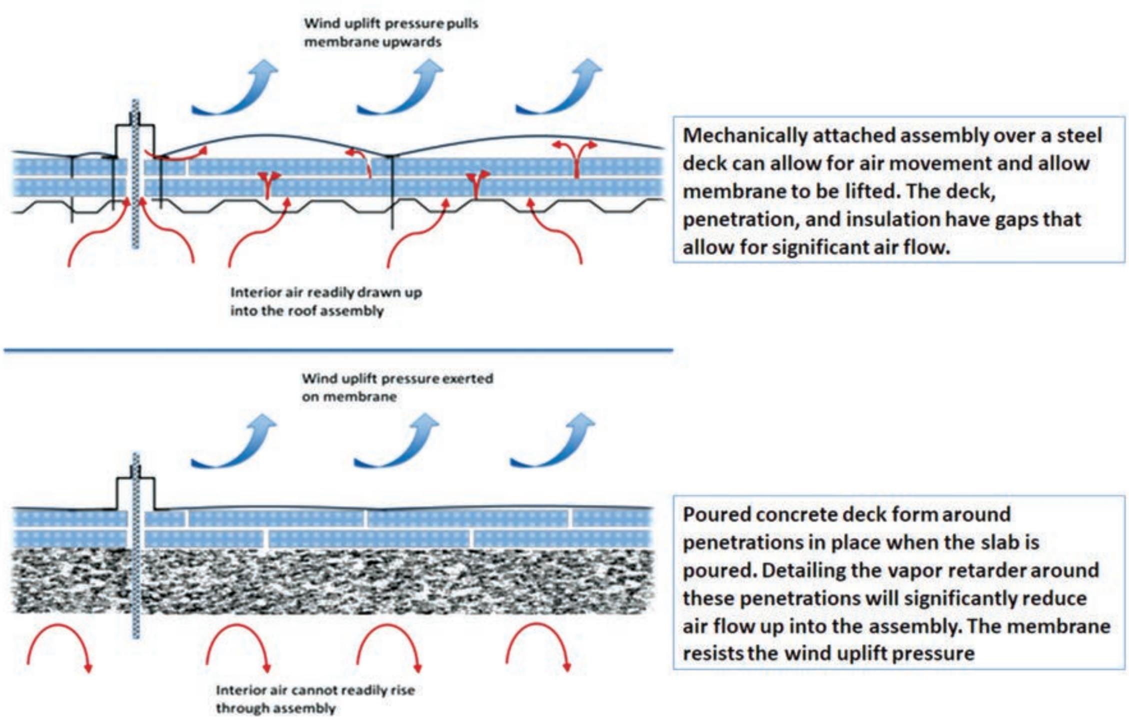

Figure 1. The relative efficacy of steel and concrete roof decks in terms of resisting air intrusion. Note that the wind uplift of the concrete deck can be further improved by adhering the insulation and membrane.

Despite the benefits of the concrete reducing the amount of air infiltration and the related transported moisture from collecting within the roof system, excessive moisture in concrete roof decks themselves can lead to poor performance of roof assemblies. The industry is still learning about the causes of these failures, and what does and does not work to mitigate the issue.

Despite the benefits of the concrete reducing the amount of air infiltration and the related transported moisture from collecting within the roof system, excessive moisture in concrete roof decks themselves can lead to poor performance of roof assemblies. The industry is still learning about the causes of these failures, and what does and does not work to mitigate the issue.

HOW THIS STARTED

Prior to the 1990s, normalweight structural concrete was used to cast roof decks over forms that were removed once the concrete achieved the specified compressive strength. Once the interior was conditioned, the residual moisture in the concrete roof deck could migrate downward into the building, gradually drying over time. Traditionally, insulation was adhered to the concrete deck with a full mopping of hot-applied asphalt. The continuous application of asphalt performed as a class 1 vapor retarder, mitigating the impact of latent moisture in the concrete on the roof system. This approach is still successfully used today.

In the 1990s, newer technologies became popular in the roofing industry, displacing the traditional asphaltic-based application methods. Insulation boards could now be installed with solvent-based and water-based adhesives, and in the 2000s, low-rise foam adhesives were introduced to the market. Engineers began specifying lightweight structural concrete more often, metal deck forms were often left in place, and low-rise foam applied in a spatter pattern or ribbons was used to secure the roof insulation. This approach introduces a significant amount of moisture, does not provide the ability for downward drying of the deck, and does not provide a vapor retarder to prevent the moisture in the concrete from migrating into the roof system.

Interestingly, removable forms are currently making a comeback, replacing steel decking. This development is driven by the steel market, which can be volatile in terms of cost and timing. Contractors are more confident in the cost of concrete, and often construction of a concrete deck is just as quick, if not quicker, than the use of steel.

EXAMINATION OF INDUSTRY ISSUES SURROUNDING MOISTURE IN CONCRETE

Around 2010, there was an increase in reported moisture-related issues with roofs installed over new concrete roof decks. While the primary function of a roof system is to keep water out of the building, moisture accumulation within the roof system can negatively affect the roof system's performance and long-term durability. Moisture accumulation can lead to adhesion loss; adhesive issues with water-based and low-volatile organic compound adhesives; material degradation of roof system components, including loss of strength; metal and fastener corrosion; insulation *R*-value loss; and microbial growth.[6] Also, restrictions on volatile organic compound content resulted in the greater use of water-based adhesives, which can be "much more susceptible to re-emulsification when exposed to moisture, depending on the adhesive formulation."[7]

When moisture accumulation affects the attachment of the roof system, the damage can lead to failure if left unchecked. There is a risk of significant property loss from wind-uplift damage, dimensional changes or crushing of the substrate, blistering or splitting of the roof membrane, and biological growth.

Several technical advisories have been issued to raise awareness about the potential for moisture issues associated with concrete roof decks. These include publications by IIBEC,[7] the National Roofing Contractors Association (NRCA),[8] the Asphalt Roofing Manufacturers Association,[9] the Single-Ply Roofing Institute,[10] the Polyisocyanurate Insulation Manufacturers Association,[11] and many roof manufacturers.

FACT OR FICTION?

Is Moisture in Concrete Only an Issue with Lightweight Structural Concrete?

As the industry began to pay attention to increased reports of moisture-related issues with roofs installed over new concrete roof decks around 2010, it was noted that many of these roof failures involved lightweight structural concrete roof decks.

Lightweight aggregates absorb up to 30% water by weight, whereas normalweight concrete aggregates typically absorb less than 2% water by weight. NRCA's calculations[6] indicate

	Lightweight structural concrete, perm-in.		Normalweight concrete, perm-in.	
Age	Wet cup	Dry cup	Wet cup	Dry cup
28 days	1.48	0.78	3.42	1.05
60 days	1.45	0.47	2.03	1.13

Table 3. Permeability of concrete decks evaluated per ASTM E96

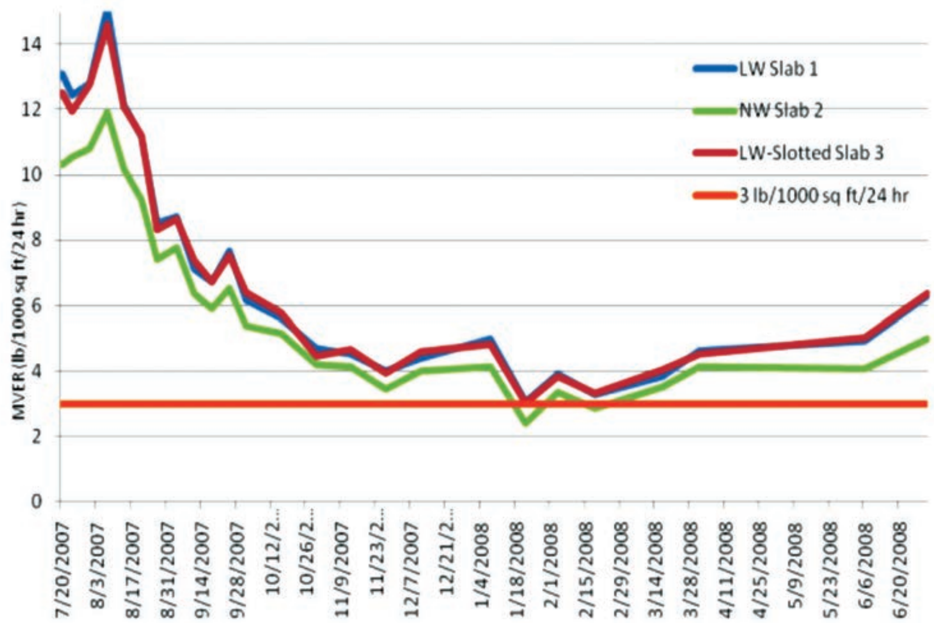

Figure 2. Moisture vapor emission rate (MVER) for lightweight (LW) structural and normalweight (NW) concrete test slabs in a nonconditioned environment.[12]

that after the 28-day cure time, the amount of free water present in a 6 in. (150 mm) lightweight structural concrete deck can be nearly three times the amount in a normalweight concrete deck. This conclusion is supported by the calculations in Table 2.

Additionally, as concrete cures, its permeability is reduced, as shown in **Table 3**.[8] While lightweight structural concrete is placed with more water than normalweight structural concrete and has two to three times more water remaining after the initial 28-day cure, it also has about half the permeability of normalweight structural concrete. This implies that lightweight structural concrete will dry at a slower rate than normalweight concrete.

Although the increase in moisture-related issues was initially associated with lightweight structural concrete, by 2015 the number of lightweight structural concrete cases was proportional to that of normalweight structural concrete cases, indicating that the extra free evaporative moisture in the lightweight aggregate was not the sole cause of the moisture-related roof failures.[8]

Craig and Wolfe[12] evaluated moisture levels and relative humidity levels in two lightweight structural concrete test slabs and one normalweight concrete test slabs in a nonconditioned environment. While the normalweight concrete slab did dry to a lower moisture vapor emission rate (MVER) level than the lightweight concrete slabs, the differences were reasonably small, as shown in **Fig. 2**. During the 13-month study, neither the normalweight or lightweight concrete slabs recorded an internal relative humidity level below 80%.

The MVER results in **Table 4** show all three test slabs following a similar drying pattern. While the normalweight concrete did record a lower MVER than the lightweight slabs, the difference was only about 1 lb (4.45 N) after the first two months of drying time. Note that slab 3 incorporated vented steel decking, which had no effect on the MVER.

Even though it is known that there are moisture-related risks with both normalweight and lightweight concrete roof decks, NRCA and some manufacturers still recommend avoiding lightweight concrete in roofing applications.

Similarly, FM Global's Loss Prevention Data Sheet (LPDS) 1-29[13] provides additional requirements for situations when a lightweight structural concrete roof deck is necessary, stating that "a great deal of moisture will be released for several months after the concrete has hardened and will be absorbed by above-deck components. This will damage and weaken those components, resulting in damage from winds below design speeds, or premature deterioration requiring replacement."

Regardless, both normalweight and lightweight concrete types are known to be a risk factor for new roof systems. Therefore, roof systems should be designed to accommodate this moisture, regardless of the type of concrete used.

Are Concrete Decks Ready to Roof after a 28-Day Cure?

Water takes a long time to diffuse out of what is typically a 4- to 6-in.-thick (100- to 150-mm thick) composite concrete deck, and the time can be extended if the deck is exposed to wet weather during the construction period. The inherent moisture migration in the concrete structure is exacerbated by concrete mixture proportions and the cascading adhesion

MVER test results, lb/1000 ft²/24 hr					
Drying time, days	Ambient temperature, °F	Ambient RH, %	Slab 1 (LW)	Slab 2 (NW)	Slab 3 (LW)
30	76.0	62.0	12.3	10.3	12.7
48	85.0	74.0	15.7	12.6	15.5
90	74.7	60.0	7.9	6.5	7.9
174	65.4	41.0	4.9	4.0	4.8
216	53.3	29.0	3.2	2.6	3.2
281	66.1	38.1	4.4	3.5	4.4

Note: LW = lightweight concrete; MVER = moisture vapor emission rate; NW = normalweight concrete; RH = relative humidity.

Table 4. Moisture vapor emission rate for lightweight structural and normalweight concrete test slabs in a nonconditioned environment[12]

problems that can occur in roof systems. Significant amounts of water remain after curing is completed, even more so when lightweight aggregates are incorporated into the mixture.

The conventional 28-day cure period for concrete is to achieve appropriate compressive strength. In concrete roof decks, there is very little correlation between cure time and the amount of water remaining. Guideline "rules of thumb" such as not installing the roof system until a minimum of 30 days after concrete placing and forming are not particularly effective at reducing or eliminating issues.

When a concrete deck is placed, some of the mixture's water is used up by the curing process, and some evaporates. However, because the rate of evaporation is slow, large quantities of water remain stored within the concrete for extended periods. Moisture retention is exacerbated by construction methods that install concrete over nonremovable, nonvented metal forms or other impermeable substrates. While the concrete itself is generally not damaged by this moisture, the moisture typically migrates into the roofing system, where it is absorbed by materials that are more moisture sensitive.

Among the many variables that affect the concrete drying rate are location, the volume of mixing water, and any rewetting from rain exposure during construction (the latter will extend the drying time). In the late 1990s, Hedenblad concluded that it can take three to six months, or longer, for a new concrete roof deck to be dry enough to roof over.[14,15] However, it is important to understand that schedules for construction projects do not permit sufficient time for the concrete roof deck to reach the level of "dryness" defined in Hedenblad's work. Therefore, roof systems installed over concrete must be designed to perform despite residual moisture within the roof deck.

Do Vented Composite Decks Significantly Enhance Downward Drying?

The use of nonremovable forms or composite steel and concrete decks has significantly increased in the past 30 years. These decks allow for much shorter construction timelines, eliminating much of the expense of building and stripping temporary form structures, and they are structurally efficient. However, by leaving the steel formwork in place at the bottom of the concrete slab, the concrete cannot dry to the underside. Therefore, the roof deck retains a significant amount of water, as there are very limited pathways to allow for drying, as shown in Fig. 3.

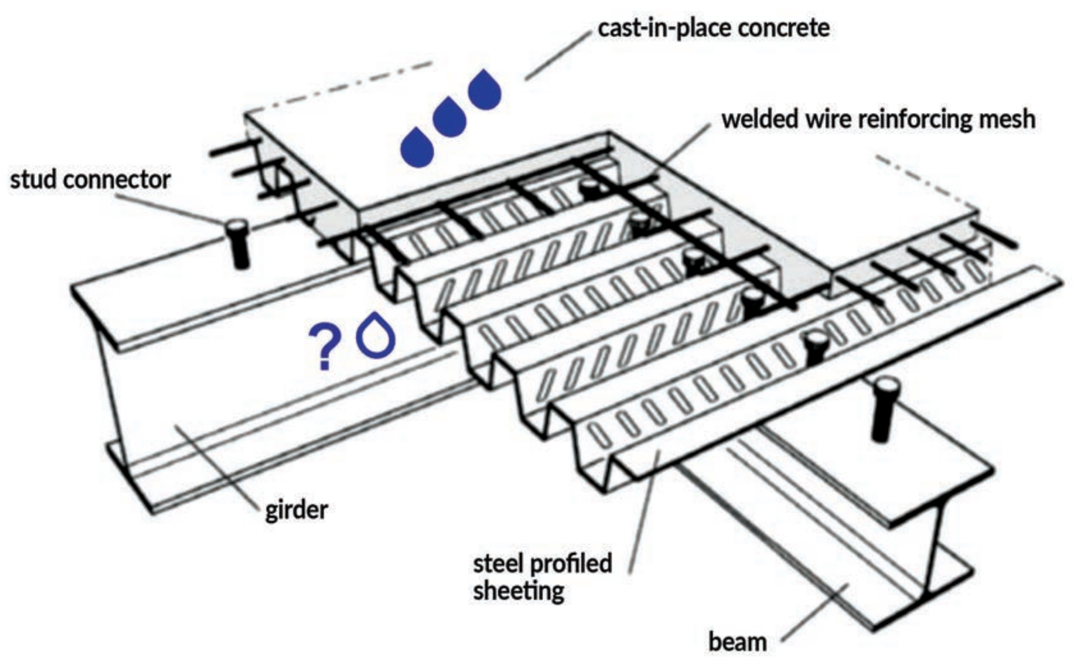

Figure 3. The actual venting achieved by vented metal decks is not yet quantified.

There is an option to vent the steel form deck, which may facilitate some amount of downward drying. However, according to IIBEC Technical Advisory 020-2021,[7] "steel pan decks, whether vented or non-vented, function essentially as a vapor retarder located beneath the concrete, which significantly reduces the amount of drying that can occur from the bottom side of the concrete." Despite this commentary, the IIBEC bulletin also recommends the use of vented metal decks.

There is only one source of published data to quantify the actual venting achieved with the use of vented metal decks. The Steel Deck Institute's position statement "Venting of Composite Steel Floor Deck"[16] states, "The steel deck acts as a vapor barrier . . . a hypothetical 1.5% open area will increase the diffusion of water by 1.5%, an inconsequential amount." According to IIBEC, the venting is presumed to be of "minimal value with respect to downward drying."[7] FM Global's LPDS 1-29[13] states that vented metal decks "will have limited impact on moisture reduction" and requires additional design considerations beyond a vented metal deck. Despite the acknowledgement from various industry organizations, manufacturers, and FM Global that vented metal decks contribute minimally to the drying of concrete roof decks, current best practice is to use vented metal decks to allow for downward drying, especially when lightweight concrete is used.

ROOF ASSEMBLY COMPONENTS VULNERABLE TO THE MOISTURE

While the roof system needs to be considered in its entirety, it is also important to understand how various components within the roof assembly are vulnerable to and can be affected by the moisture inherent in concrete roof decks. Best practice is to assume that there will be moisture in the roof assembly from the concrete roof deck and to design and install the roof accordingly. Designers and contractors alike should be aware of these vulnerabilities and mitigate the risks associated with concrete roof decks, starting from the specifications, through value-engineering and cost-reduction processes, to installation.

Vapor retarders are often included in roof assemblies over concrete roof decks. There is no industry consensus on how to determine the right time to begin installation of the roof system, and some project teams have experienced early failure of newly installed vapor retarders. Moisture can accumulate under the vapor retarder and inhibit the initial bond between the vapor retarder and the concrete deck. Fastening down a vapor retarder can provide redundancy to keep the vapor retarder, and the roof system that is adhered to it, in place.

When selecting insulation, there are several elements to consider. Beyond meeting the required *R*-value for the project, selection of an insulation that will not be damaged by moisture is the first step. Moisture can negatively affect the bond of the organic or paper facers on insulation boards, which may result in uplift failures for wind loads well below the design wind pressures. Due to their absorptive characteristics, organic or paper facers may not maintain their bond to the insulation board once wet and can also support biological growth by providing a food source once wet. Coated-glass facers (CGFs) can help provide enhanced protection against moisture and biological growth, as well as potentially increase wind-uplift resistance and fire performance.

There are some considerations surrounding the attachment of the insulation and membrane. Roof assemblies over concrete decks are typically adhered because drilling fasteners into the concrete is more expensive and takes longer (and is more disruptive to tenants for reroofing projects). Traditionally, hot asphalt was used as an adhesive to install the insulation and became an integral part of the roof membrane, setting felt plies into the hot asphalt. However, over the past 20 years, water-based and solvent-based adhesives have largely displaced the use of hot asphalt to reduce installation times and remove kettles from the roof.

Water-based adhesives often require primers over concrete, and functionality of both the adhesive and the primer depends on them not being exposed to elevated moisture levels once they are installed. These water-based materials can soften and revert when they are exposed to moisture after installation. Therefore, in situations where there is a potential for the primer and/or adhesives to be rewetted, solvent-based materials can provide a more durable solution. Low-rise foam adhesives for insulation and roof membrane attachment perform better in these conditions, as they do not rely on moisture in the air to cure and the bonding strength can result in systems that achieve high wind-uplift ratings without mechanical attachment.

There are discussions about the long-term effects of the moisture and alkalinity of concrete on fasteners. Stainless steel fasteners with an AISI Type 304 or 305 designation or corrosion-resistant, ceramic-coated carbon steel fasteners are often specified to provide extra corrosion resistance and extend the life of the fastener in a damp and alkaline condition. Additionally, FM Global LPDS 1-29[13] requires the use of a mechanically fastened base sheet or a "dry" deck prior to installation of the roof when using a lightweight structural concrete roof deck.

The selection of cover board materials poses similar challenges to the selction of insulation. When using a cover board in the roof assembly over a concrete deck, it is important to consider moisture durability. Gypsum-based cover boards generally do not perform well with extended exposure to moisture. The gypsum can soften and lose its strength over time. This can reduce the uplift resistance of the roof assembly as well as the impact resistance of the assembly to hail, storm debris, and even foot traffic. Cementitious boards provide more protection than gypsum boards against moisture. Additionally, the consideration of organic versus inorganic facers is the same for cover boards as it is for insulation. Inorganic facers and CGFs perform better in roof systems over concrete decks than organic and paper facers. Lastly, like insulation, cover boards are usually adhered in these roof assemblies; therefore, the conversation about water-based versus solvent-based adhesives applies here as well.

FACT OR FICTION?
Are Vapor Barriers the Solution to Roofing over Wet Concrete Decks?

Traditionally, the first layer of a low-slope roof system was a layer of hot asphalt, applied directly to the new concrete deck. That layer of hot asphalt would act as an effective vapor retarder. Today's roof systems use adhesives or low-rise foam in ribbon patterns or spatter attachment. These types of attachment methods do not inherently have a vapor retarder on the deck, potentially allowing the moisture in the new concrete deck to migrate into the roof system.

Vapor retarders are designed to reduce vapor diffusion. A class 1 vapor retarder has a perm rating of 0.1 perms or less, and is often referred to as a vapor barrier. A class 1 vapor retarder installed on the concrete is necessary for expected roof system performance in all climate zones, except possibly ASHRAE Climate Zone 1, given the right conditions.[4] NRCA also recommends the use of a class 1 vapor retarder in roof systems over concrete roof decks in all climate zones because of its ability to prevent moisture from entering the roof system. However, there are no industry guidelines on when to install the vapor retarder during the construction process, which leaves all parties to point at each other to take responsibility for the "correct time" to install the vapor retarder, which is often in conflict with the construction schedule.

Specifying a class 1 vapor retarder over the concrete deck is certainly part of the solution, but the answer isn't quite that simple. While the initial bond of the self-adhered vapor retarder to a "wet deck" may result in acceptable adhesion, no formal studies have been conducted to evaluate the adhesion over time when exposed to upward vapor drive from curing concrete, though it has been recommended by researchers.[17] It is possible that the bond would be insufficient over time as the moisture migrates out of the roof concrete slab over a period of years, as demonstrated by SRI Consultants.[8]

To make matters worse, subsequent layers of roof insulation and roof membrane are often also adhered together, relying on the initial self-adhered vapor retarder's bond to the "wet deck" to attach the entire roof system.

While vapor retarders can be a necessary part of roof systems installed over concrete decks, the traditional rules of thumb may not be enough. The concerns around long-term adhesion to the concrete deck are leading contractors and designers to consider additional steps to keep the roof system attached to the building. In a 2020 article,[18] Pierce and Crowe provide six alternative design configurations and attachment methods to navigate various scenarios and the attachments, assembly layers, and the fundamental physics at work across the interconnected structure and roof systems. **Figure 4** shows an example of one of the scenarios provided, with the nontraditional design elements highlighted in red for clarity. Mechanical attachment of the vapor retarder provides redundancy to help keep the vapor retarder secured to the roof deck, and the roof system that is adhered to the vapor retarder, in place.

While industry guidance points toward the use of a vapor retarder over concrete decks, which includes two plies of hot-mopped asphalt or self-adhered asphaltic membranes, there are continued concerns regarding the potential for moisture to be trapped between the vapor retarder at the deck level and the roof membrane, which also acts as a class 1 vapor retarder. However, the risk of not using a vapor retarder at the deck level exceeds the risk of trapping moisture within the roof system, which would be a potential risk with poor design and/or installation.

Are Manufacturers Responsible for Providing Roof Assemblies That Work with Concrete Roof Decks?

While manufacturers must provide rated roof systems that meet code and industry standards, the designer of record is responsible for the design of the roof system. Individual responsibilities and considerations for each contributor to a roofing project are discussed here.

Designer

To design a durable roof system and mitigate the risk of failure, best practice is for designers of the roof system to assume that the concrete roof deck will be wet for an extended period of time. The design must specify how the moisture and vapor drive within the concrete deck, as well as environmental conditions, will be addressed. The concrete roof deck is rewetted each time it rains during the construction process, and the evaporation of moisture is slowed in the winter. There is no current means to evaluate a concrete deck for "dryness," nor is there sufficient time in any construction project to pause for the drying of the concrete roof deck.

General Contractor

The general contractor is responsible for coordinating the concrete and roofing subcontractors. The general contractor must also understand the potential consequences of construction methods that may use of additives, curing agents, nonremovable forms, temporary protection, or temporary heat. Another general contractor responisiblity is to determine whether value-engineering and cost-reduction strategies within the roof assembly—including any treatments to the underside of the concrete roof deck such as paints and epoxy coatings for exposed ceilings—may inhibit the concrete deck's ability for downward drying.

Roofing Contractor

The roofing contractor is responsible for installing the roof system as designed and per the manufacturer's written instructions. However, without consensus on a quantitative industry standard to assess the moisture content in a concrete roof deck, the roofing contractor may not be capable of assessing the moisture within the concrete roof deck.

NRCA recommends the use of the following contractual provision to protect roofing contractors from misplaced liability for determining whether the substrate is acceptable (that is, for determining thatthe concrete deck is "dry" and ready to receive roofing):

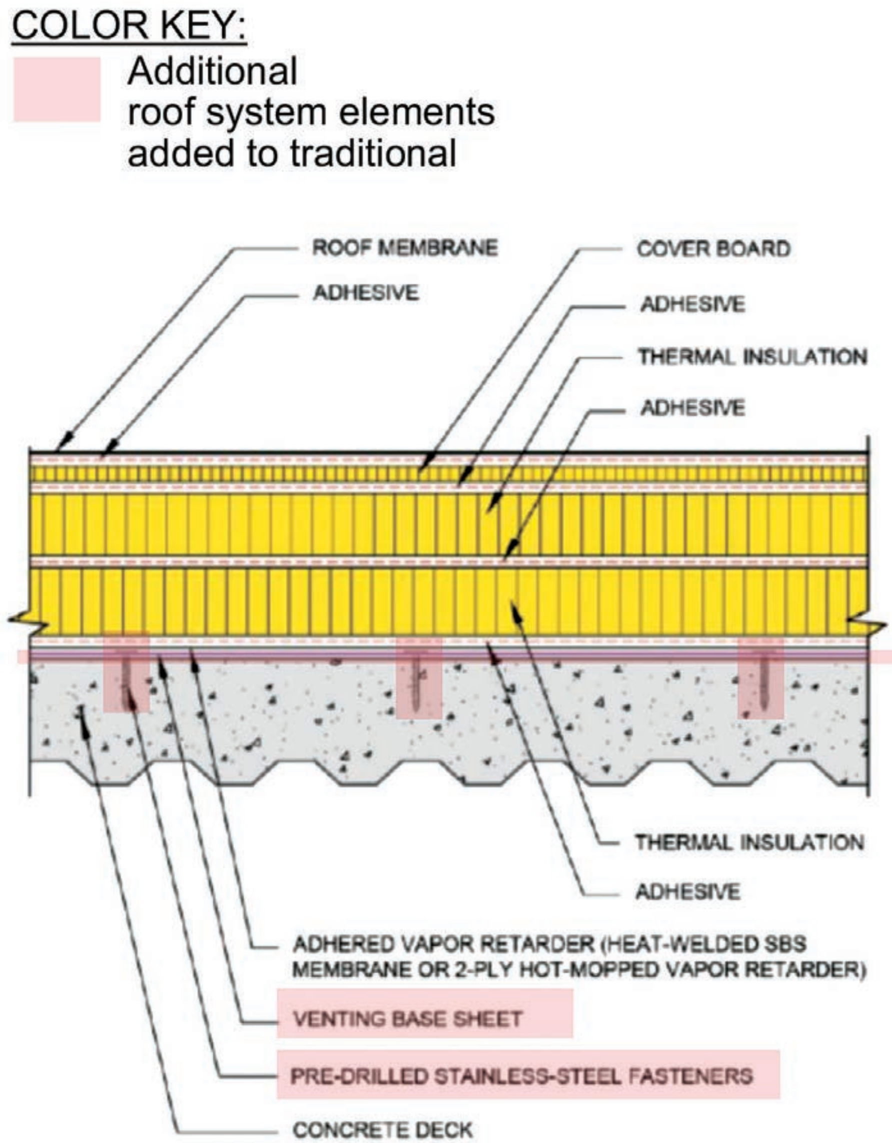

Figure 4. Example of added roof complexity from evolving structural design. Note: SBS = styrene-butadiene-styrene.

> Roofing Contractor is not responsible to test or assess the moisture content of the deck or evaluate the likelihood of condensation from moisture drive within the building. Roofing Contractor recommends that roofing not commence until probes in concrete decks show moisture content is no greater than 75% relative humidity when there is no organic content within the roofing materials. Wood fiberboard, perlite and organic paper facers on polyisocyanurate insulation will generate mold with relative humidity as low as about 65-70%.[19]

The overall roof system design needs to account for the moisture within the concrete roof slab for successful performance. This is primarily the responsibility of the roof designer, whether that be an architect, a roof consultant, or a roofing contractor who is providing the roof design, which is more common in reroofing projects than in new construction. If the roofing contractor notices risk in the roof system design, they could reduce their risk in the project by submitting a request for information and suggesting a project team meeting to discuss the potential risks. A roof consultant could also be a worthwhile investment to address concerns with roof design.

When the roofing contractor acts as the designer in a reroof project, the contractor takes on the responsibility for the design, even when replacing the roof with the same system as originally installed on the building.

Roofing Manufacturer

Roofing manufacturers are responsible for providing installation instructions for their products, but they do not determine when the concrete is "dry enough" for installation. Warranties or guarantees typically provide for the repair of covered leaks, which may not include leaks or other failures due to improper design. Additionally, given the inherent risks when roofing is installed over lightweight structural concrete, manufacturers may have an exclusion for moisture in the roof substrate or additional requirements for such projects, or they could reduce the duration of the warranty or guarantee.

If the roof fails prematurely, all parties likely will be brought to the table. Ultimately, the designer of record is responsible for designing a roof system that accounts for the likelihood of moisture in a concrete deck, and the roofing contractor is responsible for installing the roof system as designed and per the manufacturer's written instructions.

DESIGN CONSIDERATIONS TO ADDRESS MOISTURE-RELATED RISKS

As we have established, the time required for a concrete roof deck to "dry out" is unpredictable, it is unreasonable to expect that any construction schedule will allow for the time needed to "dry out," and it can be challenging to determine when a concrete roof deck is ready for roofing. Thefore, the design must assume the worst-case scenario: a wet roof deck.

There are several design options to consider. Working with the structural engineer is often the first opportunity to open the conversation regarding the use of structural concrete for the roof deck. The following are questions for the roof designer to ask early in the project:

- If the roof deck does not need to incorporate concrete for structural, fire, or other reasons, is it possible to use a roof deck material other than concrete? Opening the conversation to other structural considerations could bypass the concerns with moisture in the concrete roof deck.
- If the design call for a concrete deck, can normalweight structural concrete be used in lieu of lightweight structural concrete? The use of normalweight concrete could reduce the amount of water in the roof deck by using less porous aggregates, and reducing the amount of water could reduce the potential risk of moisture in the roof system. However, normalweight concrete could increase the weight of the structure, which may be cost prohibitive.
- Can the *w/cm* (for either normalweight or lightweight concrete) be limited? Again, reducing the volume of water in the mixture, regardless of the type of concrete, will reduce the available moisture within the concrete roof deck, which ultimately could reduce the potential risk. Incorporating fly ash and slag into the mixture might increase the time required to reach design strength and potentially reduce the amount of moisture in the concrete deck to an acceptable level.
- Can the concrete be placed into a strippable form instead of using a nonremovable formed deck? If the design calls for a composite deck, can the metal deck be vented? While this might seem like a means-and-methods discussion, removable forms can facilitate drying of the concrete roof deck to the interior of the building. Note that the amount of drying potential may be nominal with vented forms.
- Can the concrete specification exclude the use of additives or curing agents? There are admixtures marketed to reduce the amount of cure time, necessary water in the mixture, and moisture vapor movement within the concrete slab. However, these materials can negatively affect the adhesive bond of vapor retarders and insulation adhesives to the concrete roof deck.
- Can the level of surface finish be specified to provide some texture to facilitate adhesion? A slightly roughened surface such as a broom finish or level 3 concrete surface profile[20] will facilitate a mechanical bond between the concrete roof deck and a self-adhered vapor retarder, asphalt application, or adhesive. (Verify surface preparation requirements with the vapor retarder manufacturer.) Additionally, the rougher finish provides more surface area for moisture within the slab to escape.
- Does the structure have the capacity for an inverted roof membrane assembly roof? Having the waterproofing layer directly installed to the concrete deck bypasses some of the issues with moisture degrading other elements within the roof system, such as insulation and cover boards.

In addition to the opportunities to influence the structural engineer's design decisions, the roof designer has two approaches to consider when working with a concrete roof deck: venting the moisture or encapsulating the moisture. Venting the moisture in the concrete roof deck includes the use of a vented base sheet with perimeter venting or the use of a ballasted roof membrane with venting to provide a path for the moisture to escape. Note that a vented membrane cannot perform as the air barrier in the roof system. A continuous air barrier is required on all six sides of the structure in accordance with the IECC.[5]

Encapsulating the moisture involves the installation of a class 1 vapor retarder with a perm rating of less than 0.01 perms direct to the concrete roof deck. Given that the long-term adhesion of self-adhered vapor retarders with an upward vapor drive has not been evaluated, and the uplift resistance of the roof assembly is reliant on that bond, project teams have been adding mechanical attachment of the vapor retarder and first layer of insulation into the concrete deck for redundancy.

An impermeable epoxy coating could also be considered. However, this approach requires additional deck preparation, specialty applicators, consideration of ultraviolet-light stability, and adhesion of the insulation, as well as a budget for this costly approach. Another option for encapsulating the moisture includes a two-part, water-based, trowel-applied epoxy that is integral with the concrete roof deck. Pepper Construction has successfully used this approach on several projects.

The specification of material is the responsibility of the designer of record, who must make appropriate design accommodations to address high moisture content encountered with concrete roof decks. Design and installation considerations include the following:

- Elimination or reduction of the number of penetrations in the roof, as is done for some data centers and manufacturing facilities. This reduces the risk of air leakage, which can carry the moisture from the concrete roof deck into the roof system.
- Mechanical attachment of the vapor retarder and first layer of insulation for redundancy and added protection since long-term adhesion is unknown.
- The use of solvent-based primers and adhesives instead of water-based primers and adhesives for the insulation and roof membrane attachment. As discussed earlier, water-based materi-

als are more susceptible to re-emulsification when exposed to moisture. Solvent-based primers and low-rise foam adhesives are more tolerant to residual moisture.
- The use of moisture-tolerant facers instead of paper-faced insulation and cover boards. Paper facers can be weakened by moisture absorption, which may compromise the wind-uplift performance of the roof system. Wet paper facers may also facilitate microbial growth. Boards with CGFs perform better in damp environments. Gypsum-based cover boards can lose strength with extended exposure to moisture. Cementitious boards and high-density polyiso boards tend to stand up better to moisture.
- Limiting the materials installed directly below the concrete roof deck, including the metal deck; foil-faced insulation attached to the underside of the deck; and epoxy coatings or paint on the bottom of the deck, which can obstruct the downward movement of moisture.

It is important to specify a roof manufacturer's specific assembly that is designed and tested for wind-uplift resistance over concrete decks. Additionally, consider the long term adhesion performance of the vapor retarder when the assembly relies on the adhesion for wind-uplift resistance.

FACT OR FICTION?

Will Moisture-Vapor-Reducing Admixtures Prevent Moisture-Related Issues?

Curing compounds, air entrainment, water reducers, accelerants, and retarders do not have a known history of negatively affecting roof performance. However, some surface-applied compounds can interfere with adhesion of the roof system, which can negatively affect the system's long-term performance.

Moisture-vapor-reducing admixtures (MVRAs) are admixtures that effectively shutting down moisture-vapor movement through the concrete, and MVRAs purportedly deliver a slab that requires no further moisture tests and no additional topical moisture mitigation systems.

The concept is to turn the concrete slab into a vapor retarder, slowing the release of its own moisture into the roof system. However, there currently is little to no technical data to substantiate marketing claims made by MRVA vendors that these additives significantly lower the water-vapor transmission of concrete.

In fact, when NRCA partnered with RDH Building Science Laboratories[21] to conduct roofing-industry-specific research on MVRAs, the investigators found that the vapor-permeability values of the concrete roof deck cores with MVRA were about two times greater than those without MVRA, meaning the MVRA renders the concrete more "vapor open." These test results contradict marketing claims that MVRAs minimize the concrete's ability to release moisture vapor. These results mirror the findings in the independent testing conducted by Pepper Construction several years prior.

To date, MVRAs have been shown in the laboratory and field to have no effect on moisture issues in roof systems. Therefore, their use is *not* recommended to address the moisture in concrete concerns for roof decks.[6,13]

Are Roofing Issues with Concrete Roof Decks Limited to New Construction?

Given the volume of water in newly placed concrete decks, the risks are certainly greater in new construction than in reroofing. However, there are potential moisture-related risks when reroofing over an existing concrete roof deck. Complicating matters, the amount of water contained within the existing deck is unknown.

Moisture can accumulate in existing concrete roof decks from exposure to long-term leakage, condensation within the roof system, residual moisture from the original placement of the concrete, or rewetting from precipitation during construction. While a history of leakage is a strong indicator that the concrete roof deck could be wet, an absence of leakage does not provide assurance that the deck is dry.

To protect the building and its occupants, existing roof systems are quickly removed and the new systems are installed without providing sufficient time to adequately dry a wet concrete deck. The risk of precipitation during the reroofing effort and the importance of nighttime terminations to prevent construction-related moisture from negatively affecting the installation of the new roof system are critical.

Investigations conducted by qualified roof consultants, in combination with core cuts and moisture surveys, are best practice for reroofing projects. These efforts will inform the designer and help them weigh the potential risks associated with moisture accumulation in the existing concrete roof deck.

A case study[22] of a reroofing project over an existing concrete roof deck highlights the risks. The 13-year-old roof of an office tower in the Midwest was replaced. The existing built-up roof with wood fiberboard insulation adhered to the concrete deck with mopping asphalt was removed down to the deck. Large sections of the existing fiberboard insulation were wet. A new adhered single-ply system with polyisocyanurate (polyiso) insulation and a glass-faced gypsum protection board was installed. Within a few years, the surface of the cover board within the new roof system was damp. An investigation revealed that condensation due to air migration was highly unlikely to be the source of the moisture, and it was determined that the concrete roof deck was the source of the moisture. The remediation cost to replace the roof system and include a vapor retarder at the concrete deck was six times more than the cost would have been to install a vapor retarder in the original reroofing effort. This cost estimate does not include the consulting and attorney fees that were incurred throughout the process.

NRCA recommends the use of a high-bond-strength vapor retarder adhered directly to existing lightweight structural concrete roof decks and in situations where there is evidence of concrete-deck-related moisture. A more conservative approach considered by contractors and consultants alike includes the use of the vapor retarder adhered to existing normal-weight concrete roof decks, as the moisture risks still exist.

EVALUATION OF THE CONCRETE DECK

Traditionally, the roofing contractor accepted the substrate once the roof installation began. However, the task of analyzing the moisture content within the concrete roof deck and determining whether it is acceptable to commence roofing is above and beyond acceptance of the substrate. The designer is primarily responsible for providing a roof system that can be installed and will perform over a wet concrete deck.

There is no current industry consensus on an acceptable standard for evaluating moisture content in concrete roof decks, let alone the levels that are deemed acceptable. Historically, the roofing industry used three qualitative test methods that were thought to provide visual evidence of unacceptable moisture levels to evaluate concrete roof decks:

- The plastic mat test (ASTM D4263, *Standard Test Method for Indicating Moisture in Concrete by the Plastic Sheet Method*[23])

- Hot asphalt pour and peel test (NRCA test method)[24]
- Calcium chloride dome test (ASTM F1869, *Standard Test Method for Measuring Moisture Vapor Emission Rate of Concrete Subfloor Using Anhydrous Calcium Chloride*)[25]

Today, these test methods are no longer considered reliable to evaluate concrete roof decks. The plastic mat test involves securing a plastic sheet to the roof deck and observing condensation accumulation over a 24-hour period. It is difficult to provide an airtight seal around the edges, and the temperature differential can result in a false "dryness" due to the lack of vapor pressure.

The hot asphalt pour and peel test method involves pouring hot asphalt onto the roof deck, watching for bubbles or frothing, and examining the quality of the adhesion. If the asphalt did not react, the roof was deemed dry enough to commence roofing.

The calcium chloride dome test involves placing a canister of the powder under a plastic dome and measuring the amount of water evaporation collected over a 24-hour period. It is difficult to provide an airtight seal around the edges and the test can provide variable results under different climatic conditions. The standard also requires testing to be performed in an environmentally stable condition, which the roof is not.

A key point to understand about all three of these testing procedures is that the evaluation methods only assess surface moisture, which varies as it is exposed to weather, including precipitation and temperature variations. Surface dryness is necessary for adhesives to adhere to the concrete. However, if the roof system is not designed to perform long term over a wet concrete deck, the evaluation of surface dryness is not enough.

The roofing industry has been exploring the standards used by the flooring industry to evaluate moisture in concrete floor slabs. The standards and acceptable threshold levels do not directly translate, as the concrete roof deck does not exist within conditioned space and is exposed to the elements. The flooring standards require conditioning of both the concrete slab and the air above it to a constant service temperature and relative humidity for at least 48 hours, which is not feasible for a roof deck. The in-place probes used in ASTM F2170[26] have been found to be useful with existing concrete decks but problematic with new concrete decks, as there can be too much moisture that can short out the probes.

CONSTRUCTION-PHASE CONSIDERATIONS

Contractors who know the inherent risks of roofing over concrete roof decks have developed several approaches to mitigate the risks when influencing the design is not successful. The following elements may be included in the bid as an alternative to bring awareness to the issue and reduce liability:

- Vapor retarder
- CGF for insulation and cover boards
- Adhesives that are not water based

Additionally, some contractors will take an even more conservative approach on projects. Conservative measures include the following:

- Fastening down the first layer of insulation to ensure long-term securement of the self-adhered vapor retarder
- Installing the roof in sections such that the vapor retarder is not exposed for an extended period of time
- Shot blasting the concrete and sealing it with an impermeable epoxy coating to reduce water-vapor migration through the top of the roof deck. Compatibility with the adhesive and proper adhesion would need to be evaluated. Installation would need to consider the sensitivity of epoxy to ultraviolet light, temperature, and wind as encountered during the construction period.
- Troweling on an epoxy-based, two-component, water-based additive to the newly placed concrete to reduce water-vapor emission
- Placing a rapid-drying concrete that is designed to eliminate moisture-related issues. This approach would require approval from the structural engineer and is very costly.

Such conservative measures can significantly add to the cost per square foot of the roof system. However, the cost of failure can be infinitely greater, so contractors rely on these options as insurance.

TODAY'S BEST PRACTICE

Concrete decks have a number of advantages over steel decks, including improved fire ratings and wind-uplift ratings. Care must be taken to ensure that moisture in concrete decks is prevented from moving upward into the roof assembly. The industry is continually learning more about the long-term performance of roof systems over concrete decks. More research is needed to better understand the appropriate timing of initial application and which design and installation approaches are most effective over time. In the interim, the following are some of the best practices based on the industry information available to date:

- Work with the structural engineer to limit the *w/cm* (for either normal-weight or lightweight concrete) to reduce the volume of water in the concrete.
- Lobby for strippable forms instead of a composite deck to facilitate drying of the concrete roof deck to the interior of the building.
- Specify slightly roughened surface preparation such as a level 3 concrete surface profile to facilitate a mechanical bond between the concrete roof deck and the vapor retarder.
- Include a class 1 vapor retarder with a perm rating of less than 0.01 perms direct to the concrete roof deck in the design. Consider mechanical attachment of the first layer of insulation to provide long-term attachment in case the adhesion of the vapor retarder is compromised over time.
- Specify products that are more tolerant to residual moisture, including
  - Solvent-based primers and adhesives such as low-rise foam
  - Coated glass–faced insulation boards
  - Cementitious boards or high-density polyiso boards
- Design all details, penetrations, and transitions to ensure continuity of the air control layer, which will be the vapor retarder in most instances, to reduce the risk of air-carried moisture from infiltrating the roof system.
- Do not specify the application of materials to the underside of the concrete roof deck that could reduce permeability. This includes the application of epoxy coatings, paint, and foil-faced insulation.

It is important to specify a roof manufacturer's specific assembly that is designed and tested for wind-uplift resistance over concrete decks. Keep in mind that the performance of the entire roof system, in terms of moisture vapor and wind uplift, depends on the long-term adhesion of the vapor retarder, or the first layer of the assembly that is adhered to the concrete deck.

CONCLUSION

To resolve the challenges associated with roofing over concrete decks, it is essential to educate designers, general contractors, roofing contractors, and owners about the risks to the roof system that may occur due to moisture migration from the concrete deck. A collaborative effort with all parties is necessary to mitigate project risk.

After the 28-day cure period for concrete to reach the specified compressive strength, new concrete will still contain most of its initial mix water. The construction industry needs to accept this fact and design roofs that can withstand a wet substrate and maintain long-term performance.

REFERENCES

1. National Roofing Contractors Association (NRCA). *NRCA 2015–16 Market Survey*. Rosemont, IL: NRCA.
2. ASTM International. 2017. *Standard Specification for Lightweight Aggregates for Structural Concrete*. ASTM C330/C330M-17. West Conshohocken, PA: ASTM International.
3. ASTM International. 2017. *Standard Specification for Lightweight Aggregates for Insulating Concrete*. ASTM C332-17. West Conshohocken, PA: ASTM International.
4. Condren, S. J., J. P. Piñon, and P. C. Scheiner. 2012. "What You Can't See Can Hurt You: Moisture in Concrete Roof Decks Can Result in Premature Roof System Failure." *Professional Roofing* 42 (8). https://www.professionalroofing.net/Articles/What-you-can-t-see-can-hurt-you--08-01-2012/2126.
5. International Code Council (ICC). 2018. *International Energy Conservation Code*. Country Club Hills, IL: ICC.
6. Graham, M. S. 2017. "Moisture in Concrete Roof Decks." *Professional Roofing* 47 (9). https://www.professionalroofing.net/Articles/Moisture-in-concrete-roof-decks--09-01-2017/4082.
7. International Institute of Building Enclosure Consultants (IIBEC). 2021. *Roof Covering Systems and New Concrete Roof Decks*. IIBEC Technical Advisory Bulletin 020-2021. Raleigh, NC: IIBEC. https://iibec.org/publication-post/iibec-technical-advisory-no-020-2021-rooftop-equipment-including-communication-equipment.
8. SRI Consultants. 2020. *Moisture in New Concrete Roof Decks*. Rosemont, IL: NRCA.
9. Asphalt Roofing Manufacturers Association (ARMA). 2021. "ARMA Lightweight Structural Concrete Roof Decks Statement." https://www.asphaltroofing.org/arma-lightweight-structural-concrete-roof-decks-statement.
10. Single-Ply Roofing Institute (SPRI). 2017. "Moisture Concerns in Roofing Systems Applied Over Lightweight Structural Concrete Roof Decks." SPRI Industry Information Bulletin 2-13. https://www.spri.org/wpfb-file/spri-bulletin-2-13-moisture-concerns-pdf.
11. Polyisocyanurate Insulation Manufacturers Association (PIMA). 2019. "Moisture Control with Polyiso CI." PIMA Technical Bulletin 303. https://cdn.ymaws.com/www.polyiso.org/resource/resmgr/tech_bulletins/2019/tb303_Sept2019.pdf.
12. Craig, P., and B. Wolfe. 2012. "Another Look at the Drying of Lightweight Concrete." *Concrete International* 34 (1): 53-58.
13. FM Global. 2020. *Roof Deck Securement and Above-Deck Roof Components*. FM Global Property Loss Prevention Data Sheet 1-29. Johnston, RI: Factory Mutual Insurance Company. https://www.fmglobal.com/-/media/Documentum/Data-Sheet-Individual/01-Construction/FMDS0129.pdf
14. Hedenblad, G. 1997. *Drying of Construction Water in Concrete: Drying Times and Moisture Measurement*. Lund, Swedent: Swedish Council for Building Research.
15. Hedenblad, G. 1997. "Concrete Drying Time," *Concrete Technology Today* 19 (2): 4-5.
16. Steel Deck Instutite. 2013. "Position Statement: Venting of Composite Steel Floor Deck." http://www.sdi.org/wp-content/uploads/2013/11/PPVENTR2.pdf
17. G. R. Doelp and M. K. Donlon. 2020. "Effects of Moisture in Concrete Roof Decks on Vapor Retarder Adhesion." in *Roofing Research and Standards Development: 9th Volume*. ed. S. Molleti and W. Rossiter. West Conshohocken, PA: ASTM International. https://doi.org/10.1520/STP162120190044
18. Helene Hardy Pierce and Joan Crowe. 2020. "Structural Concrete Decks, Vapor Retarders, and Moisture—Rethinking What We Know." *Interface*. February. Raleigh, NC: IIBEC.
19. NRCA. 2018. "Contract Provision Addresses Installation of Roof System Over Concrete Deck." https://nrca.net/legal/contractprovisions.
20. International Concrete Repair Institute (ICRI). 2013. *Selecting and Specifying Concrete Surface Preparation for Sealers, Coatings, Polymer Overlays, and Concrete Repair*. ICRI Technical Guideline No 310-2. St. Paul, MN: ICRI.
21. Graham. M. S. 2020. "Putting it to the Test: NRCA Conducts Testing of Moisture Vapor Reduction Admixtures." *Professional Roofing* 50 (2). https://www.professionalroofing.net/Articles/Putting-it-to-the-test--02-01-2020/4615.
22. Condren, S., J. Schwetz, and S. Graveline. 2016. "Concrete Deck Moisture Issues: Causes and Preventative Measures." In *RCI International Convention Proceedings (2016). Proceedings of the RCI 31st International Convention & Trade Show. March 10–15, 2016, Rosen Shingle Creek Resort, Orlando, FL*. Raleigh, NC: IIBEC. https://iibec.org/wp-content/uploads/2016-cts-condren-schwetz.pdf.
23. ASTM International. 2018. *Standard Test Method for Indicating Moisture in Concrete by the Plastic Sheet Method*. ASTM D4263-83(2018). West Conshohocken, PA: ASTM International.
24. Hot Asphalt Pour and Peel Test (NRCA Test Method)
25. ASTM International. 2016. *Standard Test Method for Measuring Moisture Vapor Emission Rate of Concrete Subfloor Using Anhydrous Calcium Chloride*. ASTM F1869-16a. West Conshohocken, PA: ASTM International.
26. ASTM International. 2019. *Standard Test Method for Determining Relative Humidity in Concrete Floor Slabs Using in situ Probes*. ASTM F2170-19a. West Conshohocken, PA: ASTM International.

Evolution of Sheet Metal Window Sill Flashing: Lessons Learned that Lead to Better Performance

Rocco C. Romero, AIA, NCARB

Wiss, Janney, Elstner Associates Inc. | Seattle, WA

rromero@wje.com

IIBEC 2022 - Building for the Future

International Convention and Trade Show

March 17–22, 2022 | Orlando, FL

ABSTRACT

Flashings are often the most challenging aspect of aluminum window system design and installation on both new and replacement projects. Although the aluminum window system and its performance are often well detailed by the window manufacturer, it can be challenging to provide a waterproof transition of the window frame to cladding system interface. Metal sill flashings have been used in the construction industry as a supplemental element in window systems (in addition to the manufacturer's standard sill design). However, inadequate attention to sill flashing detailing can result in water leakage into the exterior enclosure and even into the building interior. Historically, metal sill flashing was often continued into the rough opening of the window, and this method is sometimes still used today. This presentation addresses how going beyond the standardized approach to detailing, and taking into consideration the installers' sequencing of components during installation, can minimize potential pathways for water intrusion.

SPEAKER

Rocco C. Romero, AIA, NCARB

Wiss, Janney, Elstner Associates Inc. | Seattle, WA

Rocco C. Romero is a registered architect and principal with Wiss, Janney, Elstner Associates Inc. (WJE) in Seattle, Washington. He has more than 30 years of experience and has investigated hundreds of building enclosure systems. Romero specializes in water leakage investigations, assessment, diagnostic testing, and repair design and construction document preparation in contemporary and vintage buildings and structures. He provides professional consulting services to owners, architects, and general contractors related to the design, performance, and constructability of new and retrofit building enclosure systems. Romero also provides expert witness and litigation support services on existing buildings.

Evolution of Sheet Metal Window Sill Flashing: Lessons Learned that Lead to Better Performance

Flashing can be one of the most challenging aspects of design when integrating windows with building cladding systems. Because window–to–cladding system interfaces are some of the most repeated conditions in a facade, deficiencies in either design or installation can have detrimental effects, one of which is water intrusion into the building interior.

The standard installation and performance criteria of manufacturer's windows and cladding systems are often graphically detailed in publications by each system manufacturer. However, depending on the complexity of the facade design, applying some of these details at the window-to-cladding interface can be challenging. Where is the window set in the rough opening? Does the window extend over the cladding or is it inset at the cladding? Are there window wells? How is the window attached to the structure? The answers to these questions and other design conditions must be carefully considered to design a watertight window–to–air/weather barrier interface.

From a waterproofing perspective, the window-to-cladding interface is often poorly detailed in design and construction documents. In addition, the windows and cladding are often installed by separate subcontractors, and the sequencing of installation can lead to coordination issues during construction that may result in incomplete or conflicting interface installations. Overcoming such challenges is important because the design detailing and construction of components at the interface between the window frame and cladding can be one of the most critical aspects of a watertight assembly. If designed and constructed properly, windowsill flashing is one part of the window-to-cladding interface that can help attain the goal of a watertight exterior wall assembly.

When constructing the window-to-cladding interface, on-site mock-ups can be an invaluable tool for assessing constructability of flashing systems and determining whether supplemental flashing is needed.

UNCONTROLLED WATER INTRUSION

Inadequate attention to the interface between the window and substrate can result in uncontrolled water leakage into the exterior wall system, which can then find its way into the occupied spaces of the building interior. The use of flashing systems (flashing) as part of an exterior wall system, while not specific to windows, provides a mechanism, component, or assembly that helps direct water that infiltrates the wall assembly to drain to the exterior. Flashing that helps protect a rough opening in an exterior wall where a window will be installed from water infiltration can take many forms, including, but not limited to, simple sheet metal, complex metal trim, mechanically attached or self-adhered sheet-applied membranes, fluid-applied elastomeric products that when cured become a monolithic continuous membrane, or any combination of these components.

Building and energy codes commonly require air- and weather-resistive barriers (air/weather barriers) for exterior wall systems as part of the building enclosure. The proper integration of these systems at window rough openings is necessary to help establish continuity of the air/weather barrier system; with proper waterproofing, this integration can also be relied on to help make window rough openings weathertight.

WINDOW-RELATED WATER LEAKAGE

Wet interior carpets below a window can be a telltale sign of water leakage related to the window, whether leakage is from the window installation or from its interface with the cladding system. Often, these types of window

When constructing the window-to-cladding interface, on-site mock-ups can be an invaluable tool for assessing constructability of flashing systems and determining whether supplemental flashing is needed.

leaks go on for years. Building maintenance staff may aim to fix the leak by having their window washing contractors apply sealant to exposed glazing joints and gaskets at both the interior and exterior of the window system; however, this type of repair does not necessarily provide a long-term solution. One of the most damaging aspects of uncontrolled

Figure 1. Decaying wood below a window frame.

Figure 2. Corrosion of metal track and studs.

water leakage is that it can enter the wall system below the window. This water might be absorbed by interior drywall and wood sheathing and framing, or if the wall is framed with metal studs, it can collect in the stud tracks. Long-term water intrusion can result in substantial damage to the exterior wall, including decay of wood framing, deterioration and erosion of fire-rated gypsum drywall or sheathing, organic growth, and corrosion of structural metal wall framing (**Fig. 1** and **2**).

LEAKY WINDOWSILLS

When investigating leaky windowsill conditions, it can be useful to create interior openings in the drywall below the sill to evaluate concealed conditions and to track and observe the leakage during diagnostic water testing. If organic growth is suspected or found within the wall cavity, the owner should consider retaining the services of a certified industrial hygienist to establish protocols for containment, air sampling and testing, organic growth removal, cleaning, indoor air monitoring, and other remediation issues.

In a framed window system that uses a sill component, water that infiltrates is expected to drain to the exterior through weep holes. However, deficient installation of the sill can result in water intrusion into the exterior wall cavity. In a ribbon-type storefront window system, the window system can be installed in a continuous horizontal band application, with individual glazing units captured at the sides by vertical mullions. The vertical mullions are attached to the horizontal sill mullion (sill), and either clipped into the subsill or attached to the substrate with anchor clips. Water that enters the glazing pocket of a storefront system is directed to the sill/subsill components, where it is drained to the exterior through weep holes. When a subsill system is used, this component is typically anchored to the substrate with fasteners that penetrate the horizontal portion of the subsill (**Fig. 3**). With this type of installation, there are generally three installation-related conditions that can be potential sources of water leakage: poorly sealed gaps at butt joints between adjacent subsill components; poorly sealed anchors that penetrate the horizontal portion of the sill and any pan flashing beneath; and poorly sealed end dams at the jamb-to-sill termination (**Fig. 4**).

SUBSILL COMPONENT UPGRADES

A watertight subsill component is important to achieve a weathertight window interface with the air/weather barrier. When installing a window manufacturer's subsill component, sealing the gap between butt joints can be accomplished by fabrication and installation of butt joint covers, set in sealant at each end of the joint, that match the profile

Figure 3. Fastener penetration through a subsill.

Figure 4. A loose end dam at the end of a sill.

Figure 5. A subsill butt joint cover.

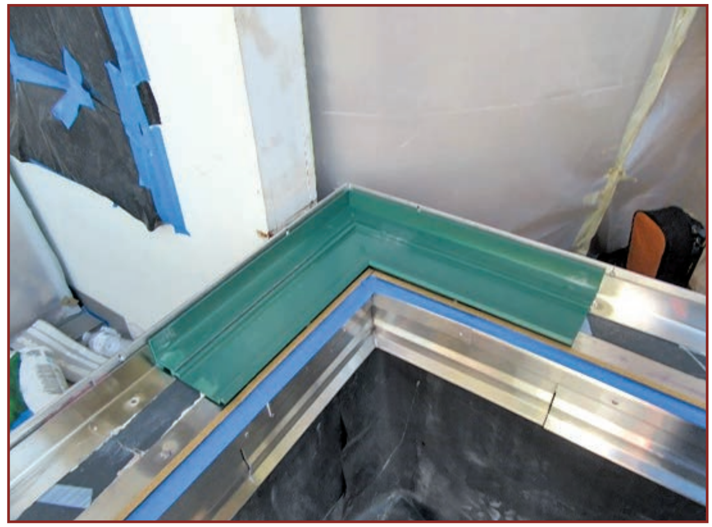

Figure 6. A one-component inside corner subsill.

of the sill component (**Fig. 5**). At inside and outside corners, the corner can be shop fabricated as a single component, welded together at the miter joint (**Fig. 6**), and then sealed with sealant. The butt joints at either side of the L-shaped corner component are then more easily waterproofed, with the use of a butt joint cover at each side of the shop-fabricated corner. The L-shaped end dams at subsill-to-wall terminations can be set in a full bed of sealant at the underside of the subsill component, mechanically attached, and with another bead of sealant applied and tooled at the inside of the end dam–to–subsill interface (**Fig. 7**).

Where there is a high probability of water infiltration and resulting damage to substrate materials, it may be worthwhile to install metal angles or clips at the interior surface of the window frame to attach through the vertical surface of the windowsill frame (**Fig. 8**). The height of the vertical leg of the attachment angle should be determined based on the water-resistance performance of the window system since this performance is dependent on the vertical back leg of the sill and flashing. For this same reason, fasteners should not penetrate the vertical leg at a point that is lower than the height required to provide the specified water resistance for the window system. These fabrications should be of the same metal as the window system, or incorporate a separator if the metals are not compatible, to help prevent galvanic corrosion. This approach avoids penetration of the horizontal surface of the manufacturer's sill as well as the pan flashing or rough opening flashing (if either are present).

Figure 7. A subsill end dam.

Figure 8. An angle bracket.

ONE-COMPONENT SHEET METAL PAN FLASHING

Before the development of contemporary air/weather barrier membrane flashing systems, a sheet metal pan flashing (pan) system was commonly used as supplemental flashing below window frames. Pans are often constructed as one-component stainless steel flashing with end dams and back dams that can be shop fabricated and soldered watertight, or sealed with sealant at the end dam–to–back dam inside corner transitions. The main idea is to create a three-sided "pan" or reservoir that can collect water that infiltrates below the window system and direct it to drain to the exterior. Pans are intended to extend through the entire depth of the rough opening, with the drip edge exposed at the exterior side of the wall and the upturned vertical back leg located at the interior side of the window frame. As these are a non–thermally broken through-wall component, they are subject to both the exterior and interior temperatures and relative humidity. Although the frame of the window system may be thermally broken, the one-component sheet metal pan is not, and

Figure 9. The drip edge of a pan exposed at the exterior.

Figure 10. A pan is reverse-sloped toward the interior.

this leads to a thermal bridge from the exterior to the interior, which, under some conditions, can lead to the formation of condensation at the interior.

When a pan is used, a drainage route to the exterior is needed for water that collects on the horizontal surface of the pan underneath the window. Therefore, the window frame should be shimmed above the pan so that a sealant joint can be installed between these components, with regularly spaced weep slots that are baffled.

The following are among the construction deficiencies observed with pans:

- End dam–to–back dam joints that are not sealed watertight, and thus leak at the corners to the interior
- A poor seal between the sill pan and the air/weather barrier
- Short back dams, which allow the pan to easily overflow
- The weight of the window itself produces a reverse slope of the pan toward the building interior

Water that collects on the pan can infiltrate at poorly sealed windowsill fasteners that penetrate through the horizontal surface of the pan directly below the window. These unsealed anchor holes offer a direct pathway for water into the interior and wall cavity below.

FLASHING AT MULLION ANCHORAGE CLIPS

Aluminum window wall systems are designed so that if water enters the glazing pocket, it is directed to drain to the exterior at individual glazing locations through the horizontal mullions. The glazing pocket at the vertical mullion–to–horizontal mullion interface is typically sealed with sealant and rubber plugs. The aim is to keep water localized to each individual glazing unit, where it is directed to drain at weep holes in the pressure plates or other portion of the horizontal mullions. With window walls of this type, there is no sill component at the base of the window wall to collect water from the entire wall system. At the base of the window wall, T-clips or F-clips anchor either the vertical mullion or the horizontal mullion to the adjacent wall or floor slab; thus, these systems have limited options for supplemental flashing systems. When clip-type anchorage is used, the window system relies on the exterior perimeter sealant joint between the rough-opening flashing and the window frame as the primary seal to keep the interface weathertight. If the clips protrude too far into the sealant adhesion area, which typically can occur at the base of the vertical mullions, the integrity of the primary seal may be in jeopardy.

In an investigation by the author of a 1980s' vintage window wall system that was anchored to the concrete floor slab with clips at vertical mullions, water leakage regularly occurred along the sill-to-slab interface. When the system was viewed from the exterior, a sheet metal drip edge of a pan extending beyond the sill was visible (**Fig. 9**). Diagnostic water testing reproduced the reported water leakage immediately. After one of the sill components was deglazed and removed, it was evident that the pan terminated underneath the sill component and was reverse-sloped toward the interior (**Fig. 10**).

During construction, portions of the back dam of the pan had been cut so that the pan could fit around the vertical mullions and anchor clips. The reverse slope of the pan directed water to the areas where the back dam was removed, which in turn provided a direct path for water leakage to the interior (**Fig. 11**). The sealant joint between the sill and the pan was installed in a haphazard manner, resulting in a discontinuous and ineffective sealant joint, particularly at the vertical mullion locations. In this case, the typical one-component pan was discontinuous due to the obstructions created by the vertical mullion anchor clips.

Figure 11. The back dam of the pan was cut to fit around the mullion and anchor clip.

CONTEMPORARY WINDOW FLASHING SOLUTIONS

In contemporary designs, using an air/weather barrier membrane as part of a window rough-opening flashing system can help provide an integrated system and weathertight performance at component transitions.

In this type of system, the air/weather barrier membrane (flashing membrane) should be fully adhered to the rough-opening substrate to eliminate potential pathways between the flashing membrane and the rough-opening substrate. The window frame should be sized so that the sealant joint width will be ½ in. (13 mm) minimum between the edge of the window frame and the installed flashing membrane. Because the window perimeter sealant joint must adhere to both the flashing membrane and the window frame, mock-up sealant adhesion tests should be performed to evaluate adhesion with and without manufacturer-recommended primers. If proper sealant adhesion can be attained without using primer, priming the adhesion surface areas may not be necessary. Once the primary sealant joint is properly installed, the transition between the window frame and the flashing membrane should be weathertight. Any surface of the flashing membrane that is exposed to potential ponding water at the exterior side of the window frame should be made waterproof if it is not already waterproofed by the nature of the flashing membrane material. Some membrane sheets are not fully waterproof, and ponding water can soak through the sheet. Some flashings are vapor permeable, which means vapor diffusion can allow water to damage rough-opening framing. Thus, an additional waterproofing top layer is required. Some fluid-applied air/weather barrier manufacturers include sheet metal flashing in their standard details to account for this risk. Water that reaches the flashing membrane at the sill of the rough opening should be directed to the exterior, either into the drainage space of a drainable cladding system or, preferably, over the exterior-side surface of the cladding.

Figure 13. An end cap installed at a gap between the head and jamb and fastened in place.

Figure 12. A gap between head and jamb frame components.

If the window system has a head compensation channel, where the window frame is set into a separate head component, or if there is a gap at the head-to-jamb transition in the frame (**Fig. 12**), the exterior perimeter sealant will not have adequate surface adhesion area on the window frame for sealant adhesion. An end cap should be fabricated and installed in a full bed of sealant to cover the gap (**Fig. 13**).

For this system to be successful, the window system itself must function and perform as a watertight assembly, with no unsealed gaps in the frame. In addition, the perimeter sealant joint must be continuous, properly designed and installed, and fully adhered. Water testing should be performed on trial mock-up installations to verify that the performance meets the design criteria for water-leakage resistance. If the water testing proves that the installation is watertight, with no leakage into the wall or the interior, additional supplemental sheet metal flashing may not be necessary.

Two-Component Supplemental Flashing for Punched and Ribbon-Type Windows

To help address the thermal bridging issue of one-component sheet metal pans, two-component supplemental flashing can be constructed. This flashing uses two components: a sheet metal drip at the exterior of the rough opening and a separate back dam component (**Fig. 14**). Each component should have integrated side end dams at the termination to the rough-opening jamb. The area between the metal flashing components can be made watertight with the application of trowel- or fluid-applied elastomeric-type waterproofing

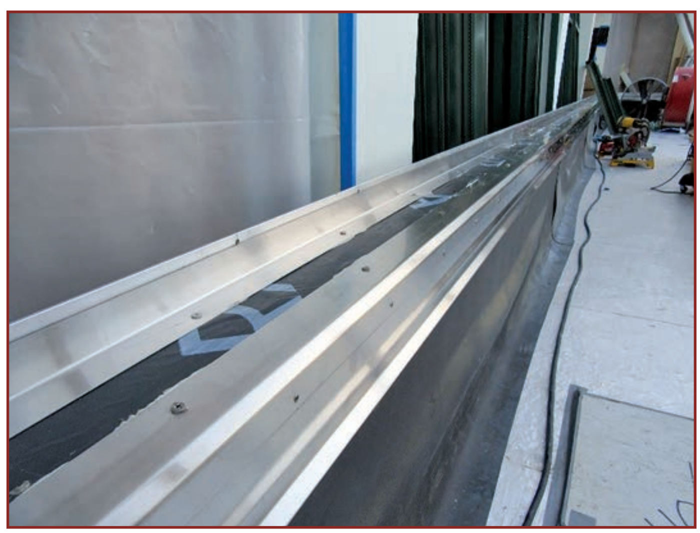

Figure 14. A two-component metal flashing system.

Figure 15. Fluid-applied elastomeric waterproofing troweled in place between metal flashing components.

Figure 16. A subsill set and shimmed in place.

that is mixed in the field and cures to a rubber-like material (**Fig. 15**). The back dam component can also be formed with membrane or fluid flashing installed over a vertical step formed in sill of the rough opening. Another advantage of this approach is that the back dam can be continuous along the entire run of the window frame at the interior. This is particularly useful when there is a stepped configuration (change in elevation) at the rough opening. An aluminum angle can be used to attach the vertical leg of the windowsill frame to the substrate; this will not penetrate the waterproofing below the window. After the waterproofing has cured, the windowsill is set into the two-component flashing system and then shimmed in place (**Fig. 16**). The shims below the sill provide a gap to allow for the installation of a continuous sealant joint between the windowsill frame and the drip edge of the sheet metal flashing with baffled weeps to allow for drainage.

Integrated Supplemental Metal Flashing for Mullion Base Plate–Connected Systems

When clips are required to attach the base of mullions to the wall structure, T-clips and F-clips, or some version thereof, are typically used. As the names imply, the clips are respectively shaped like the letters *T* and *F* (**Fig. 17**). The preferred anchorage clip in flashing scenarios is the one that does not fully protrude into and obstruct the sealant adhesion area of the perimeter sealant joint, as this sealant joint is the primary weather seal for the window frame interface with the wall opening.

As a supplemental measure, sheet metal flashing can be used to shield the sealant joint at the window frame sill from contact with water. For a horizontal mullion, it is advisable to select a component profile that has both a mullion tongue to attach the pressure plate and a glazing pocket directly below because this profile can allow for installation of supplemental sheet metal flashing. In this design, a sheet metal flashing can be installed with a vertical leg that fits in the space below the mullion tongue. However, for the flashing to be continuous, a portion of the vertical mullion tongue must be removed (**Fig. 18** and **19**). The metal flashing is fabricated to be continuous across the vertical mullion profile, which is the most vulnerable area of the system when attempting to install a continuous sealant joint between the mullion and rough opening.

To accomplish this construction, an L-shaped pressure plate is needed, as the pressure plate and gasket are provided to hold the metal flashing in place. Fasteners that attach the vertical leg of the metal flashing to the horizontal mullion can also be added, as well as a cleat at the drip edge of the metal flashing for added mechanical securement. The integrated sheet metal flashing provides another layer of protection from weather at the most vulnerable area of the windowsill assembly.

CONSTRUCTION DRAWINGS

The interface between the windows and cladding system should be a priority during the design development of the project. This interface condition will affect the performance requirements for the exterior enclosure, the technical specifications, and the details in the construction drawings. The interface of windows and cladding systems should not be generic; instead, it should be developed based on the systems and their project-specific connections. Illustrated details of interfaces should not be limited to a single section cut through the most basic sill location. Rather, they should present a well-thought-out process of how the systems transition to one another and turn corners, and how they are installed. The manufacturer's published details often do not cover conditions that meet the specific requirements of every project, or follow the water drainage path of systems other than

Figure 17. A T-clip to be installed into base of mullion.

Figure 18. The portion of mullion tongue removed.

Figure 19. Supplemental flashing set into a glazing pocket under the mullion tongue.

their own. Therefore, consideration should be given to development of job-specific details, including step-by-step drawings that illustrate the components incorporated in the construction process.

From a general contractor's perspective, it is imperative to have detailed drawings before specialty subcontractors are retained for the work. If the drawings do not show adequate detailing, the installation subcontractor's "low-bid" price can be the basis for award of the contract. However, once shop drawings and subsequent mock-ups are performed, problems with the low-bid work can become apparent, potentially leading to higher price-change orders.

Subcontractors often use the construction drawings to develop shop drawings. Thus, ensuring that the construction drawings clearly illustrate essential information improves the chance that the shop drawings correctly address the design conditions being considered. If the design drawings do not show specific details, chances are that these details will not be considered by the contractor. The right time to address these details is during bidding; the wrong time to figure this out is when materials have been ordered and mock-ups are being constructed.

CONSTRUCTIBILITY MOCK-UPS AND PERFORMANCE TESTING

Mock-ups play a key role in assessing constructibility and evaluating water-testing performance before systems are implemented throughout a project. Mock-ups should be considered a work in progress and an opportunity for all those involved to visualize the actual construction and the process required to implement it. Often, several attempts are needed to achieve successful mock-ups. Once they are successfully completed and approved, the mock-ups become the standard for acceptable installation. It is always advisable to have the actual installers for the project construct all aspects of the mock-up to avoid getting the best installer for the mock-up but later having a less-experienced installer perform the actual work on the project. Specifications can require that the installers who perform the mock-ups shall be those who will perform the overall work. The reviewed and accepted mock-ups help establish the learning curve that takes place with all fieldwork, determine the quality of construction required for the project, and define the expectations of all parties. Because one of the purposes of constructing mock-ups is to confirm constructibility of the systems as designed, it is recommended that mock-ups be performed before all materials are ordered for the project. The mock-up should remain in place during the course of construction to establish the standard of work. It can also be used as a training tool and reference for new workers on site.

Mock-ups can also help project stakeholders understand the local weather conditions anticipated during construction, and whether some materials, such as sealants, are better applied and cured during specific conditions. The experience and familiarity of the installers with these products, as well as the compatibility of sealant materials with the window frame, sheet metal flashing, and air/weather resistive barrier, can also be evaluated in the mock-ups.

Air- and water-infiltration testing can be performed on completed mock-ups to verify performance of the completed assembly. Mock-ups also provide an opportunity for manufacturers to verify material compatibility, perform adhesion testing of sealants, confirm warranty requirements, and provide other input and recommendations. The owner and architect or engineer can review the mock-ups for aesthetic effect and to validate the performance of the design. Overall, the mock-up period should be coordinated far in advance of the full-scale work on the building to allow the project team time to acquire other products if necessary and to refine details and perform additional mock-ups as necessary.

CONCLUSION

The initial basis for successful performance of a window system is the selection of appropriate windows for the building type and location, as well as all the proper installation and performance of all components of the window system. This includes a frame system that is installed weathertight and a properly performing perimeter sealant joint between the window frame and the substrate.

Window flashing systems have evolved over time, with new approaches and materials being introduced to the marketplace to help provide more enhanced performance and more energy-efficient systems. Window flashing design is not achieved through a one-size-fits-all approach—having a thorough understanding of how the systems are intended to perform is crucial to constructing a weathertight system. ASTM E2112, *Standard Practice for Installation of Exterior Windows, Doors, and Skylights*,[1] is a useful resource for additional window flashing information.

Numerous investigations of leaky window and cladding system transitions have helped identify many of the pitfalls that may be encountered when designing and constructing interfaces and flashings to help produce weathertight systems. Many installations have unique aspects, and approaches should be tailored to specific on-site conditions. Thorough development of detailing, including full consideration of the sequencing of component installation, together with use of mock-ups to evaluate the installation, can help minimize potential pathways for water intrusion into the building interior at window and cladding interfaces.

REFERENCE

1. ASTM International. 2019. *Standard Practice for Installation of Exterior Windows, Doors, and Skylights*. ASTM E2112-19c. West Conshohocken, PA: ASTM International. https://doi.org/10.1520/E2112-19C.

Wind Performance of Buildings: The Building Enclosure and Rooftop Equipment Challenge

Thomas Lee Smith, AIA, RRC, F.SEI

TLSmith Consulting Inc. | Rockton, IL

tlsmith@hughes.net

IIBEC 2022 - Building for the Future

International Convention and Trade Show

March 17–22, 2022 | Orlando, FL

ABSTRACT

This paper describes the state of building enclosure wind performance before and at the time of Hurricanes Hugo (1989) and Andrew (1992); explains the reasons for improved wind performance of building enclosures and rooftop equipment during the past 30 years; and presents the challenges (obstacles) for further improvement of the wind performance of building enclosures. The paper also presents roles and opportunities for building enclosure designers and consultants, manufacturers, contractors, and IIBEC to enhance the wind performance of building enclosures.

SPEAKER

Thomas Lee Smith, AIA, RRC, F.SEI

TLSmith Consulting Inc. | Rockton, IL

Thomas L. Smith specializes in forensic architecture and architectural technology and research, with an emphasis on roof systems and wind performance of buildings. He has served on the American Society of Civil Engineers' ASCE 7 subcommittee on wind loads since 1990. He has performed building performance investigations after 16 hurricanes and 6 tornado outbreaks and has coauthored 13 wind design guides. He received the Carl G. Cash Award from ASTM International in 2013 for his body of work regarding wind damage investigations. Also in 2013, he was named a fellow of ASCE's Structural Engineering Institute.

Wind Performance of Buildings: The Building Enclosure and Rooftop Equipment Challenge

PROBLEM STATEMENT

The following statement from the Federal Emergency Management Agency's (FEMA's) *Mitigation Assessment Team Report: Hurricane Michael in Florida*[1] captures the current building enclosure problem:

> Overall, the MAT's assessments of buildings impacted by Hurricane Michael and other recent hurricanes show that structural systems of buildings built to modern building codes are performing well. As performance of structural systems has improved, the vulnerability of the building envelope has become increasingly apparent.

This point is illustrated by the poor enclosure performance at a relatively new hospital (**Fig. 1** and **2**[1]). The hospital was evacuated the day after Hurricane Michael made landfall along the Florida panhandle as a Category 5 storm on October 10, 2018. As provided in the American Society of Civil Engineers' *Minimum Design Loads and Associated Criteria for Buildings and Other Structures* (ASCE 7-16),[2] the basic (design) wind speed for this site is 147 mph. The estimated wind speed was 130 mph, or 88% of the basic speed. (Note: All wind speeds in this paper are 3-second gusts at 33 ft above grade in exposure C.)

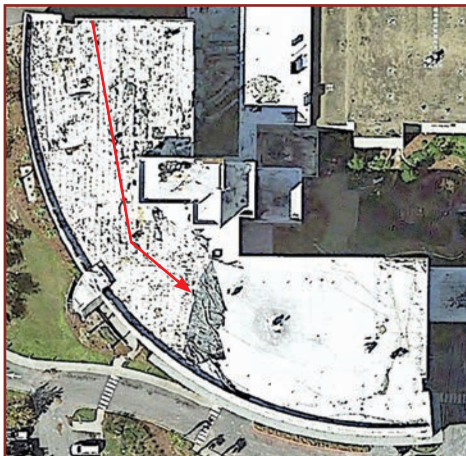

Figure 1. Aerial view of a hospital building constructed in 2010. The red line indicates where the roof membrane blew off. Several acoustical ceiling panels at the fifth floor were wetted by roof leakage and collapsed. Source: Federal Emergency Management Agency (FEMA P-2077).[1]

Figure 2. By the time this photo was taken, the damaged roof membrane shown in Fig. 1 had been replaced (red line). In addition to roof membrane damage, rooftop equipment and exterior insulation and finish system were blown off.

DEFINITIONS

Building enclosure (envelope): Exterior doors, exterior glazing (including skylights) and storm shutters, exterior walls (including load-bearing and non-load-bearing), wall coverings, soffits, roof assemblies, and attic vents.

Building wind performance: A building's adequate resistance to wind pressure as well as its adequate resistance to or accommodation of wind-borne debris and wind-driven rain.

Critical facilities: Buildings that are essential for the delivery of vital services or protection of a community such as emergency operations centers, healthcare facilities, police and fire stations, schools, and power stations.[3]

Fully engineered: In common use, this term relates wind damage susceptibility of the main wind force resisting system. In addition to fully engineered, buildings may be pre-engineered, marginally engineered, or non-engineered. The fully engineered category comprises buildings that receive individualized design and construction attention from professional engineers and architects; they are considered to perform better than other building types during windstorms. Fully engineered examples include mid- and high-rise buildings, and large hospitals.[8]

Rooftop equipment: HVAC units (also known as rooftop units), exhaust fans, relief air hoods, condensers, exposed ductwork, boiler and exhaust stacks, natural gas lines, condensate drain lines, cooling towers, exposed electrical conduits, lightning protection systems, solar panel arrays, communication antennas and towers, equipment screens, and satellite dishes.

Wind-resilient building: A building that is capable of resisting damage from wind and wind-driven rain; furthermore, if damaged, the building can be readily repaired so that important functions are maintained during and/or after a windstorm.

Figure 3. Detached roof membrane on a new police station in the Midwest. The winds were well below the basic wind speed. Source: Federal Emergency Management Agency (FEMA P-2062).[4]

Figure 4. The roof on this school in Palmer, Alaska, blew off during cold weather in the late 1970s, thus increasing the repair costs. Membrane lifting at the edge flashing initiated the failure. The membrane was not clamped by the metal edge flashing.

INTRODUCTION

During Hurricanes Hugo (South Carolina, 1989) and Andrew (Florida, 1992), and in earlier hurricanes, failure of structural elements such as roof decks and roof trusses was common. In that era, structural failures overshadowed building enclosure issues. In the aftermath of Hurricane Andrew, greater attention to the design and construction of the main wind force resisting system (MWFRS) led to improved structural performance. Hence after Hurricane Andrew, many residential and nonresidential buildings did not experience structural failure in subsequent strong hurricanes such as Hurricanes Charley (Florida, 2004), Harvey (Texas, 2017), Irma (US Virgin Islands, 2017) and Michael (Florida, 2018). However, many of these buildings did experience interior wind or water damage (or both) due to insufficient resistance of the building enclosure and rooftop equipment to wind, wind-borne debris (WBD), or wind-driven rain.

The wind performance of building enclosures has significantly improved during the past 30 years. However after Hurricane Andrew, a very large percentage of buildings—including critical facilities—have experienced significant damage due to building enclosure failure. Most of the damage occurred because various elements of the enclosure had insufficient resistance to wind, WBD, and/or wind-driven rain; this lack of sufficient resistance resulted from inadequate design, poor installation, insufficient or lack of adequate test methods, or material deterioration.[3]

There are significant challenges for further improving the wind performance of building enclosures and rooftop equipment. To address these challenges, this paper proposes an ensemble of approaches that aim to dramatically improve enclosure performance on the inventory of current and future buildings.

Of all the storm types, a hurricane can devastate the largest geographical area and affect the largest number of people. Hurricanes are also problematic because they can be of long duration (thus inducing fatigue). Furthermore, the winds change direction (thus increasing the potential for winds approaching from critical angles), rainfall is often heavy, and a large amount of WBD can be generated. However, it is important to realize that wind performance issues are not limited to the hurricane-prone regions defined in ASCE 7.[2] Storms other than hurricanes can damage building enclosures.[4] Historically, when such damage occurred, the wind speed was typically well below the basic speed given in ASCE 7, as illustrated by **Fig. 3** and **4**.

BUILDING ENCLOSURE WIND PERFORMANCE PRIOR TO 1993

In the aftermath of the F5 tornado that struck Lubbock, Texas, in 1970, Texas Tech University (TTU) established the Institute for Disaster Research (now the National Wind Institute). TTU engineering faculty and students investigated that event and pioneered field research investigations of tornadoes and hurricanes.

Early Research

Before Hurricane Hugo (1989), storm damage research investigations by TTU and others focused on the MWFRS. However, in that era, there was some documentation of building enclosure performance:

- TTU's Dr. Minor reported on glazing and roof covering damage at the 1977 Symposium on Roofing Technology.[5] The paper was based on 28 windstorm investigations.

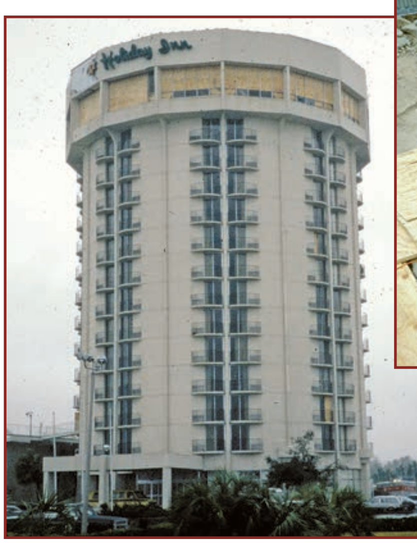

Figure 5. Roof deck damage (inset photo) at a midrise building. The estimated wind speed was around 100 mph. Source: Institute for Disaster Research, Texas Tech University.[7]

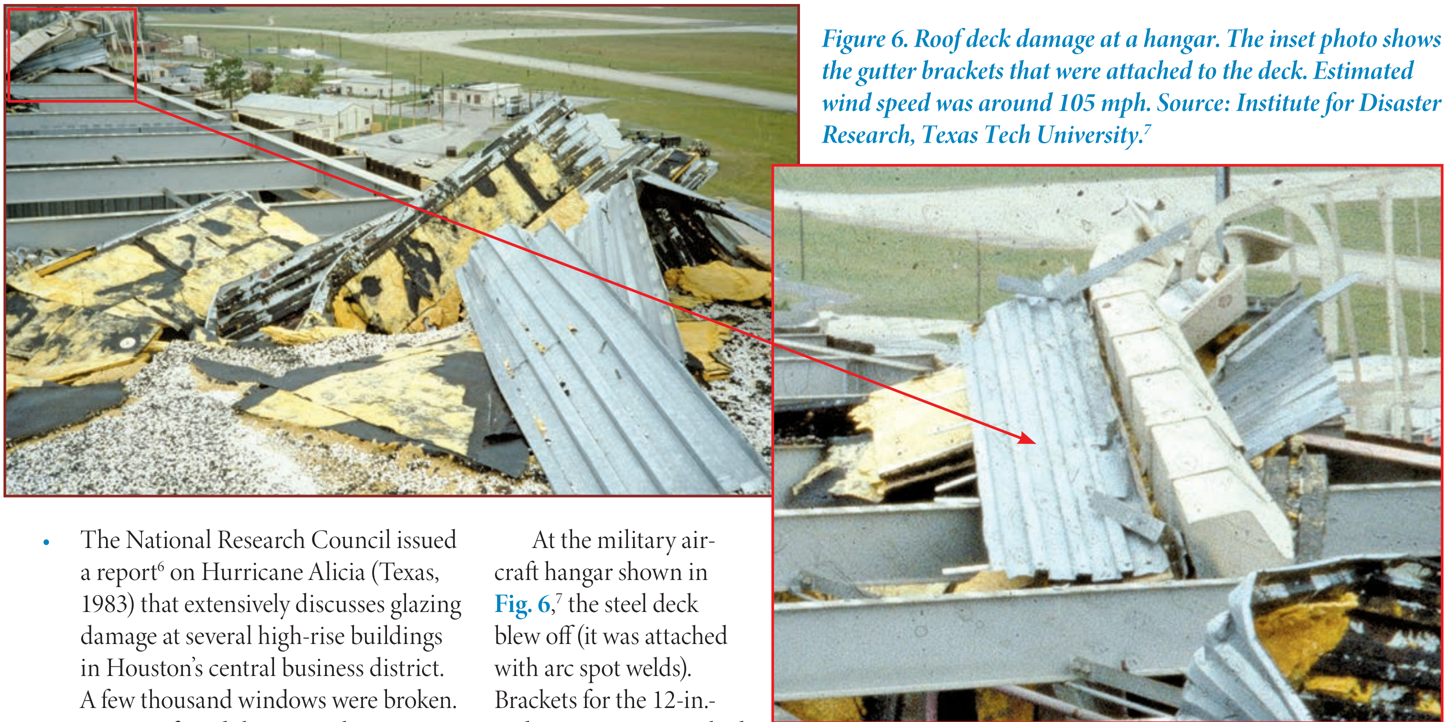

Figure 6. Roof deck damage at a hangar. The inset photo shows the gutter brackets that were attached to the deck. Estimated wind speed was around 105 mph. Source: Institute for Disaster Research, Texas Tech University.[7]

- The National Research Council issued a report[6] on Hurricane Alicia (Texas, 1983) that extensively discusses glazing damage at several high-rise buildings in Houston's central business district. A few thousand windows were broken. A survey found that more than 80% of the damage was caused by WBD. Much of the WBD was aggregate from built-up roofs. The report mentions glazing damage outside of the central business district, as well as damage to brick veneer, brick non-load-bearing walls, doors, exterior insulation and finish systems (EIFSs), and roof coverings. However, the report does not include specific information about these enclosure failures.

Hurricane Hugo (1989)

TTU's report on the performance of roof systems in Hurricane Hugo[7] was the first relatively comprehensive US report on hurricane performance of roof systems. It covered residential and nonresidential buildings (including critical facilities).

Hugo caused significant structural damage at a large number of low-rise buildings. Fully engineered buildings typically did not experience structural damage, but some did.

At the 14-story hotel shown in Fig. 5,[7] the roof deck failed. The deck was lightweight insulating concrete (LWIC) over a steel form deck. The reinforcing mesh was at the bottom of the LWIC. The 6-ft-high parapet kept deck and roof membrane debris from blowing off the roof. Wind pressure broke most of the windows at the top floor.

At the military aircraft hangar shown in Fig. 6,[7] the steel deck blew off (it was attached with arc spot welds). Brackets for the 12-in.-wide gutter were attached to the steel deck. It was apparent that the deck attachment had not accounted for the uplift load imparted by the gutter. This example illustrates importance of load path, and the critical need for effective communication between the structural engineer and the building enclosure designer. The aggregate surface built-up roof was over two layers of insulation (the first layer was mechanically attached to the deck).

The TTU report[7] documented door, glazing, and wall damage, but it concentrated on roof system performance. The following roof systems were investigated: asphalt shingles, built-up roof, metal panels (architectural and structural), metal shingles, modified bitumen, single-ply systems (adhered, mechanically attached, aggregate-ballasted), slate, and tile. The report was widely circulated and served as an initial wake-up call to the roofing industry.

A key finding of the TTU investigation was importance of metal edge flashings and copings. A subsequent paper[9] analyzed then current codes and design guides and provided recommendations for improving the wind performance of these elements.

Hurricane Andrew (1992)

After Hurricane Andrew struck, several storm-damage research teams, including a team under the auspices of the Wind Engineering Research Council (now the American Association for Wind Engineering), deployed to south Florida. As with Hurricane Hugo, significant structural damage was observed at a large number of low-rise residen-

Figure 7. Poor structural performance overshadowed the performance of the building enclosure.

Figure 8. Most of the glazing in the red circles was broken by built-up roof aggregate. Further information on the glazing damage is given in Crandell and Smith.[10] This damage is reminiscent of glazing damage in the Houston, Texas, central business district during Hurricane Alicia (1993). The building on the right had a steep-slope roof; most of the mechanically attached single-ply membrane blew off. Estimated wind speeds were 145 to 170 mph.

tial (**Fig. 7**) and nonresidential buildings. Fully engineered buildings typically did not experience structural damage (**Fig. 8**[10]).

Also as with Hurricane Hugo, Hurricane Andrew caused significant building enclosure damage (Fig. 8, **9**,[11,13] and **10**). In the area that received very high winds (from south of Kendall to Homestead), it was estimated that more than 95% of the low- and steep-slope roof coverings received some damage; more than 70% were estimated to be significantly damaged.[12]

Figure 9. This building experienced glazing damage, roof covering damage, and blow-off of roof pavers. Further information on the pavers is given in Mooneghi and Smith.[11] Estimated wind speed was in excess of 175 mph.[13]

REASONS FOR IMPROVED WIND PERFORMANCE SINCE 1992

Many major hurricanes (Categories 3 through 5 on the Saffir-Simpson Hurricane Wind Scale) have struck the US mainland (**Fig. 11**).[14] However, prior to Hurricanes Hugo and Andrew, the wind resistance of building enclosures and rooftop equipment did not typically receive increased attention in the aftermath of hurricanes. That aftermath scenario changed when Hurricane Hugo (Category 4) and Hurricane Andrew (Category 5) affected populated areas within three years. A variety of factors contributed to awareness that improved wind performance was needed. One of the key factors was the economic impact of the hurricanes. The estimated building damage loss from Hurricane Andrew is $42 billion (adjusted for inflation).[15] It was reported that Hurricane Andrew pushed eight insurance companies to

Figure 10. The collapse of the antenna tower (red arrow) at this school caused progressive peeling of the adhered single-ply membrane. Also note that the exhaust fan blew off the curb (blue arrow), but the high parapet kept it from blowing off the roof. Source: Federal Emergency Management Agency (FEMA 543).[3]

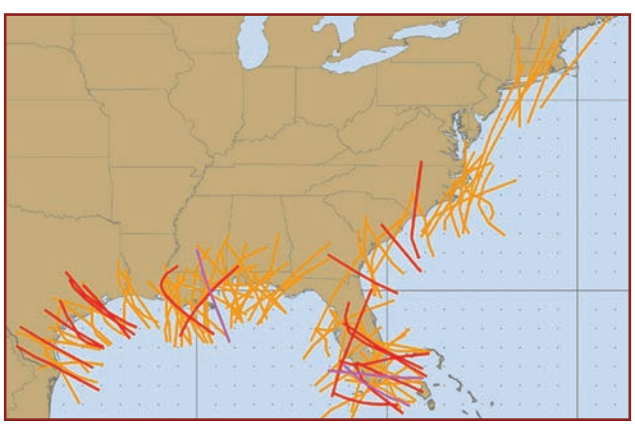

Figure 11. Major hurricane strikes, 1851–2010. Orange = Category 3; red = Category 4; purple = Category 5. Source: NOAA Technical Memorandum NWS NHC-6.[14]

Figure 12. The rooftop equipment on this new federal courthouse in Mississippi blew away during Hurricane Katrina (2005) because fans were resting on vibration isolators that provided lateral resistance but no uplift resistance. Two large openings through the roof were left after the ducts blew away. The resulting water infiltration caused extensive interior damage. The building was not occupied for several months while repairs were underway. Source: Federal Emergency Management Agency (FEMA 543).[3]

insolvency.[16] In addition to the cost of building damage, the social fabric of the communities affected was seriously disrupted.

Another factor contributing to awareness of wind performance issues was the number of teams that studied building performance. Whereas building performance research following previous hurricanes was limited, many teams deployed to learn from Hurricane Andrew (including a team from Australia). These teams included academic researchers and representatives of industry trade associations. Much of the field research focused on the MWFRS, but there was a significant amount of building enclosure and rooftop equipment investigation. The research findings from Hurricanes Hugo and Andrew, as well as other storms, were then used to inform various wind design guides that were subsequently developed.

As the economic impact of the hurricanes became clearer and field research on building performance grew, there emerged a critical mass of individuals, organizations, and associations that championed improved wind performance of building enclosures and rooftop equipment. An understanding emerged that the wind performance problem is complex and requires many people with diverse expertise and many professional and industry organizations and government to participate in finding solutions. Establishment of a wind load test facility at Clemson University led to building enclosure research, and helped spawn development of research facilities at other universities.

Since 1992, improvements have been to existing test standards and new test standards have been developed. Also since 1992, wind requirements have been added to model building codes (which previously had very few wind provisions related to nonstructural building enclosures); new products have been introduced; some existing products have been improved; new building enclosure and rooftop equipment wind design guides have been published;[3, 17-25] and designers and other parties involved in construction have become more aware of wind performance issues.

Observations of building performance have been made after many hurricanes since 1995. Between 1995 and 2018, the following trends were observed:

- Failures of structural systems have decreased.
- The number of buildings that have building enclosures and rooftop equipment that are sufficiently wind resistant has increased (although problems are still frequent).
- The number of existing buildings that have been mitigated—that is, retrofitted to improve wind resistance—has increased (although many facilities are still in need of mitigation).
- The challenge to resist entrance of wind-driven rain has been recognized.
- The building insurance industry has taken a proactive approach in reducing wind damage.

Clearly, much has improved since 1989. However, as shown by the poor performance of several relatively new buildings (Fig. 1, 2, and **12**[3]), enclosures and rooftop equipment on many buildings (including critical facilities) still lack sufficient resilience. The *International Building Code* (IBC),[26] *International Residential Code* (IRC),[27] and *Florida Building Code*[28] lack sufficient requirements to reasonably ensure that buildings will be resilient when exposed to hurricanes.[29]

CHALLENGES FOR FURTHER IMPROVING WIND PERFORMANCE

Except for strong and violent tornadoes (EF2–EF5), poor performance of the MWFRS (such as that shown in Fig. 5, 6, and 7) has generally been eliminated for buildings that are designed and constructed in accordance with the IBC,[26] IRC,[27] or *Florida Building Code*.[28] Of course, significant design or construction

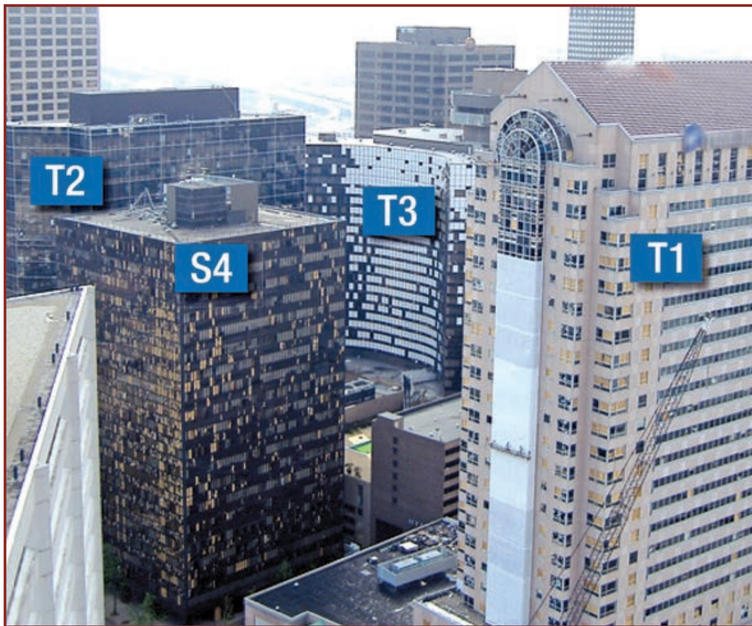

Figure 13. During Hurricane Katrina (2005), three office buildings (T1, T2, and S4) and a hotel (T3) in New Orleans had extensive glazing damage that was primarily caused by wind-borne roof aggregate. It took more than a year to replace the glazing at T1. The inset shows hotel guest rooms at T3. After the glazing was breached, development of high internal air pressure collapsed the walls between the guest rooms. The estimated wind speed was 105 mph. Source: Federal Emergency Management Agency (FEMA 549).[30]

errors or significant deterioration of structural elements (such as corrosion, wood decay, or termite attack) can and has caused MWFRS failure in buildings designed and contructed to meet code. However, observations of building performance after many hurricanes between 2004 and 2018 have shown that many buildings are still being designed and constructed with inadequate resilience. Hence, in lieu of being readily repaired so that they can serve their intended purpose, buildings are often so extensively damaged that they cannot be occupied for many weeks or months (Fig. 2, 12, and 13[30]).

The following sections identify challenges (obstacles) and opportunities for achieving building resiliency.

Building Owner Education and Input

Most building owners do not have a realistic perception of their building's vulnerability, and/or they do not believe their building will be affected by a damaging storm. An overly optimistic perception or belief can preclude an owner from mitigating an existing building or incorporating enhancements in the design and construction of a new building. Knowledgeable design professionals can play a key role in educating their clients.

A realistic perception of vulnerability should shape an owner's risk behavior. After an owner understands their building's vulnerability, the next step is for them to determine their desired level of resilience for the building through dialogue with their design professional. For example, for an office or retail building, an owner could be willing to accept damage that would result in the building being unoccupied for many months (Fig. 13[30]). Alternatively, the building owner could desire a higher level of performance and therefore be willing to accept only localized damage that would result in the building being unoccupied for a few days or a few weeks while repairs were made (Fig. 14). If a building (such as a hospital) needs to be fully operational during and after a storm, the owner may not be willing to accept water infiltration except at specific areas that do not affect facility functions (such as leakage at lobby vestibules).

The owner's desired level of building resilience should dictate mitigation actions for existing buildings and what design and construction enhancements are needed for new ones. The challenge for design professionals is to convince the building owner to invest now to ensure improved recovery if a damaging storm occurs.

Figure 14. During Hurricane Irma (2017), relatively minor roof damage resulted in leakage that collapsed acoustical ceiling panels and wetted carpet at a school auditorium in the US Virgin Islands. Source: Federal Emergency Management Agency (FEMA) Mitigation Assessment Team.

Figure 15. View of a negative pressure test apparatus that is used with test methods ASTM E907[33] and FM Global Property Loss Prevention Data Sheet 1-52.[34]

Figure 16. View of an exterior insulation and finish system field pull-test apparatus that is used with test method ASTM E2359.[35] Source: Federal Emergency Management Agency (FEMA P-2062).[4]

As part of educating a building owner, design professionals should discuss the importance of periodic inspection of the building enclosure and rooftop equipment, maintenance, and replacing systems and equipment before they reach the end of their effective service life.

Knowledgeable Design Professionals

To meet the challenge of educating building owners and adequately obtaining their input, it is essential that design professionals involved with building enclosures and rooftop equipment be knowledgeable of wind performance issues related to these elements.

Field Diagnostic Tools

A few diagnostic tools for assessing in situ conditions are available. For example, various techniques such as electric field vector mapping or infrared thermography can find moisture entrapped during construction or from leaks. ASTM D7877[31] is a guide for using electrical conductance measurement methods to locate leaks, and ASTM C1153[32] is a practice for locating wet insulation using infrared imaging. The field uplift resistance of some types of roof systems can be evaluated with a negative pressure test apparatus (**Fig. 15**[33,34]), and the suction resistance of EIFS can be evaluated with a field pull-test (**Fig. 16**[4,35]). Water resistance of windows, skylights, doors, and curtainwalls can be evaluated by the ASTM E1105 test method,[36] which uses uniform or cyclic static air pressure and water from a spray grid.

However, many more diagnostic tools need to be developed for systems and components that currently cannot be evaluated in the field. Without diagnostic tools, it is difficult to assess the wind and wind-driven rain performance of new construction and the vulnerability of existing buildings.

One example of a new field tool that would be beneficial is an apparatus to help evaluate the wind resistance of edge flashings, copings, and gutters. FEMA's *Guidelines for Wind Vulnerability Assessments of Existing Critical Facilities*[4] provides guidance for evaluation of edge flashings by hand rotation. The guidance notes that experienced investigators can detect weak edge flashings and copings easily. However, it also notes that an edge flashing or coping may be very resistant to rotation, which could be incorrectly interpreted as having adequate wind resistance. Thus, an apparatus to provide a more definitive evaluation would be enormously helpful in identifying vulnerable edgings.

Another example of a possible field tool would be a nondestructive apparatus that could evaluate the integrity of foam ribbon adhesive. Use of such an apparatus could dramatically reduce the amount of wind damage caused by inadequate adhesive bonds. Imagine something similar to medical imaging equipment. By rolling such an apparatus over insulation shortly after installation, it could be immediately known whether the adhesive bonds were adequate. If they were not, corrective action at the weak area could be performed, and work practices for the remainder of the roof could be modified, thus avoiding a vulnerable installation.

Water Infiltration

Improved wind resistance of building enclosures and rooftop equipment has revealed the problem of wind-driven rain. The FEMA report on Hurricane Charley (Florida, 2004)[37] noted that as building performance improved, water infiltration due to failed enclosures has been reduced, but the damage due to wind-driven rain infiltration is becoming more pronounced. That finding is illustrated by **Fig. 17**[20] and **18**.[1] Additional research, new and improved test methods, expanded design guidance, and product improvements are needed to successfully respond to this extremely challenging problem.

Wind-borne Debris

Criteria for protection of glazing was added to the 1995 edition of ASCE 7. Protected glazing consists of shutter or glazing assemblies that have been tested in accordance with ASTM E1886,[38] using test missiles specified in ASTM E1996.[39] Protected glazing is required in WBD regions, as defined in ASCE 7.[2] The purpose of protected glazing is to avoid breaching by debris and subsequent development of high internal air pressure and entrance of wind-driven rain.

WBD criteria are needed for roof systems, as illustrated by **Fig. 19** and **20.**[40] Most roof coverings are easily penetrated by WBD (even low-momentum debris such as a small tree branch). Unless there is a secondary membrane (as discussed in FEMA's *Design Guide for Improving Critical Facility Safety from Flooding and High Winds*[3]), water can leak into the building when the roof covering is punctured.

WBD testing research using the protocol given

Figure 17. At this Louisiana hospital, water leaked into the building along the base of many of the brick veneer walls during Hurricane Katrina (2005). It was believed that rain was blown into the wall cavity, where it overwhelmed the capacity of the weeps and inundated the through-wall flashings. Source: Federal Emergency Management Agency (FEMA 577).[20]

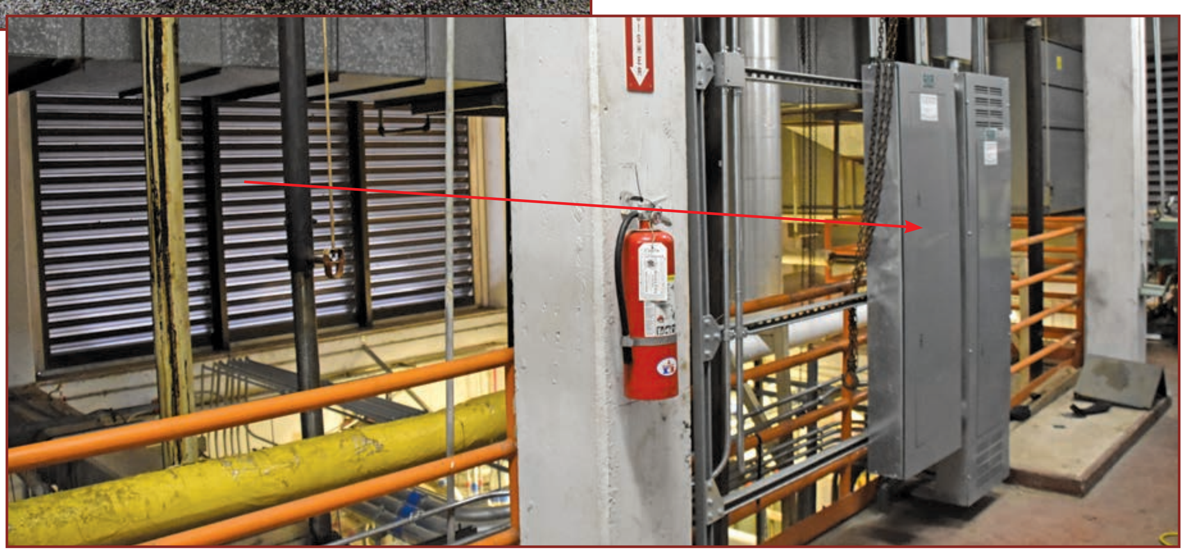

Figure 18. Although the estimated wind speed at this Florida hospital was only 115 mph, rain was driven several feet past the louvers and wetted the electric panels, which caused the circuit breakers to trip. Source: Federal Emergency Management Agency (FEMA P-2077).[1]

Figure 19. During Hurricane Marilyn (1995), a piece of 2x4 lumber penetrated the metal roof panel and 1x wood deck at a school in the US Virgin Islands. Source: Federal Emergency Management Agency Hazard Mitigation Technical Assistance Program.

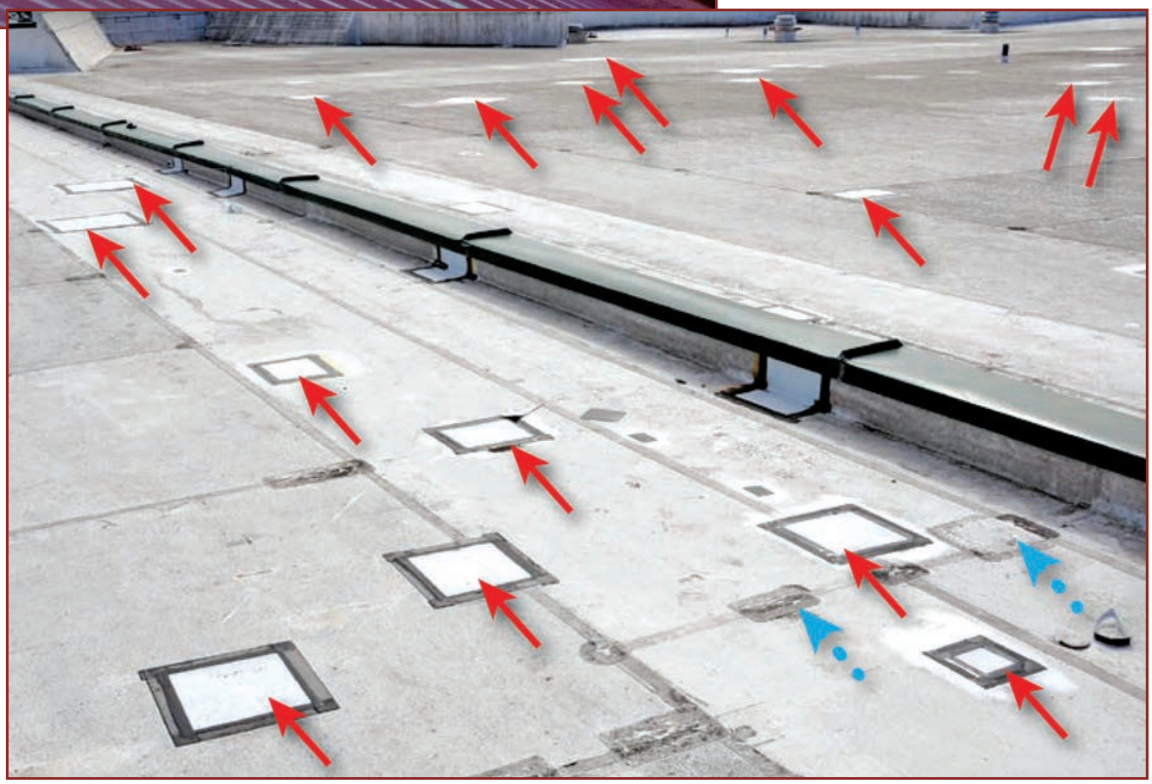

Figure 20. The red arrows indicate patches that were made after wind-borne debris punctured this Texas school's roof membrane during Hurricane Harvey (2017). The dark patches (blue dotted arrows) are old patches. Source: Federal Emergency Management Agency (FEMA P-2022).[40]

ASCE's *Prestandard for Performance-Based Wind Design*[23] is needed to quantify the qualitative secondary membrane recommendations given in the FEMA *Design Guide*.[3] The ASCE test protocol evaluates the ability of a roof assembly to prevent water leakage into the building's interior after an assembly is struck by debris.

Because much less water is likely to enter at an opening through a vertical surface than a horizontal surface, puncture of door or wall assemblies that are not glazed is typically less problematic than puncture of roof assemblies. For those buildings where puncture of door or wall assemblies is to be avoided, WBD resistance of door and wall assemblies can be evaluated by the hurricane shelter criteria given in the *ICC/NSSA Standard for the Design and Construction of Storm Shelters*.[41]

Existing Test Methods

The adequacy of laboratory and field test methods to evaluate wind and wind-driven rain resistance over the effective service life of an assembly is unknown, particularly for those assemblies that experience in-service dynamic loading but are statically tested. Comprehensive reevaluation research is needed to identify limitations of existing test methods and, where limitations are found, modify the tests so that they provide realistic evaluation on an assembly.

Examples of research questions include the following:

- Can the negative pressure test apparatus used with ASTM E907[33] and FM Global 1-52[34] (Fig. 15) adequately evaluate the attachment of a bottom insulation board in an assembly that has three or more layers of insulation and a cover board? Does the apparatus frame pushing down on the upper layers of the system preclude adequately loading the bottom board?
- ANSI/SPRI/FM 4435/ES-1, *Test Standard for Edge Systems Used with Low Slope Roofing Systems*,[42] is a static test. However, many edge flashings and copings are quite flexible and experience a large number of cyclical load cycles during a strong storm. Are assemblies that pass this test susceptible to fatigue failure during their effective service life?

Climate Change

Reference 43 states that "climate change has the potential to adversely affect wind pressures on roof assemblies, by producing

The current inventory of existing buildings is huge. A large number of these building have enclosures and rooftop equipment that are very vulnerable to wind pressure, WBD, and/or wind-driven rain.

windstorms that have: 1) greater speed, 2) longer storm duration, and/or 3) increased frequency of occurrence. Each of these three factors present greater wind resistance demand on roof assemblies. The demand is amplified when more than one of these factors occur simultaneously ... One approach to address climate change impact on windstorms is to increase the design wind speed. However, the magnitude of a reasonable increase is currently unknown. Also, increasing the design wind speed does not account for changes in storm duration nor frequency, which are also unknowns." Reference 43 recommends that attention be given to enhancing the reliability of roof assembly resistance, rather than simply just increasing the design wind speed. Reference 43 pertains to roof assemblies, but the concepts are applicable to the entire building enclosure and rooftop equipment. Numerous examples of efforts to enhance reliability are given in this paper and elsewhere.[3,17-25]

Performance-Based Wind Design

Chapter 8 of ASCE's *Prestandard for Performance-Based Wind Design*[23] addresses the building enclosure and rooftop equipment and specifies performance objectives. However, Chapter 8 notes that standardized test methods and other criteria for demonstrating that the performance objectives can be met do not exist for many of the objectives. Accordingly, judgment-based guidance for meeting each of the performance objectives is given in the Commentary. Research is needed to replace the judgment-based guidance with new test methods and other criteria for demonstrating compliance with the objectives.

Target Reliability

Chapter 1 of ASCE 7[2] provides target reliabilities (performance goals) for structural elements as a function of building risk categories. However, target reliabilities for building enclosures and rooftop equipment have not been established. Research and analysis are needed to establish target reliabilities for these important building elements.

Workmanship

Layered on top of the previously mentioned challenges is the challenge of achieving adequate workmanship. Storm damage investigations have revealed that workmanship defects are the root cause of many wind failures. While there have been improvements over the past three decades, workmanship defects remain one of the main causes of failure.

Certification of workers that install building enclosures and rooftop equipment should reduce the incidence of failures caused by installation defects. For example, in the National Roofing Contractors Association's (NRCA's) ProCertification initiative, experienced workers who demonstrate substantial roofing skills and knowledge can become certified in specific roof system installations.[44] The Vinyl Siding Institute also has a certification program for vinyl siding installers.[45]

Figure 21. This Florida fire station was constructed in 1978. Around 2001, it was retrofitted with storm shutters (red arrows) and new apparatus bay doors (which failed during Hurricane Michael in 2018). These mitigations were unsuccessful because several of the cementitious wood-fiber deck panels blew off. The fire station was demolished after the storm. The ASCE 7-16[2] basic wind speed for this building is 146 mph. Estimated wind speed was 132 mph (90% of the basic speed). Source: Federal Emergency Management Agency.[46]

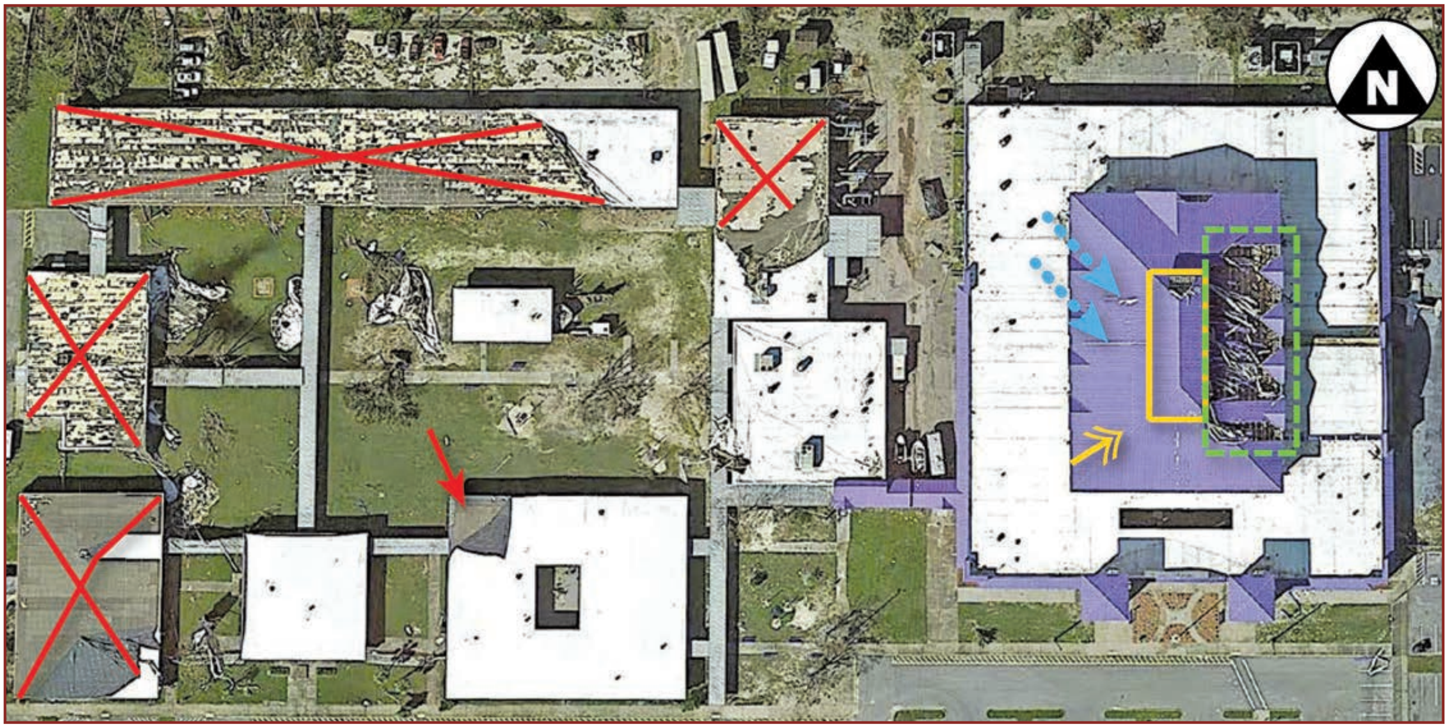

Figure 22. The red lines and arrows indicate where roof membranes blew off during Hurricane Michael (Florida, 2018). The green dashed rectangle indicates where metal roof panels blew off. The blue dotted arrows indicate where standing seams opened up. The ASCE 7-16[2] basic wind speed for this building is 143 mph. Estimated wind speed was 126 mph (88% of the basic speed). Source: Federal Emergency Management Agency (FEMA P-2077).[1]

Imagine the positive impact if every building enclosure and rooftop equipment worker on a jobsite were certified for the systems that they are installing.

Existing Buildings

Challenges presented thus far pertain to the design and construction of new buildings, as well as existing buildings. However, existing buildings present additional significant challenges.

Mitigation work on structural elements and/or the building enclosure is often needed because deterioration has occurred over time. Mitigation is also necessary when an existing building has inadequate strength to resist current design winds.

Many buildings constructed before the 1990s have insufficient uplift resistance of decks and/or deck support structures (Fig. 5, 6, 7 and **21**[46]). The roof systems on most of these buildings have been replaced; however, strengthening the deck or deck support structure was often not part of the reroofing work. When working on these older buildings, it is important to be aware of model building code criteria from the era when the building was designed. If a building were designed to the 1979 (or earlier) edition of the *Uniform Building Code* or the *Standard Building Code*, or the 1984 (or earlier) edition of the *Basic/National Building Code*, a uniform uplift pressure was used throughout the entire roof area. Therefore, decks and the deck support structure on buildings designed to these code editions are often substantially underdesigned in perimeter and corner areas when compared with current design uplift loads. Reference 47 has tables that illustrate the magnitude of the difference between loads derived from the 1998 edition of ASCE 7 and these older codes. Reference 47 also gives recommendations for enhancing roof deck attachment during reroofing work.

Section 706.3.2 of the *International Existing Building Code* (IEBC)[48] has structural requirements for reroofing projects when a building is located where the basic wind speed is greater than 130 mph. Roof diaphragms, connections of the diaphragm to the roof framing members, and roof-to-wall connections are required to be evaluated for wind loads specified in the IBC,[26] including uplift. If these elements are not capable of resisting 75% of those loads, they are to be replaced or strengthened. Buildings that comply with the wind load provisions of the 1988 or later edition of ASCE 7 are exempt.

When reroofing, the above requirement is reasonable for many buildings. However, for those buildings where the owner desires a very high level of performance (such as an occupied hospital), resistance much greater than 75% would be prudent. If a new roof system can resist 100% of current design loads, a storm approaching design conditions could result in deck blow-off if the deck only has a capacity of 75%.

For mitigation to be effective, it must be comprehensive, with all significant wind vulnerabilities addressed by the retrofit. FEMA's Hurricane Michael Mitigation Assessment Team reported on the performance of 19 buildings that had been retrofitted for the purpose of improving wind performance.[1] Most of the retrofit projects were ultimately ineffective at limiting significant damage to the buildings or their contents. Substantial building damage and occupancy disruption occurred because not all significant wind vulnerabilities were addressed by the wind retrofit project. Figures 21 and **22** show two of the studied buildings.

The school shown at Fig. 22 was constructed in phases between 1968 and 1979. It was reroofed in 2004. After 1998, it was retrofitted with storm shutters to allow the building to be used as a post-hurricane recovery shelter. However, because of widespread significant roof covering and interior water damage during Hurricane Michael, it could not be opened for that purpose. A portion of the facility opened 26 days after hurricane landfall.

FEMA published key wind retrofit guidelines for buildings that have recently been damaged by wind, as well as for buildings

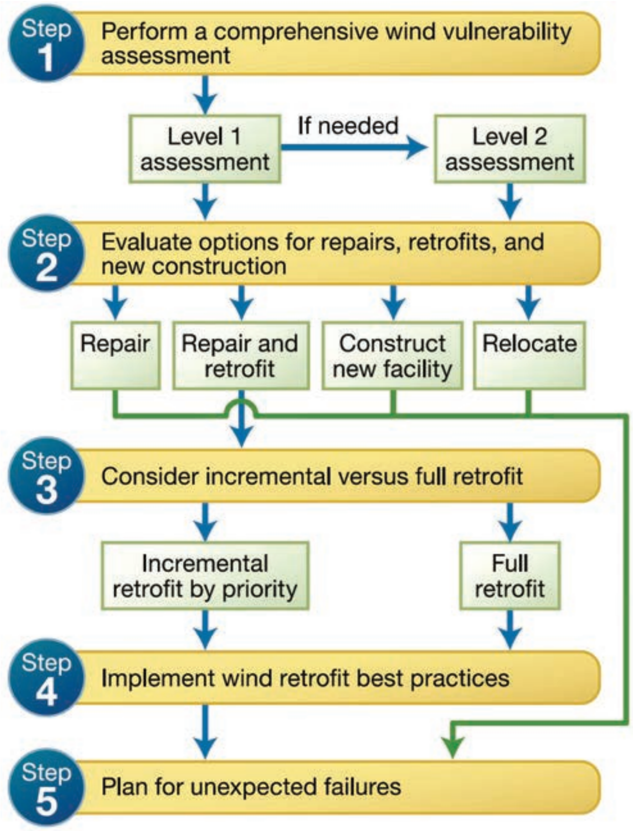

Figure 23. Flowchart showing a five-step approach to improving wind performance of existing buildings. Source: Federal Emergency Management Agency.[46]

that have not experienced wind damage.[46] The guidelines are intended to help building owners and designers prevent or limit wind damage and water infiltration during high-wind events. The guidelines include a five-step process for developing a comprehensive plan (Fig. 23). A key element of the process is performing a comprehensive wind vulnerability assessment, including the MWFRS, building enclosure, and rooftop equipment. FEMA's *Guidelines for Wind Vulnerability Assessments of Existing Critical Facilities*[4] provide design professionals with guidelines for assessing the vulnerability of buildings to wind pressure, WBD, and wind-driven rain.

Figure 24[1] illustrates the importance of conducting a comprehensive vulnerability assessment. The nailer at this medical office building had inadequate wind resistance. The nailer was part of the original construction, but its attachment was apparently not checked when the building was reroofed. FEMA[4] provides guidance for assessing nailer attachment, and Smith[49] provides design guidance for existing nailers.

CODE-PLUS DESIGN

With respect to wind performance of building enclosures, current editions of the IBC,[26] IRC,[27] and *Florida Building Code*[28] are significantly better than the editions of building codes at the time of Hurricane Andrew. However, some aspects of performance are still not addressed. These codes also do not adequately address inspection and testing during construction. To reasonably ensure that a high level of wind performance is achieved, design enhancements (that is, "code-plus") and increased inspection during construction are needed.

STAKEHOLDER ROLES AND OPPORTUNITIES

To dramatically improve the wind performance of building enclosures and rooftop equipment, significant effort is needed by a variety of stakeholders.

Building Owners

Owners desiring a high level of performance need to budget for appropriate design enhancements[29] (such as those identified in guidance[3,17-25]). Owners also need to invest in increased inspection and testing during construction, periodic inspection during the life of the building, maintenance, and replacing systems and equipment before they reach the end of their effective service life. The magnitude of the additional costs for design enhancements and increased inspection and testing is a function of the wind hazard where the building is located and the owner's desired level of resilience. Figures 25 and 26 illustrate the importance of design enhancements and inspection during construction.

Residential building owners who desire a high level of performance should consider the Insurance Institute for Business & Home Safety (IBHS) Fortified Home program.[50,51]

Design Professionals

It is apparent that many design professionals (architects, structural, mechanical, and electrical engineers, and building enclosure consultants) are not implementing known best practices to achieve good wind performance of building enclosures and rooftop equipment. It is also apparent that many practitioners are either infrequently or not specifying inspection and field testing during construction (for example, nondestructive testing for moisture, uplift testing, and water spray testing). These shortcomings with regard to implementing best practices and performing inspection and testing may be due to lack of awareness on the

Figure 24. During Hurricane Michael (Florida, 2018), the nailer lifted and caused progressive lifting and peeling of the roof membrane. The ASCE 7-16[2] basic wind speed for this building is 147 mph. Estimated wind speed was 130 mph (88% of the basic speed). Source: Federal Emergency Management Agency (FEMA P-2021).[1]

Figure 25. Damage that occurred during Hurricane Ivan (Alabama, 2004) to an exterior insulation and finish system (EIFS) at a residential building. The gypsum board typically detached from the studs. In some areas, the interior gypsum board was also blown off. EIFS can perform well, but wind damage is common. (EIFS damage also occurred at the hospital shown in Fig. 2.) Use of precast concrete wall panels would be a conservative design enhancement. Source: Federal Emergency Management Agency (FEMA 489).[52]

Figure 26. In the mid-1980s, the roof on this new school in Anchorage, Alaska, blew off during moderate winds soon after it was installed. It failed even though it was a robust system because of a major installation error.

practitioner's part, or it could be that building owners are unwilling to budget for these expenses. To adequately serve clients, design professionals should make the effort to be aware of current knowledge and the importance of inspection and field testing. They also should seek to educate their clients about their buildings' vulnerabilities and ascertain the level of resilience they desire for their buildings.

When architects are involved in a project, they should either have adequate building enclosure expertise or engage a qualified engineer or consultant. Architects should also ensure that their mechanical and electrical engineering consultants are adequately addressing rooftop equipment, including wind-driven rain entrances at wall louvers and equipment. A FEMA *Recovery Advisory*[24] published after Hurricanes Irma and Maria struck the US Virgin

Figure 28. The fan in the foreground was struck by wind-borne debris. The fan's disconnect switch bracket was not adequately anchored. The green dotted arrow indicates a detached lightning protection system conductor. The blue arrow indicates detached base flashing. This damage occurred at the Florida hospital shown at Fig. 2 during Hurricane Michael (2018). Source: Federal Emergency Management Agency (FEMA P-2077).[1]

Figure 27. Although this 18,000-lb heating, ventilation, and air-conditioning unit was attached to its curb with 16 straps, the unit blew off during Hurricane Ivan (2004) because the attachment was inadequate. The Alabama medical office building was less than one year old. The estimated wind speed was 85 to 95 mph. Source: Federal Emergency Management Agency (FEMA 489).[52]

Figure 29. Brick veneer failure at a 12-story Texas condominium during Hurricane Harvey (2017). Before the storm, repairs had been made in the failed area using helical ties. The ASCE 7-16[2] basic wind speed for this building is 149 mph. The estimated wind speed was 140 mph (94% of the basic speed). Source: Federal Emergency Management Agency (FEMA P-2022).[40]

Islands (2017) and **Fig. 27**[52] and **28**[1] illustrate rooftop equipment performance problems.

Manufacturers

Product and equipment manufacturers can play a key role in educating design professionals and contractors about their products and equipment, and they can highlight various design enhancements that could be applicable to specific projects. Manufacturers should also help fund needed research.

Manufacturers should *not* advocate for the elimination of important enhancements specified by design professionals. Statements such as "You don't need to do that to get our warranty" can lead to less-resilient buildings.

Contractors

It is important that contractors employ workers who are adequately trained, and ensure that installed systems/equipment comply with the contract documents. Contractors should also implement quality control. For systems where worker certification programs exist (such as NRCA's ProCertification[44]), contractors should employ certified workers.

On privately funded projects, replacement of existing systems and equipment is often performed by contractors working directly with the building owner, and a design professional is not involved. When working on these types of projects, the contractor needs to be responsible for duties performed by a design professional, or they should recommend that the building owner retain the services of a design professional.

Appropriate design and installation are needed to avoid failures such as the example shown at **Fig. 29**.[40]

Figure 30. During Hurricane Marilyn (US Virgin Islands, 1995), a displaced air terminal punctured the roof membrane in several locations. Source: Federal Emergency Management Agency (FEMA 543).[2]

Trade and Professional Organizations

Trade associations should implement worker certification programs (such as NRCA's ProCertification[44]) and develop quality control documents (such as NRCA's *Quality Control and Quality-Assurance Guidelines for the Application of Membrane Roof Systems*[53]).

Trade and professional organizations should help fund needed research, and they should work to add needed provisions (such as WBD criteria for roof systems in WBD regions) to building codes and standards.

The Lightning Protection Institute (LPI) should work to incorporate wind-resistance criteria into LPI-175,[54] NFPA 780,[55] and UL 96A[56] installation standards. (Until wind-related criteria are incorporated into these standards, guidance for attachment provided by FEMA[18] is recommended.) Numerous storm damage investigations have found detached lightning protection systems (**Fig. 30**[3]), some of which have resulted in significant water leakage damage.

Figure 31. The sheet metal enclosure (cabinet) blew off this heating, ventilation, and air-conditioning unit during Hurricane Irma (US Virgin Islands, 2017). An access panel was also blown off. It appeared that wind-blown enclosure debris caused roof membrane tears. Source: Federal Emergency Management Agency (FEMA P-2021).[57]

RESEARCH UNIVERSITIES

Notable wind-related research universities in north America include Florida International University (Facility Overview | DesignSafe-CI), University of Florida (UF Experimental Facility Overview | DesignSafe-CI), University of Notre Dame, Texas Tech University (National Wind Institute | National Wind Institute | TTU), Western University (Wind Engineering – Research – Faculty of Engineering – Western University) and WindEEE Research Institute, Western University (WindEEE Research Facility—Canada's most advanced research facility in wind engineering, energy and environment). Other research entities include the IBHS Research Center (IBHS Research Center – Insurance Institute for Business & Home Safety) and the National Research Council of Canada.

ASHRAE should take a more active role in working to improve the wind performance of rooftop equipment in terms of anchorage of equipment and equipment integrity (**Fig. 31**[57]).

Universities

Universities that offer architectural and/or engineering (civil, structural, mechanical, and electrical) degrees should address wind performance of building enclosures and rooftop equipment by devoting at least an hour to this topic during a student's tenure at the university. Research universities should continue to perform research that is needed to improve the wind performance of building enclosures and rooftop equipment. Research should contribute to new solutions, add to the depth of knowledge, and/or contribute to development/advancement of codes and standards (see "Research Universities" sidebar). Key items in need of research, as previously enumerated, are development of field diagnostic tools, water infiltration, WBD criteria for roof systems, reevaluation of existing test methods, criteria for demonstrating compliance with the performance objectives given in ASCE's *Prestandard for Performance-Based Wind Design*,[23] and target reliabilities.

To implement research, significant funding is needed. Potential funding sources include the US federal government (via the National Windstorm Impact Reduction Program[58]), trade and professional organizations, and manufacturers.

In addition to research needs listed previously, adequate research of new materials and systems before they are commercialized is

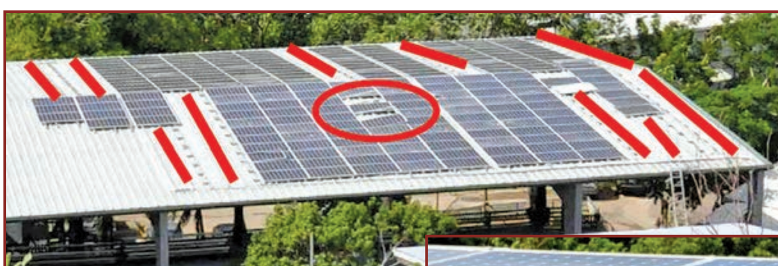

Figure 32. The red lines indicate where several adjacent solar panels were blown off during Hurricane Irma (US Virgin Islands, 2017). The area within the red oval in the left photo is the focus of the right photo, where the red arrows indicate the polyvinyl film detached from the panel frame. Some panels lifted but did not blow away (yellow arrows). Some panels were damaged by wind-borne debris (blue arrows). Source: Federal Emergency Management Agency.[25]

Figure 33. During Hurricane Irma (US Virgin Islands, 2017), there was no apparent damage to this building enclosure (the interior was not evaluated for entrance of wind-driven rain). The estimated wind speed was approximately 175 mph (including wind speed-up due to an abrupt change in topography). Source: Federal Emergency Management Agency (FEMA P-2021).[57]

needed to avoid poor wind performance. For example, when Hurricanes Irma and Maria struck the US Virgin Islands in 2017, many rooftop solar panels exhibited poor wind performance (**Fig .32**[25]). (For information on design, installation and maintenance guidance for rooftop solar panels, see FEMA's *Recovery Advisory.*[25])

Design Guides

FEMA and other entities have published useful design guides.[3,17-25] Many of these are several years old. While most of the guidance in these documents is still valid, these guides do not reference test methods that have been developed since the guides were published. These guides also do not capture changes that have been made to ASCE 7 since the guides were published. These documents should be updated. Also, the sections pertaining to remedial work on existing buildings in FEMA's design guides for hospitals,[3] schools,[18] and critical facilities safety[20] should be expanded to provide more in-depth guidance.

IIBEC Credentialing Program

IIBEC's credential program currently offers seven credentials, including Registered Roof Consultant (RRC), Registered Exterior Wall Consultant (REWC), and Registered Building Enclosure Consultant (RBEC).[59]

IIBEC should consider adding a wind performance registration to its credential program. This new program would be similar to a master's degree. For example, someone with an RRC, REWC, or RBEC could augment that registration with a wind performance registration.

The new credentials should be based on a robust understanding of wind/building interactions and an in-depth knowledge of what it takes to achieve a wind-resilient building. A cadre of people with the new credentials could be instrumental in further improving wind performance of building enclosures and rooftop equipment.

SUMMARY

Achieving good, reliable performance is difficult. It takes design and construction attention, and a commitment of adequate funding to achieve the desired resilience. However, when buildings remain operational, the payoff is enormous.[29] This is illustrated by the building in **Fig. 33**, which was not damaged when Hurricane Irma struck the US Virgin Islands in 2017. This building has a corrugated metal panel roof with integral gutter that appeared to comply with the US Virgin Islands Stronger Home Guide, which was developed by FEMA and the US Virgin Islands building department soon after Hurricane Marilyn in 1995 and is now in its fourth edition.[60]

REFERENCES

1. Federal Emergency Management Agency (FEMA). 2020. *Mitigation Assessment Team Report: Hurricane Michael in Florida Building Performance Observations, Recommendations, and Technical Guidance.* FEMA P-2077. https://www.fema.gov/sites/default/files/2020-07/mat-report_hurricane-michael_florida.pdf.
2. American Society of Civil Engineers (ASCE). 2016. *Minimum Design Loads and Associated Criteria for Buildings and Other Structures.* ASCE 7-16. Reston, VA: ASCE.
3. FEMA. 2007. *Design Guide for Improving Critical Facility Safety from Flooding and High Winds.* FEMA 543. https://www.fema.gov/sites/default/files/2020-08/fema543_design_guide_complete.pdf.
4. FEMA. 2019 *Guidelines for Wind Vulnerability Assessments of Existing Critical Facilities.* FEMA P-2062. https://www.fema.gov/sites/default/files/2020-07/guidelines-wind-vulnerability.pdf.
5. Minor, J. E. 1977. "Performance of Roofing Systems in Wind Storms." In *NRCA/NBS Proceedings of the Symposium on Roofing Technology,* pp. 124-132. https://nrcawebstorage.blob.core.windows.net/files/TechnicalLibraryNRCA/255.pdf.
6. National Research Council. 1984. *Hurricane Alicia, Galveston and Houston, Texas, August 17-18, 1983.* Washington, DC: National Academies Press. https://doi.org/10.17226/19411.
7. McDonald, J. R., and T. L. Smith. 1990. *Performance of Roofing Systems in Hurricane Hugo.* Lubbock: Institute for Disaster Research, Texas Tech University.
8. Minor, J. E., J. R. McDonald, and K. C. Mehta. 1977 (reprinted 1993). *The Tornado: An Engineering-Oriented Perspective.* National Oceanic and Atmospheric Administration Technical Memorandum ERL NSSL-82. US Department of Commerce. https://repository.library.noaa.gov/view/noaa/7227.
9. Smith, T. 1990 "Hurricane Hugo's Effects on Edge Flashings." *International Journal of Roofing Technology* 2: 65-70.
10. Crandell, J. H., and T. L. Smith. 2009. "Design Method Improvements to Prevent Roof Aggregate Blow-off." In *Proceedings of the Hurricane Hugo 20th Anniversary Symposium* (CD).

Charleston, SC: Applied Technology Council.
11. Mooneghi, M. A., and T. L. Smith. 2017. "Concrete Roof Pavers: Wind Uplift Aerodynamic Mechanisms and Design Guidelines—A Proposed Addition to ANSI/SPRI RP-4." *Proceedings of the 32nd RCI International Convention and Trade Show, March 2017.* http://iibec.org/wp-content/uploads/2017-cts-mooneghi-smith-irwin-chowdhury.pdf.
12. Smith, T. L. 1994. "Causes of Roof Covering Damage and Failure Modes: Insights Provided by Hurricane Andrew." In *Hurricanes of 1992: Lessons Learned and Implications for the Future*, edited by R. A. Cook. Reston, VA: ASCE.
13. Powell, M. D., S. H. Houston, and T. A. Reinhold. 1996. "Hurricane Andrew's Landfall in South Florida. Part 1: Standardizing Measurements for Documentation of Surface Wind Fields." *Weather and Forecasting* 11 (3): 304–328. https://doi.org/10.1175/1520-0434(1996)011%3C0304:HALISF%3E2.0.CO;2.
14. Blake, E. S., and E. J. Gibney. 2011. *The Deadliest, Costliest, and Most Intense United States Tropical Cyclones from 1851 to 20210 (and Other Frequently Requested Hurricane Facts).* NOAA Technical Memorandum NWS NHC-6. https://www.nhc.noaa.gov/pdf/nws-nhc-6.pdf.
15. Davis, R. J. 2021. "Risk Associated with Extreme Wind Events from a Property Insurance Standpoint" (webinar). Florida International University. https://interact.fiu.edu/webinars/webinar-series-archives/risk-associated-with-extreme-wind-events-from-a-property-insurance-standpoint/fiu-webinar-march-12-2021.pdf.
16. Law Offices of Kanner and Pintaluga. n.d. "Hurricane Andrew's Impact on the Insurance Industry in Florida" (blog post). Accessed December 30, 2021. https://hurricanedamage.com/blog/hurricane-andrew-cost-insurance-industry.
17. FEMA. 2011. *Coastal Construction Manual: Principles and Practices of Planning, Siting, Designing, Constructing, and Maintaining Residential Buildings in Coastal Areas (Fourth Edition)*, vol. I and II. FEMA P-55. https://www.fema.gov/sites/default/files/2020-08/fema55_voli_combined.pdf.
18. FEMA. 2010. *Design Guide for Improving School Safety in Earthquakes, Floods, and High Winds.* FEMA P-424. https://www.fema.gov/pdf/plan/prevent/rms/424/fema424_cvr-toc.pdf.
19. FEMA. 2010. *Home Builder's Guide to Coastal Construction, Technical Fact Sheet Series.* FEMA P-499. https://www.fema.gov/sites/default/files/2020-08/fema499_2010_edition.pdf.
20. FEMA.2007. *Design Guide for Improving Hospital Safety in Earthquakes, Floods, and High Winds.* FEMA 577. https://www.wbdg.org/FFC/DHS/fema577.pdf.
21. Baskaran, A., and T. L. Smith. 2005. *A Guide for the Wind Design of Mechanically Attached Flexible Membrane Roofs.* Ottawa, ON: National Research Council of Canada, Institute for Research in Construction.
22. Commission on Roofing Materials and Systems, International Council for Research and Innovation in Building and Construction. 2015. *Improving Roof Reliability.* CIB W083. https://www.irbnet.de/daten/iconda/CIB_DC29667.pdf.
23. ASCE. 2019. *Prestandard for Performance-Based Wind Design.* Reston, VA: ASCE. https://doi.org/10.1061/9780784482186.
24. FEMA. 2018. *Attachment of Rooftop Equipment in High-Wind Regions.* Hurricanes Irma and Maria in the U.S. Virgin Islands Recovery Advisory 2. https://www.fema.gov/sites/default/files/documents/hurricanes_irma_maria_usvi_1-5.zip.
25. FEMA. 2018. *Rooftop Solar Panel Attachment: Design, Installation, and Maintenance.* Hurricanes Irma and Maria in the U.S. Virgin Islands Recovery Advisory 5. Revised August 2018. https://www.fema.gov/sites/default/files/documents/hurricanes_irma_maria_usvi_1-5.zip.
26. International Code Council (ICC). 2021. *International Building Code.* Country Club Hills, IL: ICC.
27. ICC. 2021. *International Residential Code.* Country Club Hills, IL: ICC.
28. Florida Building Commission. 2020. *Florida Building Code.* 7th ed. Tallahassee: Florida Building Commission.
29. Smith, T. L. 2009. "Historical Performance of Critical Facilities Exposed to Hurricanes: Lessons Learned and Opportunities for Improvement." In *Proceedings of the Hurricane Hugo 20th Anniversary Symposium* (CD). Charleston, SC: Applied Technology Council.
30. FEMA. 2006. *Hurricane Katrina in the Gulf Coast Mitigation Assessment Team Report: Building Performance Observations, Recommendations, and Technical Guidance.* FEMA 549. https://www.fema.gov/emergency-managers/risk-management/building-science/publications?name=%22549%22.
31. ASTM International. 2016. *Standard Guide for Electronic Methods for Detecting and Locating Leaks in Waterproof Membranes.* ASTM D7877-14. West Conshohocken, PA: ASTM International. https://doi.org/10.1520/D7877-14.
32. ASTM International. 2016. *Standard Practice for Location of Wet Insulation in Roofing Systems Using Infrared Imaging.* ASTM C1153-10(2015). West Conshohocken, PA: ASTM International. https://doi.org/10.1520/C1153-10R15.
33. ASTM International. 2013. *Standard Test Method for Field Testing Uplift Resistance of Adhered Membrane Roofing Systems (Withdrawn 2013).* ASTM E907-96(2004). West Conshohocken, PA: ASTM International.
34. FM Global. 2021. *Field Verification of Roof Wind Uplift Resistance.* FM Global Property Loss Prevention Data Sheet 1-52. Johnston, RI: FM Global.
35. ASTM International. 2018. *Standard Test Method for Field Pull Testing of an In-Place Exterior Insulation and Finish System Clad Wall Assembly.* E2359/E2359M-13(2018). West Conshohocken, PA: ASTM International. https://doi.org/10.1520/E2359_E2359M-13R18.
36. ASTM International. 2016. *Standard Test Method for Field Determination of Water Penetration of Installed Exterior Windows, Skylights, Doors, and Curtain Walls, by Uniform or Cyclic Static Air*

Pressure Difference. ASTM E1105-15. West Conshohocken, PA: ASTM International. https://doi.org/10.1520/E1105-15.
37. FEMA.2005. *Mitigation Assessment Team Report Hurricane Charley in Florida: Observations, Recommendations, and Technical Guidance*. FEMA 488. https://www.fema.gov/sites/default/files/2020-08/fema488_mat_report_hurricane_charley_fl.pdf.
38. ASTM International. 2019. *Standard Test Method for Performance of Exterior Windows, Curtain Walls, Doors, and Impact Protective Systems Impacted by Missile(s) and Exposed to Cyclic Pressure Differentials*. ASTM E1886-19. West Conshohocken, PA: ASTM International. https://doi.org/10.1520/E1886-19.
39. ASTM International. 2020. *Standard Specification for Performance of Exterior Windows, Curtain Walls, Doors, and Impact Protective Systems Impacted by Windborne Debris in Hurricanes*. ASTM E1996-20. West Conshohocken, PA: ASTM International.
40. FEMA. 2019. *Mitigation Assessment Team Report Hurricane Harvey in Texas: Building Performance Observations, Recommendations, and Technical Guidance*. FEMA P-2022. Homeland Security Digital Library. https://www.hsdl.org/?abstract&did=822658.
41. ICC and National Storm Shelter Association (NSSA). 2020. *ICC/NSSA Standard for the Design and Construction of Storm Shelters*. ICC 500-2020. Country Club Hills, IL: ICC.
42. American National Standards Institute (ANSI) and Small-Ply Roofing Industry (SPRI). 2017 *Test Standard for Edge Systems Used with Low Slope Roofing Systems*. ANSI/SPRI/FM 4435/ES-1 2017. Waltham, MA: SPRI. https://www.spri.org/download/ansi-spri_standards_2020_restructure/es-1/ANSI_SPRI_FM-4435-ES-1_2017_080420.pdf.
43. Smith, T. L. 2017. *Adapting to Climate Change, New Build and Retrofit Options for Steep-Slope Residential Roofs*. Ottawa, ON: National Research Council of Canada.
44. National Roofing Contractors Association (NRCA). n.d. “NRCA ProCertification.” Accessed December 30, 2021. https://www.nrca.net/pro-certification.
45. Vinyl Siding Institute. n.d. “Certified Installer Program.” Accessed December 30, 2021. https://www.vinylsiding.org/careers-training/become-certified-installer.
46. FEMA. 2019. *Successfully Retrofitting Buildings for Wind Resistance*. Hurricane Michael in Florida Recovery Advisory 1. https://www.fema.gov/sites/default/files/2020-07/retrofitting-buildings-wind-resistance_hurricane-michael_florida.pdf.
47. Smith, T.L. 2001. “Uplift Resistance of Existing Roof Decks: Recommendations for Enhanced Attachment During Reroofing Work.” In *Proceedings of the International Conference on Building Envelope Systems and Technologies*. Raleigh, NC: IIBEC. An article that was adapted from this paper is available at: https://iibec.org/wp-content/uploads/2016/04/2003-01-smith.pdf.
48. ICC. 2021. *International Existing Building Code*. Country Club Hills, IL: ICC.
49. Smith, T. L. 2015. “Facing the Wind: Nailer Attachment Is One Key to Achieving Good Wind-Uplift Performance.” *Professional Roofing* 45 (3). https://www.professional-roofing.net/Articles/Facing-the-wind--03-01-2015/3612.
50. Insurance Institute for Business & Home Safety. n.d. “Fortified Construction Standards.” Accessed December 30, 2021. https://ibhs.org/fortified.
51. Rupar, M. 2014. “Building Stronger Buildings: The Insurance Industry Gives Homeowners and Building Owners Incentives to Fortify Their Structures.” *Professional Roofing* 44 (6). https://www.professionalroofing.net/Articles/Building-stronger-buildings--06-01-2014/2471.
52. FEMA. 2005. *Mitigation Assessment Team Report Hurricane Ivan in Alabama and Florida: Observations, Recommendations, and Technical Guidance*. FEMA 489. https://www.fema.gov/sites/default/files/2020-08/fema_489__hurricane_ivan_bpat_.pdf.
53. NRCA. 2017. *Quality Control and Quality-Assurance Guidelines for the Application of Membrane Roof Systems*. Rosemont, IL: NRCA.
54. Lightning Protection Institute (LPI). 2020. *Standard for the Design–Installation–Inspection of Lightning Protection Systems*. LPI 175–2020. Libertyville, IL: LPI.
55. National Fire Protection Association (NFPA). 2020. *Standard for the Installation of Lightning Protection Systems*. NFPA 780. Quincy, MA: NFPA.
56. UL Standards. 2016. *Standard for Installation Requirements for Lightning Protection Systems*. UL-96A. Northbrook, IL: UL Standards.
57. FEMA. 2018. *Mitigation Assessment Team Report Hurricanes Irma and Maria in the U.S. Virgin Islands: Building Performance Observations, Recommendations, and Technical Guidance*. FEMA P-2021. https://www.fema.gov/sites/default/files/2020-07/mat-report_hurricane-irma-maria_virgin-islands.pdf.
58. National Windstorm Impact Reduction Program. 2018. *Strategic Plan for the National Windstorm Impact Reduction Program*. https://www.nist.gov/system/files/documents/2018/09/24/nwirp_strategic_plan.pdf.
59. International Institute of Building Enclosure Consultants. n.d. “Credentials.” Accessed December 30, 2021. https://iibec.org/credentials.
60. US Virgin Islands Department of Planning and Natural Resources and FEMA. 2018. *Construction Information for a Stronger Home*. 4th ed. http://www.vitema.vi.gov/docs/default-source/response-recovery-documents/(1)-construction-information-for-a-stronger-home-4th-edition.pdf?sfvrsn=c52995d_2.

Resisting Water Infiltration from Cladding Attachment Penetrations in Wall Assemblies

Andrea Wagner Watts, LEED Green Associate

DuPont Performance Building Solutions | East Aurora, NY

a.wagnerwatts@dupont.com

IIBEC 2022 - Building for the Future

International Convention and Trade Show

March 17–22, 2022 | Orlando, FL

ABSTRACT

How do you make sure penetrations through your already installed air and water barrier are watertight? The method of sealing of cladding attachments through the wall assembly is critical to the building performance. To create a relevant, data-backed solution, a robust test plan was developed using a statistical test design and implemented to test all the variables of interest. Then, a statistical model was built to predict the probability of leaks with various sealing solutions. The process was used to determine which type of flashing and sealing solution is best to ensure watertightness after cladding attachments are installed over polyisocyanurate insulating sheathing. This presentation shares the basis of the test plan and research methodology as well as the findings on sealing penetrations through this system.

SPEAKER

Andrea Wagner Watts, LEED Green Associate

DuPont Performance Building Solutions | East Aurora, NY

Andrea Wagner Watts is the commercial application leader for DuPont Performance Building Solutions. In the 15 years, she has worked in the construction industry, she has successfully helped develop multiple sealants and air/water barrier system solutions. Currently, she focuses on improving the overall performance of the building enclosure through application innovation and new product development. Watts has published on building science, interfaces, durability, and resiliency. She has two patents, is a LEED Green Associate, and is the Technical Committee co-chair for the Air Barrier Association of America. Watts holds a bachelor of science degree in civil engineering from Cornell University.

Nonpresenting Coauthors

Piyush Soni

Piyush Soni is a research investigator for DuPont Performance Building Solutions in Midland, Michigan.

Wenyu Su

Wenyu Su is a statistician for DuPont Water Solutions in Midland, Michigan.

Resisting Water Infiltration from Cladding Attachment Penetrations in Wall Assemblies

Air infiltration is an ever-growing concern for buildings, and it is the focus of new codes and regulations in each code cycle. Water, which was previously a priority, seems to now be forgotten until it is too late. The water-resistant barrier (WRB) is very frequently the same product as the air barrier, and sometimes the same as the thermal barrier. These barriers are the final layer of defense before unwanted water or air enters the building, and they are intended to be continuous. The problem is that they are not designed to be the final aesthetic, ultraviolet light–durable covering for the building. When cladding is attached to the building after the WRB is installed, numerous holes are punched through the once-continuous barrier. The question is how to ensure that these penetrations remain watertight, safeguarding that water does not make its way through the wall assembly and into the finished structure.

The current testing of air and water barrier performance varies by material. Self-adhered membranes and fluid-applied membranes are typically tested for nail sealability per Section 8.9 of ASTM D1970, *Standard Specification for Self-Adhering Polymer Modified Bituminous Sheet Materials Used as Steep Roofing Underlayment for Ice Dam Protection.*[1] This standard tests the ability of a membrane to resist waterhead after the membrane is applied to plywood and penetrated by a roofing nail.

There is disagreement in the industry about the effectiveness of the ASTM D1970 test method in predicting the in-service success of WRBs tested to this standard. Common construction practices typically use either wood screws or self-tapping screws to secure cladding to the structure. These screws behave very differently from nails when going through a membrane. As a result, industry associations such as the Air Barrier Association of America and the Fenestration & Glazing Industry Alliance are working to develop better standards to test this property. Insulated sheathing used as an air and weather barrier and mechanically fastened WRBs currently do not have any material-only test requirements for nail or fastener sealability. However, these two types of materials are tested for water penetration as full systems per their ICC Evaluation Service (ICC-ES) code acceptance criteria. This testing includes the recommended fasteners used to attach the WRB and as well as other penetrations in the wall assembly.

Building codes require all air barriers to be tested for air leakage as part of an assembly per ASTM E2357, *Standard Test Method for Determining Air Leakage Rate of Air Barrier Assemblies.*[2] This test method specifies exact designs of the wall assembly to be tested, including penetrations, a window opening, and brick ties. The assembly is tested for air leakage per ASTM E283, *Standard Test Method for Determining Rate of Air Leakage Through Exterior Windows, Skylights, Curtain Walls, and Doors Under Specified Pressure Differences Across the Specimen,*[3] both before and after wind pressure conditioning to ensure the system leakage is less than the maximum amount allowed. The *International Building Code* (IBC)[4] includes no requirement for testing additional types of penetrations such as the large fasteners usually required to attach cladding.

The IBC includes additional requirements for WRBs. The code acceptance criteria for WRBs often require an assembly similar to the ASTM E2357[2] penetrated assembly to be tested for water infiltration per ASTM E331, *Standard Test Method for Water Penetration of Exterior Windows, Skylights, Doors, and Curtain Walls by Uniform Static Air Pressure Difference.*[5] The exact pressures and length of the testing, along with the type of wall assembly to be tested, vary by material.

As suppliers of materials with a shorter history make performance claims about air and water resistance, questions arise about the watertight performance of those materials after the entire facade is complete. The question then becomes how to test for these products' in-service properties.

The water-resistant barrier is very frequently the same product as the air barrier, and sometimes the same as the thermal barrier. These barriers are the final layer of defense before unwanted water or air enters the building, and they are intended to be continuous. The problem is that they are not designed to be the final aesthetic, ultraviolet light–durable covering for the building.

One of the products that is the subject of such questions is foil-faced polyisocyanurate (ISO) insulation, which can be used as an air, water, and thermal barrier when the joints of the insulation boards are sealed. ICC-ES AC71, *Acceptance Criteria for Foam Plastic Sheathing Panels Used as Water-Resistive Barriers*,[6] is designed to address many of these questions. It requires wall assemblies similar to those found in ASTM E2357[2] to be tested for water penetration per ASTM E331[5] for two hours at a differential pressure of 6.24 lb/ft^2 (300 Pa). This requirement is the same as the IBC requirements for exceptions to the use of a WRB. Even with this standardized testing for water infiltration, there are questions about what happens when the foil face of the insulation is punctured when cladding is later installed—there is concern that water can migrate through to the interior side of the insulation and subsequently into the building.

This paper details a study that was performed to determine how foil-faced ISO insulation performs after cladding attachments, specifically rain screen attachments, are installed onto the face. Previous assembly and project-specific testing of WRBs with fastener penetrations has shown that sealing at the point of penetration of the air barrier provides the greatest chance of success. We predicted that it would be the same for these systems. Unfortunately, it is often easiest to seal fasteners after they have been installed, instead of before. To minimize the potential of workmanship errors, the potential sealing solutions included in the study were selected to balance the predicted likelihood of success with the ease of installation in the field.

Several potential solutions were evaluated using a wall assembly test methodology. These tests examined different variables, such as girt system type, orientations of the attachments, and ways to seal the penetrations using different types of fluid and self-adhered flashing. Because of the large number of included variables, the study was divided into two phases. A statistical test design was used to limit the number of experiments for small-scale testing in phase I. Phase I testing focused only on pressurized water leakage through small-scale samples to quickly evaluate the critical pass/fail probability of each variable combination. This was done because water infiltration was chosen as the main criterion for passing the final evaluation. The results of phase I were used to develop a probability-of-leaks model to predict results for the full range of variables, which then helped to refine the plan for larger-scale testing in phase II. The second phase of the testing included additional stresses on the wall assembly to better predict long-term performance of the sealing solution in actual construction. This study design allowed us to quickly understand which solutions would likely work best for implementation in the field.

EXPERIMENTAL STRATEGY

The objective of the experiments was to find the most effective way to flash girts installed over foil-faced ISO insulation boards. One of the most representative ways to test wall assemblies to predict in-field performance for water infiltration is to use pressurized water leakage testing per ASTM E331.[5] In theory, this process is straightforward: walls are built with the different girt and sealing configurations, pressurized water leakage testing is conducted, and then the flashing configurations that did not show water leaks are selected for use. However, there were so many variables in this scenario that it was not possible to allot all the time and resources necessary to test each combination. To reduce the number of full-scale tests, an experimental strategy was created and implemented. Three key challenges and strategies to mitigate them were identified. The experimental strategy is explained as follows.

Challenge #1: Large Number of Experiments

It was ideal to keep the study as broad as possible because construction practices and materials vary widely across regions and building types. Consider the following questions:

- What is the most effective way to flash a hat channel girt? What if the hat channel is applied upside down? What about a Z channel or other proprietary rainscreen systems?
- What is the most effective way to flash a girt in the horizontal orientation? Or in the vertical orientation?
- Which flashing works better: fluid applied or self-adhered?
- Should the fluid-applied flashing be wet or should it be allowed to cure before installing the girt?
- Will the flashing recommendations change with insulation board thickness?

It was resource prohibitive to study every variable combination individually, so the variables were prioritized and factor levels for each variable were combined. (Variables or factors of the study are the characteristics that differentiate the treatments from one another such as the insulation thickness or girt type in this experiment. The factor levels, or simply levels, are the different treatments of the factor such as the three different insulation thicknesses being studied.[7]) For example, "hat down" girt (the hat channel applied with the long continuous side against the sheathing) was eliminated because it is essentially the same as a Z-girt at the point of contact with the insulation (**Fig. 1**). Hence, it was reasoned that the recommendations for Z-girts will also be watertight for hat down girts.

Similarly, levels of each variable were scrutinized to minimize the total number that would need to be tested while still including those that would have the greatest impact. A list of final primary variables and their factor levels are as follows:

1. ISO insulation thickness: 0.625 in. (15.9 mm), 1.55 in. (39.4 mm), 3 in. (76.2 mm)
2. Girt type: hat, Z, proprietary horizontal attachment system with large openings predrilled for fasteners, proprietary vertical attachment system with large predrilled openings for fasteners
3. Girt orientation: horizontal, vertical
4. Flashing material: no flashing, silicone fluid-applied flashing, water-based acrylic flashing, self-adhered flashing with a polyolefin top sheet, STPE (silyl-terminated polyether) fluid-applied flashing
5. Flashing on edge: no material, top only, all ("Top only" includes only

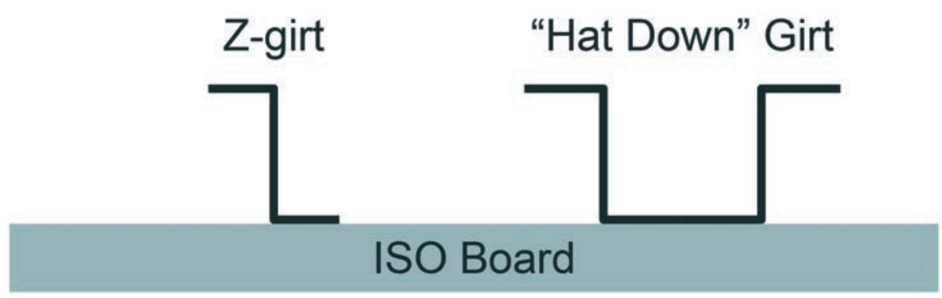

Figure 1. Z-girt and "hat down" girt connect to the sheathing in the same way.

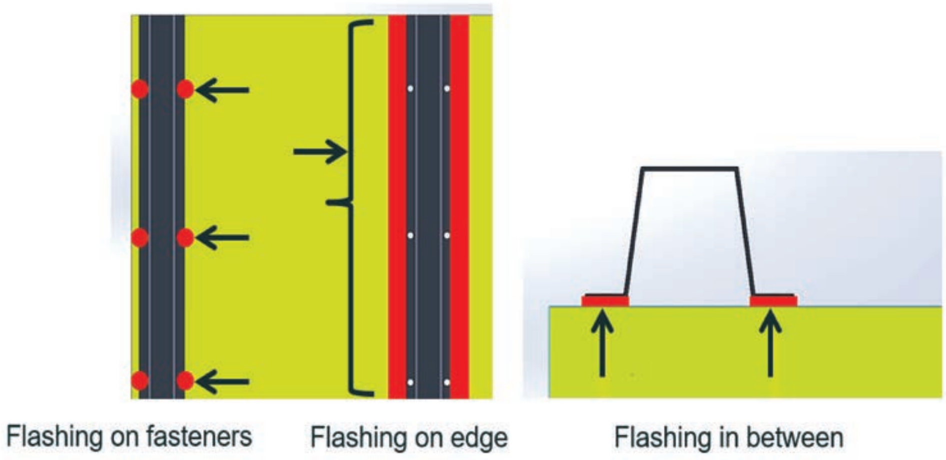

Figure 2. Flashing locations "on fasteners," "on edge," and "in between" shown by arrows.

the top edge of a horizontal girt. "All" includes both top and bottom edges. This definition is only for horizontal girts because there is no physical significance of top/bottom for vertical girts. Whereas there could be differences between top- and bottom-edge sealing in horizontal girts, there is no expected difference between left- and right-edge sealing of a vertical girt.)

6. Flashing on fasteners: no material, top only, all
7. Flashing in between (girt and ISO): no material, wet material, cured material

All flashing material used for the testing passes ASTM D1970[1] as defined in AAMA 714-19 (for fluid applied materials)[8] and AAMA 711-13 (for self-adhered materials).[9] The testing was completed prior to the introduction of the new fastener sealability test method in AAMA 711-20.[10] Variables 5, 6, and 7 in the previous list define where the flashing material is applied on the girt (**Fig. 2**).

A simple calculation shows that a full factorial experimental design would require 3240 test combinations.[11] It was not feasible to test that many combinations, let alone with any replication. Therefore, an experiment was designed to minimize the number of test combinations. The final experiment design with 36 test combinations allowed investigators to study the main effect of each primary variable. The designed experiment was a complex split-plot design consisting of many categorical factors and restricted design space. A split-plot design is used when some of the variables are difficult to change such that the study cannot be completely randomized.[11] For this study, it was difficult to change the insulation board thickness within the same board; therefore a split-plot design was an appropriate choice.

Challenge #2: Resource-Intensive Study

Standard ASTM E331[5] tests are highly resource intensive, as they require building and testing large walls (typically 8 × 8 ft [2.4 × 2.4 m]) along with the use of large-scale test equipment. To counteract this challenge, the study was conducted in two phases. In the first phase, screening tests were conducted on small walls (3 × 3 ft [0.9 × 0.9 m]). Only a subset of variable combinations was then carried forward to phase II, where the full test protocol was tested on larger walls (8 × 8 ft) with replication of each solution. This approach allowed for efficient implementation of the study.

Challenge #3: Inferring and Communicating Results

We hypothesized that without statistical analysis, it would be very difficult to infer and communicate results. Statistical models make it easy to communicate results quantitatively. Statistical analysis also allowed multiple team members to make informed decisions about which combinations were carried forward from phase I to phase II.

Table 1 summarizes the three challenges and the ideas for how to counteract each one.

PHASE I EXPERIMENT METHODS: SCREENING TESTS ON SMALL WALLS

A small-scale pressurized water infiltration test based on ASTM E331[5] was used in phase I testing of 3 × 3 ft (0.9 × 0.9 m) walls. Each wall was able to fit three test conditions. Because the final experiment design had 36 test combinations, there were a total of 12 small walls. Each condition was replicated at least three times, with five replicates for most variables tested. Refer to **Table A1** in the **Appendix** for the full set of variable combinations tested. Only one variation of the fluid-applied, water-based acrylic flashing (Type A) was included in phase I.

Walls were built using 4 in. (100 mm), 18-gauge steel studs spaced approximately 9 in. (230 mm) on center with ISO insulating sheathing attached directly to the studs. Templates were built to ensure alignment between the girt location on the sheathing and the steel stud frame. Girts were attached with the flashing applied as per the defined test combinations. All flashing was allowed to cure for two weeks at standard laboratory conditions before being tested. **Figure 3** shows the step-by-step process of building the small-scale walls.

After the flashing cured, the wall was transferred into a small chamber equipped with a vacuum pump and spray head. Water was sprayed on the entire wall under the pull of vacuum pressure. Water was sprayed at a rate of 5.0 US gal/ft^2 · hr (3.4 L/m^2 · min) per the standard. It was sprayed for two hours under a negative pressure of 6.24 lb/ft^2 (300 Pa) per ICC-ES AC71.[6] The vacuum pressure was then increased to 15 lb/ft^2 (720 Pa) for an additional 15 minutes, which is similar to the testing done on many window systems. While the higher vacuum pressure is greater than what is tested for most WRBs, it is in line with the pressures required of windows being tested to the same standard. If fasteners did not leak during the entire protocol, they were recorded as a pass.

The backside of the walls was examined throughout the testing, and leaks were

Challenge	Counteracting idea
Large number of experiments	Prioritize variables and combine levels Statistically designed experiments
Resource-intensive study	Two-phase testing
Inferring and communicating results	Use statistical models to infer and communicate results

Table 1. Experiment strategy formed by counteracting ideas to the challenges

(a) Make steel stud frame

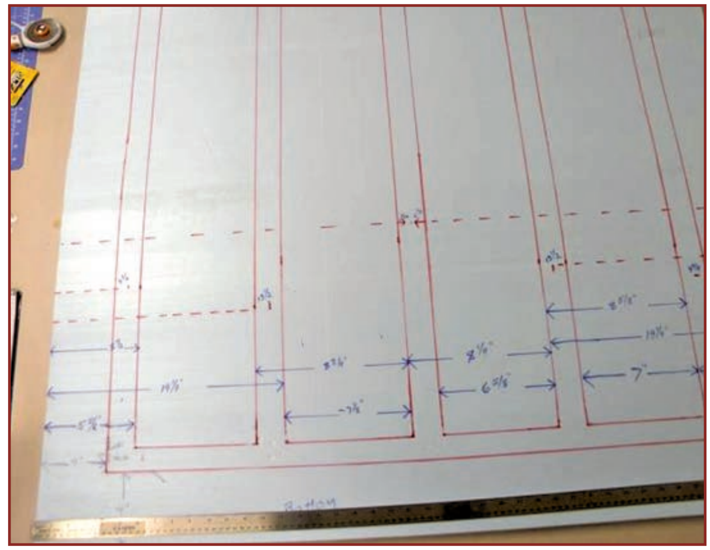

(b) Make templates for placement of girts

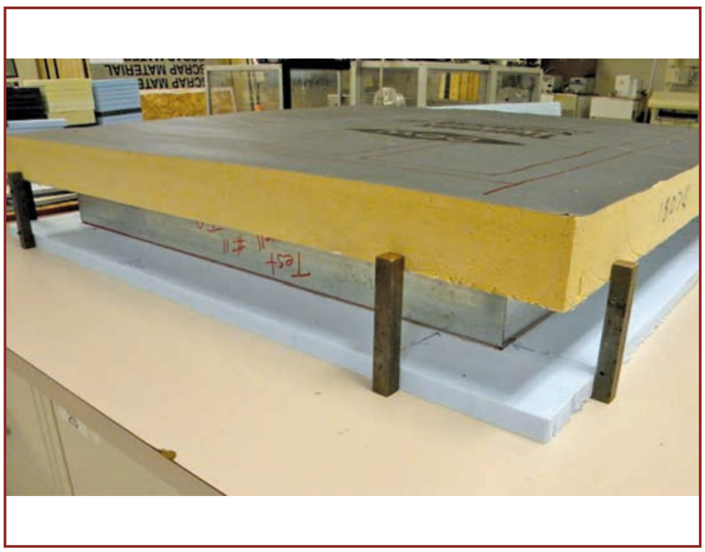

(c) Make wall with insulation sheathing

(d) Attach girts and flashing as per test plan

Figure 3. Step-by-step process to make a wall.

recorded. To make it easier to dentify leaks at the source, the water was infused with red dye and small pieces of paper were attached underneath every penetration between the steel stud frame and ISO insulation—a piece of paper marked with the colored water indicated a leak. In the absence of the paper, a leak might go undetected at the source or the source might be misidentified. For example, water can run down between the stud and the sheathing until it shows at another spot below the actual location of the leak. The indicator paper guarded against such instances. The test chamber, spray nozzle, and paper arrangement are shown in **Fig. 4**.

Two data points were recorded for analysis during the first phase of testing: one was a binary response for water leaks (yes/no) and the second response was a proportion of penetrations of that configuration that leaked (percent leaks). The data were entered into JMP Pro 14.2.0 software for further analysis. The binary response was used to predict the water penetration through a specific combination of variables. The percent leak response was used to identify the most important variables (and consequently the least important variables).

The percent leaks response was analyzed using an ordinary least-squares technique.[12] The *P* value from the hypothesis testing of each variable is shown in **Fig. 5**. The null hypothesis for such a test states that the factor is not important. Hence, wherever there was a low *P* value, the null hypothesis could safely be rejected. For example, it was found that the location where the flashing was applied and the flashing material itself were important factors.

The binary response for leaks (yes/no) was analyzed using a ridge regression model[13] along with the "leave-one-out" validation method. The output of this analysis was a probability-of-leaks model. The misclassification rates are 0.09 for the training data set and 0 for the validation data set. This indicates that the model is a decent model for prediction purposes. A lower probability of leaks (leaks = yes) is desirable. When the probability of this response (leaks = yes) is less than 0.5, the selected combination of variables is considered likely not to leak in future testing.

An interactive graphical model was created using this information. The model allowed the various combinations to be predicted for leaks by changing the input levels of each variable.

(a) Wall inside test frame: front view

(b) Wall inside test frame: back view

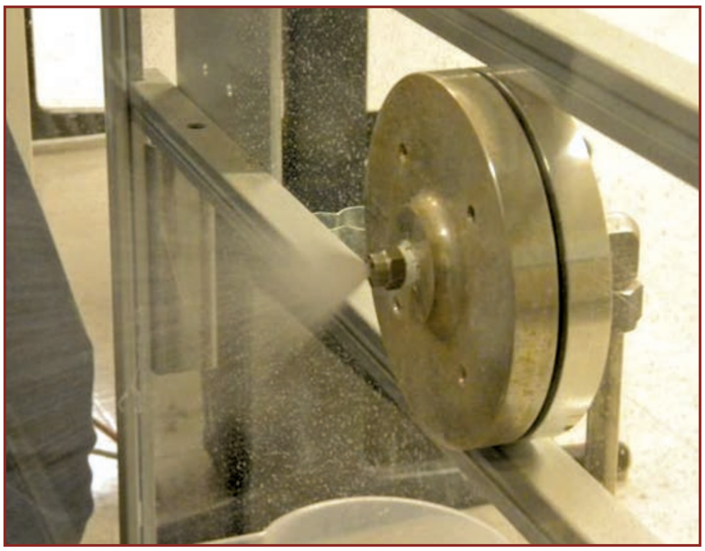

(c) Close-up of spray nozzle inside the test chamber

(d) Wall being tested with colored water

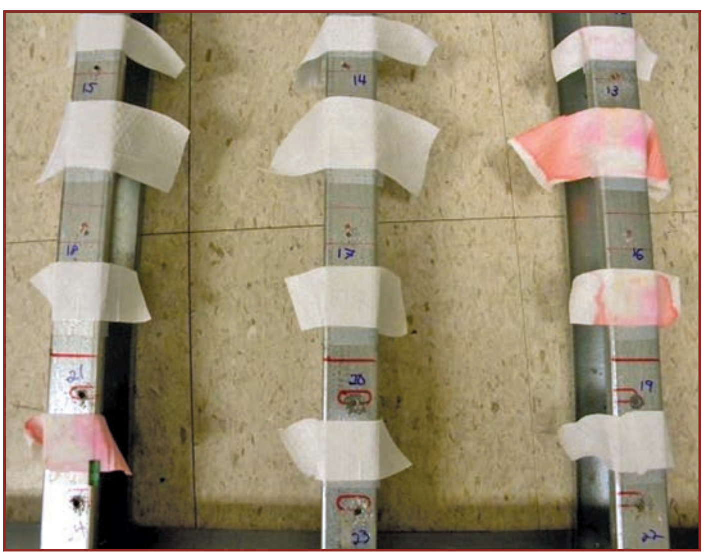

(e) Post test photo of paper pieces that help in accurate leak detection

Figure 4. Test setup and paper detectors.

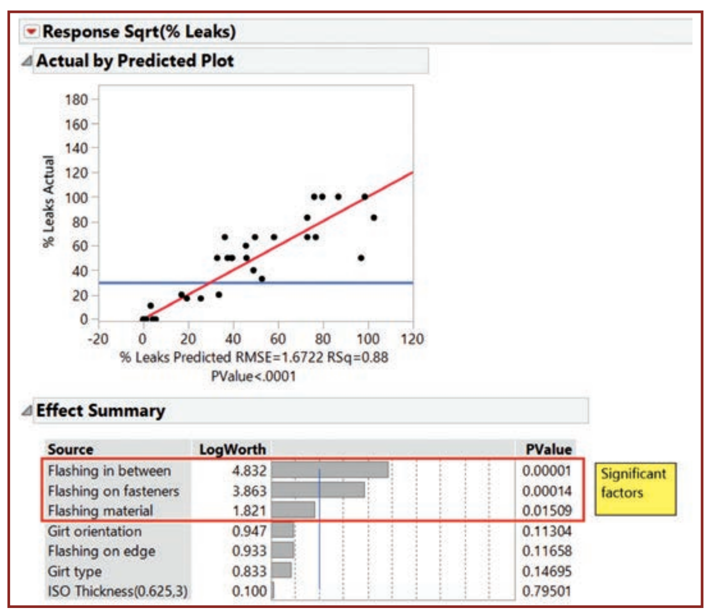

Figure 5. Least-squares model for percent leaks and hypothesis test for each of the model variables.

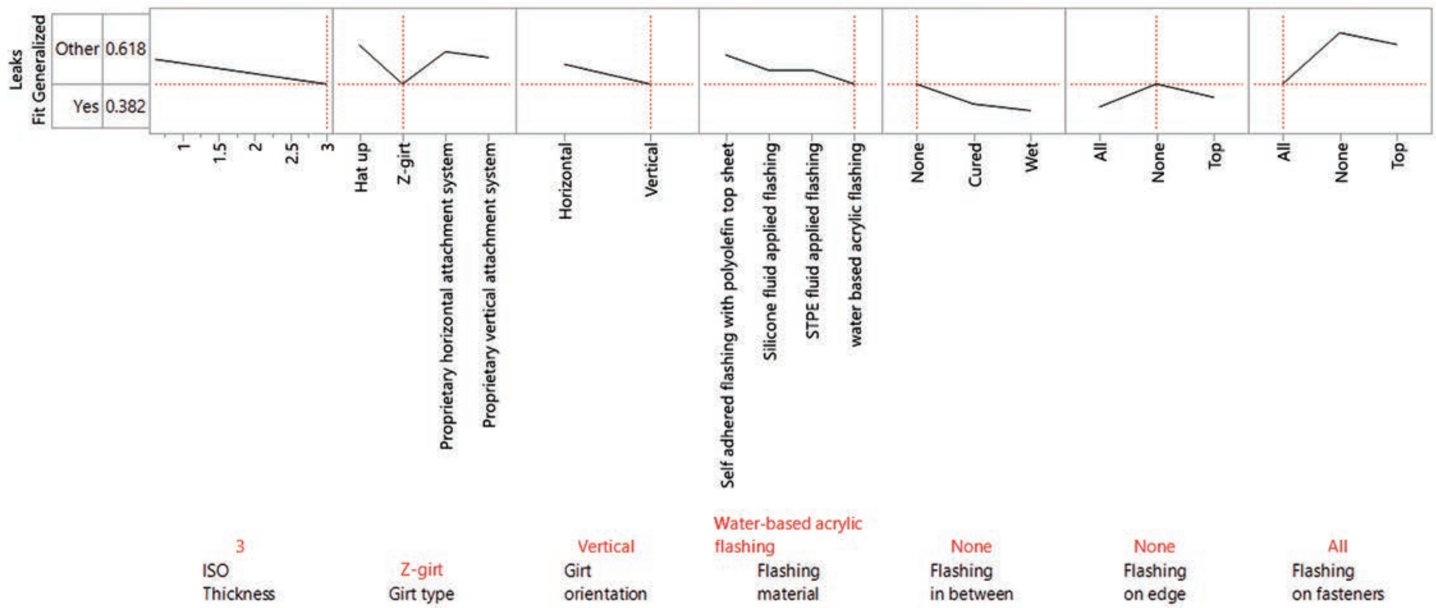

Figure 6. Interactive profiler to predict the probability of leaks based on various input variable selections.

Figure 6 shows the output of a specific set of variables. This scenario shows the prediction that a vertical Z-girt with a water-based acrylic flashing applied only on the fasteners is most likely not going to leak (the probability of "leaks = yes" is 0.38, which is less than 0.5). The interactive profiler was used to predict the effectiveness of multiple combinations. The most promising combinations based on the model, along with additional evaluation based on probability of applicator acceptance and repeatability of the technique between multiple systems, were taken to phase II for full-scale wall assembly testing.

PHASE I RESULTS

All variables from the study were analyzed using the interactive profiler tool. Based on the phase I results, the following factors were found to have the largest impact on percent leaks compared with other factors: flashing being in between the girt and ISO insulation, flashing being on the fasteners, and the type of flashing material used. Girt orientation did not seem to have a strong impact; however, there was a trend of reduced leaks for girts in the vertical direction. The phase I results also showed that the thickness of the insulation had no effect on the results of the configuration. Therefore, this variable was excluded in phase II testing.

Based on previous testing, current field recommendations for various systems, and common assumptions about the performance of self-adhered membranes and fastener sealability, we expected that the self-adhered flashing would be one of the best solutions for sealing behind the fasteners in this wall assembly. However, there were multiple water leaks for this solution in phase I. Therefore, we did not include self-adhered membranes in the phase II test combinations.

PHASE II EXPERIMENTAL METHODS: VALIDATION TESTING WITH FULL-SCALE WALLS

To determine which solutions would be tested in phase II, we used data from the predicted leak probability model, and we also considered both the ease of installation in the field and the desire to have a single recommendation for all types of cladding attachments. As such, we anticipated that some of the configurations tested in phase II would likely fail. We concluded that this expectation was necessary given the ease-of-use and consistency-of-recommendation requirements for the project. This approach would also help to further validate the model.

Two additional variables were added to phase II testing based on the results of phase I. First, a second water-based acrylic fluid-applied flashing material was added (referred to as Type B). The goal was to see whether the performances of Type B and Type A would be similar because of their similar base chemistry or if there would be a difference in performance between the types based on their property differences: Type A passes crack bridging testing, whereas Type B does not.

Second, we had concerns about the ability to get a watertight seal using the proprietary horizontal and vertical cladding attachment systems chosen for the study, as no solutions passed phase I. Therefore, a new technique of wet-dipping the threads and shanks of the screws into the fluid-applied silicone flashing before installing the fastener through the girt/foam sheathing was added for that system. The other tested combinations that were tested in phase II are summarized in **Table A2** of the Appendix.

Once the new set of variable sets was identified for further evaluation, two 8 × 8 ft (2.4 × 2.4 m) walls were assembled. ISO insulating sheathing with a 4.0 mil (0.1 mm) embossed foil facer was secured to 6 in. (150 mm), 18-gauge steel studs at 16 in. (410 mm) on center using standard fasteners recommended by the insulation manufacturer. Due to the number of additional fasteners going into the assembly, the fastening pattern of the insulation fasteners was reduced to the perimeter of the boards only. No exterior gypsum was installed between the insulation and the studs. The joints in the insulation boards were sealed using a silicone fluid-applied flashing. Each wall was assembled such that five fasteners were installed for each configuration to determine repeatability of the solution. A solution that would be implemented in the field to help ensure risks of water infiltration through the fasteners needed to achieve a 100% passing rate.

The walls were tested to a full testing protocol like that used for evaluation of some air barriers and WRBs, with additional testing for better assurance of long-term robustness. The overall series of tests is similar to those proposed in AAMA 504, *Voluntary Laboratory Test Method to Qualify Fenestration Installation*

Figure 7. Wall shown in the test setup. Various girts are attached with different flashing configurations. A spray rack is in front of the wall.

Figure 8. Side view of the wall during test. Water is seen coming out of various nozzles on the spray rack.

Procedures,[14] for testing the installation of window assemblies. The same wall assembly is tested through the entire protocol. This helps determine whether any of the stresses such as wind pressure conditioning cause the assembly to become more porous to air or, more imporA tantly for this study, water. It is not uncommon for wall assemblies that pass the current code limits for air infiltration to have issues with water leakage when tested to this protocol.

The test protocol followed for this study is as follows:

- Conduct air infiltration testing per ASTM E283[3] up to 6.24 lb/ft^2 (300 Pa) pressure differential, with special focus on the code compliance level of 1.57 lb/ft^2 (75 Pa).
- Conduct water infiltration testing per ASTM E331[5] under negative pressure ramping up to 6.24 lb/ft^2, where the wall assembly is held for two hours; then increase the pressure at three additional levels up to 15 lb/ft^2 (720 Pa), with the assembly being held at each of the intermittent and maximum pressures for 15 minutes each.
- Conduct wind pressure conditioning per ASTM E2357.[2]
- Repeat air filtration testing per ASTM E283.
- Repeat water infiltration testing per ASTM E331.
- Conduct thermal cycling per ASTM E2264-05(2013), *Standard Practice for Determining the Effects of Temperature Cycling on Fenestration Products* Method A, Level 2.[14]
- Repeat air filtration testing per ASTM E283.
- Repeat water infiltration testing per ASTM E331.
- Perform forensic evaluation of assemblies.

The pass/fail criterion used for this testing was an air leakage rate less than 0.04 cfm/ft^2 (0.2 L/s·m^2) at a pressure differential of 1.57 lb/ft^2 (75 Pa) and no water observed on the interior

Girt	Flashing	Application
Hat	Silicone fluid-applied flashing	Flashing in between—wet material and flashing on fasteners
	Water-based acrylic flashing A	Flashing in between—cured material and flashing on fasteners
Z-horizontal	Water-based acrylic flashing A Water-based acrylic flashing B	Flashing in between—cured material and flashing on fasteners
Z-vertical	Water-based acrylic flashing A	Flashing in between—cured material and flashing on fasteners
	Silicone fluid-applied flashing	Flashing in between—wet or cured material and flashing on fasteners
Proprietary vertical attachment system	Silicone fluid-applied flashing	Wet-dipped screws
Proprietary horizontal attachment system	Silicone fluid-applied flashing	Wet-dipped screws
	Water-based acrylic flashing A	Flashing in between—cured material and flashing on fasteners

Table 2. Passing results—girt/flashing configuration

side of the wall assembly at any point during the water infiltration testing. The wall assembly was inspected for water leakage after each round of water testing and the conditions were documented. Figures 7 and 8 show the wall assemblies installed in the testing chamber.

Once the complete test protocol was finished, the wall assemblies were put under negative pressure and sprayed using dyed water. The wall assemblies were then taken apart and further examined for evidence of water infiltration through the fastener onto the backside of the sheathing.

PHASE II RESULTS

During phase II, most of the fasteners that leaked during the testing did so early during the first round of water penetration testing, often during the two hours of water spray with 6.24 lb/ft^2 (300 Pa) negative pressure on the assembly. A few additional fasteners leaked during the second round, with all but one of them leaking at differential pressure equal to or greater than 12.5 lb/ft^2 (600 Pa). Two fasteners leaked for the first time during the final round of water penetration testing after thermal cycling.

While all of the flashing materials tested in phase II successfully passed the nail penetration testing currently required by AAMA 714,[8] which is based on ASTM D1970,[1] they did not all perform the same. The two water-based acrylic flashing materials exhibited different results when tested under the same conditions. Type A was more likely to pass water penetration testing throughout the entire protocol than Type B. In fact, Type A performed more similarly to the silicone fluid-applied flashing.

The phase II test results identified a common solution for the standard hat channel and Z-girt systems regardless of orientation: use of a Type A water-based acrylic flashing that is cured in between the girt and the sheathing and sealing the fastener heads. This successful result was predicted by the model. Given the study size limitations and current construction practices, phase II did not include the Type A flashing installed wet in between the girt and sheathing. However, the predictive model shows wet flashing in this location always has a lower probability of leaks than cured flashing. This solution could be fully tested in a large-scale assembly to provide additional flexibility in construction operations.

Phase II testing also provided a successful result for the proprietary attachment system. Table 2 presents all of the girt/flashing/application combinations that showed zero water leakage throughout the entire test protocol from phase II.

There were a few surprising results during phase II testing that were not predicted by the model:

- The biggest surprise was the use of silicone fluid-applied flashing applied wet between the girt and the sheathing with additional flashing on the fastener heads on hat channels. The model predicted that this solution would likely fail. It was included in phase II because the model showed this treatment was likely to be successful for Z-girts and there was a desire to have a consistent solution for the treatment of all systems. This method of sealing the hat channel girts was successful.
- Despite predicted success on the horizontal Z-girt system, this application of silicone fluid-applied flashing applied wet between the girt and the sheathing with additional flashing on the fastener heads was not 100% successful for all fasteners, as there was a late water leak on one fastener at 12.5 lb/ft^2 (600 Pa) negative pressure after thermal cycling. Although this solution did not pass the full criteria for this study, it would likely be acceptable for most building types.
- Like all models, this model has some uncertainty around its predictions. When the model predicts probability lower than 0.5 but close to it, there is still potential for the solution to leak. For example, the model predicted success of only treating the fasteners on the Z-girts in a vertical orientation. The probability of leaks in the model was 0.42. This configuration was included in phase II because of its simplicity, but it leaked during testing.

STUDY LIMITATIONS AND FUTURE WORK

While this study included a large number of conditions and scenarios, it was not comprehensive of all variables found in exterior wall construction. Additional testing is required to continue assessing the impact of additional variables such as different sizes of self-driven screws and different facers of the ISO boards.

The current study also did not address the impact of the weight of the cladding on the girts and rotation of the fasteners during both installation and service. It also did not evaluate the impact of thinner-gauge or smaller steel studs. These variables could allow for more movement of the fasteners and the entire wall assembly.

It would also be interesting to investigate whether these same fastener sealing solutions provide a watertight solution for attaching girts to wall assemblies where the insulation is a different layer from the air and water barrier, such as is found in a more traditional wall assembly with gypsum being installed to the steel stud followed by a WRB and the insulation. Additionally, this work could be repeated on wood-based structures. Finally, there is a need to evaluate the wet-dipped screw option for other systems and other types of fluid-applied flashings given its ease of use in the field.

CONCLUSION

The use of statistical design greatly reduced the test effort required for this study, and building a validated predictive model for leaks improved the quality of the results. The probability-of-leakage model allowed the team to evaluate several variables, compare expected results, and evaluate key candidates for a second phase of more robust testing. Learnings from each phase of the testing were included in the next round of testing to continually improve the proposed solutions and quickly reach final field recommendations.

The study found the following factors have significantly affect leak resistance:

- Location of flashing. The testing affirmed the hypothesis that sealing at the point of penetration is important to keep water out of the full assembly. Specifically, it was more beneficial to apply the flashing on the fasteners and in between the girt and ISO insulating sheathing. Wet-set flashing performed better than cured-set flashing in between the girt and ISO insulating sheathing.
- Flashing material. Fluid-applied flashing performed better than self-adhered flashing. The performance of the fluid-applied flashing solutions tested also varied. The difference in performance between the two water-based acrylic flashing materials included in the study indicates that performance cannot be assumed based on the base chemistry of the material alone. None of the tested materials had known self-healing properties, but all are able to pass the roofing nail water-penetration test.

The statistical model suggested that girt orientation did not have a strong impact on leaks. However, all vertical girts had fewer leaks than horizontal ones; there is a trend toward fewer leaks on vertical girts. Additionally, the thickness of the ISO insulation did not have any effect on leaks.

This study has provided data-based flashing recommendations to end users of ISO insulation as to how best to install cladding attachments over the insulation boards to prevent future water penetration.

ACKNOWLEDGMENTS

The authors would like to acknowledge the following building scientists with DuPont for their direct contributions in completing this study: Mae Drzyzga, Shanot Kelty, Kim LeBlanc, Anson Wong, and Gary Parsons.

REFERENCES

1. ASTM International. 2021. *Standard Specification for Self-Adhering Polymer Modified Bituminous Sheet Materials Used as Steep Roofing Underlayment for Ice Dam Protection*. ASTM D1970/D1970M-21. West Conshohocken, PA: ASTM International. https://doi.org/10.1520/D1970_D1970M-21.
2. ASTM International. 2018. *Standard Test Method for Determining Air Leakage Rate of Air Barrier Assemblies*. ASTM E2357-18. West Conshohocken, PA: ASTM International. https://doi.org/10.1520/E2357-18.
3. ASTM International. 2019. *Standard Test Method for Determining Rate of Air Leakage Through Exterior Windows, Skylights, Curtain Walls, and Doors Under Specified Pressure Differences Across the Specimen*. ASTM E283/E283M-19. West Conshohocken, PA: ASTM International. https://doi.org/10.1520/E0283_E0283M-19.
4. International Code Council (ICC). 2021. *International Building Code*. Country Club Hills, IL: ICC.
5. ASTM International. 2016. *Standard Test Method for Water Penetration of Exterior Windows, Skylights, Doors, and Curtain Walls by Uniform Static Air Pressure Difference*. ASTM E331-00(2016). West Conshohocken, PA: ASTM International. https://doi.org/10.1520/E0331-00R16.
6. ICC Evaluation Service (ICC-ES). 2018. *Acceptance Criteria 71: Foam Plastic Sheathing Panels Used as Weather-Resistive Barriers*. ICC-ES AC71. Brea, CA: ICC-ES.
7. Devore, J. L. 2004. *Probability and Statistics for Engineering and the Sciences*. 6th ed. Belmont, CA: Brooks/Cole-Thomson Learning.
8. Fenestration and Glazing Industry Alliance (FGIA). 2018. *Voluntary Specification for Liquid Applied Flashing Used to Create a Water-Resistive Seal Around Exterior Wall Openings in Buildings*. AAMA 714-19. Schaumburg, IL: FGIA.
9. American Architectural Manufacturers Association (AAMA). 2013. *Voluntary Specification for Self Adhered Flashing Used for Installation of Exterior Wall Fenestration Products*. AAMA 711-13. Schaumburg, IL: AAMA.
10. FGIA. 2020. *Voluntary Specification for Self-Adhering Flashing Used for Installation of Exterior Wall Fenestration Products*. AAMA 711-20. Schaumburg, IL: FGIA.
11. Montgomery, D. C. 2005. *Design and Analysis of Experiments*. 6th ed. New York, NY: John Wiley & Sons.
12. Neter, J., M. Kutner, W. Wasserman, and C. Nachtsheim. 1996. *Applied Linear Statistical Models*. 4th ed. New York, NY: McGraw-Hill/Irwin.
13. Hastie, T., R. Tibshirani, and J. Friedman. 2001. *The Element of Statistical Learning: Data Mining, Inference, and Prediction*. New York, NY: Springer.
14. FGIA. 2020. *Voluntary Laboratory Test Method to Qualify Fenestration Installation Procedures*. AAMA 504-20. Schaumburg, IL: FGIA.
15. ASTM International. 2013. *Standard Practice for Determining the Effects of Temperature Cycling on Fenestration Products*. ASTM E2264-05(2013). West Conshohocken, PA: ASTM International.

APPENDIX

Table A1. Variable combinations tested in phase I

Insulation thickness, in	Girt	Flashing	Flashing
0.625	Proprietary horizontal system	Self-adhered flashing	On fasteners only
		STPE flashing	On fasteners and top edge
			Both edges
	Proprietary vertical system	Silicone fluid-applied flashing	Flashing in between—cured
	Hat	Self-adhered flashing	Flashing in between
		Water-based acrylic fluid-applied flashing A	On fasteners and top edge
	Z—horizontal	Silicone fluid-applied flashing	Flashing in between—wet and on fasteners
	Z—vertical	Silicone fluid-applied flashing	Flashing in between—cured
		STPE flashing	Flashing in between—cured and on fasteners and edges
1.55	Proprietary horizontal system	Silicone fluid-applied flashing	Flashing in between—wet and on fasteners and both edges
			Flashing in between—cured and on fasteners and both edges
		Self-adhered flashing	Flashing in between and on both edges
		None	None
		Water-based acrylic fluid-applied flashing A	On fasteners only
			Flashing in between—cured and on top edge
	Proprietary vertical system	None	None
	Hat	None	None
		Silicone fluid-applied flashing	On fasteners and top edge
		STPE flashing	Flashing in between—cured and on fasteners
	Z—horizontal	STPE flashing	Flashing in between—wet and on fasteners
			On edge only
	Z—vertical	None	None
		Water-based acrylic fluid-applied flashing A	On fasteners and on edge
		STPE flashing	On edge only
		Self-adhered flashing	On fasteners only

APPENDIX

Table A1. Variable combinations tested in phase I (continued)

<table>
<tr><th>Insulation thickness, in</th><th>Girt</th><th>Flashing</th><th>Flashing</th></tr>
<tr><td rowspan="13">3</td><td rowspan="3">Proprietary horizontal system</td><td>STPE flashing</td><td>Flashing in between—wet, on fasteners and on top edge</td></tr>
<tr><td>Silicone fluid-applied flashing</td><td>Flashing in between—cured and on top edge</td></tr>
<tr><td>Self-adhered flashing</td><td>On fasteners and top edge</td></tr>
<tr><td>Proprietary vertical system</td><td>Silicone fluid-applied flashing</td><td>Flashing in between—wet</td></tr>
<tr><td rowspan="4">Hat</td><td rowspan="2">Water-based acrylic fluid-applied flashing A</td><td>On fasteners only</td></tr>
<tr><td>Flashing in between—wet, on fasteners and on both edges</td></tr>
<tr><td>STPE flashing</td><td>Flashing in between—cured and top fasteners</td></tr>
<tr><td>Self-adhered flashing</td><td>Flashing in between, on fasteners and on both edges</td></tr>
<tr><td rowspan="2">Z—horizontal</td><td>Water-based acrylic fluid-applied flashing A</td><td>Flashing in between—cured, on fasteners and on both edges</td></tr>
<tr><td>Silicone fluid-applied flashing</td><td>On edges only</td></tr>
<tr><td rowspan="2">Z—vertical</td><td>Water-based acrylic fluid-applied flashing A</td><td>Flashing in between—wet</td></tr>
<tr><td>Self-adhered flashing</td><td>Flashing in between—cured, on fasteners and on edges</td></tr>
</table>

Note: STPE = silyl-terminated polyether. 1 in. = 25.4 mm.

APPENDIX

Table A2. Variable combinations tested in phase II

Girt	Flashing	Application
Hat	Water-based acrylic fluid-applied flashing A	On fasteners only
		Flashing in between—cured material and flashing on fasteners
	Water-based acrylic fluid-applied flashing B	Flashing in between—cured material and flashing on fasteners
	Silicone fluid-applied flashing	Flashing in between—wet material, flashing on fasteners and on edges
		Flashing in between—wet material and flashing on fasteners
Z—horizontal	Water-based acrylic fluid-applied flashing A	Flashing in between—cured material and flashing on fasteners
		On fasteners only
	Silicone fluid-applied flashing	Flashing in between—cured material and flashing on fasteners
		Flashing in between—wet material and flashing on fasteners
	Water-based acrylic fluid-applied flashing B	Flashing in between—cured material and flashing on fasteners
Z—vertical	Water-based acrylic fluid-applied flashing A	Flashing in between—cured material and flashing on fasteners
		On fasteners only
	Silicone fluid-applied flashing	Flashing in between—cured material and flashing on fasteners
		Flashing in between—wet material and flashing on fasteners
	Water-based acrylic fluid-applied flashing B	Flashing in between—cured material and flashing on fasteners
Proprietary horizontal system	Water-based acrylic fluid-applied flashing A	Flashing in between—cured material and flashing on fasteners
	Silicone fluid-applied flashing	Wet-dipped screws
Proprietary vertical system	Water-based acrylic fluid-applied flashing A	Flashing in between—cured material and flashing on fasteners
	Silicone fluid-applied flashing	Wet-dipped screws

Scan this QR Code into your smartphone to find out more about IIBEC